



Universiteit  
Leiden  
The Netherlands

## A chemical biology approach for targeting of ligand-drug conjugates

Hoogendoorn, S.

### Citation

Hoogendoorn, S. (2014, January 23). *A chemical biology approach for targeting of ligand-drug conjugates*. Retrieved from <https://hdl.handle.net/1887/23082>

Version: Corrected Publisher's Version

License: [Licence agreement concerning inclusion of doctoral thesis in the Institutional Repository of the University of Leiden](#)

Downloaded from: <https://hdl.handle.net/1887/23082>

**Note:** To cite this publication please use the final published version (if applicable).

Cover Page



Universiteit Leiden



The handle <http://hdl.handle.net/1887/23082> holds various files of this Leiden University dissertation.

**Author:** Hoogendoorn, Sascha

**Title:** A chemical biology approach for targeting of ligand-drug conjugates

**Issue Date:** 2014-01-23

# A Chemical Biology Approach for Targeting of Ligand-Drug Conjugates

---

PROEFSCHRIFT

ter verkrijging van  
de graad van Doctor aan de Universiteit Leiden,  
op gezag van Rector Magnificus prof. mr. dr. C. J. J. M. Stolker,  
volgens besluit van het College voor Promoties  
te verdedigen op donderdag 23 januari 2014  
klokke 11.15 uur

door

**Sascha Hoogendoorn**

Geboren te Amsterdam in 1984

## Promotiecommissie

Promotores: Prof. dr. H. S. Overkleef  
Prof. dr. G. A. van der Marel

Co-promotor: Dr. R. G. Boot

Overige leden: Prof. dr. J. J. Neefjes  
Prof. dr. J. Brouwer  
Prof. dr. J. Lugtenburg  
Dr. K. M. Bongers  
Dr. M. van der Stelt



# Table of Contents

|  |     |
|--|-----|
| List of Abbreviations  | iv  |
| 1 General introduction   | 1   |
| 2 Targeted pH-dependent fluorescent activity-based cathepsin probes  | 17  |
| 3 Synthesis of pH-activatable red fluorescent BODIPY dyes with distinct functionalities                                    | 37  |
| 4 Targeted delivery of Heat shock protein 70 by sortase-mediated ligation with a synthetic mannose receptor-binding ligand | 55  |
| 5 Multivalent MPR ligand for endolysosomal targeting of an activity-based cathepsin probe                                  | 71  |
| 6 Structure-activity relationship studies towards functionalization of dihydropyridine FSHR agonists                       | 87  |
| 7 Small-molecule fluorescent agonists for the follicle-stimulating hormone receptor  | 123 |
| 8 Small-molecule FSHR agonists as targeting agents for BNCT  | 147 |
| 9 From LMW to HMW ligands: fluorescently tagged FSH by sortase-mediated ligation   | 171 |
| 10 Summary, Work in Progress and Future Prospects  | 187 |
| Samenvatting   | 207 |
| List of Publications   | 210 |
| Curriculum Vitae   | 211 |

# List of Abbreviations

|                    |   |          |   |
|--------------------|---|----------|---|
| ab                 | antibody  | Cy       | cyanine dye   |
| ABP                | activity-based probe                                      | d        | doublet   |
| Ac                 | acetyl  | $\delta$ | chemical shift  |
| ACN                | acetonitrile  | DBU      | 1,8-diazabicyclo[5.4.0]undec-7-ene  |
| AcOH               | acetic acid   | DC       | dendritic cell  |
| Ahx                | aminohexanoic acid  | DC       | dual color molecular weight marker SDS-PAGE                                     |
| aq                 | aqueous   | DC-SIGN  | dendritic cell-specific intercellular adhesion molecule-3-grabbing non-integrin |
| ar                 | aromatic  | DCE      | dichloroethane  |
| ATP                | adenosine triphosphate                                    | DCM      | dichloromethane   |
| BAIB               | bis(acetoxy)iodobenzene                                   | dd       | double doublet  |
| BDP                | BODIPY  | DDQ      | 2,3-dichloro-5,6-dicyano-1,4-benzoquinone                                       |
| BMP                | bis(monoacylglycero)phosphate                             | DHP      | dihydropyridine   |
| BNCT               | boron neutron capture therapy                             | DIAD     | diisopropyl azodicarboxylate  |
| Boc                | <i>tert</i> -butoxycarbonyl                               | DiPEA    | <i>N,N</i> -diisopropylethylamine   |
| Boc <sub>2</sub> O | <i>tert</i> -butoxycarbonyl anhydride                     | DMAP     | 4-( <i>N,N</i> -dimethylamino)-pyridine   |
| BODIPY             | 4,4-difluoro-4-bora-3a,4a-diaza- <i>s</i> -indacene       | DMEM     | Dulbecco's modified eagle's medium  |
| BSA                | bovine serum albumin                                      | DMF      | <i>N,N</i> -dimethylformamide   |
| BSH                | <i>closo</i> -borane mercaptoundecahydrododecaborate      | DMSO     | dimethylsulfoxide   |
| Bu                 | butyl   | DNJ      | deoxynojirimycin  |
| calcd.             | calculated  | DOX      | doxorubicin   |
| cAMP               | cyclic adenosine monophosphate                            | dt       | double triplet  |
| cat.               | catalytic   | DTT      | dithiothreitol  |
| CBB                | coomassie brilliant blue                                  | EDC      | 1-ethyl-3-(3-dimethylaminopropyl)-carbodiimide                                  |
| CBE                | conditrol beta epoxide                                    | EDTA     | ethylenediaminetetraacetate   |
| CD                 | circular dichroism  | EEDQ     | 2-ethoxy-1-ethoxycarbonyl-1,2-dihydroquinoline                                  |
| CD-MPR             | cation-dependent mannose-6-phosphate receptor             | ELISA    | enzyme-linked immunosorbent assay   |
| CHAPS              | 3-[(3-cholamidopropyl)dimethylammonio]-1-propanesulfonate | eq       | molar equivalents   |
| CHO                | chinese hamster ovary (cells)                             | ER       | endoplasmic reticulum   |
| CI-MPR             | cation-independent mannose-6-phosphate receptor           | ERT      | enzyme replacement therapy  |
| CPZ                | chlorpromazine  | ESI      | electrospray ionization   |
| CRD                | carbohydrate recognition domain                           | Et       | ethyl   |
| CRE                | cAMP response element                                     | EtOAc    | ethyl acetate   |
| CTLD               | C-type lectin-like domain                                 | FACS     | fluorescence-activated cell sorting   |
| CV                 | column volume   | FCS      | fetal calf serum  |
|                    |   | FITC     | fluorescein isothiocyanate  |

|            |  |            |   |
|------------|--|------------|---|
| Fmoc       | (9 <i>H</i> -fluoren-9-yl)methoxycarbonyl  | MeOH       | methanol  |
| FR         | folate receptor  | MFI        | mean fluorescence intensity   |
| FRET       | fluorescence resonance energy transfer   | min        | minute(s)   |
| FSC        | forward scatter  | MPR        | mannose-6-phosphate receptor  |
| FSH(R)     | follicle-stimulating hormone (receptor)  | MR         | mannose receptor  |
| FT         | flow-through   | MWCO       | molecular weight cutoff   |
| (e)GFP     | (enhanced) green fluorescent protein   | NBD        | 7-nitrobenz-2-oxa-1,3-diazol-4-yl ( <i>dye</i> )                    |
| GBA1       | $\beta$ -glucocerebrosidase 1  | NBD        | nucleotide binding domain ( <i>protein</i> )                        |
| GnRH       | gonadotropin-releasing hormone   | NBS        | newborn bovine calf serum   |
| GPCR       | G protein-coupled receptor   | NMP        | <i>N</i> -methyl-2-pyrrolidone                                      |
| GRK        | G protein-coupled receptor kinase  | NMR        | nuclear magnetic resonance  |
| GSL        | glycosphingolipid  | NPD        | Niemann-Pick disease  |
| h          | hour(s)  | NPY        | neuropeptide Y  |
| HBTU       | 2-(1 <i>H</i> -Benzotriazole-1-yl)-1,1,3,3-tetramethyluronium hexafluorophosphate          | NTD        | N-terminal domain   |
| hCG        | human chorionic gonadotropin   | o/n        | overnight   |
| HCTU       | 2-(6-chloro-1 <i>H</i> -benzotriazole-1-yl)-1,1,3,3-tetramethyluronium hexafluorophosphate | <i>o</i> - | <i>ortho</i> -  |
| HEK293     | human embryonic kidney (cells)   | obsd.      | observed  |
| HMW        | high molecular weight  | <i>p</i> - | <i>para</i> -   |
| HOBt       | <i>N</i> -hydroxybenzotriazole   | PAGE       | polyacrylamide gel electrophoresis                                  |
| HRMS       | high resolution mass spectrometry  | PBS        | phosphate buffered saline   |
| HRP        | horseradish peroxidase   | PE         | petroleum ether   |
| Hsp        | heat shock protein   | PEG        | polyethylene glycol   |
| Hz         | hertz  | pen/strep  | penicillin/streptomycin   |
| IGF-II     | insulin-like growth factor-2   | PeT        | photoinduced electron transfer                                      |
| IMDM       | Iscove's modified Dulbecco's medium  | Ph         | phenyl  |
| <i>J</i>   | coupling constant  | ppm        | parts per million   |
| LC/MS      | liquid chromatography/ mass spectrometry   | PyBOP      | (benzotriazol-1-yloxy)tripyrrolidinophosphonium hexafluorophosphate |
| LH(R)      | luteinizing hormone (receptor)   | q          | quartet   |
| LMW        | low molecular weight   | quant      | quantitative  |
| LSD        | lysosomal storage disorder   | $R_f$      | retention factor  |
| M          | molar  | rFSH       | recombinant FSH   |
| m          | multiplet  | RhoB       | rhodamine B dye   |
| M6P        | mannose-6-phosphate  | rpm        | revolutions per minute  |
| M6PC       | mannose-6-phosphate cluster  | rt         | room temperature  |
| M6Pn       | mannose-6-phosphonate  | s          | singlet   |
| <i>m/z</i> | mass to charge ratio   | SAR        | structure-activity relationship                                     |
| <i>m</i> - | <i>meta</i> -  | sat        | saturated   |
| man        | mannose  | SBD        | substrate binding domain ( <i>protein</i> )                         |
| MC         | mannose cluster  | SDS        | sodium dodecyl sulfate  |
| Me         | methyl   | SPPS       | solid-phase peptide synthesis                                       |
|            |  | SrtA       | sortase A   |
|            |  | SSC        | side scatter  |
|            |  | sst        | somatostatin receptor   |
|            |  | t          | triplet   |
|            |  | $t_R$      | retention time  |
|            |  | TBAF       | tetrabutylammonium fluoride   |

|        |                                   |        |   |
|--------|-----------------------------------|--------|---|
| TBAI   | tetrabutylammonium iodide         | TLC    | thin layer chromatography                 |
| TBDMS  | <i>tert</i> -butyl dimethylsilyl  | Tris   | 2-amino-2-(hydroxymethyl)-1,3-propanediol |
| TBDPS  | <i>tert</i> -butyl diphenylsilyl  | trz    | triazole                                  |
| TBS(T) | Tris-buffered saline (+ Tween 20) | TSH(R) | thyroid-stimulating hormone (receptor)    |
| TEA    | triethylamine                     | WB     | western blot                              |
| TEMPO  | 2,2,6,6-tetramethylpiperidinyloxy | WT     | wildtype                                  |
| TFA    | trifluoroacetic acid              | (e)YFP | (enhanced) yellow fluorescent protein     |
| THF    | tetrahydrofuran                   |        |   |
| THQ    | tetrahydroquinoline               |        |   |
| TIS    | triisopropyl silane               |        |   |

Note: The one or three letter codes for the amino acids follow the recommendations of IUPAC. *J. Biol. Chem.* **1968**, 243, 3557-3559 and *J. Biol. Chem.* **1972**, 247, 977-983.





# 1

## General introduction

Many complex biological processes are regulated by cell signaling, where a secreted ligand travels short or long distances through an organism or tissue until it is recognized by a cell surface receptor. These receptors, proteins residing in the cellular membrane, function as a communication channel between the extra- and intracellular space, translating the binding of a ligand into a variety of signaling cascades which ultimately lead to a cellular response. Receptor expression is cell-type specific so that the ligands that bind them exert a localized effect. This principle is essential for maintaining normal tissue homeostasis and dysregulation of cellular communication lies at the basis of a variety of diseases, such as cancer or autoimmune diseases. In his pioneering work in the early 20th century, Paul Ehrlich proposed the presence of a ligand-receptor interaction and the possibilities that this provides for selective targeting of chemotherapeutics.<sup>1</sup> With his studies on the cellular localization of colored dyes he laid the groundwork for the realisation that the chemical properties of a compound, in combination with the cell on which it acts, determine the effects. He recognized the potential of organic chemistry as a means to create those molecules that interact with a specific cellular target as indicated by his statement "wir müssen zielen lernen, chemisch zielen lernen" ("we have to learn how to aim, aim chemically").<sup>2,3</sup> More than a hundred years later, the search for Ehrlich's "magic bullet" has not ceased and the area of drug targeting approaches is still very much alive. In this chapter, current strategies for the targeted delivery of imaging or therapeutic agents that employ ligand-receptor interactions will be highlighted. In line with the projects discussed in the later chapters of this thesis, the focus will be on those examples that make use of synthetic approaches to reach this goal.

## General principles of receptor-mediated targeted delivery

When discussing targeted delivery, it is important to distinguish which kind of targeting is envisaged, systemic, intracellular or both. In the ideal case, the ligand-drug conjugate enters the circulation, and accumulates at the site where its action is needed by being captured by the surface receptors. For this to happen, the affinity of the ligand and the expression levels of the receptor should be sufficiently high. Ideally, the receptor is only expressed on the diseased cells, such as tumor cells, because even when overexpressed, the lower levels on the more abundant healthy cells will compete for binding and can thus act as a sink. Non-specific interaction with surrounding cells should preferably be very low.

Once arrived at the site of action, multiple options for further, intracellular, delivery exist, depending on the nature of the ligand and the design of the ligand-drug conjugate. Ligands are generally classified as agonists, which activate receptors, or antagonists, which block the receptor and thereby prevent activation. Over the years it has become clear that this classification does not cover all possibilities, with ligands being able to induce full or partial effects that can even be opposite to that generated by an endogenous agonist.<sup>4</sup> Moreover, besides the orthosteric binding site where the endogenous ligand binds, there are often other, allosteric, sites where ligand binding can occur. Some receptors contain multiple ligand recognition domains, leading to enhanced affinity for multivalent ligands, examples of which will be discussed in more detail later on. Binding of a ligand, typically an agonist, to the receptor might result in receptor-ligand internalization. Depending on the type of targeted therapy, this might be an advantage or a disadvantage. The two-step antibody-directed enzyme prodrug therapy (ADEPT) is designed such that an enzyme, required to release the active drug, is delivered to the binding site so that the drug can then freely diffuse into the tissue.<sup>5</sup>

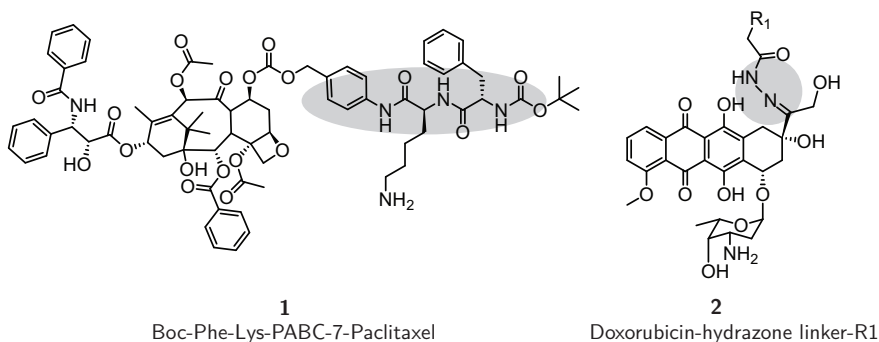


**Figure 1.1:** Strategies for controlled release in the lysosomes of paclitaxel or doxorubicin by employing Cathepsin B-cleavable (Phe-Lys) or acid labile (hydrazone) linkers. PABC: self-immolative *p*-aminobenzylcarbamate linker. Linker regions are indicated in grey.

In most cases drugs or drug formulations need to be delivered intracellularly by receptor-mediated endocytosis to exert their effect. For some therapies, such as enzyme replacement therapy for lysosomal storage disorders, the endolysosomal pathway is the endpoint of the delivery. In many other cases, the drug needs to be released from the endolysosomes



to reach its intracellular target, requiring alternative strategies such as synthetic cleavable linkers between the ligand and the drug. The use of a cathepsin B cleavable dipeptide linker (1, Figure 1.1) has been used to release the cytotoxic anticancer drugs paclitaxel (acting on microtubules), doxorubicin (DOX) (a DNA intercalator), and mitomycin C (a DNA crosslinker) from the lysosomes.<sup>6,7</sup> Making use of the increasingly acidic pH of the endolysosomes is another means of controlled drug release as shown by the introduction of an acid labile hydrazone linkage onto DOX, which was released in the lysosomes (2, Figure 1.1).<sup>8,9</sup> In case of targeted delivery for diagnostic purposes, such as a fluorescent dye or a radiotracer, it will depend on the final goal whether an antagonist or an agonist is the preferred ligand. Antagonists are the ligands of choice to visualize a receptor population on the cell membrane without inducing a direct effect, whereas if receptor-ligand internalization and trafficking are the subjects of interest, agonists are preferred.

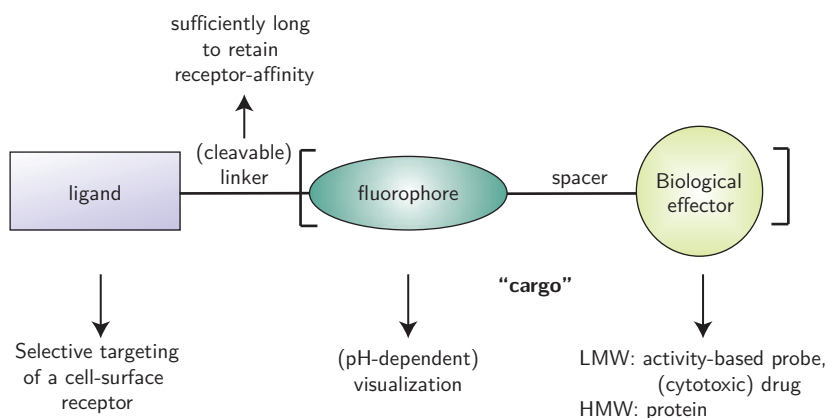


**Figure 1.2:** General structure of constructs for targeted drug delivery.

The general structure of the (bio)molecules employed for targeted delivery thus consists of the receptor-binding ligand, a (cleavable) linker and 'cargo' (Figure 1.2). The cargo could involve a therapeutic agent such as a drug or a protein and alternatively it could be a reporter group, such as a fluorescent dye, to visualize and study the delivery process and/or an activity-based probe to assess the activity of an intracellular enzyme. This general structure forms the basis of the synthesized constructs that are presented in this thesis. In Chapters 2 and 5 fluorescent DCG-04, an activity-based probe for lysosomal cathepsins was introduced as cargo, in Chapter 4 the protein Hsp70, and in Chapters 7-9 fluorescent dyes for visualization and carboranes as potential drugs. The ligands that are found in the literature can be divided in two main categories: antibodies (or fragments thereof) directed to a specific cell receptor or antigen, or non-antibody receptor ligands, spanning a wide variety of synthetic and endogenous ligands. Even though the antibody category has its distinct advantages in the sense of affinity and selectivity, the synthetic ligands hold a lot of promise because of the relatively easy access to large amounts of defined material which can be chemically tuned to contain the properties of interest (see Chapters 2, 4-8).

In the following sections selected literature examples of synthetic ligands that are used as targeting devices are discussed, based on the receptor type that they bind.

## G protein-coupled receptors

The large family of G protein-coupled receptors (GPCRs) is one of the most druggable and many synthetic small molecules or peptides have been developed that are able to act on these receptors.<sup>10,11</sup> Endogenous ligands for GPCRs span a wide range of biomolecules, from small compounds such as neurotransmitters to large protein hormones. Although the structural features of individual GPCRs vary considerably, they are all characterized by a seven-transmembrane domain (Figure 1.3). A heterotrimeric G-protein is bound to the C-terminus which dissociates upon activation of the receptor. Depending on the nature of the  $\alpha$ -subunit of the G-protein ( $G_s$ ,  $G_i$ ,  $G_q$  or  $G_{12/13}$ ) distinct intracellular signaling cascades are set in motion.<sup>12</sup> An elaborate desensitization/resensitization mechanism is used to prevent overstimulation of the system. G protein-coupled receptor kinases (GRKs) phosphorylate the receptor,<sup>13</sup> enabling the binding of  $\beta$ -arrestins. Arrestin binding prevents the binding of G-proteins, thereby desensitizing the receptor for further stimulation. In a next step, the receptor is sequestered from the cell membrane in clathrin-coated vesicles. This can either lead to resensitization, in which the receptor is dephosphorylated and recycled back to the surface in an active form, or to downregulation of the receptor from the cell membrane by degradation in the endolysosomal pathway.<sup>14</sup> The fate of the ligand upon endocytosis varies. If the receptor-ligand complex is stable, the ligand might recycle back to the membrane together with the receptor where it is released into the extracellular space. If the receptor-ligand complex is unstable, the ligand might be released into the endolysosomal pathway where it is degraded and the drug is released.

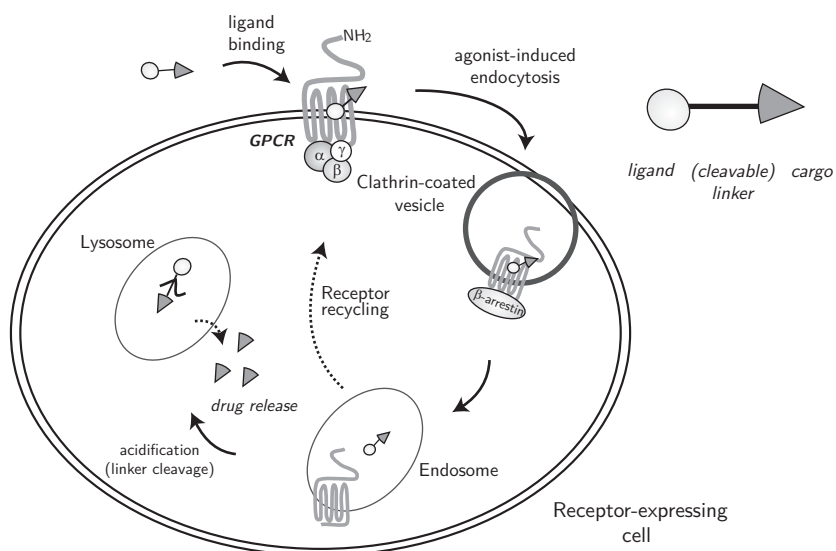


**Figure 1.3:** Graphic representation of agonist-induced internalization of GPCRs and a possible trafficking route of the ligand-drug conjugate.

Alternatively, the ligand dissociates from the receptor in the endolysosomal pathway. It is then either trafficked further to the lysosomes, or it diffuses out of the vesicles into the cytoplasm (Figure 1.3).

The discovery of allosteric binding sites, topographically distant from the orthosteric site, created novel opportunities for the design and development of structurally diverse ligands.<sup>15–17</sup> The glycoprotein hormone receptors, follicle-stimulating hormone receptor (FSHR), luteinizing hormone receptor (LH/hCGR) and thyroid-stimulating hormone receptor (TSHR), for example have a large N-terminal hormone binding domain and an allosteric binding site in the seven-transmembrane domain.<sup>18</sup> Many low molecular weight ligands that bind to the allosteric sites of these receptors have been developed<sup>19–22</sup> to interfere with their biological activity. There are, however, only limited examples of small-molecule GPCR ligands that are used for targeting purposes. One of the reasons for this is that structural alterations, required to introduce a chemical ligation handle needed for attachment of a label or a drug, can have a large influence on the affinity, potency and selectivity of a small molecule. For this approach to work, detailed structure-activity relationship (SAR) studies are often needed to arrive at the most optimal structure that still complies with these criteria.<sup>23</sup> Based on a low molecular weight dihydropyridine (DHP) agonist of the FSHR,<sup>24,25</sup> a SAR study was conducted to find the optimal length and positioning of a ligation handle-containing PEG-spacer (see Chapter 6). The optimal structure obtained from this was employed in the synthesis of DHP-analogues containing a fluorescent dye, with the aim to develop a diagnostic tool to visualize receptor binding, internalization and trafficking (see Chapter 7).

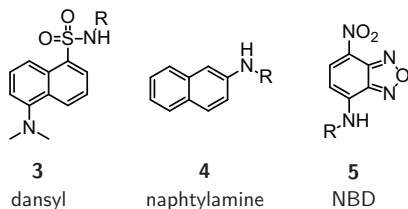


**Figure 1.4:** Structures of small fluorophores dansyl, naphthylamine and NBD.

Fluorescent ligands for several GPCRs have been reported in the literature, sometimes with unexpected changes in the pharmacological profile from agonist to antagonist.<sup>26,27</sup> Most examples make use of relatively small fluorophores such as dansyl **3**, naphthylamine **4** or NBD **5** (7-nitrobenz-2-oxa-1,3-diazol-4-yl) (Figure 1.4) to diminish the influence of the dye on the binding properties of the ligand. A drawback hereof is that these dyes consequently have

short emission and excitation wavelengths, limiting their use in a cell- or tissue-based system because of high levels of autofluorescence (Figure 1.4).<sup>26,28</sup> Some recent studies have successfully employed red-emitting dyes in the synthesis of low molecular weight fluorescent ligands to visualize receptors. Holtke *et al.* synthesized a near-infrared Cy5.5-conjugate of the nonpeptidyl selective endothelin A receptor antagonist PD156707 (**6**, Figure 1.5) which was shown to bind to the receptor with similar affinity as the lead compound and could be used to visualize the receptor on different cell types.<sup>29</sup> By introduction of a conjugation handle onto the core of SR144528, a cannabinoid CB<sub>2</sub> receptor ligand, Bai *et al.* could introduce a near-infrared dye. No thorough studies were performed on the phar-

macological properties of the resulting fluorescent ligand NIR-mbc94 (**7**, Figure 1.5), but it was shown that receptor expressing cells were much more fluorescent than wildtype cells and that this fluorescence could be competed with non-labeled SR144528.<sup>30</sup> In a follow-up study, NIR-mbc94 was shown to be indeed a selective ligand for the CB<sub>2</sub> receptor albeit with a much lower binding affinity than the lead SR144528 ( $K_i = 260$  nM vs 1 nM). Endogenous levels of receptor could be fluorescently labeled and quantified using this fluorescent ligand, showing its potential for use in a high-throughput screen for novel CB<sub>2</sub> receptor ligands.<sup>31</sup> The potential of fluorescent ligands when used together with advanced confocal fluorescence microscopy techniques, such as fluorescence correlation spectroscopy (FCS), has been shown with fluorescently labeled adenosine A1 and A3 receptor ligands. In these studies, the ligand-receptor interactions could be thoroughly studied which led to the identification of two distinct agonist-occupied receptor populations, based on their motility in the membranes of living cells.<sup>32,33</sup>

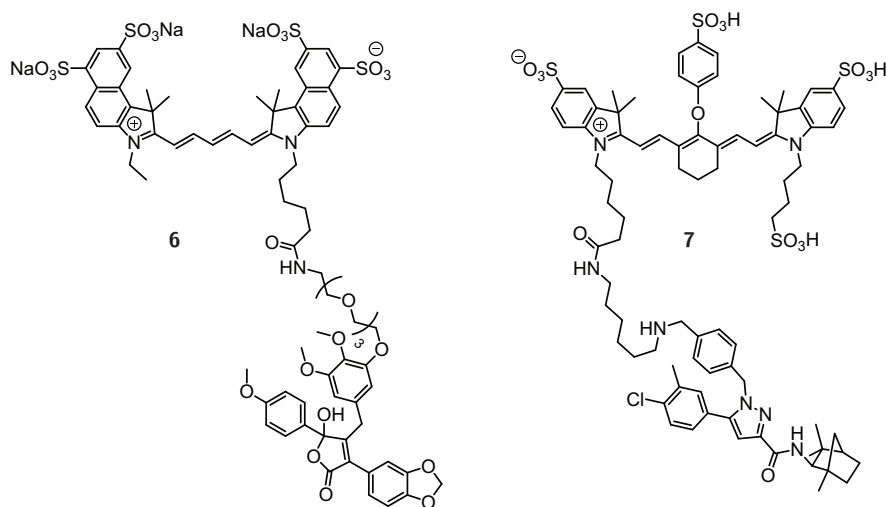


**Figure 1.5:** Near-infrared fluorescent GPCR ligands Cy5.5-PD156707 **6** and NIR-mbc94 **7**.

GPCRs that have endogenous peptide or protein ligands have been more often explored for targeted delivery, because of the ease of access to a synthetic peptide (fragment) by solid-phase peptide synthesis (SPPS). Besides, SPPS enables peptide modification by extension of its N- or C- terminus or by introduction of an unnatural amino acid. The Y receptor family is regulated by abundantly present endogenous neuropeptide Y (NPY) ligands.<sup>34</sup> Shorter fragments of the endogenous peptides or peptide-like structures resembling the C-terminus have been synthesized and were shown to be antagonist or agonists for the different subtypes of Y receptors.<sup>35</sup> The scope of the use of NPY ligands has expanded by the discovery of the presence of the Y<sub>1</sub>-receptor subtype on breast and metastatic tumors.<sup>36</sup> Radiolabeled Y<sub>1</sub>-selective peptides were subsequently used *in vitro* as well as *in vivo* as a diagnostic tool to visualize the overexpressed receptor in breast tumor tissue and metastases sites.<sup>37</sup> This result prompted the researchers to investigate the use of NPY ligands

to deliver a cytotoxic agent to the tumor site. In an approach analogous to that described in Chapter 8, the agent of choice was an *o*-carborane moiety. Carboranes are boron-rich lipophilic polyhedral structures with potential application in a binary anti-cancer therapy named boron-neutron capture therapy (BNCT).<sup>38</sup> Both individual components (carboranes and thermal neutrons) are relatively non-toxic in themselves, whereas a combination of both leads to a nuclear reaction and release of high energy particles that are detrimental for the cells which are exposed to it. A prerequisite for effective therapy is a high concentration of boron preferentially accumulated in tumor cells as opposed to healthy cells. Intracellular delivery would allow for the most efficient approach, since the trajectory of energy release by the formed  $\alpha$ -particles is estimated to coincide with the average diameter of a cell.<sup>39</sup>

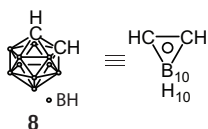


**Figure 1.6:** Different depictions of *o*-carborane

Attachment of *o*-carborane (**8**, Figure 1.6) to a  $Y_1R$  selective  $[F^7, P^{34}]$ -NPY derivative via the  $\epsilon$ -amino group of lysine-4 resulted in a slight loss in binding affinity and diminished activity compared to  $[F^7, P^{34}]$ -NPY. Affinity and activity were still in the nanomolar range, however, and the ligand was shown to be selective for the  $Y_1R$  over the  $Y_2R$  subtypes. This peptide was also capable of inducing receptor-internalization of only  $Y_1R$  as seen by microscopy studies on HEK293 cells transiently expressing human

$Y_1R$  conjugated to enhanced yellow fluorescent protein (EYFP). It remains elusive what the fate of the carborane-containing ligand was in this system, since it could not be visualized.<sup>40</sup>

The overexpression of peptide hormone receptors such as the somatostatin receptor and the gonadotropin-releasing hormone (GnRH) receptor in various tumor tissues has also been established.<sup>41</sup> The activities of toxic conjugates of a peptide-based GnRH receptor agonist with doxorubicin or an analogue hereof, 2-pyrrolino-DOX, were compared with that of the cytotoxic drug alone. Targeted analogues were shown to be much less toxic *in vivo* while having significantly more antitumor activity on tumors that did express the receptor.<sup>42,43</sup> The doxorubicin containing analogue (AN-152) is currently being evaluated in clinical trials.<sup>44</sup> The somatostatin receptor (sst) is present on many neuroendocrine tumors.<sup>45</sup> Synthetic analogues with enhanced plasma stability and affinity towards sst compared to endogenous somatostatin peptides have been described. These analogues, octreotates, consist of the pharmacophoric part of somatostatin and contain a threonine at the C-terminus (**9**, Figure 1.7). Various radiolabeled octreotate analogues have been reported that find use as radiotracers or in radionuclide therapy.<sup>46,47</sup> Conjugation of a cyanine dye to octreotate yielded a fluorescent analogue (**10**, Figure 1.7) that was shown to be internalized in sst-expressing cells and accumulated specifically in primary human neuroendocrine tumor cells. This example shows the potential of synthetic ligands for tumor visualization.<sup>48</sup> The use of octreotate as a tumor targeting entity for BNCT has also been explored. Mier *et al.* have attached *closo*-borane mercaptoundecahydrododecaborate (BSH) to maleimide-conjugated Tyr<sup>3</sup>-octreotate, but no biological studies were conducted.<sup>49</sup> In a more recent

study by Betzel and co-workers, one or two *o*-carboranes were attached to octreotate via linkers of different size. *In vitro* radioligand binding studies showed these analogues to be potent binders of the various sst-subtypes with enhanced selectivity for the sst<sub>2</sub>-subtype compared to the reference peptide somatostatin 28 (SRIF-28). Binding was shown to be dependent on spacer length, with increased binding at longer length, and on the number of carboranes attached, with one (**11**, Figure 1.7) being favored over two (**12**, Figure 1.7). Although these compounds show potential for use as targeting agents for BNCT, no specificity or internalization data is currently available.<sup>50</sup>

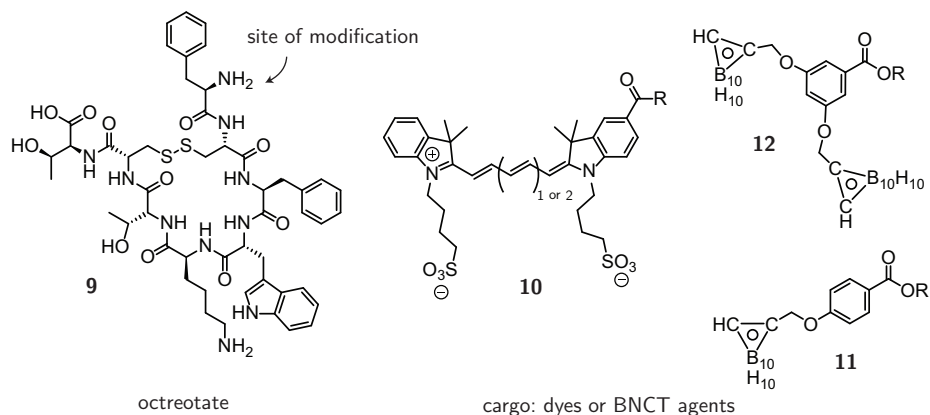


**Figure 1.7:** Synthetic somatostatin analogue (octreotate) used to target fluorescent dyes or carboranes for BNCT to sst-expressing tissues.

## Lectin receptors

Proteins that are able to recognize and bind carbohydrates such as glycan chains present on glycoproteins, are collectively named lectins. These can be soluble or membrane-bound, and the latter category encompasses an increasing variety of lectin receptors.<sup>51</sup> With the advancements in carbohydrate synthesis, such as solid-phase methods, more complex oligosaccharide structures have become within reach. Although the lectin binding properties of these oligosaccharides have often been investigated, little work has been done on the use of synthetic carbohydrates as targeting entities.<sup>52</sup> In analogy with the work discussed above and in Chapter 8, some work on carbohydrate-carborane compounds as targeted BNCT-agents has been performed. An additional advantage of the use of carbohydrates in this context is their hydrophilicity, thereby somewhat compensating the hydrophobic nature of the carborane cage. Orlova *et al.* conjugated the disaccharide lactose to *o*-carboranylacetic acid with the aim of targeting lactose-binding lectins on melanoma cells. No biological evaluation of the compounds was conducted however, and in a follow-up study it was found that *o*-carborane at the  $\alpha$ -position of a carbonyl results in deboronation to the corresponding *nido* compound when dissolved in water or methanol.<sup>53</sup> Tietze *et al.* have published several papers on the subject of glycoside modified carboranes for BNCT.<sup>54,55</sup> In their studies, carboranes were introduced by the reaction of decaborane with a terminal or in-

ternal alkyne on either *O*- or *C*-glycosides. *In vitro* studies on C6 rat glioma cells and B-16 melanoma cells showed dose-dependent uptake of a maltoside-carborane construct resulting in much higher intracellular boron levels than obtained with currently approved BNCT agents. *In vivo* studies in rat showed accumulation in brain tumor tissue, but similar concentrations were found in the blood, resulting in unwanted side-effects.<sup>54</sup> It remains elusive whether these constructs are taken up by cells in a receptor-dependent fashion and if so, which receptor is responsible for the uptake.

Cells of the immune system, especially dendritic cells (DCs) and macrophages, express different *C*-type lectin receptors which are characterized by their calcium dependency in ligand binding and conserved carbohydrate recognition domains (CRD). An important member is the macrophage mannose receptor (MR, CD206) which recognizes oligosaccharides terminating in mannose, fucose or *N*-acetylglucosamine. The receptor contains eight CRDs (Figure 1.8), which have been re-named *C*-type lectin-like domains (CTLDs) because most of the domains lack ligand binding activity.<sup>56,57</sup> Both CTLD4 and CTLD5 have been implied as the domains involved in ligand binding.<sup>58</sup> Having two ligand binding domains within one polypeptide chain allows for a stronger interaction with multivalent ligands and possibly ligand specificity, although the MR is also able to capture antigens with single mannose residues.<sup>59,60</sup> Besides the MR, dendritic cells express other mannose-binding *C*-type lectins, such as dendritic cell-specific intercellular adhesion molecule-3-grabbing non-integrin (DC-SIGN, CD209) (Figure 1.8).

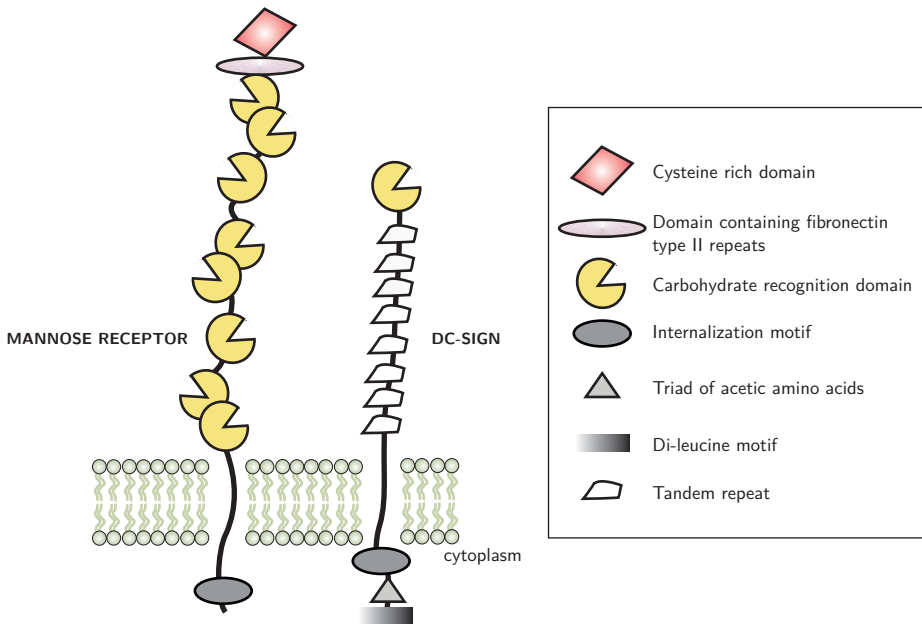


**Figure 1.8:** Schematic representation of the mannose receptor and DC-SIGN.

DC-SIGN belongs to type II C-type lectins, with an intracellular N-terminus, whereas the MR is a type I receptor, with an extracellular N-terminus. DC-SIGN contains only one CRD, but has been shown to multimerize in order to bind multivalent ligands with high affinity.<sup>59,61</sup> Furthermore, structural examination of DC-SIGN bound to either a high-mannose *N*-linked oligosaccharide or a complex-type *N*-linked glycan showed an unexpected interaction between the receptor and internal mannose residues.<sup>62</sup> Both receptors share an intracellular motif that allows internalization of the receptor in clathrin-coated pits. Targeting of either receptor might thus result in the selective internalization of ligands into the endolysosomal pathway of professional antigen-presenting cells.

Kikkeri *et al.* used carbohydrate modified quantum dots which showed enhanced uptake in liver cells when used *in vivo* compared to unmodified quantum dots. This finding suggests that receptor-mediated uptake, via the mannose receptor when using mannose or the asialoglycoprotein receptor when using D-galactose conjugated to quantum dots, plays a role in their endocytosis.<sup>63</sup> In a study by Hillaert *et al.*, six propargyl mannoses were clicked onto an azide-modified peptide scaffold in order to obtain a multivalent 'mannose cluster'. This cluster was conjugated to the fluorescent activity-based probe (ABP) BODIPY-DCG-04 with the aim to deliver the ABP to the lysosomes of DCs and macrophages. It was indeed shown that incorporation of the cluster led to temperature-dependent internalization of the compound **13** (Figure 1.9), indicating a receptor-mediated process. Uptake and subsequent cathepsin labeling by the ABP could be blocked by addition of mannan, a natural occurring oligomannoside, to the medium of DCs, further establishing the receptor dependency. In Chapter 2 an extension of this work is described. Instead of a regular BODIPY dye, a pH-activatable BODIPY dye was incorporated in the mannose cluster-BODIPY-DCG-04 construct.

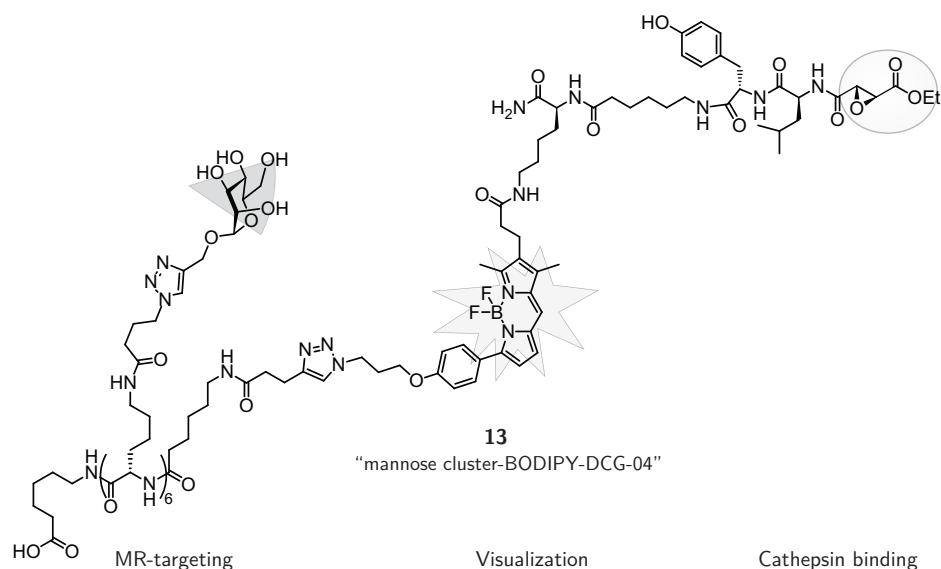


**Figure 1.9:** Targeted fluorescent activity-based probe for cathepsins.



The pH at which the BODIPY dye becomes fluorescent is dependent on the alkyl-substituents on the *meso*-aniline group and is thus synthetically tunable (see also Chapter 3). With the use of multiple constructs incorporating BODIPY dyes with differing pH-dependencies, live-cell imaging experiments could be performed to study the trafficking of these compounds in the endolysosomal pathway.<sup>64</sup>

Targeting of larger cargo, such as proteins, to lysosomes of specific cell-types lies at the basis of therapeutic intervention in lysosomal storage disorders. Enzyme replacement therapy (ERT) relies on the uptake of recombinant lysosomal enzyme into the endolysosomal pathway of disease-affected cells, to restore normal lysosomal function. In case of Gaucher disease,  $\beta$ -glucocerebrosidase (GBA1) is the enzyme of interest which needs to be targeted to mannose-binding lectins on macrophage (Gaucher) cells. Current ERTs for Gaucher use different approaches for glycan remodeling in order to expose core mannose or high mannose glycan chains on the recombinant GBA1. In Chapter 4 an alternative approach is investigated to target a protein to dendritic cells. Recombinant heat shock protein 70 (Hsp70) containing a C-terminal 'sortase sequence' (LPETGG) was conjugated to GGG-BODIPY-mannose cluster by employing the bacterial enzyme Sortase A. Uptake of the resulting Hsp70-BDP-MC in DCs was studied by confocal microscopy and gel analysis, showing that a relatively small synthetic entity such as the mannose cluster can function as a targeting device for a large protein.

In Chapter 5 the mannose cluster is modified to contain mannose-6-phosphate residues instead of mannoses, with the aim of targeting the mannose-6-phosphate receptor (MPR). The main role of the MPRs is to route newly synthesized lysosomal proteins from the *trans*-Golgi network to the lysosomes. Although mainly localized intracellularly, a fraction of the receptor population is continuously recycling between the cell membrane and the intracellular environment. Zhu *et al.* have used synthetic M6P-containing oligosaccharides to target recombinant acid  $\alpha$ -glucosidase to M6PR-expressing muscle cells affected by Pompe disease.<sup>65,66</sup> Dephosphorylation of M6P by serum phosphatases, yielding mannose, results in enhanced uptake by MR-expressing liver cells and less or no selective delivery to the intended target site. More stable M6P analogues that do have receptor affinity but are not a substrate for phosphatases are therefore interesting alternatives. Several isosteric and non-isosteric analogues of M6P have been synthesized and tested for their receptor binding affinities.<sup>67</sup> Isosteric mannose-6-phosphonate (M6Pn) was shown to have similar affinity for the CI-M6PR as M6P and would be a suitable alternative as targeting entity.<sup>68</sup> As an example hereof, Barragan *et al.* have shown that vesicles containing M6Pn coupled to a steroid are targeted to MCF-7 breast cancer cells. Although promising, conclusive experiments for the involvement of the CI-M6PR in their uptake have not been conducted as yet.<sup>69</sup>

## Folate receptor

The best studied example of a small molecule used to target a cell membrane receptor is likely that of folic acid targeting the folate receptor. Folic acid is the oxidized form of folate, an essential vitamin for mammals. Capturing of exogenous folate by cells is thus of great importance. Two transporters for folate have been identified, the "reduced-folate carrier" system, a low affinity carrier which is present on virtually all cells, and the folate receptor (FR), a high affinity binder of folic acid and highly overexpressed on various tumor cells.<sup>70</sup> The low affinity of the reduced-folate carrier system for folic acid, combined with the favorable expression pattern of the FR makes folic acid a highly suited organic molecule for tumor targeting.<sup>71</sup> Furthermore, folic acid retains its high affinity for the FR when conjugated through its  $\gamma$ -carboxyl group, is stable, readily available and cheap.<sup>72</sup> Leamon and Low demonstrated for the first time that covalent attachment of folic acid to macromolecules such as serum albumin or horseradish peroxidase results in their uptake in living cells via the folate receptor.<sup>73,74</sup> Since then many examples have appeared in the literature of folic acid-conjugates for various application such as radiotherapy, contrast agents and immuno- or chemotherapy.<sup>70,75,76</sup> A near-infrared dye was conjugated to folic acid, resulting in a tumor-targeted imaging agent that was shown to accumulate in ovarian cancer tissue *in vivo*.<sup>77</sup>

FR-mediated endocytosis occurs in caveolae, in a clathrin-independent fashion.<sup>78</sup> The resulting endosomes have been shown to be recycling and because folic acid retains its high receptor-affinity inside endosomes, the amount of folate-conjugated drug which is released inside the cell is limited. The pH of the FR-containing endosomes remains relatively high (average  $\sim 6.5$ ) and folate-drug conjugates that rely on an acid-cleavable linker system for drug release have been shown to be ineffective.<sup>76,79</sup> A better strategy is to make use of the reducing properties of the endosome by introduction of a self-immolative disulfide linker between folic acid and a drug of choice.<sup>80</sup> The applicability of this approach was shown by Yang *et al.* who introduced a FRET pair (BODIPY-FL/rhodamine) onto folic acid via an S-S linkage (14, Figure 1.10). Upon cleavage of the disulfide linker in the endosomes, the two dyes are dissociated resulting in loss of the FRET signal and recovery of the green fluorescent signal.<sup>81</sup> Conjugation of the maytansinoid DM1, a highly cytotoxic drug, to folic acid via an S-S-containing linker led to selective targeting of and cytotoxicity in FR-expressing cells.<sup>82</sup> The many successful *in vitro* and *in vivo* examples of folate receptor-mediated targeting open up the way for clinical trials to further investigate the potential of folate conjugates as targeted immuno- or chemo-therapeutic agents.

## Conclusion

The examples highlighted in this chapter show that small-molecule synthetic ligands hold a lot of promise as targeting entities. Organic chemistry allows for a thorough evaluation of possible sites of ligand modification and linker systems and for the development of new classes of ligands for unexplored receptors. Furthermore, synthetic dyes have greatly advanced the imaging applications and synthetic approaches to cytotoxic molecules such as carboranes for BNCT are ever expanding. To arrive at clinically relevant targeting entities,

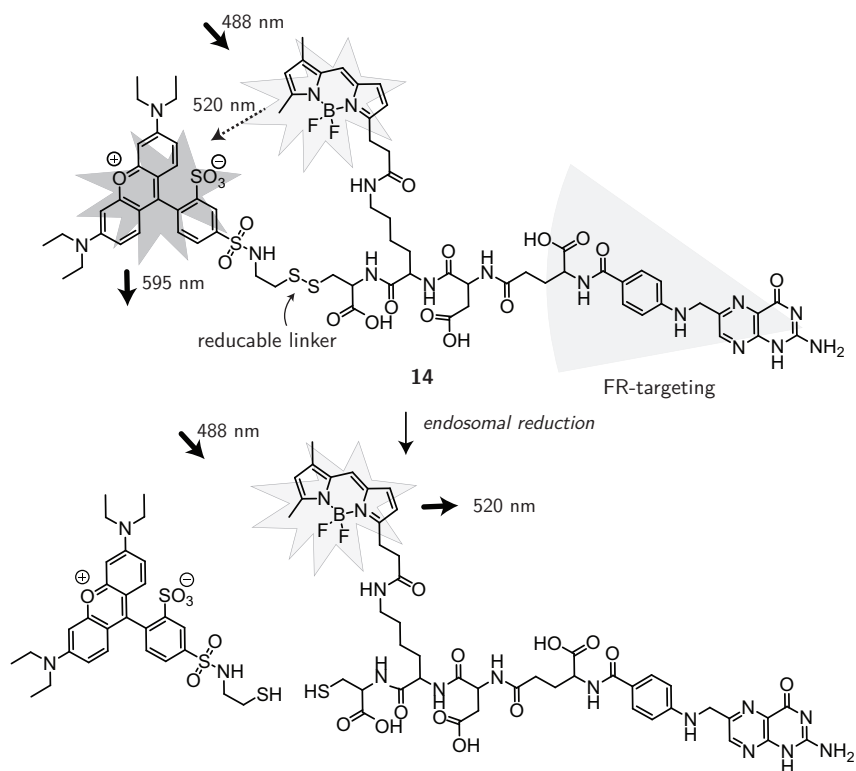


**Figure 1.10:** Endosomal uptake via the folate receptor was studied using a FRET dye pair linked to folic acid via an S-S linker. Irradiation with 488 nm light resulted in a red (595 nm) FRET signal. Upon cleavage of the disulfide bridge under endosomal reducing conditions, the two dyes were dissociated and fluorescence emission changed to green (520 nm).

either as diagnostics or therapies, however, *in vitro* binding assays to assess the ligand-receptor interaction are insufficient. Biochemical experiments addressing receptor pharmacology, and the behaviour of the ligand-cargo constructs in a more complex setting such as cells, tissue or *in vivo* are essential. When chemistry and biology are highly integrated much can be gained, as shown by the few examples that have resulted in well-defined receptor-ligand pairs that can be used for efficient targeting. In that way, a variety of ‘magic bullets’, each with its own target can be accomplished.

### Aim and outline of this thesis

The research described in this thesis aims at the development of constructs containing a receptor-targeting entity covalently bound to biologically active cargo. Chemical and biological approaches are combined to arrive at the ultimate goal: selective delivery of the cargo to a cell-type, tissue or organelle of interest. In all cases, a fluorescent dye is incorporated to visualize the construct by fluorescence microscopy or in-gel fluorescence scanning. In Chapters 2, 3 and 8, pH-dependent BODIPY dyes are investigated with the aim to selectively visualize intracellular acidic compartments. Targeted receptors that will be

discussed include mannose-binding lectins (Chapters 2 and 4), the mannose-6-phosphate receptor (Chapter 5) and the follicle-stimulating hormone receptor (Chapters 6-9). With the exception of the work described in Chapter 9, where recombinant FSH is used as the targeting entity, the ligands that are employed are synthetic and (relatively) low molecular weight in nature. A variety of cargo is introduced, ranging from an activity-based probe (Chapters 2 and 5), carboranes for BNCT (Chapter 8) to the protein Hsp70 (Chapter 4). In the concluding Chapter 10 the findings are summarized and alternative and future strategies towards targeted delivery of these receptors are discussed. Broader applications of some of the synthesized entities, such as pH-dependent dyes and functionalized carboranes, are presented here as well.

## References

- [1] Ehrlich, P. *Proc. Roy. Soc. London* **1899**, *66*, 424–448.
- [2] Strebhardt, K.; Ullrich, A. *Nat. Rev. Cancer* **2008**, *8*, 473–480.
- [3] Ehrlich, P. *Berichte der deutschen chemischen Gesellschaft* **1909**, *42*, 17–47.
- [4] Smith, N. J.; Bennett, K. A.; Milligan, G. *Mol. Cell. Endocrinol.* **2011**, *331*, 241–247.
- [5] Niculescu-Duvaz, I.; Springer, C. *Adv. Drug Delivery Rev.* **1997**, *26*, 151–172.
- [6] Dubowchik, G. M.; Mosure, K.; Knipe, J. O.; Firestone, R. A. *Bioorg. Med. Chem. Lett.* **1998**, *8*, 3347–3352.
- [7] Dubowchik, G. M.; Firestone, R. A.; Padilla, L.; Willner, D.; Hofstead, S. J.; Mosure, K.; Knipe, J. O.; Lasch, S. J.; Trail, P. A. *Bioconjug. Chem.* **2002**, *13*, 855–869.
- [8] Kratz, F.; Beyer, U.; Roth, T.; Tarasova, N.; Collery, P.; Lechenault, F.; Cazabat, A.; Schumacher, P.; Unger, C.; Falken, U. *J. Pharm. Sci.* **1998**, *87*, 338–346.
- [9] Ulbrich, K.; Šubr, V. *Adv. Drug Delivery Rev.* **2004**, *56*, 1023–1050.
- [10] Hopkins, A. L.; Groom, C. R. *Nat. Rev. Drug Discovery* **2002**, *1*, 727–730.
- [11] Lagerström, M. C.; Schiöth, H. B. *Nat. Rev. Drug Discovery* **2008**, *7*, 339–357.
- [12] Neves, S. R.; Ram, P. T.; Iyengar, R. *Science* **2002**, *296*, 1636–1639.
- [13] Pitcher, J. A.; Freedman, N. J.; Lefkowitz, R. J. *Annu. Rev. Biochem.* **1998**, *67*, 653–692.
- [14] Claing, A.; Laporte, S. A.; Caron, M. G.; Lefkowitz, R. J. *Prog. Neurobiol.* **2002**, *66*, 61–79.
- [15] Christopoulos, A. *Nat. Rev. Drug Discovery* **2002**, *1*, 198–210.
- [16] Leach, K.; Sexton, P. M.; Christopoulos, A. *Trends Pharmacol. Sci.* **2007**, *28*, 382–389.
- [17] May, L. T.; Leach, K.; Sexton, P. M.; Christopoulos, A. *Annu. Rev. Pharmacol. Toxicol.* **2007**, *47*, 1–51.
- [18] Vassart, G.; Pardo, L.; Costagliola, S. *Trends Biochem. Sci.* **2004**, *29*, 119–126.
- [19] Jäschke, H.; Neumann, S.; Moore, S.; Thomas, C. J.; Colson, A.-O.; Costanzi, S.; Kleinau, G.; Jiang, J.-K.; Paschke, R.; Raaka, B. M.; Krause, G.; Gershengorn, M. C. *J. Biol. Chem.* **2006**, *281*, 9841–9844.
- [20] Moore, S.; Jaeschke, H.; Kleinau, G.; Neumann, S.; Costanzi, S.; Jiang, J.-k.; Childress, J.; Raaka, B. M.; Colson, A.; Paschke, R.; Krause, G.; Thomas, C. J.; Gershengorn, M. C. *J. Med. Chem.* **2006**, *49*, 3888–3896.
- [21] Heitman, L. H.; IJzerman, A. P. *Med. Res. Rev.* **2008**, *28*, 975–1011.
- [22] van Koppen, C. J.; Zaman, G. J.; Timmers, C. M.; Kelder, J.; Mosselman, S.; van de Lage-maat, R.; Smit, M. J.; Hanssen, R. G. *Naunyn. Schmiedebergs Arch. Pharmacol.* **2008**, *378*, 503–514.
- [23] Leopoldo, M.; Lacivita, E.; Berardi, F.; Perrone, R. *Drug discov. today* **2009**, *14*, 706–712.
- [24] Grima Poveda, P. M.; Karstens, W. F. J.; Timmers, C. M. *WO Patent* **2006**, 2006117368(A1).
- [25] van Koppen, C. J.; Verbost, P. M.; van de Lagemaat, R.; Karstens, W.-J. F.; Loozen, H. J.; van Achterberg, T. A.; van Amstel, M. G.; Brands, J. H.; van Doornmalen, E. J.; Wat, J.; Mulder, S. J.; Raafs, B. C.; Verkaik, S.; Hanssen, R. G.; Timmers, C. M. *Biochem. Pharmacol.* **2013**, *85*, 1162–1170.

- [26] Berque-Bestel, I.; Soulier, J.-L.; Giner, M.; Rivail, L.; Langlois, M.; Sicsic, S. *J. Med. Chem.* **2003**, *46*, 2606–2620.
- [27] Kuder, K.; Kiec-Kononowicz, K. *Curr. Med. Chem.* **2008**, *15*, 2132–2143.
- [28] Leopoldo, M.; Lacivita, E.; Passafiume, E.; Contino, M.; Colabufo, N. A.; Berardi, F.; Perrone, R. *J. Med. Chem.* **2007**, *50*, 5043–5047.
- [29] Höltkke, C.; von Wallbrunn, A.; Kopka, K.; Schober, O.; Heindel, W.; Schäfers, M.; Bremer, C. *Bioconjug. Chem.* **2007**, *18*, 685–694.
- [30] Bai, M.; Sexton, M.; Stella, N.; Bornhop, D. *J. Bioconjug. Chem.* **2008**, *19*, 988–992.
- [31] Sexton, M.; Woodruff, G.; Horne, E. A.; Lin, Y. H.; Muccioli, G. G.; Bai, M.; Stern, E.; Bornhop, D. J.; Stella, N. *Chem. Biol.* **2011**, *18*, 563–568.
- [32] Briddon, S.; Middleton, R.; Cordeaux, Y.; Flavin, F.; Weinstein, J.; George, M.; Kellam, B.; Hill, S. *Proc. Natl. Acad. Sci. U. S. A.* **2004**, *101*, 4673–4678.
- [33] Cordeaux, Y.; Briddon, S.; Alexander, S.; Kellam, B.; Hill, S. *FASEB J.* **2008**, *22*, 850–860.
- [34] Michel, M. C.; Beck-Sickinger, A.; Cox, H.; Doods, H. N.; Herzog, H.; Larhammar, D.; Quirion, R.; Schwartz, T.; Westfall, T. *Pharmacol. Rev.* **1998**, *50*, 143–150.
- [35] Cabrele, C.; Beck-Sickinger, A. G. *J. Pept. Sci.* **2000**, *6*, 97–122.
- [36] Reubi, J. C.; Gugger, M.; Waser, B.; Schaer, J.-C. *Cancer Res.* **2001**, *61*, 4636–4641.
- [37] Khan, I. U.; Zwanziger, D.; Böhme, I.; Javed, M.; Naseer, H.; Hyder, S. W.; Beck-Sickinger, A. G. *Angew. Chem. Int. Ed. Engl.* **2010**, *49*, 1155–1158.
- [38] Sivaev, I. B.; Bregadze, V. V. *Eur. J. Inorg. Chem.* **2009**, *2009*, 1433–1450.
- [39] Barth, R. F.; Coderre, J. A.; Vicente, M. G. H.; Blue, T. E. *Clin. Cancer Res.* **2005**, *11*, 3987–4002.
- [40] Ahrens, V. M.; Frank, R.; Stadlbauer, S.; Beck-Sickinger, A. G.; Hey-Hawkins, E. *J. Med. Chem.* **2011**, *54*, 2368–2377.
- [41] Mezo, G.; Manea, M. *Expert Opin. Drug Deliv.* **2010**, *7*, 79–96.
- [42] Nagy, A.; Schally, A. V.; Armatis, P.; Szepeshazi, K.; Halmos, G.; Kovacs, M.; Zarandi, M.; Groot, K.; Miyazaki, M.; Jungwirth, A.; Horvath, J. *Proc. Natl. Acad. Sci. U. S. A.* **1996**, *93*, 7269–7273.
- [43] Nagy, A.; Schally, A. V. *Biol. Reprod.* **2005**, *73*, 851–859.
- [44] Limonta, P.; Manea, M. *Cancer Treat. Rev.* **2013**, *39*, 647–663.
- [45] Reubi, J.; Lang, W.; Maurer, R.; Koper, J.; Lamberts, S. *Cancer Res.* **1987**, *47*, 5758–5764.
- [46] de Jong, M.; Breeman, W. A.; Bernard, B. F.; Bakker, W. H.; Schaar, M.; van Gameren, A.; Bugaj, J. E.; Erion, J.; Schmidt, M.; Srinivasan, A.; Krenning, E. P. *Int. J. Cancer* **2001**, *92*, 628–633.
- [47] Breeman, W. A.; de Jong, M.; Kwekkeboom, D. J.; Valkema, R.; Bakker, W. H.; Kooij, P. P.; Visser, T. J.; Krenning, E. P. *Eur. J. Nucl. Med.* **2001**, *28*, 1421–1429.
- [48] Becker, A.; Hassenius, C.; Licha, K.; Ebert, B.; Sukowski, U.; Semmler, W.; Wiedenmann, B.; Gröttinger, C. *Nat. Biotechnol.* **2001**, *19*, 327–331.
- [49] Mier, W.; Gabel, D.; Haberkorn, U.; Eisenhut, M. Z. *Anorg. Allg. Chem.* **2004**, *630*, 1258–1262.
- [50] Betzel, T.; Heß, T.; Waser, B.; Reubi, J.-C.; Roesch, F. *Bioconjug. Chem.* **2008**, *19*, 1796–1802.
- [51] Bies, C.; Lehr, C.-M.; Woodley, J. F. *Adv. Drug Delivery Rev.* **2004**, *56*, 425–435.
- [52] Ratner, D. M.; Adams, E. W.; Disney, M. D.; Seeberger, P. H. *ChemBioChem* **2004**, *5*, 1375–1383.
- [53] Kononov, L. O.; Orlova, A. V.; Zinin, A. I.; Kimel, B. G.; Sivaev, I. B.; Bregadze, V. I. *J. Organomet. Chem.* **2005**, *690*, 2769–2774.
- [54] Tietze, L. F.; Bothe, U.; Griesbach, U.; Nakaichi, M.; Hasegawa, T.; Nakamura, H.; Yamamoto, Y. *Bioorg. Med. Chem.* **2001**, *9*, 1747–1752.
- [55] Tietze, L. F.; Griesbach, U.; Schubert, I.; Bothe, U.; Marra, A.; Dondoni, A. *Chem. Eur. J.* **2003**, *9*, 1296–1302.
- [56] East, L.; Isacke, C. M. *Biochim. Biophys. Acta* **2002**, *1572*, 364–386.
- [57] Taylor, M. E.; Conary, J.; Lennartz, M.; Stahl, P. D.; Drickamer, K. *J. Biol. Chem.* **1990**, *265*, 12156–12162.
- [58] Taylor, M. E.; Bezouska, K.; Drickamer, K. *J. Biol. Chem.* **1992**, *267*, 1719–1726.
- [59] Figdor, C. G.; van Kooyk, Y.; Adema, G. J. *Nat. Rev. Immunol.* **2002**, *2*, 77–84.
- [60] Taylor, M. E.; Drickamer, K. *J. Biol. Chem.* **1993**, *268*, 399–404.
- [61] Mitchell, D. A.; Fadden, A. J.; Drickamer, K. *J. Biol. Chem.* **2001**, *276*, 28939–28945.
- [62] Feinberg, H.; Mitchell, D. A.; Drickamer, K.; Weis, W. I. *Science* **2001**, *294*, 2163–2166.
- [63] Kikkeri, R.; Lepenies, B.; Adibekian, A.; Laurino, P.; Seeberger, P. H. *J. Am. Chem. Soc.* **2009**, *131*, 2110–2112.

- [64] Hoogendoorn, S.; Habets, K. L.; Passemaid, S.; Kuiper, J.; van der Marel, G. A.; Florea, B. I.; Overkleeft, H. S. *Chem. Commun.* **2011**, *47*, 9363–9365.
- [65] Zhu, Y.; Jiang, J.-L.; Gumlaw, N. K.; Zhang, J.; Bercury, S. D.; Ziegler, R. J.; Lee, K.; Kudo, M.; Canfield, W. M.; Edmunds, T.; Jiang, C.; Mattaliano, R. J.; Cheng, S. H. *Mol. Ther.* **2009**, *17*, 954–963.
- [66] Zhu, Y.; Li, X.; Mcvie-Wylie, A.; Jiang, C.; Thurberg, B.; Raben, N.; Mattaliano, R.; Cheng, S. *Biochem. J* **2005**, *389*, 619–628.
- [67] Gary-Bobo, M.; Nirdé, P.; Jeanjean, A.; Morère, A.; Garcia, M. *Curr. Med. Chem.* **2007**, *14*, 2945.
- [68] Vidil, C.; Morère, A.; Garcia, M.; Barragan, V.; Hamdaoui, B.; Rochefort, H.; Montero, J.-L. *Eur. J. Org. Chem.* **1999**, *1999*, 447–450.
- [69] Barragan, V.; Menger, F. M.; Caran, K. L.; Vidil, C.; Morère, A.; Montero, J.-L. *Chem. Commun.* **2001**, 85–86.
- [70] Leamon, C. P.; Low, P. S. *Drug discov. today* **2001**, *6*, 44–51.
- [71] Antony, A. *Blood* **1992**, *79*, 2807–2820.
- [72] Lu, Y.; Low, P. S. *Adv. Drug Delivery Rev.* **2012**, *64*, 342–352.
- [73] Leamon, C. P.; Low, P. S. *Proc. Natl. Acad. Sci. U. S. A.* **1991**, *88*, 5572–5576.
- [74] Low, P. S.; Henne, W. A.; Doorneweerd, D. D. *Acc. Chem. Res.* **2007**, *41*, 120–129.
- [75] Sudimack, J.; Lee, R. J. *Adv. Drug Delivery Rev.* **2000**, *41*, 147–162.
- [76] Xia, W.; Low, P. S. *J. Med. Chem.* **2010**, *53*, 6811–6824.
- [77] Tung, C.-H.; Lin, Y.; Moon, W. K.; Weissleder, R. *ChemBioChem* **2002**, *3*, 784–786.
- [78] Anderson, R.; Kamen, B. A.; Rothberg, K. G.; Lacey, S. W. *Science* **1992**, *255*, 410–411.
- [79] Yang, J.; Chen, H.; Vlahov, I. R.; Cheng, J.-X.; Low, P. S. *J. Pharmacol. Exp. Ther.* **2007**, *321*, 462–468.
- [80] Vlahov, I. R.; Leamon, C. P. *Bioconjug. Chem.* **2012**, *23*, 1357–1369.
- [81] Yang, J.; Chen, H.; Vlahov, I. R.; Cheng, J.-X.; Low, P. S. *Proc. Natl. Acad. Sci. U. S. A.* **2006**, *103*, 13872–13877.
- [82] Ladino, C. A.; Chari, R. V.; Bourret, L. A.; Kedersha, N. L.; Goldmacher, V. S. *Int. J. Cancer* **1997**, *73*, 859–864.

# 2

## Targeted pH-dependent fluorescent activity-based cathepsin probes<sup>1</sup>

**B**ifunctional, pH-activatable BODIPY dyes were developed in this chapter and incorporated in mannose cluster-containing activity-based probes for cysteine proteases. Mannose receptor-dependent uptake of the probes in dendritic cells, followed by trafficking to acidic cellular compartments resulted in fluorescence as seen by live-cell imaging, and subsequent cathepsin inhibition.

## 2.1 Introduction

Fluorescent dyes are applied in many different areas of chemical biology. Among these dyes, boron-dipyromethene (BODIPY) derivatives are frequently used due to their excellent photochemical properties and relative stability under physiological conditions.<sup>2,3</sup> For example, covalent attachment of a BODIPY dye to an activity-based probe (ABP) facilitates the study of its target enzyme, by means of fluorescence scanning and microscopy.<sup>4-9</sup> Urano *et al.* recently developed a series of acidic pH-activatable BODIPY dyes.<sup>10</sup> Due to photoinduced electron transfer (PeT) of the meso aniline substituent toward the BODIPY fluorophore, fluorescence is quenched at neutral or basic pH.<sup>11-13</sup> Upon protonation of the aniline nitrogen, fluorescence is restored. Depending on the choice of alkyl substituents on the aniline nitrogen, the  $pK_a$  and thus the pH-dependency of the fluorophore can be tuned.<sup>10</sup> A great advantage of these kind of fluorophores is that they do not fluoresce when unprotonated, making them convenient tools to study in-cell processes with fluorescence microscopy. Since a (slightly) acidic pH is a prerequisite for fluorescence, these fluorophores are ideally suited for incorporation in probes that are transported to acidic cellular compartments like lysosomes.

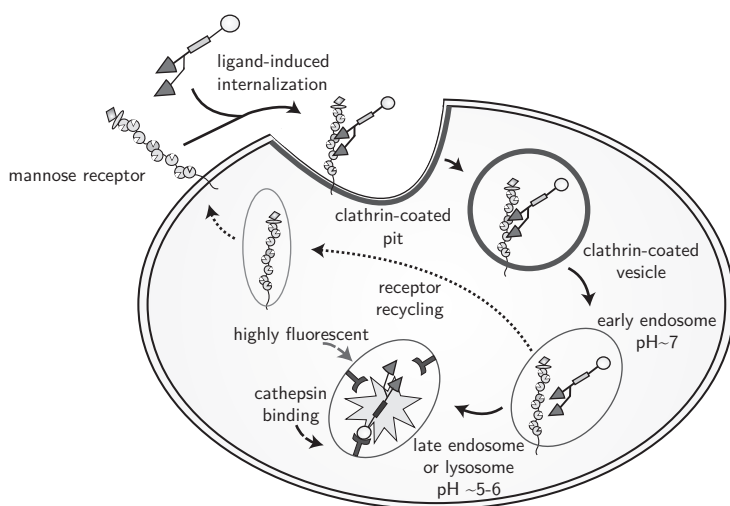


**Figure 2.1:** Schematic overview of the expected internalization and fluorescence properties of the constructs described in this chapter in mannose-receptor expressing cells.

In a previous study, Hillaert *et al.* have shown that lysosomal targeting of the epoxy-succinate activity-based probe DCG-04<sup>14</sup> can be accomplished by attachment of a synthetic mannose cluster.<sup>4</sup> This mannose cluster binds to the mannose receptor, which is predominantly present on professional antigen-presenting cells such as dendritic cells and macrophages. Mannose receptor-mediated internalization of the construct is followed by trafficking in the endocytic pathway towards the lysosomes. Subsequently, multiple lysosomal cysteine proteases of the cathepsin<sup>15</sup> family are covalently and irreversibly addressed

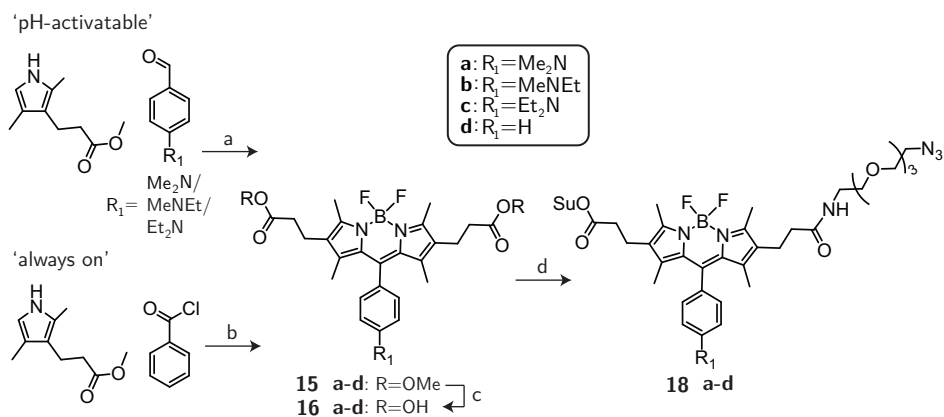


by the ABP. In this chapter the incorporation of a pH-activatable fluorophore in the previously reported mannose-cluster-BODIPY-DCG-04 construct (**13**, Figure 1.9) is described. The aim is to investigate whether this leads to less background because of selective fluorescence in the cellular compartments of interest as depicted in Figure 2.1. The synthesis of bifunctional pH-dependent BODIPY dyes with orthogonal ligation handles, needed for incorporation in the larger construct, is reported and their spectroscopic properties are investigated. Furthermore, the uptake and (pH-dependent) fluorescence of constructs **21a-d** in dendritic cells is studied.

## 2.2 Results and Discussion

**Synthesis.** To obtain the large mannose cluster-pH-dependent-DCG-04 constructs, a modular synthetic approach was followed, in which the constructs were assembled from three building blocks in the two final steps. The mannose cluster **20** and cathepsin inhibitor DCG-04-amine were synthesized as previously reported.<sup>4,14</sup> To obtain bifunctional pH-dependent BODIPY dyes, the synthetic route of Urano and coworkers<sup>10</sup> was modified and extended (Scheme 2.1).

**Scheme 2.1:** Synthesis of asymmetric, bifunctional (pH-activatable) BODIPY dyes **18a-d**.



Reagents and conditions: [a] i) cat. TFA, DCM; ii) DDQ; iii) base,  $\text{BF}_3 \cdot \text{OEt}_2$ , a: 28%, b, c: 19%; [b] i) DCE, reflux; ii) TEA,  $\text{BF}_3 \cdot \text{OEt}_2$ , d: 23%; [c] NaOH (aq), MeOH/dioxane, a: quant, b: 88%, c: 45%, d: 53%; [d] i) EDC · HCl, HOBt, TEA, DMF, spacer **17a**; ii) *N*-hydroxysuccinimide, EDC · HCl, DCM, a: 34%, b: 52%, c: 43%, d: 33%.

Starting from commercially available *N,N*-dialkylaminobenzaldehydes and methyl 2,4-dimethyl-3-pyrrolepropionate,<sup>16</sup> symmetrical pH-dependent dyes **15a-c** were obtained by a three-step, one-pot procedure. The "always on" control dye **15d** was synthesized from benzoyl chloride and methyl 2,4-dimethyl-3-pyrrolepropionate, followed by reaction with  $\text{BF}_3 \cdot \text{OEt}_2$  and base to yield the BODIPY core. The methyl esters were saponified using sodium hydroxide in MeOH/dioxane, providing symmetrical dicarbonyl BODIPYs **16**.



BODIPYs **18a-d** and DCG-04 amine followed by ligation to the mannose cluster **20** by copper(I) catalyzed Huisgen 1,3-cycloaddition<sup>17,18</sup> gave constructs **21a-d** (Figure 2.2).

To assess the fluorescence properties of the dyes, fluorescence-pH curves of probes **21a-d** in a citric acid/phosphate buffer system were measured (Figure 2.3A, B). The resulting curves for **21a-c** (Figure 2.3B) were shifted to the left as compared to the curves reported by Urano *et al.*,<sup>10</sup> indicative of a shift in  $pK_a$  values. Upon addition of a low amount (0.2%) of the detergent sodium dodecyl sulphate (SDS) the values resembled the expected  $pK_a$ 's. Since the pH of the lysosomes in antigen-presenting cells such as macrophages is estimated to be 4.5-4.9<sup>19</sup> probe **21c**, with  $pK_a \sim 5.1$  was expected to be the best candidate for imaging in living cells.

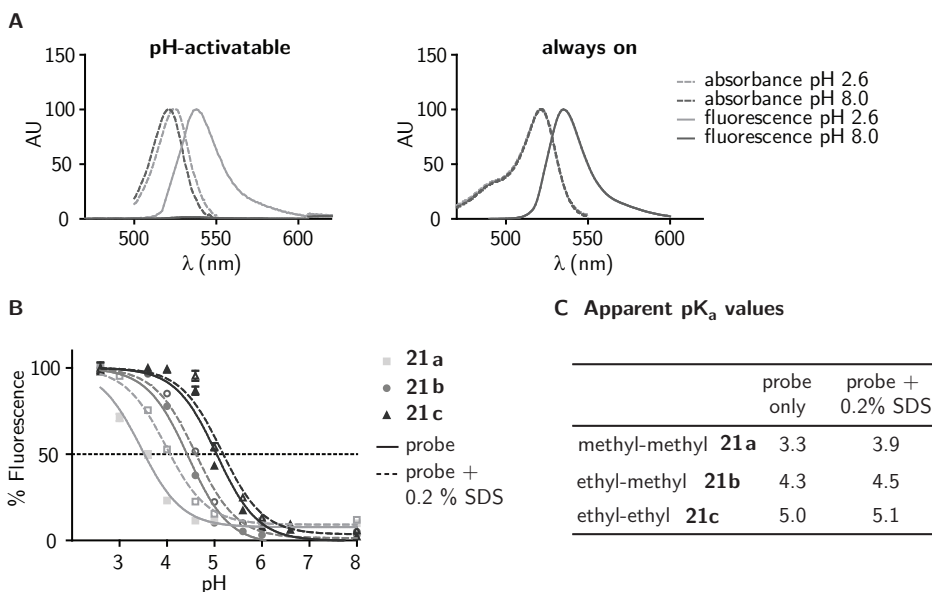


**Figure 2.3: pH-dependency of compounds 21a-c.** A) Normalized absorption and emission spectra of pH-activatable compounds **21a-c** and the "always on" control **21d**. B) Fluorescence measurements as a function of pH in citrate/phosphate buffer with or without 0.2% SDS. C) Apparent  $pK_a$  values (50% fluorescence) as determined by the curves shown in B).

**Biological evaluation.** The ability of probes **21a-d** to label lysosomal cysteine proteases was first examined by incubation of mouse liver lysates with various concentrations of the construct, followed by resolution of the proteins on SDS-PAGE. The bands could be visualized by overnight incubation of the gel in acidic fixing solution (MeOH/H<sub>2</sub>O/acetic acid), thereby lowering the pH to allow in-gel fluorescence scanning. Labeling was shown to be concentration-dependent and the profile corresponded well with that seen for the previously reported mannose cluster-BODIPY-DCG-04 probe, with a MW-shift of 3-4 kDa compared to BODIPY-DCG-04<sup>4,20</sup> **22** ( $\beta$ -DCG-04; Figure 2.4), consistent with the molecular weight of the probes (Figure 2.4).<sup>4</sup> In a competition experiment with  $\beta$ -DCG-04 **22** it was shown that the constructs competed for the same set of cysteine proteases.

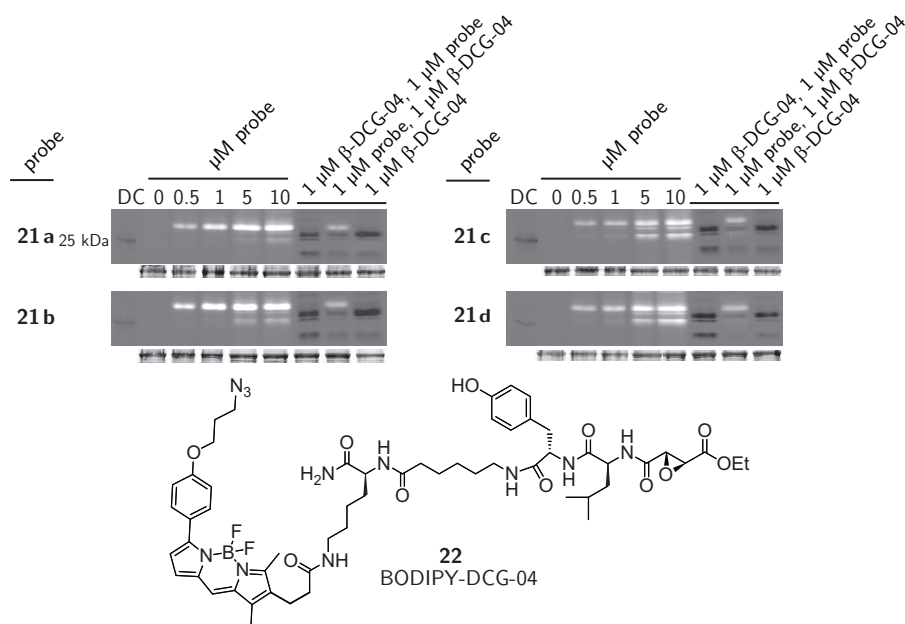


**Figure 2.4: Liver lysate cathepsin labeling.** 12.5% SDS-PAGE analysis; fluorescence scanning images (upper, white bands: Cy2 BODIPY fluorescence; black: Cy3 fluorescence) and coomassie staining for total protein (lower) are shown. DC: dual color prestained protein marker. Incubation of mouse liver lysate with probes **21a-d** showed concentration-dependent labeling of cathepsins (white bands, lanes 2-6). The probes competed for the same set of cathepsins as the known cathepsin inhibitor  $\beta$ -DCG-04 (black bands, lanes 7-9) and the bands were shifted consistent with the molecular weight of the probes.

Next, the behaviour of probes **21a-d** in living cells was investigated. Immature mouse dendritic cells (DCs) were incubated with 1  $\mu$ M of probe and studied with live-cell fluorescence microscopy. Brightly fluorescent vesicles appeared inside the cells after 30 min of incubation, with increasing fluorescence upon prolonged exposure to the probe. In contrast to the "always on" construct **21d**, no background signal was detected for the pH-activatable probes **21a-c** and therefore cells could be imaged without any additional washing steps (Figure 2.5). In accordance with the observed  $pK_a$  values, the signal for the methyl-methyl (**21a**) and methyl-ethyl (**21b**) probes was less strong and took longer to appear (Figure 2.5B). This clearly indicates that the probes were indeed trafficked to increasingly acidic cellular compartments over time. Subsequent cell lysis and SDS-PAGE analysis showed a labeling profile of cysteine proteases identical to that found in lysates (Figure 2.6B).

Dendritic cells, being professional antigen-presenting cells, can take up macromolecules from the environment by macropinocytosis.<sup>21</sup> Therefore, incubation times for follow-up experiments were set to two hours, to diminish the amount of probe internalized by means other than mannose receptor-mediated internalization. Indeed, under these conditions, pre-incubation of the cells with mannan, a naturally occurring polymannoside that binds the mannose receptor, abolished the uptake of the probes and subsequent labeling of cathep-

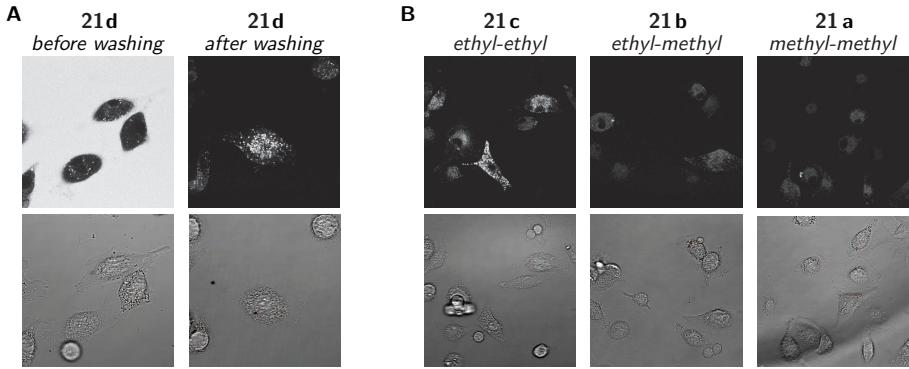


**Figure 2.5: Fluorescence (upper) and brightfield phase contrast images (lower) of immature dendritic cells treated with the different probes 21a-d.** A) The "always on" control probe cannot be used without washing due to a large amount of background. B) After 3 h of treatment, fluorescence intensities for the diethyl probe 21c were strongest of all pH-activatable probes.

sins (Figure 2.6, cond. 2). Pre-incubation of the cells with non-fluorescent azido-DCG-04 23 (Figure 5.2) did not prevent the probes from entering the cell, as seen by live-cell imaging. However, no labeling of cathepsins was seen on SDS-PAGE, indicating that the probes were taken up by the mannose receptor, trafficked to the lysosomes, but unable to bind to,

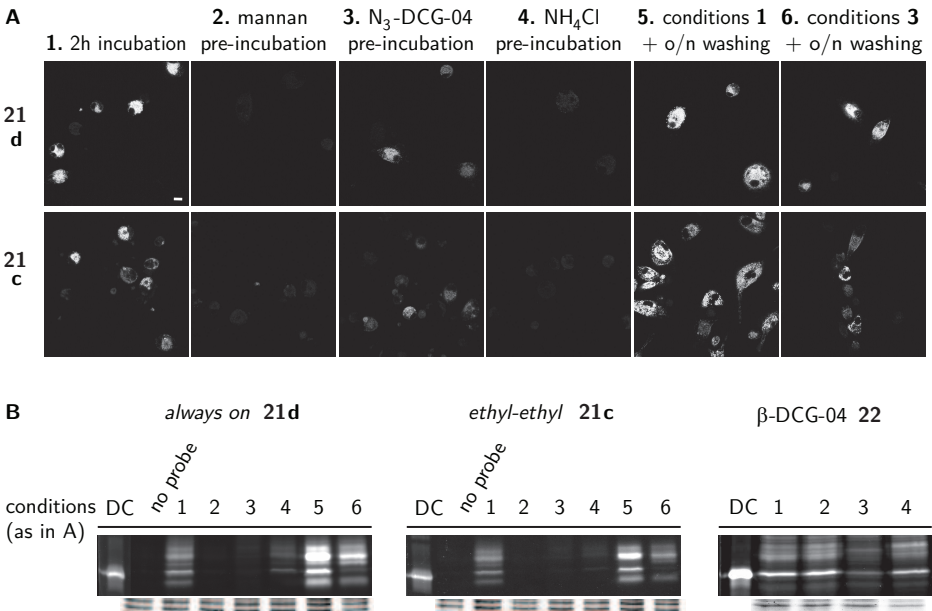


**Figure 2.6: Uptake and cathepsin labeling in live dendritic cells.** A) Confocal microscopy images of DCs incubated for 2 h with probes 21c or 21d, under different conditions (1-6) show mannose receptor-dependent uptake of the constructs. Scale bar (white) corresponds to 10  $\mu$ m. B) Cell lysis and analysis of cells treated as in A) shows inhibition of cathepsin labeling by azido-DCG-04, which is partly restored after overnight washing.

the already blocked, cathepsins (Figure 2.6, cond. 3). Interestingly, in-cell fluorescence remained even after prolonged washing of the cells (Figure 2.6A, cond. 6). To further investigate this, cells were lysed after washing and analyzed by SDS-PAGE. As shown in Figure 2.6B, cond. 6, labeling of cathepsins was largely restored. Also, more cathepsins were labeled after overnight washing compared to immediate lysis in the control experiment (Figure 2.6B, cond. 5). Because of their size, the probes were probably retained in the cells, where they could bind any newly formed cathepsins.

In a next experiment, the intracellular pH was increased by addition of ammonium chloride to the medium.<sup>22</sup> Ammonia passively diffuses into the cell and acts as a weak base, thereby increasing the pH up to 6 in lysosomes in a reversible manner.<sup>19,23</sup> Almost no in-cell fluorescence was detectable for both the ethyl-ethyl (**21c**) and control probe (**21d**) after pre-incubation with 10 mM NH<sub>4</sub>Cl, even after extensive washing at normal pH, indicating that the levels of internalized probe were low (Figure 2.6A, cond. 4). This is in accordance with the postulation of Tietze *et al.*, that an increased cellular pH decreases receptor recycling, which leads to lower levels of cell surface receptors.<sup>24</sup> SDS-PAGE analysis on the other hand, revealed that not all cathepsin activity was gone, as seen by, albeit weak, labeling on gel (Figure 2.6B, cond. 5). This finding illustrates the efficiency with which the probes were internalized and processed in the endocytic pathway.

## 2.3 Conclusion

In this chapter a series of pH-activatable fluorophores that contain orthogonal ligation handles were developed. These dyes were incorporated in large mannose cluster containing ABPs, thereby facilitating their imaging without influencing their uptake or distribution in dendritic cells. These kind of molecules might find use in studies concerning antigen cross-presentation and the role of cysteine proteases herein. Moreover, the ease of access to the panel of bifunctional, tunable, pH-activatable dyes should allow their incorporation in bioconjugates quite different from those presented here. Potential drawbacks of the dyes, such as their spectral properties (absorption and emission maxima between standard Cy2 and Cy3 laser/filter settings) and their symmetry, which makes mono-functionalization difficult are addressed in Chapter 3. The ability of the mannose cluster to function as a targeting device to deliver (bio)molecules other than ABPs to dendritic cells will be examined in Chapter 4. The modular synthetic approach followed here allows for easy exchange of the different parts of the construct. In this fashion, alternative receptors (such as the mannose-6-phosphate receptor (Chapter 5)) can be targeted to specifically deliver cargo to endocytic compartments with the aim to interfere with a variety of subcellular targets.

## 2.4 Experimental Section

**Absorption and Fluorescence Spectroscopy.** All spectroscopic experiments were performed in citrate/phosphate buffer (McIlvaine)<sup>25</sup> at a concentration of ca. 1  $\mu$ M (absorption) or 100 nM (flu-

orescence) of **21a-d**. Measurements were conducted on a Shimadzu UV1700 pharماسpec UV-VIS spectrophotometer (absorbance) and a Shimadzu RF-5301PC spectrofluorometer (fluorescence). For pH-fluorescence curves, the pH was set using different ratios of citric acid (0.1 M stock solution) vs phosphate buffer (0.2 M stock solution). The excitation wavelength was set equal to the maximum of the corresponding absorption spectrum and the emission spectrum recorded. Experiments were conducted at a concentration of 25 nM in a total volume of 2 mL and performed in quadruplicate. SDS was added to a final concentration of 0.2% from a 10% stock solution in water.

**Cell culture of primary cells.** Immature dendritic cells were obtained from the bone marrow of C75BL/6 mice. The use of animals was approved by the ethics committee of Leiden University. Mice were sedated, bone marrow of tibiae and femurs was flushed out and washed with PBS. Cells were grown in dendritic cell selection medium (IMDM containing granulocyte-macrophage colony stimulating factor (GM-CSF) 2:1 vol/vol) containing 8% FCS, penicillin/streptomycin (100 units/mL), glutamax (2 mM) and beta-mercaptoethanol (20  $\mu$ M). Cells were selected for 10 days (37 °C; 5% CO<sub>2</sub>) after which they were either used directly or frozen and stored at -80 °C until further use.

**Live-cell microscopy.** Experiments were conducted on a Leica TCS SPE confocal microscope, using GFP or dsRed filter settings ( $\lambda_{\text{ex}}$  488 or 532 nm). Immature dendritic cells (DCs, 30-75  $\times$  10<sup>4</sup> cells/well) were seeded onto sterile Labtek II 4- or 8-chamber borosilicate coverglass systems (Fisher Emergo). Stock solutions of probes and other reagents were prepared in conditioned DC medium. For time-course experiments cells were treated with 10  $\mu$ M of probe **21a-d**, incubated for the indicated time (37 °C; 5% CO<sub>2</sub>) and imaged. Removal of the probe-containing medium followed by addition of fresh cell culture medium was required for the "always on" control probe **21d**. Experiments that required pre-treatment were conducted as follows: cells were incubated (37 °C; 5% CO<sub>2</sub>) with mannan (3 mg/mL), NH<sub>4</sub>Cl (10 mM), or N<sub>3</sub>-DCG-04 (10  $\mu$ M) for 2 h. Probes **21a-d** (1  $\mu$ M) were added directly to the medium, and incubation was continued for 2 h, after which the medium was refreshed and cells imaged. Alternatively, cells were washed with PBS (2  $\times$  0.5 mL) incubated overnight in medium and imaged after 16 h. All experiments were performed at least in duplicate.

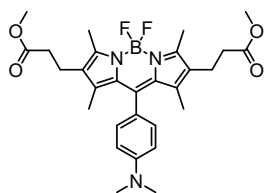
**SDS-PAGE analysis - Labeling of cathepsins in lysate.** Mouse liver lysate (40  $\mu$ g) in 25 mM MES buffer pH 5.0 was incubated with 0, 0.5, 1, 5 or 10  $\mu$ M of probes **21a-d** for 1 h at 37 °C. For competition experiments, lysate was pre-incubated with BODIPY-DCG-04 (1  $\mu$ M) for 1 h at 37 °C, followed by incubation with probes **21a-d** (1  $\mu$ M). Subsequently, samples were boiled with 4x Laemli's sample buffer under reducing conditions and resolved on a 12.5% SDS-PAGE gel. To visualize the pH-dependent probes, gels were fixed overnight in MeOH/H<sub>2</sub>O/acetic acid (50/40/10). After washing with H<sub>2</sub>O/acetic acid (90/10), gels were imaged on a Typhoon 2000 imager (GE Healthcare) using the Cy2 ( $\lambda_{\text{ex}}$  532 nm;  $\lambda_{\text{em}}$  526 nm) and TAMRA ( $\lambda_{\text{ex}}$  532 nm;  $\lambda_{\text{em}}$  580 nm) settings. After imaging, gels were stained with coomassie brilliant blue to visualize total protein loaded. Gel images were coloured with ImageJ.

**Labeling of cathepsins in live-cells.** Immature mouse dendritic cells were seeded onto tissue-coated 24-wells plates for same-day experiments or on borosilicate 4-chamber microscope slides for overnight experiments (2  $\times$  10<sup>5</sup> cells/well). Stock solutions of probes and other reagents were prepared in conditioned DC medium. For labeling experiments cells were treated with 1  $\mu$ M of probe **21a-d**, incubated for 2 h (37 °C; 5% CO<sub>2</sub>), washed with ice-cold PBS (2 $\times$  0.5 mL) and lysed (35  $\mu$ L Invitrogen complete cell extraction buffer). Experiments that required pre-treatment were conducted as follows: cells were incubated (37 °C; 5% CO<sub>2</sub>) with mannan (3 mg/mL), NH<sub>4</sub>Cl (10 mM), or N<sub>3</sub>-DCG-04 (10  $\mu$ M) for 2 h. Probes **21a-d** (1  $\mu$ M) were added directly to the medium, and incubation was continued for 2 h. Cells were washed with ice-cold PBS (2 $\times$  0.5 mL) and lysed in

35  $\mu\text{L}$  lysis buffer (Invitrogen cell extraction buffer, supplemented with 1 mM PMSF and protease inhibitor cocktail (Roche)). For the overnight time-point, cells were incubated in fresh medium after the washing step for 16 h before lysis. Lysates were collected, centrifuged (4  $^{\circ}\text{C}$ , 14,000 rpm, 10 min) and stored at -80  $^{\circ}\text{C}$  until further use. Lysates were thawed and the protein concentration was determined by a DC (detergent-compatible) protein assay (Biorad). Samples (20  $\mu\text{g}$  protein/well) were boiled with 4x Laemli's sample buffer under reducing conditions and resolved on a 12.5% SDS-PAGE gel. To visualize the pH-dependent probes, gels were fixed overnight in MeOH/ $\text{H}_2\text{O}$ /acetic acid (50/40/10). After washing with  $\text{H}_2\text{O}$ /acetic acid (90/10), gels were imaged on a Typhoon 2000 imager (GE Healthcare) using the Cy2 settings ( $\lambda_{\text{ex}}$  532 nm;  $\lambda_{\text{em}}$  526 nm). After imaging, gels were stained with coomassie brilliant blue to visualize total protein loaded. Gel images were coloured with ImageJ.

## Synthesis

**General.** All reagents were of commercial grade and used as received unless stated otherwise. Reaction solvents were of analytical grade and when used under anhydrous conditions stored over flame-dried 3  $\text{\AA}$  molecular sieves. Dichloromethane was distilled over  $\text{CaH}_2$  prior to use. Solvents used for column chromatography were of technical grade and distilled before use. All moisture and oxygen sensitive reactions were performed under an argon atmosphere. Flash chromatography was performed on silica gel (Screening Devices BV, 0.04-0.063 mm, 60  $\text{\AA}$ ). Reactions were routinely monitored by TLC analysis on DC-alufolien (Merck, Kieselgel60, F254) with detection by UV-absorption (254/366 nm) where applicable and spraying with a solution of  $(\text{NH}_4)_6\text{Mo}_7\text{O}_{24} \cdot 4\text{H}_2\text{O}$  (25 g/l) and  $(\text{NH}_4)_4\text{Ce}(\text{SO}_4)_4 \cdot 2\text{H}_2\text{O}$  (10 g/l) in 10% sulfuric acid in water followed by charring at  $\sim 150$   $^{\circ}\text{C}$ .  $^1\text{H}$  and  $^{13}\text{C}$  NMR spectra were recorded on a Bruker AV-400 (400 MHz) or Bruker DMX-600 (600 MHz). Chemical shifts are given in ppm ( $\delta$ ) relative to the residual solvent peak or TMS (0 ppm) as internal standard. Coupling constants are given in Hz. Peak assignments are based on 2D  $^1\text{H}$ -COSY and  $^{13}\text{C}$ -HSQC NMR experiments. IR measurements (thin film) were conducted on an IRAffinity-1 apparatus and evaluated using IRRSolutions software (Shimadzu, Kyoto, Japan). LC-MS measurements were conducted on a Thermo Finnigan LCQ Advantage MAX ion-trap mass spectrometer (ESI+) coupled to a Surveyor HPLC system (Thermo Finnigan) equipped with a standard C18 (Gemini, 4.6 mmD  $\times$  50 mmL, 5  $\mu$  particle size, Phenomenex) analytical column and buffers A:  $\text{H}_2\text{O}$ , B: ACN, C: 0.1% aq. TFA. High resolution mass spectra were recorded on a LTQ Orbitrap (Thermo Finnigan) mass spectrometer equipped with an electrospray ion source in positive mode (source voltage 3.5 kV, sheath gas flow 10  $\text{mL min}^{-1}$ , capillary temperature 250  $^{\circ}\text{C}$ ) with resolution  $R=60000$  at  $m/z$  400 (mass range  $m/z=150-2000$ ) and dioctylphthalate ( $m/z = 391.28428$ ) as a "lock mass". The high resolution mass spectrometer was calibrated prior to measurements with a calibration mixture (Thermo Finnigan). For reversed-phase HPLC purification of the final compounds an automated HPLC system equipped with a C18 semiprep column (Gemini C18, 250 $\times$ 10 mm, 5  $\mu$  particle size, Phenomenex) was used.

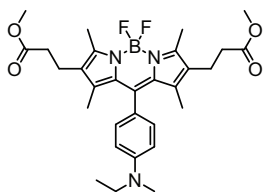


### 1, 3, 5, 7-Tetramethyl-2,6-bis-(2-methoxycarbonyl)ethyl)-8-[4-(*N,N*-dimethylamino)phenyl]-4, 4-difluoro-4-bora-3a, 4a-diaza-*s*-indacene (15a).

Methyl 2,4-dimethyl-3-pyrrolepropionate (1.43 g, 7.9 mmol, 2.2 eq) and *N,N*-dimethylaminobenzaldehyde (0.54 g, 3.6 mmol, 1 eq) were dissolved in dry dichloromethane (100 mL) followed by addition of a catalytic amount of TFA. The reaction mixture was stirred overnight at room temperature under an argon atmosphere. 2,3-Dichloro-5,6-dicyanobenzoquinone (DDQ, 0.98 g, 4.3 mmol, 1.2 eq) was added and stirring was continued for 1 h. The reaction was concentrated *in vacuo*, dissolved in dichloroethane (100 mL) followed by addition

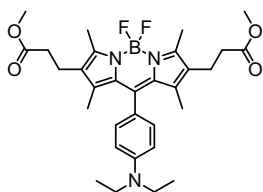


of diisopropylethylamine (DIPEA, 2.5 mL, 14.4 mmol, 4 eq) and  $\text{BF}_3 \cdot \text{OEt}_2$  (2.5 mL, 20 mmol, 5.5 eq). The mixture was stirred for 2h, washed with water ( $2 \times 50$  mL), dried ( $\text{MgSO}_4$ ), filtered and concentrated under reduced pressure. Purification by silica column chromatography (1  $\rightarrow$  13% EtOAc in toluene) gave the product as an orange powder (0.53 g, 1 mmol, 28%).  $R_f = 0.6$  (4:1 toluene: EtOAc)  $^1\text{H NMR}$  (400 MHz,  $\text{CDCl}_3$ ):  $\delta$  7.06 (d,  $J = 8.7$  Hz, 2H,  $2 \times \text{CH}_{\text{ar}}$ ), 6.80 (d,  $J = 8.7$  Hz, 2H,  $2 \times \text{CH}_{\text{ar}}$ ), 3.68 (s, 6H,  $2 \times \text{CH}_3$ ), 3.05 (s, 6H,  $2 \times \text{CH}_3$ ), 2.71 - 2.63 (m, 4H,  $2 \times \text{CH}_2$ ), 2.56 (s, 6H,  $2 \times \text{CH}_3$ ), 2.42 - 2.33 (m, 4H,  $2 \times \text{CH}_2$ ), 1.43 (s, 6H,  $2 \times \text{CH}_3$ ).  $^{13}\text{C NMR}$  (101 MHz,  $\text{CDCl}_3$ ):  $\delta$  173.30, 153.41, 150.81, 142.49, 139.74, 131.78, 128.96, 128.84, 122.69, 112.51, 51.78, 40.48, 34.42, 19.50, 12.66, 12.27. ESI-HRMS ( $m/z$ ): calcd. for  $[\text{C}_{29}\text{H}_{36}\text{BF}_2\text{N}_3\text{O}_4 + \text{H}]^+$  540.28449; obsd. 540.28420.



**1, 3, 5, 7-Tetramethyl-2,6-bis-(2-methoxycarbonyl)ethyl)-8-[4-(*N,N*-ethylmethylamino)phenyl] -4, 4-difluoro-4-bora-3a, 4a-diaza-s-indacene (15b).**

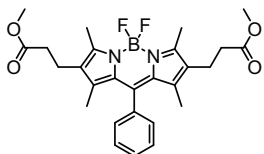
Methyl 2,4-dimethyl-3-pyrrolepropionate (1.23 g, 6.8 mmol, 2.2 eq) and *N,N*-ethylmethylaminobenzaldehyde (0.49 g, 3.0 mmol, 1 eq) were dissolved in dry dichloromethane (100 mL) followed by addition of a catalytic amount of TFA. The reaction mixture was stirred overnight at room temperature under an argon atmosphere. DDQ (0.82 g, 3.6 mmol, 1.2 eq) was added and stirring was continued for 1 h. The reaction was concentrated *in vacuo*, dissolved in dichloroethane (100 mL) followed by addition of TEA (1.25 mL, 9 mmol, 3 eq) and  $\text{BF}_3 \cdot \text{OEt}_2$  (1.9 mL, 15 mmol, 5 eq). The mixture was refluxed for 40 min, cooled to room temperature, washed with water ( $2 \times 50$  mL), dried ( $\text{MgSO}_4$ ), filtered and concentrated under reduced pressure. Purification by repeated silica column chromatography (1  $\rightarrow$  25% EtOAc in toluene/ 1  $\rightarrow$  25% EtOAc in PE + 1% AcOH) gave the product as orange crystals (0.31 g, 0.56 mmol, 19%).  $R_f = 0.6$  (4:1 toluene: EtOAc)  $^1\text{H NMR}$  (400 MHz,  $\text{CDCl}_3$ ):  $\delta$  7.02 (d,  $J = 8.6$  Hz, 2H,  $2 \times \text{CH}_{\text{ar}}$ ), 6.77 (d,  $J = 8.6$  Hz, 2H,  $2 \times \text{CH}_{\text{ar}}$ ), 3.65 (s, 6H,  $2 \times \text{CH}_3$ ), 3.46 (q,  $J = 7.0$  Hz, 2H,  $\text{CH}_2$ ), 2.97 (s, 3H,  $\text{CH}_3$ ), 2.68 - 2.60 (m, 4H,  $2 \times \text{CH}_2$ ), 2.53 (s, 6H,  $2 \times \text{CH}_3$ ), 2.39 - 2.32 (m, 4H,  $2 \times \text{CH}_2$ ), 1.42 (s, 6H,  $2 \times \text{CH}_3$ ), 1.16 (t,  $J = 7.0$  Hz, 3H,  $\text{CH}_3$ ).  $^{13}\text{C NMR}$  (101 MHz,  $\text{CDCl}_3$ ):  $\delta$  173.28, 153.39, 149.57, 142.62, 139.75, 131.84, 129.11, 128.86, 122.39, 112.60, 51.75, 46.96, 37.55, 34.45, 19.55, 12.66, 12.27, 11.15. ESI-HRMS ( $m/z$ ): calcd. for  $[\text{C}_{30}\text{H}_{38}\text{BF}_2\text{N}_3\text{O}_4 + \text{H}]^+$  554.30015; obsd. 554.29979.



**1, 3, 5, 7-Tetramethyl-2,6-bis-(2-methoxycarbonyl)ethyl)-8-[4-(*N,N*-diethylamino)phenyl] -4, 4-difluoro-4-bora-3a, 4a-diaza-s-indacene (15c).**

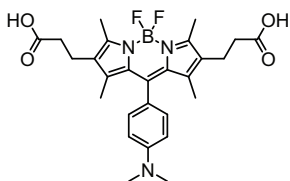
Methyl 2,4-dimethyl-3-pyrrolepropionate (1.81 g, 10 mmol, 2.2 eq) and *N,N*-diethylaminobenzaldehyde (0.83 g, 4.7 mmol, 1 eq) were dissolved in dry DCM (100 mL) followed by addition of a catalytic amount of TFA. The reaction mixture was stirred overnight at room temperature under an argon atmosphere. DDQ (1.18 g, 5.2 mmol, 1.1 eq) was added and stirring was continued for 1 h. The reaction was concentrated *in vacuo*, dissolved in dichloroethane (100 mL) followed by addition of TEA (1.96 mL, 14.1 mmol, 3 eq) and  $\text{BF}_3 \cdot \text{OEt}_2$  (2.95 mL, 23.5 mmol, 5 eq). The mixture was refluxed for 40 min, cooled to room temperature, washed with water ( $2 \times 50$  mL), dried ( $\text{MgSO}_4$ ), filtered and concentrated under reduced pressure. Purification by repeated silica column chromatography (1  $\rightarrow$  25% EtOAc in PE + 1% AcOH) gave the product as orange crystals (0.50 g, 0.87 mmol, 19%).  $R_f = 0.75$  (3:1 toluene: EtOAc)  $^1\text{H NMR}$  (400 MHz,  $\text{CDCl}_3$ ):  $\delta$  6.99 (d,  $J = 8.7$  Hz, 2H,  $2 \times \text{CH}_{\text{ar}}$ ), 6.74 (d,  $J = 8.7$  Hz, 2H,  $2 \times \text{CH}_{\text{ar}}$ ), 3.65 (s, 6H,  $2 \times \text{CH}_3$ ), 3.41 (q,  $J = 7.0$  Hz, 4H,  $2 \times \text{CH}_2$ ), 2.72 - 2.57 (m, 4H,  $2 \times \text{CH}_2$ ), 2.53 (s,

6H, 2 × CH<sub>3</sub>), 2.41 - 2.29 (m, 4H, 2 × CH<sub>2</sub>), 1.44 (s, 6H, 2 × CH<sub>3</sub>), 1.20 (t, *J* = 7.0 Hz, 6H, 2 × CH<sub>3</sub>). <sup>13</sup>C NMR (101 MHz, CDCl<sub>3</sub>): δ 173.26, 153.19, 148.24, 142.73, 139.71, 131.78, 129.09, 128.73, 121.62, 112.09, 51.73, 44.45, 34.38, 19.46, 12.60, 12.44, 12.28. ESI-HRMS (*m/z*): calcd. for [C<sub>31</sub>H<sub>40</sub>BF<sub>2</sub>N<sub>3</sub>O<sub>4</sub> + H]<sup>+</sup> 568.31528; obsd. 568.31547.



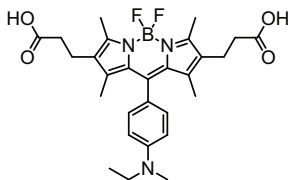
**1, 3, 5, 7-Tetramethyl-2,6-bis(2-methoxycarbonyl)ethyl-8-phenyl-4,4-difluoro-4-bora-3a,4a-diaza-s-indacene (15d).**

Methyl 2,4-dimethyl-3-pyrrolepropionate (0.9 g, 5 mmol, 2.2 eq) was dissolved in dichloroethane (20 mL). Benzoyl chloride (0.29 mL, 2.5 mmol, 1 eq) was added and the mixture was heated to reflux for 3 h. After cooling to room temperature, TEA (1.04 mL, 7.5 mmol, 3 eq) and BF<sub>3</sub> · OEt<sub>2</sub> (1.57 mL, 12.5 mmol, 5 eq) were added and the reaction mixture was stirred for 16 h. The mixture was washed with water (2 × 50 mL), dried (MgSO<sub>4</sub>), filtered and concentrated under reduced pressure. Purification by repeated silica column chromatography (1 → 12% EtOAc in PE) gave the product as an orange powder (0.29 g, 0.58 mmol, 23%). *R<sub>f</sub>* = 0.8 (1:1 toluene: EtOAc). <sup>1</sup>H NMR (400 MHz, CDCl<sub>3</sub>): δ 7.52 - 7.45 (m, 3H, 3 × CH<sub>ar</sub>), 7.28 - 7.23 (m, 2H, 2 × CH<sub>ar</sub>), 3.65 (s, 6H, 2 × CH<sub>3</sub>), 2.67 - 2.57 (m, 4H, 2 × CH<sub>2</sub>), 2.55 (s, 6H, 2 × CH<sub>3</sub>), 2.39 - 2.32 (m, 4H, 2 × CH<sub>2</sub>), 1.29 (s, 6H, 2 × CH<sub>3</sub>). <sup>13</sup>C NMR (101 MHz, CDCl<sub>3</sub>): δ 173.20, 154.16, 141.02, 139.59, 135.54, 131.02, 129.30, 129.25, 129.08, 128.19, 51.81, 34.35, 19.45, 12.74, 11.95. ESI-HRMS (*m/z*): calcd. for [C<sub>27</sub>H<sub>31</sub>BF<sub>2</sub>N<sub>2</sub>O<sub>4</sub> + H]<sup>+</sup> 497.24225; obsd. 497.24199.



**1,3,5,7-Tetramethyl-2,6-bis(2-carboxyethyl)-8-[4-(*N,N*-dimethylamino)phenyl]-4,4-difluoro-4-bora-3a,4a-diaza-s-indacene (16a).**

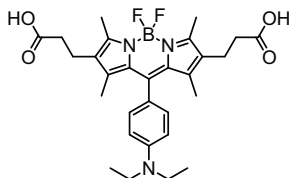
**15a** (230 mg, 0.43 mmol) was dissolved in methanol/dioxane (1:1, 20 mL). NaOH (aq, 1M, 5 mL) was added and the mixture was heated to 40 °C for 50 min. The mixture was neutralized with HCl (aq, 1M, 5.5 mL), followed by addition of water and extraction with EtOAc. The mixture was dried (MgSO<sub>4</sub>), filtered and concentrated *in vacuo* to give the product as an orange powder in quantitative yield (217 mg, 0.43 mmol, quant.). *R<sub>f</sub>* = 0.3 (2:1 toluene: EtOAc + AcOH) <sup>1</sup>H NMR (400 MHz, CDCl<sub>3</sub>/MeOD): δ 7.06 (d, *J* = 8.7 Hz, 2H, 2 × CH<sub>ar</sub>), 6.85 (d, *J* = 8.7 Hz, 2H, 2 × CH<sub>ar</sub>), 3.03 (s, 6H, 2 × CH<sub>3</sub>), 2.65 (t, *J* = 7.8 Hz, 4H, 2 × CH<sub>2</sub>), 2.51 (s, 6H, 2 × CH<sub>3</sub>), 2.34 (t, *J* = 7.8 Hz, 4H, 2 × CH<sub>2</sub>), 1.45 (s, 6H, 2 × CH<sub>3</sub>). <sup>13</sup>C NMR (101 MHz, CDCl<sub>3</sub>/MeOD): δ 176.28, 154.10, 151.98, 143.53, 140.61, 132.48, 129.95, 129.68, 123.38, 113.37, 40.60, 35.15, 20.16, 12.69, 12.51. ESI-HRMS (*m/z*): calcd. for [C<sub>27</sub>H<sub>32</sub>BF<sub>2</sub>N<sub>3</sub>O<sub>4</sub> + H]<sup>+</sup> 512.25315; obsd. 512.25291.



**1,3,5,7-Tetramethyl-2,6-bis(2-carboxyethyl)-8-[4-(*N,N*-ethylmethylamino)phenyl]-4,4-difluoro-4-bora-3a,4a-diaza-s-indacene (16b).**

Compound **15b** (37 mg, 0.067 mmol) was dissolved in methanol/dioxane (1:1, 3 mL). NaOH (aq, 1M, 0.84 mL) was added and the mixture was heated to 40 °C for 1 h. The mixture was neutralized with HCl (aq, 1M, 1 mL), followed by addition of water and extraction with EtOAc. The mixture was dried (MgSO<sub>4</sub>), filtered and concentrated *in vacuo*. Pure product (31 mg, 0.059 mmol, 88%) was obtained by silica column chromatography (10 → 30% EtOAc in toluene + 1% AcOH). *R<sub>f</sub>* = 0.3 (2:1 toluene: EtOAc + AcOH) <sup>1</sup>H NMR (400 MHz, CDCl<sub>3</sub>/MeOD): δ 7.00 (d, *J* = 8.4 Hz, 2H, 2 × CH<sub>ar</sub>), 6.83 (d, *J* = 8.5 Hz, 2H, 2 × CH<sub>ar</sub>), 3.47 (q, *J* = 6.8 Hz, 2H, CH<sub>2</sub>), 2.96 (s, 3H, CH<sub>3</sub>), 2.64 (t, *J* = 7.6 Hz, 4H, 2 × CH<sub>2</sub>),

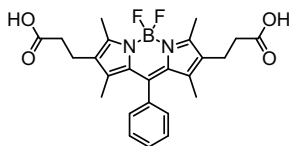
2.49 (s, 6H, 2 × CH<sub>3</sub>), 2.33 (t, *J* = 7.6 Hz, 4H, 2 × CH<sub>2</sub>), 1.45 (s, 6H, 2 × CH<sub>3</sub>), 1.14 (t, *J* = 6.9 Hz, 3H, CH<sub>3</sub>). <sup>13</sup>C NMR (101 MHz, CDCl<sub>3</sub>/MeOD): δ 176.35, 154.18, 150.67, 143.76, 140.66, 132.58, 130.06, 129.92, 123.03, 113.41, 47.49, 37.73, 35.20, 20.21, 12.68, 12.52, 11.24. ESI-HRMS (*m/z*): calcd. for [C<sub>28</sub>H<sub>34</sub>BF<sub>2</sub>N<sub>3</sub>O<sub>4</sub> + H]<sup>+</sup> 526.26882; obsd. 526.26792.



**1,3,5,7-Tetramethyl-2,6-bis-(2-carboxyethyl) -8-[4-(*N,N*-diethylamino)phenyl] -4, 4-difluoro-4-bora-3a, 4a-diaza-*s*-indacene (15c).**

Compound **15c** (0.45 g, 0.8 mmol) was dissolved in methanol/dioxane (1:1, 20 mL). NaOH (aq, 4M, 2.4 mL) was added and the mixture was heated to 40 °C for 1h. The mixture was neutralized with HCl (aq, 1M, 10 mL), followed by addition of water and extraction with EtOAc. The mixture was dried (MgSO<sub>4</sub>), filtered and concentrated *in vacuo*. Pure product (0.2 g, 0.36 mmol, 45%) was

obtained by silica column chromatography (10 → 20% EtOAc in toluene + 1% AcOH). *R<sub>f</sub>* = 0.3 (2:1 toluene: EtOAc + AcOH) <sup>1</sup>H NMR (400 MHz, CDCl<sub>3</sub>/MeOD): δ 6.99 (d, *J* = 8.7 Hz, 2H, 2 × CH<sub>ar</sub>), 6.79 (d, *J* = 8.7 Hz, 2H, 2 × CH<sub>ar</sub>), 3.47 - 3.36 (m, 4H, 2 × CH<sub>2</sub>), 2.65 (t, *J* = 7.9 Hz, 4H, 2 × CH<sub>2</sub>), 2.52 (s, 6H, 2 × CH<sub>3</sub>), 2.35 (t, *J* = 7.9 Hz, 4H, 2 × CH<sub>2</sub>), 1.47 (s, 6H, 2 × CH<sub>3</sub>), 1.20 (t, *J* = 7.0 Hz, 6H, 2 × CH<sub>3</sub>). <sup>13</sup>C NMR (101 MHz, CDCl<sub>3</sub>/MeOD): δ 176.08, 153.75, 148.95, 143.50, 140.46, 132.32, 129.69, 129.66, 122.19, 112.83, 45.01, 34.97, 19.98, 12.68, 12.58, 12.54. ESI-HRMS (*m/z*): calcd. for [C<sub>29</sub>H<sub>36</sub>BF<sub>2</sub>N<sub>3</sub>O<sub>4</sub> + H]<sup>+</sup> 540.28449; obsd. 540.28417.

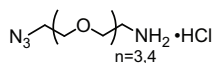


**1,3,5,7-Tetramethyl-2,6-bis-(2-carboxyethyl) -8-phenyl-4,4-difluoro-4-bora-3a,4a-diaza-*s*-indacene (15d).**

Compound **15d** (30 mg, 0.06 mmol) was dissolved in methanol/dioxane (1:1, 4 mL). NaOH (aq, 1M, 0.84 mL) was added and the mixture was heated to 40 °C for 15 min. The mixture was neutralized with HCl (aq, 1M, 1 mL), followed by addition of water and extraction with EtOAc. The mixture was dried (MgSO<sub>4</sub>), filtered

and concentrated *in vacuo*. Pure product (15 mg, 0.032 mmol, 53%) was obtained by silica column chromatography (10 → 20% EtOAc in toluene + 1% AcOH). *R<sub>f</sub>* = 0.45 (1:1 toluene: EtOAc + AcOH). <sup>1</sup>H NMR (400 MHz, CDCl<sub>3</sub>): δ 7.59 - 7.46 (m, 3H, 3 × CH<sub>ar</sub>), 7.35 - 7.21 (m, 2H, 2 × CH<sub>ar</sub>), 2.65 (t, *J* = 7.8 Hz, 4H, 2 × CH<sub>2</sub>), 2.53 (s, 6H, 2 × CH<sub>3</sub>), 2.35 (t, *J* = 7.8 Hz, 4H, 2 × CH<sub>2</sub>), 1.34 (s, 6H, 2 × CH<sub>3</sub>). <sup>13</sup>C NMR (101 MHz, CDCl<sub>3</sub>): δ 176.05, 168.66, 154.79, 141.95, 140.41, 136.19, 131.65, 130.25, 129.97, 129.80, 128.90, 96.94, 34.98, 20.03, 12.75, 12.17 ESI-HRMS (*m/z*): calcd. for [C<sub>25</sub>H<sub>27</sub>BF<sub>2</sub>N<sub>2</sub>O<sub>4</sub> + H]<sup>+</sup> 469.21092; obsd. 469.21079.

**General procedure for the monoreduction of diazido-PEG spacers (17a,b).**

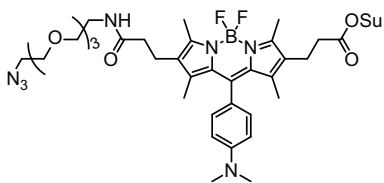


To a cooled (0 °C) solution of diazido-PEG spacers (5 mmol) in toluene (15 mL), 5% aq HCl (15 mL) was added, followed by the addition of PPh<sub>3</sub> (4.75 mmol, 0.95 eq). The mixture was warmed to rt and stirred for 16 h. The

waterlayer, containing the product, was separated, concentrated and co-evaporated with toluene (3×) to give a colorless oil.

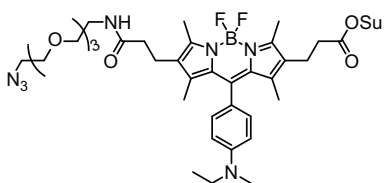
**11-azido-3,6,9-trioxaundecan-1-amine hydrochloride (17a).** Yield: 1.2 g, 4.7 mmol, 94%. *R<sub>f</sub>* = 0.7 (9:1 MeOH:NH<sub>4</sub>OH). <sup>1</sup>H NMR (400 MHz, MeOD): δ 3.75 - 3.70 (m, 2H, CH<sub>2</sub>), 3.68 (d, *J* = 5.5 Hz, 10H, 5 × CH<sub>2</sub>), 3.43 - 3.37 (m, 2H, CH<sub>2</sub>), 3.16 - 3.10 (m, 2H, CH<sub>2</sub>). <sup>13</sup>C NMR (101 MHz, MeOD): δ 71.57, 71.47, 71.36, 71.20, 71.01, 67.80, 51.77, 40.68. FT-IR (thin film) *v* 3052, 2878, 2360, 2344, 2102, 1560, 1116 cm<sup>-1</sup>.

**14-azido-3,6,9,12-tetraoxatetradecan-1-amine hydrochloride (17b).** Yield: 1.32 g, 4.4 mmol, 89%.  $R_f = 0.7$  (9:1 MeOH:NH<sub>4</sub>OH). <sup>1</sup>H NMR (400 MHz, MeOD):  $\delta$  3.72 - 3.67 (m, 2H, CH<sub>2</sub>), 3.64 (d,  $J = 4.2$  Hz, 14H, 7  $\times$  CH<sub>2</sub>), 3.40 - 3.34 (m, 2H, CH<sub>2</sub>), 3.13 - 3.08 (m, 2H, CH<sub>2</sub>). <sup>13</sup>C NMR (101 MHz, MeOD):  $\delta$  71.47, 71.43, 71.38, 71.11, 70.98, 67.82, 51.79, 40.66. FT-IR (thin film)  $\nu$  3036, 2866, 2360, 2343, 2106, 1118 cm<sup>-1</sup>.



**1,3,5,7-Tetramethyl-2-(2-(1-azidotetraethyleneglycol) aminocarbonyl) ethyl)-6-(2-succinimidylloxycarbonyl) ethyl)-8-[4-(*N,N*-dimethylamino)- phenyl]-4,4-difluoro-4-bora-3a,4a-diaza-s-indacene (18a).**

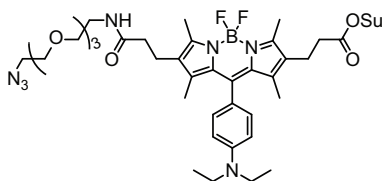
**16a** (97 mg, 0.19 mmol, 1 eq) was dissolved in DMF (10 mL). PEG-spacer **17a** (43 mg, 0.17 mmol, 0.9 eq), triethylamine (40  $\mu$ L, 0.29 mmol, 1.5 eq) and HOBt (23 mg, 0.17 mmol, 0.9 eq) were added, the mixture was cooled to 0 °C and EDC · HCl (32 mg, 0.17 mmol, 0.9 eq) was added. After stirring for 16 h at ambient temperature, DMF was evaporated and the solids were dissolved in DCM (, 20 mL). *N*-hydroxysuccinimide (175 mg, 1.52 mmol, 8 eq) and EDC · HCl (291 mg, 1.52 mmol, 8 eq) were added and after 3h stirring at room temperature, the reaction was finished according to TLC. The mixture was washed with HCl (aq, pH 3) and water, dried (MgSO<sub>4</sub>), filtered and concentrated. Pure compound (53 mg, 0.065 mmol) was obtained by silica column chromatography (0  $\rightarrow$  1% MeOH in DCM) in 34% yield.  $R_f = 0.75$  (10:1 DCM: MeOH) <sup>1</sup>H NMR (400 MHz, CDCl<sub>3</sub>):  $\delta$  7.04 (d,  $J = 8.7$  Hz, 2H, 2  $\times$  CH<sub>ar</sub>), 6.78 (d,  $J = 8.7$  Hz, 2H, 2  $\times$  CH<sub>ar</sub>), 6.30 (s, 1H, NH), 3.73 - 3.56 (m, 10H, 5  $\times$  CH<sub>2</sub>), 3.53 (t,  $J = 5.0$  Hz, 2H, CH<sub>2</sub>), 3.41 (dd,  $J = 10.1, 5.1$  Hz, 2H, CH<sub>2</sub>), 3.39 - 3.34 (m, 2H, CH<sub>2</sub>), 3.03 (s, 6H, 2  $\times$  CH<sub>3</sub>), 2.83 (d,  $J = 8.4$  Hz, 4H, 2  $\times$  CH<sub>2</sub>), 2.79 - 2.70 (m, 2H, CH<sub>2</sub>), 2.71 - 2.61 (m, 4H, 2  $\times$  CH<sub>2</sub>), 2.53 (s, 6H, 2  $\times$  CH<sub>3</sub>), 2.30 - 2.18 (m, 2H, CH<sub>2</sub>), 1.42 (s, 6H, 2  $\times$  CH<sub>3</sub>). <sup>13</sup>C NMR (101 MHz, CDCl<sub>3</sub>):  $\delta$  172.43, 171.94, 169.21, 167.85, 154.42, 152.37, 150.80, 142.64, 140.33, 139.36, 132.00, 131.49, 129.75, 128.88, 127.27, 122.43, 112.50, 70.70, 70.65, 70.52, 70.28, 70.06, 69.92, 50.72, 40.45, 39.45, 36.70, 31.32, 25.67, 25.55, 25.47, 20.02, 19.13, 12.74, 12.62, 12.33, 12.29. ESI-HRMS ( $m/z$ ): calcd. for [C<sub>39</sub>H<sub>52</sub>BF<sub>2</sub>N<sub>8</sub>O<sub>8</sub> + Na]<sup>+</sup> 831.37900; obsd. 831.37902.



**1,3,5,7-Tetramethyl-2-(2-(1-azidotetraethyleneglycol) aminocarbonyl) ethyl)-6-(2-succinimidylloxycarbonyl) ethyl)-8-[4-(*N,N*-ethylmethylamino)- phenyl]-4,4-difluoro-4-bora-3a,4a-diaza-s-indacene (18b).**

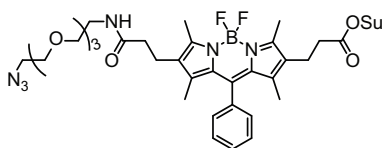
**16b** (63 mg, 0.12 mmol, 1 eq) was dissolved in DMF (5 mL). PEG-spacer **17a** (28 mg, 0.11 mmol, 0.9 eq), TEA (15  $\mu$ L, 0.11 mmol, 0.9 eq) and HOBt (15 mg, 0.11 mmol, 0.9 eq) were added, the mixture was cooled to 0 °C and EDC · HCl (21 mg, 0.11 mmol, 0.9 eq) was added. After stirring for 16 h at ambient temperature, DMF was evaporated and the solids were dissolved in DCM (10 mL). *N*-hydroxysuccinimide (115 mg, 0.96 mmol, 8 eq) and EDC · HCl (184 mg, 0.96 mmol, 8 eq) were added and after 2 h stirring at room temperature, the reaction was finished according to TLC. The mixture was washed with HCl (aq, pH 3) and water, dried (MgSO<sub>4</sub>), filtered and concentrated. Pure compound (51 mg, 0.062 mmol) was obtained by silica column chromatography (0  $\rightarrow$  1% MeOH in DCM) in 52% yield.  $R_f = 0.6$  (15:1 DCM: MeOH) <sup>1</sup>H NMR (600 MHz, CDCl<sub>3</sub>):  $\delta$  7.02 (s, 2H, 2  $\times$  CH<sub>ar</sub>), 6.78 (s, 2H, 2  $\times$  CH<sub>ar</sub>), 5.99 (t,  $J = 5.2$  Hz, 1H, NH), 3.66 - 3.56 (m, 10H, 5  $\times$  CH<sub>2</sub>), 3.52 (t,  $J = 5.1$  Hz, 2H, CH<sub>2</sub>), 3.47 (dd,  $J = 13.8, 6.8$  Hz, 2H, CH<sub>2</sub>), 3.44 - 3.39 (m, 2H, CH<sub>2</sub>), 3.38 - 3.33 (m, 2H, CH<sub>2</sub>), 2.98 (s, 3H, CH<sub>3</sub>), 2.83 (s, 4H, 2  $\times$  CH<sub>2</sub>), 2.78 - 2.71 (m, 2H, CH<sub>2</sub>), 2.70 - 2.59 (m, 4H, 2  $\times$  CH<sub>2</sub>), 2.52 (d,  $J = 16.9$

H<sub>2</sub>, 6H, 2 × CH<sub>3</sub>), 2.24 - 2.17 (m, 2H, CH<sub>2</sub>), 1.43 (s, 6H, 2 × CH<sub>3</sub>), 1.17 (t, *J* = 6.9 Hz, 3H, CH<sub>3</sub>). <sup>13</sup>C NMR (151 MHz, CDCl<sub>3</sub>): δ 172.04, 169.15, 167.88, 154.41, 152.45, 149.57, 142.78, 140.29, 139.39, 132.07, 131.57, 129.84, 129.09, 127.34, 122.15, 112.58, 70.82, 70.77, 70.65, 70.42, 70.17, 69.97, 50.79, 39.46, 36.82, 31.39, 25.72, 20.01, 19.21, 12.81, 12.67, 12.38, 12.33, 11.16. ESI-HRMS (*m/z*): calcd. for [C<sub>40</sub>H<sub>53</sub>BF<sub>2</sub>N<sub>8</sub>O<sub>8</sub> + Na]<sup>+</sup> 845.39466; obsd. 845.39463.



**1,3,5,7-Tetramethyl-2-(2-(1-azidotetraethyleneglycol)aminocarbonyl)-6-(2-succinimidoxycarbonyl)-8-[4-(*N,N*-diethylamino)phenyl]-4,4-difluoro-4-bora-3a,4a-diaza-*s*-indacene (18c).**

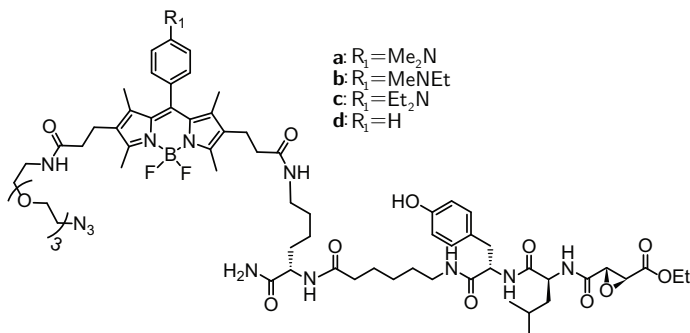
Compound **16c** (35 mg, 0.064 mmol, 1 eq) was dissolved in DMF (3 mL). PEG-spacer **17a** (17 mg, 0.06 mmol, 0.9 eq), TEA (8 μL, 0.06 mmol, 0.9 eq) and HOBt (8 mg, 0.06 mmol, 0.9 eq) were added, the mixture was cooled to 0 °C and EDC · HCl (12 mg, 0.06 mmol, 0.9 eq) was added. After stirring for 16 h at ambient temperature, DMF was evaporated and the solids were dissolved in DCM (10 mL). *N*-hydroxysuccinimide (37 mg, 0.32 mmol, 5 eq) and EDC · HCl (61 mg, 0.32 mmol, 5 eq) were added and after 2 h stirring at room temperature, the reaction was finished according to TLC. The mixture was washed with HCl (aq, pH 3) and water, dried (MgSO<sub>4</sub>), filtered and concentrated. Pure compound (23 mg, 0.027 mmol) was obtained by silica column chromatography (0 → 2% MeOH in DCM) in 43% yield. *R*<sub>f</sub> = 0.8 (15:1 DCM: MeOH) <sup>1</sup>H NMR (400 MHz, CDCl<sub>3</sub>): δ 6.99 (d, *J* = 8.6 Hz, 2H, 2 × CH<sub>ar</sub>), 6.74 (d, *J* = 8.7 Hz, 2H, 2 × CH<sub>ar</sub>), 6.09 (s, 1H, NH), 3.72 - 3.57 (m, 10H, 5 × CH<sub>2</sub>), 3.52 (t, *J* = 4.9 Hz, 2H, CH<sub>2</sub>), 3.47 - 3.34 (m, 8H, 4 × CH<sub>2</sub>), 2.89 - 2.79 (m, 4H, 2 × CH<sub>2</sub>), 2.79 - 2.72 (m, 2H, CH<sub>2</sub>), 2.71 - 2.60 (m, 4H, 2 × CH<sub>2</sub>), 2.54 (s, 6H, 2 × CH<sub>3</sub>), 2.22 (t, *J* = 7.7 Hz, 2H, CH<sub>2</sub>), 1.45 (s, 6H, 2 × CH<sub>3</sub>), 1.20 (t, *J* = 7.0 Hz, 6H, 2 × CH<sub>3</sub>). <sup>13</sup>C NMR (101 MHz, CDCl<sub>3</sub>): δ 171.99, 169.15, 169.07, 167.76, 154.17, 152.15, 148.20, 142.82, 140.21, 139.28, 131.98, 131.47, 129.63, 128.98, 127.12, 121.35, 112.00, 70.66, 70.62, 70.49, 70.25, 70.02, 69.85, 50.64, 44.38, 39.31, 36.68, 31.25, 25.59, 19.90, 19.08, 12.38, 12.32, 12.26. ESI-HRMS (*m/z*): calcd. for [C<sub>41</sub>H<sub>55</sub>BF<sub>2</sub>N<sub>8</sub>O<sub>8</sub> + Na]<sup>+</sup> 859.41033; obsd. 859.41055.



**1,3,5,7-Tetramethyl-2-(2-(1-azidotetraethyleneglycol)aminocarbonyl)-6-(2-succinimidoxycarbonyl)-8-phenyl-4,4-difluoro-4-bora-3a,4a-diaza-*s*-indacene (18d).**

Compound **15d** (27 mg, 0.06 mmol, 1 eq) was dissolved in DMF (2 mL). PEG-spacer **17a** (16 mg, 0.054 mmol, 0.9 eq), TEA (7.5 μL, 0.054 mmol, 0.9 eq) and HOBt (7 mg, 0.054 mmol, 0.9 eq) were added, the mixture was cooled to 0 °C and EDC · HCl (10.5 mg, 0.054 mmol, 0.9 eq) was added. After stirring for 24 h at ambient temperature, DMF was evaporated and the solids were dissolved in DCM (5 mL). *N*-hydroxysuccinimide (55 mg, 0.48 mmol, 8 eq) and EDC · HCl (92 mg, 0.48 mmol, 8 eq) were added and after 2 h stirring at room temperature, the reaction was finished according to TLC. The mixture was washed with HCl (aq, pH 3) and water, dried (MgSO<sub>4</sub>), filtered and concentrated. Pure compound (15 mg, 0.02 mmol) was obtained by silica column chromatography (0 → 1% MeOH in DCM) in 33% yield. *R*<sub>f</sub> = 0.7 (15:1 DCM: MeOH) <sup>1</sup>H NMR (400 MHz, CDCl<sub>3</sub>): δ 7.56 - 7.44 (m, 3H, 3 × CH<sub>ar</sub>), 7.35 - 7.23 (m, 2H, 2 × CH<sub>ar</sub>), 6.02 (s, 1H, NH), 3.70 - 3.56 (m, 10H, 5 × CH<sub>2</sub>), 3.53 (t, *J* = 5.0 Hz, 2H, CH<sub>2</sub>), 3.45 - 3.40 (m, 2H, CH<sub>2</sub>), 3.39 - 3.31 (m, 2H, CH<sub>2</sub>), 2.84 (s, 4H, 2 × CH<sub>2</sub>), 2.77 - 2.70 (m, 2H, CH<sub>2</sub>), 2.70 - 2.58 (m, 4H, 2 × CH<sub>2</sub>), 2.55 (s, 6H, 2 × CH<sub>3</sub>), 2.20 (t, *J* = 7.7 Hz, 2H, CH<sub>2</sub>), 1.30 (s, 6H, 2 × CH<sub>3</sub>). <sup>13</sup>C

NMR (101 MHz,  $\text{CDCl}_3$ ):  $\delta$  171.90, 169.01, 167.68, 155.10, 153.07, 141.06, 140.02, 139.15, 135.28, 132.06, 130.66, 130.11, 129.22, 129.05, 128.03, 127.56, 70.67, 70.62, 70.50, 70.26, 70.04, 69.81, 50.64, 39.34, 36.56, 31.19, 29.71, 25.59, 19.82, 19.01, 12.74, 12.61, 11.92, 11.87. ESI-HRMS ( $m/z$ ): calcd. for  $[\text{C}_{37}\text{H}_{46}\text{BF}_2\text{N}_7\text{O}_8 + \text{Na}]^+$  788.33677; obsd. 788.33660.



#### General procedure for BODIPY-DCG-04 derivatives (19a-d).

BODIPY **18a-d** (~20  $\mu\text{mol}$ , 1 eq) was dissolved in DMF (0.5 mL) and DIPEA (1 eq) was added. A solution of DCG-04 amine<sup>14</sup> (0.95 eq) in DMF was dropwise added. The mixture was stirred for 3 h

at room temperature, concentrated and isolated using silica column chromatography (3  $\rightarrow$  7% MeOH in DCM). The product was lyophilized from *t*-butanol/ $\text{H}_2\text{O}$  to give a hygroscopic orange powder.

#### *N,N*-dimethylamino BODIPY-DCG-04 (19a).

Yield: 10 mg (7.3  $\mu\text{mol}$ , 37%).  $R_f = 0.45$  (10:1 DCM:MeOH).  $^1\text{H}$  NMR (600 MHz, MeOD):  $\delta$  7.05 (d,  $J = 8.4$  Hz, 2H, 2  $\times$   $\text{CH}_{\text{ar}}$ ), 7.01 (d,  $J = 8.3$  Hz, 2H, 2  $\times$   $\text{CH}_{\text{ar}}$ ), 6.88 (d,  $J = 8.8$  Hz, 2H, 2  $\times$   $\text{CH}_{\text{ar}}$ ), 6.69 (d,  $J = 8.2$  Hz, 2H, 2  $\times$   $\text{CH}_{\text{ar}}$ ), 4.45 (t,  $J = 7.6$  Hz, 1H, CH), 4.41 - 4.36 (m, 1H, CH), 4.31 - 4.21 (m, 3H,  $\text{CH}_2$ , CH), 3.68 - 3.51 (m, 12H, 5  $\times$   $\text{CH}_2$ , 2  $\times$  CH), 3.47 (t,  $J = 5.5$  Hz, 2H,  $\text{CH}_2$ ), 3.34 - 3.32 (m, 4H, 2  $\times$   $\text{CH}_2$ ), 3.17 - 3.07 (m, 3H,  $\text{CH}_2$ ,  $\text{CH}_2\text{-H}^{\text{a}}$ ), 3.08 - 2.99 (m, 7H, 2  $\times$   $\text{CH}_3$ ,  $\text{CH}_2\text{-H}^{\text{b}}$ ), 2.99 - 2.93 (m, 1H,  $\text{CH}_2\text{-H}^{\text{a}}$ ), 2.85 - 2.78 (m, 1H,  $\text{CH}_2\text{-H}^{\text{b}}$ ), 2.65 (dd,  $J = 13.5$ , 7.2 Hz, 4H, 2  $\times$   $\text{CH}_2$ ), 2.49 (s, 6H, 2  $\times$   $\text{CH}_3$ ), 2.28 - 2.17 (m, 6H, 3  $\times$   $\text{CH}_2$ ), 1.81 - 1.73 (m, 1H,  $\text{CH}_2\text{-H}^{\text{a}}$ ), 1.67 - 1.60 (m, 1H,  $\text{CH}_2\text{-H}^{\text{b}}$ ), 1.60 - 1.32 (m, 18H, 6  $\times$   $\text{CH}_2$ , 2  $\times$   $\text{CH}_3$ ), 1.30 (t,  $J = 7.2$  Hz, 3H,  $\text{CH}_3$ ), 1.25 - 1.16 (m, 2H,  $\text{CH}_2$ ), 0.93 (d,  $J = 6.4$  Hz, 3H,  $\text{CH}_3$ ), 0.89 (d,  $J = 6.4$  Hz, 3H,  $\text{CH}_3$ ).  $^{13}\text{C}$  NMR (151 MHz, MeOD):  $\delta$  177.16, 176.12, 175.14, 174.97, 173.67, 173.08, 169.22, 168.35, 157.31, 154.81, 154.57, 152.56, 143.88, 141.04, 140.85, 132.79, 132.73, 131.36, 130.55, 130.44, 130.10, 128.90, 123.71, 116.24, 113.68, 71.61, 71.56, 71.47, 71.31, 71.11, 70.60, 63.22, 56.46, 54.41, 54.24, 53.40, 53.04, 51.75, 41.65, 40.57, 40.52, 40.20, 40.18, 38.20, 37.44, 37.27, 36.66, 32.79, 30.01, 29.84, 27.41, 26.50, 25.88, 24.34, 23.31, 22.03, 21.28, 21.18, 14.37, 12.79, 12.56, 12.53. ESI-HRMS ( $m/z$ ): calcd. for  $[\text{C}_{68}\text{H}_{98}\text{BF}_2\text{N}_{13}\text{O}_{14} + \text{H}]^+$  1370.75011; obsd. 1370.75147.

#### *N,N*-ethylmethylamino BODIPY-DCG-04 (19b).

Yield: 9 mg (6.5  $\mu\text{mol}$ , 43%).  $R_f = 0.45$  (10:1 DCM:MeOH).  $^1\text{H}$  NMR (600 MHz, MeOD):  $\delta$  7.06 - 6.98 (m, 4H, 4  $\times$   $\text{CH}_{\text{ar}}$ ), 6.87 (d,  $J = 8.8$  Hz, 2H, 2  $\times$   $\text{CH}_{\text{ar}}$ ), 6.69 (d,  $J = 8.5$  Hz, 2H, 2  $\times$   $\text{CH}_{\text{ar}}$ ), 4.45 (t,  $J = 7.6$  Hz, 1H, CH), 4.39 (dd,  $J = 9.1$ , 5.9 Hz, 1H, CH), 4.31 - 4.19 (m, 3H,  $\text{CH}_2$ , CH), 3.67 - 3.56 (m, 10H, 4  $\times$   $\text{CH}_2$ , 2  $\times$  CH), 3.56 - 3.52 (m, 2H,  $\text{CH}_2$ ), 3.52 - 3.44 (m, 4H, 2  $\times$   $\text{CH}_2$ ), 3.34 - 3.32 (m, 4H, 2  $\times$   $\text{CH}_2$ ), 3.18 - 3.08 (m, 3H,  $\text{CH}_2$ ,  $\text{CH}_2\text{-H}^{\text{a}}$ ), 3.07 - 3.01 (m, 1H,  $\text{CH}_2\text{-H}^{\text{b}}$ ), 2.99 - 2.93 (m, 4H,  $\text{CH}_3$ ,  $\text{CH}_2\text{-H}^{\text{a}}$ ), 2.85 - 2.79 (m, 1H,  $\text{CH}_2\text{-H}^{\text{b}}$ ), 2.66 (dd,  $J = 13.8$ , 7.2 Hz, 4H, 2  $\times$   $\text{CH}_2$ ), 2.47 (s, 6H, 2  $\times$   $\text{CH}_3$ ), 2.28 - 2.19 (m, 6H, 3  $\times$   $\text{CH}_2$ ), 1.81 - 1.73 (m, 1H,  $\text{CH}_2\text{-H}^{\text{a}}$ ), 1.67 - 1.60 (m, 1H,  $\text{CH}_2\text{-H}^{\text{b}}$ ), 1.59 - 1.32 (m, 18H, 6  $\times$   $\text{CH}_2$ , 2  $\times$   $\text{CH}_3$ ), 1.30 (t,  $J = 7.1$  Hz, 3H,  $\text{CH}_3$ ), 1.23 - 1.17 (m, 2H,  $\text{CH}_2$ ), 1.15 (t,  $J = 7.0$  Hz, 3H,  $\text{CH}_3$ ), 0.93 (d,  $J = 6.4$  Hz, 3H,  $\text{CH}_3$ ), 0.89 (d,  $J = 6.4$  Hz, 3H,  $\text{CH}_3$ ).

173.08, 168.73, 168.41, 157.31, 154.76, 154.51, 151.09, 143.97, 141.03, 140.85, 132.82, 132.76, 131.36, 130.53, 130.42, 130.23, 128.90, 123.28, 116.24, 113.64, 71.61, 71.56, 71.48, 71.32, 71.11, 70.61, 63.21, 56.48, 54.38, 54.24, 53.39, 53.18, 51.75, 47.62, 41.65, 40.52, 40.20, 40.18, 38.20, 37.76, 37.44, 37.27, 36.66, 32.79, 30.01, 29.84, 27.42, 26.50, 25.89, 24.34, 23.31, 22.02, 21.29, 21.19, 14.36, 12.78, 12.56, 12.53, 11.24. ESI-HRMS ( $m/z$ ): calcd. for  $[C_{69}H_{100}BF_2N_{13}O_{14} + H]^+$  1384.76578; obsd. 1384.76725.

#### ***N,N*-diethylamino BODIPY-DCG-04 (19c).**

Yield: 12 mg (8.6  $\mu$ mol, 31%).  $R_f = 0.3$  (10:1 DCM:MeOH).  $^1H$  NMR (600 MHz,  $CDCl_3/MeOD$ ):  $\delta$  7.03 - 6.95 (m, 4H, 4  $\times$   $CH_{ar}$ ), 6.77 (d,  $J = 8.7$  Hz, 2H, 2  $\times$   $CH_{ar}$ ), 6.74 - 6.69 (m, 2H, 2  $\times$   $CH_{ar}$ ), 4.45 (t,  $J = 7.5$  Hz, 1H, CH), 4.40 (t,  $J = 7.3$  Hz, 1H, CH), 4.33 - 4.23 (m, 3H,  $CH_2$ , CH), 3.67 - 3.60 (m, 9H, 4  $\times$   $CH_2$ , CH), 3.60 - 3.56 (m, 2H,  $CH_2$ ), 3.55 (d,  $J = 1.8$  Hz, 1H, CH), 3.50 (t,  $J = 5.3$  Hz, 2H,  $CH_2$ ), 3.42 (q,  $J = 7.0$  Hz, 4H, 2  $\times$   $CH_2$ ), 3.39 - 3.32 (m, 4H, 2  $\times$   $CH_2$ ), 3.20 - 3.08 (m, 3H,  $CH_2$ ,  $CH_2-H^a$ ), 3.05 - 2.98 (m, 1H,  $CH_2-H^b$ ), 2.94 (dd,  $J = 13.7, 7.8$  Hz, 1H,  $CH_2-H^a$ ), 2.89 - 2.81 (m, 1H,  $CH_2-H^b$ ), 2.64 (dd,  $J = 15.2, 7.0$  Hz, 4H, 2  $\times$   $CH_2$ ), 2.50 (s, 6H, 2  $\times$   $CH_3$ ), 2.26 - 2.17 (m, 6H, 3  $\times$   $CH_2$ ), 1.81 - 1.73 (m, 1H,  $CH_2-H^a$ ), 1.66 - 1.58 (m, 1H,  $CH_2-H^b$ ), 1.58 - 1.49 (m, 6H, 3  $\times$   $CH_2$ ), 1.46 (s, 6H, 2  $\times$   $CH_3$ ), 1.40 - 1.29 (m, 7H, 2  $\times$   $CH_2$ ,  $CH_3$ ), 1.22 - 1.17 (m, 6H, 2  $\times$   $CH_3$ ), 1.17 - 1.10 (m, 2H,  $CH_2$ ), 0.91 (d,  $J = 5.9$  Hz, 3H,  $CH_3$ ), 0.88 (d,  $J = 5.8$  Hz, 3H,  $CH_3$ ).  $^{13}C$  NMR (151 MHz,  $CDCl_3/MeOD$ ):  $\delta$  176.00, 175.08, 174.02, 173.68, 172.45, 171.84, 167.90, 167.20, 156.22, 153.71, 153.62, 148.82, 143.21, 140.42, 140.33, 132.14, 130.74, 129.73, 129.66, 129.46, 129.37, 127.93, 121.89, 115.78, 115.72, 112.62, 70.99, 70.89, 70.54, 70.44, 70.04, 62.88, 55.50, 53.96, 53.20, 52.82, 52.29, 51.06, 44.84, 41.11, 39.79, 39.54, 39.49, 37.76, 36.93, 36.84, 36.18, 32.05, 29.19, 29.00, 26.60, 25.74, 25.69, 25.19, 23.40, 23.07, 21.85, 20.68, 20.57, 14.19, 12.62, 12.53, 12.44, 12.40. ESI-HRMS ( $m/z$ ): calcd. for  $[C_{70}H_{102}BF_2N_{13}O_{14} + H]^+$  1398.78144; obsd. 1398.78302.

#### **Phenyl BODIPY-DCG-04 (19d).**

Yield: 8.4 mg (6  $\mu$ mol, 31%).  $R_f = 0.3$  (10:1 DCM:MeOH).  $^1H$  NMR (600 MHz,  $CDCl_3/MeOD$ ):  $\delta$  7.54 - 7.47 (m, 3H, 3  $\times$   $CH_{ar}$ ), 7.27 - 7.22 (m, 2H, 2  $\times$   $CH_{ar}$ ), 7.01 (d,  $J = 8.5$  Hz, 2H, 2  $\times$   $CH_{ar}$ ), 6.73 (d,  $J = 8.5$  Hz, 2H, 2  $\times$   $CH_{ar}$ ), 4.49 - 4.39 (m, 2H, 2  $\times$  CH), 4.39 - 4.23 (m, 3H,  $CH_2$ , CH), 3.69 - 3.64 (m, 9H, 4  $\times$   $CH_2$ , CH), 3.61 - 3.56 (m, 2H,  $CH_2$ ), 3.54 - 3.49 (m, 3H,  $CH_2$ , CH), 3.39 - 3.33 (m, 4H, 2  $\times$   $CH_2$ ), 3.24 - 3.06 (m, 3H,  $CH_2$ ,  $CH_2-H^a$ ), 3.05 - 2.97 (m, 1H,  $CH_2-H^b$ ), 2.96 - 2.82 (m, 2H,  $CH_2$ ), 2.69 - 2.60 (m, 4H, 2  $\times$   $CH_2$ ), 2.53 (s, 6H, 2  $\times$   $CH_3$ ), 2.27 - 2.12 (m, 6H, 3  $\times$   $CH_2$ ), 1.85 - 1.73 (m, 1H,  $CH_2-H^a$ ), 1.69 - 1.58 (m, 1H,  $CH_2-H^b$ ), 1.57 - 1.41 (m, 6H, 3  $\times$   $CH_2$ ), 1.36 - 1.28 (m, 13H, 3  $\times$   $CH_3$ , 2  $\times$   $CH_2$ ), 1.16 - 1.05 (m, 2H,  $CH_2$ ), 0.96 - 0.86 (m, 6H, 2  $\times$   $CH_3$ ).  $^{13}C$  NMR (151 MHz,  $CDCl_3/MeOD$ ):  $\delta$  175.56, 174.67, 173.46, 171.97, 171.43, 167.49, 166.70, 155.91, 141.15, 139.96, 139.86, 135.49, 131.08, 130.49, 129.97, 129.83, 129.43, 129.29, 128.22, 127.61, 115.53, 70.77, 70.68, 70.64, 70.26, 70.19, 69.87, 62.69, 55.25, 53.80, 52.78, 52.71, 51.82, 50.83, 40.99, 39.50, 39.34, 39.18, 38.13, 37.62, 36.64, 36.52, 35.98, 31.79, 29.33, 28.90, 28.69, 26.24, 25.37, 24.96, 23.03, 22.91, 21.74, 20.33, 20.21, 14.05, 12.54, 11.86. ESI-HRMS ( $m/z$ ): calcd. for  $[C_{66}H_{93}BF_2N_{12}O_{14} + H]^+$  1327.70789; obsd. 1327.70956.

#### **General procedure for mannose cluster-BODIPY-DCG-04 derivatives (21a-d).**

BODIPY-DCG-04 derivative **19a-d** (~5  $\mu$ mol, 1 eq) dissolved in DMF (degassed, 1 mL) was added to mannose cluster **20<sup>4</sup>** (0.9 eq) in  $H_2O$  (degassed, 1 mL) under an argon atmosphere. Sodium ascorbate (1 eq) and  $CuSO_4$  (10 mol%), as solution in water (degassed), were added to the mixture followed by heating to 80  $^\circ C$  for 12 h. The reaction was monitored by LC-MS. When needed, additional sodium ascorbate and  $CuSO_4$  were added. Upon prolonged heating (>48 h), decomposition of starting



materials was observed, and so the reaction was terminated by concentration under reduced pressure and semi-preparative HPLC (C18 column, solvent A: 0.2% TFA in H<sub>2</sub>O; solvent B: acetonitrile) purification. HPLC fractions containing the product were combined and lyophilized, yielding the compound as a hygroscopic orange/reddish powder.

#### Mannose cluster -*N,N*-dimethylamino BODIPY-DCG-04 (21a).

Hydrolysis of the ethyl ester of DCG-04 was observed and this compound was isolated besides the title compound. HPLC (27–41% B in 12', 450 μL injection) yielded 13% (2.5 mg, 0.55 μmol) product and 10% (1.9 mg, 0.42 μmol) hydrolyzed product. ESI-HRMS (*m/z*): calcd. for [C<sub>199</sub>H<sub>312</sub>BF<sub>2</sub>N<sub>45</sub>O<sub>66</sub> + 3H]<sup>3+</sup> 1370.75011; obsd. 1370.75147.

#### Mannose cluster -*N,N*-ethylmethylamino BODIPY-DCG-04 (21b).

HPLC (27–41% B in 12', 450 μL injection) yielded 29% (6.2 mg, 1.4 μmol) product. ESI-HRMS (*m/z*): calcd. for [C<sub>200</sub>H<sub>314</sub>BF<sub>2</sub>N<sub>45</sub>O<sub>66</sub> + 3H]<sup>3+</sup> 1485.43157; obsd. 1485.43328.

#### Mannose cluster -*N,N*-diethylamino BODIPY-DCG-04 (21c).

This reaction proceeded very sluggishly, and was terminated after 24 h to prevent decomposition of the formed product as well as remaining starting materials. HPLC (21–36% B in 12', 450 μL injection) yielded 4% (0.56 mg, 0.13 μmol) product. ESI-HRMS (*m/z*): calcd. for [C<sub>201</sub>H<sub>316</sub>BF<sub>2</sub>N<sub>45</sub>O<sub>66</sub> + 3H]<sup>3+</sup> 1490.10345; obsd. 1490.10513.

#### Mannose cluster -phenyl BODIPY-DCG-04 (21d).

HPLC (27–41% B in 12', 450 μL injection) yielded 20% (3.3 mg, 0.75 μmol) product. ESI-HRMS (*m/z*): calcd. for [C<sub>197</sub>H<sub>307</sub>BF<sub>2</sub>N<sub>44</sub>O<sub>66</sub> + 3H]<sup>3+</sup> 1466.41228; obsd. 1466.41367.

## References

- [1] Hoogendoorn, S.; Habets, K. L.; Passemard, S.; Kuiper, J.; van der Marel, G. A.; Florea, B. I.; Overkleeft, H. S. *Chem. Commun.* **2011**, *47*, 9363–9365.
- [2] Loudet, A.; Burgess, K. *Chem. Rev.* **2007**, *107*, 4891–932.
- [3] Ulrich, G.; Ziesel, R.; Harriman, A. *Angew. Chem. Int. Ed. Engl.* **2008**, *47*, 1184–201.
- [4] Hillaert, U.; Verdoes, M.; Florea, B.; Saragliadis, A.; Habets, K.; Kuiper, J.; Van Calenbergh, S.; Ossendorp, F.; van der Marel, G.; Driessen, C.; Overkleeft, H. *Angew. Chem. Int. Ed. Engl.* **2009**, *48*, 1629.
- [5] Witte, M. D. et al. *Nat. Chem. Biol.* **2010**, *6*, 907–913.
- [6] Blum, G.; Mullins, S. R.; Keren, K.; Fonovič, M.; Jedeszko, C.; Rice, M. J.; Sloane, B. F.; Bogyo, M. *Nat. Chem. Biol.* **2005**, *1*, 203–209.
- [7] Li, X.; Cao, J.-H.; Li, Y.; Rondard, P.; Zhang, Y.; Yi, P.; Liu, J.-F.; Nan, F.-J. *J. Med. Chem.* **2008**, *51*, 3057–3060.
- [8] Saghatelian, A.; Jessani, N.; Joseph, A.; Humphrey, M.; Cravatt, B. F. *Proc. Natl. Acad. Sci. U. S. A.* **2004**, *101*, 10000–10005.
- [9] Yee, M.-C.; Fas, S. C.; Stohlmeyer, M. M.; Wandless, T. J.; Cimprich, K. A. *J. Biol. Chem.* **2005**, *280*, 29053–29059.
- [10] Urano, Y.; Asanuma, D.; Hama, Y.; Koyama, Y.; Barrett, T.; Kamiya, M.; Nagano, T.; Watanabe, T.; Hasegawa, A.; Choyke, P. L.; Kobayashi, H. *Nat. Med.* **2009**, *15*, 104–9.
- [11] Kollmannberger, M.; Rurack, K.; Resch-Genger, U.; Daub, J. *J. Phys. Chem. A* **1998**, *102*, 10211–10220.
- [12] de Silva, A. P.; Gunaratne, H. Q. N.; Gunnlaugsson, T.; Huxley, A. J. M.; McCoy, C. P.; Rademacher, J. T.; Rice, T. E. *Chem. Rev.* **1997**, *97*, 1515–1566.
- [13] Sunahara, H.; Urano, Y.; Kojima, H.; Nagano, T. *J. Am. Chem. Soc.* **2007**, *129*, 5597–5604.



- [14] Greenbaum, D.; Medzihradzky, K. F.; Burlingame, A.; Bogyo, M. *Chem. Biol.* **2000**, *7*, 569–581.
- [15] Brix, K.; Dunkhorst, A.; Mayer, K.; Jordans, S. *Biochimie* **2008**, *90*, 194–207.
- [16] Boiadjiev, S. E.; Lightner, D. A. *J. Heterocycl. Chem.* **2003**, *40*, 181–185.
- [17] Rostovtsev, V. V.; Green, L. G.; Fokin, V. V.; Sharpless, K. B. *Angew. Chem. Int. Ed. Engl.* **2002**, *41*, 2596–2599.
- [18] Tornøe, C. W.; Christensen, C.; Meldal, M. *J. Org. Chem.* **2002**, *67*, 3057–3064.
- [19] Ohkuma, S.; Poole, B. *Proc. Natl. Acad. Sci. U. S. A.* **1978**, *75*, 3327–3331.
- [20] Verdoes, M.; Florea, B. I.; Hillaert, U.; Willems, L. I.; van der Linden, W. A.; Sae-Heng, M.; Filippov, D. V.; Kisselev, A. F.; van der Marel, G. A.; Overkleeft, H. S. *ChemBioChem* **2008**, *9*, 1735–1738.
- [21] Sallusto, F.; Cella, M.; Danieli, C.; Lanzavecchia, A. *J. Exp. Med.* **1995**, *182*, 389–400.
- [22] Dean, R. T.; Jessup, W.; Roberts, C. R. *Biochem. J* **1984**, *217*, 27–40.
- [23] Seglen, P. O.; Grinde, B.; Solheim, A. E. *Eur. J. Biochem.* **1979**, *95*, 215–225.
- [24] Tietze, C.; Schlesinger, P.; Stahl, P. *Biochem. Biophys. Res. Commun.* **1980**, *93*, 1–8.
- [25] McIlvaine, T. C. *J. Biol. Chem.* **1921**, *49*, 183–186.



# 3

## Synthesis of pH-activatable red fluorescent BODIPY dyes with distinct functionalities<sup>1</sup>

This chapter describes the synthesis of a series of tunable pH-dependent BODIPY dyes that were functionalized using a Knoevenagel-type condensation reaction. In this fashion, monofunctional dyes containing an alkyne, azide or carboxylic acid (masked as its methyl ester) as ligation sites as well as asymmetrical bifunctional dyes were obtained, without compromising their pH-dependency. In addition, fluorescence excitation and emission maxima for these dyes were shown to be significantly red-shifted in comparison to their tetramethyl precursors.

## 3.1 Introduction

In recent years fluorescent dyes have found widespread use in chemical biology applications. An important class of dyes are those based on the 4,4-difluoro-4-bora-3a,4a-diaza-s-indacene (BODIPY) scaffold. BODIPY dyes usually show excellent photochemical properties, such as high molar absorption coefficients, high quantum yields and narrow emission bandwidths. Moreover, they are relatively stable under physiological conditions.<sup>2-4</sup>

Synthetic efforts have been directed towards the formation of analyte-sensitive dyes and numerous reports can be found in the literature.<sup>4</sup> Particularly useful examples are the pH-sensitive BODIPY dyes that are responsive to protonation.<sup>5-9</sup> Intracellular pH is an important factor in many physiological processes and by using a pH-activatable dye selective visualization of processes in acidic cellular compartments becomes possible. pH-sensitivity is usually accomplished by incorporation of a *p*-(*N,N*-dialkyl)aniline moiety at the *meso*-position of the BODIPY core.<sup>7,10-13</sup> Due to photo-induced electron transfer (PeT) fluorescence is quenched at neutral or basic pH.<sup>13-15</sup> Upon protonation of the aniline nitrogen fluorescence intensity increases drastically.

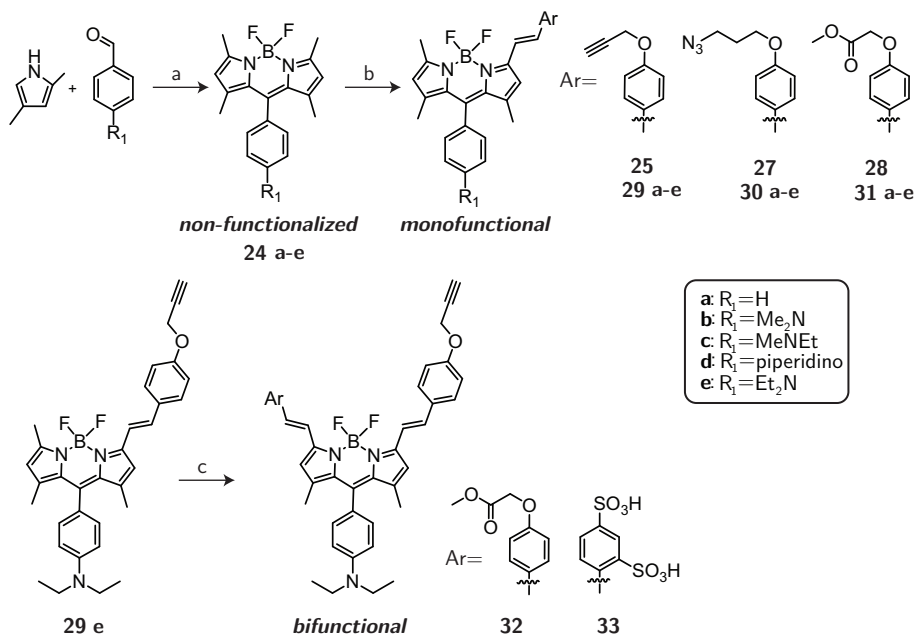
In a recent paper by Urano *et al.*, the development of a series of pH-activatable dyes with varying pK<sub>a</sub>-values is described.<sup>11</sup> These can be easily transformed into bifunctional dyes, but for mono-conjugation they are less convenient due to their symmetry, as described in Chapter 2.<sup>12</sup> Other groups have investigated the tetramethyl-BODIPY scaffold with a *meso*-aniline substituent.<sup>10,13,16</sup> The methyl groups adjacent to the nitrogens are susceptible to a Knoevenagel-type condensation with benzaldehydes, yielding dyes with red-shifted absorption and emission maxima.<sup>5-7,9,17-21</sup> The potential of the Knoevenagel reaction to extend the conjugated system is widely acknowledged and the reaction has been used to construct large libraries of (pH-independent) BODIPY dyes.<sup>22-25</sup> The use of the Knoevenagel reaction to incorporate ligation handles in the BODIPY dye has not been employed, although that would allow covalent attachment to other (bio-active) molecules, which is vital for applications in chemical biology. Often used ligation reactions comprise the Staudinger-Bertozzi ligation (involving azides),<sup>26</sup> the copper(I) catalyzed Huisgen 1,3-cycloaddition (involving azides or alkynes)<sup>27,28</sup> and, in a more traditional fashion, amide/ester formation (involving carboxylic acids). This chapter concerns the synthesis of a series of pH-dependent BODIPY dyes that are functionalized by means of the Knoevenagel reaction. The pH-dependency and spectroscopic properties of these novel dyes are investigated. Finally, one of the dyes is subjected to a ligation reaction to study the synthetic stability of these dyes.

## 3.2 Results and Discussion

Starting from commercially available *N,N*-dialkylamino benzaldehydes (or benzaldehyde in case of **24a**, the "always on" dye) and 2,4-dimethylpyrrole synthesis of non-functionalized BODIPY dyes **24a-e** proved straightforward, with yields ranging between 32 and 50% (Scheme 7.1).<sup>13,29</sup> To obtain mono-functional BODIPY dyes **29-31a-e**, three benzaldehydes

were synthesized, containing either an alkyne (**25**),<sup>30</sup> azide (**27**)<sup>31</sup> or a methyl ester (**28**)<sup>32</sup> as the functional group. The use of a tert-butyl ester has been reported in a related study,<sup>18</sup> however, literature precedence shows that methyl esters can be saponified using (mild) basic conditions while leaving the BODIPY core intact.<sup>1,11,33</sup> Subsequently, these benzaldehydes were used in a Knoevenagel condensation reaction with BODIPYs **24a-e**.

**Scheme 3.1:** Synthesis of non-functionalized, monofunctional and bifunctional BODIPY dyes



Reagents and conditions: [a] i) cat. TFA, DCM; ii) DDQ; iii) DiPEA, BF<sub>3</sub> · OEt<sub>2</sub>, 32-50%; [b] ArCHO **25-28**, pyrrolidine, acetic acid, EtOH or MeOH, microwave, 13-35%; [c] ArCHO, pyrrolidine, acetic acid, EtOH or MeOH, microwave, **32**: 42%, **33**: 12%

Reaction times using classical Knoevenagel conditions (refluxing in toluene in the presence of piperidine/ acetic acid) can be extensive (12-24 h).<sup>3,4,18</sup> Recent reports show that the use of microwave irradiation considerably shortens reaction times (5-20 min).<sup>25,34</sup> Therefore, microwave conditions were used in this study, in order to synthesize various BODIPYs in a relatively short period of time. In case of benzaldehyde **28**, the reaction solvent was changed from ethanol to methanol to prevent transesterification of the methyl ester. Typically, reaction yields of the Knoevenagel reaction are low,<sup>5,6,17,18,34</sup> and although this case forms no exception, the envisaged 15 mono-functional BODIPYs **29-31a-e** were all readily obtained. Importantly, a significant amount (30-50%) of unreacted starting material could easily be recovered by silica column chromatography.

BODIPY dyes **24a-e** contain two reactive methyl groups (at the 3 and 5 positions) and the main byproduct observed in the reaction was indeed the symmetrical distyryl substituted BODIPY. Under these conditions, no formation of tetrastryl substituted BODIPY

dyes was observed.<sup>19,21</sup> Taking advantage of the acidity of the second methyl group, mono-functional dye **29e** was subjected to another cycle of Knoevenagel condensation with benzaldehyde **28** to obtain bifunctional BODIPY dye **32**, containing two orthogonal ligation handles. As an alternative strategy, the second methyl group can be used to alter the solubility properties of the dye. BODIPY dyes tend to be fairly lipophilic and poorly water-soluble, which can be improved by introduction of polar moieties such as sulfonic acids<sup>37–39</sup> or polyethylene glycol.<sup>19,20</sup> By introduction of a disulfonic acid-containing styryl moiety via the Knoevenagel reaction water-soluble BODIPY dye **33** was synthesized in 12% yield. The low yield of this reaction was mostly due to extensive purification procedures to separate the product from pyrrolidinium acetate.

Evaluation of the spectroscopic properties of the dyes (Table 3.1) revealed small Stokes shifts, characteristic of BODIPY dyes, and moderate to excellent relative quantum yields\*. The fluorescence absorption and emission maxima of the dyes were shifted approximately 70 nm towards the red end of the spectrum with each Knoevenagel reaction (Table 3.1, Figure 3.1A). For biological applications such as live-cell fluorescence microscopy this is a great advantage, since levels of autofluorescence are lower at the red end of the spectrum. Besides, as a result of their narrow absorbance and emission peaks, the bifunctional dyes are compatible for use in the same experiment as other pH-dependent dyes, such as the ones described in Chapter 2.

**Table 3.1:** Spectroscopic properties measured in TFA (135 mM) /methanol

|            | $\lambda_{\text{abs}}$ (nm) | $\lambda_{\text{em}}$ (nm) | $\Phi_f^{b,c}$    | $pK_d^e$                |
|------------|-----------------------------|----------------------------|-------------------|-------------------------|
| <b>24a</b> | 497                         | 510                        | 0.63 <sup>b</sup> | -                       |
| <b>24b</b> | 500                         | 514                        | 0.35 <sup>b</sup> | 4.49 <sup>a</sup> /2.14 |
| <b>24c</b> | 500                         | 513                        | 0.44 <sup>b</sup> | 5.10 <sup>a</sup> /2.95 |
| <b>24d</b> | 500                         | 514                        | 0.40 <sup>b</sup> | 5.06 <sup>a</sup> /3.97 |
| <b>24e</b> | 500                         | 513                        | 0.56 <sup>b</sup> | 5.81 <sup>a</sup> /4.05 |
| <b>29a</b> | 563                         | 574                        | 1.09 <sup>c</sup> | -                       |
| <b>29b</b> | 567                         | 582                        | 0.66 <sup>c</sup> | 2.13                    |
| <b>29c</b> | 569                         | 582                        | 0.84 <sup>c</sup> | 2.93                    |
| <b>29d</b> | 568                         | 582                        | 0.85 <sup>c</sup> | 3.92                    |
| <b>29e</b> | 568                         | 582                        | 0.84 <sup>c</sup> | 4.07                    |
| <b>30a</b> | 564                         | 578                        | 1.01 <sup>c</sup> | -                       |
| <b>30b</b> | 568                         | 586                        | 0.59 <sup>c</sup> | 2.08                    |
| <b>30c</b> | 568                         | 586                        | 0.69 <sup>c</sup> | 2.93                    |
| <b>30d</b> | 570                         | 586                        | 0.81 <sup>c</sup> | 3.91                    |
| <b>30e</b> | 570                         | 587                        | 0.82 <sup>c</sup> | 4.05                    |
| <b>31a</b> | 562                         | 574                        | 1.10 <sup>c</sup> | -                       |
| <b>31b</b> | 566                         | 580                        | 0.67 <sup>c</sup> | 2.08                    |
| <b>31c</b> | 567                         | 581                        | 0.78 <sup>c</sup> | 2.96                    |
| <b>31d</b> | 567                         | 581                        | 0.87 <sup>c</sup> | 3.94                    |
| <b>31e</b> | 567                         | 581                        | 0.87 <sup>c</sup> | 4.10                    |
| <b>32</b>  | 640                         | 655                        | . <sup>d</sup>    | 4.10                    |
| <b>33</b>  | 643 <sup>a</sup>            | 660 <sup>a</sup>           | . <sup>d</sup>    | 5.81 <sup>a</sup>       |

<sup>a</sup> Measured in citric acid/phosphate buffer. <sup>b</sup> Relative quantum yield ( $\pm 0.1$ ) with fluorescein ( $\Phi_f = 0.925 \pm 0.015$  in 0.1 M NaOH)<sup>35</sup> as standard. <sup>c</sup> Relative quantum yield ( $\pm 0.1$ ) with rhodamine 101 ( $\Phi_f = 1.00 \pm 0.02$  in ethanol)<sup>36</sup> as standard. <sup>d</sup> No standard available. <sup>e</sup> Apparent dissociation constant determined from curves of fluorescence vs p[TFA] (in MeOH) or pH ( $pK_a = -\log K_d$ ).

\*Some controversy about the actual quantum yield of rhodamine 101 exists in the literature.<sup>40,41</sup> Since quantum yields reported here are relative values, this would explain the values greater than

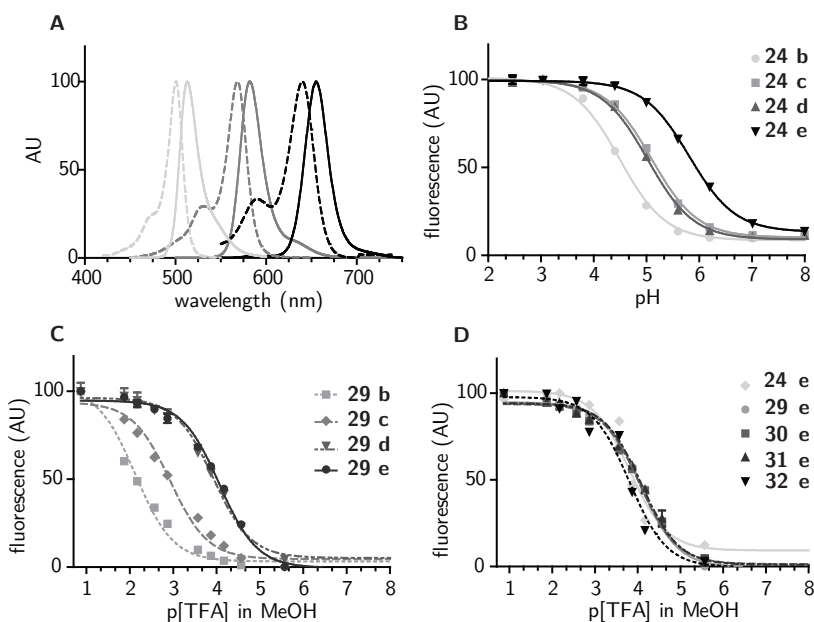


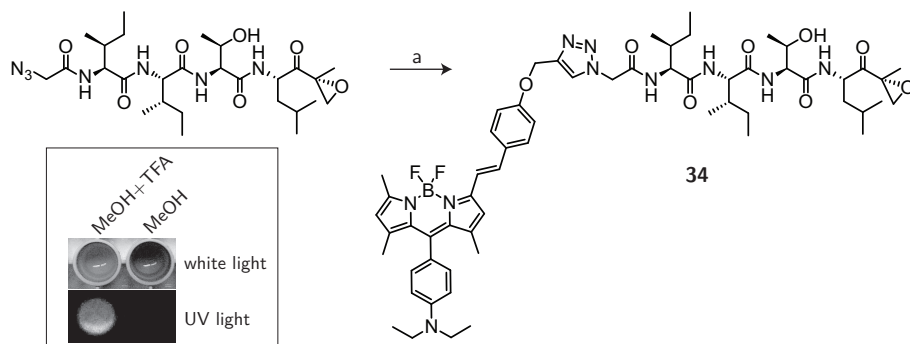
**Figure 3.1:** A) Absorbance (dashed line) and emission (solid line) spectra of compounds **24a-e** (left), **29-31a-e** (middle) and **32, 33** (right) in TFA/methanol. B) Fluorescence intensity vs pH curves for compounds **24b-e**. C, D) Fluorescence intensity vs p[TFA] curves for compounds **29b-e** and for non-functionalized (**24e**), monofunctional (**29-31e**) and bifunctional (**32**) diethylaniline derivatives.

To assess whether modifications of the BODIPY core by one or two Knoevenagel reactions would lead to any change in pH-dependency, the fluorescence intensities at different pH-values were measured for all pH-activatable fluorophores (Figure 3.1B-D). Since the water-solubility of dyes **29-31** was low, their fluorescence was determined as a function of the concentration of trifluoroacetic acid (TFA) in methanol. The apparent  $pK_a$  (in aq. buffer) or  $pK_d$  (in methanol/TFA)<sup>4</sup> of the dyes decreases in the order diethyl > piperidino > ethylmethyl > dimethyl (Figure 3.1B,C, Table 3.1), which corresponds to the electron-donating properties of the substituted amines and the trend found for previously reported pH-dependent dyes (2).<sup>11,12,16</sup> No change in pH-dependency was observed for the various mono- and bifunctional dyes compared to their non-functionalized counterparts (Figure 3.1D, Table 3.1). It is therefore likely that attachment of these dyes via their ligation handle to (bio)active molecules will result in constructs with the same advantageous fluorescence characteristics as the original dyes.

Finally, to examine the stability of the dyes when used in a ligation reaction, dye **29e** was used in a traditional copper(I) catalyzed Huisgen 1,3-cycloaddition<sup>27,28</sup> with the azide-modified proteasome inhibitor epoxomicin.<sup>42</sup> This resulted in the pH-dependent BODIPY-epoxomicin **34** in good yield (Scheme 3.2).

unity (although within the estimated error of measurement) for dyes **29-31a**.

**Scheme 3.2:** Synthesis of pH-dependent BODIPY-epoxomicin. Inset: pH-dependent fluorescence of compound **34**.



Reagents and conditions: [a] **29e**, sodium ascorbate,  $\text{CuSO}_4$ ,  $\text{H}_2\text{O}/\text{toluene}/t\text{-BuOH}$ ,  $80^\circ\text{C}$ , 89%

### 3.3 Conclusion

This chapter describes a series of tunable pH-dependent BODIPY dyes that contain a (bio-)conjugation handle for incorporation in larger constructs. The Knoevenagel-type condensation reaction that was used provides a fast and easy means to a large variety of red-shifted BODIPY dyes. Because of the red-shift in the fluorescence properties of these dyes, they should be more suited for live-cell fluorescence microscopy than their greener counterparts discussed in Chapter 2, as non-invasive tools to selectively image cellular compartments of interest, based on their acidity. Because of the generality of the approach, the methodology can be extended towards the development of many other (analyte-sensitive) BODIPY dyes containing the functionality or property of interest, an example hereof will be discussed in Chapter 8.

### 3.4 Experimental Section

**Absorption and Fluorescence Spectroscopy.** All spectroscopic experiments were performed in 135 mM TFA in methanol (spectroscopic grade) or a citric acid/phosphate buffer pH 1.8, at a concentration of  $1\ \mu\text{M}$  (absorption) or  $100\ \text{nM}$  (fluorescence). For fluorescence experiments the excitation wavelength was set equal to the maximum of the corresponding absorption spectrum and the emission spectrum recorded. Measurements were conducted on a Shimadzu UV1700 pharماسpec UV-VIS spectrophotometer (absorbance) and a Shimadzu RF-5301PC spectrofluorometer (fluorescence). For the determination of relative quantum yields the slit width was set to 3 nm for both excitation and emission. For the determination of relative quantum yields the slit width was set to 3 nm for both excitation and emission. Quantum yields were calculated using equation 3.1\*:

\*Quantum yields were determined according to the method described in: <http://www.jobinyvon.com/usadivisions/Fluorescence/applications/quantumyieldstrad.pdf>



$$\Phi_x = \Phi_{st} \frac{Grad_x \eta_x^2}{Grad_{st} \eta_{st}^2} \quad (3.1)$$

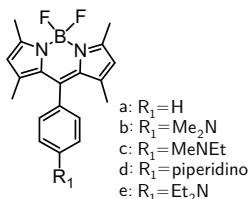
where  $x$  denotes the unknown and  $st$  the standard.  $\Phi$  is the quantum yield,  $Grad$  is the gradient from the plot of integrated fluorescence vs absorbance (absorbances between 0.01 and 0.1) and  $\eta$  is the refractive index of the solvent used (1.3288 for methanol, 1.36 for ethanol and 1.333 for water). Quantum yields were determined with rhodamine 101 ( $\Phi_f = 1.00 \pm 0.02$  in ethanol)<sup>36</sup> and fluorescein ( $\Phi_f = 0.925 \pm 0.015$  in 0.1 M NaOH)<sup>35</sup> as standards. The error in the measurements is estimated to be  $\pm 0.1$ .

**Determination of pH-dependency.** Fluorescence intensity was measured on a FLUOstar Optima platereader (BMG Labtech) using the following filter settings:

Dyes **24b-e**:  $\lambda_{ex}$  480-12;  $\lambda_{em}$  505-10; Dyes **29-31b-e**:  $\lambda_{ex}$  520-10;  $\lambda_{em}$  570-10; Dyes **32, 33**:  $\lambda_{ex}$  620-10;  $\lambda_{em}$  660-10. All compounds were prepared as a stock solution in DMSO (100  $\mu$ M). Intensity was measured of 1  $\mu$ M solutions of compounds **24a-e**, **29a-e**, **30a-e**, **31a-e** and **32** in freshly prepared solutions of trifluoroacetic acid in methanol in a 96-wells plate. Alternatively, for compounds **24a-e** and **33** measurements were conducted in a citric acid/phosphate buffer of different pH, containing 0.2% SDS. All experiments were conducted at least in triplicate. Data was analyzed using GraphPad Prism 5.0 and curves were corrected for background fluorescence of the solvent.

## Synthesis

**General.** All reagents were of commercial grade and used as received unless stated otherwise. Reaction solvents were of analytical grade and when used under anhydrous conditions stored over flame-dried 3 Å molecular sieves. Dichloromethane was distilled over CaH<sub>2</sub> prior to use. Solvents used for column chromatography were of technical grade and distilled before use. All moisture and oxygen sensitive reactions were performed under an argon atmosphere. Flash chromatography was performed on silica gel (Screening Devices BV, 0.04-0.063 mm, 60 Å). Reactions were routinely monitored by TLC analysis on DC-alufolien (Merck, Kieselgel60, F254) with detection by UV-absorption (254/366 nm) where applicable and spraying with a solution of (NH<sub>4</sub>)<sub>6</sub>Mo<sub>7</sub>O<sub>24</sub> · 4 H<sub>2</sub>O (25 g/l) and (NH<sub>4</sub>)<sub>4</sub>Ce(SO<sub>4</sub>)<sub>4</sub> · 2 H<sub>2</sub>O (10 g/l) in 10% sulfuric acid in water followed by charring at ~150 °C. <sup>1</sup>H and <sup>13</sup>C NMR spectra were recorded on a Bruker AV-400 (400 MHz) or Bruker DMX-600 (600 MHz). Chemical shifts are given in ppm ( $\delta$ ) relative to the residual solvent peak or TMS (0 ppm) as internal standard. Coupling constants are given in Hz. Peak assignments are based on 2D <sup>1</sup>H-COSY and <sup>13</sup>C-HSQC NMR experiments. IR measurements (thin film) were conducted on an IRaffinity-1 apparatus and evaluated using IRSolutions software (Shimadzu, Kyoto, Japan). LC-MS measurements were conducted on a Thermo Finnigan LCQ Advantage MAX ion-trap mass spectrometer (ESI+) coupled to a Surveyor HPLC system (Thermo Finnigan) equipped with a standard C18 (Gemini, 4.6 mmD × 50 mmL, 5  $\mu$  particle size, Phenomenex) analytical column and buffers A: H<sub>2</sub>O, B: ACN, C: 0.1% aq.TFA. High resolution mass spectra were recorded on a LTQ Orbitrap (Thermo Finnigan) mass spectrometer equipped with an electrospray ion source in positive mode (source voltage 3.5 kV, sheath gas flow 10 mL min<sup>-1</sup>, capillary temperature 250 °C) with resolution R=60000 at m/z 400 (mass range m/z=150-2000) and dioctylphthalate (m/z = 391.28428) as a "lock mass". The high resolution mass spectrometer was calibrated prior to measurements with a calibration mixture (Thermo Finnigan). For reversed-phase HPLC purification of the final compounds an automated HPLC system equipped with a C18 semiprep column (Gemini C18, 250x10 mm, 5  $\mu$  particle size, Phenomenex) was used. Microwave syntheses were conducted in a Personal Chemistry Emrys Optimizer automated microwave synthesizer.



### General procedure for the synthesis of non-functionalized BODIPYs (24a-e).

To a solution of 2,4-dimethylpyrrole (0.5 mL, 0.46 g, 4.4 mmol, 2 eq) in dry DCM (100 mL) the appropriate benzaldehyde (2.2 mmol, 1 eq) was added followed by a catalytic amount of trifluoroacetic acid (TFA). After overnight stirring of the resulting reddish solution, 2,3-dichloro-5,6-dicyanobenzoquinone (DDQ, 1.2 eq) was added and the mixture stirred for 1 h. If TLC analysis (4:1 PE:EtOAc + 1% triethylamine) revealed incomplete oxidation, another 0.5 eq of DDQ was added. All reactions were complete after 2 h, upon which *N,N*-diisopropylethylamine (DIPEA, 3 mL) and  $\text{BF}_3 \cdot \text{OEt}_2$  (3.5 mL) were added. After 1 h the mixture was concentrated *in vacuo*, redissolved in EtOAc and washed with water. The water layer was extracted with EtOAc and the combined organic layers were dried ( $\text{MgSO}_4$ ), filtered and concentrated under reduced pressure. Silica column chromatography (toluene) yielded **24a-e** as orange powders.  $R_f = 0.5$  (4:1 PE:EtOAc)

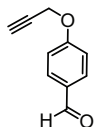
**1, 3, 5, 7-Tetramethyl-8-phenyl-4,4-difluoro-4-bora-3a,4a-diaza-s-indacene (24a).** Yield: 287 mg, 0.89 mmol, 40%.  $^1\text{H NMR}$  (400 MHz,  $\text{CDCl}_3$ ):  $\delta$  7.67 - 7.36 (m, 3H, 3  $\times$   $\text{CH}_{\text{ar}}$ ), 7.38 - 7.10 (m, 2H, 2  $\times$   $\text{CH}_{\text{ar}}$ ), 5.98 (s, 2H, 2  $\times$  CH), 2.56 (s, 6H, 2  $\times$   $\text{CH}_3$ ), 1.37 (s, 6H, 2  $\times$   $\text{CH}_3$ ).  $^{13}\text{C NMR}$  (101 MHz,  $\text{CDCl}_3$ ):  $\delta$  155.55, 143.29, 141.85, 135.11, 131.56, 129.26, 129.06, 128.05, 121.33, 14.73, 14.48. FT-IR (thin film)  $\nu$  2922, 1533, 1504, 1301, 1177, 1150, 1051, 966, 718  $\text{cm}^{-1}$ . ESI-HRMS ( $m/z$ ): calcd. for  $[\text{C}_{19}\text{H}_{19}\text{BF}_2\text{N}_2 + \text{H}]^+$  325.16821; obsd. 325.16822.

**1, 3, 5, 7-Tetramethyl-8-[4-(*N,N*-dimethylamino)phenyl]-4,4-difluoro-4-bora-3a,4a-diaza-s-indacene (24b).** Yield: 350 mg, 0.95 mmol, 32%; based on 3 mmol benzaldehyde.  $^1\text{H NMR}$  (400 MHz,  $\text{CDCl}_3$ ):  $\delta$  7.15 - 7.00 (m, 2H, 2  $\times$   $\text{CH}_{\text{ar}}$ ), 6.77 (d,  $J = 8.7$  Hz, 2H, 2  $\times$   $\text{CH}_{\text{ar}}$ ), 5.97 (s, 2H, 2  $\times$  CH), 3.02 (s, 6H, 2  $\times$   $\text{NCH}_3$ ), 2.55 (s, 6H, 2  $\times$   $\text{CH}_3$ ), 1.49 (s, 6H, 2  $\times$   $\text{CH}_3$ ).  $^{13}\text{C NMR}$  (101 MHz,  $\text{CDCl}_3$ ):  $\delta$  154.86, 150.83, 143.37, 132.34, 128.88, 122.33, 120.96, 112.47, 40.46, 14.82, 14.69. FT-IR (thin film)  $\nu$  2916, 2854, 1610, 1504, 1302, 1182, 1153, 1074, 1047, 974, 806  $\text{cm}^{-1}$ . ESI-HRMS ( $m/z$ ): calcd. for  $[\text{C}_{21}\text{H}_{24}\text{BF}_2\text{N}_3 + \text{H}]^+$  368.21041; obsd. 368.21077.

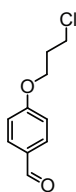
**1, 3, 5, 7-Tetramethyl-8-[4-(*N,N*-ethylmethylamino)phenyl]-4,4-difluoro-4-bora-3a,4a-diaza-s-indacene (24c).** Yield: 420 mg, 1.1 mmol, 50%.  $^1\text{H NMR}$  (400 MHz,  $\text{CDCl}_3$ ):  $\delta$  7.03 (d,  $J = 8.6$  Hz, 2H, 2  $\times$   $\text{CH}_{\text{ar}}$ ), 6.76 (d,  $J = 8.6$  Hz, 2H, 2  $\times$   $\text{CH}_{\text{ar}}$ ), 5.97 (s, 2H, 2  $\times$  CH), 3.45 (q,  $J = 7.1$  Hz, 2H,  $\text{NCH}_2$ ), 2.96 (s, 3H,  $\text{NCH}_3$ ), 2.55 (s, 6H, 2  $\times$   $\text{CH}_3$ ), 1.50 (s, 6H, 2  $\times$   $\text{CH}_3$ ), 1.15 (t,  $J = 7.1$  Hz, 3H,  $\text{CH}_3$ ).  $^{13}\text{C NMR}$  (101 MHz,  $\text{CDCl}_3$ ):  $\delta$  154.75, 149.45, 143.36, 132.31, 128.93, 121.86, 120.93, 112.43, 46.90, 37.51, 14.82, 14.69, 11.17. FT-IR (thin film)  $\nu$  2918, 2850, 1732, 1543, 1263, 1195, 1083, 734, 704  $\text{cm}^{-1}$ . ESI-HRMS ( $m/z$ ): calcd. for  $[\text{C}_{22}\text{H}_{26}\text{BF}_2\text{N}_3 + \text{H}]^+$  382.22606; obsd. 382.22656.

**1, 3, 5, 7-Tetramethyl-8-[4-(piperidino)phenyl]-4,4-difluoro-4-bora-3a,4a-diaza-s-indacene (24d).** Yield: 382 mg, 0.94 mmol, 43%.  $^1\text{H NMR}$  (400 MHz,  $\text{CDCl}_3$ ):  $\delta$  7.07 (d,  $J = 8.7$  Hz, 2H, 2  $\times$   $\text{CH}_{\text{ar}}$ ), 7.00 (d,  $J = 8.8$  Hz, 2H, 2  $\times$   $\text{CH}_{\text{ar}}$ ), 5.96 (s, 2H, 2  $\times$  CH), 3.28 - 3.15 (m, 4H, 2  $\times$   $\text{NCH}_2$ ), 2.54 (s, 6H, 2  $\times$   $\text{CH}_3$ ), 1.80 - 1.69 (m, 4H, 2  $\times$   $\text{CH}_2$ ), 1.66 - 1.55 (m, 2H,  $\text{CH}_2$ ), 1.46 (s, 6H, 2  $\times$   $\text{CH}_3$ ).  $^{13}\text{C NMR}$  (101 MHz,  $\text{CDCl}_3$ ):  $\delta$  154.98, 152.56, 143.35, 142.88, 132.12, 128.76, 124.87, 121.02, 116.32, 50.19, 25.75, 24.36, 14.75, 14.67. FT-IR (thin film)  $\nu$  2916, 2850, 1730, 1543, 1263, 1157, 1060, 732, 704  $\text{cm}^{-1}$ . ESI-HRMS ( $m/z$ ): calcd. for  $[\text{C}_{24}\text{H}_{28}\text{BF}_2\text{N}_3 + \text{H}]^+$  408.24171; obsd. 408.24179.

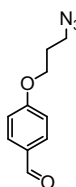
**1, 3, 5, 7-Tetramethyl-8-[4-(*N,N*-diethylamino)phenyl]-4,4-difluoro-4-bora-3a,4a-diaza-*s*-indacene (24e).** Yield: 332 mg, 0.84 mmol, 38%.  $^1\text{H NMR}$  (400 MHz,  $\text{CDCl}_3$ ):  $\delta$  7.01 (d,  $J = 8.7$  Hz, 2H,  $2 \times \text{CH}_{\text{ar}}$ ), 6.73 (d,  $J = 8.7$  Hz, 2H,  $2 \times \text{CH}_{\text{ar}}$ ), 5.96 (s, 2H,  $2 \times \text{CH}$ ), 3.40 (q,  $J = 7.0$  Hz, 4H,  $2 \times \text{NCH}_2$ ), 2.54 (s, 6H,  $2 \times \text{CH}_3$ ), 1.51 (s, 6H,  $2 \times \text{CH}_3$ ), 1.19 (t,  $J = 7.0$  Hz, 6H,  $2 \times \text{CH}_3$ ).  $^{13}\text{C NMR}$  (101 MHz,  $\text{CDCl}_3$ ):  $\delta$  154.68, 148.28, 143.38, 132.38, 129.02, 121.27, 120.90, 112.04, 44.47, 14.86, 14.69, 12.51. FT-IR (thin film)  $\nu$  2924, 2878, 1726, 1603, 1501, 1466, 1265, 1192, 1044, 970, 814  $\text{cm}^{-1}$ . ESI-HRMS ( $m/z$ ): calcd. for  $[\text{C}_{23}\text{H}_{28}\text{BF}_2\text{N}_3 + \text{H}]^+$  396.24171; obsd. 396.24170.



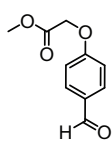
**4-(propargyloxy)-benzaldehyde (25).**<sup>30</sup> 4-hydroxybenzaldehyde (6.1 g, 50 mmol) was dissolved in acetone (250 mL). Potassium carbonate (9.7 g, 70 mmol, 1.4 eq) was added and the mixture was refluxed for 30 minutes before propargylbromide (11.1 mL, 100 mmol, 2 eq) was added. After 2 h of refluxing, the solvent was evaporated *in vacuo*. The residue was dissolved in water and extracted with EtOAc ( $4 \times 75$  mL). The combined organic layers were washed with water and brine, dried over  $\text{MgSO}_4$ , filtered and concentrated under reduced pressure. The crude mixture was purified by silica column chromatography (0  $\rightarrow$  10% EtOAc in toluene) resulting in compound **25** in 98% yield (7.8 g, 48.9 mmol).  $R_f = 0.8$  (5:1 toluene:EtOAc)  $^1\text{H NMR}$  (400 MHz,  $\text{CDCl}_3$ ):  $\delta$  9.91 (s, 1H, HCO), 7.93 - 7.80 (m, 2H,  $2 \times \text{CH}_{\text{ar}}$ ), 7.10 (d,  $J = 7.2$  Hz, 2H,  $2 \times \text{CH}_{\text{ar}}$ ), 4.79 (s, 2H,  $\text{CH}_2$ ), 2.58 (s, 1H, CH).  $^{13}\text{C NMR}$  (101 MHz,  $\text{CDCl}_3$ ):  $\delta$  190.91, 162.47, 132.02, 130.71, 115.29, 109.74, 77.66, 76.50, 56.07. FT-IR (thin film)  $\nu$  3205, 2121, 1678, 1600, 1573, 1238, 1168, 1006, 825, 651  $\text{cm}^{-1}$ . ESI-HRMS ( $m/z$ ): calcd. for  $[\text{C}_{10}\text{H}_8\text{O}_2 + \text{H}]^+$  161.05971; obsd. 161.05952.



**4-(3-chloropropoxy)benzaldehyde (26).** To a solution of 4-hydroxybenzaldehyde (6.1 g, 50 mmol) in acetone (50 mL)  $\text{K}_2\text{CO}_3$  (8.1 g, 55 mmol, 1.1 eq) was added and the solution was heated to reflux. After 30 minutes 1-bromo-3-chloropropane (5.45 mL, 55 mmol, 1.1 eq) was added and the mixture was refluxed overnight. The solvent was evaporated *in vacuo*, the residue dissolved in EtOAc, washed with water, dried ( $\text{MgSO}_4$ ), filtered and concentrated. Silica column chromatography (0  $\rightarrow$  10% EtOAc in PE) afforded pure compound **26** (9.76 g, 49 mmol) as an oil in 98% yield.  $R_f = 0.7$  (3:1 PE:EtOAc).  $^1\text{H NMR}$  (400 MHz,  $\text{CDCl}_3$ ):  $\delta$  9.89 (s, 1H, COH), 7.99 - 7.70 (m, 2H,  $2 \times \text{CH}_{\text{ar}}$ ), 7.10 - 6.87 (m, 2H,  $2 \times \text{CH}_{\text{ar}}$ ), 4.21 (t,  $J = 5.9$  Hz, 2H,  $\text{CH}_2$ ), 3.76 (t,  $J = 6.2$  Hz, 2H,  $\text{CH}_2$ ), 2.28 (p,  $J = 6.0$  Hz, 2H,  $\text{CH}_2$ ).  $^{13}\text{C NMR}$  (101 MHz,  $\text{CDCl}_3$ ):  $\delta$  190.87, 163.80, 132.10, 130.19, 114.85, 64.70, 41.32, 32.08. FT-IR (thin film)  $\nu$  1686, 1600, 1578, 1508, 1253, 1160  $\text{cm}^{-1}$ .

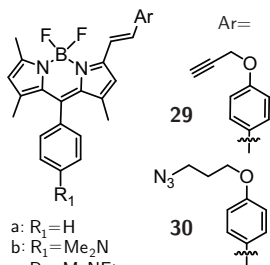


**4-(3-azidopropoxy)benzaldehyde (27).**<sup>31</sup> Compound **26** (9.65 g, 48.7 mmol) was dissolved in DMF (50 mL). Sodium azide (3.9 g, 60 mmol, 1.2 eq) was added and the mixture heated to 95  $^\circ\text{C}$  for 16 h. The solvent was evaporated under reduced pressure, the residue was taken up in DCM (50 mL), washed with water and brine, dried over  $\text{MgSO}_4$ , filtered and concentrated *in vacuo*. The crude product was purified by silica column chromatography (0  $\rightarrow$  13% EtOAc in PE) resulting in compound **27** as a yellowish oil in 88% yield (8.87 g, 43 mmol).  $R_f = 0.55$  (4:1 PE:EtOAc).  $^1\text{H NMR}$  (400 MHz,  $\text{CDCl}_3$ ):  $\delta$  9.86 (s, 1H, COH), 7.82 (d,  $J = 7.9$  Hz, 2H,  $2 \times \text{CH}_{\text{ar}}$ ), 6.99 (d,  $J = 7.8$  Hz, 2H,  $2 \times \text{CH}_{\text{ar}}$ ), 4.12 (d,  $J = 5.4$  Hz, 2H,  $\text{CH}_2$ ), 3.53 (d,  $J = 6.0$  Hz, 2H,  $\text{CH}_2$ ), 2.08 (d,  $J = 5.8$  Hz, 2H,  $\text{CH}_2$ ).  $^{13}\text{C NMR}$  (101 MHz,  $\text{CDCl}_3$ ):  $\delta$  190.62, 163.56, 131.84, 129.95, 114.63, 64.81, 47.91, 28.45. FT-IR (thin film)  $\nu$  2094 ( $\text{N}_3$ ), 1684, 1598, 1576, 1508, 1250, 1157  $\text{cm}^{-1}$ . ESI-HRMS ( $m/z$ ): calcd. for  $[\text{C}_{10}\text{H}_{11}\text{N}_3\text{O}_2 + \text{H}]^+$  206.09240; obsd. 206.09220.



**4-((1-methylacetate)oxy)-benzaldehyde (28).**<sup>32</sup> To a solution of 4-hydroxybenzaldehyde (6.1 g, 50 mmol) in acetone (125 mL) potassium carbonate (11 g, 80 mmol, 1.6 eq) was added and the mixture was stirred vigorously. Methylbromoacetate (5.7 mL, 60 mmol, 1.2 eq) was added and the mixture was stirred for 3.5 h at room temperature. The mixture was concentrated *in vacuo*, dissolved in EtOAc, washed with H<sub>2</sub>O, dried (Na<sub>2</sub>SO<sub>4</sub>), filtered and concentrated under reduced pressure yielding the product as a colorless oil that solidified over time (9.7 g, 50 mmol, quant).  $R_f = 0.4$  (6:1 toluene:EtOAc). <sup>1</sup>H NMR (400 MHz, CDCl<sub>3</sub>):  $\delta$  9.90 (s, 1H, HCO), 7.85 (d,  $J = 8.8$  Hz, 2H, 2  $\times$  CH<sub>ar</sub>), 7.01 (d,  $J = 8.8$  Hz, 2H, 2  $\times$  CH<sub>ar</sub>), 4.73 (s, 2H, CH<sub>2</sub>), 3.82 (s, 3H, CH<sub>3</sub>). <sup>13</sup>C NMR (101 MHz, CDCl<sub>3</sub>):  $\delta$  190.68, 168.50, 162.53, 131.97, 130.78, 114.87, 65.08, 52.45. FT-IR (thin film)  $\nu$  2959, 1749, 1693, 1682, 1600, 1580, 1508, 1207, 1163, 1080, 820, 613 cm<sup>-1</sup>. ESI-HRMS ( $m/z$ ): calcd. for [C<sub>10</sub>H<sub>10</sub>O<sub>4</sub> + H]<sup>+</sup> 195.06519; obsd. 195.06509.

### General procedure for the synthesis of monofunctional BODIPYs (29 and 30a-e).



a: R<sub>1</sub>=H  
b: R<sub>1</sub>=Me<sub>2</sub>N  
c: R<sub>1</sub>=MeNEt  
d: R<sub>1</sub>=piperidino  
e: R<sub>1</sub>=Et<sub>2</sub>N

BODIPY **24a-e** (~0.15 mmol) was dissolved in dry ethanol (0.7 mL). Benzaldehyde **25** or **27** (1 eq) was added, followed by acetic acid (10 eq) and pyrrolidine (10 eq). The mixture was put under an argon atmosphere before it was subjected to microwave irradiation (10 min, 130 °C, 1 min pre-stirring). After removal of the solvent under reduced pressure the mixture was purified by silica column chromatography (2 (starting material) → 4 (product) → 10% (double substituted) acetone in PE) In most cases 40-50% unreacted starting material could be recovered. Mono-substituted products compound-pHBDPalka-e and **30a-e** were crystallized from DCM/hexanes to give

purple crystals.  $R_f = 0.35$  (4:1 PE: EtOAc)

**1, 5, 7-Trimethyl-3-[4-(propargyloxy)styryl]-8-phenyl-4,4-difluoro-4-bora-3a,4a-diaza-s-indacene (29a).** Yield: 16 mg, 0.035 mmol, 23%. <sup>1</sup>H NMR (400 MHz, CDCl<sub>3</sub>):  $\delta$  7.55 (s, 3H, 2  $\times$  CH<sub>ar</sub>, CH=), 7.48 (s, 3H, 3  $\times$  CH<sub>ar</sub>), 7.30 (s, 2H, 2  $\times$  CH<sub>ar</sub>), 7.19 (d,  $J = 15.9$  Hz, 1H, CH=), 6.98 (s, 2H, 2  $\times$  CH<sub>ar</sub>), 6.58 (s, 1H, CH), 6.00 (s, 1H, CH), 4.72 (s, 2H, CH<sub>2</sub>), 2.59 (s, 3H, CH<sub>3</sub>), 2.54 (s, 1H, CH), 1.42 (s, 3H, CH<sub>3</sub>), 1.38 (s, 3H, CH<sub>3</sub>). <sup>13</sup>C NMR (101 MHz, CDCl<sub>3</sub>):  $\delta$  158.24, 154.95, 153.11, 142.52, 140.17, 135.66, 135.13, 132.80, 131.74, 130.26, 129.08, 128.92, 128.21, 121.18, 117.56, 117.46, 115.19, 78.26, 75.80, 55.86, 14.72, 14.60, 14.36. FT-IR (thin film)  $\nu$  2965, 1597, 1535, 1493, 1296, 1196, 1173, 938, 725 cm<sup>-1</sup>. ESI-HRMS ( $m/z$ ): calcd. for [C<sub>29</sub>H<sub>25</sub>BF<sub>2</sub>N<sub>2</sub>O + H]<sup>+</sup> 467.21008; obsd. 467.20989.

**1, 5, 7-Trimethyl-3-[4-(propargyloxy)styryl]-8-[4-(*N,N*-dimethylamino)phenyl]-4,4-difluoro-4-bora-3a,4a-diaza-s-indacene (29b).** Yield: 16 mg, 0.031 mmol, 21%. <sup>1</sup>H NMR (400 MHz, CDCl<sub>3</sub>):  $\delta$  7.61 - 7.51 (m, 3H, 2  $\times$  CH<sub>ar</sub>, CH=), 7.17 (d,  $J = 16.3$  Hz, 1H, CH=), 7.08 (d,  $J = 8.6$  Hz, 2H, 2  $\times$  CH<sub>ar</sub>), 6.97 (d,  $J = 8.7$  Hz, 2H, 2  $\times$  CH<sub>ar</sub>), 6.78 (d,  $J = 8.6$  Hz, 2H, 2  $\times$  CH<sub>ar</sub>), 6.58 (s, 1H, CH), 5.99 (s, 1H, CH), 4.72 (d,  $J = 2.3$  Hz, 2H, CH<sub>2</sub>), 3.02 (s, 6H, 2  $\times$  NCH<sub>3</sub>), 2.58 (s, 3H, CH<sub>3</sub>), 2.54 (s, 1H, CH), 1.53 (s, 3H, CH<sub>3</sub>), 1.50 (s, 3H, CH<sub>3</sub>). <sup>13</sup>C NMR (101 MHz, CDCl<sub>3</sub>):  $\delta$  158.23, 154.54, 152.62, 150.81, 142.89, 142.79, 141.86, 135.18, 133.70, 132.68, 130.55, 129.09, 128.96, 122.44, 121.00, 117.92, 117.22, 115.30, 112.44, 78.43, 75.90, 56.01, 40.49, 15.09, 14.86. FT-IR (thin film)  $\nu$  2887, 1614, 1523, 1462, 1232, 1198, 1157, 1045, 818 cm<sup>-1</sup>. ESI-HRMS ( $m/z$ ): calcd. for [C<sub>31</sub>H<sub>30</sub>BF<sub>2</sub>N<sub>3</sub>O + H]<sup>+</sup> 510.25228; obsd. 510.25240.

**1, 5, 7-Trimethyl-3-[4-(propargyloxy)styryl]-8-[4-(*N,N*-ethylmethylamino)phenyl]-4,4-difluoro-4-bora-3a,4a-diaza-*s*-indacene (29c).** Yield: 15 mg, 0.029 mmol, 19%.  $^1\text{H NMR}$  (400 MHz,  $\text{CDCl}_3$ ):  $\delta$  7.61 - 7.50 (m, 3H,  $2 \times \text{CH}_{\text{ar}}$ , CH=), 7.17 (d,  $J = 16.3$  Hz, 1H, CH=), 7.06 (d,  $J = 8.5$  Hz, 2H,  $2 \times \text{CH}_{\text{ar}}$ ), 6.97 (d,  $J = 8.6$  Hz, 2H,  $2 \times \text{CH}_{\text{ar}}$ ), 6.77 (d,  $J = 8.6$  Hz, 2H,  $2 \times \text{CH}_{\text{ar}}$ ), 6.58 (s, 1H, CH), 5.99 (s, 1H, CH), 4.72 (d,  $J = 2.0$  Hz, 2H,  $\text{CH}_2$ ), 3.46 (q,  $J = 6.9$  Hz, 2H,  $\text{NCH}_2$ ), 2.96 (s, 3H,  $\text{NCH}_3$ ), 2.58 (s, 3H,  $\text{CH}_3$ ), 2.54 (s, 1H, CH), 1.55 (s, 3H,  $\text{CH}_3$ ), 1.51 (s, 3H,  $\text{CH}_3$ ), 1.16 (t,  $J = 7.0$  Hz, 3H,  $\text{CH}_3$ ).  $^{13}\text{C NMR}$  (101 MHz,  $\text{CDCl}_3$ ):  $\delta$  158.21, 154.48, 152.56, 149.50, 142.88, 142.80, 141.97, 135.14, 133.70, 132.70, 130.55, 129.18, 128.94, 122.05, 120.98, 117.91, 117.21, 115.28, 112.46, 78.43, 75.90, 55.99, 46.93, 37.53, 15.07, 14.84, 11.19. FT-IR (thin film)  $\nu$  2924, 1734, 1463, 1373, 1265, 1242, 1045, 734, 704  $\text{cm}^{-1}$ . ESI-HRMS ( $m/z$ ): calcd. for  $[\text{C}_{32}\text{H}_{32}\text{BF}_2\text{N}_3\text{O} + \text{H}]^+$  524.26793; obsd. 524.26814.

**1, 5, 7-Trimethyl-3-[4-(propargyloxy)styryl]-8-[4-(piperidino)phenyl]-4,4-difluoro-4-bora-3a,4a-diaza-*s*-indacene (29d).** Yield: 11 mg, 0.02 mmol, 16%.  $^1\text{H NMR}$  (400 MHz,  $\text{CDCl}_3$ ):  $\delta$  7.64 - 7.54 (m, 3H,  $2 \times \text{CH}_{\text{ar}}$ , CH=), 7.21 (d,  $J = 16.3$  Hz, 1H, CH=), 7.13 (d,  $J = 8.6$  Hz, 2H,  $2 \times \text{CH}_{\text{ar}}$ ), 7.06 - 6.97 (m, 4H,  $4 \times \text{CH}_{\text{ar}}$ ), 6.60 (s, 1H, CH), 6.02 (s, 1H, CH), 4.75 (d,  $J = 2.3$  Hz, 2H,  $\text{CH}_2$ ), 3.31 - 3.21 (m, 4H,  $2 \times \text{NCH}_2$ ), 2.61 (s, 3H,  $\text{CH}_3$ ), 2.57 (t,  $J = 2.3$  Hz, 1H, CH), 1.82 - 1.72 (m, 4H,  $2 \times \text{CH}_2$ ), 1.69 - 1.60 (m, 2H,  $\text{CH}_2$ ), 1.55 (s, 3H,  $\text{CH}_3$ ), 1.51 (s, 3H,  $\text{CH}_3$ ).  $^{13}\text{C NMR}$  (101 MHz,  $\text{CDCl}_3$ ):  $\delta$  158.12, 154.53, 152.63, 152.45, 142.71, 141.24, 135.20, 133.31, 132.34, 130.36, 128.88, 128.84, 124.91, 120.94, 117.70, 117.17, 116.19, 115.15, 78.28, 75.79, 55.86, 50.11, 25.65, 24.26, 14.91, 14.67. FT-IR (thin film)  $\nu$  2926, 1735, 1458, 1373, 1236, 1157, 1045, 985, 736  $\text{cm}^{-1}$ . ESI-HRMS ( $m/z$ ): calcd. for  $[\text{C}_{34}\text{H}_{34}\text{BF}_2\text{N}_3\text{O} + \text{H}]^+$  550.28358; obsd. 550.28326.

**1, 5, 7-Trimethyl-3-[4-(propargyloxy)styryl]-8-[4-(*N,N*-diethylamino)phenyl]-4,4-difluoro-4-bora-3a,4a-diaza-*s*-indacene (29e).** Yield: 22 mg, 0.041 mmol, 27%.  $^1\text{H NMR}$  (400 MHz,  $\text{CDCl}_3$ ):  $\delta$  7.61 - 7.53 (m, 3H,  $2 \times \text{CH}_{\text{ar}}$ , CH=), 7.17 (d,  $J = 16.3$  Hz, 1H, CH=), 7.03 (d,  $J = 8.4$  Hz, 2H,  $2 \times \text{CH}_{\text{ar}}$ ), 6.97 (d,  $J = 8.5$  Hz, 2H,  $2 \times \text{CH}_{\text{ar}}$ ), 6.74 (d,  $J = 8.5$  Hz, 2H,  $2 \times \text{CH}_{\text{ar}}$ ), 6.58 (s, 1H, CH), 5.99 (s, 1H, CH), 4.72 (d,  $J = 1.8$  Hz, 2H,  $\text{CH}_2$ ), 3.40 (q,  $J = 7.0$  Hz, 4H,  $2 \times \text{NCH}_2$ ), 2.58 (s, 3H,  $\text{CH}_3$ ), 2.54 (s, 1H, CH), 1.56 (s, 3H,  $\text{CH}_3$ ), 1.53 (s, 3H,  $\text{CH}_3$ ), 1.20 (t,  $J = 7.0$  Hz, 6H,  $2 \times \text{CH}_3$ ).  $^{13}\text{C NMR}$  (101 MHz,  $\text{CDCl}_3$ ):  $\delta$  158.22, 154.44, 152.51, 148.34, 142.91, 142.81, 142.17, 135.07, 133.74, 132.75, 130.60, 129.28, 128.94, 121.48, 120.97, 117.97, 117.19, 115.31, 112.10, 111.87, 78.45, 75.89, 56.01, 44.50, 15.10, 14.88, 12.54. FT-IR (thin film)  $\nu$  2974, 1604, 1487, 1196, 1159, 986, 808  $\text{cm}^{-1}$ . ESI-HRMS ( $m/z$ ): calcd. for  $[\text{C}_{33}\text{H}_{34}\text{BF}_2\text{N}_3\text{O} + \text{H}]^+$  538.28358; obsd. 538.28383.

**1, 5, 7-Trimethyl-3-[4-((3-azidopropyl)oxy)styryl]-8-phenyl-4,4-difluoro-4-bora-3a,4a-diaza-*s*-indacene (30a).** Yield: 26 mg, 0.051 mmol, 35%.  $^1\text{H NMR}$  (400 MHz,  $\text{CDCl}_3$ ):  $\delta$  7.62 - 7.42 (m, 6H,  $5 \times \text{CH}_{\text{ar}}$ , CH=), 7.33 - 7.27 (m, 2H,  $2 \times \text{CH}_{\text{ar}}$ ), 7.19 (d,  $J = 16.3$  Hz, 1H, CH=), 6.89 (d,  $J = 8.5$  Hz, 2H,  $2 \times \text{CH}_{\text{ar}}$ ), 6.58 (s, 1H, CH), 5.99 (s, 1H, CH), 4.08 (t,  $J = 5.9$  Hz, 2H,  $\text{CH}_2$ ), 3.53 (t,  $J = 6.6$  Hz, 2H,  $\text{CH}_2$ ), 2.59 (s, 3H,  $\text{CH}_3$ ), 2.11 - 2.01 (m, 2H,  $\text{CH}_2$ ), 1.42 (s, 3H,  $\text{CH}_3$ ), 1.38 (s, 3H,  $\text{CH}_3$ ).  $^{13}\text{C NMR}$  (101 MHz,  $\text{CDCl}_3$ ):  $\delta$  159.63, 154.89, 153.46, 142.74, 142.51, 140.21, 136.07, 135.29, 132.97, 131.83, 129.78, 129.21, 129.18, 129.05, 128.37, 121.26, 117.61, 117.32, 114.90, 64.76, 48.36, 28.91, 14.84, 14.73, 14.47. FT-IR (thin film)  $\nu$  2927, 2097 ( $\text{N}_3$ ), 1599, 1537, 1497, 1196, 1173, 1157, 986  $\text{cm}^{-1}$ . ESI-HRMS ( $m/z$ ): calcd. for  $[\text{C}_{29}\text{H}_{28}\text{BF}_2\text{N}_5\text{O} + \text{H}]^+$  512.24277; obsd. 512.24259.

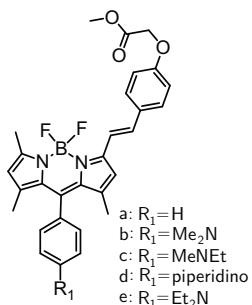
**1, 5, 7-Trimethyl-3-[4-((3-azidopropyl)oxy)styryl]-8-[4-(*N,N*-dimethylamino)phenyl]-4,4-difluoro-4-bora-3a,4a-diaza-*s*-indacene (30b).** Yield: 16 mg, 0.029 mmol, 20%.  $^1\text{H NMR}$  (400 MHz,  $\text{CDCl}_3$ ):  $\delta$  7.59 - 7.48 (m, 3H,  $2 \times \text{CH}_{\text{ar}}$ , CH=), 7.17 (d,  $J = 16.3$  Hz, 1H, CH=), 7.08 (d,  $J = 8.6$  Hz, 2H,

2 × CH<sub>ar</sub>), 6.88 (d, *J* = 8.6 Hz, 2H, 2 × CH<sub>ar</sub>), 6.78 (d, *J* = 8.6 Hz, 2H, 2 × CH<sub>ar</sub>), 6.57 (s, 1H, CH), 5.99 (s, 1H, CH), 4.08 (t, *J* = 5.9 Hz, 2H, CH<sub>2</sub>), 3.53 (t, *J* = 6.6 Hz, 2H, CH<sub>2</sub>), 3.02 (s, 6H, 2 × NCH<sub>3</sub>), 2.59 (s, 3H, CH<sub>3</sub>), 2.11 - 1.99 (m, 2H, CH<sub>2</sub>), 1.53 (s, 3H, CH<sub>3</sub>), 1.50 (s, 3H, CH<sub>3</sub>). <sup>13</sup>C NMR (101 MHz, CDCl<sub>3</sub>): δ 159.47, 154.33, 152.81, 150.80, 142.85, 142.73, 141.76, 135.45, 133.69, 132.61, 129.90, 129.09, 129.07, 122.45, 120.93, 117.51, 117.23, 114.85, 112.43, 64.73, 48.36, 40.46, 28.90, 15.08, 14.82. FT-IR (thin film) *v* 2926, 2096 (N<sub>3</sub>), 1600, 1537, 1524, 1494, 1196, 1173, 1159, 986 cm<sup>-1</sup>. ESI-HRMS (*m/z*): calcd. for [C<sub>31</sub>H<sub>33</sub>BF<sub>2</sub>N<sub>6</sub>O + H]<sup>+</sup> 555.28497; obsd. 555.28508.

**1, 5, 7-Trimethyl-3-[4-((3-azidopropyl)oxy)styryl] -8-[4-(*N,N*-ethylmethylanino)phenyl] -4,4-difluoro-4-bora-3a,4a-diaza-*s*-indacene (30c).** Yield: 19 mg, 0.033 mmol, 22%. <sup>1</sup>H NMR (400 MHz, CDCl<sub>3</sub>): δ 7.60 - 7.49 (m, 3H, 2 × CH<sub>ar</sub>, CH=), 7.17 (d, *J* = 16.3 Hz, 1H, CH=), 7.06 (d, *J* = 8.5 Hz, 2H, 2 × CH<sub>ar</sub>), 6.88 (d, *J* = 8.6 Hz, 2H, 2 × CH<sub>ar</sub>), 6.77 (d, *J* = 8.6 Hz, 2H, 2 × CH<sub>ar</sub>), 6.58 (s, 1H, CH), 5.99 (s, 1H, CH), 4.08 (t, *J* = 5.9 Hz, 2H, CH<sub>2</sub>), 3.53 (t, *J* = 6.6 Hz, 2H, CH<sub>2</sub>), 3.46 (q, *J* = 7.0 Hz, 2H, NCH<sub>2</sub>), 2.96 (s, 3H, NCH<sub>3</sub>), 2.59 (s, 3H, CH<sub>3</sub>), 2.06 (m, 2H, CH<sub>2</sub>), 1.55 (s, 3H, CH<sub>3</sub>), 1.51 (s, 3H, CH<sub>3</sub>), 1.16 (t, *J* = 7.0 Hz, 3H, CH<sub>3</sub>). <sup>13</sup>C NMR (101 MHz, CDCl<sub>3</sub>): δ 159.48, 154.30, 152.78, 149.53, 142.86, 142.75, 141.89, 135.42, 133.74, 132.66, 129.93, 129.21, 129.07, 122.10, 120.93, 117.55, 117.23, 114.87, 112.47, 64.75, 48.37, 46.94, 37.53, 28.92, 15.08, 14.83, 11.19. FT-IR (thin film) *v* 2926, 2096 (N<sub>3</sub>), 1601, 1537, 1524, 1510, 1495, 1198, 1173, 1159, 986 cm<sup>-1</sup>. ESI-HRMS (*m/z*): calcd. for [C<sub>32</sub>H<sub>35</sub>BF<sub>2</sub>N<sub>6</sub>O + H]<sup>+</sup> 569.30062; obsd. 569.30086.

**1, 5, 7-Trimethyl-3-[4-((3-azidopropyl)oxy)styryl] -8-[4-(piperidino)phenyl] -4,4-difluoro-4-bora-3a,4a-diaza-*s*-indacene (30d).** Yield: 12 mg, 0.020 mmol, 17%. <sup>1</sup>H NMR (400 MHz, CDCl<sub>3</sub>): δ 7.60 - 7.49 (m, 3H, 2 × CH<sub>ar</sub>, CH=), 7.17 (d, *J* = 16.3 Hz, 1H, CH=), 7.10 (d, *J* = 8.6 Hz, 2H, 2 × CH<sub>ar</sub>), 7.01 (d, *J* = 8.7 Hz, 2H, 2 × CH<sub>ar</sub>), 6.89 (d, *J* = 8.7 Hz, 2H, 2 × CH<sub>ar</sub>), 6.57 (s, 1H, CH), 5.99 (s, 1H, CH), 4.08 (t, *J* = 5.9 Hz, 2H, CH<sub>2</sub>), 3.53 (t, *J* = 6.6 Hz, 2H, CH<sub>2</sub>), 3.27 - 3.19 (m, 4H, 2 × NCH<sub>2</sub>), 2.58 (s, 3H, CH<sub>3</sub>), 2.11 - 2.00 (m, 2H, CH<sub>2</sub>), 1.79 - 1.70 (m, 4H, 2 × CH<sub>2</sub>), 1.64 - 1.59 (m, 2H, CH<sub>2</sub>), 1.52 (s, 3H, CH<sub>3</sub>), 1.48 (s, 3H, CH<sub>3</sub>). <sup>13</sup>C NMR (101 MHz, CDCl<sub>3</sub>): δ 159.50, 154.45, 152.95, 152.57, 142.83, 142.69, 141.27, 135.60, 133.50, 132.41, 129.86, 129.09, 129.03, 125.05, 121.00, 117.45, 117.31, 116.32, 114.86, 64.73, 50.25, 48.36, 28.91, 25.78, 24.39, 15.04, 14.83, 14.78. FT-IR (thin film) *v* 2927, 2096 (N<sub>3</sub>), 1600, 1539, 1496, 1197, 1172, 985 cm<sup>-1</sup>. ESI-HRMS (*m/z*): calcd. for [C<sub>34</sub>H<sub>37</sub>BF<sub>2</sub>N<sub>6</sub>O + H]<sup>+</sup> 595.31627; obsd. 595.31622.

**1, 5, 7-Trimethyl-3-[4-((3-azidopropyl)oxy)styryl] -8-[4-(*N,N*-diethylamino)phenyl] -4,4-difluoro-4-bora-3a,4a-diaza-*s*-indacene (30e).** Yield: 18 mg, 0.031 mmol, 21%. <sup>1</sup>H NMR (400 MHz, CDCl<sub>3</sub>): δ 7.59 - 7.50 (m, 3H, 2 × CH<sub>ar</sub>, CH=), 7.17 (d, *J* = 16.3 Hz, 1H, CH=), 7.03 (d, *J* = 8.6 Hz, 2H, 2 × CH<sub>ar</sub>), 6.88 (d, *J* = 8.6 Hz, 2H, 2 × CH<sub>ar</sub>), 6.74 (d, *J* = 8.6 Hz, 2H, 2 × CH<sub>ar</sub>), 6.58 (s, 1H, CH), 5.99 (s, 1H, CH), 4.07 (t, *J* = 5.9 Hz, 2H, CH<sub>2</sub>), 3.53 (t, *J* = 6.6 Hz, 2H, CH<sub>2</sub>), 3.40 (q, *J* = 7.0 Hz, 4H, 2 × NCH<sub>2</sub>), 2.59 (s, 3H, CH<sub>3</sub>), 2.11 - 2.02 (m, 2H, CH<sub>2</sub>), 1.56 (s, 3H, CH<sub>3</sub>), 1.53 (s, 3H, CH<sub>3</sub>), 1.20 (t, *J* = 7.0 Hz, 6H, 2 × CH<sub>3</sub>). <sup>13</sup>C NMR (101 MHz, CDCl<sub>3</sub>): δ 159.43, 154.19, 152.67, 148.29, 142.85, 142.74, 142.05, 135.34, 133.75, 132.67, 129.90, 129.25, 129.05, 121.44, 120.88, 117.52, 117.18, 114.83, 112.04, 64.71, 48.35, 44.48, 28.90, 15.12, 14.87, 12.52. FT-IR (thin film) *v* 2930, 2097 (N<sub>3</sub>), 1601, 1540, 1522, 1510, 1497, 1198, 1173, 1159, 988 cm<sup>-1</sup>. ESI-HRMS (*m/z*): calcd. for [C<sub>33</sub>H<sub>37</sub>BF<sub>2</sub>N<sub>6</sub>O + H]<sup>+</sup> 583.31627; obsd. 583.31633.



**General procedure for the synthesis of monofunctional BODIPYs (31a-e).** BODIPY **24a-e** (~0.15 mmol) was dissolved in dry methanol (0.7 mL). Benzaldehyde **28** (1 eq) was added, followed by acetic acid (10 eq) and pyrrolidine (10 eq). The mixture was put under an argon atmosphere before it was subjected to microwave irradiation (10 min, 110 °C, 1 min pre-stirring). After removal of the solvent under reduced pressure the mixture was purified by silica column chromatography (2 (starting material) → 4 (product) → 10% (double substituted) acetone in PE) In most cases 40-50% unreacted starting material could be recovered. Mono-substituted products **31a-e** were crystallized from DCM/hexanes to give purple crystals.  $R_f = 0.30$  (4:1 PE: EtOAc)

**1, 5, 7-Trimethyl-3-[4-((1-methylacetate)oxy)styryl] -8-phenyl-4,4-difluoro-4-bora-3a,4a-diaza-s-indacene (31a).** Yield: 16 mg, 0,032 mmol, 21%.  $^1H$  NMR (400 MHz,  $CDCl_3$ ):  $\delta$  7.60 - 7.52 (m, 3H, 2 x  $CH_{ar}$ , CH=), 7.51 - 7.45 (m, 3H, 3 x  $CH_{ar}$ ), 7.32 - 7.28 (m, 2H, 2 x  $CH_{ar}$ ), 7.18 (d,  $J = 16.3$  Hz, 1H, CH=), 6.91 (d,  $J = 8.8$  Hz, 2H, 2 x  $CH_{ar}$ ), 6.58 (s, 1H, CH), 6.00 (s, 1H, CH), 4.66 (s, 2H,  $CH_2$ ), 3.82 (s, 3H,  $OCH_3$ ), 2.59 (s, 3H,  $CH_3$ ), 1.42 (s, 3H,  $CH_3$ ), 1.38 (s, 3H,  $CH_3$ ).  $^{13}C$  NMR (101 MHz,  $CDCl_3$ ):  $\delta$  169.24, 158.52, 155.17, 153.12, 142.73, 142.65, 140.35, 135.60, 135.22, 132.91, 131.88, 130.62, 129.22, 129.13, 129.06, 128.32, 121.35, 117.82, 117.58, 115.02, 65.42, 52.48, 14.85, 14.72, 14.49. FT-IR (thin film)  $\nu$  2924, 1767 (C=O), 1597, 1535, 1492, 1196, 1173, 1155, 1061, 976  $cm^{-1}$ . ESI-HRMS ( $m/z$ ): calcd. for  $[C_{29}H_{27}BF_2N_2O_3 + H]^+$  501.21556; obsd. 501.21548.

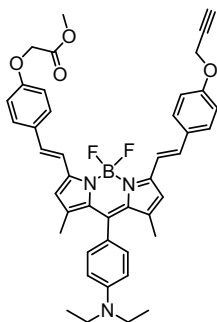
**1, 5, 7-Trimethyl-3-[4-((1-methylacetate)oxy)styryl] -8-[4-(*N,N*-dimethylamino)phenyl] -4,4-difluoro-4-bora-3a,4a-diaza-s-indacene (31b).** Yield: 12 mg, 0.022 mmol, 17%.  $^1H$  NMR (400 MHz,  $CDCl_3$ ):  $\delta$  7.60 - 7.50 (m, 3H, 2 x  $CH_{ar}$ , CH=), 7.16 (d,  $J = 16.3$  Hz, 1H, CH=), 7.08 (d,  $J = 8.6$  Hz, 2H, 2 x  $CH_{ar}$ ), 6.90 (d,  $J = 8.7$  Hz, 2H, 2 x  $CH_{ar}$ ), 6.78 (d,  $J = 8.6$  Hz, 2H, 2 x  $CH_{ar}$ ), 6.57 (s, 1H, CH), 5.99 (s, 1H, CH), 4.67 (s, 2H,  $CH_2$ ), 3.82 (s, 3H,  $OCH_3$ ), 3.02 (s, 6H, 2 x  $NCH_3$ ), 2.58 (s, 3H,  $CH_3$ ), 1.53 (s, 3H,  $CH_3$ ), 1.50 (s, 3H,  $CH_3$ ).  $^{13}C$  NMR (101 MHz,  $CDCl_3$ ):  $\delta$  169.18, 158.25, 154.50, 152.28, 150.67, 142.82, 142.60, 141.78, 134.85, 130.66, 128.94, 128.91, 122.28, 120.90, 117.93, 117.06, 114.87, 112.30, 65.32, 52.35, 40.34, 14.95, 14.73. FT-IR (thin film)  $\nu$  2916, 1767 (C=O), 1597, 1508, 1485, 1194, 1171, 1080, 986  $cm^{-1}$ . ESI-HRMS ( $m/z$ ): calcd. for  $[C_{31}H_{32}BF_2N_3O_3 + H]^+$  544.25776; obsd. 544.25758.

**1, 5, 7-Trimethyl-3-[4-((1-methylacetate)oxy)styryl] -8-[4-(*N,N*-ethylmethylamino)phenyl] -4,4-difluoro-4-bora-3a,4a-diaza-s-indacene (31c).** Yield: 9 mg, 0.017 mmol, 13%.  $^1H$  NMR (400 MHz,  $CDCl_3$ ):  $\delta$  7.60 - 7.51 (m, 3H, 2 x  $CH_{ar}$ , CH=), 7.16 (d,  $J = 16.3$  Hz, 1H, CH=), 7.06 (d,  $J = 8.5$  Hz, 2H, 2 x  $CH_{ar}$ ), 6.90 (d,  $J = 8.6$  Hz, 2H, 2 x  $CH_{ar}$ ), 6.77 (d,  $J = 8.6$  Hz, 2H, 2 x  $CH_{ar}$ ), 6.57 (s, 1H, CH), 5.99 (s, 1H, CH), 4.67 (s, 2H,  $CH_2$ ), 3.82 (s, 3H,  $OCH_3$ ), 3.46 (q,  $J = 7.0$  Hz, 2H,  $NCH_2$ ), 2.97 (s, 3H,  $NCH_3$ ), 2.58 (s, 3H,  $CH_3$ ), 1.55 (s, 3H,  $CH_3$ ), 1.52 (s, 3H,  $CH_3$ ), 1.16 (t,  $J = 7.0$  Hz, 3H,  $CH_3$ ).  $^{13}C$  NMR (101 MHz,  $CDCl_3$ ):  $\delta$  169.30, 158.38, 154.60, 152.45, 149.52, 142.99, 142.77, 142.03, 134.95, 130.80, 129.18, 129.04, 122.04, 121.03, 118.08, 117.20, 115.00, 112.46, 65.46, 52.49, 46.94, 37.54, 15.07, 14.85, 11.20. FT-IR (thin film)  $\nu$  2924, 1761 (C=O), 1521, 1508, 1197, 1174, 1080, 987  $cm^{-1}$ . ESI-HRMS ( $m/z$ ): calcd. for  $[C_{32}H_{34}BF_2N_3O_3 + H]^+$  558.27341; obsd. 558.27325.



**1, 5, 7-Trimethyl-3-[4-((1-methylacetate)oxy)styryl] -8-[4-(piperidino)phenyl] -4,4-difluoro-4-bora-3a,4a-diaza-s-indacene (31d).** Yield: 17 mg, 0.029 mmol, 23%.  $^1\text{H NMR}$  (400 MHz,  $\text{CDCl}_3$ ):  $\delta$  7.60 - 7.51 (m, 3H,  $2 \times \text{CH}_{\text{ar}}$ ,  $\text{CH}=\text{}$ ), 7.17 (d,  $J = 16.3$  Hz, 1H,  $\text{CH}=\text{}$ ), 7.10 (d,  $J = 8.6$  Hz, 2H,  $2 \times \text{CH}_{\text{ar}}$ ), 7.01 (d,  $J = 8.7$  Hz, 2H,  $2 \times \text{CH}_{\text{ar}}$ ), 6.90 (d,  $J = 8.7$  Hz, 2H,  $2 \times \text{CH}_{\text{ar}}$ ), 6.57 (s, 1H, CH), 5.99 (s, 1H, CH), 4.67 (s, 2H,  $\text{CH}_2$ ), 3.82 (s, 3H,  $\text{OCH}_3$ ), 3.27 - 3.19 (m, 4H,  $2 \times \text{NCH}_2$ ), 2.58 (s, 3H,  $\text{CH}_3$ ), 1.75 (m, 4H,  $2 \times \text{CH}_2$ ), 1.66 - 1.59 (m, 2H,  $\text{CH}_2$ ), 1.52 (s, 3H,  $\text{CH}_3$ ), 1.48 (s, 3H,  $\text{CH}_3$ ).  $^{13}\text{C NMR}$  (101 MHz,  $\text{CDCl}_3$ ):  $\delta$  169.28, 158.43, 154.79, 152.60, 142.94, 142.76, 141.45, 135.14, 132.52, 130.77, 129.07, 129.02, 125.03, 121.12, 118.03, 117.29, 116.32, 115.02, 65.47, 52.49, 50.25, 25.79, 24.41, 15.03, 14.81. FT-IR (thin film)  $\nu$  2924, 1764 ( $\text{C}=\text{O}$ ), 1595, 1489, 1298, 1157, 1080, 989  $\text{cm}^{-1}$ . ESI-HRMS ( $m/z$ ): calcd. for  $[\text{C}_{34}\text{H}_{36}\text{BF}_2\text{N}_3\text{O}_3 + \text{H}]^+$  584.28906; obsd. 584.28900.

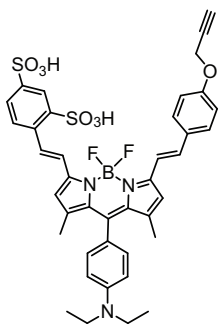
**1, 5, 7-Trimethyl-3-[4-((1-methylacetate)oxy)styryl] -8-[4-(*N,N*-diethylamino)phenyl] -4,4-difluoro-4-bora-3a,4a-diaza-s-indacene (31e).** Yield: 11 mg, 0.019 mmol, 15%.  $^1\text{H NMR}$  (400 MHz,  $\text{CDCl}_3$ ):  $\delta$  7.61 - 7.49 (m, 3H,  $2 \times \text{CH}_{\text{ar}}$ ,  $\text{CH}=\text{}$ ), 7.16 (d,  $J = 16.3$  Hz, 1H,  $\text{CH}=\text{}$ ), 7.03 (d,  $J = 8.6$  Hz, 2H,  $2 \times \text{CH}_{\text{ar}}$ ), 6.90 (d,  $J = 8.7$  Hz, 2H,  $2 \times \text{CH}_{\text{ar}}$ ), 6.74 (d,  $J = 8.7$  Hz, 2H,  $2 \times \text{CH}_{\text{ar}}$ ), 6.57 (s, 1H, CH), 5.99 (s, 1H, CH), 4.67 (s, 2H,  $\text{CH}_2$ ), 3.82 (s, 3H,  $\text{OCH}_3$ ), 3.40 (q,  $J = 7.0$  Hz, 4H,  $2 \times \text{NCH}_2$ ), 2.58 (s, 3H,  $\text{CH}_3$ ), 1.56 (s, 3H,  $\text{CH}_3$ ), 1.53 (s, 3H,  $\text{CH}_3$ ), 1.20 (t,  $J = 7.0$  Hz, 6H,  $2 \times \text{CH}_3$ ).  $^{13}\text{C NMR}$  (101 MHz,  $\text{CDCl}_3$ ):  $\delta$  169.29, 158.37, 154.52, 152.37, 148.33, 142.98, 142.22, 134.88, 130.82, 129.26, 129.03, 121.43, 121.00, 118.11, 117.17, 115.00, 112.08, 65.46, 52.48, 44.50, 15.10, 14.89, 12.53. FT-IR (thin film)  $\nu$  2924, 1765 ( $\text{C}=\text{O}$ ), 1597, 1524, 1510, 1492, 1194, 1159, 1078, 988  $\text{cm}^{-1}$ . ESI-HRMS ( $m/z$ ): calcd. for  $[\text{C}_{33}\text{H}_{36}\text{BF}_2\text{N}_3\text{O}_3 + \text{H}]^+$  572.28906; obsd. 572.28959.



**1,7-dimethyl-3-[4-(propargyloxy) styryl] -5-[4-((1-methylacetate)oxy) styryl] -8-[4-(*N,N*-diethylamino) phenyl] -4,4-difluoro-4-bora-3a,4a-diaza-s-indacene (32).** BODIPY 29e (16 mg, 0.03 mmol) and benzaldehyde 28 (29 mg, 0.15 mmol, 5 eq) were dissolved in methanol (0.5 mL) and acetic acid (17  $\mu\text{L}$ , 0.3 mmol, 10 eq) and pyrrolidine (25  $\mu\text{L}$ , 0.3 mmol, 10 eq) were added. The mixture was put under an argon atmosphere before it was subjected to microwave irradiation (10 min, 110  $^\circ\text{C}$ , 1 min pre-stirring). After removal of the solvent under reduced pressure the mixture was purified by repeated silica column chromatography (3 (starting material)  $\rightarrow$  10% (product) acetone in PE and 0  $\rightarrow$  0.25% methanol in DCM). After crystallization (DCM/hexanes) product 32 was obtained as blue crystals in 42% yield (9 mg, 0.013 mmol).  $R_f = 0.7$

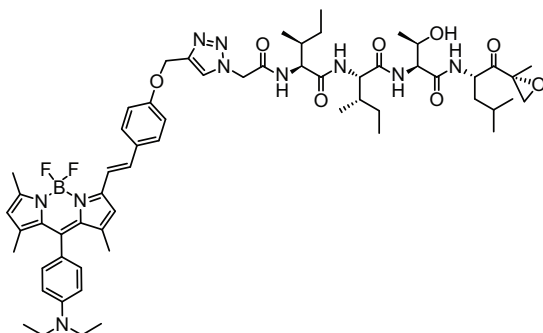
(1:1 PE:EtOAc).  $^1\text{H NMR}$  (400 MHz,  $\text{CDCl}_3$ ):  $\delta$  7.68 - 7.54 (m, 6H,  $4 \times \text{CH}_{\text{ar}}$ ,  $2 \times \text{CH}=\text{}$ ), 7.19 (d,  $J = 16.3$ , 1H,  $\text{CH}=\text{}$ ), 7.18 (d,  $J = 16.3$ , 1H,  $\text{CH}=\text{}$ ), 7.05 (d,  $J = 8.6$  Hz, 2H,  $2 \times \text{CH}_{\text{ar}}$ ), 7.01 (d,  $J = 8.7$  Hz, 2H,  $2 \times \text{CH}_{\text{ar}}$ ), 6.93 (d,  $J = 8.7$  Hz, 2H,  $2 \times \text{CH}_{\text{ar}}$ ), 6.75 (d,  $J = 8.7$  Hz, 2H,  $2 \times \text{CH}_{\text{ar}}$ ), 6.60 (s, 2H,  $2 \times \text{CH}$ ), 4.74 (d,  $J = 2.3$  Hz, 2H,  $\text{CH}_2$ ), 4.68 (s, 2H,  $\text{CH}_2$ ), 3.83 (s, 3H,  $\text{OCH}_3$ ), 3.41 (q,  $J = 7.0$  Hz, 4H,  $2 \times \text{NCH}_2$ ), 2.55 (t,  $J = 2.3$  Hz, 1H, CH), 1.58 (s, 6H,  $2 \times \text{CH}_3$ ), 1.21 (t,  $J = 7.0$  Hz, 6H,  $2 \times \text{CH}_3$ ).  $^{13}\text{C NMR}$  (101 MHz,  $\text{CDCl}_3$ ):  $\delta$  169.32, 158.37, 158.22, 152.25, 152.05, 148.31, 142.37, 142.26, 140.48, 135.06, 134.80, 134.19, 130.94, 130.68, 129.49, 129.08, 129.00, 121.55, 118.27, 118.09, 117.31, 115.32, 115.03, 112.05, 78.46, 75.92, 65.47, 56.01, 52.50, 44.51, 15.12, 12.54. FT-IR (thin film)  $\nu$  2926, 1755 ( $\text{C}=\text{O}$ ), 1595, 1510, 1450, 1196, 1157, 986  $\text{cm}^{-1}$ . ESI-HRMS ( $m/z$ ): calcd. for  $[\text{C}_{43}\text{H}_{42}\text{BF}_2\text{N}_3\text{O}_4 + \text{H}]^+$  714.33092; obsd. 714.33139.





**1,7-dimethyl-3-[4-(propargyloxy) styryl] -5-[styryl-2,4-disulfonic acid]-8-[4-(*N,N*-diethylamino)phenyl] -4,4-difluoro-4-bora-3a,4a-diaza-s-indacene (33).** BODIPY 29e (27 mg, 0.05 mmol) was dissolved in ethanol (0.7 mL). 4-Formyl-1,3-benzenedisulfonic acid, disodium salt hydrate (78 mg, 0.25 mmol, 5 eq) was added followed by acetic acid (41  $\mu$ L, 0.5 mmol, 10 eq) and pyrrolidine (27  $\mu$ L, 0.5 mmol, 10 eq). The mixture was put under an argon atmosphere before it was subjected to microwave irradiation (10 min, 130  $^{\circ}$ C, 1 min pre-stirring). After removal of the solvent under reduced pressure and co-evaporation with toluene, the mixture was purified by size exclusion chromatography (Sephadex, methanol) and crystallization from DCM/hexanes. This yielded blue compound 33 in

12% yield (5 mg, 6  $\mu$ mol).  $R_f = 0.35$  (1:1:1:1 n-BuOH:H<sub>2</sub>O:EtOAc:AcOH).  $^1\text{H NMR}$  (400 MHz, MeOD):  $\delta$  10.95 (s, 1H, SO<sub>3</sub>H), 8.58 - 8.50 (m, 2H, CH<sub>ar</sub>, SO<sub>3</sub>H), 8.40 (d,  $J = 16.2$  Hz, 1H, CH=), 8.05 - 7.97 (m, 2H, 2  $\times$  CH<sub>ar</sub>), 7.76 (d,  $J = 16.5$  Hz, 1H, CH=), 7.67 - 7.55 (m, 3H, 2  $\times$  CH<sub>ar</sub>, CH=), 7.41 (d,  $J = 16.3$  Hz, 1H, CH=), 7.14 - 7.04 (m, 4H, 4  $\times$  CH<sub>ar</sub>), 6.91 - 6.86 (m, 3H, CH<sub>ar</sub>, CH), 6.82 (s, 1H, CH), 4.81 (d,  $J = 1.9$  Hz, 2H, CH<sub>2</sub>), 3.48 (q,  $J = 7.0$  Hz, 4H, 2  $\times$  NCH<sub>2</sub>), 3.01 (t,  $J = 2.2$  Hz, 1H, CH), 1.65 (s, 3H, CH<sub>3</sub>), 1.64 (s, 3H, CH<sub>3</sub>), 1.22 (t,  $J = 7.0$  Hz, 6H, 2  $\times$  CH<sub>3</sub>).  $^{13}\text{C NMR}$  (101 MHz, MeOD):  $\delta$  160.15, 154.93, 151.99, 149.83, 144.73, 142.89, 142.49, 137.77, 137.62, 132.98, 131.50, 130.53, 129.92, 128.88, 127.40, 126.79, 126.37, 122.26, 118.93, 116.47, 113.21, 77.02, 56.72, 45.36, 15.25, 15.05, 12.68. FT-IR (thin film)  $\nu$  3600-3200 (br, OH), 2922, 1599, 1487, 1198, 1163, 1022, 991, 690  $\text{cm}^{-1}$ . ESI-HRMS ( $m/z$ ): calcd. for [C<sub>40</sub>H<sub>38</sub>BF<sub>2</sub>N<sub>3</sub>O<sub>7</sub>S<sub>2</sub> + H]<sup>+</sup> 786.22851; obsd. 786.22818.



#### pH-dependent BODIPY-epoxomicin

**(34).** BODIPY 29e (7 mg, 0.013 mmol) and azido-epoxomicin<sup>43</sup> (8 mg, 0.014 mmol, 1.1 eq) were dissolved in toluene/*t*-BuOH/H<sub>2</sub>O (1:1:1 v/v) and the solution was degassed (sonication) under argon. Sodium ascorbate (aq solution, 0.013 mmol, 1 eq) and copper sulfate (aq solution, 0.0013 mmol, 10 mol%) were added and the mixture was heated to 80  $^{\circ}$ C for 1 hour. TLC analysis showed complete conversion

of the BODIPY dye, so the mixture was concentrated and purified by silica column chromatography (0  $\rightarrow$  2.5% methanol in DCM). Additional Sephadex size exclusion (methanol) and recrystallization (DCM/hexanes) purification steps resulted in purple compound 34 in 89% yield (13 mg, 0.011 mmol).  $R_f = 0.2$  (10:1 DCM:methanol).  $^1\text{H NMR}$  (400 MHz, CDCl<sub>3</sub>/MeOD):  $\delta$  7.95 (s, 1H, CH<sub>trz</sub>), 7.60 - 7.50 (m, 3H, 2  $\times$  CH<sub>ar</sub>, CH=), 7.21 (d,  $J = 16.4$  Hz, 1H, CH=), 7.05 (d,  $J = 8.2$  Hz, 2H, 2  $\times$  CH<sub>ar</sub>), 7.00 (d,  $J = 8.3$  Hz, 2H, 2  $\times$  CH<sub>ar</sub>), 6.78 (d,  $J = 8.2$  Hz, 2H, 2  $\times$  CH<sub>ar</sub>), 6.62 (s, 1H, CH), 6.02 (s, 1H, CH), 5.23 (s, 2H, OCH<sub>2</sub>), 5.15 (q,  $J = 12.6$  Hz, 2H, CH<sub>2</sub>), 4.54 (d,  $J = 10.6$  Hz, 1H, CH), 4.26 - 4.18 (m, 2H, 2  $\times$  CH), 4.14 - 4.04 (m, 1H, CH), 3.90 (s, 1H, CH), 3.49 - 3.40 (m, 4H, 2  $\times$  NCH<sub>2</sub>), 3.31 (d,  $J = 4.6$  Hz, 1H, CH<sub>2</sub>-H<sup>a</sup>), 2.92 (d,  $J = 4.6$  Hz, 1H, CH<sub>2</sub>-H<sup>b</sup>), 2.57 (s, 3H, CH<sub>3</sub>), 1.84 (s, 2H, 2  $\times$  CH), 1.68 (s, 1H, CH), 1.64 - 1.44 (m, 11H, 3  $\times$  CH<sub>3</sub>, 2  $\times$  CH<sub>2</sub>-H<sup>a</sup>), 1.39 - 1.26 (m, 2H, CH<sub>2</sub>-H<sup>b</sup>, OH), 1.21 (t,  $J = 6.7$  Hz, 6H, 2  $\times$  CH<sub>3</sub>), 1.14 (d,  $J = 6.1$  Hz, 4H, CH<sub>3</sub>, CH<sub>2</sub>-H<sup>b</sup>), 0.99 - 0.79 (m, 18H, 6  $\times$  CH<sub>3</sub>).  $^{13}\text{C NMR}$  (101 MHz, CDCl<sub>3</sub>/MeOD):  $\delta$  208.46, 171.81, 171.77, 170.32, 165.69, 158.68, 153.99, 152.27, 148.18, 143.73, 142.80, 142.01, 135.06, 133.44, 132.41,

130.02, 128.93, 128.70, 124.93, 121.05, 120.72, 117.21, 116.97, 114.88, 111.96, 66.84, 61.45, 59.04, 58.09, 57.60, 52.23, 51.92, 50.63, 44.21, 39.15, 36.68, 36.38, 24.97, 24.68, 24.63, 22.98, 20.75, 18.23, 16.45, 15.01, 14.95, 14.66, 14.43, 14.25, 12.03, 10.64, 10.59. ESI-HRMS ( $m/z$ ): calcd. for  $[C_{60}H_{81}BF_2N_{10}O_8 + H]^+$  1119.63727; obsd. 1119.63914.

## References

- [1] Hoogendoorn, S.; Blom, A. E. M.; Willems, L. I.; van der Marel, G. A.; Overkleeft, H. S. *Org. Lett.* **2011**, *13*, 5656–5659.
- [2] Loudet, A.; Burgess, K. *Chem. Rev.* **2007**, *107*, 4891–932.
- [3] Ulrich, G.; Ziesel, R.; Harriman, A. *Angew. Chem. Int. Ed. Engl.* **2008**, *47*, 1184–201.
- [4] Boens, N.; Leen, V.; Dehaen, W. *Chem. Soc. Rev.* **2012**, *41*, 1130–1172.
- [5] He, H.; Ng, D. K. P. *Org. Biomol. Chem.* **2011**, *9*, 2610–2613, 1477–0520.
- [6] Galangau, O.; Dumas-Verdes, C.; Meallet-Renault, R.; Clavier, G. *Org. Biomol. Chem.* **2010**, *8*, 4546–4553.
- [7] Rurack, K.; Kollmannsberger, M.; Daub, J. *New J. Chem.* **2001**, *25*, 289–292, 1144–0546.
- [8] Murtagh, J.; Frimannsson, D. O.; O’Shea, D. F. *Org. Lett.* **2009**, *11*, 5386–5389.
- [9] Zheng, Q.; Xu, G.; Prasad, P. *Chem Eur J* **2008**, *14*, 5812–5819.
- [10] Ying, L.-Q.; Branchaud, B. P. *Bioorg. Med. Chem. Lett.* **2011**, *21*, 3546–3549.
- [11] Urano, Y.; Asanuma, D.; Hama, Y.; Koyama, Y.; Barrett, T.; Kamiya, M.; Nagano, T.; Watanabe, T.; Hasegawa, A.; Choyke, P. L.; Kobayashi, H. *Nat. Med.* **2009**, *15*, 104–9.
- [12] Hoogendoorn, S.; Habets, K. L.; Passemard, S.; Kuiper, J.; van der Marel, G. A.; Florea, B. I.; Overkleeft, H. S. *Chem. Commun.* **2011**, *47*, 9363–9365.
- [13] Kollmannsberger, M.; Rurack, K.; Resch-Genger, U.; Daub, J. *J. Phys. Chem. A* **1998**, *102*, 10211–10220.
- [14] de Silva, A. P.; Gunaratne, H. Q. N.; Gunnlaugsson, T.; Huxley, A. J. M.; McCoy, C. P.; Rademacher, J. T.; Rice, T. E. *Chem. Rev.* **1997**, *97*, 1515–1566.
- [15] Sunahara, H.; Urano, Y.; Kojima, H.; Nagano, T. *J. Am. Chem. Soc.* **2007**, *129*, 5597–5604.
- [16] Qin, W.; Baruah, M.; Van der Auweraer, M.; De Schrijver, F. C.; Boens, N. *J. Phys. Chem. A* **2005**, *109*, 7371–7384.
- [17] Yu, Y.-H.; Descalzo, A. B.; Shen, Z.; Rohr, H.; Liu, Q.; Wang, Y.-W.; Spieles, M.; Li, Y.-Z.; Rurack, K.; You, X.-Z. *Chem. Asian. J.* **2006**, *1*, 176–187.
- [18] Dost, Z.; Atilgan, S.; Akkaya, E. U. *Tetrahedron* **2006**, *62*, 8484 – 8488.
- [19] Bura, T.; Retailleau, P.; Ulrich, G.; Ziesel, R. *J. Org. Chem.* **2011**, *76*, 1109–1117.
- [20] Zhu, S.; Zhang, J.; Vegesna, G.; Luo, F.-T.; Green, S. A.; Liu, H. *Org. Lett.* **2011**, *13*, 438–441.
- [21] Buyukcikir, O.; Bozdemir, O. A.; Kolemen, S.; Erbas, S.; Akkaya, E. U. *Org. Lett.* **2009**, *11*, 4644–4647.
- [22] Schuller, A.; Goh, G.; Kim, H.; Lee, J.-S.; Chang, Y.-T. *Mol. Inf.* **2010**, *29*, 717–729.
- [23] Lee, J.-S.; Kang, N.-Y.; Kim, Y. K.; Samanta, A.; Feng, S.; Kim, H. K.; Vendrell, M.; Park, J. H.; Chang, Y.-T. *J. Am. Chem. Soc.* **2009**, *131*, 10077–10082.
- [24] Lee, J.-S.; Kim, H. K.; Feng, S.; Vendrell, M.; Chang, Y.-T. *Chem. Commun.* **2011**, *47*, 2339–2341.
- [25] Vendrell, M.; Krishna, G. G.; Ghosh, K. K.; Zhai, D.; Lee, J.-S.; Zhu, Q.; Yau, Y. H.; Shochat, S. G.; Kim, H.; Chung, J.; Chang, Y.-T. *Chem. Commun.* **2011**, *47*, 8424–8426.
- [26] Saxon, E.; Bertozzi, C. R. *Science* **2000**, *287*, 2007–2010.
- [27] Rostovtsev, V. V.; Green, L. G.; Fokin, V. V.; Sharpless, K. B. *Angew. Chem. Int. Ed. Engl.* **2002**, *41*, 2596–2599.
- [28] Tornøe, C. W.; Christensen, C.; Meldal, M. *J. Org. Chem.* **2002**, *67*, 3057–3064.
- [29] Gabe, Y.; Urano, Y.; Kikuchi, K.; Kojima, H.; Nagano, T. *J. Am. Chem. Soc.* **2004**, *126*, 3357–67.
- [30] Giguere, J.-B.; Thibeault, D.; Cronier, F.; Marois, J.-S.; Auger, M.; Morin, J.-F. *Tetrahedron Lett.* **2009**, *50*, 5497–5500.
- [31] Yilmaz, M. D.; Bozdemir, O. A.; Akkaya, E. U. *Org. Lett.* **2006**, *8*, 2871–2873.
- [32] Bowman, M. D.; Jeske, R. C.; Blackwell, H. E. *Org. Lett.* **2004**, *6*, 2019–2022.
- [33] Bernhard, C.; Goze, C.; Rousselin, Y.; Denat, F. *Chem. Commun.* **2010**, *46*, 8267–8269.

- [34] Baruah, M.; Qin, W.; Flors, C.; Hofkens, J.; Vallee, R. A. L.; Beljonne, D.; van der Auweraer, M.; De Borggraeve, W.; Boens, N. *J. Phys. Chem. A* **2006**, *110*, 5998–6009.
- [35] Magde, D.; Wong, R.; Seybold, P. G. *Photochem. Photobiol.* **2002**, *75*, 327–334.
- [36] Karstens, T.; Kobs, K. *J. Phys. Chem.* **1980**, *84*, 1871–1872.
- [37] Thivierge, C.; Bandichhor, R.; Burgess, K. *Org. Lett.* **2007**, *9*, 2135–2138.
- [38] Li, L.; Han, J.; Nguyen, B.; Burgess, K. *J. Org. Chem.* **2008**, *73*, 1963–1970.
- [39] Wories, H. J.; Koek, J. H.; Lodder, G.; Lugtenburg, J.; Fokkens, R.; Driessen, O.; Mohn, G. R. *Recl. Trav. Chim. Pays-Bas* **1985**, *104*, 288–291.
- [40] Pereira, E. J. N.; Berberan-Santos, M. N.; Fedorov, A.; Vincent, M.; Gallay, J.; Martinho, J. M. G. *J. Chem. Phys.* **1999**, *110*, 1600–1610.
- [41] Prazeres, T. J. V.; Fedorov, A.; Barbosa, S. P.; Martinho, J. M. G.; Berberan-Santos, M. N. *J. Phys. Chem. A* **2008**, *112*, 5034–5039.
- [42] Verdoes, M.; Florea, B. I.; van der Linden, W. A.; Renou, D.; van den Nieuwendijk, A. M. C. H.; van der Marel, G. A.; Overkleeft, H. S. *Org. Biomol. Chem.* **2007**, *5*, 1416–1426.
- [43] Verdoes, M.; Hillaert, U.; Florea, B. I.; Sae-Heng, M.; Risseeuw, M. D.; Filippov, D. V.; van der Marel, G. A.; Overkleeft, H. S. *Bioorg. Med. Chem. Lett.* **2007**, *17*, 6169 – 6171.



# 4

## Targeted delivery of Heat shock protein 70 by sortase-mediated ligation with a synthetic mannose receptor-binding ligand<sup>1</sup>

**H**eat shock protein 70 (Hsp70) is a chaperone protein that is expressed in response to cellular stress. This chapter presents a sortase-mediated ligation strategy to target exogenous recombinant Hsp70 to dendritic cells, via the mannose receptor (MR). For this, a sortagging nucleophile was synthesized, containing a BODIPY dye (BDP) for fluorescent visualization and a MR-targeting mannose cluster (MC). Using SrtA<sub>staph</sub>, recombinant Hsp70-LPETGG was transformed into Hsp70-BDP-MC. Successful uptake of this construct by dendritic cells was demonstrated to be dependent on the mannose receptor, showing the ability of the mannose cluster to ensure delivery of a large protein into the lysosomal pathway. Possible applications of targeted Hsp70 lie in the therapeutic intervention of lysosomal storage disorders, where exogenous Hsp70 could lead to decreased breakdown or enhanced activity of lysosomal enzymes.

## 4.1 Introduction

The family of heat shock proteins (Hsp) functions as molecular chaperones that assist in the quality control and folding of newly synthesized proteins.<sup>2</sup> Some of the family members are constitutively expressed such as Hsc70 (heat shock cognate protein), whereas others such as the 70 kDa protein Hsp70 (also known as Hsp72 or HSPA1A) are expressed in response to cellular stress.<sup>3</sup> The protein isoforms are highly conserved across species. For example, *E. coli* derived Hsp70, called DnaK, shares an approximate 50% sequence homology with the human protein.<sup>4,5</sup> The structure of Hsp70 contains two major domains, an N-terminal nucleotide binding domain (NBD) of ~45 kDa that binds ATP and a C-terminal substrate binding domain (SBD) of ~25 kDa that binds short peptides as well as the nascent chain of newly formed proteins. Both domains are connected by a short linker sequence.<sup>5</sup> The ability of Hsp70 to bind and release polypeptide chains is closely linked to its ATPase activity, and several co-chaperones have been identified that are essential for enhancing the ATPase activity and thus proper functioning of Hsp70.<sup>2,5,6</sup> While Hsp70 isoforms can be found in all cellular compartments, the majority of expressed Hsp70/Hsc70 is located in the cytosol.<sup>5</sup> However, especially in tumor cells, Hsp70 is also found in lysosomes, where it enhances lysosome stability by preventing lysosomal membrane permeabilization and subsequent release of cysteine cathepsins into the cytosol.<sup>7,8</sup>

Lysosomes are acidic vesicles containing a plethora of lytic enzymes such as proteases, glycosidases, nucleases, and lipases, and function as the metabolic center of the cell. Lysosomal storage disorders (LSD) are a group of rare but severe diseases in which one of the key enzymes in lipid metabolism is dysfunctioning, leading to accumulation of cellular constituents in the lysosomes (ie (glyco)lipids in case of lipidoses).<sup>9</sup> As shown schematically in Figure 4.1A, parts of the plasma membrane, containing glycosphingolipids (GSL), are engulfed by a variety of processes and transported through the endolysosomal pathway. Along the pathway, both the pH and the amount of cholesterol in the membrane decrease, whereas the amount of bis(monoacylglycero)phosphate (BMP, Figure 4.1A,B) increases.<sup>10</sup> Lysosomes are confined by a limiting membrane, which is secured from proteolytical degradation by the presence of a glycocalix. Inside the lysosomes, the remains of the endocytosed plasma membrane (consisting mainly of BMP and GSL) form intralysosomal vesicles and the membranes of these vesicles are the main site of GSL catabolism. Enzymes that are responsible for the breakdown of GSLs are usually water-soluble and present in the lysosomal lumen.<sup>10,11</sup> BMP, along with sphingolipid activator proteins (Saposins), forms a bridge between the internal membrane containing the substrate and the hydrolytic enzymes in the lumen, enabling the catalytic breakdown of GSLs.<sup>12-14</sup>

A recent study by Kirkegaard *et al.* has shown that Hsp70 is able to stabilize lysosomes by binding with its amino-terminal NBD domain to the negatively charged BMP, especially at acidic pH (corresponding to the lysosomal environment, Figure 4.1A). They have shown that this has important implications for at least one of the lysosomal storage disorders, Niemann-Pick disease (NPD).<sup>16</sup> Treatment of NPD fibroblasts with exogenous

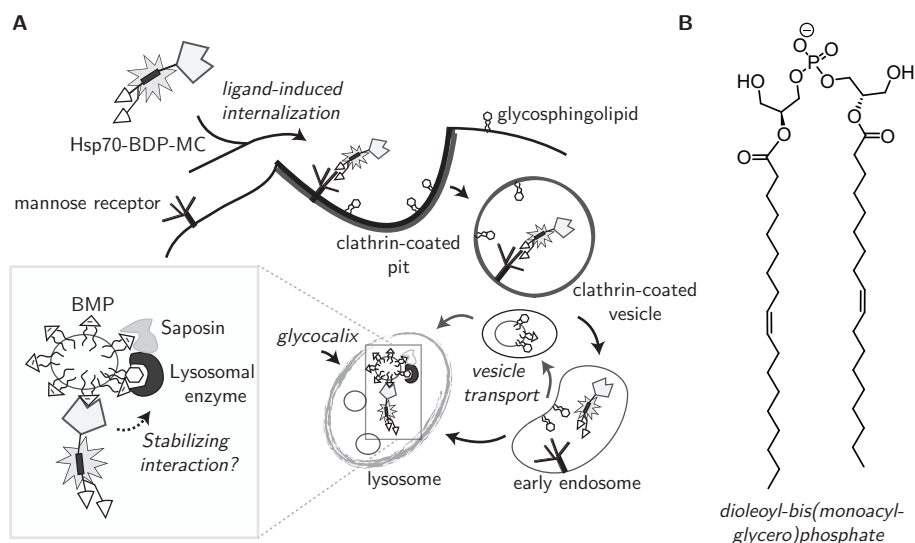


**Figure 4.1: Proposed mechanism of Hsp70 targeting.** A) Schematic representation of MR-dependent uptake and trafficking of Hsp70-BDP-MC. Also shown is the formation of intralysosomal vesicles, consisting mainly of glycosphingolipids and BMP. Zoom in shows the working model by Petersen *et al.* for the Hsp70-mediated stabilization of lysosomes by binding to BMP.<sup>15,16</sup> B) Example structure of BMP, containing oleic acid residues.

recombinant Hsp70 resulted in the stimulation of acid sphingomyelinase, stabilization of the lysosomes and reversal of the associated NPD pathology.<sup>15,16</sup> It is not known whether the lysosomal stabilization of Hsp70 has a beneficial effect on other LSDs as well. It is not unlikely that this effect exists, either by a general mechanism (stabilization of the lysosomes as a whole) or via direct binding interaction between Hsp70 and a lysosomal enzyme, thereby stabilizing it to prevent proteolytical degradation. To study this, efficient uptake of recombinant Hsp70 into the endolysosomal pathway is a requirement. Targeting of cell surface receptors that are constitutively or ligand-induced internalized, provides a point of entry into this pathway. In a previous study by Hillaert *et al.* and a follow-up study, described in Chapter 2, a synthetic mannose cluster has been used as a targeting ligand for mannose receptors on dendritic cells and macrophages, enabling the delivery of cargo attached to the cluster into the lysosomes.<sup>17,18</sup> In Gaucher disease, an LSD where  $\beta$ -glucocerebrosidase is deficient, macrophage-like cells form the main population of affected cells (Gaucher cells) and current enzyme replacement therapies use glycan remodeling to expose mannoses on the enzyme for delivery to the mannose receptor.<sup>19,20</sup>

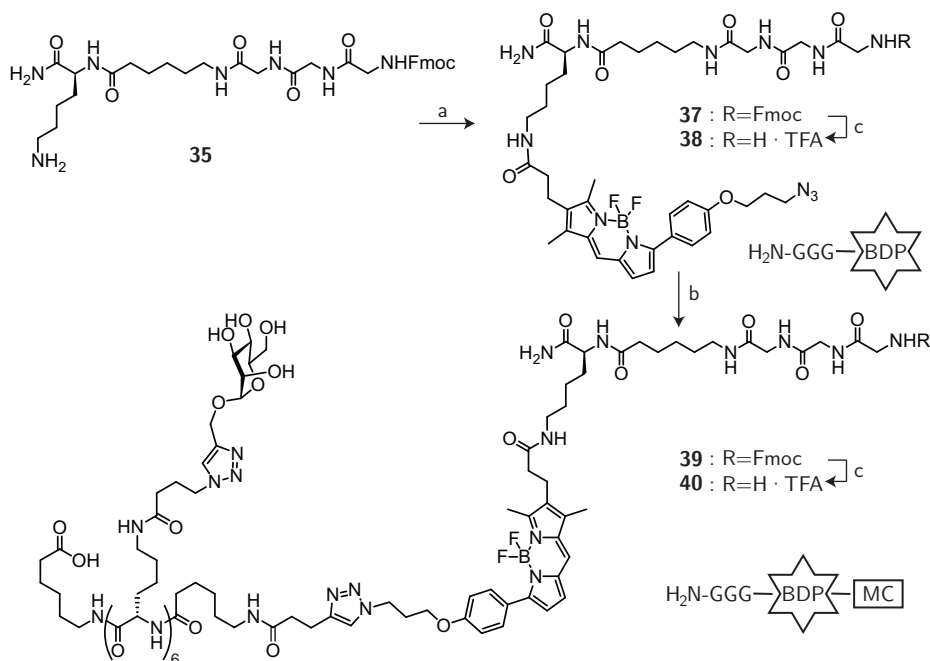
The research described in this chapter is aimed at the delivery of Hsp70 to the lysosomes via the mannose receptor, by ligation to the synthetic mannose cluster. For this the enzymatic ligation method termed 'sortagging' is used, which employs the bacterial enzyme Sortase A (SrtA).<sup>21,22</sup> This approach combines organic synthesis, to create the sortagging nucleophile, with molecular biology to obtain recombinant Hsp70 that contains the SrtA recognition sequence. Optimization of the sortase reaction is described, followed by

an investigation of the ability of the synthetic ligand to function as a targeting device for a macromolecule such as Hsp70 in dendritic cells.

## 4.2 Results and Discussion

**Synthesis.** The bacterial enzyme Sortase A (SrtA) catalyzes the transpeptidation between a glycine nucleophile and a polypeptide substrate containing a C-terminal recognition sequence, as shown schematically in Figure 4.2A.<sup>23</sup> The triglycine sortagging nucleophile **35** was synthesized by standard solid-phase peptide (SPPS) procedures and cleaved from the resin using acidic conditions. Under these conditions, the Boc-protected lysine was deprotected, whereas the Fmoc group on the N-terminal glycine was still in place. This allowed for selective modification of the  $\epsilon$ -amino group of lysine with azido-BODIPY-OSu **36**<sup>24</sup> (Scheme 4.1), resulting in Fmoc-protected **37** in 91% yield. This intermediate was deprotected using DBU in DMF, followed by quenching with HOBT and immediate purification by RP-HPLC. The HPLC fractions were lyophilized resulting in the TFA salt of sortase ligand "GGG-BDP" **38** in 16% yield. Other purification procedures, yielding the free amine, resulted in significant degradation of the BODIPY dye, whereas the TFA salt proved to be stable.

**Scheme 4.1:** Synthesis of the sortagging nucleophiles GGG-BDP (**38**) and GGG-BDP-MC (**40**).



Reagents and conditions: [a]  $N_3$ -BODIPY-OSu **36**,<sup>24</sup> DiPEA, DMF, 91%; [b] mannose cluster **20**,  $CuSO_4$ , sodium ascorbate, DMF/ $H_2O$ ; [c] i) DBU, DMF; ii) RP-HPLC purification, **38**: 16%; **40**: 24% over 2 steps.



Alternatively, compound **37** was used in a Cu(I)-catalyzed Huisgen cycloaddition<sup>25,26</sup> with mannose cluster **20**.<sup>17</sup> After Fmoc removal with DBU and RP-HPLC purification, the envisaged sortagging ligand "GGG-BDP-MC" **40** was obtained in 24% (two steps).

**Sortase-mediated ligation.** Sortase A from *Staphylococcus aureus* lacking the membrane anchoring domain (SrtA<sub>staph</sub>Δ59, referred to here as "WT") has been shown to catalyze the transpeptidation reaction between a triglycine nucleophile and protein *in vitro*.<sup>27</sup> In case of C-terminal sortagging, the protein of interest needs to contain the sortase recognition sequence (LPXTGG, where X can be any amino acid)<sup>28</sup> near its C-terminus. Recombinant Hsp70 was designed with an LPETGG sortase sequence, followed by a His<sub>6</sub> tag for purification purposes at its C-terminus. As depicted in Figure 4.2A, reaction of "Hsp70-LPETGG" with either one of the sortagging nucleophiles **38** or **40** (Scheme 4.1) would result in the

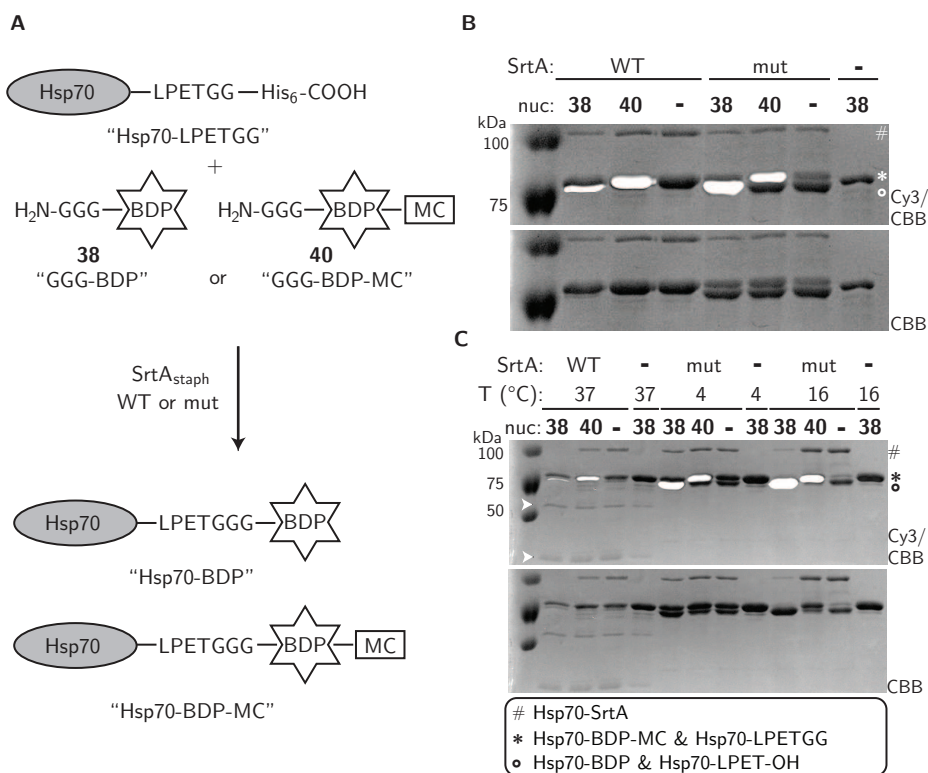


**Figure 4.2: Optimization of the sortase-mediated ligation of Hsp70 and a triglycine nucleophile.** A) Schematic representation of sortase-mediated ligation of Hsp70-LPETGG with GGG-BDP or GGG-BDP-MC using either wild-type SrtA<sub>staph</sub>-Δ59 (WT) or P94S/D160N/K196T triple mutant SrtA<sub>staph</sub> (mut). B) 7.5% SDS-PAGE of the reaction between Hsp70-LPETGG (1 μg, 1 eq), SrtA WT or mut (5 eq) and GGG-BDP **38** or GGG-BDP-MC **40** (25 eq), 16 h, 37 °C. C) 7.5% SDS-PAGE of Hsp70-LPETGG (1 μg, 1 eq), SrtA WT or mut (5 eq) and GGG-BDP **38** or GGG-BDP-MC **40** (25 eq) samples that were reacted for 65 h at different temperatures. White bands correspond to the BODIPY fluorescence signal (Cy3), black bands to Coomassie brilliant blue staining (CBB). Arrowheads: unidentified degradation products.

formation of fluorescently labeled Hsp70, with (Hsp70-BDP-MC) or without (Hsp70-BDP) a targeting entity. A recent report by Chen *et al.* has identified a sortase triple mutant (P94S/ D160N/ K196T, here referred to as "mut") with enhanced affinity for the LPETGG sequence and higher catalytic activity allowing for much more efficient transpeptidation.<sup>29</sup>

Hsp70-LPETGG, SrtA-WT and SrtA-mut were expressed in *E. coli* and purified using nickel-affinity chromatography on an automated AKTA system. Fractions containing the protein of interest were pooled and buffer exchanged to 50 mM Tris, 150 mM NaCl, pH 8.0. All proteins were sufficiently pure after chromatography to be used directly in the transpeptidation reaction. The ability of the novel triglycine compounds **38** and **40** to function as a nucleophile in the sortagging reaction with Hsp70-LPETGG was first tested on a small scale. Briefly, Hsp70-LPETGG (1  $\mu$ g, 1 eq) was reacted with GGG-BDP or GGG-BDP-MC (25 eq) in the presence of SrtA-WT or SrtA-mut for 16 h, 37 °C in SrtA reaction buffer (10  $\mu$ L 50 mM Tris, 150 mM NaCl, 10 mM CaCl<sub>2</sub>, pH 7.5). The proteins were resolved on 7.5% SDS-PAGE and the gel slabs scanned for fluorescence of the BODIPY, before total protein staining with coomassie brilliant blue. As shown in Figure 4.2B, more product was formed in case of the mutant enzyme (lane 5), compared to wild-type (lane 2), when using GGG-BDP **38**. For the larger nucleophile GGG-BDP-MC **40** it was more difficult to assess the progress of the reaction, because of similar molecular weights of the starting protein Hsp70-LPETGG (lane 8) and the product Hsp70-BDP-MC (lanes 3, 6). When the nucleophile was excluded from the reaction mixture (lanes 4 and 7), no reaction was observed in case of the WT enzyme (lane 4) whereas almost all starting Hsp70-LPETGG was converted to a lower molecular weight protein by the mutant enzyme (lane 7). The lower molecular weight protein most likely corresponds to the hydrolyzed Hsp70-LPET-OH, which is formed by nucleophilic attack of H<sub>2</sub>O on the SrtA-Hsp70 intermediate. It was also formed when nucleophile was included in the reaction, as judged by the presence of a lower running band in lane 6. In case of nucleophile **38** the product and by-product have similar molecular weights, so these could not be distinguished.

Figure 4.3 shows the proposed mechanism for sortase-mediated ligation.<sup>30</sup> Most of the steps in this mechanism are equilibria and thus reversible. The only irreversible step is the hydrolysis reaction, leading to the unwanted Hsp70-LPET-OH as the end-point of the reaction. For wild-type SrtA<sub>staph</sub>, the formation of the acyl-enzyme intermediate is the rate-limiting step, and water is recognized very poorly as the nucleophile.<sup>30,31</sup> The greater rate of hydrolysis for the mutant enzyme is likely explained by its enhanced affinity for the LPXTGG sequence, thereby accelerating the formation of the acyl-enzyme intermediate. Both loss of selectivity for the nucleophile and slower rates for the transpeptidation reaction might contribute to the increased formation of the hydrolysed product.<sup>29</sup> In order to increase the amount of product formation for SrtA-WT and decrease the amount of hydrolysis in favor of product formation for SrtA-mut, reactions were performed at different temperatures for longer periods of time (Figure 4.2C). Prolonged (65 h) reaction times at 37 °C with the wildtype enzyme led to degradation of Hsp70, as seen by multiple bands of lower molecular weight on SDS-PAGE. A similar degradation pattern can be observed in lane 4

(Figure 4.2C), where no enzyme was present, indicating that it reflects inherent instability of Hsp70. Remarkably, SrtA-mut was still able to catalyze the transpeptidation reaction at 4 °C, albeit slower than at 16 °C. At 16 °C, complete reaction of Hsp70-LPETGG with GGG-BDP was observed, but both the mixture containing GGG-BDP-MC 40 or no nucleophile again showed a lower running band, corresponding to hydrolysis. Since all residues C-terminally of the threonine of the sortase sequence are removed in the transpeptidation or hydrolysis reaction, only the starting Hsp70-LPETGG contained a His<sub>6</sub>-tag. To be able to purify the envisaged product Hsp70-BDP-MC, removal of unreacted starting protein with nickel-affinity chromatography seemed more promising than removal of untagged Hsp70-LPET-OH by for instance size exclusion chromatography. Therefore, wildtype sortase was chosen as the most convenient enzyme for large scale transpeptidation reactions, even though it was anticipated that the reaction would not go to completion.

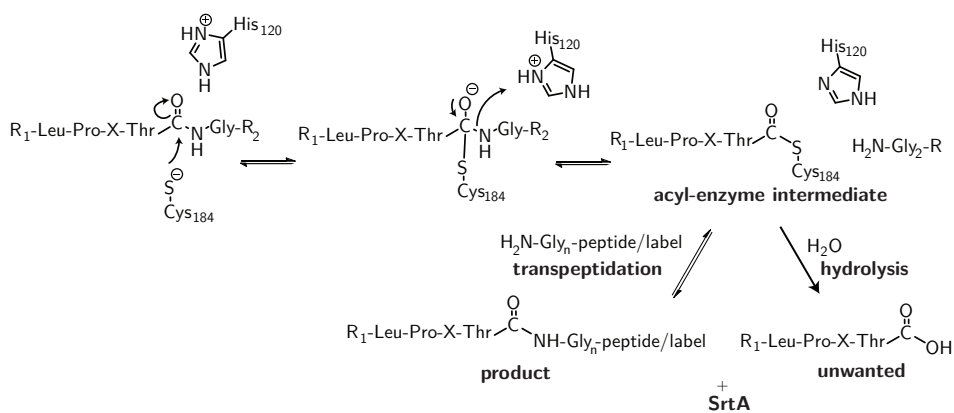
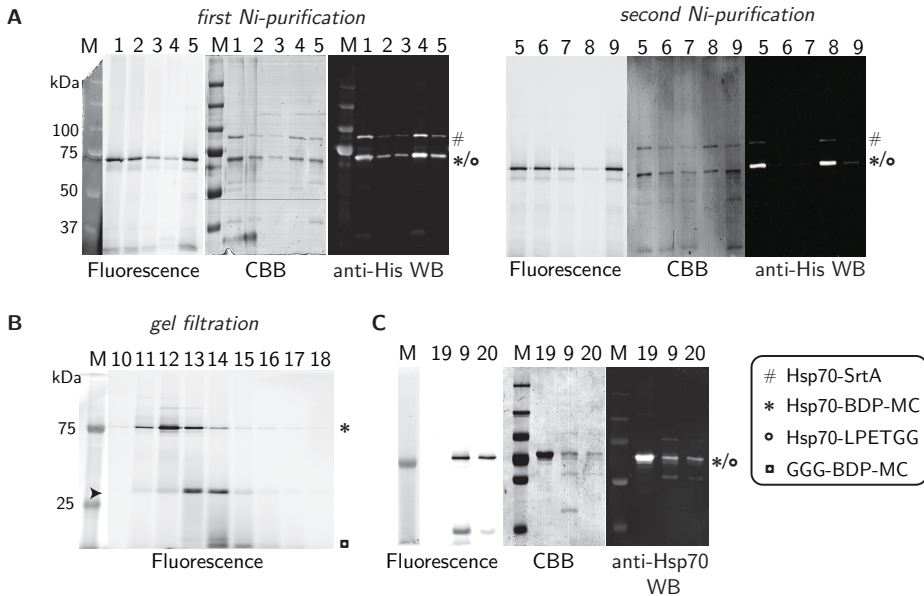


**Figure 4.3:** Proposed mechanism for the SrtA-mediated ligation of a target protein containing the C-terminal LPXTGG recognition sequence and a glycine nucleophile.<sup>30</sup>

Preparative scale sortagging was performed on Hsp70-LPETGG (0.5 mg) with GGG-BDP-MC 40 (25 eq) in the presence of SrtA<sub>staph</sub>-WT (5 eq) for 20 h at 37 °C in sortase reaction buffer. A small amount (0.05%) of Tween-80 was included in the reaction buffer and in buffers of all subsequent steps to prevent aspecific interactions of the amphiphilic sortagging nucleophile with tubes, proteins or beads. After the reaction, all His-tagged proteins (unreacted Hsp70-LPETGG, SrtA and SrtA-Hsp70 intermediate) were removed by nickel-affinity chromatography. From each step of the purification, a small sample was analyzed by SDS-PAGE, followed by fluorescence scanning, Coomassie brilliant blue staining or anti-His western blotting. As shown in Figure 4.4A (left), one Ni-column was not sufficient to remove all His-tagged proteins and therefore the flow-through of the first column was subjected to a second nickel purification step (Figure 4.4A, right), which resulted in a mixture free of any His-tagged proteins as judged by an anti-His western blot (WB). All fluorescent signal, corresponding to the product Hsp70-BDP-MC was found in the flow-through and washing steps, indicating that indeed the His-tag was lost during the reaction and that aspecific interaction of the protein with the beads was negligible under the conditions

used. Removal of excess nucleophile **40** was attempted using 30 kDa MWCO filters, but this did not succeed, probably due to formation of HMW aggregates or a lack of globularity of the molecule. Therefore, the mixture was subjected to gel filtration to remove the excess of nucleophile. Fractions were analyzed for the presence of fluorescent protein using in-gel fluorescence scanning. As shown in Figure 4.4B, the first fractions contained a ~75 kDa protein, corresponding to the MW of Hsp70-BDP-MC, and later fractions contained an unknown degradation product of about 30 kDa and finally the excess of nucleophile. Fractions containing pure Hsp70-BDP-MC were pooled, concentrated and again analyzed on SDS-PAGE. As can be seen in Figure 4.4C, final sample "20" contained one major band, as seen by fluorescence and coomassie staining, which was positively immunostained by an anti-Hsp70 antibody. In conclusion, Hsp70-BDP-MC was successfully obtained by sortase-mediated ligation between Hsp70-LPETGG and GGG-BDP-MC **40**, in 27% overall yield of sortagging and purification procedures.



Samples: 1) Sortase reaction mixture; 2, 6) Flow-through Ni-NTA; 3, 7) Wash Ni-NTA; 4, 8) Elution Ni-NTA; 5, 9) Concentrated FT Ni-NTA; 10-18) Elution fractions Vision; 19) Hsp70-LPETGG; 20) Hsp70-BDP-MC purified and concentrated

**Figure 4.4: Large scale sortase-mediated ligation of Hsp70-LPETGG with GGG-BDP-MC and purification of Hsp70-BDP-MC.** A) Hsp70-LPETGG (0.5 mg) was treated with SrtA<sub>staph</sub> WT (5 eq) and GGG-BDP-MC **40** (25 eq) for 20 h at 37 °C. Unreacted Hsp70-LPETGG, Hsp70-SrtA intermediate and SrtA were removed with two subsequent Ni-NTA agarose columns. Shown are 10% SDS-PAGE gels of samples taken from the Ni-purification steps, followed by in-gel fluorescence scanning, Coomassie brilliant blue staining or anti-His Western blotting. B) The semi-pure Hsp70-BDP-MC obtained was subjected to gel filtration using a Vision chromatography system to remove excess nucleophile. Shown is a 12% SDS-PAGE in-gel fluorescence scan of fractions eluted from the Vision. Arrowhead: unidentified degradation products. C) 10% SDS-PAGE of Hsp70-LPETGG and Hsp70-BDP-MC before and after Vision gel filtration, followed by in-gel fluorescence scanning, Coomassie brilliant blue staining or anti-Hsp70 immunoblotting.

Next, it was investigated whether the synthetic mannose cluster could function as a targeting agent for Hsp70. For this, immature mouse dendritic cells (DCs) were incubated with 10  $\mu\text{g}/\text{mL}$  purified Hsp70-BDP-MC for 2 h, 37 °C. Cells were extensively washed, fixed with 4 % formaldehyde, nuclei were stained with Draq5<sup>32</sup> and imaged using a confocal fluorescence microscope. Bright intracellular vesicles were observed, as shown in Figure 4.5A. Moreover, entry of Hsp70-BDP-MC could be completely blocked by pre-incubation with the yeast polymannoside mannan (3 mg/mL), indicating that the internalization was mediated by mannose-binding lectins such as the mannose receptor (MR). An alternative control experiment would be to make use of Hsp70-BDP, with the fluorophore suited for microscopy, but without the mannose cluster for targeting, to study the efficiency of MR-dependent uptake. Purification of Hsp70-BDP from remaining nucleophile GGG-BDP proved to be cumbersome, and not enough material of good purity could be obtained

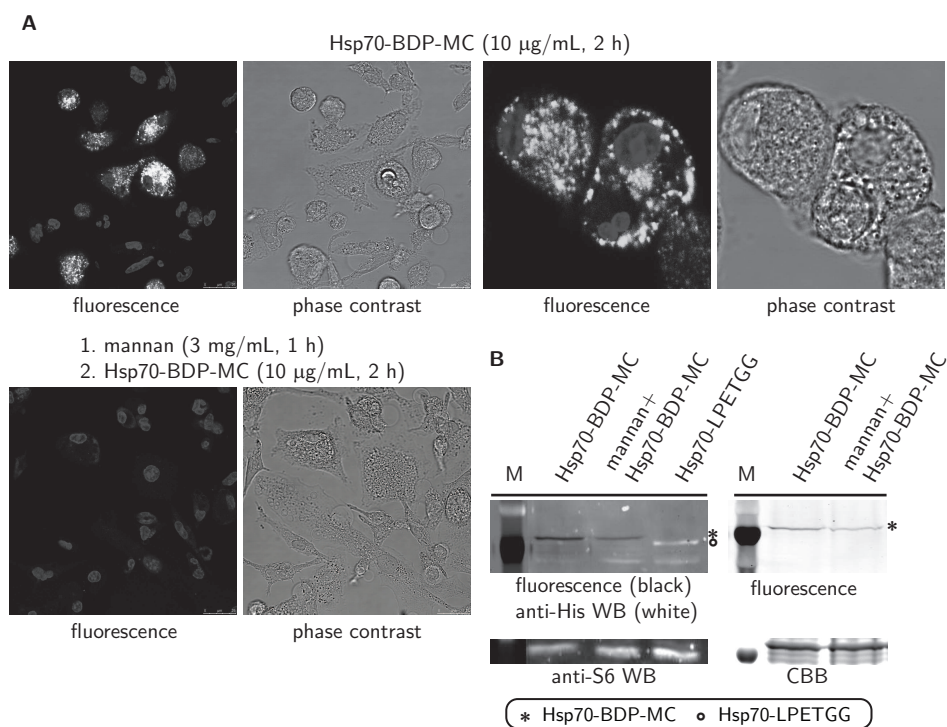


**Figure 4.5: MR-dependent uptake of Hsp70-BDP-MC in immature dendritic cells.** A) Representative micrographs of immature mouse dendritic cells that were treated for 2 h with purified Hsp70-BDP-MC (10  $\mu\text{g}/\text{mL}$ ) or pre-incubated for 1 h with mannan (3 mg/mL) followed by 2 h treatment with Hsp70-BDP-MC. Cells were washed with PBS, fixed (4 % formaldehyde in PBS), nuclei were stained with Draq5 (dark grey) and cells imaged for BODIPY fluorescence (white). B) Cells were treated as in A), or with unsorted Hsp70-LPETGG (10  $\mu\text{g}/\text{mL}$ ) instead of Hsp70-BDP-MC. After incubation, cells were washed with PBS and PBS containing ovalbumin (1 mg/mL) to reduce aspecific binding. Cells were lysed and analyzed by 7.5 % SDS-PAGE, followed by fluorescence scanning/anti-His WB and CBB staining of total protein or anti-S6 (ribosomal protein) WB as loading control. M: molecular weight protein marker, thick black band corresponds to 70 kDa.

to conduct this experiment. In a next experiment, cells were treated using the same conditions, and unsorted Hsp70-LPETGG was included as a control. Instead of imaging, cells were washed with PBS containing ovalbumin (1 mg/mL, to reduce aspecific binding) and lysed. The lysates were analyzed by 7.5% SDS-PAGE. Gels were scanned for fluorescence, and either stained with Coomassie brilliant blue or immunoblotted against His<sub>6</sub> to show Hsp70-LPETGG (Figure 4.5B). In-gel fluorescence showed the presence of a ~75 kDa band corresponding to Hsp70-BDP-MC both in samples with and without pre-incubation with mannan. Quantification of the fluorescent signal, normalized against total protein, showed that ~2.5-fold more Hsp70-BDP-MC was present in lysates of DCs that were untreated compared to those that were treated with mannan. Unexpectedly, immunoblotting showed the presence of Hsp70-LPETGG.

The discrepancy between the SDS-PAGE analysis and the microscopy results, where no signal was detected upon pre-treatment with mannan, can be explained by several factors. Hsp70, being a chaperone, can be expected to interact with a variety of macromolecules present in the medium or on the cell membrane. For example, it has been shown that Hsp70 is able to bind to scavenger receptors such as LOX-1 on dendritic cells.<sup>33,34</sup> Even though the cells were washed several times before lysis in the presence of a large excess of ovalbumin, it is quite likely that some Hsp70-BDP-MC or Hsp70-LPETGG remained, which was then included in the cell lysate. The fluorescence signal in intracellular vesicles is much easier to detect using confocal microscopy than a diffuse binding pattern on the cell membrane, which might explain the lack of fluorescence in mannan-treated cells. Overall, it can be concluded that the synthetic mannose cluster, although low molecular weight compared to Hsp70, is able to ensure its targeted delivery into dendritic cells in a mannose-binding lectin-dependent fashion.

## 4.3 Conclusion

A sortagging nucleophile containing a BODIPY dye and a synthetic mannose cluster for targeting of the mannose receptor was successfully synthesized and employed in a sortase-mediated ligation reaction with recombinant Hsp70-LPETGG. The ensuing Hsp70-BDP-MC protein could be purified by repeated nickel-affinity and gel filtration chromatography. Treatment of immature dendritic cells with the purified protein resulted in MR-mediated internalization as shown by confocal microscopy and SDS-PAGE analysis. Sortase-mediated modification of a protein with a receptor-targeting, fully synthetic ligand, thus enables selective uptake of the macromolecule into the endolysosomal pathway. The next step would be to determine what the functional consequences are of targeted delivery of Hsp70 to cells that are affected by a lysosomal storage disorder. The current construct, Hsp70-BDP-MC, is ideally suited for delivery to Gaucher cells, and because of the flexible synthetic nature of the sortagging nucleophile, targeting of other receptors is within easy reach.



## 4.4 Experimental Section

**Cloning, expression and purification of Hsp70-LPETGG-His<sub>6</sub>.** Wild-type *Hsp70* RNA was isolated from HEK293T cells using RNA-Bee (Bio Connect) and converted to cDNA by RT-PCR. The *HSP* gene was then PCR amplified using the following primers: 5'-CATATGGCCAAAGCCGCGGCG-3' (sense) and 5'-GCGGCCGCTAATCTACCTCCTCAATGGT-3' (anti-sense) containing *Nde*I and *Not*I restriction sites, respectively. The PCR product (2000 bp) was ligated into the pGEM-T plasmid (Promega). The C-terminal LPETGG-sequence was then introduced by PCR amplification using the following primers: sense primer '5-CATATGGCCAAAGCCGCGGCG-3' and anti-sense primer 5'-GCGGCCGCTCCGCGGTCTCGGGCAGATCTACCTCCTCAATGGTGGG-3' containing *Nde*I and *Not*I restriction sites, respectively. The PCR product (2000 bp) was again ligated into the pGEM-T plasmid and then cloned into the expression plasmid Pet21A(+) (Novagen) using the *Not*I and *Nde*I restriction sites. The resulting construct containing a C-terminal His<sub>6</sub>-tag after the LPETGG sequence was transformed into competent *E. coli* BL21(DE3) cells for expression of the recombinant protein. Therefore, two 50 mL cultures in LB-Amp medium were grown overnight at 37 °C, inoculated into 500 mL LB-Amp medium and grown again at 37 °C to an OD<sub>600</sub> of ~0.6. Protein expression was induced by addition of isopropyl β-D-1-thiogalactopyranoside (IPTG, 1 mM) and cultures were grown for 4 h before the cells were pelleted (10,000 g, 4 °C, 2 × 15 min). The pellets were each lysed for 2 h at 4 °C in 20 mL lysis buffer (50 mM NaH<sub>2</sub>PO<sub>4</sub>, 300 mM NaCl, 10 mM imidazole, 0.1% (v/v) Triton X-100, 100 μM EDTA, 0.5 mg/mL lysozyme, 0.4 μg/mL leupeptin and Roche protease inhibitor cocktail) while rotating. The cells were then sonicated on ice (10 × 10 s with 30 s intervals) and centrifuged at 10,000 g for 10 min at 4 °C, after which the supernatant was collected (43 mL). For protein purification, 5 mL 10x binding buffer (500 mM Na<sub>2</sub>HPO<sub>4</sub>, 1.5 M NaCl, 100 mM imidazole, pH 8.0) was added to the lysates and the mixture was filtered over a 0.45 μm filter. The protein was then purified on a nickel column (HisPur Ni-NTA chromatography cartridge, Thermo Scientific) using the AKTA Prime Plus System (HisTag purification program with a linear imidazole gradient of 10 → 500 mM in 50 mM Tris, 150 mM NaCl, pH 8.0). Fractions containing the Hsp70-LPETGG-His<sub>6</sub> protein were combined, concentrated using 30 kDa MWCO filter tubes (Millipore) and buffer exchanged to 50 mM Tris, 150 mM NaCl, pH 8.0, yielding a total of 6 mg protein (1 mL, 6 mg/mL).

**Cloning, expression and purification of SrtA<sub>staph</sub> wild-type or P94S/D160N/K196T mutant.**

SrtA<sub>staph</sub> Δ59 (wild-type minus the membrane anchoring domain) in PET28A plasmid was a gift from H. Ploegh (Whitehead institute, MIT, Boston, USA) and was expressed in *E. coli* as described previously.<sup>27</sup> Mutant P94S/D160N/K196T sortase<sup>29</sup> was obtained by multi-site mutagenesis using the following primers: CCAGGACCAGCAACATCTGAACAATTAATAGAGG (P94S); GACAAGTATAA-GAAATGTTAAGCCTACAGATGTAGGAG (D160N); GACAGCGTTTTGGGAAACACGTAAAATCTT-TGTAGC (K196T) and the QuikChange Lightning Multi Site-Directed Mutagenesis Kit (Agilent Technologies) per manufacturers' instructions. Both recombinant sortases contain a His<sub>6</sub>-tag for purification purposes. For protein purification 10x binding buffer (500 mM Na<sub>2</sub>HPO<sub>4</sub>, 1.5 M NaCl, 100 mM imidazole, pH 8.0) was added to the lysates and the lysate was clarified by filtration over a 0.45 μm filter. The protein was then purified on a nickel column (HisPur Ni-NTA chromatography cartridge, Thermo Scientific) using the AKTA Prime Plus System (HisTag purification program with a linear imidazole gradient of 10 → 500 mM in 50 mM Tris, 150 mM NaCl, pH 8.0). Fractions containing sortase A were combined, concentrated using 10 kDa MWCO filter tubes (Millipore) and buffer exchanged to 50 mM Tris, 150 mM NaCl, pH 8.0 using a desalting column (HiTrap Desalting, GE Healthcare). Fractions were pooled, concentrated and glycerol was added to a final concentration of 10% before storage at -80 °C.

**Analytical scale sortase-mediated ligation of Hsp70-LPETGG-His<sub>6</sub>.** To find the optimal conditions for sortase-mediated ligation of Hsp70, small scale transpeptidation reactions under varying conditions were performed. A typical reaction contained Hsp70-LPETGG (1  $\mu$ g, 14 pmol, 1 eq), SrtA<sub>staph</sub> WT or mutant (5 eq) and triglycine nucleophile **38** or **40** (25 eq) in sortase-reaction buffer (10  $\mu$ L 50 mM Tris, 150 mM NaCl, 10 mM CaCl<sub>2</sub>, pH 7.5). Reaction times were varied, together with the temperature. Aspecific interactions between the nucleophile and Hsp70 were examined by excluding SrtA enzyme from the reaction mixture. Hydrolysis was determined in the absence of nucleophile. After reaction, 5x Laemli's sample buffer (including  $\beta$ -mercaptoethanol) was added and the samples were boiled (100 °C, 5 min) and resolved on 7.5% SDS-PAGE. Gels were scanned on a Typhoon 2000 imager (GE Healthcare) using the Cy3 ( $\lambda_{\text{ex}}$  532 nm;  $\lambda_{\text{em}}$  580 nm) settings. Total protein loading was determined by staining with Coomassie brilliant blue.

**Preparative scale sortase-mediated ligation of Hsp70-LPETGG-His<sub>6</sub> and subsequent purification of Hsp70-BDP-MC.** Hsp70-LPETGG-His<sub>6</sub> (7.1 nmol, 0.50 mg, 83  $\mu$ L 6 mg/mL in Tris buffer pH 8.0) was treated with StrA<sub>staph</sub>  $\Delta$ 59 (36 nmol, 0.60 mg, 0.46 mL 1.3 mg/mL in Tris buffer pH 8.0, 5 eq) and GGG-BDP-MC **40** (178 nmol, 9  $\mu$ L 20 mM in DMSO, 25 eq) in the presence of sortase reaction buffer (65  $\mu$ L 10x buffer: 500 mM Tris, 1.5 M NaCl, 100 mM CaCl<sub>2</sub>, pH 7.5) and 0.05% Tween-80 (33  $\mu$ L 1% in 50 mM Tris pH 8.0). The reaction mixture (0.65 mL) was incubated 20 h at 37 °C while rotating. After reaction, both unreacted Hsp70-LPETGG-His<sub>6</sub> and Sortase A could be removed by Ni-affinity purification. To avoid extensive sticking of the product Hsp70-BDP-MC to the nickel column, Tween-80 was included in all buffers. Hence, the reaction mixture was diluted with 75  $\mu$ L 10x binding buffer (500 mM Na<sub>2</sub>HPO<sub>4</sub>, 1.5 M NaCl, 100 mM imidazole, pH 8.0) and 800  $\mu$ L 1x binding buffer (50 mM Na<sub>2</sub>HPO<sub>4</sub>, 150 mM NaCl, 10 mM imidazole, pH 8.0) containing 0.05% Tween-80, before being applied on top of a Ni-NTA agarose (Qiagen) column (0.5 mL column volume; prewashed 3x with binding buffer and 2x with binding buffer + 0.05% Tween-80). The flow-through was collected and the column was washed with binding buffer + 0.05% Tween-80 (1.5 mL). The combined flow-through and washes were concentrated using 30 kDa MWCO filter tubes (Millipore) and buffer-exchanged 3x with 50 mM Tris, 150 mM NaCl and 0.05% Tween-80, pH 7.5 (10x sample volume). The Ni-affinity purification procedure was repeated to further purify the protein, giving a final volume of 250  $\mu$ L. Finally, the excess of low molecular weight nucleophile was removed by applying the sample to a Vision (BioCad, Applied Biosciences) gel filtration column, using a buffer containing 50 mM Tris and 150 mM NaCl, pH 8.0. The elution fractions containing the desired protein were combined and concentrated using 30 kDa MWCO filter epps (Millipore) to give a final volume of 200  $\mu$ L containing 135  $\mu$ g Hsp70-BDP-MC (1.9 nmol, 27%). Each step of the above procedure was monitored by SDS-PAGE analysis of samples containing an estimated 0.5  $\mu$ g of Hsp70, followed by fluorescence scanning on a Typhoon 2000 imager (GE Healthcare). The gels were then either stained with Coomassie brilliant blue for total protein, or the protein was transferred onto a nitrocellulose membrane using a Bio-Rad Trans-Blot SD Semi-Dry Transfer Cell (1 h, 12V). The membrane was then blocked (1 h, 2% milk in TBST), and incubated (o/n, 4 °C) with primary antibody (1:500 mouse monoclonal  $\alpha$ -His IgG (R&D systems, MAB050) or 1:500 mouse  $\alpha$ -Hsp70/72 (Enzo life sciences, mAb C92F3A-5)), followed by washing (3x 20 min TBST) and incubation with secondary antibody (1:15000 goat  $\alpha$ -mouse IRdye 800CW in 2% milk TBST, 1 h, rt, in the dark). After another wash cycle (3x 20 min TBST + 20 min TBS) the membrane was scanned on an Odyssey scanner (Licor).

**Cell culture of primary cells.** Immature dendritic cells were obtained from the bone marrow of C75BL/6 mice and were a gift from the Biopharmaceutical Department (Leiden University). The use of animals was approved by the ethics committee of Leiden University. Mice were sedated, bone



marrow of tibiae and femurs was flushed out and washed with PBS. Cells were grown in dendritic cell selection medium (IMDM containing granulocyte-macrophage colony stimulating factor (GM-CSF) 2:1 vol/vol) containing 8% FCS, penicillin/streptomycin (100 units/mL), glutamax (2 mM) and beta-mercaptoethanol (20  $\mu$ M). Cells were selected for 10 days (37 °C; 5% CO<sub>2</sub>) and subcultured every 2-3 days before use in the assays.

**Uptake of Hsp70-BDP-MC - Confocal fluorescence microscopy.** Experiments were conducted on a Leica TCS SPE confocal microscope, using dsRed filter settings ( $\lambda_{\text{ex}}$  532 nm) for BODIPY fluorescence and Cy5 filter settings ( $\lambda_{\text{ex}}$  635 nm) to detect Draq5 nuclear stain (Fisher Scientific). Cells (30-75  $\times$  10<sup>4</sup> cells/well, 250-400  $\mu$ L medium) were seeded onto sterile Labtek II 4- or 8-chamber borosilicate coverglass systems (Fisher Emergo). Dendritic cells were allowed to attach for 2 h before pre-incubation with mannan (3 mg/mL) (1 h, 37°C, 5% CO<sub>2</sub>) and subsequent incubation with Hsp70-BDP-MC (10  $\mu$ g/mL, 2 h). Cells were then thoroughly washed (PBS), fixed (4% formaldehyde in PBS), washed again with PBS, nuclei stained with Draq5 and imaged. All experiments were performed at least in triplicate.

**Uptake of Hsp70-BDP-MC - SDS-PAGE analysis.** Immature mouse dendritic cells (200.000 cells/well) were seeded on a 24-wells plate (300  $\mu$ L medium) and cultured for 2 h (37 °C; 5% CO<sub>2</sub>) before start of the experiment. For competition experiments, cells were pre-treated with mannan (3 mg/mL) for 1 h. After subsequent incubation with Hsp70-BDP-MC (10  $\mu$ g/mL, 250  $\mu$ L) or Hsp70-LPETGG-His<sub>6</sub> (10  $\mu$ g/mL, 250  $\mu$ L) for 2 h, cells were washed (2 $\times$  0.5 mL PBS, 1 $\times$  0.2 mL PBS + 1 mg/mL ovalbumin (Sigma)) and lysed (35  $\mu$ L Invitrogen complete cell extraction buffer). Proteins were resolved on 7.5% SDS-PAGE, followed by fluorescence scanning and either Coomassie brilliant blue staining or anti-His WB as described above. Rabbit  $\alpha$ -S6 ribosomal protein (1:4000) primary antibody was included as a loading control for total protein. After washing, the membrane was incubated with secondary antibodies (1:15000 goat  $\alpha$ -mouse IRdye 800CW and 1:15000 goat  $\alpha$ -rabbit IRdye 680CW in 2% milk TBST, 1 h, rt, in the dark). Fluorescence intensities were quantified using ImageJ, and normalized against total protein to correct for differences in protein levels.

## Synthesis

**General.** All reagents were of commercial grade and used as received unless stated otherwise. Reaction solvents were of analytical grade and when used under anhydrous conditions stored over flame-dried 3 Å molecular sieves. Dichloromethane was distilled over CaH<sub>2</sub> prior to use. Solvents used for column chromatography were of technical grade and distilled before use. All moisture and oxygen sensitive reactions were performed under an argon atmosphere. Flash chromatography was performed on silica gel (Screening Devices BV, 0.04-0.063 mm, 60 Å). Reactions were routinely monitored by TLC analysis on DC-alufolien (Merck, Kieselgel60, F254) with detection by UV-absorption (254/366 nm) where applicable and spraying with a solution of (NH<sub>4</sub>)<sub>6</sub>Mo<sub>7</sub>O<sub>24</sub> · 4 H<sub>2</sub>O (25 g/l) and (NH<sub>4</sub>)<sub>4</sub>Ce(SO<sub>4</sub>)<sub>4</sub> · 2 H<sub>2</sub>O (10 g/l) in 10% sulfuric acid in water followed by charring at ~150 °C. <sup>1</sup>H and <sup>13</sup>C NMR spectra were recorded on a Bruker AV-400 (400 MHz) or Bruker AV-500 (500 MHz). Chemical shifts are given in ppm ( $\delta$ ) relative to the residual solvent peak or TMS (0 ppm) as internal standard. Coupling constants are given in Hz. Peak assignments are based on 2D <sup>1</sup>H-COSY and <sup>13</sup>C-HSQC NMR experiments. LC-MS measurements were conducted on a Thermo Finnigan LCQ Advantage MAX ion-trap mass spectrometer (ESI+) coupled to a Surveyor HPLC system (Thermo Finnigan) equipped with a standard C18 (Gemini, 4.6 mmD  $\times$  50 mmL, 5 $\mu$  particle size, Phenomenex) analytical column and buffers A: H<sub>2</sub>O, B: ACN, C: 0.1% aq.TFA. High resolution mass spectra were recorded on a LTQ Orbitrap (Thermo Finnigan) mass spectrometer equipped with an electrospray ion source in positive

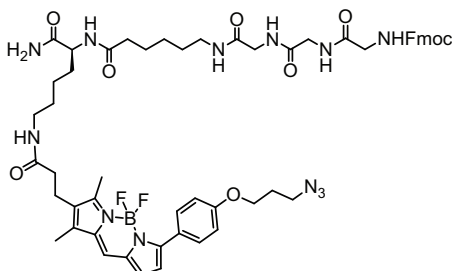
mode (source voltage 3.5 kV, sheath gas flow 10 mL min<sup>-1</sup>, capillary temperature 250 °C) with resolution R=60000 at m/z 400 (mass range m/z=150-2000) and dioctylphthalate (m/z = 391.28428) as a "lock mass". The high resolution mass spectrometer was calibrated prior to measurements with a calibration mixture (Thermo Finnigan). For reversed-phase HPLC purification of the final compounds an automated HPLC system equipped with a C18 semiprep column (Gemini C18, 250x10 mm, 5 μ particle size, Phenomenex) was used.

### Synthesis of LysAhxGly<sub>3</sub>Fmoc (35).

The peptide was synthesized using standard solid-phase peptide synthesis protocols. Starting from Rink amide resin HL (100-200 mesh, 0.78 mmol/g) the following steps were followed:

- Removal of the Fmoc-group with 20% piperidine in NMP for 20 min.
- NMP (3x), DCM (3x), NMP (1x) wash.
- Coupling of the appropriate amino acid (2 eq) with HBTU (2 eq) as the coupling agent, DiPEA (4 eq) as the base, in NMP as the solvent for 5-16 h.
- NMP (3x), DCM (3x), NMP (1x) wash.

Each coupling was monitored by LC/MS analysis and Kaiser test<sup>35</sup> for completion. After the final coupling step, all acid-labile protecting groups were removed and the peptide cleaved from the resin by treatment with TFA/H<sub>2</sub>O/TIS (95:2.5:2.5; v/v/v) for 1 h. The peptide was crystallized from ice-cold Et<sub>2</sub>O and collected by centrifugation as a white solid (40 mg, 0.061 mmol, 85%). *R*<sub>f</sub> = 0.1 (1:1 DCM:MeOH + TEA). <sup>1</sup>H NMR (500 MHz, CDCl<sub>3</sub>/MeOD): δ 7.78 (d, *J* = 7.5 Hz, 2H, 2 × CH<sub>ar</sub>), 7.65 (d, *J* = 7.4 Hz, 2H, 2 × CH<sub>ar</sub>), 7.40 (t, *J* = 7.5 Hz, 2H, 2 × CH<sub>ar</sub>), 7.31 (t, *J* = 7.5 Hz, 2H, 2 × CH<sub>ar</sub>), 4.39 (d, *J* = 7.0 Hz, 2H, CH<sub>2</sub>), 4.35 (dd, *J* = 8.8, 5.3 Hz, 1H, CH), 4.23 (t, *J* = 6.8 Hz, 1H, CH), 3.90 (s, 2H, CH<sub>2</sub>), 3.84 (s, 4H, 2 × CH<sub>2</sub>), 3.21 - 3.13 (m, 2H, CH<sub>2</sub>), 2.92 - 2.87 (m, 2H, CH<sub>2</sub>), 2.24 (t, *J* = 7.3 Hz, 2H, CH<sub>2</sub>), 1.88 - 1.80 (m, 1H, CH<sub>2</sub>-H<sup>a</sup>), 1.69 - 1.59 (m, 5H, 2 × CH<sub>2</sub>, CH<sub>2</sub>-H<sup>b</sup>), 1.54 - 1.48 (m, 2H, CH<sub>2</sub>), 1.47 - 1.38 (m, 2H, CH<sub>2</sub>), 1.33 - 1.28 (m, 2H, CH<sub>2</sub>). <sup>13</sup>C NMR (126 MHz, CDCl<sub>3</sub>/MeOD): δ 174.86, 174.29, 171.45, 170.23, 169.49, 157.51, 143.27, 140.77, 127.13, 126.45, 124.42, 119.28, 66.65, 52.03, 46.54, 43.55, 42.29, 41.85, 38.78, 38.52, 35.04, 30.71, 28.02, 26.21, 25.49, 24.56, 21.95. LC/MS analysis (linear gradient 10 → 90% ACN) *t*<sub>R</sub>: 4.92 min, ESI-MS (*m/z*): [M + H]<sup>+</sup>: 652.5. ESI-HRMS (*m/z*): calcd. for [C<sub>33</sub>H<sub>45</sub>N<sub>7</sub>O<sub>7</sub> + H]<sup>+</sup> 652.34532; obsd. 652.34536.

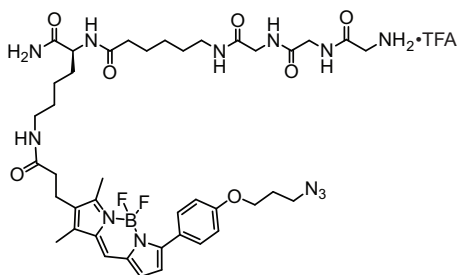


### Synthesis of protected sortase nucleophile BODIPY-Gly<sub>3</sub>Fmoc (37).

Peptide **35** (65 mg, 0.10 mmol) was dissolved in dry DMF (10 mL) and azido-BODIPY-OSu **36**<sup>24</sup> (56 mg, 0.10 mmol) and DiPEA (36 μL, 0.20 mmol, 2 eq) were added. After 2 h, LC/MS revealed complete consumption of starting materials, toluene was added and the solvents removed *in vacuo*. Pure product was obtained by silica column chromatography (0 → 100 % MeOH in DCM) followed by crystallization from DMF/Et<sub>2</sub>O as a dark-

purple solid (100 mg, 91 μmol, 91%). <sup>1</sup>H NMR (400 MHz, DMF-d<sub>7</sub>): δ 8.47 (t, *J* = 5.2 Hz, 1H, NH), 8.24 (t, *J* = 5.6 Hz, 1H, NH), 8.01 - 7.90 (m, 5H, NH, 4 × CH<sub>ar</sub>), 7.86 (d, *J* = 8.0 Hz, 1H, NH), 7.82 - 7.73 (m, 5H, CH<sub>2</sub>, 3 × CH<sub>ar</sub>), 7.51 - 7.44 (m, 3H, NH, 2 × CH<sub>ar</sub>), 7.38 (t, *J* = 7.4 Hz, 2H, 2 × CH<sub>ar</sub>), 7.22 (d, *J* = 4.0 Hz, 1H, CH<sub>ar</sub>), 7.10 (d, *J* = 8.8 Hz, 2H, 2 × CH<sub>ar</sub>), 7.05 (s, 1H, NH), 6.77 (d, *J* = 4.0 Hz, 1H, CH<sub>ar</sub>), 4.40 - 4.26 (m, 3H, CH<sub>2</sub>, CH), 4.21 (t, *J* = 6.1 Hz, 2H, CH<sub>2</sub>), 3.92

(t,  $J = 5.2$  Hz, 4H,  $2 \times \text{CH}_2$ ), 3.84 (d,  $J = 5.8$  Hz, 2H,  $\text{CH}_2$ ), 3.68 - 3.64 (m, 2H,  $\text{CH}_2$ ), 3.19 - 3.10 (m, 4H,  $2 \times \text{CH}_2$ ), 2.74 (s, 2H,  $\text{CH}_2$ ), 2.56 (s, 3H,  $\text{CH}_3$ ), 2.37 (t,  $J = 7.5$  Hz, 2H,  $\text{CH}_2$ ), 2.31 (s, 3H,  $\text{CH}_3$ ), 2.24 (t,  $J = 7.4$  Hz, 2H,  $\text{CH}_2$ ), 2.11 (p,  $J = 6.4$  Hz, 2H,  $\text{CH}_2$ ), 1.83 - 1.71 (m, 1H,  $\text{CH}_2\text{-H}^a$ ), 1.67 - 1.53 (m, 3H,  $\text{CH}_2$ ,  $\text{CH}_2\text{-H}^b$ ), 1.53 - 1.26 (m, 8H,  $4 \times \text{CH}_2$ ).  $^{13}\text{C}$  NMR (101 MHz,  $\text{DMF-d}_7$ ):  $\delta$  174.50, 172.68, 171.53, 170.49, 169.54, 168.86, 160.09, 159.65, 157.17, 154.35, 144.28, 141.20, 140.93, 135.29, 134.62, 131.69, 130.74, 128.25, 127.80, 127.22, 125.72, 125.50, 124.09, 120.16, 118.00, 114.29, 66.60, 65.04, 52.88, 48.17, 47.11, 44.21, 42.83, 42.44, 38.85, 35.58, 32.03, 29.22, 28.58, 26.40, 25.34, 23.28, 20.15, 12.64, 8.91. LC/MS analysis (linear gradient 10  $\rightarrow$  90% ACN)  $t_R$ : 9.13 min, ESI-MS ( $m/z$ ):  $[\text{M} + \text{H}]^+$ : 1101.33. ESI-HRMS ( $m/z$ ): calcd. for  $[\text{C}_{56}\text{H}_{67}\text{BF}_2\text{N}_{12}\text{O}_9 + \text{H}]^+$  1101.52878; obsd. 1101.53115.



(linear gradient 0  $\rightarrow$  90% ACN)  $t_R$ : 7.72 min, ESI-MS ( $m/z$ ):  $[\text{M} + \text{H}]^+$ : 879.33. ESI-HRMS ( $m/z$ ): calcd. for  $[\text{C}_{41}\text{H}_{57}\text{BF}_2\text{N}_{12}\text{O}_7 + \text{H}]^+$  879.46071; obsd. 879.46174.

#### Synthesis of GGG-BDP-MC (40).

Mannose cluster **20** (11.6 mg, 3.8  $\mu\text{mol}$ ) and peptide **37** (4.2 mg, 4.7  $\mu\text{mol}$ , 1.2 eq) were dissolved in DMF (2 mL) and aqueous solutions of sodium ascorbate (76  $\mu\text{L}$  100 mM, 2 eq) and  $\text{CuSO}_4$  (19  $\mu\text{L}$  100 mM, 0.5 eq) were added. The resulting mixture was heated to 75  $^\circ\text{C}$  for 24 h. Toluene was added and the Fmoc-protected peptide **39** was collected by centrifugation and used without further purification. LC/MS analysis (linear gradient 0  $\rightarrow$  90% ACN)  $t_R$ : 6.60 min, ESI-MS ( $m/z$ ):  $[\text{M} + 3\text{H}]^{3+}$ : 1391.00. The peptide was again dissolved in DMF and DBU (1.2  $\mu\text{L}$ , 8  $\mu\text{mol}$ , 2 eq) was added. After 2 h at room temperature, HOBt (5.2 mg, 38  $\mu\text{mol}$ , 10 eq) was added to quench the reaction and the solvent was removed under reduced pressure. The product was purified by RP-HPLC (A: 0.2 % TFA in  $\text{H}_2\text{O}$ , B: linear gradient 20  $\rightarrow$  30 % ACN in 12',  $t_R$ : 11.5 min) and lyophilized from water to give the corresponding TFA salt as a purple powder (3.5 mg, 0.9  $\mu\text{mol}$ , 24%). LC/MS analysis (linear gradient 10  $\rightarrow$  90% ACN)  $t_R$ : 4.88 min, ESI-MS ( $m/z$ ):  $[\text{M} + 2\text{H}]^{2+}$ : 1974.40. ESI-HRMS ( $m/z$ ): calcd. for  $[\text{C}_{172}\text{H}_{271}\text{BF}_2\text{N}_{44}\text{O}_{59} + 2\text{H}]^{2+}$  1974.99159; obsd. 1974.99467; calcd. for  $[\text{C}_{172}\text{H}_{271}\text{BF}_2\text{N}_{44}\text{O}_{59} + 3\text{H}]^{3+}$  1316.99682; obsd. 1316.99846.

## References

- [1] Hoogendoorn, S.; Willems, L. I.; Verhoek, M.; Boot, R.; van der Marel, G. A.; Aerts, J. M. F. G.; Overkleeft, H. S. contributed to the work described in this chapter.
- [2] Hartl, F. U. *Nature* **1996**, *381*, 571–579.

- [3] Callahan, M. K.; Chaillot, D.; Jacquin, C.; Clark, P. R.; Ménoret, A. *J. Biol. Chem.* **2002**, *277*, 33604–33609.
- [4] Daugaard, M.; Rohde, M.; Jäättelä, M. *FEBS Lett.* **2007**, *581*, 3702–3710.
- [5] Evans, C. G.; Chang, L.; Gestwicki, J. E. *J. Med. Chem.* **2010**, *53*, 4585–4602.
- [6] Laufen, T.; Mayer, M. P.; Beisel, C.; Klostermeier, D.; Mogk, A.; Reinstein, J.; Bukau, B. *Proc. Natl. Acad. Sci. U. S. A.* **1999**, *96*, 5452–5457.
- [7] Gyrd-Hansen, M.; Nylandsted, J.; Jäättelä, M. *Cell Cycle* **2004**, *3*, 1484–1485.
- [8] Nylandsted, J.; Gyrd-Hansen, M.; Danielewicz, A.; Fehrenbacher, N.; Lademann, U.; Høyer-Hansen, M.; Weber, E.; Multhoff, G.; Rohde, M.; Jäättelä, M. *J. Exp. Med.* **2004**, *200*, 425–435.
- [9] Kolter, T.; Sandhoff, K. *Biochim. Biophys. Acta* **2006**, *1758*, 2057–2079.
- [10] Kolter, T.; Sandhoff, K. *FEBS Lett.* **2010**, *584*, 1700–1712.
- [11] Schulze, H.; Sandhoff, K. *Cold Spring Harb Perspect Biol* **2011**, *3*.
- [12] Linke, T.; Wilkening, G.; Lansmann, S.; Moczall, H.; Bartelsen, O.; Weisgerber, J.; Sandhoff, K. *Biol. Chem.* **2001**, *382*, 283–290.
- [13] Fürst, W.; Sandhoff, K. *Biochim. Biophys. Acta* **1992**, *1126*, 1–16.
- [14] Wilkening, G.; Linke, T.; Sandhoff, K. *J. Biol. Chem.* **1998**, *273*, 30271–30278.
- [15] Petersen, N. H.; Kirkegaard, T.; Olsen, O. D.; Jäättelä, M. *Cell Cycle* **2010**, *9*, 2305–2309.
- [16] Kirkegaard, T.; Roth, A. G.; Petersen, N. H.; Mahalka, A. K.; Olsen, O. D.; Moilanen, I.; Zyllicz, A.; Knudsen, J.; Sandhoff, K.; Arenz, C.; Kinnunen, P. K.; Nylandsted, J.; Jäättelä, M. *Nature* **2010**, *463*, 549–553.
- [17] Hillaert, U.; Verdoes, M.; Florea, B.; Saragliadis, A.; Habets, K.; Kuiper, J.; Van Calenbergh, S.; Ossendorp, F.; van der Marel, G.; Driessen, C.; Overkleeft, H. *Angew. Chem. Int. Ed. Engl.* **2009**, *48*, 1629.
- [18] Hoogendoorn, S.; Habets, K. L.; Passemard, S.; Kuiper, J.; van der Marel, G. A.; Florea, B. I.; Overkleeft, H. S. *Chem. Commun.* **2011**, *47*, 9363–9365.
- [19] Boven, L. A.; van Meurs, M.; Boot, R. G.; Mehta, A.; Boon, L.; Aerts, J. M.; Laman, J. D. *Am. J. Clin. Pathol.* **2004**, *122*, 359–369.
- [20] Barton, N. W.; Brady, R. O.; Dambrosia, J. M.; Di Bisceglie, A. M.; Doppelt, S. H.; Hill, S. C.; Mankin, H. J.; Murray, G. J.; Parker, R. I.; Argoff, C. E.; Grewal, R. P.; Yu, K.-T. *N. Engl. J. Med.* **1991**, *324*, 1464–1470.
- [21] Popp, M. W.; Antos, J. M.; Grotenbreg, G. M.; Spooner, E.; Ploegh, H. L. *Nat. Chem. Biol.* **2007**, *3*, 707–708.
- [22] Tsukiji, S.; Nagamune, T. *ChemBioChem* **2009**, *10*, 787–798.
- [23] Mazmanian, S. K.; Liu, G.; Ton-That, H.; Schneewind, O. *Science* **1999**, *285*, 760–763.
- [24] Verdoes, M.; Florea, B. I.; Hillaert, U.; Willems, L. I.; van der Linden, W. A.; Sae-Heng, M.; Filippov, D. V.; Kisselev, A. F.; van der Marel, G. A.; Overkleeft, H. S. *ChemBioChem* **2008**, *9*, 1735–1738.
- [25] Tornøe, C. W.; Christensen, C.; Meldal, M. *J. Org. Chem.* **2002**, *67*, 3057–3064.
- [26] Rostovtsev, V. V.; Green, L. G.; Fokin, V. V.; Sharpless, K. B. *Angew. Chem. Int. Ed. Engl.* **2002**, *41*, 2596–2599.
- [27] Antos, J. M.; Chew, G.-L.; Guimaraes, C. P.; Yoder, N. C.; Grotenbreg, G. M.; Popp, M. W.-L.; Ploegh, H. L. *J. Am. Chem. Soc.* **2009**, *131*, 10800–10801.
- [28] Kruger, R. G.; Otvos, B.; Frankel, B. A.; Bentley, M.; Dostal, P.; McCafferty, D. G. *Biochemistry* **2004**, *43*, 1541–1551.
- [29] Chen, I.; Dorr, B. M.; Liu, D. R. *Proc. Natl. Acad. Sci. U. S. A.* **2011**, *108*, 11399–11404.
- [30] Frankel, B. A.; Kruger, R. G.; Robinson, D. E.; Kelleher, N. L.; McCafferty, D. G. *Biochemistry* **2005**, *44*, 11188–11200.
- [31] Huang, X.; Aulabaugh, A.; Ding, W.; Kapoor, B.; Alksne, L.; Tabei, K.; Ellestad, G. *Biochemistry* **2003**, *42*, 11307–11315.
- [32] Smith, P. J.; Blunt, N.; Wiltshire, M.; Hoy, T.; Teesdale-Spittle, P.; Craven, M. R.; Watson, J. V.; Amos, W. B.; Errington, R. J.; Patterson, L. H. *Cytometry* **2000**, *40*, 280–291.
- [33] Delneste, Y.; Magistrelli, G.; Gauchat, J.-F.; Haeuw, J.-F.; Aubry, J.-P.; Nakamura, K.; Kawakami-Honda, N.; Goetsch, L.; Sawamura, T.; Bonnefoy, J.-Y.; Jeannin, P. *Immunity* **2002**, *17*, 353–362.
- [34] Thériault, J. R.; Mambula, S. S.; Sawamura, T.; Stevenson, M. A.; Calderwood, S. K. *FEBS Lett.* **2005**, *579*, 1951–1960.
- [35] Kaiser, E.; Colescott, R.; Bossinger, C.; Cook, P. *Anal. Biochem.* **1970**, *34*, 595–598.

# 5

## Multivalent MPR ligand for endolysosomal targeting of an activity-based cathepsin probe<sup>1</sup>

**M**annose-6-phosphate receptors (MPR) are ubiquitously expressed intracellular receptors that sort newly synthesized lysosomal enzymes to the lysosomes. A small population of the receptors recycle to the plasma membrane to recapture missorted phosphorylated proteins. This chapter describes the development of a synthetic, multivalent, mannose-6-phosphate (M6P) glycopeptide. Conjugation of this cluster to fluorescent DCG-04, an activity-based cysteine cathepsin probe, enabled fluorescent readout of the receptor targeting properties of this ligand. The large M6P cluster-BODIPY-DCG-04 **52** was still able to label cathepsins, as determined by lysate cathepsin labeling experiments. The probe was shown to be taken up in dendritic cells as well as COS cells and trafficking along the endocytic pathway ensured very efficient cathepsin labeling. The uptake in COS cells was completely inhibited by addition of mannose-6-phosphate, concluding that the mannose-6-phosphate cluster indeed targets the MPR and ensures targeted delivery of cargo bound to the cluster into the endolysosomal pathway.

## 5.1 Introduction

The 300 kDa cation-independent mannose-6-phosphate receptor (CI-MPR) and its smaller 46 kDa homolog, the cation-dependent mannose 6-phosphate receptor (CD-MPR) are essential for the correct trafficking of newly synthesized lysosomal enzymes from the *trans*-Golgi network to the lysosomes. Most of the receptor population resides intracellularly, but a small ( $\sim 10\%$ ) fraction of the receptors shuttles continuously between the cell membrane and the endocytic pathway (Figure 5.1A).<sup>2</sup> Besides mannose-6-phosphate (M6P)-containing ligands such as transforming growth-factor  $\beta$ <sup>3</sup> and granzyme B,<sup>4</sup> the CI-MPR has been shown to bind non-M6P ligands at the cell surface. These include insulin-like growth factor II (IGF-II, hence it is also named M6P/IGFII-R),<sup>5</sup> retinoic acid,<sup>6</sup> urokinase-type plasminogen activator receptor and plasminogen.<sup>7</sup> The extracellular region of the CI-MPR consists of 15 homology domains that are similar in size and tertiary structure (Figure 5.1A).<sup>8</sup> Two of those, domains 3 and 9, have been shown to be the mannose-6-phosphate binding domains.<sup>9</sup> In addition, domain 5 has weak affinity for mannose-6-phosphate but is able to bind to Man-P-GlcNAc phosphodiester<sup>10</sup> and domain 11 is the reported IGF-II binding domain.<sup>11</sup> X-ray crystal structures of the extracytoplasmic domain of the CD-MPR in absence or presence of mannose-6-phosphate ligands show dimeric structures with one M6P binding site per monomer (Figure 5.1A).<sup>12,13</sup> The CI-MPR has relatively low affinity towards M6P ( $K_d=7 \mu\text{M}$ ), compared to glycoproteins that contain multiple phosphorylated mannoses ( $K_d=2\text{-}20 \text{ nM}$ ).<sup>14</sup> This could either be contributed to multivalent interaction of one multimeric ligand with the two separate binding domains on the receptor, or by receptor oligomerization, as shown in Figure 5.1B. Evidence points into the direction of the latter explanation, since Byrd *et al.* were able to isolate receptor dimers in the absence of ligand.<sup>15</sup> Furthermore, after mutation of the binding site in domain 9, high affinity binding of a multivalent ligand was still observed, although with reduced stoichiometry.<sup>16</sup> Another study by York *et al.* shows that  $\beta$ -glucuronidase, which contains multiple mannose-6-phosphate residues, enhances CI-MPR internalization rates compared to IGFII, also when one of the receptor binding domains is mutated.<sup>17</sup>

The notion that multivalency increases the affinity of mannose-6-phosphate-containing ligands towards the receptor, has prompted several groups to investigate synthetic ligands, since these allow for defined structures both of the glycan chain as well as the spacing between the phosphate residues. Distler *et al.* synthesized a series of linear or biantennary di- tri- and oligomannosides with  $\alpha(1,2)$ ,  $\alpha(1,3)$  or  $\alpha(1,6)$  linkages and terminal or internal phosphorylation. Only structures with a terminal mannose-6-phosphate were inhibitors of the MPRs, and  $\alpha(1,2)$  linkage was preferred between the ultimate and penultimate residues. Biantennary structures containing two terminal M6P residues were the most potent inhibitors in this study. Interestingly, p-nitrophenyl- $\alpha$  M6P was a slightly better inhibitor than M6P which indicates that the aglycone portion of the mannoside does not interfere with receptor binding.<sup>20</sup> Franzyk and Christensen followed a different approach where they attached one or two phosphorylated mono- or di-saccharides to a peptide back-

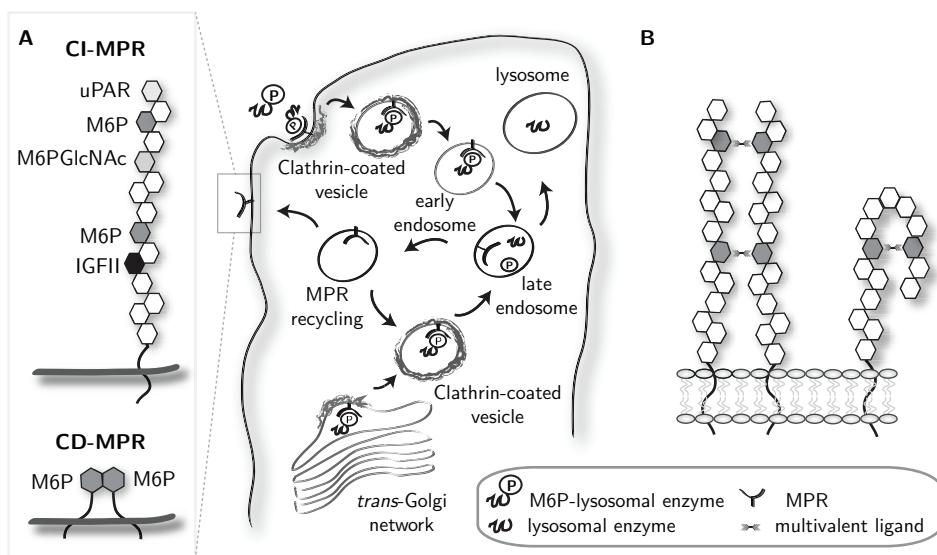


**Figure 5.1:** A) Schematic representations of left: the extracytoplasmic domains of the cation-dependent (CD) and cation-independent (CI) mannose-6-phosphate receptors (MPR), including the different binding domains. Each polygon represents one of the homology domains.<sup>2</sup> right: intracellular trafficking of the MPRs which sorts newly synthesized phosphorylated lysosomal enzymes to the lysosomes. Lowering of the pH in the late endosomes leads to dissociation of the receptor-ligand complex. The receptor then either shuttles back to the *trans*-Golgi network or is re-routed to the plasma membrane.<sup>18</sup> B) Proposed models for multivalent receptor binding. left: Multivalent ligands bound to a CI-MPR dimer; right: multivalent ligand bound to both domain 3 and domain 9 on the same receptor.<sup>19</sup>

bone. Again, structures containing  $\alpha(1,2)$ -linked mannose disaccharides were more potent than their monosaccharide counterparts and the presence of two mannose-6-phosphate residues resulted in a large increase in potency.<sup>21,22</sup>

Insights into the molecular requirements for optimal receptor binding are especially useful when employed to target M6P-bearing molecules to the endolysosomal pathway of MPR-expressing cells. Current enzyme replacement therapies for lysosomal storage disorders such as Fabry and Pompe make use of the binding interaction between M6P residues on the complex *N*-glycan chains of enzymes recombinantly expressed in CHO cells and membrane-bound CI-MPRs.<sup>23,24</sup> Internalization of recombinant enzyme bound to the CI-MPR ensures delivery into the endolysosomal pathway of cells deficient in the lysosomal enzyme.

In Chapter 2 a synthetic mannose cluster<sup>25</sup> is described that contains six mannoses that are flexibly spaced and which functions as a ligand for mannose-binding lectins on dendritic cells. This chapter describes the synthesis and biological evaluation of an analogous mannose-6-phosphate cluster (M6PC, 51 Scheme 5.1) with the aim of targeting the mannose-6-phosphate receptor. For this, a propargyl mannose-6-phosphate building block was designed and synthesized that contained acid-labile *t*-butyl protective groups on the phosphate and base-labile benzyl groups on the hydroxyls that were compatible with solid-



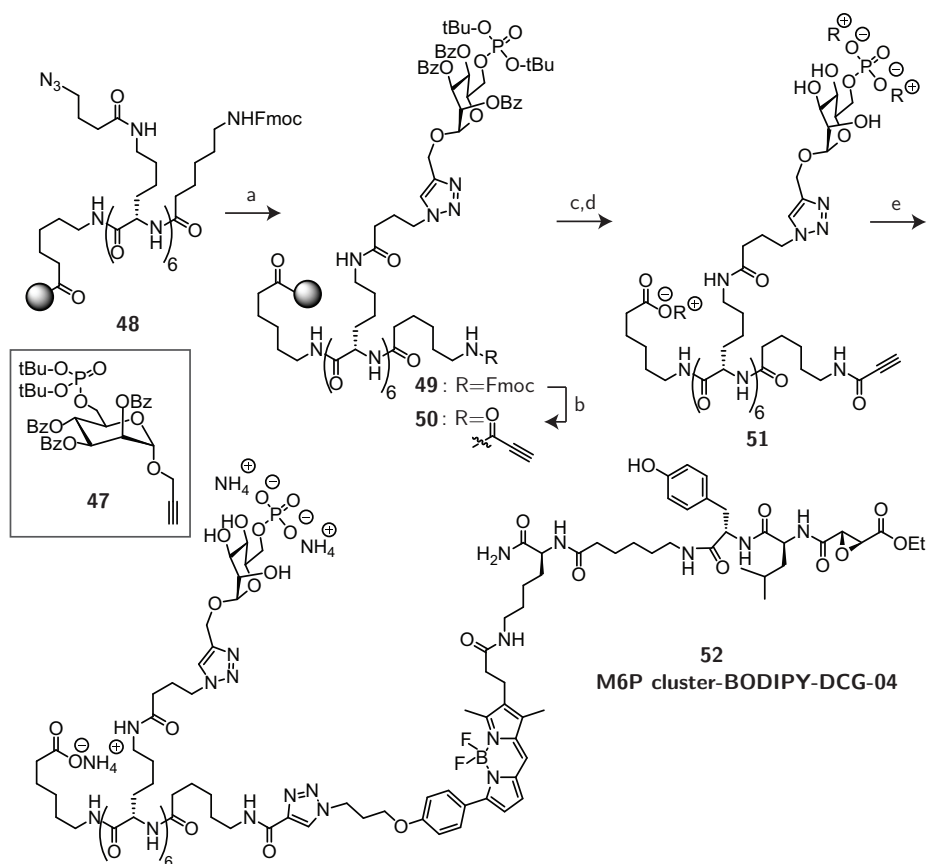
phase peptide synthesis conditions. The flexible nature of the cluster might enable multivalent binding interactions, thereby increasing the potency and possibly receptor internalization.<sup>17</sup> To investigate the MPR targeting properties of this ligand, the cluster was conjugated to fluorescent BODIPY-DCG-04, an activity-based probe for cysteine cathepsins. The ability of the M6P-BODIPY-DCG-04 probe **52** (Scheme 5.1) to label cathepsins was investigated in lysates, followed by *in situ* analysis of uptake, trafficking and cathepsin inhibition in both dendritic cells and COS cells, a fibroblast-like cell line.

## 5.2 Results and Discussion

**Synthesis.** The same peptide scaffold as reported for the mannose cluster<sup>25</sup> **20** (Chapter 2) was used as a starting point for the solid-phase peptide synthesis (SPPS) approach to mannose-6-phosphate cluster **51** (Scheme 5.1). Protected propargyl mannose-6-phosphate **47** was attached six times to the peptide **48** on solid support by Cu(I)-catalyzed Huisgen 1,3-cycloaddition.<sup>26,27</sup> Next, the Fmoc group was removed and propionic acid was coupled to the primary amine by EEDQ coupling. The ensuing terminal alkyne is more electron-deficient than the pentynoic chain that was incorporated as a click handle in the mannose cluster **20**. A drawback hereof is its relative instability to strong (nucleophilic) acid and base conditions, whereas the advantage is its expected greater reactivity in the click reaction allowing for much milder reaction conditions than those used in Chapter 2. The peptide was cleaved from the resin using acidic conditions, which also ensured complete deprotection of the phosphate groups. This is a great advantage compared to previous methods with either 2,2,2-trichloroethyl (Tce) protection of the phosphate group, which requires harsh solution phase conditions for cleavage,<sup>21</sup> or the use of unprotected phosphate, which results in electronic repulsion and coupling difficulties.<sup>22</sup> Global deprotection was accomplished using a saturated solution of K<sub>2</sub>CO<sub>3</sub> in methanol, followed by mild acidic quenching with citric acid. The glycopeptide was purified under neutral NH<sub>4</sub>OAc conditions and lyophilized to give the ammonium salt of **51**. <sup>31</sup>P NMR analysis showed a very broad peak, indicative of multiple salt forms of the peptide. Therefore, the peptide was ion-exchanged to the sodium form using Chelex-Na<sup>+</sup> resin, which resulted in a homogeneous salt form as seen by a sharp phosphate peak in NMR. However, final compound M6P cluster-BODIPY-DCG-04 **52** was only successfully synthesized using the heterogeneous NH<sub>4</sub><sup>+</sup>-phosphate cluster, because of solubility issues of either the starting material or the product. In contrast to the conditions necessary to click the mannose cluster to BODIPY(TMR)-DCG-04 (elevated temperatures, long reaction times), the click reaction of peptide **51** and BODIPY(TMR)-DCG-04 (**22**, Chapter 2) proceeded at room temperature and was finished within one hour. Purification by MS-HPLC under NH<sub>4</sub>OAc conditions provided the (mostly) ammonium salt form of probe **52** in 26% yield, which was used without further cation-exchange procedures.



Scheme 5.1: Synthesis of M6P cluster-BODIPY-DCG-04



Reagents and conditions: [a] mannose **47**, sodium ascorbate,  $\text{CuSO}_4$ ,  $\text{DCM}/\text{H}_2\text{O}$ ; [b] i) 20% piperidine/NMP; ii) propiolic acid, EEDQ; [c] TFA/TIS (98/2, v/v); [d]  $\text{K}_2\text{CO}_3$ , MeOH, RP-HPLC ( $\text{R}=\text{NH}_4^+$ , used for [e]), Chelex- $\text{Na}^+$  ( $\text{R}=\text{Na}^+$ ); [e] BODIPY(TMR)-DCG-04 **22**, sodium ascorbate,  $\text{CuSO}_4$ ,  $\text{DMF}/\text{H}_2\text{O}$ , 26%

**Biological evaluation.** To study the uptake and trafficking of the phosphorylated glycopeptide probe **52** in mammalian cells, labeling of cathepsins along the endolysosomal route was the envisaged read-out. The ability of compound **52** to function as an activity-based probe for cathepsins was first investigated in lysate labeling experiments. For this, increasing concentrations of the probe were added to lysates of different origin (mouse liver, mouse dendritic cells or monkey COS cells) at pH 5.5, the optimal pH for most of the cathepsin activities.<sup>28</sup> As shown in Figure 5.2A, concentration-dependent labeling of active cathepsins was observed. Inactivation of the cathepsins by pre-incubation with 1 or 10  $\mu\text{M}$  of known cathepsin inhibitors AS44<sup>25</sup> or various DCG-04 derivatives<sup>29</sup> (Figure 5.2B) resulted in loss of labeling with probe **52**, indicating that the probe competes for the same set of cathepsins.

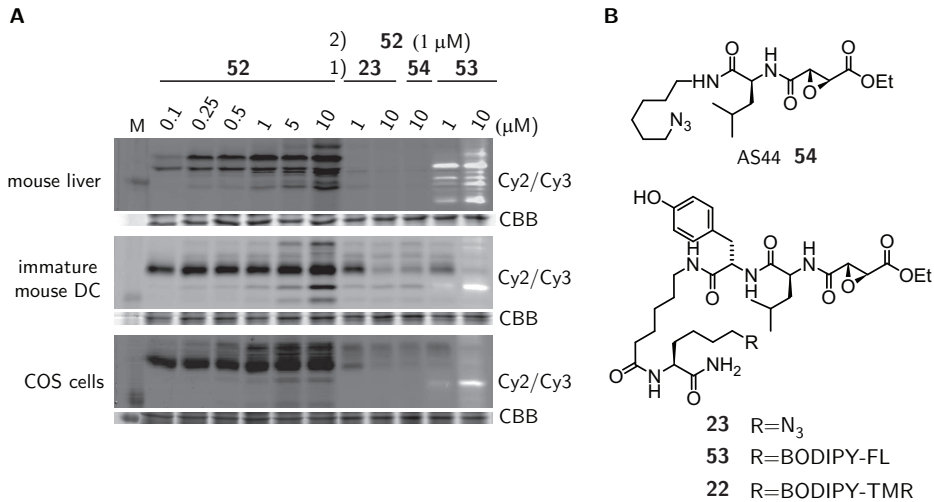


**Figure 5.2: Lysate cathepsin labeling** A) Mouse liver, immature mouse DC or COS cell lysate (10–20  $\mu\text{g}$  total protein) was incubated (1 h, 37  $^{\circ}\text{C}$ ) with increasing concentration of probe **52** at pH 5.5. Alternatively, lysates were incubated (1 h, 37  $^{\circ}\text{C}$ ) with azido-DCG-04 (**23**, 1 or 10  $\mu\text{M}$ ), AS44 (**54**, 10  $\mu\text{M}$ ) or BODIPY(FL)-DCG-04 (**53**, 1 or 10  $\mu\text{M}$ ), before treatment with **52** (1  $\mu\text{M}$ , 1 h, 37  $^{\circ}\text{C}$ ). Proteins were resolved on 12.5% SDS-PAGE, followed by fluorescence scanning (Cy2: BODIPY(FL), Cy3: BODIPY(TMR)) and total protein staining with CBB. B) Chemical structures of cathepsin inhibitors AS44 (**54**) and various DCG-04 derivatives (**22**, **23** and **53**) that were used in competition experiments.

Having established that attachment of the mannose-6-phosphate cluster did not interfere with cathepsin profiling, the new probe was compared head-to-head with the previously reported mannose cluster-BODIPY-DCG-04 probe **13** (Figure 1.9).<sup>25</sup> Immature mouse dendritic cells (DCs) were incubated with 0.1, 0.5 or 1  $\mu\text{M}$  of either probe for 2 h at 37  $^{\circ}\text{C}$ . After cell lysis, the proteome was resolved on SDS-PAGE and the gel was scanned for fluorescence. Similar concentration-dependent labeling profiles were found for both probes (Figure 5.3A). Pre-incubation with 20  $\mu\text{M}$  of non-fluorescent, cell-permeable azido-DCG-04 **23** abolished all labeling for both probes, indicating that indeed cathepsins were labeled. Blocking of the mannose-binding lectins present on dendritic cells with the yeast oligomannoside mannan resulted in inhibition of the uptake of mannose-cluster probe **13**, as previously reported.<sup>25,30</sup> Uptake and cathepsin binding of phosphorylated probe **52** was not inhibited by mannan, showing that the uptake of this probe is mediated by means other than via the mannose receptor. An attempt at uptake inhibition by addition of 1 mM of mannose-6-phosphate to the medium, did not succeed. The presence of MPRs on mouse dendritic cells has not been investigated, although it has been shown that rabbit alveolar macrophages express MPRs on the cell surface.<sup>31</sup> Since the affinity of monovalent mannose-6-phosphate for the receptor is low, the used concentration of 1 mM might have been insufficient to block the binding of probe **52**. Dendritic cells have been shown to be highly endocytotically active, complicating the experimental design, since other processes besides receptor-mediated endocytosis, such as macropinocytosis, might play a role.<sup>32</sup> Confocal fluorescence microscopy of dendritic cells treated with 1  $\mu\text{M}$  of probe **13** or **52**, in the pre-

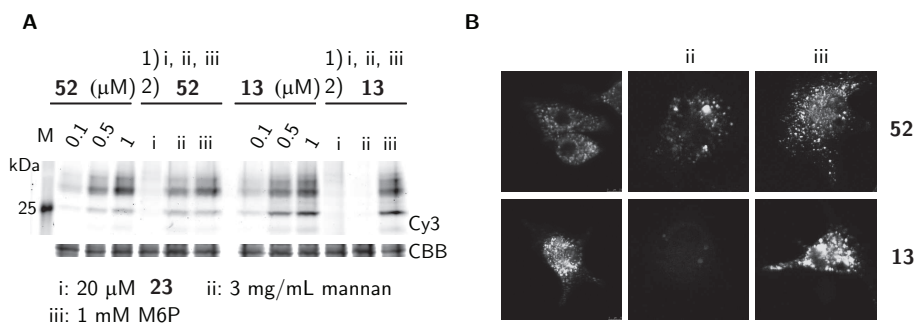


**Figure 5.3: Comparison of uptake and cathepsin labeling of M6PC-BDP-DCG-04 52 and MC-BDP-DCG-04 13 in immature mouse dendritic cells.** A) DCs were treated with varying concentrations of **52** or **13** (2 h, 37 °C) or pre-incubated (1 h, 37 °C) with azido-DCG-04 **23** (20 μmol), mannan (3 mg/mL) or mannose-6-phosphate (1 mM), followed by addition of **52** or **13** (1 μM, 2 h, 37 °C), washed with PBS, lysed and resolved on 12.5% SDS PAGE. In-gel fluorescence of BODIPY (Cy3) and total protein stain (CBB) are shown. B) Representative confocal microscope images of DCs treated with 1 μM of probes **52** or **13** (left panels) or with mannan (ii, middle) or M6P (iii, right) for 1 h, followed by treatment with the probes. After treatment, cells were washed with PBS, fixed with 4% formaldehyde and images using the Cy3 ( $\lambda_{\text{ex}}$  532 nm) settings.

sence or absence of mannan (3 mg/mL) or M6P (1 mM), confirmed the results found by SDS-PAGE analysis (Figure 5.3B). In conclusion, these experiments showed that 6-*O*-phosphorylation of the mannoses present in the mannose cluster changes its internalization properties, without altering its trafficking and subsequent cathepsin labeling in live dendritic cells.

To further elucidate whether the compound could bind the mannose-6-phosphate receptor, experiments were conducted using COS cells, an african green monkey fibroblast-like cell line. Cells were incubated for 16 h with 0.5 μM of mannose receptor-targeted probe **13**, mannose-6-phosphate targeted probe **52** or cell-permeable fluorescent DCG-04 **22** and subsequently analyzed by fluorescence-activated cell sorting (FACS). As shown in Figure 5.4A, only cells that were treated with probes **52** or **22** showed a shift in population fluorescence, indicative of probe uptake. Uptake of probe **52** was time-dependent (50% positive after 6 h, compared to 74% after 16 h of incubation) and was almost completely inhibited in the presence of 1 mM M6P. COS cells treated for 6 h with 0.5 μM of probe **52** and imaged, using a confocal fluorescence microscope, showed bright intracellular fluorescent vesicles, establishing that the compound was taken up in the endocytic pathway (Figure 5.4B). Next, cathepsin labeling was determined, as additional proof for MPR-dependent uptake and trafficking of the probe towards the lysosomes. Cells were treated under various conditions, washed and lysed. Total cell lysates were analyzed by 12.5% SDS-PAGE followed by in-gel fluorescence scanning. In agreement with the FACS data, no labeling was observed for mannose cluster-BODIPY-DCG-04 **13**, in accordance with its selectivity for mannose-binding lectins. The mannose-6-phosphate probe **52**, on the other hand, showed both concentration and time-dependent labeling of cathepsins (Figure 5.4C,D). As shown in Figure 5.4E, cathepsin labeling was inhibited by using increasing concentrations

of mannose-6-phosphate, with almost complete inhibition at 1 mM concentration. Even when taking into account that the probe contains six mannose-6-phosphate residues, a large molar excess of monovalent M6P is needed to inhibit its binding and uptake. Pre-treatment of the cells with non-fluorescent azido-DCG-04 **23** did not result in inhibition of cathepsin labeling by the targeted probe. This is in agreement with COS cathepsin labeling studies with fluorescent non-targeted DCG-04 **53**, which only gave background bands and not the expected labeling as seen in lysates (Figure 5.2) (data not shown). The most likely explanation for this would be that the non-targeted probes are not able to diffuse into the endolysosomal compartments of COS cells, in contrast to dendritic cells, where punctate

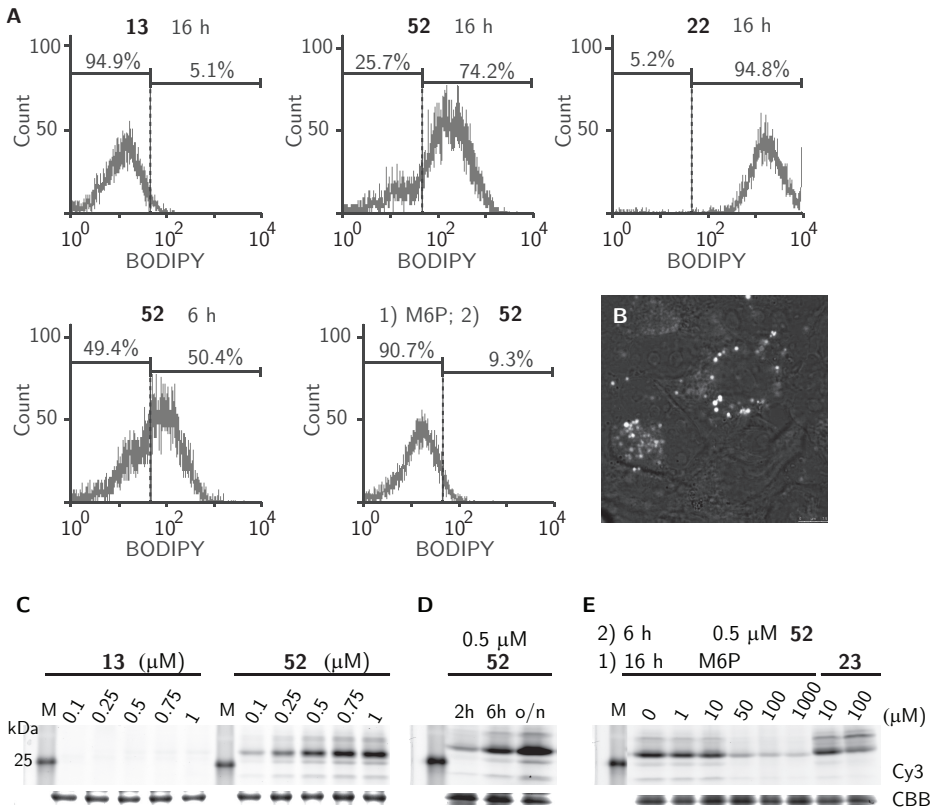


**Figure 5.4: Uptake and cathepsin labeling of M6PC-BDP-DCG-04 (52) in COS cells.** A) FACS analysis of COS cells that were treated with 0.5 μM M6PC-BDP-DCG-04 (**52**, 6 h or 16 h), MC-BDP-DCG-04 (**13**, 16 h), the non-targeted probe BODIPY(TMR)-DCG-04 (**22**, 16 h) or first with 1 mM M6P (16 h), followed by treatment with probe **52** for 6 h. Mean percentages of cells in negative (left) and positive (right) populations from 3 independent experiments are given. B) Representative confocal microscope image of live COS cells treated with probe **52** (0.5 μM) for 6 h, showing fluorescently labeled intracellular compartments. C, D) COS cells were treated with increasing concentrations of probe **52** or MC-BDP-DCG **13** for 16 h (C) or with a 0.5 μM concentration of **52** for different times (D), washed, lysed and analyzed by 12.5% SDS-PAGE. Representative fluorescence scans (Cy3) and total protein stains (CBB) are depicted. E) Competition experiments between different concentrations of mannose-6-phosphate (M6P) or azido-DCG-04 (**23**) (16 h, 37 °C) and **52** (0.5 μM, 6 h, 37 °C). After treatment, cells were washed with PBS, lysed and resolved on a 12.5% SDS-PAGE gel.

cathepsin labeling has been described.<sup>33</sup> This finding does highlight the efficiency by which the targeted probe was taken up by MPR-mediated endocytosis and trafficked to the endolysosomal compartments, leading to inactivation of cathepsins.

### 5.3 Conclusion

Modification of the previously reported mannose cluster **20** by attachment of six propargyl mannose-6-phosphates instead of mannoses on the peptide scaffold resulted in a multivalent mannose-6-phosphate glycopeptide. To assess the receptor-binding and internalization properties of this ligand, it was 'clicked' to the fluorescent activity-based probe BODIPY-DCG-04 **22**. Attachment of the cluster had no effect on cathepsin labeling as seen by lysate labeling experiments and thus the probe was used on live dendritic cells to compare it with the mannose cluster-BODIPY-DCG-04 probe (**13**). Indeed, both compounds were internalized by the cells, and able to label cathepsins along the endocytic pathway, but only for the mannose-cluster containing probe could this process be inhibited by blockage of mannose-binding lectins by mannan. In COS cells that do not express the mannose receptor, only the novel mannose-6-phosphate construct **52** was endocytosed in a process that was inhibited by addition of mannose-6-phosphate to the medium. Taken together, these results showed that 6-*O*-phosphorylation of the mannoses in the MR-ligand completely altered the targeting properties of the ligand, from the mannose receptor to the mannose-6-phosphate receptor. Since this receptor is widely expressed on a variety of cells and tissues, the M6P-cluster provides an efficient means of broad targeted delivery. Conjugation of this M6P-cluster to other biological entities, such as recombinant lysosomal enzymes, might therefore be a suitable alternative for their targeted delivery into various cell types affected by a lysosomal storage disorder such as Pompe or Fabry disease.

### 5.4 Experimental Section

**Cell culture conditions** COS-7 cells, a monkey fibroblast-like cell line, were a kind gift from the Medicinal Biochemistry department (AMC, the Netherlands) and were maintained in Iscove's Modified Dulbecco's Medium (IMDM) containing 5% FCS, 2 mM glutamax (Gibco) and 0.1 mg/mL penicillin/streptomycin at 37 °C, 5% CO<sub>2</sub>.

**Cell culture of primary cells.** Immature dendritic cells were obtained from the bone marrow of C75BL/6 mice and were a gift from the Biopharmaceutical Department (Leiden University). The use of animals was approved by the ethics committee of Leiden University. Mice were sedated, bone marrow of tibiae and femurs was flushed out and washed with PBS. Cells were grown in dendritic cell selection medium (IMDM containing granulocyte-macrophage colony stimulating factor (GM-CSF) 2:1 vol/vol) containing 8% FCS, penicillin/streptomycin (100 units/mL), glutamax (2 mM) and beta-mercaptoethanol (20 μM). Cells were selected for 10 days (37 °C; 5% CO<sub>2</sub>) and subcultured every 2-3 days before use in the assays.

**Labeling of cathepsins in mouse liver, immature dendritic cell or COS cell lysate.** Lysates (10-20  $\mu\text{g}$  total protein, determined on a Qubit 2.0 fluorometer, Life Technologies-Invitrogen) in 50 mM sodium citrate pH 5.5, 5 mM DTT, 0.2 % CHAPS, and 0.1% Triton X-100, were incubated with the indicated concentration of probe (total volume: 10  $\mu\text{L}$ ) for 1 h at 37 °C. For competition experiments, lysates were first incubated with  $\text{N}_3$ -DCG-04 (1 or 10  $\mu\text{M}$ ), AS44<sup>25</sup> (10  $\mu\text{M}$ ) or BDP(FL)-DCG-04 (**53**, 1 or 10  $\mu\text{M}$ ) for 1 h, 37 °C, before addition of the probe and continued incubation for 1 h. After treatment, 5x Laemli's sample buffer (including  $\beta$ -mercaptoethanol) was added and the samples were boiled (100 °C, 5 min) and resolved on 12.5% SDS-PAGE. Gels were scanned on a Typhoon 2000 imager (GE Healthcare) using the Cy2 ( $\lambda_{\text{ex}}$  532 nm;  $\lambda_{\text{em}}$  526 nm) and Cy3 ( $\lambda_{\text{ex}}$  532 nm;  $\lambda_{\text{em}}$  580 nm) settings. Total protein loading was determined by staining with Coomassie brilliant blue and subsequent scanning on a BioRad GS800 calibrated densitometer. Image processing was done with ImageJ, representative gels from at least three independent experiments are shown.

#### Labeling of cathepsins in live-cells

**Immature mouse dendritic cells:** Cells were seeded onto tissue-culture coated 24-wells plates (200.000 cells/well, 250  $\mu\text{L}$  medium) and allowed to attach for 2 h (37 °C; 5%  $\text{CO}_2$ ), before addition of inhibitor or probe to the medium. Pre-incubations with  $\text{N}_3$ -DCG-04 (20  $\mu\text{M}$ ), mannan (3 mg/mL) or mannose-6-phosphate (1 mM) were conducted for 1 h, followed by addition of compound **52** or **13** (1  $\mu\text{M}$ ) and continued incubation for 2 h. For direct labeling experiments, cells were cultured for 2 h (37 °C; 5%  $\text{CO}_2$ ) in the presence of probes **52** or **13** (0.1, 0.5 or 1  $\mu\text{M}$ ). After incubation, cells were washed with PBS (2x), lysed (35  $\mu\text{L}$  Invitrogen complete cell extraction buffer) and proteins resolved on 12.5 % SDS-PAGE, followed by fluorescence scanning (Cy3 settings) and CBB staining.

**COS cells:** Cells (200.000 cells/well) were cultured in full medium (300  $\mu\text{L}$ ) on a tissue-culture coated 24-wells plate for 24-48 h (confluency ~80-90%). Cells were gently washed with PBS and (pre)-incubations were started by addition of compounds/inhibitors in serum-free medium. Concentration-dependent labeling of cathepsins was conducted by incubation with increasing concentrations (0.1, 0.25, 0.5, 0.75 or 1  $\mu\text{M}$ ) of compound **52** or **13**, for 16 h (37 °C; 5%  $\text{CO}_2$ ). For time-course experiments, cells were changed to serum-free medium on  $t=0$ , which was also the start of the o/n (~20 h) incubation time-point, followed by addition of probe (0.5  $\mu\text{M}$ ) after 14 h (start of 6 h) or 18 h (start of 2 h). For competition experiments, cells were cultured in the presence of M6P (0, 1, 10, 50, 100  $\mu\text{M}$  or 1 mM) or  $\text{N}_3$ -DCG-04 (10 or 100  $\mu\text{M}$ ) for 16 h in serum-free medium (250  $\mu\text{L}$ ) before treatment with **52** (0.5  $\mu\text{M}$ ) for 6 h. At the end of the incubation period, medium was removed and the cells were washed twice with ice-cold PBS. Cells were harvested in PBS, centrifuged (1500 rpm, 5 min) and the pellet was lysed in 30  $\mu\text{L}$  lysis buffer (25 mM KPi pH 6.5, 0.1% Triton X-100, 20  $\mu\text{M}$  **23**, protease inhibitor cocktail (Roche)). Labeling was analyzed on 12.5% SDS-PAGE as described above.

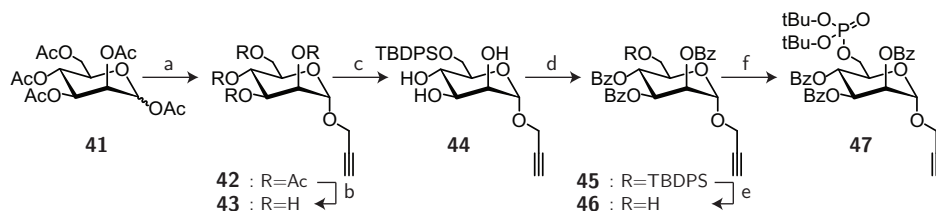
**Confocal fluorescence microscopy.** Experiments were conducted on a Leica TCS SPE confocal microscope, using dsRed filter settings ( $\lambda_{\text{ex}}$  532 nm). Cells (30-75  $\times 10^4$  cells/well) were seeded onto sterile Labtek II 4- or 8-chamber borosilicate coverglass systems (Fisher Emerge). Dendritic cells were allowed to attach for 2 h before pre-incubation with M6P (1 mM) or mannan (3 mg/mL) (1 h, 37°C, 5%  $\text{CO}_2$ ) and subsequent probe incubation (1  $\mu\text{M}$ , 2 h). Cells were then thoroughly washed (PBS), fixed (4% formaldehyde in PBS), washed again with PBS and imaged. COS cells were cultured on chamberslides for 24-48 h (~90% confluent), before incubation with probe **52** (0.5  $\mu\text{M}$ , 6 h) in serum-free medium. Cells were washed with PBS, new medium (without phenol-red) was added and cells were imaged. All experiments were performed at least in triplicate.

**Fluorescence activated cell sorting (FACS) analysis.** COS cells were cultured on 12-wells plates for 24 h, before being subjected to 16 h M6P (1 mM) or compounds **52**, **13** or **22** (0.5  $\mu\text{M}$ ) in

IMDM without FCS. The next day, probe **52** (0.5  $\mu$ M) was added to the M6P-containing medium and incubation was continued for 6 h. The cells were washed with PBS (2x) and harvested in PBS. The resulting single-cell suspension (50  $\mu$ L,  $0.5 \times 10^6$  cells/mL) was analyzed on a Beckman Coulter Cell Lab Quanta SC flow cytometer. The forward scatter (FSC) and side scatter (SSC) were detected simultaneously and the FSC threshold was adjusted to exclude cell debris. Cells that were positive for BODIPY were detected in the FL2 channel ( $\lambda_{\text{ex}}$ :488 nm,  $\lambda_{\text{em}}$ : 575 BP filter). Analysis was performed using the Quanta SC software and based on  $5\text{--}10 \times 10^3$  events per sample and three independent experiments.

## Synthesis

**Scheme 5.2:** Synthesis of protected propargyl mannose-6-phosphate



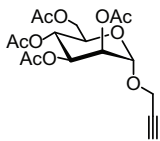
Reagents and conditions: [a] propargyl alcohol,  $\text{BF}_3 \cdot \text{OEt}_2$ , DCM, reflux, 89%; [b] NaOMe, MeOH, 80%; [c] TBDPSCI, imidazole, DMF, quant; [d] benzoyl chloride, pyridine,  $0^\circ\text{C} \rightarrow \text{rt}$ , 97%; [e] TBAF, THF, 99%; [f] i) phenyltetrazole, di-*t*-butylphosphoramidite, DCM; ii)  $\text{H}_2\text{O}_2$ , TEA,  $0^\circ\text{C} \rightarrow \text{rt}$ , 41%<sup>34</sup>

**General.** All reagents were of commercial grade and used as received unless stated otherwise. Reaction solvents were of analytical grade and when used under anhydrous conditions stored over flame-dried 3 Å molecular sieves. Dichloromethane was distilled over  $\text{CaH}_2$  prior to use. Solvents used for column chromatography were of technical grade and distilled before use. All moisture and oxygen sensitive reactions were performed under an argon atmosphere. Flash chromatography was performed on silica gel (Screening Devices BV, 0.04–0.063 mm, 60 Å). Reactions were routinely monitored by TLC analysis on DC-alufolien (Merck, Kieselgel60, F254) with detection by UV-absorption (254/366 nm) where applicable and spraying with a solution of  $(\text{NH}_4)_6\text{Mo}_7\text{O}_{24} \cdot 4 \text{H}_2\text{O}$  (25 g/l) and  $(\text{NH}_4)_4\text{Ce}(\text{SO}_4)_4 \cdot 2 \text{H}_2\text{O}$  (10 g/l) in 10% sulfuric acid in water followed by charring at  $\sim 150^\circ\text{C}$ .  $^1\text{H}$ ,  $^{13}\text{C}$  NMR and  $^{31}\text{P}$  spectra were recorded on a Bruker AV-400 (400 MHz) or Bruker DMX-600 (600 MHz). Chemical shifts are given in ppm ( $\delta$ ) relative to the residual solvent peak or TMS (0 ppm) as internal standard. Coupling constants are given in Hz. Peak assignments are based on 2D  $^1\text{H}$ -COSY and  $^{13}\text{C}$ -HSQC NMR experiments. Chloroform was neutralized by filtration over basic  $\text{Al}_2\text{O}_3$  before use with *t*-butyl-protected phosphates. IR measurements (thin film) were conducted on an IRAffinity-1 apparatus and evaluated using IR Solutions software (Shimadzu, Kyoto, Japan). LC-MS measurements were conducted on a Thermo Finnigan LCQ Advantage MAX ion-trap mass spectrometer (ESI+) coupled to a Surveyor HPLC system (Thermo Finnigan) equipped with a standard C18 (Gemini, 4.6 mmD  $\times$  50 mmL, 5  $\mu$  particle size, Phenomenex) analytical column and buffers A:  $\text{H}_2\text{O}$ , B: ACN, C: 0.1% aq. TFA. High resolution mass spectra were recorded on a LTQ Orbitrap (Thermo Finnigan) mass spectrometer equipped with an electrospray ion source in positive mode (source voltage 3.5 kV, sheath gas flow 10  $\text{mL min}^{-1}$ , capillary temperature  $250^\circ\text{C}$ ) with resolution  $R=60000$  at  $m/z$  400 (mass range  $m/z=150\text{--}2000$ ) and dioctylphthalate ( $m/z = 391.28428$ ) as a "lock mass". The high resolution mass spectrometer was calibrated prior to measurements with a calibration mixture (Thermo Finnigan). For reversed-phase HPLC purification of the final compounds an automated HPLC system equipped with a



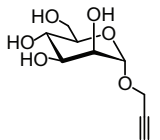
C18 semiprep column (Gemini C18, 250x10 mm, 5 $\mu$  particle size, Phenomenex) was used. HPLC-MS purifications were performed on an Agilent Technologies 1200 series automated HPLC system with a Quadropole MS 6130, equipped with a semi-preparative Gemini C18 column (Phenomenex, 250x10, 5 $\mu$  particle size). Optical rotations were measured on a Propol automatic polarimeter (Sodium D-line,  $\lambda = 589$  nm).

#### Propargyl-2,3,4,6-Tetra-*O*-acetyl- $\alpha$ -D-mannopyranoside (42).



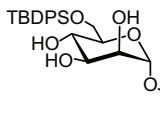
To a solution of peracetylated mannose **41** (19.5 g, 50 mmol, 1 eq) in dry DCM (300 mL) propargyl alcohol (4.4 mL, 75 mmol, 1.5 eq) and  $\text{BF}_3 \cdot \text{OEt}_2$  (9.3 mL, 75 mmol, 1.5 eq) were added. The mixture was refluxed for 20 h, after which the reaction was cooled to rt and quenched by addition of powdered  $\text{K}_2\text{CO}_3$  (13.5 g, 100 mmol, 2 eq). After stirring for 30 min, the solution was filtered over a glass filter and concentrated *in vacuo*. Silica column chromatography (0  $\rightarrow$  10% EtOAc in toluene) afforded compound **42** in 89% yield (16.5 g, 44 mmol)  $R_f = 0.5$  (1:1 PE:EtOAc). All analytical data were in full accordance with those published previously.<sup>35</sup>

#### Propargyl- $\alpha$ -D-mannopyranoside (43).



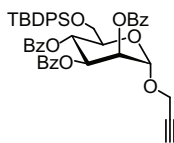
Acetylated propargyl mannose **42** (16.5 g, 44 mmol) was dissolved in MeOH (45 mL) and a solution of NaOMe (30% in MeOH, 0.79 mL, 0.1 eq) was added. Upon completion of the reaction (1 h), Dowex- $\text{H}^+$  was added till pH $\sim$ 7, the solution was filtered over a small plug of silica and concentrated under reduced pressure. Crystallization from EtOH/heptane yielded propargyl mannose **43** (7.67 g, 35 mmol, 80%) as white crystals. Analytical data were in full accordance with those previously published.<sup>36</sup>

#### Propargyl 6-*O*-(*tert*-butyldiphenylsilyl)- $\alpha$ -D-mannopyranoside (44).

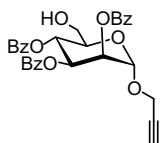


Propargyl mannose **43** (0.21 g, 0.96 mmol) was dissolved in dry DMF (5 mL) and imidazole (0.13 g, 2 mmol, 2 eq) was added. After dropwise addition of *tert*-butyldiphenylsilyl chloride (0.28 mL, 1.05 mmol, 1.1 eq) the reaction was stirred for 1 h at room temperature, before being concentrated *in vacuo*. The residue was dissolved in chloroform (10 mL), washed with HCl (aq, pH 3, 2  $\times$  20 mL) and water (20 mL). The aqueous layers were extracted with DCM (2  $\times$  30 mL) and the combined organic layers were dried over  $\text{MgSO}_4$ , filtered and concentrated under reduced pressure. Pure product was obtained by silica column chromatography (10  $\rightarrow$  50% EtOAc in pentane) as a colorless oil in quantitative yield (0.44 g, 0.96 mmol).  $R_f = 0.7$  (EtOAc).  $^1\text{H}$  NMR (400 MHz,  $\text{CDCl}_3$ ):  $\delta$  7.72 - 7.62 (m, 4H, 4  $\times$   $\text{CH}_{\text{ar}}$ ), 7.41 - 7.33 (m, 6H, 6  $\times$   $\text{CH}_{\text{ar}}$ ), 4.93 (s, 1H, H-1), 4.38 (s, 1H, OH), 4.11 (s, 2H,  $\text{CH}_2$ ), 3.93 (dd,  $J = 10.6, 4.2$  Hz, 1H, H-6), 3.89 - 3.65 (m, 6H, H-6, H-2, H-3, H-4, 2  $\times$  OH), 3.65 - 3.57 (m, 1H, H-5), 2.32 (t,  $J = 2.2$  Hz, 1H,  $\text{CH}\equiv$ ), 1.03 (s, 9H, 3  $\times$   $\text{CH}_3$ ).  $^{13}\text{C}$  NMR (101 MHz,  $\text{CDCl}_3$ ):  $\delta$  135.69, 133.05, 132.96, 129.92, 127.87, 98.05, 78.78, 75.04, 72.06, 71.71, 70.32, 69.43, 64.82, 53.98, 26.87, 19.24. FT-IR (thin film)  $\nu$  3418, 3303, 2930, 2857, 1106, 1043  $\text{cm}^{-1}$ .  $[\alpha]_D^{20} = +54^\circ$  ( $c = 1, \text{CHCl}_3$ ). ESI-HRMS ( $m/z$ ): calcd. for  $[\text{C}_{25}\text{H}_{32}\text{O}_6\text{Si} + \text{Na}]^+$  479.18604; obsd. 479.18581.

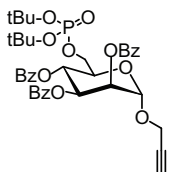




**Propargyl 2, 3, 4-tri-*O*-benzoyl-6-*O*-(*tert*-butyldiphenylsilyl)- $\alpha$ -D-mannopyranoside (45).** Compound 44 (0.40 g, 0.88 mmol) was dissolved in pyridine (10 mL) and benzoyl chloride (1.02 mL, 8.8 mmol, 10 eq) was dropwise added at 0 °C. The mixture was stirred for 2 h at room temperature, before quenching of the reaction with sat aq NaHCO<sub>3</sub> (30 mL). The water layer was extracted with EtOAc (3 × 20 mL), dried (MgSO<sub>4</sub>), filtered and concentrated *in vacuo*. Silica column chromatography (0 → 10% EtOAc in pentane) yielded compound 45 as a colorless oil (0.65 g, 0.85 mmol, 97%). *R*<sub>f</sub> = 0.9 (6:1 pentane:EtOAc). <sup>1</sup>H NMR (400 MHz, CDCl<sub>3</sub>):  $\delta$  8.16 (d, *J* = 6.9 Hz, 2H, 2 × CH<sub>ar</sub>), 7.94 (d, *J* = 7.0 Hz, 2H, 2 × CH<sub>ar</sub>), 7.88 (d, *J* = 7.0 Hz, 2H, 2 × CH<sub>ar</sub>), 7.75 (d, *J* = 5.8 Hz, 2H, 2 × CH<sub>ar</sub>), 7.61 (d, *J* = 6.4 Hz, 2H, 2 × CH<sub>ar</sub>), 7.57 - 7.46 (m, 2H, 2 × CH<sub>ar</sub>), 7.44 - 7.38 (m, 2H, 2 × CH<sub>ar</sub>), 7.38 - 7.08 (m, 11H, 11 × CH<sub>ar</sub>), 6.25 (t, *J* = 9.9 Hz, 1H, H-4), 5.91 (d, *J* = 9.5 Hz, 1H, H-3), 5.80 (s, 1H, H-2), 5.36 (s, 1H, H-1), 4.37 (s, 2H, CH<sub>2</sub>), 4.21 (d, *J* = 9.0 Hz, 1H, H-5), 4.04 - 3.83 (m, 2H, H-6), 2.48 (s, 1H, CH $\equiv$ ), 1.10 (s, 9H, 3 × CH<sub>3</sub>). <sup>13</sup>C NMR (101 MHz, CDCl<sub>3</sub>):  $\delta$  165.57, 165.50, 165.26, 135.72, 135.54, 133.77, 133.50, 133.27, 133.12, 132.94, 132.83, 130.03, 129.78, 129.74, 129.70, 129.64, 129.35, 129.30, 129.15, 128.59, 128.42, 128.30, 127.70, 127.63, 96.24, 78.27, 75.56, 71.87, 70.57, 70.50, 66.45, 62.31, 54.76, 26.67, 19.24. [ $\alpha$ ]<sub>D</sub><sup>20</sup> = +82° (c = 2, CHCl<sub>3</sub>). ESI-HRMS (*m/z*): calcd. for [C<sub>46</sub>H<sub>44</sub>O<sub>9</sub>Si + Na]<sup>+</sup> 791.26468; obsd. 791.26460.

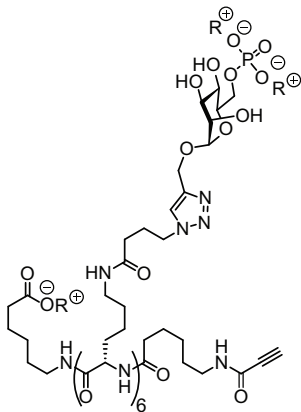


**Propargyl 2, 3, 4-tri-*O*-benzoyl- $\alpha$ -D-mannopyranoside (46).** Compound 45 (0.57 g, 0.74 mmol) was dissolved in THF (10 mL) and acetic acid (0.21 mL, 3.7 mmol, 5 eq) and TBAF (1 M in THF, 1.11 mL, 1.11 mmol, 1.5 eq) were added. After 72 h, deprotection was complete and brine was added to the mixture, followed by extraction with EtOAc. The organic layer was dried (MgSO<sub>4</sub>), filtered and concentrated under reduced pressure. Silica column chromatography (0 → 50% EtOAc in pentane) yielded compound 128 as a colorless oil (0.39 g, 0.73 mmol, 99%). *R*<sub>f</sub> = 0.3 (2:1 pentane:EtOAc). <sup>1</sup>H NMR (400 MHz, CDCl<sub>3</sub>):  $\delta$  8.12 (d, *J* = 7.4 Hz, 2H, 2 × CH<sub>ar</sub>), 7.98 (d, *J* = 7.5 Hz, 2H, 2 × CH<sub>ar</sub>), 7.84 (d, *J* = 7.4 Hz, 2H, 2 × CH<sub>ar</sub>), 7.57 (t, *J* = 7.4 Hz, 1H, CH<sub>ar</sub>), 7.50 - 7.43 (m, 3H, 3 × CH<sub>ar</sub>), 7.40 - 7.31 (m, 3H, 3 × CH<sub>ar</sub>), 7.21 (t, *J* = 7.8 Hz, 2H, 2 × CH<sub>ar</sub>), 6.02 (dd, *J* = 10.1, 3.3 Hz, 1H, H-3), 5.92 (t, *J* = 10.0 Hz, 1H, H-4), 5.77 (dd, *J* = 2.9, 1.6 Hz, 1H, H-2), 5.35 (s, 1H, H-1), 4.39 (d, *J* = 2.1 Hz, 2H, CH<sub>2</sub>), 4.17 (d, *J* = 9.5 Hz, 1H, H-5), 3.95 - 3.76 (m, 2H, H-6), 3.05 (s, 1H, OH), 2.57 (t, *J* = 2.2 Hz, 1H, CH $\equiv$ ). <sup>13</sup>C NMR (101 MHz, CDCl<sub>3</sub>):  $\delta$  166.19, 165.31, 165.29, 133.57, 133.51, 133.12, 129.80, 129.73, 129.53, 129.00, 128.86, 128.53, 128.40, 128.18, 96.29, 78.12, 75.74, 71.40, 70.20, 69.53, 66.96, 61.09, 55.01. FT-IR (thin film)  $\nu$  3418, 3303, 2930, 1724, 1450, 1260, 1107, 1065 cm<sup>-1</sup>. [ $\alpha$ ]<sub>D</sub><sup>20</sup> = -118° (c = 1, CHCl<sub>3</sub>). ESI-HRMS (*m/z*): calcd. for [C<sub>30</sub>H<sub>26</sub>O<sub>9</sub> + Na]<sup>+</sup> 553.14690; obsd. 553.14673.



**Propargyl 2, 3, 4-tri-*O*-benzoyl-6-*O*-(*di-tert*-butoxyphosphoryl)- $\alpha$ -D-mannopyranoside (47).** Compound 46 (0.52 g, 0.98 mmol) was co-evaporated with dioxane (2x), dissolved in dry DCM (10 mL) and added to a flame-dried flask with activated molecular sieves. Phenyltetrazole (287 mg, 2 mmol, 2 eq) and *di-tert*-butylphosphoramidite (0.49 mL, 1.5 mmol, 1.5 eq) were added. After 30 minutes at room temperature, TLC (*R*<sub>f</sub> = 0.95, 2:1 pentane:EtOAc) indicated complete conversion of the starting material, so the mixture was cooled to 0 °C and TEA (1 mL, 7.5 eq) and H<sub>2</sub>O<sub>2</sub> (aq, 30%, 0.35 mL, 3.1 eq) were added. TLC indicated complete oxidation after 1 h at room temperature. DCM was added and the organic layer was washed with H<sub>2</sub>O and NaHCO<sub>3</sub> (aq, sat), dried over Na<sub>2</sub>SO<sub>4</sub>, filtered and concentrated. Silica column chromatography (0 → 30 % EtOAc in PE + 1% pyridine) yielded protected mannose-6-phosphate 47 as a yellowish oil

(0.29 g, 0.4 mmol, 41%).  $R_f = 0.15$  (2:1 pentane:EtOAc).  $^1\text{H NMR}$  (400 MHz,  $\text{CDCl}_3$ ):  $\delta$  8.11 (d,  $J = 7.3$  Hz, 2H, 2  $\times$   $\text{CH}_{\text{ar}}$ ), 7.96 (d,  $J = 7.4$  Hz, 2H, 2  $\times$   $\text{CH}_{\text{ar}}$ ), 7.83 (d,  $J = 7.4$  Hz, 2H, 2  $\times$   $\text{CH}_{\text{ar}}$ ), 7.61 (t,  $J = 7.4$  Hz, 1H,  $\text{CH}_{\text{ar}}$ ), 7.49 (q,  $J = 7.2$  Hz, 3H, 3  $\times$   $\text{CH}_{\text{ar}}$ ), 7.44 - 7.33 (m, 3H, 3  $\times$   $\text{CH}_{\text{ar}}$ ), 7.25 (t,  $J = 7.8$  Hz, 2H, 2  $\times$   $\text{CH}_{\text{ar}}$ ), 5.93 - 5.85 (m, 2H, H-3, H-4), 5.73 (s, 1H, H-2), 5.33 (s, 1H, H-1), 4.42 (d,  $J = 2.3$  Hz, 2H,  $\text{CH}_2$ ), 4.38 (s, 1H, H-5), 4.24 - 4.19 (m, 2H, H-6), 2.55 (t,  $J = 2.3$  Hz, 1H,  $\text{CH}\equiv$ ), 1.45 (s, 9H, 3  $\times$   $\text{CH}_3$ ), 1.42 (s, 9H, 3  $\times$   $\text{CH}_3$ ).  $^{13}\text{C NMR}$  (101 MHz,  $\text{CDCl}_3$ ):  $\delta$  165.39, 165.36, 133.56, 133.47, 133.17, 129.92, 129.74, 129.70, 129.23, 129.01, 128.93, 128.58, 128.43, 128.27, 95.92, 82.69 (d,  $J = 3$  Hz, Cq tBut), 82.61 (d,  $J = 3$  Hz, Cq tBut), 78.00, 75.82, 70.37, 70.21 (d,  $J = 8$  Hz, C-5), 70.03, 66.82, 65.28 (d,  $J = 6$  Hz, C-6), 54.95, 29.80, 29.76, 29.72.  $^{31}\text{P NMR}$  (162 MHz,  $\text{CDCl}_3$ ):  $\delta$  -9.42. FT-IR (thin film)  $\nu$  2980 2934, 1726, 1450, 1250, 1105, 1067, 991  $\text{cm}^{-1}$ .  $[\alpha]_D^{20} = -73^\circ$  (c = 2,  $\text{CHCl}_3$ ). LC/MS analysis (linear gradient 50%  $\rightarrow$  90% ACN)  $t_R$ : 7.94 min, ESI-MS ( $m/z$ ):  $[\text{M} + \text{H}]^+$ : 722.93. ESI-HRMS ( $m/z$ ): calcd. for  $[\text{C}_{38}\text{H}_{43}\text{O}_{12}\text{P} + \text{Na}]^+$  745.23843; obsd. 745.23858.

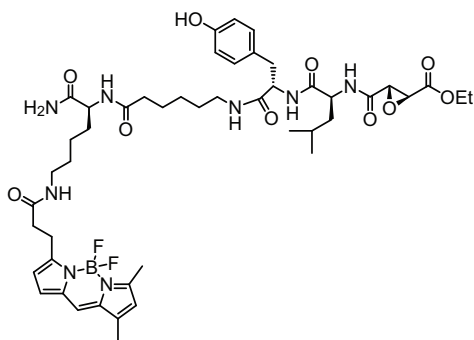


**Synthesis of mannose-6-phosphate cluster (51).** Tentagel S-HMPB-Ahx-Lys(spacerN<sub>3</sub>)<sub>6</sub>-Ahx-Fmoc (**48**, obtained as reported previously<sup>25</sup>) (0.5 g, 0.08-0.1 mmol), propargyl mannose **47** (667 mg, 0.92 mmol, 9.2 eq), sodium ascorbate (160 mg in 1 mL H<sub>2</sub>O, 0.8 mmol, 8 eq) and CuSO<sub>4</sub> (100 mg in 1 mL H<sub>2</sub>O, 0.4 mmol, 4 eq) in DCM (5 mL) were shaken for 72 h. The supernatant was collected, the resin washed with DCM and H<sub>2</sub>O and the combined supernatants were extracted to recover unreacted mannose **47** (recovered yield: 0.3 mmol, 221 mg, after silica column chromatography). The resin was washed with NMP, MeOH, DCM, H<sub>2</sub>O and Et<sub>2</sub>O for drying. Dry resin **49** (1 eq) was swollen again in DCM, washed with NMP and subsequently deprotected with 20% piperidine in NMP. After washing (NMP, DCM, NMP, all 2x), EEDQ (10 eq) and propionic acid (10 eq) were added in DCM and the mixture was shaken for 1.5 h. Resin **50** was washed again

(NMP, DCM, NMP, all 2x) and subjected to a cocktail of TFA/TIS (98/2, v/v, 3  $\times$  15') to deprotect the *t*-butyl groups and cleave the peptide from the resin. The cleaved peptide was crashed from icecold Et<sub>2</sub>O and collected by centrifugation. (ESI-HRMS ( $m/z$ ): calcd. for  $[\text{C}_{255}\text{H}_{288}\text{N}_{32}\text{O}_{88}\text{P}_6 + 3\text{H}]^{3+}$  1799.25964; obsd. 1799.25926). The crude peptide was debenzoylated by addition of a solution of K<sub>2</sub>CO<sub>3</sub> (50 mM) in MeOH and subsequent stirring for 24 h at room temperature. The reaction was quenched by careful addition of citric acid (aq) to pH~5 and the solvents removed *in vacuo*. The residue was taken up in *t*-BuOH/H<sub>2</sub>O/MeCN (1:1:1), purified by RP-HPLC (A: 50 mM NH<sub>4</sub>OAc, B: linear gradient 5  $\rightarrow$  15% ACN in 12',  $t_R$ : 10.5 min) and lyophilized to give mannose-6-phosphate cluster **51** (R = NH<sub>4</sub><sup>+</sup>, this salt form is required for successful use in the subsequent click reaction, due to solubility issues) as a hygroscopic white powder. The peptide was dissolved in H<sub>2</sub>O and ion-exchanged to the sodium form **51** (R = Na<sup>+</sup>) by flushing it over a plug of Chelex-Na<sup>+</sup>.  $^1\text{H NMR}$  (600 MHz, D<sub>2</sub>O):  $\delta$  8.19 (s, 5H, 6  $\times$  CH<sub>trz</sub>), 5.08 (s, 6H, 6  $\times$  H-1), 4.96 (d,  $J = 12.4$  Hz, 6H, CH<sub>2</sub>-H<sup>a</sup>), 4.79 (d,  $J = 12.4$  Hz, 6H, CH<sub>2</sub>-H<sup>b</sup>), 4.59 - 4.53 (m, 12H, 6  $\times$  CH<sub>2</sub>), 4.44 - 4.35 (m, 6H, 4  $\times$  CH<sub>α</sub>), 4.31 - 4.27 (m, 2H, 2  $\times$  CH<sub>α</sub>), 4.26 - 4.17 (m, 6H, 6  $\times$  H-6), 4.07 - 4.00 (m, 19H, 6  $\times$  H-2, H-4, H-6, 1  $\times$  CH≡), 3.92 (dd,  $J = 10.0, 3.1$  Hz, 6H, 6  $\times$  H-3), 3.81 (d,  $J = 9.6$  Hz, 6H, 6  $\times$  H-4), 3.37 - 3.17 (m, 16H, 8  $\times$  CH<sub>2</sub>), 2.42 - 2.25 (m, 26H, 13  $\times$  CH<sub>2</sub>), 1.94 - 1.80 (m, 12H, 6  $\times$  CH<sub>2</sub>), 1.74 - 1.55 (m, 24H, 12  $\times$  CH<sub>2</sub>), 1.55 - 1.34 (m, 36H, 18  $\times$  CH<sub>2</sub>).  $^{13}\text{C NMR}$  (151 MHz, D<sub>2</sub>O):  $\delta$  184.53, 182.40, 180.23, 177.87, 175.50, 174.28, 171.95, 171.60, 169.16, 144.40, 144.18, 126.13, 100.61, 76.15 (HSQC cross-coupling), 73.39 (d,  $J = 6$  Hz, C-5) 70.99, 70.95, 66.78, 63.36 (d,  $J$

= 4.5 Hz, C-6), 60.66, 54.95, 54.56, 50.56, 40.12, 40.01, 38.42, 36.15, 33.40, 31.39, 29.03, 28.75, 26.93, 26.66, 26.42, 23.38.  $^{31}\text{P}$  NMR (162 MHz,  $\text{D}_2\text{O}$ ):  $\delta$  5.03. LC/MS analysis (linear gradient 0%  $\rightarrow$  90% ACN)  $t_R$ : 4.71 min, ESI-MS ( $m/z$ ):  $[\text{M} + 2\text{H}]^{2+}$ : 1760.93.

**Synthesis of M6P cluster-BODIPY-DCG-04 (52).** Peptide **51** (2.64 mg, 700 nmol) was dissolved in  $\text{H}_2\text{O}$  (400  $\mu\text{L}$ ) and BODIPY-DCG-04 **22** (0.9 mg, 800 nmol, 1.14 eq) in DMF (400  $\mu\text{L}$ ) was added, followed by sodium ascorbate (35  $\mu\text{L}$ , 100 mM in  $\text{H}_2\text{O}$ , 5 eq) and  $\text{CuSO}_4$  (3.5  $\mu\text{L}$ , 100 mM in  $\text{H}_2\text{O}$ , 0.5 eq). The resulting mixture was stirred for 1 h at room temperature, before being concentrated and co-evaporated with toluene. Purification by HPLC-MS (A: 25 mM  $\text{NH}_4\text{OAc}$ , B: linear gradient 20  $\rightarrow$  35% ACN in 12') and lyophilization from  $\text{H}_2\text{O}$  yielded the final compound (0.85 mg, 180 nmol, 26%).  $^1\text{H}$  NMR (600 MHz,  $\text{D}_2\text{O}$ ):  $\delta$  8.52 (s, 1H,  $\text{CH}_{\text{trz}}$ ), 8.17 - 8.08 (m, 6H, 6  $\times$   $\text{CH}_{\text{trz}}$ ), 7.80 (d,  $J$  = 8.3 Hz, 2H, 2  $\times$   $\text{CH}_{\text{ar}}$ ), 7.58 (s, 1H,  $\text{CH}_{\text{ar}}$ ), 7.23 (d,  $J$  = 3.6 Hz, 1H,  $\text{CH}_{\text{ar}}$ ), 7.12 (d,  $J$  = 8.4 Hz, 2H, 2  $\times$   $\text{CH}_{\text{ar}}$ ), 6.92 - 6.82 (m, 4H, 4  $\times$   $\text{CH}_{\text{ar}}$ ), 6.69 (d,  $J$  = 3.8 Hz, 1H,  $\text{CH}_{\text{ar}}$ ), 5.07 (s, 6H, 6  $\times$  H-1), 4.96 - 4.91 (m, 6H, 6  $\times$   $\text{CH}_2\text{-H}^a$ ), 4.76 (t,  $J$  = 10.9 Hz, 6H, 6  $\times$   $\text{CH}_2\text{-H}^b$ ), 4.59 - 4.46 (m, 13H, 6  $\times$   $\text{CH}_2$ , CH), 4.46 - 4.43 (m, 1H, CH), 4.41 - 4.31 (m, 6H, 6  $\times$  CH), 4.30 - 4.25 (m, 1H, CH), 4.25 - 4.17 (m, 8H, 6  $\times$  H-6,  $\text{CH}_2$ ), 4.15 - 4.11 (m, 2H,  $\text{CH}_2$ ), 4.08 - 3.99 (m, 18H, 6  $\times$  H-6, H-2, H-4), 3.91 (d,  $J$  = 9.7 Hz, 7H, 6  $\times$  H-3, CH), 3.86 (d,  $J$  = 1.7 Hz, 1H, CH), 3.80 (d,  $J$  = 9.5 Hz, 6H, 6  $\times$  H-5), 3.45 (d,  $J$  = 6.9 Hz, 2H,  $\text{CH}_2$ ), 3.34 - 3.28 (m, 2H,  $\text{CH}_2$ ), 3.25 - 2.90 (m, 18H, 9  $\times$   $\text{CH}_2$ ), 2.85 (d,  $J$  = 3.7 Hz, 2H,  $\text{CH}_2$ ), 2.58 - 2.50 (m, 7H, 2  $\times$   $\text{CH}_2$ ,  $\text{CH}_3$ ), 2.38 - 2.19 (m, 33H, 15  $\times$   $\text{CH}_2$ ,  $\text{CH}_3$ ), 1.93 - 1.06 (m, 90H, CH, 43  $\times$   $\text{CH}_2$ ,  $\text{CH}_3$ ), 0.95 (d,  $J$  = 6.0 Hz, 3H,  $\text{CH}_3$ ), 0.90 (d,  $J$  = 6.0 Hz, 3H,  $\text{CH}_3$ ).  $^{31}\text{P}$  NMR (162 MHz,  $\text{D}_2\text{O}$ ):  $\delta$  4.67 (very broad). LC/MS analysis (linear gradient 0%  $\rightarrow$  90% ACN)  $t_R$ : 6.41 min, ESI-MS ( $m/z$ ):  $[\text{M} + 3\text{H}]^{3+}$ : 1549.73. ESI-HRMS ( $m/z$ ): calcd. for  $[\text{C}_{185}\text{H}_{290}\text{BF}_2\text{N}_{43}\text{O}_{81}\text{P}_6 + 3\text{H}]^{3+}$  1549.62113; obsd. 1549.62215.



**Synthesis of BODIPY(FL)-DCG-04 (53).** DCG-04 amine (5.9 mg, 8.7  $\mu\text{mol}$ ), BODIPY(FL)-OSu (3.4 mg, 8.7  $\mu\text{mol}$ ) and DiPEA (1.6  $\mu\text{L}$ , 8.7  $\mu\text{mol}$ ) were dissolved in DMF (1 mL) and stirred for 2 h at room temperature. The product was crashed from  $\text{Et}_2\text{O}$ , collected and lyophilized to give the product as an orange powder (7.9 mg, 8.3  $\mu\text{mol}$ , 95%).  $R_f$  = 0.5 (10:1 DCM:MeOH).  $^1\text{H}$  NMR (600 MHz,  $\text{CDCl}_3/\text{MeOD}$ ):  $\delta$  7.22 (s, 1H,  $\text{CH}_{\text{ar}}$ ), 6.98 (d,  $J$  = 8.1 Hz, 2H, 2  $\times$   $\text{CH}_{\text{ar}}$ ), 6.92 (d,  $J$  = 3.8 Hz, 1H,  $\text{CH}_{\text{ar}}$ ), 6.70 (d,  $J$  = 8.1 Hz, 2H, 2  $\times$   $\text{CH}_{\text{ar}}$ ), 6.26 (d,  $J$  = 3.8 Hz, 1H,

$\text{CH}_{\text{ar}}$ ), 6.14 (s, 1H,  $\text{CH}_{\text{ar}}$ ), 4.43 (t,  $J$  = 7.4 Hz, 1H, CH), 4.38 (t,  $J$  = 7.0 Hz, 1H, CH), 4.33 - 4.17 (m, 3H,  $\text{CH}_2$ , CH), 3.64 (s, 1H,  $\text{CH}_{\text{epox}}$ ), 3.53 (s, 1H,  $\text{CH}_{\text{epox}}$ ), 3.22 (t,  $J$  = 7.6 Hz, 2H,  $\text{CH}_2$ ), 3.18 - 3.10 (m, 3H,  $\text{CH}_2$ ,  $\text{CH}_2\text{-H}^a$ ), 3.04 - 2.96 (m, 1H,  $\text{CH}_2\text{-H}^b$ ), 2.96 - 2.89 (m, 1H,  $\text{CH}_2\text{-H}^a$ ), 2.86 - 2.79 (m, 1H,  $\text{CH}_2\text{-H}^b$ ), 2.58 (t,  $J$  = 7.6 Hz, 2H,  $\text{CH}_2$ ), 2.51 (s, 3H,  $\text{CH}_3$ ), 2.25 (s, 3H,  $\text{CH}_3$ ), 2.17 (d,  $J$  = 8.7 Hz, 2H,  $\text{CH}_2$ ), 1.82 - 1.72 (m, 1H,  $\text{CH}_2\text{-H}^a$ ), 1.66 - 1.56 (m, 1H,  $\text{CH}_2\text{-H}^b$ ), 1.56 - 1.45 (m, 7H, 3  $\times$   $\text{CH}_2$ , CH), 1.38 - 1.24 (m, 7H,  $\text{CH}_3$ , 2  $\times$   $\text{CH}_2$ ), 1.14 - 1.09 (m, 2H,  $\text{CH}_2$ ), 0.90 - 0.84 (m, 6H, 2  $\times$   $\text{CH}_3$ ).  $^{13}\text{C}$  NMR (151 MHz,  $\text{CDCl}_3/\text{MeOD}$ ):  $\delta$  176.14, 175.22, 173.74, 172.57, 171.96, 167.99, 167.32, 160.81, 157.67, 156.32, 144.97, 135.82, 134.01, 130.80, 128.95, 128.03, 124.78, 120.99, 117.27, 115.84, 115.78, 62.91, 55.59, 54.01, 53.39, 52.85, 52.43, 41.17, 39.63, 39.47, 37.81, 36.22, 35.73, 32.07, 29.31, 29.07, 26.68, 25.77, 25.26, 25.20, 23.39, 23.09, 21.88, 14.99, 14.21, 11.37. ESI-HRMS ( $m/z$ ): calcd. for  $[\text{C}_{47}\text{H}_{65}\text{BF}_2\text{N}_8\text{O}_{10} + \text{H}]^+$  951.49575; obsd. 951.49761.

## References

- [1] Hoogendoorn, S.; van Puijvelde, G. H. M.; Kuiper, J.; van der Marel, G. A.; Overkleeft, H. S. contributed to the work described in this chapter.
- [2] Ghosh, P.; Dahms, N. M.; Kornfeld, S. *Nat. Rev. Mol. Cell Biol.* **2003**, *4*, 202–213.
- [3] Dennis, P. A.; Rifkin, D. B. *Proc. Natl. Acad. Sci. U. S. A.* **1991**, *88*, 580–584.
- [4] Motyka, B.; Korbitt, G.; Pinkoski, M. J.; Heibin, J. A.; Caputo, A.; Hobman, M.; Barry, M.; Shostak, I.; Sawchuk, T.; Holmes, C. F.; Gauldie, J.; Bleackley, R. C. *Cell* **2000**, *103*, 491–500.
- [5] Tong, P. Y.; Tollefsen, S. E.; Kornfeld, S. *J. Biol. Chem.* **1988**, *263*, 2585–2588.
- [6] Kang, J. X.; Li, Y.; Leaf, A. *Proc. Natl. Acad. Sci. U. S. A.* **1997**, *94*, 13671–13676.
- [7] Godár, S.; Hořejší, V.; Weidle, U. H.; Binder, B. R.; Hansmann, C.; Stockinger, H. *Eur. J. Immunol.* **1999**, *29*, 1004–1013.
- [8] Lobel, P.; Dahms, N.; Kornfeld, S. *J. Biol. Chem.* **1988**, *263*, 2563–2570.
- [9] Hancock, M. K.; Haskins, D. J.; Sun, G.; Dahms, N. M. *J. Biol. Chem.* **2002**, *277*, 11255–11264.
- [10] Chavez, C. A.; Bohnsack, R. N.; Kudo, M.; Gotschall, R. R.; Canfield, W. M.; Dahms, N. M. *Biochemistry* **2007**, *46*, 12604–12617.
- [11] Brown, J.; Delaine, C.; Zaccheo, O. J.; Siebold, C.; Gilbert, R. J.; van Boxel, G.; Denley, A.; Wallace, J. C.; Hassan, A. B.; Forbes, B. E.; Jones, Y. E. *EMBO J* **2007**, *27*, 265–276.
- [12] Roberts, D. L.; Weix, D. J.; Dahms, N. M.; Kim, J.-J. P. *Cell* **1998**, *93*, 639–648.
- [13] Olson, L. J.; Zhang, J.; Dahms, N. M.; Kim, J.-J. P. *J. Biol. Chem.* **2002**, *277*, 10156–10161.
- [14] Tong, P. Y.; Gregory, W.; Kornfeld, S. *J. Biol. Chem.* **1989**, *264*, 7962–7969.
- [15] Byrd, J. C.; Park, J. H.; Schaffer, B. S.; Garmroudi, F.; MacDonald, R. G. *J. Biol. Chem.* **2000**, *275*, 18647–18656.
- [16] Byrd, J. C.; MacDonald, R. G. *J. Biol. Chem.* **2000**, *275*, 18638–18646.
- [17] York, S. J.; Arneson, L. S.; Gregory, W. T.; Dahms, N. M.; Kornfeld, S. *J. Biol. Chem.* **1999**, *274*, 1164–1171.
- [18] Desnick, R. J.; Schuchman, E. H. *Nat. Rev. Genet.* **2002**, *3*, 954–966.
- [19] Fei, X.; Connelly, C. M.; MacDonald, R. G.; Berkowitz, D. B. *Bioorg. Med. Chem. Lett.* **2008**, *18*, 3085–3089.
- [20] Distler, J. J.; Guo, J.; Jourdain, G. W.; Srivastava, O. P.; Hindsgaul, O. *J. Biol. Chem.* **1991**, *266*, 21687–21692.
- [21] Christensen, M. K.; Meldal, M.; Bock, K.; Cordes, H.; Mouritsen, S.; Elsner, H. *J. Chem. Soc. Perkin Trans. 1* **1994**, 1299–1310.
- [22] Franzyk, H.; Christensen, M. K.; Jørgensen, R. M.; Meldal, M.; Cordes, H.; Mouritsen, S.; Bock, K. *Bioorg. Med. Chem.* **1997**, *5*, 21–40.
- [23] Ioannou, Y. A.; Bishop, D. F.; Desnick, R. J. *J. Cell Biol.* **1992**, *119*, 1137–1150.
- [24] Van Hove, J.; Yang, H. W.; Wu, J.-Y.; Brady, R. O.; Chen, Y.-T. *Proc. Natl. Acad. Sci. U. S. A.* **1996**, *93*, 65–70.
- [25] Hillaert, U.; Verdoes, M.; Florea, B.; Saragliadis, A.; Habets, K.; Kuiper, J.; Van Calenbergh, S.; Ossendorp, F.; van der Marel, G.; Driessen, C.; Overkleeft, H. *Angew. Chem. Int. Ed. Engl.* **2009**, *48*, 1629.
- [26] Rostovtsev, V. V.; Green, L. G.; Fokin, V. V.; Sharpless, K. B. *Angew. Chem. Int. Ed. Engl.* **2002**, *41*, 2596–2599.
- [27] Tornøe, C. W.; Christensen, C.; Meldal, M. *J. Org. Chem.* **2002**, *67*, 3057–3064.
- [28] Brix, K.; Dunkhorst, A.; Mayer, K.; Jordans, S. *Biochimie* **2008**, *90*, 194–207.
- [29] Greenbaum, D.; Medzihradzky, K. F.; Burlingame, A.; Bogyo, M. *Chem. Biol.* **2000**, *7*, 569–581.
- [30] Hoogendoorn, S.; Habets, K. L.; Passemard, S.; Kuiper, J.; van der Marel, G. A.; Florea, B. I.; Overkleeft, H. S. *Chem. Commun.* **2011**, *47*, 9363–9365.
- [31] Shepherd, V.; Freeze, H.; Miller, A.; Stahl, P. *J. Biol. Chem.* **1984**, *259*, 2257–2261.
- [32] Sallusto, F.; Cella, M.; Danielli, C.; Lanzavecchia, A. *J. Exp. Med.* **1995**, *182*, 389–400.
- [33] Greenbaum, D.; Baruch, A.; Hayrapetian, L.; Darula, Z.; Burlingame, A.; Medzihradzky, K. F.; Bogyo, M. *Mol. Cell. Proteomics* **2002**, *1*, 60–68.
- [34] Swarbrick, J. M.; Potter, B. V. *J. Org. Chem.* **2012**, *77*, 4191–4197.
- [35] Bergeron-Brlek, M.; Shiao, T. C.; Trono, M. C.; Roy, R. *Carbohydr. Res.* **2011**, *346*, 1479 – 1489.
- [36] Daly, R.; Vaz, G.; Davies, A. M.; Senge, M. O.; Scanlan, E. M. *Chem. Eur. J.* **2012**, *18*, 14671–14679.

# 6

## Structure-activity relationship studies towards functionalization of dihydropyridine FSHR agonists<sup>1</sup>

Low molecular weight agonists for the follicle-stimulating hormone receptor (FSHR) are promising lead candidates for profertility treatments. Dihydropyridine (DHP) ligands have been shown to be nanomolar potent, allosteric agonists for the FSHR. Modification of the DHP core to introduce a ligation handle for further conjugation to a fluorescent moiety or cytotoxic drug might enable selective targeting of fluorescent ligands or therapeutic agents to tissues that express the FSHR. A structure-activity relationship study to find the optimum positioning and length of an azide-containing spacer on the DHP core is presented, which resulted in the identification of a nanomolar potent FSHR agonist *m-74a*. Attachment of a bulky group (another DHP, peptide or fluorophore) to this monomeric ligand was shown to be possible with minor loss of potency. This study provides a strong basis for further employment of the DHP-agonist for targeting of the FSHR.

## 6.1 Introduction

G protein-coupled receptors (GPCRs) are a large family of heptahelical transmembrane receptors that respond to a variety of extracellular signals, such as odorants, pheromones, neurotransmitters and hormones. Upon binding of the ligand, a conformational change takes place in the receptor which leads to exchange of GDP to GTP on the  $\alpha$ -subunit of the trimeric G-protein bound to the receptor. This in turn enables the dissociation of the  $\alpha$ -subunit from the  $\beta/\gamma$ -subunits. Both parts of the G-protein induce a diverse array of downstream intracellular signaling events.<sup>2,3</sup>

The glycoprotein hormone receptors belong to the rhodopsin-like family of GPCRs and are characterized by a large N-terminal hormone-binding ectodomain.<sup>4</sup> The glycoprotein hormones, luteinizing hormone (LH), follicle-stimulating hormone (FSH), thyroid-stimulating hormone (TSH) and human chorionic gonadotropin (hCG), all share a common alpha subunit, but have a unique beta-subunit, which confers receptor-selectivity (except for LH and hCG that share a receptor).<sup>5</sup> The luteinizing hormone/choriogonadotropin receptor (LH/CGR) and the follicle-stimulating hormone receptor (FSHR) are the key receptors in regulating human reproduction,<sup>6-8</sup> whereas the thyroid-stimulating hormone receptor (TSHR) is important for thyroid function.<sup>9</sup> Current fertility treatments involve the use of recombinant FSH (rFSH), but drawbacks hereof are the heterogeneity of the protein preparation in terms of glycosylation and sialylation, the instability of the protein at higher temperatures and the lack of oral bio-availability. In addition, the long half-life of rFSH increases the risk of ovarian hyperstimulation syndrome when used in controlled ovarian stimulation protocols.

In the last years, research has been directed to the development of low molecular weight (LMW) ligands for the LH/CGR and FSHR as modulators of human fertility.<sup>10,11</sup> Several LMW agonists for the FSHR have been reported in the literature such as thienopyrimidines (also active on LHR),<sup>12</sup> thiazolidinones<sup>13-15</sup> and diketopiperazines.<sup>16,17</sup> Another class of FSHR agonists are the dihydropyridines (DHPs) that were reported by Organon in 2006.<sup>18</sup> In a recent publication by van Koppen *et al.*, the signaling properties of a member of this class of LMW ligands, Org 214444-0, were investigated. It was shown that this compound is a nanomolar potent agonist, selective for the FSHR over the LHR (>200-fold) and TSHR (>1000-fold). In addition, the compound binds to an allosteric site on the receptor and does not compete for FSH binding. Activation of the FSHR by this small molecule leads to increased levels of the second messenger cyclic AMP (cAMP) as shown by a CRE-luciferase assay and to production of estradiol in human granulosa cells. Stimulation of U2OS cells expressing an eGFP-tagged FSHR with this small molecule led to the translocation of the FSHR from the plasma membrane to intracellular vesicles, albeit with an  $EC_{50}$  value  $\sim 2$  orders of magnitude higher than that for the stimulation of cAMP. *In vivo* studies in rats showed that this compound has similar action as FSH in supporting the follicular phase.<sup>19</sup>

The research described in this chapter, as well as in Chapters 7 and 8 involves the synthesis and biological evaluation of a variety of DHP analogues. As schematically depicted

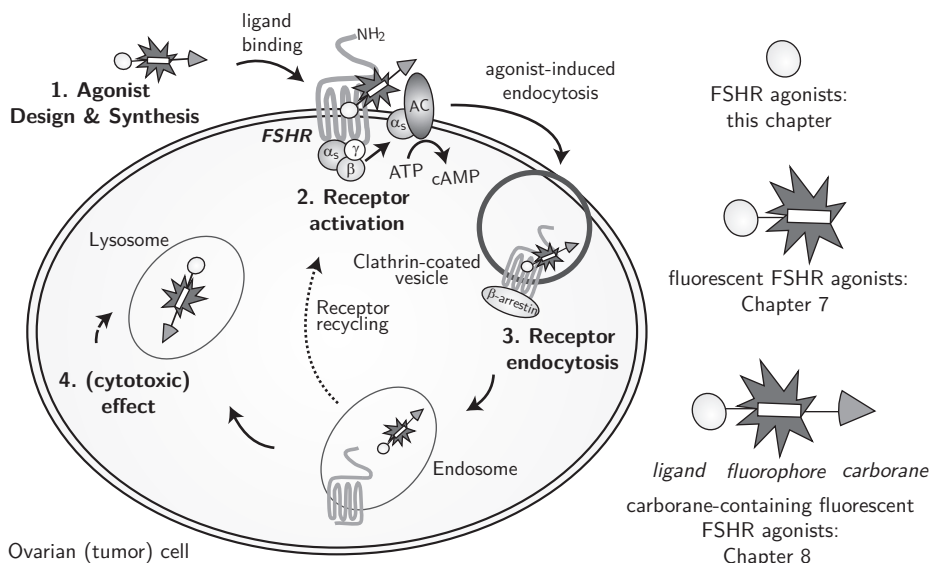


**Figure 6.1: Proposed agonist-induced internalization of the FSHR as a means of selective drug targeting.** Upon binding of the ligand, the receptor is activated which ultimately leads to internalization of the receptor-ligand complex, thereby delivering the agent for boron neutron capture therapy (BNCT) into the FSHR expressing cells. Synthesis and evaluation of agonists with a conjugation handle will be discussed in this chapter, followed by fluorescent agonists in Chapter 7 and carborane-containing fluorescent agonists in Chapter 8.

In Figure 6.1, the ultimate goal is to arrive at ligands that are taken up into the endocytic pathway of cells that express the FSHR. Since the expression of the FSHR in mammals is limited to the ovaries (in females) and the testis (in males),<sup>20</sup> this could provide a very selective targeting methodology for these tissues. Furthermore, the presence of the FSHR on blood vessels that are formed by tumor angiogenesis implicates the FSHR as potential tumor marker.<sup>21</sup> Fluorescent ligands for the FSHR could therefore be used as diagnostic tools, whereas attachment of a cytostatic drug to the DHP targeting ligand could allow for targeted anti-cancer therapy of, for example, ovarian tumors. These possibilities will be examined in Chapters 7 and 8, respectively.

Alterations of a small molecule, such as the incorporation of a fluorescent tag or drug, can result in big changes in its ability to bind to and activate receptors. So thorough pharmacological evaluation of the final constructs for their agonistic potencies on the FSHR is a requirement. This chapter explores a potential structure-activity relationship for the incorporation of a ligation handle onto the DHP 55 core. A general overview of the compounds that are presented in this chapter (as well as Chapters 7 and 8) is shown in Figure 6.2. The synthesis of four different analogues is described, followed by the attachment of a PEG spacer of varying length ( $n=3$ ,  $n=4$ ). The resulting azide-containing monomeric ligands are further conjugated to another FSHR agonist to provide dimeric ligands or to a BODIPY dye to give a first series of fluorescent ligands. All synthesized compounds are evaluated for their ability to activate the FSHR in a CRE-luciferase assay.



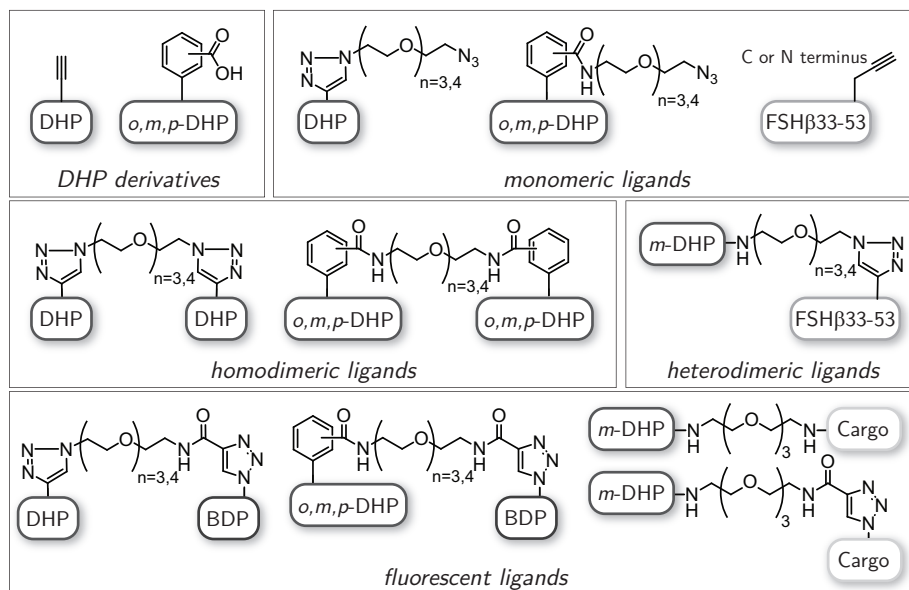


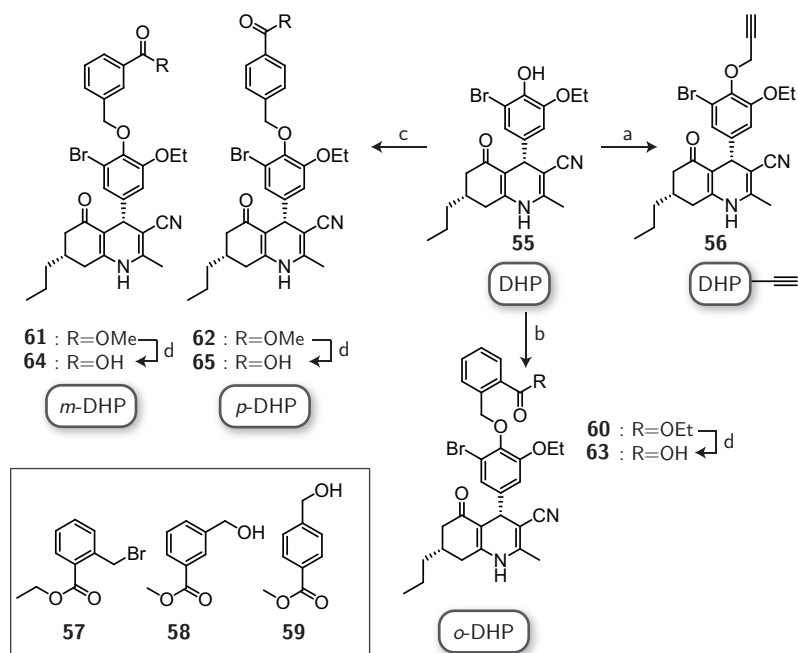
**Figure 6.2: General overview of the low molecular weight FSHR agonists described in this thesis.** Detailed structures can be found in Scheme 6.1, Scheme 6.2 and Scheme 6.3. Fluorescent (carborane-containing) agonists will also be discussed in Chapters 7 and 8.

## 6.2 Results and Discussion

**Synthesis.** Lead compound DHP **55**<sup>18</sup> was the starting point for all synthetic routes. Direct substitution with propargyl bromide resulted in the first derivative **56** (Scheme 6.1). The second set of analogues required *ortho*-, *meta*-, and *para*-hydroxymethyl benzoate esters for use in a DIAD/ $\text{PPh}_3$  mediated Mitsunobu reaction with DHP **55**. *Meta*- and *para*-esters **58** and **59** (Scheme 6.1) were readily obtained and used in the Mitsunobu reaction. The *ortho*-variant, however, proved unattainable due to an intramolecular esterification reaction to the more stable phthalide. Therefore ethyl 2-(bromomethyl)benzoate **57**<sup>22</sup> was used in a nucleophilic substitution reaction instead. Separation of esters **60**, **61** and **62** from unreacted starting material **55** proved difficult in this stage, but after saponification using sodium hydroxide, pure *o,m,p*-derivatives **63**, **64**, **65** were isolated. The dihydropyridine scaffold was found to be easily oxidized to the corresponding pyridine under aerobic conditions, and although these molecules were separable by column chromatography, anaerobic conditions during synthesis are recommended to keep yields high. It is important to note that the corresponding pyridine analogues do not exhibit FSHR agonistic activity.

With four analogues of DHP **55** in hand, monomeric, dimeric and fluorescent ligands could be synthesized. As shown in Scheme 6.2, compound **56** was used in a Cu(I)-catalyzed [2+3] Huisgen-cycloaddition ('click' reaction)<sup>23,24</sup> with PEG-spacers  $n = 3$  (**66a**) or  $n = 4$  (**66b**) to give monomeric ligands **67a,b** when an excess of spacer was used and predom-



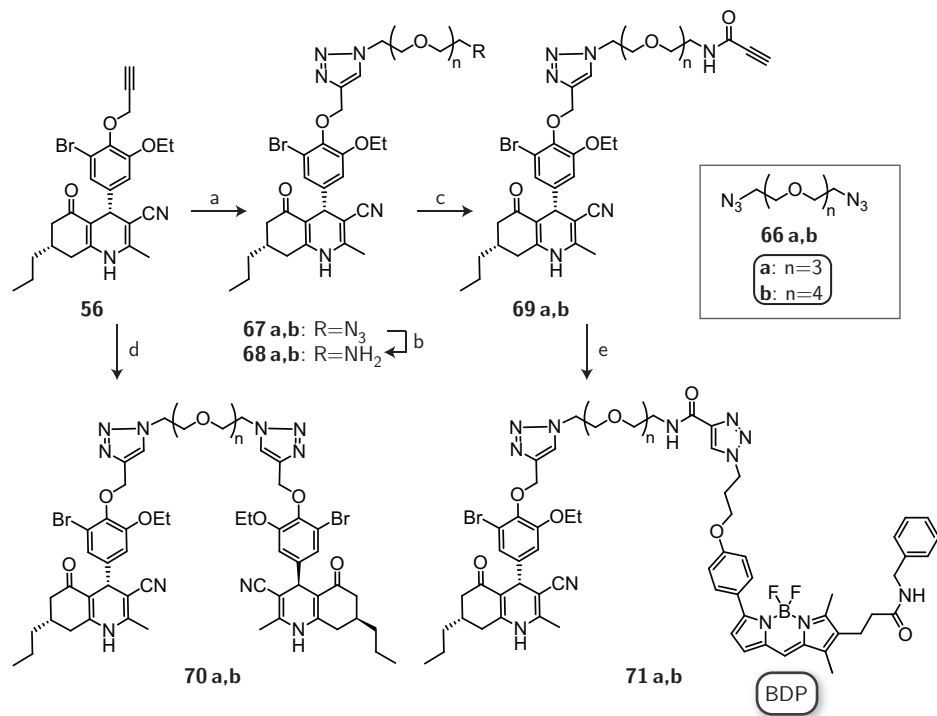
**Scheme 6.1:** Functionalization of the lead compound DHP **55**.

Reagents and conditions: [a]  $K_2CO_3$ , propargyl bromide, acetone, reflux, 75%; [b]  $K_2CO_3$ , ethyl 2-(bromomethyl)benzoate **57**, acetone, reflux; [c] hydroxymethylbenzoate **58** or **59**,  $PPh_3$ , DIAD, THF, *p*-**62**: 50%; [d] MeOH, NaOH, 40 °C, *o*-**63**: 52% (2 steps), *m*-**64**: 65% (2 steps), *p*-**65**: 85%.

inantly dimeric ligands **70a,b** when 0.5 eq of spacer was used. Staudinger reduction of the monomeric azides **67a,b** with  $PPh_3$ , followed by EEDQ-coupling<sup>25</sup> of the primary amine with propiolic acid yielded alkyne ligands **69a,b** in good yields. Pre-activation of propiolic acid in the presence of other coupling agents than EEDQ resulted in rapid degradation as seen by the change in color of the solution from colorless to almost black. Click reaction of alkynes **69a,b** with azido-BODIPY-benzyl,<sup>26</sup> resulted in the first set of fluorescent ligands **71a,b** in 93% and 71% yield, respectively.

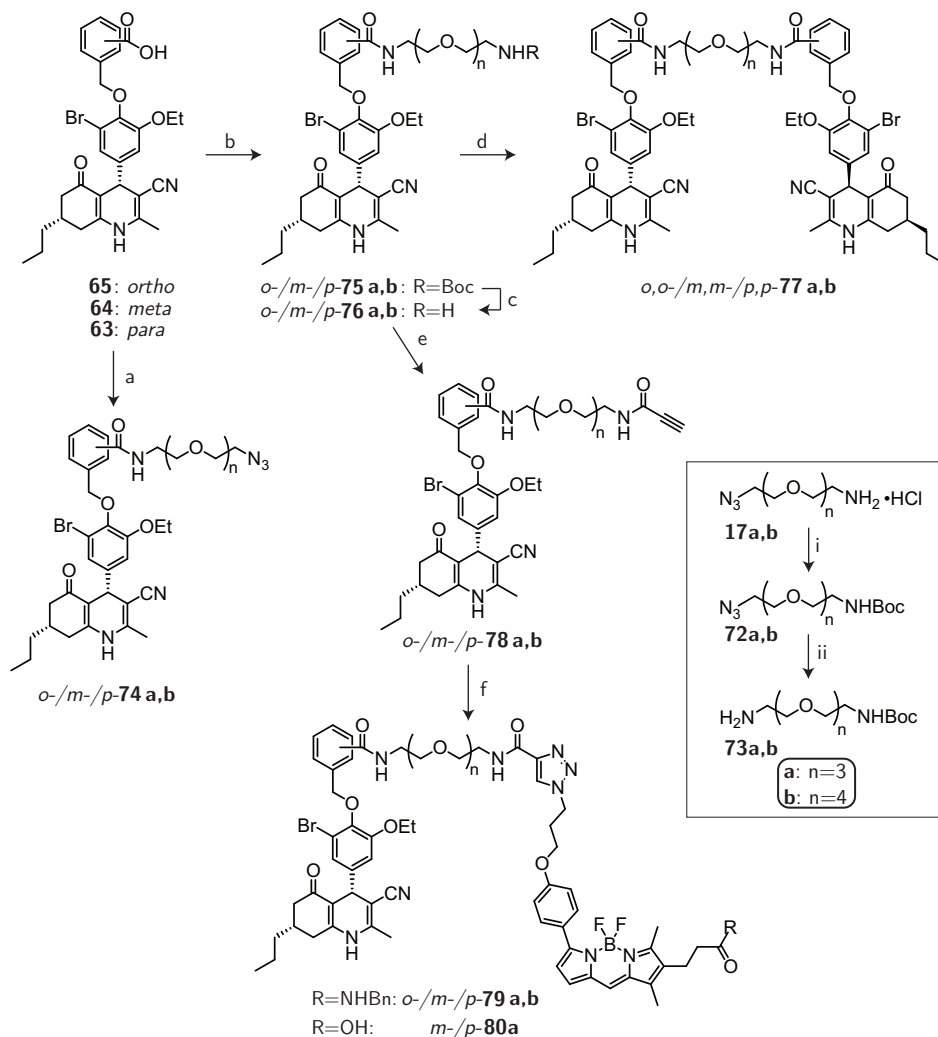
In case of *o,m,p*-substituted derivatives **63-65**, mono-amino PEG spacers  $n=3$  or  $n=4$ , were coupled to the carboxylic acid using EEDQ (Scheme 6.3). For this, bisazido-PEG spacers **66a,b** were mono-reduced using  $PPh_3$  in a two-phase system of toluene and 5% aq HCl, resulting in the HCl salt of spacers **17a,b** in good yield. Coupling of spacers **17a,b** with *o,m,p*-substituted DHPs resulted in the formation of azido-monomeric ligands *o*-/*m*-/*p*-**74a,b** in 74-91% yield. Analogous to the route described in Scheme 6.2, Staudinger reduction of the azide was attempted to obtain the primary amine **76**. Because reaction progress was slow and isolated yields were low as a result of significant byproduct formation, a different approach towards the amine was followed, as depicted in Scheme 6.3. Spacers **17** were reacted with  $Boc_2O$  resulting in mono-protected azido-spacers **72** which were again subjected to  $PPh_3$  to reduce the remaining azide. Coupling of mono-protected

**Scheme 6.2:** Synthesis of monomeric, dimeric and fluorescent ligands based on propargyl - functionalized DHP.



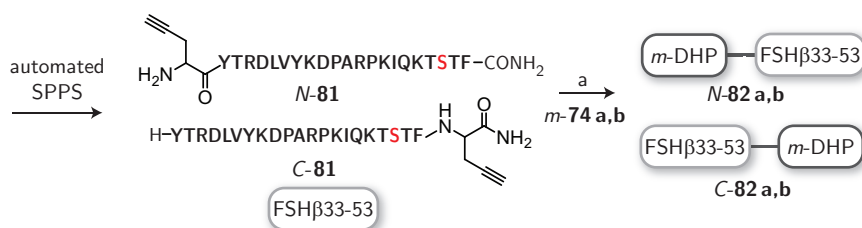
Reagents and conditions: [a] Diazido-spacer **66 a** or **66 b**, CuSO<sub>4</sub>, sodium ascorbate, *t*-BuOH/ACN/H<sub>2</sub>O, **67a**: 72%, **67b**: 92%; [b] PPh<sub>3</sub>, THF/H<sub>2</sub>O, **68a**: 66%, **68b**: 62%; [c] propionic acid, EEDQ, DCM, **69a**: 71%, **69b**: 81%; [d] Diazido-spacer **66 a** or **66 b**, CuSO<sub>4</sub>, sodium ascorbate, *t*-BuOH/ACN/H<sub>2</sub>O, **70a**: 50% + 42% monomer **67a**, **70b**: 48% + 26% monomer **67b**; [e] azido-BODIPY-benzyl, CuSO<sub>4</sub>, sodium ascorbate, *t*-BuOH/ACN/H<sub>2</sub>O, **71a**: 93%, **71b**: 71%.

diamino-PEG spacers **73a,b** to *ortho*-, *meta*- or *para*-acids **63-65**, resulted in Boc-protected intermediates *o*-/*m*-/*p*-**75a,b** in good yields. The Boc-group was easily removed with TFA to yield amine ligands *o*-/*m*-/*p*-**76a,b**. For the synthesis of homodimeric ligands, these were coupled to *o,m,p*-DHPs **63-65**, using EDC · HCl and HOBT as the coupling agents. Isolated yields for this reaction dropped because of the presence of two oxidizable core structures, giving rise to mono- and di-oxidized dimer byproducts. Alternatively, amines **76** were coupled to propionic acid using EEDQ, resulting in terminal alkynes **78a,b** that were used in a click reaction with azido-BODIPY-benzyl,<sup>26</sup> to yield the second set of fluorescent ligands **79a,b**. As discussed below, biological evaluation showed that *meta*- or *para*-substituted derivatives with spacer length *n*=3 were the most potent of the series. Therefore a third set of fluorescent ligands was synthesized based on these two compounds. Click reaction of *m*-/*p*-**78a** with azido-BODIPY-acid **88**<sup>27</sup> (see also Chapter 7) yielded compounds *m*-/*p*-**80** with a free carboxylic acid instead of a benzylamide on the BODIPY dye, with the aim to reduce the lipophilicity of the compounds.

**Scheme 6.3:** Synthesis of monomeric, dimeric and fluorescent ligands based on *ortho*-, *meta*- and *para*- functionalized DHP.

Scheme 6.4 shows the synthesis of heterodimeric ligands, based on the FSH $\beta_{33-53}$  peptide, which has been used as an FSH-derived agonist.<sup>28</sup> This peptide was synthesized using automated solid-phase peptide synthesis (SPPS), with incorporation of an N- or C-terminal propargylglycine for subsequent ligation to the LMW ligand. Attachment of DHP to either terminus of the peptide might interfere with binding of the peptide to the receptor, so both options were included to enhance the chance of finding an active heterodimer. The naturally occurring cysteine in the sequence was replaced by a serine, to prevent the formation of peptide-dimers.<sup>28</sup> Peptides C-,N-**81** were reacted with azido-monomeric ligands *m*-**74a,b** in a Cu(I)-catalyzed click reaction and purified by size-exclusion chromatography to give the four envisaged heterodimeric FSH $\beta_{33-53}$ -DHP ligands **82**.

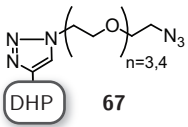
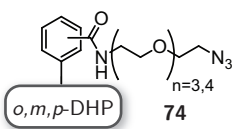
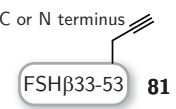
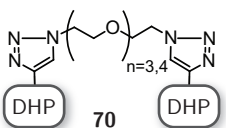
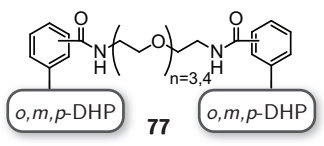
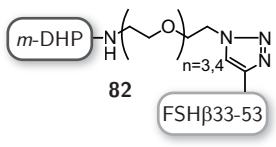
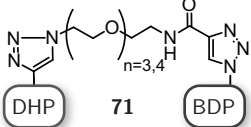
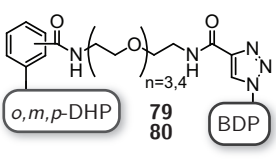
**Scheme 6.4:** Synthesis of heterodimeric FSH $\beta_{33-53}$ -DHP ligands



Reagents and conditions: [a] Azide *m*-**74a** or **b**, CuSO<sub>4</sub>, sodium ascorbate, dioxane/H<sub>2</sub>O, *N*-**82a**: 69%, *N*-**82b**: 50%, *C*-**82a**: 51%, *C*-**82b**: 69%.

**Biological evaluation.** All compounds were evaluated for their potency to activate the human FSH receptor. A CHO cell line stably expressing human FSHR (hFSHR), together with a CRE-luciferase reporter gene was used for this purpose. Recombinant FSH (200 pM, rFSH) was included in the assay and the response was normalized against the maximal effect obtained for rFSH. The pEC<sub>50</sub> values obtained from the dose-response curves were used to calculate EC<sub>50</sub> values (the concentration at which half-maximum stimulation is observed), shown in Table 6.1. The objective was to get more insight in a possible structure-activity relationship (SAR) for the various modifications on the lead compound DHP **55** (Scheme 6.1). The first variation that was introduced was the way in which the spacer was attached to the DHP core; either directly via a triazole moiety or indirectly by installment of an additional phenyl group containing an *o*, *m*, *p*-carboxylic acid handle. This was then used to connect the ligand to the spacer via an amide bond. The second variation concerned the length of the PEG-spacer, with either n=3 or n=4 ethylene glycol units. Large differences in potency were found for the monomeric DHP ligands (Table 6.1). Direct functionalization of DHP as for ligands **67** resulted in poor agonists with EC<sub>50</sub> values of 300-500 nM. Also, *ortho*-functionalized monomeric ligands *o*-**74** were ~10-fold less potent than the best agonist of the series. *Meta*- or *para*- substitution did not result in big differences. Overall, compounds with spacer length n=3 proved to be slightly better agonists than those with linker n=4. Both *para*- and *meta*-**74a** were shown to be low nanomolar potent agonists for the FSHR.

**Table 6.1:** Mean agonistic potency ( $EC_{50}$ ) values of monomeric, dimeric and fluorescent DHP analogues.

|   | spacer (n)      | $EC_{50}$ (nM) | p $EC_{50}$ | N           |    |
|---|-----------------|----------------|-------------|-------------|----|
| <i>Monomeric ligands</i>  |                 |                |             |             |    |
| <br>DHP <b>67</b>                              | <b>67a</b>      | n = 3          | 269         | 6.57        | 1  |
|   | <b>67b</b>      | n = 4          | 490         | 6.31        | 1  |
| <br><i>o,m,p</i> -DHP <b>74</b>                | <i>o</i> -74a   | n = 3          | 54          | 7.27 ± 0.05 | 1  |
|   | <i>o</i> -74b   | n = 4          | 100         | 7.00        | 1  |
|   | <i>m</i> -74a   | n = 3          | 6.0         | 8.22 ± 0.10 | 3  |
|   | <i>m</i> -74b   | n = 4          | 7.8         | 8.11 ± 0.08 | 3  |
|   | <i>p</i> -74a   | n = 3          | 8.3         | 8.08        | 1  |
|   | <i>p</i> -74b   | n = 4          | 14          | 7.86        | 1  |
| <br>C or N terminus<br>FSHβ33-53 <b>81</b>     | N-81            | -              | N.A.        | N.A.        | 2  |
|   | C-81            | -              | N.A.        | N.A.        | 2  |
| <i>Homodimeric ligands</i>  |                 |                |             |             |    |
| <br>DHP <b>70</b>                              | <b>70a</b>      | n = 3          | 2.1 μM      | 5.67        | 1  |
|   | <b>70b</b>      | n = 4          | 4.5 μM      | 5.35        | 1  |
| <br><i>o,m,p</i> -DHP <b>77</b>               | <i>o,o</i> -77a | n = 3          | 501         | 6.30        | 1  |
|   | <i>o,o</i> -77b | n = 4          | 724         | 6.14        | 1  |
|   | <i>m,m</i> -77a | n = 3          | 48          | 7.32 ± 0.10 | 3  |
|   | <i>m,m</i> -77b | n = 4          | 59          | 7.23 ± 0.10 | 3  |
|   | <i>p,p</i> -77a | n = 3          | 76          | 7.12        | 1  |
|   | <i>p,p</i> -77b | n = 4          | 102         | 6.99        | 1  |
| <i>Heterodimeric ligands</i>  |                 |                |             |             |    |
| <br><i>m</i> -DHP <b>82</b>                  | N-82a           | n = 3          | 10          | 7.98 ± 0.11 | 3  |
|   | N-82b           | n = 4          | 9.8         | 8.01 ± 0.13 | 3  |
|   | C-82a           | n = 3          | 8.7         | 8.06 ± 0.07 | 3  |
|   | C-82b           | n = 4          | 8.7         | 8.06 ± 0.11 | 3  |
| <i>fluorescent ligands</i>  |                 |                |             |             |    |
| <br>DHP <b>71</b>                            | <b>71a</b>      | n = 3          | 5.0 μM      | 5.30        | 1  |
|   | <b>71b</b>      | n = 4          | 2.4 μM      | 5.62        | 1  |
| <br><i>o,m,p</i> -DHP <b>79</b><br><b>80</b> | <i>o</i> -79a   | n = 3          | 912         | 6.04        | 1  |
|   | <i>o</i> -79b   | n = 4          | 1.5 μM      | 5.83        | 1  |
|   | <i>m</i> -79a   | n = 3          | 83          | 7.08 ± 0.07 | 4  |
|   | <i>m</i> -79b   | n = 4          | 105         | 6.98        | 1  |
|   | <i>p</i> -79a   | n = 3          | 100         | 7.00 ± 0.01 | 2  |
|   | <i>p</i> -79b   | n = 4          | 427         | 6.37        | 1  |
|   | <i>m</i> -80a   | n = 3          | 26          | 7.58 ± 0.07 | 12 |
|   | <i>p</i> -80a   | n = 3          | 21          | 7.67        | 1  |

The mean  $EC_{50}$  values are calculated from the p $EC_{50}$  (mean ± SEM) values from  $N$  independent experiments performed in duplicate. N.A. not active at 100 μM.

In contrast to earlier reports, FSH $\beta_{33-53}$  peptides **81** did not show any agonistic activity up to 100  $\mu\text{M}$  concentrations.<sup>28</sup> The predicted FSHR binding sequences in this peptide are the TRDL (aa 34-37) and KTCT (aa 49-52) residues, which are unmodified in the here described peptide, except for the cysteine residue.<sup>29</sup> It is unlikely that the cysteine to serine modification lies at the basis of this result, because the study of Santa Coloma *et al.* employed a carboxymethylated variant of the peptide which showed the same potency as the free cysteine.<sup>28</sup> In a study by Zhang *et al.*, the cysteine residue was used as a ligation handle for a fluorophore, without loss of receptor binding.<sup>30</sup> The additional propargyl glycine residue could have an influence on the agonistic potency of the peptide, which is why both C- and N-terminal modified peptides were synthesized. Since a C-terminal extended peptide is described without loss of potency, the additional residue was not expected to have a significant effect.<sup>31</sup> Most of the previous reports have used <sup>125</sup>I-FSH binding displacement, <sup>125</sup>I-FSH $\beta_{33-53}$  binding or estradiol biosynthesis in Sertoli cells as the biochemical readout for agonistic activity of these peptides, which differ from the here used luciferase assay and might lead to different EC<sub>50</sub> values.<sup>28,31</sup> For solubility reasons, no concentrations higher than 100  $\mu\text{M}$  were used in the assay, but it is possible that effects would be visible at higher concentrations of peptide. Future experiments could include circular dichroism (CD) measurements to be able to compare the structures of the peptides described here with those previously reported.

The classical view of a single receptor that is activated by a single ligand has been opposed by a large amount of studies addressing the homo- or heterodimerization and even higher oligomerization of GPCRs.<sup>32-34</sup> The crystal structure of the hormone binding domain of the FSHR (FSHR<sub>HB</sub>) in complex with FSH has been determined by Fan and Hendrickson and they reported the presence of dimers in the crystal.<sup>35</sup> With the use of bivalent ligands, containing two copies of a receptor binding ligand, the occurrence and pharmacological properties of these receptor dimer complexes can be studied. In some cases, dimeric ligands show enhanced potency compared to monomeric ligands.<sup>36,37</sup> Figure 6.3 shows possible modes of bivalent binding of dimeric ligands, either to two copies of the receptor or to two different binding sites on the same receptor. Homodimeric ligands, consisting of two copies of either *o*-, *m*- or *p*- substituted DHP, were assessed for their potency on the FSH receptor. As shown in Table 6.1, EC<sub>50</sub> values for dimers were 7-10-fold higher than for the monomers. However, the same structure-activity relationship could be deduced, with direct functionalized DHP ligands **70** being the poorest activators and *m,m*-**77a** (n=3) the best agonist. Surprisingly, heterodimeric FSH $\beta_{33-53}$ -*m*-DHP ligands **82** all showed potencies around 10 nM, which is comparable to the values found for the monomers. These dimers were designed to potentially bind the receptor as shown in Figure 6.3B, because the binding site of the peptide is believed to be in the ectodomain of the receptor, whereas the low molecular weight DHP ligand binds to an allosteric site in the transmembrane domain.<sup>19,28</sup> No differences were found in terms of spacer length (**82a** vs **b**) or orientation of the peptide and DHP (**82 N**- vs **C**-), which, especially in combination with the inactivity of precursor peptides **81** in the luciferase assay, makes a dual interaction with the receptor

unlikely. No conclusion can be drawn whether it is a bivalence effect which explains the difference in potency between hetero- and homo-dimeric ligands. Alternatively, it could be that the spatial orientation of the peptide is such that there is enough room outside the DHP-binding site in the receptor to accommodate it without loss of binding affinity, whereas the second DHP ligand might have negative (steric) interaction with the receptor. Bongers *et al.* previously reported a series of dimeric FSHR antagonists based on the low molecular tetrahydroquinoline (THQ) scaffold.<sup>38</sup> These dimeric ligands also showed a significant loss of potency upon dimerization of the ligand. The loss of potency found for both the THQ-dimeric antagonists and DHP-dimeric agonists, but not (or less) for THQ heterodimers containing one inactive copy of the ligand or DHP-peptide heterodimers (where the peptide monomer was also inactive), might be explained by a negative cooperativity effect. Upon binding of one of the ligands, the affinity for the second ligand to the receptor (dimer) is decreased.<sup>38,39</sup> However, more research is needed to fully elucidate the behavior of these dimeric ligands.

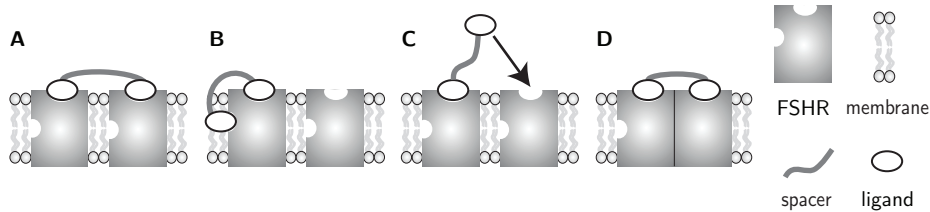


**Figure 6.3: Different modes of bivalent binding of dimeric ligands.** A) Binding of neighbouring receptors. B) Binding of two separate sites on a receptor monomer. C) Enhanced local concentration upon binding of one of the ligands. D) Ligand-induced receptor dimerization.

From the various dimeric structures it can be concluded that attachment of bulk to the DHP-ligand not necessarily leads to detrimental effects on its agonistic activity towards the FSHR. This strengthens the hypothesis that this low molecular weight ligand could be used as a targeting device to deliver cargo to cells expressing the FSH receptor. The next series of fluorescent ligands that was synthesized explored this concept further and completed the structure-activity relationship studies. Addition of azido-BODIPY-benzyl to the various monomeric ligands led to a decrease in potency that was slightly larger than that found for the homodimeric compounds. Again, spacer  $n=3$  gave somewhat better results than spacer  $n=4$  and *meta*- and *para*-substituted DHPs were superior over *ortho*-substitution or direct functionalization. In an attempt to increase the hydrophilicity of the compounds, the benzyl group of the BODIPY was removed to give the carboxylic acid (*m*-/*p*-**80a**). This resulted in a 3-4-fold increase in potency compared to compounds *m*-/*p*-**79** and resulted in fluorescent agonists of the FSHR with  $\sim 20$ - $30$  nM potency. To have a better estimate of  $EC_{50}$  values and allow comparison to the compounds in Chapters 7 and 8, luciferase assays for all *meta*-substituted ligands were repeated and *meta* substitution in combination with a PEG spacer of length  $n=3$  (*m*-/**129a**) was chosen as the lead molecule for all subsequent structural variants.

## 6.3 Conclusion

Even small synthetic modifications of a low molecular weight ligand can have large effects on its pharmacological properties. The aim of this chapter was to deduce a structure-activity relationship for possible modifications of the FSHR agonist, DHP **55**. The first objective was to find the optimal positioning on the DHP core and length of a spacer containing a ligation handle for further conjugation. The second objective was to investigate whether homo- or heterodimerization of DHP would lead to enhanced agonistic potencies. The third objective was closely related to the second, namely to examine the change in potency upon attachment of steric bulk to the DHP ligand. Four different derivatives with two different spacer lengths were designed and synthesized and further conjugated to another DHP (homodimers), an FSH $\beta_{33-53}$  peptide (heterodimers) or a fluorescent BO-DIPY dye. From the luciferase assays it became apparent that direct functionalization of the DHP or incorporation of an *ortho*-substituted phenyl ring led to a drastic decrease in agonistic potency. The use of PEG spacers with three ethylene glycol units ( $n=3$ ) led to better agonists than the longer  $n=4$  spacers. *Meta*- and *para*-substituted DHPs of all series were comparable, with a slight lead for the *meta*-compounds. Overall, it can be concluded that *meta*-substituted compounds with attachment of a PEG  $n=3$  spacer are the most promising lead candidates for future studies, such as described in Chapters 7 and 8. The dimeric ligands described in this chapter did not show enhanced potency compared to the monomeric ligands, although the heterodimers were still very potent agonists. No evidence was found that supported a bivalent interaction between these ligands and the receptor (dimer). While attachment of bulk, either a fluorophore or another DHP, in most cases led to a decrease in potency, fluorescent agonists with an  $EC_{50}$  of 20-30 nM were obtained. In conclusion, a ligation handle was successfully introduced onto the DHP core with only minor loss of agonistic potency compared to the lead compound. Attachment of a fluorophore or peptide to this ligation handle resulted in functionalized FSH ligands while preserving the agonistic activity. These insights will contribute to the development of DHP-based constructs as a means of targeted delivery to cells expressing the FSH receptor.

## 6.4 Experimental Section

**Cell culture conditions.** CHO cells stably expressing the human FSH receptor together with a luciferase reporter gene (CHO-hFSHR\_luc cells) and control cells without receptor but with luciferase gene (CHO\_luc cells) were provided by MSD, Oss, The Netherlands. Cells were cultured in Dulbecco's Modified Eagle's Medium (DMEM) and Ham's F12 medium (1:1) with glutamine, penicillin/streptomycin (0.1 mg/mL) and fetal calf serum (FCS) (5%) in a humidified atmosphere at 37 °C and 5% CO<sub>2</sub>. CHO-hFSHR\_luc cells were maintained under constant selection with Hygromycin B (0.8 mg/mL). Cells were subcultured twice weekly at a ratio of 1:10-1:15.

**Measurement of CRE-induced luciferase expression.** Protocol 1- Initial screening of compounds was



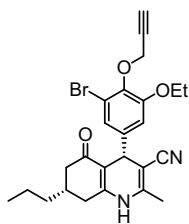
done at MSD, Oss, the Netherlands according to the following protocol: On the day of the experiment, frozen CHO-hFSHR\_luc or CHO\_luc cell aliquots were thawed, washed with assay medium (Dulbecco's MEM/Nutrient Mix F12 supplemented with 1 mg/L bovine insulin (Sigma), 5 mg/L apo-transferrin (Sigma), penicillin G (100 units/mL) and streptomycin (0.1 mg/mL)) and then resuspended in assay medium. The compounds were tested in duplicate at 10 concentrations ranging from final concentrations of 10  $\mu$ M to 0.316 nM with half log intervals. In the agonistic assays, 10  $\mu$ L of assay medium containing test compound and 3% DMSO, 10  $\mu$ L of assay medium containing 3% DMSO with rFSH (final concentration of 200 pM) or 10  $\mu$ L of assay medium containing 3% DMSO alone were added to the wells of a 384-well white culture plate followed by the addition of 10  $\mu$ L of assay medium. Then, 10  $\mu$ L of cell suspension containing 7,500 cells was added to the wells. The final concentration of DMSO was 1%. After incubation for 4 h in a humidified atmosphere in 5% CO<sub>2</sub> at 37 °C, plates were allowed to adjust to room temperature for 1 h. Then, 15  $\mu$ L of Steadylite solution (PerkinElmer) was added to the incubation mixture. Following 60 min at room temperature in the dark, luciferase activity was measured in an Envision 2102 multilabel reader (PerkinElmer). Agonistic effects of the compounds were determined as percentage of the (maximal) effect induced by rFSH. Data analysis and curve fitting was done with GraphPad Prism 5 (GraphPad Software, La Jolla, USA).

Protocol 2 - The most potent compounds as determined from the initial screen were re-tested using the following protocol: CHO\_luc or CHO-hFSHR\_luc cells were cultured to ~80% confluency before use in the assay. On the day of the experiment, cells were harvested using enzyme-free dissociation solution (Millipore), counted (Biorad TC10 automated cell counter) and resuspended in assay medium (DMEM-F12 (1:1), without phenol-red, with pen/strep (100  $\mu$ g/mL) supplied with 1  $\mu$ g/mL bovine insulin (Tebu-Bio) and 5  $\mu$ g/mL human apo-transferrin (Sigma)) to a concentration of  $7.5 \times 10^5$  cells/mL. Experiments were conducted in 96-wells white Optiplates (Perkin Elmer) and each well contained 30  $\mu$ L of test compound, recombinant FSH (200 pM, positive control) or assay medium (negative control), 30  $\mu$ L of assay medium and 30  $\mu$ L cell suspension. Final concentration of DMSO was 1% for all compounds, including controls. After 4 h of stimulation, 50  $\mu$ L Neolite (PerkinElmer) was added to each well and luminescence signal was detected on a Microbeta Trilux 1450 Luminescence Counter (PerkinElmer). To control for non-FSHR mediated effects on luciferase activity, highest compound concentrations used in the dose-response experiments were tested on CHO\_luc cells. As a positive control, forskolin (3  $\mu$ M, gift from the Medicinal Chemistry department, Leiden University) was included. Data was analyzed using GraphPad Prism 5 (GraphPad Software, La Jolla, USA), and values were normalized to the maximal effect obtained for recombinant human FSH (200 pM, rFSH, Org32489, gift from MSD, Oss, The Netherlands). Each experiment was performed on duplicate plates and mean  $\pm$  SEM values of at least three independent experiments are given.

## Synthesis

**General.** All reagents were of commercial grade and used as received unless stated otherwise. Reaction solvents were of analytical grade and when used under anhydrous conditions stored over flame-dried 3 Å molecular sieves. Dichloromethane was distilled over CaH<sub>2</sub> prior to use. Solvents used for column chromatography were of technical grade and distilled before use. All moisture and oxygen sensitive reactions were performed under an argon atmosphere. Flash chromatography was performed on silica gel (Screening Devices BV, 0.04-0.063 mm, 60 Å). Reactions were routinely monitored by TLC analysis on DC-alufolien (Merck, Kieselgel60, F254) with detection by UV-absorption (254/366 nm) where applicable and spraying with a solution of (NH<sub>4</sub>)<sub>6</sub>Mo<sub>7</sub>O<sub>24</sub> · 4 H<sub>2</sub>O (25 g/l) and (NH<sub>4</sub>)<sub>4</sub>Ce(SO<sub>4</sub>)<sub>4</sub> · 2 H<sub>2</sub>O (10 g/l) in 10% sulfuric acid in water followed by charring at ~150 °C. <sup>1</sup>H and <sup>13</sup>C NMR spectra were recorded on a Bruker AV-400 (400 MHz) or Bruker DMX-600 (600 MHz). Chemical shifts are given in ppm ( $\delta$ ) relative to the residual solvent peak or TMS (0 ppm) as internal standard. Coupling

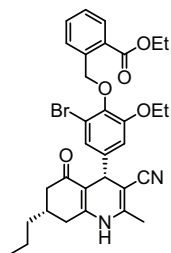
constants are given in Hz. Peak assignments are based on 2D  $^1\text{H}$ -COSY and  $^{13}\text{C}$ -HSQC NMR experiments. IR measurements (thin film) were conducted on an IRAffinity-1 apparatus and evaluated using IRSolutions software (Shimadzu, Kyoto, Japan). LC-MS measurements were conducted on a Thermo Finnigan LCQ Advantage MAX ion-trap mass spectrometer (ESI+) coupled to a Surveyor HPLC system (Thermo Finnigan) equipped with a standard C18 (Gemini, 4.6 mmD  $\times$  50 mmL, 5  $\mu$  particle size, Phenomenex) analytical column and buffers A:  $\text{H}_2\text{O}$ , B: ACN, C: 0.1% aq.TFA. High resolution mass spectra were recorded on a LTQ Orbitrap (Thermo Finnigan) mass spectrometer equipped with an electrospray ion source in positive mode (source voltage 3.5 kV, sheath gas flow 10 mL  $\text{min}^{-1}$ , capillary temperature 250  $^\circ\text{C}$ ) with resolution  $R=60000$  at  $m/z$  400 (mass range  $m/z=150-2000$ ) and dioctylphthalate ( $m/z = 391.28428$ ) as a "lock mass". The high resolution mass spectrometer was calibrated prior to measurements with a calibration mixture (Thermo Finnigan). For reversed-phase HPLC purification of the final compounds an automated HPLC system equipped with a C18 semiprep column (Gemini C18, 250 $\times$ 10 mm, 5  $\mu$  particle size, Phenomenex) was used. Optical rotations were measured on a Propol automatic polarimeter (Sodium D- line,  $\lambda = 589$  nm).



**(4*R*,7*S*)-4-(3-bromo-5-ethoxy-4-(prop-2-yn-1-yloxy)phenyl)-2-methyl-5-oxo-7-propyl-1,4,5,6,7,8-hexahydroquinoline-3-carbonitrile (56).**

Potassium carbonate (100 mg, 0.68 mmol) was added to a solution of DHP **55** (228 mg, 0.5 mmol) in acetone (50 mL) and heated to reflux for 45 min, after which propargyl bromide (80% in toluene, 0.1 mL, 1 mmol) was added and heating continued for 20 h. The solvent was evaporated *in vacuo*, the residue dissolved in EtOAc, washed with  $\text{H}_2$  and brine, dried ( $\text{MgSO}_4$ ) and concentrated. Purification by silica column chromatography (0  $\rightarrow$  30% EtOAc in PE) yielded pure compound **56** (181 mg, 0.37 mmol, 75%) as a yellowish oil.  $R_f = 0.4$  (1:1 EtOAc:PE).  $^1\text{H}$

NMR (400 MHz,  $\text{CDCl}_3$ ):  $\delta$  7.53 (s, 1H, NH), 6.85 (s, 1H,  $\text{CH}_{\text{ar}}$ ), 6.84 (s, 1H,  $\text{CH}_{\text{ar}}$ ), 4.70 (d,  $J = 2.1$  Hz, 2H, CH), 4.52 (s, 1H, CH), 4.14 - 4.02 (m, 2H, CH), 2.51 (s, 1H, CH), 2.50 - 2.36 (m, 2H, 2  $\times$  CH- $\text{H}^{\text{a}}$ ), 2.33 - 2.05 (m, 3H, 2  $\times$   $\text{CH}_2$ - $\text{H}^{\text{b}}$ , CH), 2.02 (s, 3H,  $\text{CH}_3$ ), 1.43 (t,  $J = 6.9$  Hz, 3H,  $\text{CH}_3$ ), 1.37 - 1.25 (m, 4H, 2  $\times$   $\text{CH}_2$ ), 0.90 (t,  $J = 6.7$  Hz, 3H,  $\text{CH}_3$ ).  $^{13}\text{C}$  NMR (101 MHz,  $\text{CDCl}_3$ ):  $\delta$  196.09, 152.62, 150.75, 145.50, 143.10, 142.63, 123.13, 119.36, 118.12, 112.62, 109.36, 87.68, 78.95, 75.62, 64.75, 60.10, 43.32, 38.29, 37.24, 33.67, 33.26, 19.90, 18.27, 14.80, 14.09. ESI-MS ( $m/z$ ):  $[\text{M} + \text{H}]^+$ : 483.00. ESI-HRMS ( $m/z$ ): calcd. for  $[\text{C}_{25}\text{H}_{27}\text{BrN}_2\text{O}_3 + \text{H}]^+$  483.12778; obsd. 483.12785.

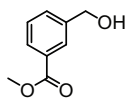


**Ethyl 2-((2-bromo-4-((4*R*,7*S*)-3-cyano-2-methyl-5-oxo-7-propyl-1,4,5,6,7,8-hexahydroquinolin-4-yl)-6-ethoxyphenoxy)methyl)benzoate (60).**

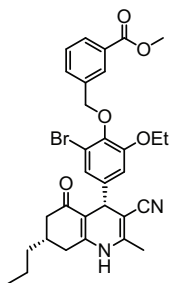
To a solution of DHP **55** (227 mg, 0.5 mmol) in acetone (25 mL)  $\text{K}_2\text{CO}_3$  (90 mg, 0.65 mmol, 1.3 eq) was added and the mixture was heated to reflux for 30 min. Ethyl 2-(bromomethyl)benzoate **57**<sup>22</sup> (155 mg, 0.65 mmol) as a solution in toluene (2 mL) was added and heating was continued for 48 h, after which the solvent was evaporated *in vacuo*. The remaining solids were dissolved in EtOAc, washed with  $\text{H}_2\text{O}$ , brine and dried over  $\text{MgSO}_4$ . Silica column chromatography (0  $\rightarrow$  30% EtOAc in PE) yielded pure product **60** (57 mg, 0.094 mmol, 19%) as well as a mixture of **60** and starting material DHP **55** (237 mg: 80:20 based on

LC/MS analysis), which was taken to the next step without any further purification.  $R_f = 0.7$  (15:1 DCM:MeOH).  $^1\text{H}$  NMR (400 MHz,  $\text{CDCl}_3$ ):  $\delta$  8.09 (d,  $J = 7.8$  Hz, 1H,  $\text{CH}_{\text{ar}}$ ), 7.98 (d,  $J = 7.8$  Hz, 1H,  $\text{CH}_{\text{ar}}$ ), 7.59 (t,  $J = 7.6$  Hz, 1H,  $\text{CH}_{\text{ar}}$ ), 7.36 (t,  $J = 7.6$  Hz, 1H,  $\text{CH}_{\text{ar}}$ ), 7.23 (s, 1H, NH), 6.86 (d,  $J = 4.3$  Hz, 2H, 2  $\times$   $\text{CH}_{\text{ar}}$ ), 5.44 (s, 2H,  $\text{CH}_2$ ), 4.54 (s, 1H, CH), 4.32 (q,  $J = 7.1$  Hz, 2H,  $\text{CH}_2$ ), 4.12 - 3.98 (m, 2H,  $\text{CH}_2$ ), 2.53 - 2.33 (m, 2H,  $\text{CH}_2$ ), 2.33 - 2.22 (m, 1H, CH), 2.21 - 2.08

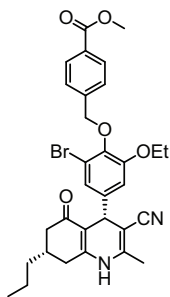
(m, 2H, CH<sub>2</sub>), 2.06 (d, *J* = 7.9 Hz, 3H, CH<sub>3</sub>), 1.37 - 1.21 (m, 10H, 2 × CH<sub>3</sub>, 2 × CH<sub>2</sub>), 0.89 (t, *J* = 6.5 Hz, 3H, CH<sub>3</sub>). <sup>13</sup>C NMR (101 MHz, CDCl<sub>3</sub>): δ 195.90, 167.14, 152.82, 149.99, 145.06, 144.75, 141.98, 140.36, 132.45, 130.26, 127.96, 127.73, 126.97, 123.04, 119.35, 118.07, 112.84, 109.86, 88.12, 72.64, 64.68, 61.09, 43.42, 38.24, 37.39, 33.83, 33.50, 19.94, 18.47, 14.77, 14.41, 14.15. FT-IR (thin film) *v* 2959, 2930, 2363, 2338, 2201, 1713, 1653, 1613, 1490, 1426, 1384, 1274, 1142, 1046 cm<sup>-1</sup>. LC/MS analysis (linear gradient 50% → 90% ACN) *t*<sub>R</sub>: 7.70 min, ESI-MS (*m/z*): [M + H]<sup>+</sup>: 606.93.



**Methyl 3-(hydroxymethyl)benzoate (58).** Dimethyl isophthalate (1.94 g, 10 mmol) was dissolved in MeOH (50 mL) and KOH (0.65 g, 12 mmol) was added. The mixture was stirred for 15 h, concentrated *in vacuo* followed by the addition of water, acidification with HCl (aq) and extraction with DCM. After drying (MgSO<sub>4</sub>), filtration and concentration, the mixture was dissolved in dry THF (20 mL) and cooled to 0 °C. BH<sub>3</sub>·THF (20 mL 1 M in THF, 20 mmol) was slowly added at 0 °C, followed by stirring at rt for 45 min, after which the mixture was cooled again and carefully quenched with acetic acid (aq, 50%). The solvent was removed under reduced pressure and the solids dissolved in EtOAc, washed with water, NaHCO<sub>3</sub> (sat aq, 4x), dried (Na<sub>2</sub>SO<sub>4</sub>) and concentrated. Silica column chromatography (0 → 30% EtOAc in PE) yielded pure compound **58** (852 mg, 5.1 mmol, 51% over 2 steps) as a colorless oil. *R*<sub>f</sub> = 0.5 (2:1 PE:EtOAc). <sup>1</sup>H NMR (400 MHz, CDCl<sub>3</sub>): δ 8.01 - 7.97 (m, 1H, CH<sub>ar</sub>), 7.92 (d, *J* = 7.8 Hz, 1H, CH<sub>ar</sub>), 7.56 - 7.51 (m, 1H, CH<sub>ar</sub>), 7.40 (t, *J* = 7.7 Hz, 1H, CH<sub>ar</sub>), 4.69 (s, 2H, CH<sub>2</sub>), 3.89 (s, 3H, CH<sub>3</sub>), 3.07 (s, 1H, OH). <sup>13</sup>C NMR (101 MHz, CDCl<sub>3</sub>): δ 167.17, 141.39, 131.41, 130.17, 128.63, 128.54, 127.88, 64.47, 52.15.

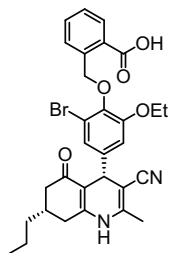


**Methyl 3-((2-bromo-4-((4*R*,7*S*)-3-cyano-2-methyl-5-oxo-7-propyl-1,4,5,6,7,8-hexahydroquinolin-4-yl)-6-ethoxyphenoxy)methyl)benzoate (61).** To a solution of DHP **55** (0.2 g, 0.45 mmol) in dry THF (10 mL) were added PPh<sub>3</sub> (polymer bound, 0.25 g, 0.75 mmol) and methyl 3-(hydroxymethyl)benzoate **58** (82 mg, 0.5 mmol) and the mixture was cooled to 0 °C. DIAD (0.1 mL, 0.5 mmol) was added dropwise and the reaction continued for 48 h at ambient temperature. LC/MS analysis (linear gradient 10% → 90% ACN/0.1% TFA/H<sub>2</sub>O, *t*<sub>R</sub>:10.2 min) showed a conversion of ~90%. The resin was filtered off, the mixture concentrated and the crude product was subjected to silica column chromatography (0 → 30% EtOAc in PE) resulting in an inseparable mixture of product **61** and starting material **55** (239 mg) which was taken to the next step without any further purification. *R*<sub>f</sub> = 0.65 (15:1 DCM:MeOH). ESI-MS (*m/z*): [M + Na]<sup>+</sup>: 615.07.



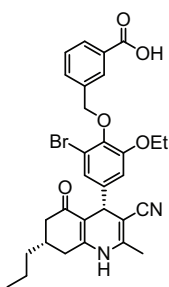
**Methyl 4-((2-bromo-4-((4*R*,7*S*)-3-cyano-2-methyl-5-oxo-7-propyl-1,4,5,6,7,8-hexahydroquinolin-4-yl)-6-ethoxyphenoxy)methyl)benzoate (62).** To a solution of DHP **55** (0.2 g, 0.45 mmol) in dry THF (10 mL) were added PPh<sub>3</sub> (polymer bound, 0.25 g, 0.75 mmol) and methyl 4-(hydroxymethyl)benzoate **59**<sup>40</sup> (82 mg, 0.5 mmol) and the mixture was cooled to 0 °C. DIAD (0.1 mL, 0.5 mmol) was added dropwise and the reaction continued for 18 h at ambient temperature. The resin was filtered off, the mixture concentrated and the product was purified by silica column chromatography (0 → 100% EtOAc in PE) resulting in pure **62** (135 mg, 0.23 mmol, 50%) and a mixture of product and starting material (90 mg), both of which were used in the subsequent step. *R*<sub>f</sub> = 0.65 (15:1 DCM:MeOH). <sup>1</sup>H NMR (400 MHz, CDCl<sub>3</sub>): δ 8.04 (d, *J* = 8.2 Hz, 2H, 2 × CH<sub>ar</sub>), 7.63 (d, *J* = 8.2 Hz, 2H, 2 × CH<sub>ar</sub>), 7.16 (s, 1H, NH), 6.88 (d, *J* = 1.7 Hz, 1H, CH<sub>ar</sub>), 6.85

(d,  $J = 1.8$  Hz, 1H, CH<sub>ar</sub>), 5.05 (s, 2H, CH<sub>2</sub>), 4.54 (s, 1H, CH), 4.16 - 4.00 (m, 2H, CH<sub>2</sub>), 3.92 (s, 3H, CH<sub>3</sub>), 2.51 - 2.23 (m, 3H, CH<sub>2</sub>, CH<sub>2</sub>-H<sup>a</sup>), 2.23 - 2.06 (m, 2H, CH<sub>2</sub>-H<sup>b</sup>, CH), 2.04 (s, 3H, CH<sub>3</sub>), 1.41 (t,  $J = 7.0$  Hz, 3H, CH<sub>3</sub>), 1.36 - 1.27 (m, 4H, 2 × CH<sub>2</sub>), 0.90 (t,  $J = 6.8$  Hz, 3H, CH<sub>3</sub>). <sup>13</sup>C NMR (101 MHz, CDCl<sub>3</sub>):  $\delta$  195.93, 167.24, 152.77, 150.15, 145.08, 144.22, 142.83, 142.33, 129.67, 129.57, 127.93, 123.11, 119.31, 118.07, 112.84, 109.72, 88.11, 73.97, 64.72, 52.24, 43.39, 38.36, 37.33, 33.76, 33.45, 19.93, 18.39, 14.88, 14.13. FT-IR (thin film)  $\nu$  2956, 2930, 2878, 2362, 2343, 2201, 1718, 1652, 1616, 1489, 1435, 1382, 1274, 1109, 1046 cm<sup>-1</sup>. ESI-MS ( $m/z$ ): [M + H]<sup>+</sup>: 593.07. ESI-HRMS ( $m/z$ ): calcd. for [C<sub>31</sub>H<sub>33</sub>BrN<sub>2</sub>O<sub>5</sub> + H]<sup>+</sup> 593.16456; obsd. 593.16389.



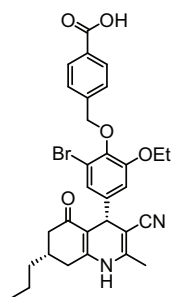
**2-((2-Bromo-4- (4R,7S) -3-cyano-2-methyl-5-oxo-7-propyl-1,4,5,6,7,8-hexahydroquinolin-4-yl)-6-ethoxyphenoxy)methyl)benzoic acid (63).** Compound **60** (237 mg, containing **55**) was dissolved in MeOH (10 mL) and degassed under argon with sonication. A degassed solution of NaOH (aq, 2 M, 2.5 mL) was added and the reaction mixture stirred for 24 h, after which more NaOH (aq, 2 M, 2.5 mL) was added and the reaction heated to 40 °C for 2 h. The reaction was acidified to pH~5 with HCl (aq, 1 M), extracted with DCM (3x), dried over MgSO<sub>4</sub> and concentrated. Silica column chromatography (30 → 100% EtOAc in PE) provided compound **63** (121 mg, 0.21 mmol, 52% over 2 steps) in pure form.  $R_f = 0.25$  (15:1 DCM:MeOH). <sup>1</sup>H NMR (400 MHz, MeOD):  $\delta$  8.06 -

7.94 (m, 2H, 2 × CH<sub>ar</sub>), 7.57 (t,  $J = 7.5$  Hz, 1H, CH<sub>ar</sub>), 7.36 (t,  $J = 7.5$  Hz, 1H, CH<sub>ar</sub>), 6.94 (s, 1H, CH<sub>ar</sub>), 6.89 (s, 1H, CH<sub>ar</sub>), 5.41 (s, 2H, CH<sub>2</sub>), 4.48 (s, 1H, CH), 4.10 - 4.00 (m, 2H, CH<sub>2</sub>), 2.54 (d,  $J = 16.9$  Hz, 1H, CH<sub>2</sub>-H<sup>a</sup>), 2.46 - 2.32 (m, 2H, CH<sub>2</sub>), 2.19 - 2.05 (m, 5H, CH<sub>3</sub>, CH, CH<sub>2</sub>-H<sup>b</sup>), 1.39 - 1.28 (m, 7H, CH<sub>3</sub>, 2 × CH<sub>2</sub>), 0.89 (s, 3H, CH<sub>3</sub>). <sup>13</sup>C NMR (101 MHz, MeOD):  $\delta$  198.36, 170.13, 153.98, 153.51, 147.35, 145.75, 144.11, 141.34, 133.23, 131.56, 129.31, 128.89, 128.01, 124.35, 120.40, 118.56, 113.91, 109.99, 88.37, 73.62, 65.71, 44.04, 39.74, 38.12, 34.75, 33.51, 20.92, 18.06, 15.04, 14.49. FT-IR (thin film)  $\nu$  2957, 2360, 2337, 2202, 1686, 1654, 1611, 1490, 1426, 1384, 1260, 1145 cm<sup>-1</sup>.  $[\alpha]_D^{20} = -135^\circ$  (c = 1, CHCl<sub>3</sub>). ESI-HRMS ( $m/z$ ): calcd. for [C<sub>30</sub>H<sub>31</sub>BrN<sub>2</sub>O<sub>5</sub> + H]<sup>+</sup> 579.14891; obsd. 579.14884.

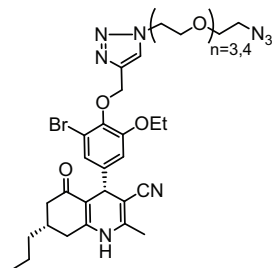


**3-((2-Bromo-4- (4R,7S) -3-cyano-2-methyl-5-oxo-7-propyl-1,4,5,6,7,8-hexahydroquinolin-4-yl)-6-ethoxyphenoxy)methyl)benzoic acid (64).** Compound **61** (239 mg, containing **55**) was dissolved in MeOH (10 mL) and degassed under argon with sonication. A degassed solution of NaOH (aq, 2 M, 5 mL) was added and the reaction mixture heated to 40 °C for 2 h. The reaction was acidified to pH~5 with HCl (aq, 1 M), extracted with DCM (3x), dried over MgSO<sub>4</sub> and concentrated. Silica column chromatography (0 → 10% MeOH in DCM) provided compound **64** (169 mg, 0.29 mmol, 65% over 2 steps) in pure form.  $R_f = 0.15$  (15:1 DCM:MeOH). <sup>1</sup>H NMR (400 MHz, MeOD):  $\delta$  8.22 (s, 1H, CH<sub>ar</sub>),

7.98 (d,  $J = 7.7$  Hz, 1H, CH<sub>ar</sub>), 7.72 (d,  $J = 7.5$  Hz, 1H, CH<sub>ar</sub>), 7.45 (t,  $J = 7.6$  Hz, 1H, CH<sub>ar</sub>), 6.92 (s, 1H, CH<sub>ar</sub>), 6.89 (s, 1H, CH<sub>ar</sub>), 5.00 (s, 2H, CH<sub>2</sub>), 4.47 (s, 1H, CH), 4.14 - 4.03 (m, 2H, CH<sub>2</sub>), 2.56 (d,  $J = 16.6$  Hz, 1H, CH<sub>2</sub>-H<sup>a</sup>), 2.47 - 2.34 (m, 2H, CH<sub>2</sub>), 2.23 - 2.03 (m, 5H, CH<sub>2</sub>-H<sup>b</sup>, CH, CH<sub>3</sub>), 1.43 (t,  $J = 6.8$  Hz, 3H, CH<sub>3</sub>), 1.35 (s, 4H, 2 × CH<sub>2</sub>), 0.91 (s, 3H, CH<sub>3</sub>). <sup>13</sup>C NMR (101 MHz, MeOD):  $\delta$  1198.36, 169.99, 154.13, 153.56, 147.44, 145.20, 144.40, 139.14, 133.85, 132.46, 130.84, 130.35, 129.37, 124.27, 120.38, 118.74, 113.72, 109.98, 88.33, 75.18, 65.71, 44.05, 39.74, 38.14, 34.80, 33.50, 20.95, 18.04, 15.18, 14.48.  $[\alpha]_D^{20} = -86^\circ$  (c = 0.42, CHCl<sub>3</sub>). ESI-HRMS ( $m/z$ ): calcd. for [C<sub>30</sub>H<sub>31</sub>BrN<sub>2</sub>O<sub>5</sub> + H]<sup>+</sup> 579.14891; obsd. 579.14882.



**4-((2-Bromo-4- (4R,7S) -3-cyano-2-methyl-5-oxo-7-propyl-1,4,5,6,7,8-hexahydroquinolin-4-yl)-6-ethoxyphenoxy)methyl)benzoic acid (65).** Compound **62** (155 mg, 0.26 mmol) was dissolved in MeOH (10 mL) and degassed under argon with sonication. A degassed solution of NaOH (aq, 2 M, 5 mL) was added and the reaction mixture heated to 40 °C for 2 h followed by stirring at rt for 15 h. The reaction was acidified to pH~5 with HCl (aq, 1 M), extracted with DCM (3x), dried over MgSO<sub>4</sub> and concentrated. Silica column chromatography (0 → 10% MeOH in DCM) provided compound **65** (128 mg, 0.22 mmol, 85%) in pure form.  $R_f = 0.3$  (15:1 DCM:MeOH). <sup>1</sup>H NMR (400 MHz, MeOD):  $\delta$  8.01 (d,  $J = 8.1$  Hz, 2H, 2 × CH<sub>ar</sub>), 7.60 (d,  $J = 8.1$  Hz, 2H, 2 × CH<sub>ar</sub>), 6.93 (s, 1H, CH<sub>ar</sub>), 6.89 (s, 1H, CH<sub>ar</sub>), 5.00 (s, 2H, CH<sub>2</sub>), 4.47 (s, 1H, CH), 4.12 - 4.01 (m, 2H, CH<sub>2</sub>), 2.59 - 2.50 (m, 1H, CH<sub>2</sub>-H<sup>a</sup>), 2.46 - 2.32 (m, 2H, CH<sub>2</sub>), 2.18 - 2.03 (m, 5H, CH<sub>3</sub>, CH, CH<sub>2</sub>-H<sup>b</sup>), 1.38 (t,  $J = 6.9$  Hz, 3H, CH<sub>3</sub>), 1.35 - 1.26 (m, 4H, 2 × CH<sub>2</sub>), 0.89 (s, 3H, CH<sub>3</sub>). <sup>13</sup>C NMR (101 MHz, MeOD):  $\delta$  198.25, 169.56, 154.03, 153.47, 147.36, 145.17, 144.39, 143.94, 131.35, 130.68, 129.05, 124.29, 120.39, 118.67, 113.76, 109.94, 88.33, 74.94, 65.67, 44.04, 39.75, 38.12, 34.73, 33.49, 20.93, 18.07, 15.17, 14.50. FT-IR (thin film)  $\nu$  2959, 2928, 2872, 2364, 2337, 2202, 1691, 1654, 1617, 1578, 1475, 1407, 1275, 1046 cm<sup>-1</sup>.  $[\alpha]_D^{20} = -87^\circ$  (c = 1, CHCl<sub>3</sub>). ESI-HRMS ( $m/z$ ): calcd. for [C<sub>30</sub>H<sub>31</sub>BrN<sub>2</sub>O<sub>5</sub> + H]<sup>+</sup> 579.14891; obsd. 579.14878.



#### General procedure for the synthesis of monomeric ligands (67a,b).

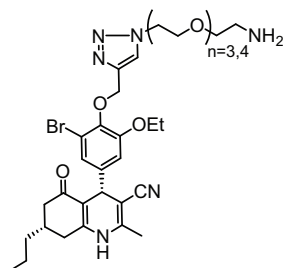
To a solution of compound **56** (50 mg, 0.1 mmol) and diazido-spacer **66a** or **66b**<sup>41</sup> (1 mmol, 10 eq) in degassed *t*-BuOH/ACN/H<sub>2</sub>O (5 mL; 2/2/1; v/v/v) were added degassed aqueous solutions of sodium ascorbate (0.25 mL 2 M, 0.5 mmol, 5 eq) and CuSO<sub>4</sub> (20  $\mu$ L 1 M, 0.02 mmol, 20 mol%) and the resulting mixture was stirred for 16 h at room temperature. DCM/MeOH (9:1; v/v) and water were added and after partitioning of the layers, the waterlayer was extracted with DCM/MeOH (9:1; v/v, 2 x). The combined organic layers were dried (MgSO<sub>4</sub>) and concentrated. Silica column chromatography (0 → 1% MeOH in DCM) afforded compound **67** as an off-white glassy solid.  $R_f = 0.45$  (9:1 DCM:MeOH). FT-IR (thin film)  $\nu$  2919, 2871, 2360, 2325, 2200, 2104, 1652, 1619, 1496, 1471, 1425, 1384, 1275, 1253, 1123, 1045 cm<sup>-1</sup>.

#### (4R,7S)-4-(4-(1-(11-azido-3,6,9-trioxaundecyl)-1H-1,2,3-triazol-4-yl) methoxy)-3-bromo-5-ethoxyphenyl)-2-methyl-5-oxo-7-propyl-1,4,5,6,7,8-hexahydroquinoline-3-carbonitrile (67a).

Yield: 52 mg, 0.072 mmol, 72%. <sup>1</sup>H NMR (400 MHz, CDCl<sub>3</sub>):  $\delta$  7.93 (s, 1H, CH<sub>triaz</sub>), 7.67 (s, 1H, NH), 6.91 (d,  $J = 1.9$  Hz, 1H, CH<sub>ar</sub>), 6.85 (d,  $J = 1.9$  Hz, 1H, CH<sub>ar</sub>), 5.15 (s, 2H, CH<sub>2</sub>), 4.62 - 4.52 (m, 3H, CH<sub>2</sub>, CH), 4.18 - 4.05 (m, 2H, CH<sub>2</sub>), 3.90 (t,  $J = 5.1$  Hz, 2H, CH<sub>2</sub>), 3.76 - 3.48 (m, 10H, 5 × CH<sub>2</sub>), 3.36 (t,  $J = 5.1$  Hz, 2H, CH<sub>2</sub>), 2.56 - 2.43 (m, 2H, CH<sub>2</sub>), 2.43 - 2.30 (m, 1H, CH<sub>2</sub>-H<sup>b</sup>), 2.23 - 2.16 (m, 1H, CH), 2.16 - 2.04 (m, 4H, CH<sub>3</sub>, CH<sub>2</sub>-H<sup>b</sup>), 1.43 (t,  $J = 6.9$  Hz, 3H, CH<sub>3</sub>), 1.37 - 1.27 (m, 4H, 2 × CH<sub>2</sub>), 0.88 (t,  $J = 6.9$  Hz, 3H, CH<sub>3</sub>). <sup>13</sup>C NMR (101 MHz, CDCl<sub>3</sub>):  $\delta$  195.87, 152.70, 150.27, 145.44, 144.52, 143.79, 142.53, 124.79, 123.07, 119.56, 118.18, 112.82, 109.74, 87.90, 70.79, 70.76, 70.70, 70.14, 69.55, 66.16, 64.66, 50.76, 50.54, 43.49, 38.19, 37.53, 33.92, 33.59, 19.92, 18.52, 14.95, 14.16.  $[\alpha]_D^{20} = -111^\circ$  (c = 0.2, CHCl<sub>3</sub>). ESI-HRMS ( $m/z$ ): calcd. for [C<sub>33</sub>H<sub>43</sub>BrN<sub>8</sub>O<sub>6</sub> + H]<sup>+</sup> 727.25617; obsd. 727.25643.

#### (4R,7S)-4-(4-(1-(14-azido-3,6,9,12-tetraoxatetradecyl)-1H-1,2,3-triazol-4-yl) methoxy)-3-bromo-5-ethoxyphenyl)-2-methyl-5-oxo-7-propyl-1,4,5,6,7,8-hexahydroquinoline-3-carbonitrile (67b).

Yield: 71 mg, 0.092 mmol, 92%.  $^1\text{H}$  NMR (400 MHz,  $\text{CDCl}_3$ ):  $\delta$  8.13 (s, 1H, NH), 7.90 (s, 1H,  $\text{CH}_{\text{trz}}$ ), 6.91 (d,  $J = 1.7$  Hz, 1H,  $\text{CH}_{\text{ar}}$ ), 6.86 (d,  $J = 1.8$  Hz, 1H,  $\text{CH}_{\text{ar}}$ ), 5.15 (s, 2H,  $\text{CH}_2$ ), 4.57 (t,  $J = 4.9$  Hz, 3H,  $\text{CH}_2$ , CH), 4.17 - 4.05 (m, 2H,  $\text{CH}_2$ ), 3.89 (t,  $J = 5.1$  Hz, 2H,  $\text{CH}_2$ ), 3.71 - 3.53 (m, 14H,  $7 \times \text{CH}_2$ ), 3.37 (t,  $J = 5.0$  Hz, 2H,  $\text{CH}_2$ ), 2.55 - 2.43 (m, 2H,  $2 \times \text{CH}_2\text{-H}^{\text{a}}$ ), 2.43 - 2.30 (m, 1H,  $\text{CH}_2\text{-H}^{\text{b}}$ ), 2.23 - 2.04 (m, 5H,  $\text{CH}_3 + \text{CH}$ ,  $\text{CH}_2\text{-H}_2$ ), 1.43 (t,  $J = 7.0$  Hz, 3H,  $\text{CH}_3$ ), 1.36 - 1.25 (m, 4H,  $2 \times \text{CH}_2$ ), 0.87 (t,  $J = 6.9$  Hz, 3H,  $\text{CH}_3$ ).  $^{13}\text{C}$  NMR (101 MHz,  $\text{CDCl}_3$ ):  $\delta$  195.77, 152.56, 150.58, 145.66, 144.29, 143.61, 142.56, 124.67, 122.98, 119.56, 118.03, 112.71, 109.38, 87.50, 70.66, 70.63, 70.60, 70.56, 70.48, 69.97, 69.43, 65.94, 64.56, 50.66, 50.44, 43.39, 38.13, 37.39, 33.77, 33.29, 19.82, 18.26, 14.84, 14.04.  $[\alpha]_D^{20} = -96^\circ$  ( $c = 0.43$ ,  $\text{CHCl}_3$ ). ESI-HRMS ( $m/z$ ): calcd. for  $[\text{C}_{35}\text{H}_{47}\text{BrN}_8\text{O}_7 + \text{H}]^+$  771.28328; obsd. 771.28291.



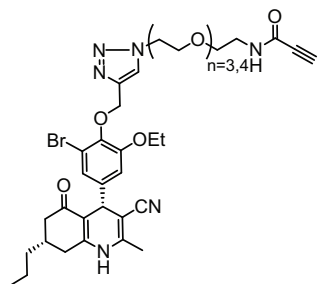
**General procedure for the Staudinger reduction of monomeric ligands (68a,b).** Compound **67** (1 eq) was dissolved in THF (5 mL) and  $\text{PPh}_3$  (3 eq) was added. Water (0.5 mL) was added after 20 h and the reaction continued for an additional 24 h, after which the solvents were removed *in vacuo* by co-evaporation with toluene. The residue was taken up in DCM and purified by silica column chromatography (2.5  $\rightarrow$  10% MeOH in DCM, followed by 10% MeOH and 1% TEA in DCM) to give compound **68** as an off-white glassy solid.  $R_f = 0.15$  (9:1:0.1 DCM:MeOH:TEA). FT-IR (thin film)  $\nu$  3200, 2924, 2872, 2360, 2199, 1651, 1622, 1500, 1474, 1385, 1275, 1124, 1045  $\text{cm}^{-1}$ .

**(4*R*,7*S*)-4-(4-(1-(11-amino-3,6,9-trioxaundecyl)-1*H*-1,2,3-triazol-4-yl) methoxy)-3-bromo-5-ethoxyphenyl)-2-methyl-5-oxo-7-propyl-1,4,5,6,7,8-hexahydroquinoline-3-carbonitrile (68a).**

Yield: 41 mg, 0.058 mmol, 66%.  $^1\text{H}$  NMR (400 MHz,  $\text{CDCl}_3$ ):  $\delta$  8.61 (s, 1H, NH), 7.88 (s, 1H,  $\text{CH}_{\text{trz}}$ ), 6.88 (d,  $J = 11.0$  Hz, 2H,  $2 \times \text{CH}_{\text{ar}}$ ), 5.15 (s, 2H,  $\text{CH}_2$ ), 4.56 (t,  $J = 4.8$  Hz, 3H,  $\text{CH}_2$ , CH), 4.22 - 4.02 (m, 2H,  $\text{CH}_2$ ), 3.88 (t,  $J = 5.0$  Hz, 2H,  $\text{CH}_2$ ), 3.61 (d,  $J = 6.0$  Hz, 8H,  $4 \times \text{CH}_2$ ), 3.51 - 3.45 (m, 2H,  $\text{CH}_2$ ), 2.85 (s, 2H), 2.61 - 2.31 (m, 5H,  $\text{CH}_2$ ,  $\text{CH}_2\text{-H}^{\text{a}}$ ,  $\text{NH}_2$ ), 2.20 - 2.05 (m, 5H,  $\text{CH}_3$ , CH,  $\text{CH}_2\text{-H}^{\text{b}}$ ), 1.43 (t,  $J = 7.0$  Hz, 3H,  $\text{CH}_3$ ), 1.37 - 1.28 (m, 4H,  $2 \times \text{CH}_2$ ), 0.88 (t,  $J = 6.8$  Hz, 3H,  $\text{CH}_3$ ).  $^{13}\text{C}$  NMR (101 MHz,  $\text{CDCl}_3$ ):  $\delta$  195.92, 152.65, 150.93, 145.93, 144.54, 143.66, 142.88, 124.64, 123.14, 119.76, 118.05, 112.83, 109.37, 87.46, 72.63, 70.69, 70.68, 70.52, 70.27, 69.57, 66.19, 64.67, 50.47, 43.52, 41.53, 38.36, 37.51, 33.87, 33.35, 19.92, 18.33, 14.94, 14.16.  $[\alpha]_D^{20} = -112^\circ$  ( $c = 0.28$ ,  $\text{CHCl}_3$ ). ESI-HRMS ( $m/z$ ): calcd. for  $[\text{C}_{33}\text{H}_{45}\text{BrN}_6\text{O}_6 + \text{H}]^+$  701.26567; obsd. 701.26568.

**(4*R*,7*S*)-4-(4-(1-(14-amino-3,6,9,12-tetraoxatetradecyl)-1*H*-1,2,3-triazol-4-yl) methoxy) -3-bromo-5-ethoxyphenyl)-2-methyl-5-oxo-7-propyl-1,4,5,6,7,8-hexahydroquinoline-3-carbonitrile (68b).**

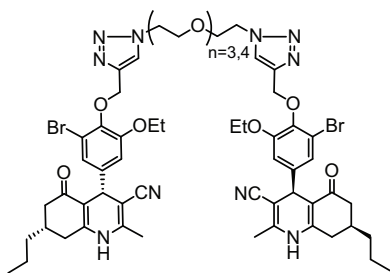
Yield: 30 mg, 0.040 mmol, 62%.  $^1\text{H}$  NMR (400 MHz,  $\text{CDCl}_3$ ):  $\delta$  9.21 (s, 1H, NH), 7.85 (s, 1H,  $\text{CH}_{\text{trz}}$ ), 6.88 (d,  $J = 1.9$  Hz, 2H,  $2 \times \text{CH}_{\text{ar}}$ ), 5.15 (s, 2H,  $\text{CH}_2$ ), 4.60 - 4.49 (m, 3H,  $\text{CH}_2 + \text{CH}$ ), 4.16 - 3.99 (m, 2H,  $\text{CH}_2$ ), 3.87 (t,  $J = 4.9$  Hz, 2H,  $\text{CH}_2$ ), 3.67 - 3.51 (m, 16H,  $7 \times \text{CH}_2$ ,  $\text{NH}_2$ ), 2.99 - 2.90 (m, 2H,  $\text{CH}_2$ ), 2.76 - 2.67 (m, 1H,  $\text{CH}_2\text{-H}^{\text{a}}$ ), 2.51 - 2.33 (m, 2H,  $\text{CH}_2$ ), 2.23 - 2.14 (m, 4H,  $\text{CH}_3$ , CH), 2.12 - 2.03 (m, 1H,  $\text{CH}_2\text{-H}^{\text{b}}$ ), 1.43 (t,  $J = 7.0$  Hz, 3H,  $\text{CH}_3$ ), 1.39 - 1.27 (m, 4H,  $2 \times \text{CH}_2$ ), 0.87 (t,  $J = 6.6$  Hz, 3H,  $\text{CH}_3$ ).  $^{13}\text{C}$  NMR (101 MHz,  $\text{CDCl}_3$ ):  $\delta$  196.09, 152.65, 151.67, 146.48, 144.56, 143.49, 143.22, 124.57, 123.19, 120.00, 117.96, 112.76, 109.03, 87.04, 70.70, 70.56, 70.49, 70.45, 70.43, 70.35, 70.02, 69.63, 66.19, 64.68, 50.36, 43.56, 40.87, 38.43, 37.54, 33.90, 33.27, 19.93, 18.31, 14.94, 14.20.  $[\alpha]_D^{20} = -126^\circ$  ( $c = 0.28$ ,  $\text{CHCl}_3$ ). ESI-HRMS ( $m/z$ ): calcd. for  $[\text{C}_{35}\text{H}_{49}\text{BrN}_6\text{O}_7 + \text{H}]^+$  745.29189; obsd. 745.29128.



**General procedure for the coupling of amines 68a,b with propiolic acid (69a,b).** Compound **68** (1 eq) was dissolved in DCM (2 mL) and a pre-activated mixture of propiolic acid (2 eq) and EEDQ (2 eq) in DCM (1 mL) was added. After 1 h, TLC indicated complete conversion of the starting material. Silica column chromatography (0 → 2.5% (n=3) or 3% (n=4) MeOH in DCM) gave pure **69** as a yellowish solid.  $R_f = 0.6$  (10:1 DCM:MeOH).

**N-(11-(4-((2-bromo-4-(4*R*,7*S*)-3-cyano-2-methyl-5-oxo-7-propyl-1,4,5,6,7,8-hexahydroquinolin-4-yl)-6-ethoxyphenoxy)methyl)-1*H*-1,2,3-triazol-1-yl)-3,6,9-trioxaundecyl) propiolamide (69a).** Yield: 16 mg, 0.021 mmol, 71%.  $^1\text{H NMR}$  (400 MHz,  $\text{CDCl}_3$ ):  $\delta$  7.93 (s, 1H,  $\text{CH}_{\text{trz}}$ ), 7.80 (s, 1H, NH), 6.98 (s, 1H, NH), 6.91 (d,  $J = 1.6$  Hz, 1H,  $\text{CH}_{\text{ar}}$ ), 6.85 (d,  $J = 1.7$  Hz, 1H,  $\text{CH}_{\text{ar}}$ ), 5.17 (s, 2H,  $\text{CH}_2$ ), 4.64 - 4.51 (m, 3H,  $\text{CH}_2$ , CH), 4.17 - 4.04 (m, 2H,  $\text{CH}_2$ ), 3.91 (t,  $J = 5.0$  Hz, 2H,  $\text{CH}_2$ ), 3.67 - 3.56 (m, 8H, 4 ×  $\text{CH}_2$ ), 3.53 (t,  $J = 5.0$  Hz, 2H,  $\text{CH}_2$ ), 3.49 - 3.38 (m, 2H,  $\text{CH}_2$ ), 2.83 (s, 1H, CH), 2.56 - 2.43 (m, 2H,  $\text{CH}_2$ ), 2.43 - 2.30 (m, 1H,  $\text{CH}_2\text{-H}^{\text{a}}$ ), 2.19 (s, 1H, CH), 2.14 - 2.02 (m, 4H,  $\text{CH}_3$ ,  $\text{CH}_2\text{-H}^{\text{b}}$ ), 1.43 (t,  $J = 7.0$  Hz, 3H,  $\text{CH}_3$ ), 1.38 - 1.28 (m, 4H, 2 ×  $\text{CH}_2$ ), 0.88 (t,  $J = 6.8$  Hz, 3H,  $\text{CH}_3$ ).  $^{13}\text{C NMR}$  (101 MHz,  $\text{CDCl}_3$ ):  $\delta$  195.90, 152.69, 152.53, 150.44, 145.52, 144.63, 143.79, 142.69, 124.74, 123.08, 119.61, 118.09, 112.89, 109.67, 87.83, 77.41, 73.85, 70.80, 70.65, 70.60, 70.37, 69.61, 69.19, 66.38, 64.70, 50.49, 43.51, 39.76, 38.31, 37.53, 33.90, 33.53, 19.93, 18.49, 14.96, 14.17.  $[\alpha]_D^{20} = -113^\circ$  (c = 0.32,  $\text{CHCl}_3$ ). ESI-HRMS ( $m/z$ ): calcd. for  $[\text{C}_{36}\text{H}_{45}\text{BrN}_6\text{O}_7 + \text{H}]^+$  753.26059; obsd. 753.26088.

**N-(14-(4-((2-bromo-4-(4*R*,7*S*)-3-cyano-2-methyl-5-oxo-7-propyl-1,4,5,6,7,8-hexahydroquinolin-4-yl)-6-ethoxyphenoxy)methyl)-1*H*-1,2,3-triazol-1-yl)-3,6,9,12-tetraoxatetradecyl) propiolamide (69b).** Yield: 15 mg, 0.019 mmol, 81%.  $^1\text{H NMR}$  (400 MHz,  $\text{CDCl}_3$ ):  $\delta$  7.91 (s, 1H,  $\text{CH}_{\text{trz}}$ ), 7.58 (s, 1H, NH), 7.03 (s, 1H, NH), 6.92 (d,  $J = 1.8$  Hz, 1H,  $\text{CH}_{\text{ar}}$ ), 6.83 (d,  $J = 1.8$  Hz, 1H,  $\text{CH}_{\text{ar}}$ ), 5.17 (s, 2H,  $\text{CH}_2$ ), 4.57 (d,  $J = 7.4$  Hz, 3H,  $\text{CH}_2$ , CH), 4.17 - 4.08 (m, 2H,  $\text{CH}_2$ ), 3.89 (t,  $J = 5.0$  Hz, 2H,  $\text{CH}_2$ ), 3.65 - 3.60 (m, 14H, 7 ×  $\text{CH}_2$ ), 3.58 - 3.55 (m, 2H,  $\text{CH}_2$ ), 3.50 - 3.45 (m, 2H,  $\text{CH}_2$ ), 2.83 (s, 1H, CH), 2.52 - 2.43 (m, 2H, 2 ×  $\text{CH}_2\text{-H}^{\text{a}}$ ), 2.43 - 2.33 (m, 1H,  $\text{CH}_2\text{-H}^{\text{b}}$ ), 2.19 (s, 1H, CH), 2.14 - 2.05 (m, 4H,  $\text{CH}_3$ ,  $\text{CH}_2\text{-H}^{\text{b}}$ ), 1.44 (t,  $J = 7.0$  Hz, 3H,  $\text{CH}_3$ ), 1.36 - 1.31 (m, 4H, 2 ×  $\text{CH}_2$ ), 0.89 (t,  $J = 6.8$  Hz, 3H,  $\text{CH}_3$ ).  $^{13}\text{C NMR}$  (101 MHz,  $\text{CDCl}_3$ ):  $\delta$  195.79, 152.71, 152.54, 150.17, 145.39, 144.66, 143.83, 142.54, 124.70, 123.01, 119.56, 118.12, 112.91, 109.79, 87.93, 73.80, 70.79, 70.72, 70.64, 70.62, 70.58, 70.38, 69.64, 69.26, 66.40, 64.72, 50.49, 43.52, 39.82, 38.22, 37.55, 33.94, 33.61, 19.94, 18.55, 14.97, 14.18.  $[\alpha]_D^{20} = -91^\circ$  (c = 0.3,  $\text{CHCl}_3$ ). ESI-HRMS ( $m/z$ ): calcd. for  $[\text{C}_{38}\text{H}_{49}\text{BrN}_6\text{O}_8 + \text{H}]^+$  797.28680; obsd. 797.28759.



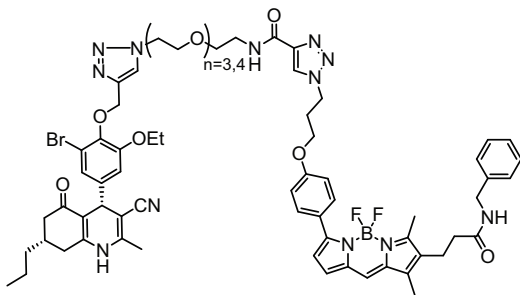
**General procedure for the synthesis of dimeric ligands (70a,b).** To a solution of compound **56** (2 eq) and diazido-spacer **66a** or **66b**<sup>41</sup> (1 eq) in degassed *t*-BuOH/ACN/ $\text{H}_2\text{O}$  (5 mL; 2/2/1; v/v/v) were added degassed aqueous solutions of sodium ascorbate (2 M, 5 eq) and  $\text{CuSO}_4$  (1 M, 20 mol%) and the resulting mixture was stirred for 16 h at room temperature. DCM/MeOH (9:1; v/v) and water were added and after partitioning of the layers, the waterlayer was extracted with DCM/MeOH (9:1; v/v, 2 ×). The combined organic layers were dried ( $\text{MgSO}_4$ ) and concentrated. After silica column chromatography (0 → 5% MeOH in DCM) both dimeric compound **70** and monomeric compound **67**, as a side-product, were isolated as slightly yellow



solids.  $R_f = 0.4$  (9:1 DCM:MeOH). FT-IR (thin film)  $\nu$  2960, 2924, 2360, 2326, 2201, 1654, 1619, 1497, 1477, 1426, 1384, 1275, 1253, 1149, 1125  $\text{cm}^{-1}$ .

**Dimeric ligand (70a).** Yield: dimer: 35 mg, 0.03 mmol, 50%, monomer: 18 mg, 0.025 mmol, 42%.  $^1\text{H}$  NMR (400 MHz, MeOD):  $\delta$  8.00 (s, 2H, 2  $\times$   $\text{CH}_{\text{trz}}$ ), 6.86 (t,  $J = 1.7$  Hz, 4H, 4  $\times$   $\text{CH}_{\text{ar}}$ ), 5.12 (s, 4H, 2  $\times$   $\text{CH}_2$ ), 4.54 (t,  $J = 4.9$  Hz, 4H, 2  $\times$   $\text{CH}_2$ ), 4.51 (s, 2H, 2  $\times$  CH), 4.18 - 4.01 (m, 4H, 2  $\times$   $\text{CH}_2$ ), 3.83 (t,  $J = 4.9$  Hz, 4H, 2  $\times$   $\text{CH}_2$ ), 3.61 - 3.54 (m, 8H, 4  $\times$   $\text{CH}_2$ ), 2.55 - 2.29 (m, 6H, 2  $\times$   $\text{CH}_2$ , 2  $\times$   $\text{CH}_2\text{-H}^{\text{a}}$ ), 2.18 (s, 2H, 2  $\times$  CH), 2.15 - 2.04 (m, 8H, 2  $\times$   $\text{CH}_3$ , 2  $\times$   $\text{CH}_2\text{-H}^{\text{b}}$ ), 1.42 (t,  $J = 6.9$  Hz, 6H, 2  $\times$   $\text{CH}_3$ ), 1.39 - 1.29 (m, 8H, 4  $\times$   $\text{CH}_2$ ), 0.90 (t,  $J = 6.7$  Hz, 6H, 2  $\times$   $\text{CH}_3$ ).  $^{13}\text{C}$  NMR (101 MHz, MeOD):  $\delta$  196.63, 152.33, 151.57, 145.90, 143.26, 142.76, 124.89, 122.83, 119.39, 117.57, 112.34, 108.76, 86.94, 70.21, 70.16, 68.89, 65.56, 64.30, 50.35, 49.09, 48.88, 48.66, 48.45, 48.24, 48.02, 47.81, 42.95, 38.10, 37.03, 33.44, 32.50, 19.54, 17.44, 14.34, 13.62.  $[\alpha]_D^{20} = -126^\circ$  ( $c = 0.84$ ,  $\text{CHCl}_3$ ). ESI-HRMS ( $m/z$ ): calcd. for  $[\text{C}_{58}\text{H}_{70}\text{Br}_2\text{N}_{10}\text{O}_9 + \text{H}]^+$  1211.37463; obsd. 1211.37644.

**Dimeric ligand (70b).** Yield: dimer: 30 mg, 0.024 mmol, 48%, monomer: 10 mg, 0.013 mmol, 26%.  $^1\text{H}$  NMR (400 MHz,  $\text{CDCl}_3$ ):  $\delta$  8.15 (s, 2H, 2  $\times$  NH), 7.91 (s, 2H, 2  $\times$   $\text{CH}_{\text{trz}}$ ), 6.89 (d,  $J = 1.6$  Hz, 2H, 2  $\times$   $\text{CH}_{\text{ar}}$ ), 6.86 (d,  $J = 1.7$  Hz, 2H, 2  $\times$   $\text{CH}_{\text{ar}}$ ), 5.15 (s, 4H, 2  $\times$   $\text{CH}_2$ ), 4.54 (d,  $J = 6.8$  Hz, 6H, 2  $\times$   $\text{CH}_2$ , 2  $\times$  CH), 4.14 - 4.06 (m, 4H, 2  $\times$   $\text{CH}_2$ ), 3.86 (t,  $J = 5.0$  Hz, 4H, 2  $\times$   $\text{CH}_2$ ), 3.58 (s, 12H, 6  $\times$   $\text{CH}_2$ ), 2.55 - 2.41 (m, 4H, 4  $\times$   $\text{CH}_2\text{-H}^{\text{a}}$ ), 2.40 - 2.25 (m, 2H, 2  $\times$   $\text{CH}_2\text{-H}^{\text{b}}$ ), 2.23 - 2.04 (m, 10H, 2  $\times$   $\text{CH}_3$ , 2  $\times$   $\text{CH}_2\text{-H}^{\text{b}}$ , 2  $\times$  CH), 1.42 (t,  $J = 7.0$  Hz, 6H, 2  $\times$   $\text{CH}_3$ ), 1.36 - 1.26 (m, 8H, 4  $\times$   $\text{CH}_2$ ), 0.86 (t,  $J = 6.8$  Hz, 6H, 2  $\times$   $\text{CH}_3$ ).  $^{13}\text{C}$  NMR (101 MHz,  $\text{CDCl}_3$ ):  $\delta$  196.01, 152.71, 150.91, 145.83, 144.46, 143.76, 142.74, 124.81, 123.10, 119.69, 118.12, 112.82, 109.44, 87.62, 70.73, 70.71, 70.55, 69.51, 66.22, 64.70, 50.53, 43.53, 38.34, 37.49, 33.88, 33.38, 19.94, 18.37, 14.97, 14.18.  $[\alpha]_D^{20} = -140^\circ$  ( $c = 0.62$ ,  $\text{CHCl}_3$ ). ESI-HRMS ( $m/z$ ): calcd. for  $[\text{C}_{60}\text{H}_{74}\text{Br}_2\text{N}_{10}\text{O}_{10} + \text{H}]^+$  1255.40084; obsd. 1255.40252.



**General procedure for the copper-catalyzed click reaction of alkyne-ligands **69** with azido-BODIPY to give fluorescent ligands (**71a,b**).** To a solution of alkynes **69** (1 eq) and azido-BODIPY-benzyl<sup>26</sup> (1.1 eq) in degassed  $t\text{-BuOH}/\text{ACN}$  (2 mL; 1/1; v/v) were added degassed aqueous solutions of sodium ascorbate (1.25 mL, 1.2 eq) and  $\text{CuSO}_4$  (0.2 mL, 20 mol%) and the resulting mixture was stirred for 24 h at room temperature. Since the conversion was not

complete, more sodium ascorbate (1 eq) and  $\text{CuSO}_4$  (20 mol%) were added and stirring was continued for 16 h. Dichloromethane and water were added, and the product was extracted with DCM (3 $\times$ ), dried ( $\text{MgSO}_4$ ) and concentrated. After silica column chromatography (0  $\rightarrow$  2.5% ( $n=3$ ) or 3% ( $n=4$ ) MeOH in DCM) the fluorescent ligand was obtained as a purple solid.

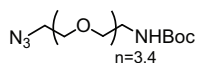
**Fluorescent ligand (71a).** Yield: 13 mg, 10  $\mu\text{mol}$ , 93%.  $R_f = 0.6$  (10:1 DCM:MeOH).  $^1\text{H}$  NMR (600 MHz,  $\text{CDCl}_3$ ):  $\delta$  8.07 (s, 1H,  $\text{CH}_{\text{trz}}$ ), 7.90 (s, 1H,  $\text{CH}_{\text{trz}}$ ), 7.85 (d,  $J = 8.8$  Hz, 2H, 2  $\times$   $\text{CH}_{\text{ar}}$ ), 7.56 (s, 1H, NH), 7.30 - 7.23 (m, 3H, 3  $\times$   $\text{CH}_{\text{ar}}$ ), 7.20 (t,  $J = 10.6$  Hz, 2H, 2  $\times$   $\text{CH}_{\text{ar}}$ ), 7.10 - 7.07 (m, 1H,  $\text{CH}_{\text{BDP}}$ ), 7.05 (s, 1H, NH), 6.97 (d,  $J = 4.0$  Hz, 1H,  $\text{CH}_{\text{ar}}$ ), 6.92 (d,  $J = 8.8$  Hz, 2H, 2  $\times$   $\text{CH}_{\text{ar}}$ ), 6.90 (d,  $J = 1.6$  Hz, 1H,  $\text{CH}_{\text{ar}}$ ), 6.80 (d,  $J = 1.7$  Hz, 1H,  $\text{CH}_{\text{BDP}}$ ), 6.55 (d,  $J = 4.0$  Hz, 1H,  $\text{CH}_{\text{BDP}}$ ), 5.94 (t,  $J = 5.4$  Hz, 1H, NH), 5.16 (s, 2H,  $\text{CH}_2$ ), 4.61 (t,  $J = 6.8$  Hz, 2H,  $\text{CH}_2$ ), 4.58 - 4.50 (m, 3H,



CH<sub>2</sub>, CH), 4.40 (d, *J* = 5.7 Hz, 2H, CH<sub>2</sub>), 4.14 - 4.04 (m, 2H, CH<sub>2</sub>), 4.03 - 3.95 (m, 2H, CH<sub>2</sub>), 3.86 (t, *J* = 5.1 Hz, 2H, CH<sub>2</sub>), 3.66 - 3.60 (m, 12H, 6 × CH<sub>2</sub>), 2.79 (t, *J* = 7.4 Hz, 2H, CH<sub>2</sub>), 2.51 (s, 3H, CH<sub>3</sub>), 2.46 - 2.38 (m, 3H, CH<sub>2</sub>, CH<sub>2</sub>-H<sup>a</sup>), 2.37 - 2.31 (m, 3H, CH<sub>2</sub>, CH<sub>2</sub>-H<sup>b</sup>), 2.31 - 2.23 (m, 1H, CH<sub>2</sub>-H<sup>b</sup>), 2.20 - 2.12 (m, 4H, CH<sub>3</sub>, CH), 2.08 - 2.02 (m, 4H, CH<sub>3</sub>, CH<sub>2</sub>-H<sup>b</sup>), 1.42 (t, *J* = 6.9 Hz, 3H, CH<sub>3</sub>), 1.34 - 1.26 (m, 4H, 2 × CH<sub>2</sub>), 0.87 (t, *J* = 6.7 Hz, 3H, CH<sub>3</sub>). <sup>13</sup>C NMR (151 MHz, CDCl<sub>3</sub>): δ 195.75, 171.59, 160.27, 159.70, 159.20, 155.38, 152.74, 149.82, 145.15, 144.68, 143.94, 143.39, 142.32, 140.29, 138.15, 135.08, 134.60, 130.92, 130.71, 128.85, 128.06, 127.88, 127.67, 126.20, 125.80, 124.68, 123.16, 122.89, 119.47, 118.49, 118.16, 114.30, 112.91, 109.93, 88.08, 70.74, 70.71, 70.57, 69.80, 69.65, 66.55, 64.71, 63.97, 50.42, 47.66, 43.83, 43.44, 39.08, 38.13, 37.52, 36.46, 33.91, 33.60, 29.94, 20.18, 19.90, 18.54, 14.94, 14.19, 13.36, 9.77. ESI-HRMS (*m/z*): calcd. for [C<sub>66</sub>H<sub>76</sub>BBBrF<sub>2</sub>N<sub>12</sub>O<sub>9</sub> + H]<sup>+</sup> 1309.51755; obsd. 1309.51908.

**Fluorescent ligand (71b).** Yield: 10 mg, 7 μmol, 71%. *R*<sub>f</sub> = 0.5 (10:1 DCM:MeOH). <sup>1</sup>H NMR (400 MHz, CDCl<sub>3</sub>): δ 8.07 (s, 1H, CH<sub>trz</sub>), 7.91 - 7.80 (m, 3H, 2 × CH<sub>2</sub>, CH<sub>trz</sub>), 7.55 (s, 1H, NH), 7.30 - 7.22 (m, 3H, 3 × CH<sub>ar</sub>), 7.20 - 7.16 (m, 2H, 2 × CH<sub>ar</sub>), 7.07 (s, 1H, CH<sub>BDP</sub>), 7.00 (s, 1H, NH), 6.96 (d, *J* = 4.1 Hz, 1H, CH<sub>ar</sub>), 6.93 (d, *J* = 8.9 Hz, 2H, 2 × CH<sub>ar</sub>), 6.90 (d, *J* = 1.9 Hz, 1H, CH<sub>ar</sub>), 6.78 (d, *J* = 1.9 Hz, 1H, CH<sub>BDP</sub>), 6.54 (d, *J* = 4.1 Hz, 1H, CH<sub>BDP</sub>), 5.87 (s, 1H, NH), 5.17 (s, 2H, CH<sub>2</sub>), 4.62 (t, *J* = 6.8 Hz, 2H, CH<sub>2</sub>), 4.55 - 4.49 (m, 3H, CH<sub>2</sub>, CH), 4.40 (d, *J* = 5.7 Hz, 2H, CH<sub>2</sub>), 4.16 - 4.05 (m, 2H, CH<sub>2</sub>), 4.01 (t, *J* = 5.7 Hz, 2H, CH<sub>2</sub>), 3.84 (t, *J* = 5.2 Hz, 2H, CH<sub>2</sub>), 3.68 - 3.54 (m, 16H, 8 × CH<sub>2</sub>), 2.79 (t, *J* = 7.5 Hz, 2H, CH<sub>2</sub>), 2.51 (s, 3H, CH<sub>3</sub>), 2.47 - 2.26 (m, 7H, 3 × CH<sub>2</sub>, CH<sub>2</sub>-H<sup>a</sup>), 2.19 - 2.12 (m, 4H, CH<sub>3</sub>, CH), 2.12 - 2.04 (m, 4H, CH<sub>3</sub>, CH<sub>2</sub>-H<sup>b</sup>), 1.42 (t, *J* = 7.0 Hz, 3H, CH<sub>3</sub>), 1.34 - 1.25 (m, 4H, 2 × CH<sub>2</sub>), 0.87 (t, *J* = 6.8 Hz, 3H, CH<sub>3</sub>). <sup>13</sup>C NMR (151 MHz, CDCl<sub>3</sub>): δ 195.72, 171.58, 160.31, 159.73, 159.18, 155.35, 152.76, 149.85, 145.20, 143.86, 142.34, 140.30, 138.16, 135.09, 134.61, 130.93, 130.72, 128.85, 128.04, 127.89, 127.67, 126.24, 125.84, 124.71, 123.16, 122.85, 119.51, 118.46, 118.22, 114.30, 112.91, 109.89, 96.64, 88.05, 70.77, 70.67, 70.58, 70.55, 69.84, 69.63, 66.48, 64.73, 63.97, 50.49, 47.69, 43.84, 43.45, 39.14, 38.13, 37.53, 36.47, 33.92, 33.58, 29.95, 20.18, 19.93, 18.52, 14.96, 14.20, 13.37, 9.78. ESI-HRMS (*m/z*): calcd. for [C<sub>68</sub>H<sub>80</sub>BBBrF<sub>2</sub>N<sub>12</sub>O<sub>10</sub> + H]<sup>+</sup> 1353.54376; obsd. 1353.54609.

#### General procedure for the Bocylation of mono-aminoPEG spacers 17 (72a,b).



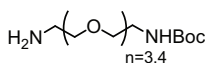
To a cooled (0 °C) solution of spacer **17** (0.5 mmol) and TEA in DCM (10 mL), Boc<sub>2</sub>O (131 mg, 0.6 mmol, 1.2 eq) was added, and the reaction stirred for 1 h at rt, after which the solvent was removed *in vacuo*.

The compound was purified by silica column chromatography (0 → 2% MeOH in DCM) to give a colorless oil.

**tert-Butyl (11-azido-3,6,9-trioxaundecyl)carbamate (72a).** Yield: 151 mg, 0.47 mmol, 95%. *R*<sub>f</sub> = 0.85 (EtOAc). <sup>1</sup>H NMR (400 MHz, CDCl<sub>3</sub>): δ 5.09 (s, 1H, NH), 3.76 - 3.59 (m, 10H, 5 × CH<sub>2</sub>), 3.54 (t, *J* = 5.2 Hz, 2H, CH<sub>2</sub>), 3.39 (t, *J* = 5.0 Hz, 2H, CH<sub>2</sub>), 3.31 (d, *J* = 4.9 Hz, 2H, CH<sub>2</sub>), 1.44 (s, 9H, 3 × CH<sub>3</sub>). <sup>13</sup>C NMR (101 MHz, CDCl<sub>3</sub>): δ 155.97, 79.08, 70.69, 70.62, 70.60, 70.24, 70.19, 70.04, 50.67, 40.38, 28.41. FT-IR (thin film) *v* 3352, 2977, 2872, 2098, 1710, 1508, 1276, 1249, 1170, 1110 cm<sup>-1</sup>. LC/MS analysis (10% → 90% ACN) *t*<sub>R</sub>: 7.04 min, ESI-MS (*m/z*): [M + H]<sup>+</sup>: 318.87.

**tert-Butyl (14-azido-3,6,9,12-tetraoxatetradecyl)carbamate (72b).** Yield: 171 mg, 0.47 mmol, 94%. *R*<sub>f</sub> = 0.85 (EtOAc). <sup>1</sup>H NMR (400 MHz, CDCl<sub>3</sub>): δ 5.09 (s, 1H, NH), 3.73 - 3.60 (m, 14H, 7 × CH<sub>2</sub>), 3.54 (t, *J* = 5.1 Hz, 2H, CH<sub>2</sub>), 3.39 (t, *J* = 5.0 Hz, 2H, CH<sub>2</sub>), 1.44 (s, 9H, 3 × CH<sub>3</sub>). <sup>13</sup>C NMR (101 MHz, CDCl<sub>3</sub>): δ 155.99, 79.15, 70.70, 70.67, 70.62, 70.60, 70.52, 70.25, 70.03, 50.69,

40.39, 28.43. FT-IR (thin film)  $\nu$  3349, 2924, 2869, 2102, 1710, 1506, 1276, 1250, 1169, 1112  $\text{cm}^{-1}$ . LC/MS analysis (10%  $\rightarrow$  90% ACN)  $t_R$ : 7.01 min, ESI-MS ( $m/z$ ):  $[M + H]^+$ : 362.93.



#### General procedure for the reduction of BocNH-PEG-azido spacers **72**

**(73a,b)**. Spacer **72** (1 eq) was dissolved in THF and  $\text{PPh}_3$  (1.2 eq) was added. After 1 h stirring at ambient temperature, water (0.5 mL) was added and stirring was continued for 20 h. Toluene was added, followed by washing

with HCl (aq, 1 M, 3x). The waterlayer was alkalized with NaOH (aq, 1 M) and extracted with EtOAc (3x) and DCM (3x). The combined organic layers were dried over  $\text{MgSO}_4$  and concentrated to afford compound **73**.

**tert-Butyl (11-amino-3,6,9-trioxaundecyl)carbamate (73a)**. Yield: 57 mg, 0.19 mmol, 72%.  $^1\text{H}$  NMR (400 MHz,  $\text{CDCl}_3$ ):  $\delta$  5.36 (s, 1H, NH), 3.72 - 3.60 (m, 8H,  $4 \times \text{CH}_2$ ), 3.54 (t,  $J = 5.1$  Hz, 4H,  $2 \times \text{CH}_2$ ), 3.31 (s, 2H,  $\text{CH}_2$ ), 2.90 (s, 2H,  $\text{CH}_2$ ), 2.39 (s, 2H,  $\text{NH}_2$ ), 1.44 (s, 9H,  $3 \times \text{CH}_3$ ).  $^{13}\text{C}$  NMR (101 MHz,  $\text{CDCl}_3$ ):  $\delta$  156.13, 79.11, 72.95, 70.58, 70.56, 70.33, 70.26, 41.56, 40.43, 28.49. LC/MS analysis (10%  $\rightarrow$  90% ACN)  $t_R$ : 4.16 min, ESI-MS ( $m/z$ ):  $[M + H]^+$ : 293.07.

**tert-Butyl (14-amino-3,6,9,12-tetraoxatetradecyl)carbamate (73b)**. Yield: 141 mg, 0.39 mmol, 78%.  $^1\text{H}$  NMR (400 MHz,  $\text{CDCl}_3$ ):  $\delta$  5.39 (s, 1H, NH), 3.70 - 3.60 (m, 12H,  $6 \times \text{CH}_2$ ), 3.57 - 3.49 (m, 4H,  $2 \times \text{CH}_2$ ), 3.34 - 3.28 (m, 2H,  $\text{CH}_2$ ), 2.88 (s, 2H,  $\text{CH}_2$ ), 2.29 (s, 2H,  $\text{NH}_2$ ), 1.44 (s, 9H,  $3 \times \text{CH}_3$ ).  $^{13}\text{C}$  NMR (101 MHz,  $\text{CDCl}_3$ ):  $\delta$  156.04, 78.97, 70.52, 70.51, 70.48, 70.47, 70.23, 70.17, 41.55, 40.32, 28.39. FT-IR (thin film)  $\nu$  3355, 2872, 1702, 1508, 1365, 1279, 1250, 1169, 1100  $\text{cm}^{-1}$ . LC/MS analysis (10%  $\rightarrow$  90% ACN)  $t_R$ : 4.52 min, ESI-MS ( $m/z$ ):  $[M + H]^+$ : 337.13.

#### General procedure for the coupling of mono-azido spacers **17** with

**ortho-, meta-, or para-functionalized DHP to give monomeric ligands**

**(o-/m-/p-74a,b)**. To a solution of **63**, **64** or **65** (30 mg, 0.052 mmol, 1 eq) in DCM (1 mL) were added spacer **17** (1 mL as a solution in DCM, 0.052 mmol, 1 eq), EEDQ (15 mg, 0.06 mmol, 1.2 eq) and DiPEA (26  $\mu\text{L}$ , 0.15 mmol, 3 eq). Reaction progress was slow, so after 24 h another 2 eq of EEDQ and 1.5 eq of spacer were added. The reaction was monitored by TLC, and upon completion, the mixture was washed with HCl (aq, 1 M, 2x), water (2x), dried ( $\text{MgSO}_4$ ) and concentrated.

Pure monomers were obtained by silica column chromatography (0  $\rightarrow$

2% MeOH in DCM).  $R_f = 0.7$  (12:1 DCM:MeOH). FT-IR (thin film)  $\nu$  3294, 2924, 2866, 2360, 2343, 2201, 2110, 1644, 1498, 1426, 1384, 1275, 1124, 1045  $\text{cm}^{-1}$ .

#### **N-(11-azido-3,6,9-trioxaundecyl)-2-((2-bromo-4-((4R,7S)-3-cyano-2-methyl-5-oxo-7-propyl-1,4,5,6,7,8-hexahydroquinolin-4-yl)-6-ethoxyphenoxy)methyl)benzamide (o-74a)**

Yield: 32 mg, 0.041 mmol, 79%.  $^1\text{H}$  NMR (400 MHz,  $\text{CDCl}_3$ ):  $\delta$  7.63 - 7.55 (m, 2H,  $\text{CH}_{\text{ar}}$ , NH), 7.52 (s, 1H, NH), 7.43 - 7.33 (m, 3H,  $3 \times \text{CH}_{\text{ar}}$ ), 6.82 (s, 2H,  $2 \times \text{CH}_{\text{ar}}$ ), 5.16 (s, 2H,  $\text{CH}_2$ ), 4.53 (s, 1H, CH), 4.02 - 3.87 (m, 2H,  $\text{CH}_2$ ), 3.69 - 3.54 (m, 14H,  $7 \times \text{CH}_2$ ), 3.37 - 3.28 (m, 2H,  $\text{CH}_2$ ), 2.49 - 2.34 (m, 2H,  $2 \times \text{CH}_2\text{-H}^{\text{a}}$ ), 2.31 - 2.20 (m, 1H,  $\text{CH}_2\text{-H}^{\text{b}}$ ), 2.17 - 2.02 (m, 5H,  $\text{CH}_3$ , CH,  $\text{CH}_2\text{-H}^{\text{b}}$ ), 1.29 (t,  $J = 6.9$  Hz, 7H,  $\text{CH}_3$ ,  $2 \times \text{CH}_2$ ), 0.88 (t,  $J = 6.7$  Hz, 3H,  $\text{CH}_3$ ).  $^{13}\text{C}$  NMR (101 MHz,  $\text{CDCl}_3$ ):  $\delta$  195.69, 169.41, 152.66, 150.11, 145.33, 143.24, 142.70, 136.81, 134.19, 130.93, 130.24, 128.55, 128.11, 123.12, 119.41, 118.03, 112.59, 109.67, 87.82, 72.68, 70.67, 70.65, 70.48, 70.03, 69.73, 64.47, 50.75, 43.48, 40.12, 38.34, 37.44, 33.82, 33.43, 19.88, 18.42, 14.66, 14.17.  $[\alpha]_D^{20} =$

-103° (c = 0.5, CHCl<sub>3</sub>). ESI-HRMS (*m/z*): calcd. for [C<sub>38</sub>H<sub>47</sub>BrN<sub>6</sub>O<sub>7</sub> + H]<sup>+</sup> 779.27624; obsd. 779.27650.

***N*-(14-azido-3, 6, 9, 12-tetraoxatetradecyl) -2-((2-bromo-4- (4*R*,7*S*) -3-cyano-2-methyl-5-oxo-7-propyl-1, 4, 5, 6, 7, 8-hexahydroquinolin-4-yl)-6-ethoxyphenoxy)methyl)benzamide (o-74b).**

Yield: 32 mg, 0.039 mmol, 75%. <sup>1</sup>H NMR (400 MHz, CDCl<sub>3</sub>): δ 7.63 - 7.57 (m, 1H, CH<sub>ar</sub>), 7.53 - 7.45 (m, 2H, 2 × NH), 7.42 - 7.35 (m, 3H, 3 × CH<sub>ar</sub>), 6.83 (s, 1H, CH<sub>ar</sub>), 6.82 (s, 1H, CH<sub>ar</sub>), 5.16 (s, 2H, CH<sub>2</sub>), 4.53 (s, 1H, CH), 4.02 - 3.87 (m, 2H, CH<sub>2</sub>), 3.72 - 3.49 (m, 18H, 9 × CH<sub>2</sub>), 3.36 (t, *J* = 5.0 Hz, 2H, CH<sub>2</sub>), 2.49 - 2.33 (m, 2H, CH<sub>2</sub>), 2.30 - 2.20 (m, 1H, CH<sub>2</sub>-H<sup>a</sup>), 2.19 - 1.99 (m, 5H, CH<sub>3</sub>, CH, CH<sub>2</sub>-H<sup>b</sup>), 1.33 - 1.20 (m, 7H, CH<sub>3</sub>, 2 × CH<sub>2</sub>), 0.88 (t, *J* = 6.5 Hz, 3H, CH<sub>3</sub>). <sup>13</sup>C NMR (101 MHz, CDCl<sub>3</sub>): δ 195.66, 169.40, 152.66, 150.05, 145.33, 143.30, 142.63, 136.76, 134.26, 130.87, 130.23, 128.51, 128.08, 123.08, 119.42, 118.03, 112.59, 109.68, 87.81, 72.66, 70.73, 70.67, 70.61, 70.57, 70.46, 70.05, 69.73, 64.47, 50.76, 43.48, 40.10, 38.28, 37.45, 33.83, 33.44, 19.88, 18.42, 14.67, 14.17. [α]<sub>D</sub><sup>20</sup> = -135° (c = 0.5, CHCl<sub>3</sub>). ESI-HRMS (*m/z*): calcd. for [C<sub>40</sub>H<sub>51</sub>BrN<sub>6</sub>O<sub>8</sub> + H]<sup>+</sup> 823.30245; obsd. 823.30316.

***N*-(11-azido-3,6,9-trioxaundecyl) -3-((2-bromo-4- (4*R*,7*S*) -3-cyano-2-methyl-5-oxo-7-propyl-1, 4, 5, 6, 7, 8-hexahydroquinolin-4-yl)-6-ethoxyphenoxy)methyl)benzamide (m-74a).**

Yield: 30 mg, 0.039 mmol, 74%. <sup>1</sup>H NMR (400 MHz, CDCl<sub>3</sub>): δ 8.07 (s, 1H, CH<sub>ar</sub>), 7.73 (d, *J* = 7.8 Hz, 1H, CH<sub>ar</sub>), 7.66 (d, *J* = 10.1 Hz, 2H, CH<sub>ar</sub>, NH), 7.45 (t, *J* = 7.7 Hz, 1H, CH<sub>ar</sub>), 7.00 (s, 1H, NH), 6.91 (d, *J* = 1.8 Hz, 1H, CH<sub>ar</sub>), 6.86 (d, *J* = 1.9 Hz, 1H, CH<sub>ar</sub>), 5.03 (s, 2H, CH<sub>2</sub>), 4.55 (s, 1H, CH), 4.19 - 4.03 (m, 2H, CH<sub>2</sub>), 3.75 - 3.54 (m, 14H, 7 × CH<sub>2</sub>), 3.40 - 3.27 (m, 2H, CH<sub>2</sub>), 2.48 - 2.23 (m, 3H, CH<sub>2</sub>, CH<sub>2</sub>-H<sup>a</sup>), 2.17 - 2.02 (m, 5H, CH<sub>3</sub>, CH, CH<sub>2</sub>-H<sup>b</sup>), 1.43 (t, *J* = 7.0 Hz, 3H, CH<sub>3</sub>), 1.33 - 1.18 (m, 4H, 2 × CH<sub>2</sub>), 0.85 (t, *J* = 6.9 Hz, 3H, CH<sub>3</sub>). <sup>13</sup>C NMR (101 MHz, CDCl<sub>3</sub>): δ 195.93, 168.01, 152.71, 150.35, 145.39, 144.04, 142.57, 138.42, 134.68, 131.34, 128.63, 127.13, 126.44, 123.14, 119.57, 118.09, 113.03, 109.70, 87.87, 74.01, 70.75, 70.67, 70.41, 70.08, 69.80, 64.68, 50.74, 43.54, 40.05, 38.43, 37.50, 33.92, 33.51, 19.84, 18.44, 14.95, 14.15. [α]<sub>D</sub><sup>20</sup> = -102° (c = 0.5, CHCl<sub>3</sub>). ESI-HRMS (*m/z*): calcd. for [C<sub>38</sub>H<sub>47</sub>BrN<sub>6</sub>O<sub>7</sub> + H]<sup>+</sup> 779.27624; obsd. 779.27652.

***N*-(14-azido-3, 6, 9, 12-tetraoxatetradecyl) -3-((2-bromo-4- (4*R*,7*S*) -3-cyano-2-methyl-5-oxo-7-propyl-1, 4, 5, 6, 7, 8-hexahydroquinolin-4-yl)-6-ethoxyphenoxy)methyl)benzamide (m-74b).**

Yield: 36 mg, 0.044 mmol, 84%. <sup>1</sup>H NMR (400 MHz, CDCl<sub>3</sub>): δ 8.08 (s, 1H, CH<sub>ar</sub>), 7.76 - 7.71 (m, 2H, NH, CH<sub>ar</sub>), 7.66 (d, *J* = 7.5 Hz, 1H, CH<sub>ar</sub>), 7.45 (t, *J* = 7.7 Hz, 1H, CH<sub>ar</sub>), 7.07 (s, 1H, NH), 6.92 (s, 1H, CH<sub>ar</sub>), 6.86 (s, 1H, CH<sub>ar</sub>), 5.03 (s, 2H, CH<sub>2</sub>), 4.55 (s, 1H, CH), 4.12 (dd, *J* = 6.9, 2.0 Hz, 2H, CH<sub>2</sub>), 3.73 - 3.55 (m, 18H, 9 × CH<sub>2</sub>), 3.35 (t, *J* = 4.8 Hz, 2H, CH<sub>2</sub>), 2.46 - 2.26 (m, 3H, CH<sub>2</sub>, CH<sub>2</sub>-H<sup>a</sup>), 2.26 - 1.99 (m, 5H, CH<sub>3</sub>, CH, CH<sub>2</sub>-H<sup>b</sup>), 1.43 (t, *J* = 6.9 Hz, 3H, CH<sub>3</sub>), 1.35 - 1.18 (m, 4H, 2 × CH<sub>2</sub>), 0.85 (t, *J* = 6.6 Hz, 3H, CH<sub>3</sub>). <sup>13</sup>C NMR (101 MHz, CDCl<sub>3</sub>): δ 195.91, 167.99, 152.69, 150.35, 145.42, 144.04, 142.56, 138.41, 134.65, 131.34, 128.61, 127.21, 126.44, 123.12, 119.58, 118.08, 113.03, 109.69, 87.84, 74.02, 70.73, 70.64, 70.41, 70.07, 69.83, 64.67, 50.75, 43.55, 40.07, 38.42, 37.50, 33.92, 33.50, 19.84, 18.44, 14.95, 14.15. [α]<sub>D</sub><sup>20</sup> = -123° (c = 0.5, CHCl<sub>3</sub>). ESI-HRMS (*m/z*): calcd. for [C<sub>40</sub>H<sub>51</sub>BrN<sub>6</sub>O<sub>8</sub> + H]<sup>+</sup> 823.30245; obsd. 823.30294.

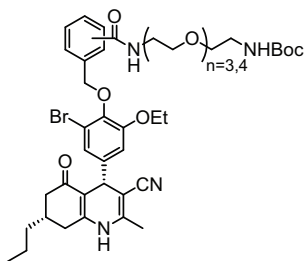
***N*-(11-azido-3,6,9-trioxaundecyl) -4-((2-bromo-4- (4*R*,7*S*) -3-cyano-2-methyl-5-oxo-7-propyl-1, 4, 5, 6, 7, 8-hexahydroquinolin-4-yl)-6-ethoxyphenoxy)methyl)benzamide (p-74a).**

Yield: 37 mg, 0.047 mmol, 91%. <sup>1</sup>H NMR (400 MHz, CDCl<sub>3</sub>): δ 7.79 (d, *J* = 8.2 Hz, 2H, 2 × CH<sub>ar</sub>), 7.62 (d, *J* = 8.3 Hz, 2H, 2 × CH<sub>ar</sub>), 7.31 (s, 1H, NH), 6.94 (d, *J* = 5.1 Hz, 1H, NH), 6.90 (d, *J* = 1.9 Hz, 1H, CH<sub>ar</sub>), 6.83 (d, *J* = 1.9 Hz, 1H, CH<sub>ar</sub>), 5.04 (s, 2H, CH<sub>2</sub>), 4.55 (s, 1H, CH), 4.16 - 4.04 (m, 2H, CH<sub>2</sub>), 3.72 - 3.58 (m, 14H, 7 × CH<sub>2</sub>), 3.38 - 3.27 (m, 2H, CH<sub>2</sub>), 2.51 - 2.38 (m, 2H, 2

$\times$  CH<sub>2</sub>-H<sup>a</sup>), 2.37 - 2.23 (m, 1H, CH<sub>2</sub>-H<sup>b</sup>), 2.22 - 2.04 (m, 5H, CH<sub>3</sub>, CH, CH<sub>2</sub>-H<sup>b</sup>), 1.42 (t,  $J$  = 7.0 Hz, 3H, CH<sub>3</sub>), 1.36 - 1.25 (m, 4H, 2  $\times$  CH<sub>2</sub>), 0.89 (t,  $J$  = 6.9 Hz, 3H, CH<sub>3</sub>). <sup>13</sup>C NMR (101 MHz, CDCl<sub>3</sub>):  $\delta$  195.79, 167.83, 152.77, 149.94, 145.11, 144.19, 142.37, 141.40, 134.05, 128.33, 127.10, 123.11, 119.41, 118.08, 113.00, 109.89, 88.13, 73.91, 70.78, 70.76, 70.69, 70.41, 70.14, 69.82, 64.72, 50.77, 43.48, 40.00, 38.32, 37.45, 33.86, 33.56, 19.93, 18.51, 14.94, 14.17.  $[\alpha]_D^{20}$  = -97° (c = 0.5, CHCl<sub>3</sub>). ESI-HRMS ( $m/z$ ): calcd. for [C<sub>38</sub>H<sub>47</sub>BrN<sub>6</sub>O<sub>7</sub> + H]<sup>+</sup> 779.27624; obsd. 779.27670.

***N*-(14-azido-3, 6, 9, 12-tetraoxatetradecyl) -4-((2-bromo-4- (4*R*,7*S*) -3-cyano-2-methyl-5-oxo-7-propyl-1, 4, 5, 6, 7, 8-hexahydroquinolin-4-yl)-6-ethoxyphenoxy)methyl)benzamide (p-74b).**

Yield: 34 mg, 0.041 mmol, 79%. <sup>1</sup>H NMR (400 MHz, CDCl<sub>3</sub>):  $\delta$  7.80 (d,  $J$  = 8.0 Hz, 2H, 2  $\times$  CH<sub>ar</sub>), 7.62 (d,  $J$  = 7.3 Hz, 3H, 2  $\times$  CH<sub>ar</sub>, NH), 7.14 - 7.08 (m, 1H, NH), 6.90 (s, 1H, CH<sub>ar</sub>), 6.84 (s, 1H, CH<sub>ar</sub>), 5.03 (s, 2H, CH<sub>2</sub>), 4.55 (s, 1H, CH), 4.19 - 3.98 (m, 2H, CH<sub>2</sub>), 3.72 - 3.58 (m, 18H, 9  $\times$  CH<sub>2</sub>), 3.34 (t,  $J$  = 5.0 Hz, 2H, CH<sub>2</sub>), 2.52 - 2.36 (m, 2H, CH<sub>2</sub>), 2.34 - 2.22 (m, 2H, CH<sub>2</sub>), 2.14 - 2.01 (m, 4H, CH<sub>3</sub>, CH), 1.42 (t,  $J$  = 6.9 Hz, 3H, CH<sub>3</sub>), 1.36 - 1.26 (m, 4H, 2  $\times$  CH<sub>2</sub>), 0.89 (t,  $J$  = 6.7 Hz, 3H, CH<sub>3</sub>). <sup>13</sup>C NMR (101 MHz, CDCl<sub>3</sub>):  $\delta$  195.82, 167.86, 152.74, 150.17, 145.27, 144.14, 142.44, 141.36, 134.00, 128.28, 127.13, 123.09, 119.48, 118.05, 112.93, 109.74, 87.95, 73.89, 70.72, 70.63, 70.38, 70.06, 69.83, 64.68, 50.73, 43.46, 40.02, 38.31, 37.42, 33.83, 33.45, 19.91, 18.42, 14.93, 14.16.  $[\alpha]_D^{20}$  = -107° (c = 0.5, CHCl<sub>3</sub>). ESI-HRMS ( $m/z$ ): calcd. for [C<sub>40</sub>H<sub>51</sub>BrN<sub>6</sub>O<sub>8</sub> + H]<sup>+</sup> 823.30245; obsd. 823.30323.



**General procedure for the coupling of mono-Boc-diaminospacers **73** with *ortho*-, *meta*-, or *para*-functionalized DHP to give Boc-protected monomeric ligands (*o*-/*m*-/*p*-75a,b).** To a solution of **63**, **64** or **65** (20 mg, 0.034 mmol, 1 eq) in DCM (1 mL) were added spacer **73** (1 mL as a solution in DCM, 0.053 mmol, 1.5 eq) and EEDQ (17 mg, 0.07 mmol, 2 eq). The reaction was monitored by TLC, and upon completion (16-36 h), the mixture was loaded onto a silica column (0  $\rightarrow$  4% MeOH in DCM) to give the Boc-protected monomers as slightly yellow solids.  $R_f$  = 0.35 (15:1 DCM:MeOH).

***tert*-Butyl (1-(2-((2-bromo-4- (4*R*,7*S*) -3-cyano-2-methyl-5-oxo-7-propyl-1, 4, 5, 6, 7, 8-hexahydroquinolin-4-yl)-6-ethoxyphenoxy)methyl) phenyl) -1-oxo-5,8,11-trioxa-2-azatridecan-13-yl) carbamate (o-75a).** Yield: 27 mg, 0.032 mmol, 93%. <sup>1</sup>H NMR (400 MHz, CDCl<sub>3</sub>):  $\delta$  7.64 - 7.58 (m, 1H, CH<sub>ar</sub>), 7.57 - 7.45 (m, 2H, 2  $\times$  NH), 7.40 - 7.34 (m, 3H, 3  $\times$  CH<sub>ar</sub>), 6.84 (d,  $J$  = 1.8 Hz, 1H, CH<sub>ar</sub>), 6.81 (d,  $J$  = 1.8 Hz, 1H, CH<sub>ar</sub>), 5.16 (s, 2H, CH<sub>2</sub>), 5.09 (s, 1H, NH), 4.54 (s, 1H, CH), 4.04 - 3.86 (m, 2H, CH<sub>2</sub>), 3.71 - 3.49 (m, 12H, 6  $\times$  CH<sub>2</sub>), 3.47 (t,  $J$  = 5.2 Hz, 2H, CH<sub>2</sub>), 3.29 - 3.22 (m, 2H, CH<sub>2</sub>), 2.49 - 2.37 (m, 2H, 2  $\times$  CH<sub>2</sub>-H<sup>a</sup>), 2.34 - 2.22 (m, 1H, CH<sub>2</sub>-H<sup>b</sup>), 2.19 - 2.02 (m, 5H, CH<sub>3</sub>, CH, CH<sub>2</sub>-H<sup>b</sup>), 1.43 (s, 9H, 3  $\times$  CH<sub>3</sub>), 1.33 - 1.26 (m, 7H, CH<sub>3</sub>, 2  $\times$  CH<sub>2</sub>), 0.89 (t,  $J$  = 6.7 Hz, 3H, CH<sub>3</sub>). <sup>13</sup>C NMR (101 MHz, CDCl<sub>3</sub>):  $\delta$  195.63, 169.36, 156.27, 152.68, 149.98, 145.27, 143.30, 142.64, 136.94, 134.12, 131.00, 130.20, 128.59, 128.25, 123.04, 119.39, 118.07, 112.63, 109.79, 87.90, 79.45, 72.76, 70.56, 70.54, 70.49, 70.27, 70.17, 69.85, 64.51, 43.50, 40.50, 40.10, 38.25, 37.48, 33.86, 33.50, 28.55, 19.90, 18.46, 14.68, 14.17.  $[\alpha]_D^{20}$  = -91° (c = 0.44, CHCl<sub>3</sub>). ESI-HRMS ( $m/z$ ): calcd. for [C<sub>43</sub>H<sub>57</sub>BrN<sub>4</sub>O<sub>9</sub> + H]<sup>+</sup> 853.33817; obsd. 853.33933.

***tert*-Butyl (1-(3-((2-bromo-4- (4*R*,7*S*) -3-cyano-2-methyl-5-oxo-7-propyl-1, 4, 5, 6, 7, 8-hexahydroquinolin-4-yl)-6-ethoxyphenoxy)methyl) phenyl) -1-oxo-5,8,11,14-tetraoxa-2-azaheptadecan-16-yl) carbamate (o-75b).** Yield: 25 mg, 0.028 mmol, 82%. <sup>1</sup>H NMR (400 MHz, CDCl<sub>3</sub>):  $\delta$  7.64 - 7.59 (m, 1H, CH<sub>ar</sub>), 7.54 (s, 2H, 2  $\times$  NH), 7.41 - 7.34 (m, 3H, 3  $\times$  CH<sub>ar</sub>), 6.84 (d,  $J$  = 1.6 Hz, 1H,

CH<sub>ar</sub>), 6.81 (d,  $J = 1.8$  Hz, 1H, CH<sub>ar</sub>), 5.16 (s, 2H, CH<sub>2</sub>), 5.12 (s, 1H, NH), 4.54 (s, 1H, CH), 3.95 (qd,  $J = 9.3, 2.2$  Hz, 2H, CH<sub>2</sub>), 3.67 (s, 4H, 2 × CH<sub>2</sub>), 3.64 - 3.52 (m, 12H, 6 × CH<sub>2</sub>), 3.50 (t,  $J = 5.1$  Hz, 2H, CH<sub>2</sub>), 3.33 - 3.24 (m, 2H, CH<sub>2</sub>), 2.48 - 2.36 (m, 2H, 2 × CH<sub>2</sub>-H<sup>a</sup>), 2.34 - 2.22 (m, 1H, CH<sub>2</sub>-H<sup>b</sup>), 2.20 - 2.03 (m, 5H, CH<sub>3</sub>, CH, CH<sub>2</sub>-H<sup>b</sup>), 1.44 (s, 9H, 3 × CH<sub>3</sub>), 1.35 - 1.24 (m, 7H, CH<sub>3</sub>, 2 × CH<sub>2</sub>), 0.89 (t,  $J = 6.5$  Hz, 3H, CH<sub>3</sub>). <sup>13</sup>C NMR (101 MHz, CDCl<sub>3</sub>):  $\delta$  195.66, 169.37, 156.26, 152.68, 150.01, 145.33, 143.32, 142.62, 136.84, 134.23, 130.89, 130.20, 128.53, 128.20, 123.02, 119.45, 118.06, 112.57, 109.74, 87.84, 79.42, 72.75, 70.59, 70.54, 70.45, 70.31, 69.86, 64.48, 43.51, 40.48, 40.08, 38.23, 37.50, 33.88, 33.49, 28.55, 19.90, 18.47, 14.69, 14.18.  $[\alpha]_D^{20} = -94^\circ$  ( $c = 0.5$ , CHCl<sub>3</sub>). ESI-HRMS ( $m/z$ ): calcd. for [C<sub>45</sub>H<sub>61</sub>BrN<sub>4</sub>O<sub>10</sub> + H]<sup>+</sup> 897.36438; obsd. 897.36608.

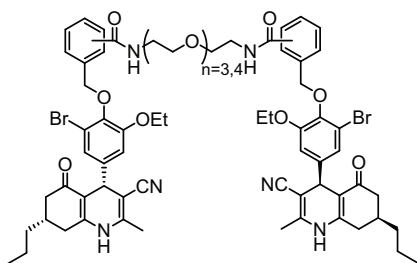
**tert-Butyl (1-(3-((2-bromo-4-((4*R*,7*S*)-3-cyano-2-methyl-5-oxo-7-propyl-1, 4, 5, 6, 7, 8-hexahydroquinolin-4-yl)-6-ethoxyphenoxy)methyl) phenyl) -1-oxo-5,8,11-trioxa-2-azatridecan-13-yl) carbamate (m-75a).** Yield: 22 mg, 0.026 mmol, 90%. <sup>1</sup>H NMR (400 MHz, CDCl<sub>3</sub>):  $\delta$  8.06 (s, 1H, CH<sub>ar</sub>), 7.75 (d,  $J = 7.5$  Hz, 1H, CH<sub>ar</sub>), 7.64 (d,  $J = 7.7$  Hz, 1H, CH<sub>ar</sub>), 7.52 (s, 1H, NH), 7.43 (t,  $J = 7.7$  Hz, 1H, CH<sub>ar</sub>), 7.00 (s, 1H, NH), 6.91 (d,  $J = 1.8$  Hz, 1H, CH<sub>ar</sub>), 6.84 (d,  $J = 1.8$  Hz, 1H, CH<sub>ar</sub>), 5.06 (t,  $J = 5.5$  Hz, 1H, NH), 5.03 (s, 2H, CH<sub>2</sub>), 4.54 (s, 1H, CH), 4.15 - 4.07 (m, 2H, CH<sub>2</sub>), 3.68 - 3.56 (m, 12H, 6 × CH<sub>2</sub>), 3.48 (t,  $J = 5.2$  Hz, 2H, CH<sub>2</sub>), 3.28 - 3.20 (m, 2H, CH<sub>2</sub>), 2.45 - 2.27 (m, 3H, CH<sub>2</sub>, CH<sub>2</sub>-H<sup>a</sup>), 2.19 - 1.99 (m, 5H, CH<sub>3</sub>, CH, CH<sub>2</sub>-H<sup>b</sup>), 1.43 (d,  $J = 6.4$  Hz, 12H, 4 × CH<sub>3</sub>), 1.30 - 1.23 (m, 4H, 2 × CH<sub>2</sub>), 0.86 (t,  $J = 6.8$  Hz, 3H, CH<sub>3</sub>). <sup>13</sup>C NMR (101 MHz, CDCl<sub>3</sub>):  $\delta$  195.83, 167.94, 156.22, 152.73, 150.12, 145.27, 144.11, 142.50, 138.33, 134.70, 131.30, 128.62, 127.05, 126.63, 123.10, 119.51, 118.09, 113.09, 109.84, 88.00, 81.79, 74.09, 70.61, 70.58, 70.43, 70.28, 69.96, 64.72, 43.55, 40.48, 40.03, 38.37, 37.53, 33.95, 33.58, 28.55, 19.87, 18.51, 14.95, 14.16.  $[\alpha]_D^{20} = -84^\circ$  ( $c = 0.44$ , CHCl<sub>3</sub>). ESI-HRMS ( $m/z$ ): calcd. for [C<sub>43</sub>H<sub>57</sub>BrN<sub>4</sub>O<sub>9</sub> + H]<sup>+</sup> 853.33817; obsd. 853.33937.

**tert-Butyl (1-(3-((2-bromo-4-((4*R*,7*S*)-3-cyano-2-methyl-5-oxo-7-propyl-1, 4, 5, 6, 7, 8-hexahydroquinolin-4-yl)-6-ethoxyphenoxy)methyl) phenyl) -1-oxo-5,8,11,14-tetraoxa-2-azahexadecan-16-yl) carbamate (m-75b).** Yield: 22 mg, 0.025 mmol, 72%. <sup>1</sup>H NMR (400 MHz, CDCl<sub>3</sub>):  $\delta$  8.07 (s, 1H, CH<sub>ar</sub>), 7.75 (d,  $J = 7.5$  Hz, 1H, CH<sub>ar</sub>), 7.66 (d,  $J = 7.3$  Hz, 2H, CH<sub>ar</sub>, NH), 7.44 (t,  $J = 7.6$  Hz, 1H, CH<sub>ar</sub>), 7.07 (s, 1H, NH), 6.92 (s, 1H, CH<sub>ar</sub>), 6.85 (s, 1H, CH<sub>ar</sub>), 5.12 (s, 1H, NH), 5.03 (s, 2H, CH<sub>2</sub>), 4.55 (s, 1H, CH), 4.18 - 4.05 (m, 2H, CH<sub>2</sub>), 3.74 - 3.52 (m, 16H, 8 × CH<sub>2</sub>), 3.50 (t,  $J = 4.9$  Hz, 2H, CH<sub>2</sub>), 3.28 (d,  $J = 4.6$  Hz, 2H, CH<sub>2</sub>), 2.48 - 2.28 (m, 3H, CH<sub>2</sub>, CH<sub>2</sub>-H<sup>a</sup>), 2.21 - 1.99 (m, 5H, CH<sub>3</sub>, CH, CH<sub>2</sub>-H<sup>b</sup>), 1.43 (s, 12H, 4 × CH<sub>3</sub>), 1.27 (m, 4H, 2 × CH<sub>2</sub>), 0.86 (t,  $J = 6.5$  Hz, 3H, CH<sub>3</sub>). <sup>13</sup>C NMR (101 MHz, CDCl<sub>3</sub>):  $\delta$  195.88, 167.94, 156.21, 152.70, 150.26, 145.38, 144.05, 142.54, 138.35, 134.67, 131.31, 128.60, 127.14, 126.56, 123.09, 119.58, 118.08, 113.02, 109.75, 87.88, 79.37, 74.05, 70.63, 70.59, 70.41, 70.34, 70.28, 69.93, 64.67, 43.56, 40.46, 40.04, 38.38, 37.53, 33.95, 33.53, 28.55, 19.86, 18.48, 14.96, 14.17.  $[\alpha]_D^{20} = -91^\circ$  ( $c = 0.44$ , CHCl<sub>3</sub>). ESI-HRMS ( $m/z$ ): calcd. for [C<sub>45</sub>H<sub>61</sub>BrN<sub>4</sub>O<sub>10</sub> + H]<sup>+</sup> 897.36438; obsd. 897.36615.

**tert-Butyl (1-(4-((2-bromo-4-((4*R*,7*S*)-3-cyano-2-methyl-5-oxo-7-propyl-1, 4, 5, 6, 7, 8-hexahydroquinolin-4-yl)-6-ethoxyphenoxy)methyl) phenyl) -1-oxo-5,8,11-trioxa-2-azatridecan-13-yl) carbamate (p-75a).** Yield: 26 mg, 0.03 mmol, 89%. <sup>1</sup>H NMR (400 MHz, CDCl<sub>3</sub>):  $\delta$  7.79 (d,  $J = 7.5$  Hz, 2H, 2 × CH<sub>ar</sub>), 7.61 (d,  $J = 7.9$  Hz, 2H, 2 × CH<sub>ar</sub>), 7.22 (s, 1H, NH), 6.90 (s, 2H, NH, CH<sub>ar</sub>), 6.82 (s, 1H, CH<sub>ar</sub>), 5.05 (s, 1H, NH), 5.02 (s, 2H, CH<sub>2</sub>), 4.55 (s, 1H, CH), 4.16 - 4.06 (m, 2H, CH<sub>2</sub>), 3.71 - 3.57 (m, 12H, 6 × CH<sub>2</sub>), 3.50 (t,  $J = 5.1$  Hz, 2H, CH<sub>2</sub>), 3.27 (d,  $J = 4.4$  Hz, 2H, CH<sub>2</sub>), 2.51 - 2.37 (m, 2H, 2 × CH<sub>2</sub>-H<sup>a</sup>), 2.37 - 2.26 (m, 1H, CH<sub>2</sub>-H<sup>b</sup>), 2.23 - 2.04 (m, 5H, CH<sub>3</sub>, CH, CH<sub>2</sub>-H<sup>b</sup>), 1.46 - 1.40 (m, 12H, 4 × CH<sub>3</sub>), 1.36 - 1.28 (m, 4H, 2 × CH<sub>2</sub>), 0.89 (t,  $J = 6.7$  Hz, 3H, CH<sub>3</sub>). <sup>13</sup>C NMR (101 MHz, CDCl<sub>3</sub>):  $\delta$  195.72, 191.97, 167.77, 157.18, 156.19, 152.76, 149.80,

146.81, 145.04, 144.21, 142.34, 141.31, 139.61, 134.07, 128.34, 127.15, 123.10, 119.39, 118.09, 113.07, 109.97, 100.11, 88.19, 81.39, 73.96, 70.62, 70.59, 70.40, 70.30, 69.97, 64.73, 43.49, 40.47, 39.99, 38.30, 37.48, 33.89, 33.61, 28.55, 19.93, 18.55, 14.95, 14.79, 14.16.  $[\alpha]_D^{20} = -77^\circ$  ( $c = 0.52$ ,  $\text{CHCl}_3$ ). ESI-HRMS ( $m/z$ ): calcd. for  $[\text{C}_{43}\text{H}_{57}\text{BrN}_4\text{O}_9 + \text{H}]^+$  853.33817; obsd. 853.33898.

**tert-Butyl (1-(4-((2-bromo-4-(4*R*,7*S*)-3-cyano-2-methyl-5-oxo-7-propyl-1,4,5,6,7,8-hexahydroquinolin-4-yl)-6-ethoxyphenoxy)methyl) phenyl)-1-oxo-5,8,11,14-tetraoxa-2-aza-hexadecan-16-yl) carbamate (**p-75b**). Yield: 24 mg, 0.027 mmol, 79%.  $^1\text{H}$  NMR (400 MHz,  $\text{CDCl}_3$ ):  $\delta$  7.82 (d,  $J = 8.1$  Hz, 2H, 2  $\times$   $\text{CH}_{\text{ar}}$ ), 7.61 (d,  $J = 8.1$  Hz, 2H, 2  $\times$   $\text{CH}_{\text{ar}}$ ), 7.42 (s, 1H, NH), 7.16 (s, 1H, NH), 6.90 (d,  $J = 1.8$  Hz, 1H,  $\text{CH}_{\text{ar}}$ ), 6.82 (d,  $J = 1.8$  Hz, 1H,  $\text{CH}_{\text{ar}}$ ), 5.18 (s, 1H, NH), 5.03 (s, 2H,  $\text{CH}_2$ ), 4.55 (s, 1H, CH), 4.18 - 4.05 (m, 2H,  $\text{CH}_2$ ), 3.69 - 3.48 (m, 18H, 9  $\times$   $\text{CH}_2$ ), 3.33 - 3.24 (m, 2H,  $\text{CH}_2$ ), 2.51 - 2.38 (m, 2H, 2  $\times$   $\text{CH}_2\text{-H}^{\text{a}}$ ), 2.37 - 2.07 (m, 6H,  $\text{CH}_3$ , CH, 2  $\times$   $\text{CH}_2\text{-H}^{\text{b}}$ ), 1.46 - 1.39 (m, 12H, 4  $\times$   $\text{CH}_3$ ), 1.35 - 1.27 (m, 4H, 2  $\times$   $\text{CH}_2$ ), 0.89 (t,  $J = 6.8$  Hz, 3H,  $\text{CH}_3$ ).  $^{13}\text{C}$  NMR (101 MHz,  $\text{CDCl}_3$ ):  $\delta$  195.77, 167.80, 156.20, 152.74, 149.95, 145.14, 144.14, 142.38, 141.27, 134.06, 128.28, 127.19, 123.05, 119.45, 118.08, 112.96, 109.87, 88.08, 79.32, 73.94, 70.64, 70.61, 70.35, 70.27, 69.98, 64.68, 43.48, 40.45, 40.00, 38.28, 37.47, 33.88, 33.55, 28.55, 19.92, 18.52, 14.95, 14.17.  $[\alpha]_D^{20} = -79^\circ$  ( $c = 0.48$ ,  $\text{CHCl}_3$ ). ESI-HRMS ( $m/z$ ): calcd. for  $[\text{C}_{45}\text{H}_{61}\text{BrN}_4\text{O}_{10} + \text{H}]^+$  897.36438; obsd. 897.36570.**



#### General procedure for the synthesis of dimeric ligands

(*o,o*-/*m,m*-/*p,p*-**77a,b**). Compound **75** (10-20  $\mu\text{mol}$ ) was subjected to DCM/TFA (2 mL, 1:1, v/v) for 30 min - 1 h, upon which TLC indicated complete removal of the Boc-group. The mixture was diluted with toluene and concentrated *in vacuo*. Silica column chromatography (2.5%  $\rightarrow$  5% MeOH in DCM + 1% TEA) afforded amine **76** ( $R_f = 0.5$  (10:1:1 DCM:MeOH:TEA)). **a**: ESI-MS ( $m/z$ ):  $[\text{M} + \text{H}]^+$ : 753.33. **b**: ESI-MS ( $m/z$ ):  $[\text{M} + \text{H}]^+$ : 797.33.). A pre-activated mixture of **63**, **64** or

**65** (1 eq), EDC (2 eq), HOBT (2 eq) and TEA (2 eq) in DCM (2 mL) was added to the corresponding *ortho*-, *meta*-, or *para*-monomeric amine **76** (1.05 eq). The reaction was monitored by TLC, and upon completion (1-2 h), DCM was added and the solution was washed with HCl (aq, 1 M, 2 $\times$ ), water (1 $\times$ ), dried ( $\text{MgSO}_4$ ) and concentrated. Pure dimeric compounds were obtained after silica column chromatography (0  $\rightarrow$  3% MeOH in DCM) as white solids.  $R_f = 0.5$  (10:1 DCM:MeOH). FT-IR (thin film)  $\nu$  3285, 2923, 2860, 2360, 2342, 2201, 1648, 1498, 1384, 1274, 1125, 1046  $\text{cm}^{-1}$ .

**Dimeric ligand (*o,o*-**77a**)**. Yield: 5.2 mg, 4  $\mu\text{mol}$ , 58%.  $^1\text{H}$  NMR (600 MHz,  $\text{CDCl}_3$ ):  $\delta$  7.62 (d,  $J = 6.6$  Hz, 2H, 2  $\times$   $\text{CH}_{\text{ar}}$ ), 7.58 (s, 2H, 2  $\times$  NH), 7.44 (s, 2H, 2  $\times$  NH), 7.39 - 7.31 (m, 6H, 6  $\times$   $\text{CH}_{\text{ar}}$ ), 6.83 (s, 2H, 2  $\times$   $\text{CH}_{\text{ar}}$ ), 6.79 (s, 2H, 2  $\times$   $\text{CH}_{\text{ar}}$ ), 5.15 (s, 4H, 2  $\times$   $\text{CH}_2$ ), 4.54 (d,  $J = 13.4$  Hz, 2H, 2  $\times$  CH), 3.93 (dd,  $J = 15.2, 7.5$  Hz, 4H, 2  $\times$   $\text{CH}_2$ ), 3.67 - 3.58 (m, 8H, 4  $\times$   $\text{CH}_2$ ), 3.49 (s, 4H, 2  $\times$   $\text{CH}_2$ ), 3.42 (s, 4H, 2  $\times$   $\text{CH}_2$ ), 2.45 (dd,  $J = 15.8, 2.9$  Hz, 2H, 2  $\times$   $\text{CH}_2\text{-H}^{\text{a}}$ ), 2.38 (d,  $J = 14.5$  Hz, 2H, 2  $\times$   $\text{CH}_2\text{-H}^{\text{a}}$ ), 2.29 - 2.23 (m, 2H, 2  $\times$   $\text{CH}_2\text{-H}^{\text{b}}$ ), 2.16 (s, 2H, 2  $\times$  CH), 2.11 - 2.05 (m, 8H, 2  $\times$   $\text{CH}_3$ , 2  $\times$   $\text{CH}_2\text{-H}^{\text{b}}$ ), 1.30 - 1.27 (m, 14H, 2  $\times$   $\text{CH}_3$ , 4  $\times$   $\text{CH}_2$ ), 0.89 (d,  $J = 6.4$  Hz, 6H, 2  $\times$   $\text{CH}_3$ ).  $^{13}\text{C}$  NMR (151 MHz,  $\text{CDCl}_3$ ):  $\delta$  195.82, 169.49, 152.69, 150.27, 145.37, 143.19, 142.66, 137.07, 133.88, 131.26, 130.33, 128.79, 128.48, 122.97, 119.46, 118.13, 112.47, 109.71, 87.93, 72.89, 70.45, 70.41, 69.78, 64.53, 43.52, 40.18, 38.18, 37.53, 33.91, 33.58, 19.92, 18.51, 14.70, 14.21.  $[\alpha]_D^{20} = -120^\circ$  ( $c = 0.1$ ,  $\text{CHCl}_3$ ). ESI-HRMS ( $m/z$ ): calcd. for  $[\text{C}_{68}\text{H}_{78}\text{Br}_2\text{N}_6\text{O}_{11} + \text{H}]^+$  1315.41476; obsd. 1315.41678.

**Dimeric ligand (o,o-77b).** Yield: 5 mg, 3.7  $\mu\text{mol}$ , 37%.  $^1\text{H}$  NMR (600 MHz,  $\text{CDCl}_3/\text{MeOD}$ ):  $\delta$  78.83 (s, 2H, 2  $\times$  NH), 7.90 (s, 2H, 2  $\times$   $\text{CH}_{\text{ar}}$ ), 7.61 - 7.54 (m, 2H, 2  $\times$   $\text{CH}_{\text{ar}}$ ), 7.43 (d,  $J$  = 6.1 Hz, 2H, 2  $\times$   $\text{CH}_{\text{ar}}$ ), 7.41 - 7.36 (m, 4H, 2  $\times$   $\text{CH}_{\text{ar}}$ , 2  $\times$  NH), 6.83 (d,  $J$  = 10.5 Hz, 4H, 4  $\times$   $\text{CH}_{\text{ar}}$ ), 5.19 - 5.12 (m, 4H, 2  $\times$   $\text{CH}_2$ ), 4.51 (s, 2H, 2  $\times$  CH), 4.07 - 3.91 (m, 4H, 2  $\times$   $\text{CH}_2$ ), 3.64 - 3.48 (m, 20H, 10  $\times$   $\text{CH}_2$ ), 2.51 - 2.42 (m, 4H, 4  $\times$   $\text{CH}_2\text{-H}^{\text{a}}$ ), 2.34 (dd,  $J$  = 16.5, 9.0 Hz, 2H, 2  $\times$   $\text{CH}_2\text{-H}^{\text{b}}$ ), 2.18 (s, 2H, 2  $\times$  CH), 2.13 - 2.06 (m, 8H, 2  $\times$   $\text{CH}_3$ , 2  $\times$   $\text{CH}_2\text{-H}^{\text{b}}$ ), 1.35 (s, 8H, 4  $\times$   $\text{CH}_2$ ), 1.30 (t,  $J$  = 6.9 Hz, 6H, 2  $\times$   $\text{CH}_3$ ), 0.91 (t,  $J$  = 6.4 Hz, 6H, 2  $\times$   $\text{CH}_3$ ).  $^{13}\text{C}$  NMR (151 MHz,  $\text{CDCl}_3/\text{MeOD}$ ):  $\delta$  196.47, 169.98, 152.52, 151.24, 145.86, 143.14, 142.79, 136.17, 134.26, 130.46, 130.15, 128.30, 127.84, 122.99, 119.52, 117.83, 112.34, 109.07, 87.18, 72.48, 70.25, 70.18, 70.06, 69.75, 64.34, 43.19, 39.91, 38.17, 37.25, 33.63, 32.76, 19.73, 17.73, 14.41, 13.90.  $[\alpha]_{\text{D}}^{20} = -120^\circ$  ( $c$  = 0.1,  $\text{CHCl}_3$ ). ESI-HRMS ( $m/z$ ): calcd. for  $[\text{C}_{70}\text{H}_{82}\text{Br}_2\text{N}_6\text{O}_{12} + \text{H}]^+$  1359.44098; obsd. 1359.44324.

**Dimeric ligand (m,m-77a).** Yield: 2.4 mg, 1.8  $\mu\text{mol}$ , 26%.  $^1\text{H}$  NMR (600 MHz,  $\text{CDCl}_3$ ):  $\delta$  8.01 (s, 2H, 2  $\times$   $\text{CH}_{\text{ar}}$ ), 7.79 (d,  $J$  = 7.7 Hz, 2H, 2  $\times$   $\text{CH}_{\text{ar}}$ ), 7.60 (d,  $J$  = 7.6 Hz, 2H, 2  $\times$   $\text{CH}_{\text{ar}}$ ), 7.42 (t,  $J$  = 7.6 Hz, 2H, 2  $\times$   $\text{CH}_{\text{ar}}$ ), 7.04 (s, 2H, 2  $\times$  NH), 6.98 (s, 2H, 2  $\times$  NH), 6.90 (d,  $J$  = 1.3 Hz, 2H, 2  $\times$   $\text{CH}_{\text{ar}}$ ), 6.80 (d,  $J$  = 1.6 Hz, 2H, 2  $\times$   $\text{CH}_{\text{ar}}$ ), 5.10 - 4.98 (m, 4H, 2  $\times$   $\text{CH}_2$ ), 4.54 (s, 2H, 2  $\times$  CH), 4.16 - 4.05 (m, 4H, 2  $\times$   $\text{CH}_2$ ), 3.65 - 3.58 (m, 16H, 8  $\times$   $\text{CH}_2$ ), 2.45 (dd,  $J$  = 16.1, 3.8 Hz, 2H, 2  $\times$   $\text{CH}_2\text{-H}^{\text{a}}$ ), 2.43 - 2.36 (m, 2H, 2  $\times$   $\text{CH}_2\text{-H}^{\text{a}}$ ), 2.31 (dd,  $J$  = 16.4, 9.2 Hz, 2H, 2  $\times$   $\text{CH}_2\text{-H}^{\text{b}}$ ), 2.17 (dd,  $J$  = 9.3, 4.8 Hz, 2H, 2  $\times$  CH), 2.11 - 2.04 (m, 8H, 2  $\times$   $\text{CH}_3$ , 2  $\times$   $\text{CH}_2\text{-H}^{\text{b}}$ ), 1.45 - 1.38 (m, 6H, 2  $\times$   $\text{CH}_3$ ), 1.34 - 1.28 (m, 8H, 4  $\times$   $\text{CH}_2$ ), 0.88 (t,  $J$  = 6.9 Hz, 6H, 2  $\times$   $\text{CH}_3$ ).  $^{13}\text{C}$  NMR (151 MHz,  $\text{CDCl}_3$ ):  $\delta$  195.91, 167.89, 152.79, 149.95, 145.05, 144.10, 142.45, 138.13, 134.70, 131.24, 128.75, 127.15, 126.60, 123.00, 119.48, 118.11, 112.97, 109.90, 88.21, 74.14, 70.64, 70.42, 69.83, 64.73, 43.51, 39.94, 38.37, 37.52, 33.92, 33.68, 19.93, 18.59, 14.97, 14.20.  $[\alpha]_{\text{D}}^{20} = -108^\circ$  ( $c$  = 0.05,  $\text{CHCl}_3$ ). ESI-HRMS ( $m/z$ ): calcd. for  $[\text{C}_{68}\text{H}_{78}\text{Br}_2\text{N}_6\text{O}_{11} + \text{H}]^+$  1315.41476; obsd. 1315.41673.

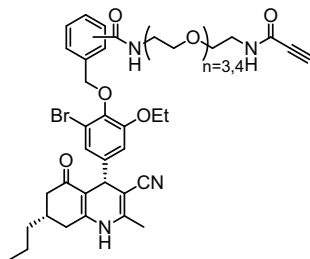
**Dimeric ligand (m,m-77b).** Yield: 4.7 mg, 3.5  $\mu\text{mol}$ , 38%.  $^1\text{H}$  NMR (600 MHz,  $\text{CDCl}_3$ ):  $\delta$  8.01 (s, 2H, 2  $\times$   $\text{CH}_{\text{ar}}$ ), 7.77 (d,  $J$  = 7.6 Hz, 2H, 2  $\times$   $\text{CH}_{\text{ar}}$ ), 7.63 (d,  $J$  = 7.6 Hz, 2H, 2  $\times$   $\text{CH}_{\text{ar}}$ ), 7.43 (t,  $J$  = 7.7 Hz, 2H, 2  $\times$   $\text{CH}_{\text{ar}}$ ), 7.37 (s, 2H, 2  $\times$  NH), 7.09 (s, 2H, 2  $\times$  NH), 6.90 (d,  $J$  = 9.2 Hz, 2H, 2  $\times$   $\text{CH}_{\text{ar}}$ ), 6.82 (d,  $J$  = 1.4 Hz, 2H, 2  $\times$   $\text{CH}_{\text{ar}}$ ), 5.07 - 4.96 (m, 4H, 2  $\times$   $\text{CH}_2$ ), 4.54 (s, 2H, 2  $\times$  CH), 4.15 - 4.02 (m, 4H, 2  $\times$   $\text{CH}_2$ ), 3.64 - 3.57 (m, 20H, 10  $\times$   $\text{CH}_2$ ), 2.48 - 2.35 (m, 4H, 2  $\times$   $\text{CH}_2\text{-H}^{\text{a}}$ ), 2.31 (dd,  $J$  = 16.4, 9.2 Hz, 2H, 2  $\times$   $\text{CH}_2\text{-H}^{\text{b}}$ ), 2.15 (d,  $J$  = 11.8 Hz, 2H, 2  $\times$  CH), 2.10 - 2.03 (m, 8H, 2  $\times$   $\text{CH}_3$ , 2  $\times$   $\text{CH}_2\text{-H}^{\text{b}}$ ), 1.42 (t,  $J$  = 6.9 Hz, 6H, 2  $\times$   $\text{CH}_3$ ), 1.33 - 1.25 (m, 8H, 4  $\times$   $\text{CH}_2$ ), 0.87 (t,  $J$  = 6.9 Hz, 6H, 2  $\times$   $\text{CH}_3$ ).  $^{13}\text{C}$  NMR (151 MHz,  $\text{CDCl}_3$ ):  $\delta$  195.99, 168.02, 152.78, 150.28, 145.28, 144.09, 142.52, 138.19, 134.68, 131.31, 128.71, 126.99, 126.81, 123.05, 119.57, 118.12, 112.94, 109.77, 88.03, 74.13, 70.58, 70.34, 69.93, 64.71, 43.53, 40.00, 38.39, 37.52, 33.93, 33.60, 19.91, 18.53, 14.98, 14.20.  $[\alpha]_{\text{D}}^{20} = -106^\circ$  ( $c$  = 0.094,  $\text{CHCl}_3$ ). ESI-HRMS ( $m/z$ ): calcd. for  $[\text{C}_{70}\text{H}_{82}\text{Br}_2\text{N}_6\text{O}_{12} + \text{H}]^+$  1359.44098; obsd. 1359.44324.

**Dimeric ligand (p,p-77a).** Yield: 4 mg, 3  $\mu\text{mol}$ , 30%.  $^1\text{H}$  NMR (600 MHz,  $\text{CDCl}_3$ ):  $\delta$  7.76 (d,  $J$  = 8.2 Hz, 4H, 4  $\times$   $\text{CH}_{\text{ar}}$ ), 7.57 (d,  $J$  = 8.1 Hz, 4H, 4  $\times$   $\text{CH}_{\text{ar}}$ ), 6.92 (s, 2H, 2  $\times$  NH), 6.90 - 6.87 (m, 4H, 2  $\times$   $\text{CH}_{\text{ar}}$ , 2  $\times$  NH), 6.80 (d,  $J$  = 1.8 Hz, 2H, 2  $\times$   $\text{CH}_{\text{ar}}$ ), 5.03 (q,  $J$  = 11.4 Hz, 4H, 2  $\times$   $\text{CH}_2$ ), 4.54 (s, 2H, 2  $\times$  CH), 4.13 - 4.03 (m, 4H, 2  $\times$   $\text{CH}_2$ ), 3.67 - 3.58 (m, 16H, 8  $\times$   $\text{CH}_2$ ), 2.45 (dd,  $J$  = 16.1, 3.8 Hz, 2H, 2  $\times$   $\text{CH}_2\text{-H}^{\text{a}}$ ), 2.38 (dd,  $J$  = 16.3, 4.3 Hz, 2H, 2  $\times$   $\text{CH}_2\text{-H}^{\text{a}}$ ), 2.29 (dd,  $J$  = 16.4, 9.2 Hz, 2H, 2  $\times$   $\text{CH}_2\text{-H}^{\text{b}}$ ), 2.22 - 2.10 (m, 2H, 2  $\times$  CH), 2.12 - 2.02 (m, 8H, 2  $\times$   $\text{CH}_3$ , 2  $\times$   $\text{CH}_2\text{-H}^{\text{b}}$ ), 1.44 - 1.39 (m, 6H, 2  $\times$   $\text{CH}_3$ ), 1.36 - 1.29 (m, 8H, 4  $\times$   $\text{CH}_2$ ), 0.89 (t,  $J$  = 6.9 Hz, 6H, 2  $\times$   $\text{CH}_3$ ).  $^{13}\text{C}$  NMR (151 MHz,  $\text{CDCl}_3$ ):  $\delta$  195.83, 167.78, 152.79, 149.80, 144.97, 144.08, 142.27, 141.13, 134.14, 128.46, 127.14, 123.05, 119.40, 118.19, 112.95, 109.97, 88.27, 74.01, 70.62, 70.35, 69.83,



64.73, 43.50, 39.90, 38.29, 37.50, 33.92, 33.69, 19.93, 18.60, 14.97, 14.19.  $[\alpha]_D^{20} = -118^\circ$  ( $c = 0.08$ ,  $\text{CHCl}_3$ ). ESI-HRMS ( $m/z$ ): calcd. for  $[\text{C}_{68}\text{H}_{78}\text{Br}_2\text{N}_6\text{O}_{11} + \text{H}]^+$  1315.41476; obsd. 1315.41639.

**Dimeric ligand (*p,p*-77b).** Yield: 2.8 mg, 2.1  $\mu\text{mol}$ , 34%.  $^1\text{H}$  NMR (600 MHz,  $\text{CDCl}_3$ ):  $\delta$  7.79 (d,  $J = 8.1$  Hz, 4H, 4  $\times$   $\text{CH}_{\text{ar}}$ ), 7.58 (d,  $J = 8.1$  Hz, 4H, 4  $\times$   $\text{CH}_{\text{ar}}$ ), 7.07 (s, 2H, 2  $\times$  NH), 6.89 (s, 2H, 2  $\times$   $\text{CH}_{\text{ar}}$ ), 6.81 (d,  $J = 1.5$  Hz, 2H, 2  $\times$   $\text{CH}_{\text{ar}}$ ), 6.77 (s, 2H, 2  $\times$  NH), 5.10 - 4.99 (m, 4H, 2  $\times$   $\text{CH}_2$ ), 4.55 (d,  $J = 9.4$  Hz, 2H, 2  $\times$  CH), 4.16 - 4.04 (m, 4H, 2  $\times$   $\text{CH}_2$ ), 3.65 - 3.58 (m, 20H, 10  $\times$   $\text{CH}_2$ ), 2.46 (dd,  $J = 16.1$ , 3.6 Hz, 2H, 2  $\times$   $\text{CH}_2\text{-H}^{\text{a}}$ ), 2.38 (dd,  $J = 16.2$ , 4.0 Hz, 2H, 2  $\times$   $\text{CH}_2\text{-H}^{\text{a}}$ ), 2.30 (dd,  $J = 16.3$ , 9.2 Hz, 2H, 2  $\times$   $\text{CH}_2\text{-H}^{\text{b}}$ ), 2.18 (d,  $J = 4.2$  Hz, 2H, 2  $\times$  CH), 2.13 - 2.06 (m, 8H, 2  $\times$   $\text{CH}_3$ , 2  $\times$   $\text{CH}_2\text{-H}^{\text{b}}$ ), 1.42 (t,  $J = 6.9$  Hz, 6H, 2  $\times$   $\text{CH}_3$ ), 1.36 - 1.29 (m, 8H, 4  $\times$   $\text{CH}_2$ ), 0.91 - 0.86 (m, 6H, 2  $\times$   $\text{CH}_3$ ).  $^{13}\text{C}$  NMR (151 MHz,  $\text{CDCl}_3$ ):  $\delta$  195.79, 167.73, 152.80, 149.67, 144.87, 144.11, 142.24, 141.10, 134.17, 128.42, 127.22, 123.03, 119.35, 118.17, 112.96, 110.06, 88.37, 74.03, 70.63, 70.32, 69.94, 64.73, 43.50, 39.93, 38.28, 37.51, 33.93, 33.75, 19.94, 18.66, 14.98, 14.19.  $[\alpha]_D^{20} = -129^\circ$  ( $c = 0.06$ ,  $\text{CHCl}_3$ ). ESI-HRMS ( $m/z$ ): calcd. for  $[\text{C}_{70}\text{H}_{82}\text{Br}_2\text{N}_6\text{O}_{12} + \text{H}]^+$  1359.44098; obsd. 1359.44285.



#### General procedure for the synthesis of alkyne-monomeric ligands

**(*o*-/*m*-/*p*-78a,b).** Compound **75** (10-20  $\mu\text{mol}$ ) was subjected to  $\text{DCM}/\text{TFA}$  (2 mL, 1:1, v/v) for 30 min - 1 h, upon which TLC indicated complete removal of the Boc-group. The mixture was diluted with toluene and concentrated *in vacuo*. Silica column chromatography (2.5%  $\rightarrow$  5% MeOH in  $\text{DCM}$  + 1% TEA) afforded amine **76** ( $R_f = 0.5$  (10:1:1  $\text{DCM}:\text{MeOH}:\text{TEA}$ ). a: ESI-MS ( $m/z$ ):  $[\text{M} + \text{H}]^+$ : 753.33. b: ESI-MS ( $m/z$ ):  $[\text{M} + \text{H}]^+$ : 797.33). A pre-activated mixture of propionic acid (1.2 eq) and EEDQ (2 eq) in  $\text{DCM}$  (2 mL) was added to monomeric amine **76** (1 eq). Upon

completion of the reaction (1-2 h), the mixture was loaded onto a silica column and purified (0  $\rightarrow$  4% MeOH in  $\text{DCM}$ ). Title compounds were obtained as yellowish solids.  $R_f = 0.5$  (10:1  $\text{DCM}:\text{MeOH}$ ). FT-IR (thin film)  $\nu$  3285, 2920, 2855, 2360, 2344, 1648, 1497, 1381, 1275, 1125, 1047  $\text{cm}^{-1}$ .

**2-((2-bromo-4-((4*R*,7*S*)-3-cyano-2-methyl-5-oxo-7-propyl-1, 4, 5, 6, 7, 8-hexahydroquinolin-4-yl)-6-ethoxyphenoxy) methyl)-*N*-(13-oxo-3, 6, 9-trioxa-12-azapentadec-14-yn-1-yl) benzamide (*o*-78a).** Yield: 6 mg, 7.5  $\mu\text{mol}$ , 68%.  $^1\text{H}$  NMR (600 MHz,  $\text{CDCl}_3$ ):  $\delta$  7.65 (dd,  $J = 7.4$ , 1.2 Hz, 1H,  $\text{CH}_{\text{ar}}$ ), 7.56 (s, 1H, NH), 7.40 - 7.33 (m, 2H, 2  $\times$   $\text{CH}_{\text{ar}}$ ), 7.31 (d,  $J = 7.3$  Hz, 1H,  $\text{CH}_{\text{ar}}$ ), 6.88 - 6.84 (m, 2H, 2  $\times$  NH), 6.80 (d,  $J = 1.8$  Hz, 1H,  $\text{CH}_{\text{ar}}$ ), 6.68 (s, 1H,  $\text{CH}_{\text{ar}}$ ), 5.16 (s, 2H,  $\text{CH}_2$ ), 4.55 (s, 1H, CH), 4.03 - 3.89 (m, 2H,  $\text{CH}_2$ ), 3.69 (d,  $J = 9.1$  Hz, 4H, 2  $\times$   $\text{CH}_2$ ), 3.64 - 3.61 (m, 2H,  $\text{CH}_2$ ), 3.59 - 3.57 (m, 2H,  $\text{CH}_2$ ), 3.56 - 3.54 (m, 2H,  $\text{CH}_2$ ), 3.53 - 3.51 (m, 2H,  $\text{CH}_2$ ), 3.49 (t,  $J = 5.1$  Hz, 2H,  $\text{CH}_2$ ), 3.43 - 3.40 (m, 2H,  $\text{CH}_2$ ), 2.80 (s, 1H, CH), 2.51 - 2.32 (m, 3H,  $\text{CH}_2$ ,  $\text{CH}_2\text{-H}^{\text{a}}$ ), 2.20 (s, 1H, CH), 2.15 (s, 3H,  $\text{CH}_3$ ), 2.13 - 2.07 (m, 1H,  $\text{CH}_2\text{-H}^{\text{b}}$ ), 1.36 - 1.32 (m, 4H, 2  $\times$   $\text{CH}_2$ ), 1.30 (t,  $J = 7.0$  Hz, 3H,  $\text{CH}_3$ ), 0.90 (t,  $J = 6.9$  Hz, 3H,  $\text{CH}_3$ ).  $^{13}\text{C}$  NMR (151 MHz,  $\text{CDCl}_3$ ):  $\delta$  195.62, 169.24, 152.73, 152.53, 149.46, 144.86, 143.22, 142.51, 137.26, 133.82, 131.23, 130.18, 128.77, 128.57, 122.98, 119.24, 118.13, 112.57, 110.09, 88.31, 77.44, 73.74, 72.96, 70.61, 70.58, 70.50, 70.34, 69.96, 69.14, 64.50, 43.49, 40.07, 39.75, 38.23, 37.51, 33.91, 33.79, 19.93, 18.73, 14.69, 14.19.  $[\alpha]_D^{20} = -83^\circ$  ( $c = 0.12$ ,  $\text{CHCl}_3$ ). ESI-HRMS ( $m/z$ ): calcd. for  $[\text{C}_{41}\text{H}_{49}\text{BrN}_4\text{O}_8 + \text{H}]^+$  805.28065; obsd. 805.28146.

**2-((2-bromo-4-((4*R*,7*S*)-3-cyano-2-methyl-5-oxo-7-propyl-1, 4, 5, 6, 7, 8-hexahydroquinolin-4-yl)-6-ethoxyphenoxy) methyl)-*N*-(16-oxo-3, 6, 9, 12-tetraoxa-15-azaoctadec-17-yn-1-yl) benzamide**



**(o-78b).** Yield: 10 mg, 12  $\mu$ mol, 78%.  $^1\text{H}$  NMR (600 MHz,  $\text{CDCl}_3$ ):  $\delta$  7.63 (d,  $J = 3.6$  Hz, 1H,  $\text{CH}_{\text{ar}}$ ), 7.57 (s, 1H, NH), 7.37 (d,  $J = 10.6$  Hz, 3H,  $3 \times \text{CH}_{\text{ar}}$ ), 7.24 (s, 1H, NH), 7.12 (s, 1H, NH), 6.85 (s, 1H,  $\text{CH}_{\text{ar}}$ ), 6.81 (s, 1H,  $\text{CH}_{\text{ar}}$ ), 5.16 (s, 2H,  $\text{CH}_2$ ), 4.54 (s, 1H, CH), 4.02 - 3.89 (m, 2H,  $\text{CH}_2$ ), 3.68 (s, 4H,  $2 \times \text{CH}_2$ ), 3.65 - 3.50 (m, 14H,  $7 \times \text{CH}_2$ ), 3.49 - 3.41 (m, 2H,  $\text{CH}_2$ ), 2.83 (s, 1H, CH), 2.49 - 2.42 (m, 2H,  $2 \times \text{CH}_2\text{-H}^{\text{a}}$ ), 2.38 - 2.30 (m, 1H,  $\text{CH}_2\text{-H}^{\text{b}}$ ), 2.16 - 2.06 (m, 5H,  $\text{CH}_3$ , CH,  $\text{CH}_2\text{-H}^{\text{b}}$ ), 1.36 - 1.27 (m, 7H,  $\text{CH}_3$ ,  $2 \times \text{CH}_2$ ), 0.90 (t,  $J = 6.9$  Hz, 3H,  $\text{CH}_3$ ).  $^{13}\text{C}$  NMR (151 MHz,  $\text{CDCl}_3$ ):  $\delta$  195.73, 169.36, 152.71, 149.93, 145.25, 143.27, 142.63, 136.99, 134.10, 131.04, 130.21, 128.64, 128.41, 123.00, 119.43, 118.07, 112.58, 109.86, 87.98, 77.45, 73.85, 72.84, 70.55, 70.44, 70.34, 69.95, 69.27, 64.52, 43.51, 40.07, 39.78, 38.21, 37.51, 33.90, 33.63, 19.93, 18.61, 14.70, 14.21.  $[\alpha]_D^{20} = -73^\circ$  ( $c = 0.2$ ,  $\text{CHCl}_3$ ). ESI-HRMS ( $m/z$ ): calcd. for  $[\text{C}_{43}\text{H}_{53}\text{BrN}_4\text{O}_9 + \text{H}]^+$  849.30687; obsd. 849.30779.

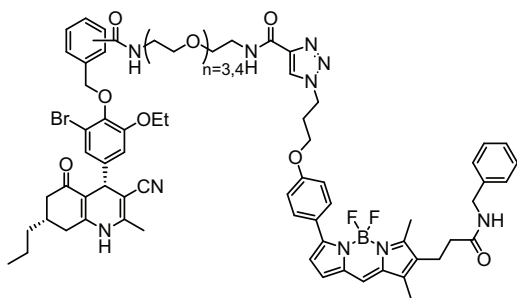
**3-((2-bromo-4-((4R,7S)-3-cyano-2-methyl-5-oxo-7-propyl-1, 4, 5, 6, 7, 8-hexahydroquinolin-4-yl)-6-ethoxyphenoxy) methyl)-N-(13-oxo-3,6,9-trioxa-12-azapentadec-14-yn-1-yl)benzamide (m-78a).** Yield: 8 mg, 10  $\mu$ mol, 90%.  $^1\text{H}$  NMR (600 MHz,  $\text{CDCl}_3$ ):  $\delta$  8.03 (s, 1H,  $\text{CH}_{\text{ar}}$ ), 7.78 (d,  $J = 7.8$  Hz, 1H,  $\text{CH}_{\text{ar}}$ ), 7.65 (d,  $J = 7.6$  Hz, 1H,  $\text{CH}_{\text{ar}}$ ), 7.45 (t,  $J = 7.6$  Hz, 1H,  $\text{CH}_{\text{ar}}$ ), 7.03 (s, 1H, NH), 6.95 (s, 1H, NH), 6.92 (d,  $J = 1.6$  Hz, 1H,  $\text{CH}_{\text{ar}}$ ), 6.83 (d,  $J = 1.8$  Hz, 1H,  $\text{CH}_{\text{ar}}$ ), 6.81 (s, 1H, NH), 5.04 (s, 2H,  $\text{CH}_2$ ), 4.55 (s, 1H, CH), 4.17 - 4.09 (m, 2H,  $\text{CH}_2$ ), 3.71 - 3.66 (m, 8H,  $4 \times \text{CH}_2$ ), 3.65 - 3.62 (m, 2H,  $\text{CH}_2$ ), 3.59 - 3.56 (m, 2H,  $\text{CH}_2$ ), 3.48 (t,  $J = 5.2$  Hz, 2H,  $\text{CH}_2$ ), 3.41 - 3.36 (m, 2H,  $\text{CH}_2$ ), 2.79 (s, 1H, CH), 2.50 - 2.34 (m, 3H,  $\text{CH}_2$ ,  $\text{CH}_2\text{-H}^{\text{a}}$ ), 2.22 - 2.16 (m, 1H, CH), 2.14 (s, 3H,  $\text{CH}_3$ ), 2.12 - 2.05 (m, 1H,  $\text{CH}_2\text{-H}^{\text{b}}$ ), 1.44 (t,  $J = 7.0$  Hz, 3H,  $\text{CH}_3$ ), 1.34 - 1.28 (m, 4H,  $2 \times \text{CH}_2$ ), 0.91 - 0.87 (m, 3H,  $\text{CH}_3$ ).  $^{13}\text{C}$  NMR (151 MHz,  $\text{CDCl}_3$ ):  $\delta$  195.84, 167.88, 152.77, 152.53, 149.82, 145.01, 144.06, 142.48, 138.18, 134.78, 131.41, 128.72, 126.97, 126.91, 123.02, 119.45, 118.11, 112.96, 110.00, 88.25, 79.71, 74.17, 73.81, 70.63, 70.60, 70.38, 70.34, 69.99, 69.20, 64.69, 43.52, 39.97, 39.68, 38.35, 37.53, 33.94, 33.72, 19.91, 18.66, 14.97, 14.19.  $[\alpha]_D^{20} = -63^\circ$  ( $c = 0.16$ ,  $\text{CHCl}_3$ ). ESI-HRMS ( $m/z$ ): calcd. for  $[\text{C}_{41}\text{H}_{49}\text{BrN}_4\text{O}_8 + \text{H}]^+$  805.28065; obsd. 805.28139.

**3-((2-bromo-4-((4R,7S)-3-cyano-2-methyl-5-oxo-7-propyl-1, 4, 5, 6, 7, 8-hexahydroquinolin-4-yl)-6-ethoxyphenoxy) methyl)-N-(16-oxo-3, 6, 9, 12-tetraoxa-15-azaoctadec-17-yn-1-yl) benzamide (m-78b).** Yield: 4 mg, 4.7  $\mu$ mol, 47%.  $^1\text{H}$  NMR (600 MHz,  $\text{CDCl}_3$ ):  $\delta$  8.04 (s, 1H,  $\text{CH}_{\text{ar}}$ ), 7.80 (d,  $J = 7.7$  Hz, 1H,  $\text{CH}_{\text{ar}}$ ), 7.65 (d,  $J = 7.6$  Hz, 1H,  $\text{CH}_{\text{ar}}$ ), 7.44 (t,  $J = 7.7$  Hz, 1H,  $\text{CH}_{\text{ar}}$ ), 7.07 (d,  $J = 10.6$  Hz, 3H  $3 \times \text{NH}$ ), 6.93 (d,  $J = 1.6$  Hz, 1H,  $\text{CH}_{\text{ar}}$ ), 6.83 (d,  $J = 1.8$  Hz, 1H,  $\text{CH}_{\text{ar}}$ ), 5.05 (s, 2H,  $\text{CH}_2$ ), 4.56 (s, 1H, CH), 4.17 - 4.08 (m, 2H,  $\text{CH}_2$ ), 3.70 - 3.66 (m, 10H,  $5 \times \text{CH}_2$ ), 3.64 - 3.61 (m, 2H,  $\text{CH}_2$ ), 3.57 (s, 4H,  $2 \times \text{CH}_2$ ), 3.52 (t,  $J = 5.0$  Hz, 2H,  $\text{CH}_2$ ), 3.45 - 3.41 (m, 2H,  $\text{CH}_2$ ), 2.81 (s, 1H, CH), 2.49 - 2.33 (m, 3H,  $\text{CH}_2$ ,  $\text{CH}_2\text{-H}^{\text{a}}$ ), 2.18 (d,  $J = 3.9$  Hz, 1H, CH), 2.15 (s, 3H,  $\text{CH}_3$ ), 2.13 - 2.05 (m, 1H,  $\text{CH}_2\text{-H}^{\text{b}}$ ), 1.44 (t,  $J = 7.0$  Hz, 3H,  $\text{CH}_3$ ), 1.36 - 1.30 (m, 4H,  $2 \times \text{CH}_2$ ), 0.89 (t,  $J = 6.0$  Hz, 3H,  $\text{CH}_3$ ).  $^{13}\text{C}$  NMR (151 MHz,  $\text{CDCl}_3$ ):  $\delta$  195.81, 167.84, 152.77, 152.58, 149.78, 145.05, 144.11, 142.43, 138.18, 134.76, 131.36, 128.68, 127.01, 123.01, 119.47, 118.09, 113.01, 110.03, 88.22, 77.47, 74.19, 73.76, 70.64, 70.62, 70.39, 70.32, 70.11, 69.33, 64.71, 43.54, 40.00, 39.74, 38.31, 37.54, 33.97, 33.74, 19.92, 18.68, 14.99, 14.20.  $[\alpha]_D^{20} = -100^\circ$  ( $c = 0.08$ ,  $\text{CHCl}_3$ ). ESI-HRMS ( $m/z$ ): calcd. for  $[\text{C}_{43}\text{H}_{53}\text{BrN}_4\text{O}_9 + \text{H}]^+$  849.30687; obsd. 849.30767.

**4-((2-bromo-4-((4R,7S)-3-cyano-2-methyl-5-oxo-7-propyl-1, 4, 5, 6, 7, 8-hexahydroquinolin-4-yl)-6-ethoxyphenoxy) methyl)-N-(13-oxo-3,6,9-trioxa-12-azapentadec-14-yn-1-yl)benzamide (p-78a).** Yield: 6.1 mg, 7.6  $\mu$ mol, 63%.  $^1\text{H}$  NMR (600 MHz,  $\text{CDCl}_3$ ):  $\delta$  7.80 (d,  $J = 8.2$  Hz, 2H,  $2 \times \text{CH}_{\text{ar}}$ ), 7.60 (d,  $J = 8.1$  Hz, 2H,  $2 \times \text{CH}_{\text{ar}}$ ), 6.91 (d,  $J = 1.6$  Hz, 1H,  $\text{CH}_{\text{ar}}$ ), 6.85 (t,  $J = 4.9$  Hz, 1H, NH), 6.80 (d,  $J = 1.8$  Hz, 1H,  $\text{CH}_{\text{ar}}$ ), 6.71 (d,  $J = 5.2$  Hz, 1H, NH), 6.30 (s, 1H, NH), 5.04 (d,  $J = 7.3$  Hz, 2H,  $\text{CH}_2$ ), 4.55 (s, 1H, CH), 4.19 - 4.05 (m, 2H,  $\text{CH}_2$ ), 3.71 - 3.67 (m, 8H,  $4 \times \text{CH}_2$ ), 3.66 - 3.63 (m,

2H, CH<sub>2</sub>), 3.61 - 3.58 (m, 2H, CH<sub>2</sub>), 3.51 (t,  $J = 5.1$  Hz, 2H, CH<sub>2</sub>), 3.43 - 3.37 (m, 2H, CH<sub>2</sub>), 2.76 (s, 1H, CH), 2.52 - 2.32 (m, 3H, CH<sub>2</sub>, CH<sub>2</sub>-H<sup>a</sup>), 2.26 - 2.08 (m, 5H, CH<sub>3</sub>, CH, CH<sub>2</sub>-H<sup>b</sup>), 1.43 (t,  $J = 6.9$  Hz, 3H, CH<sub>3</sub>), 1.38 - 1.31 (m, 4H, 2 × CH<sub>2</sub>), 0.91 (t,  $J = 7.0$  Hz, 3H, CH<sub>3</sub>). <sup>13</sup>C NMR (151 MHz, CDCl<sub>3</sub>):  $\delta$  195.72, 167.67, 152.80, 152.48, 149.36, 144.68, 144.10, 142.24, 141.19, 134.16, 128.50, 128.39, 127.28, 127.19, 123.03, 119.29, 118.18, 113.01, 110.20, 88.53, 74.01, 73.66, 70.64, 70.60, 70.37, 70.35, 69.97, 69.30, 64.71, 43.48, 39.93, 39.66, 38.31, 37.51, 33.93, 33.85, 19.95, 18.77, 14.97, 14.19.  $[\alpha]_D^{20} = -51^\circ$  ( $c = 0.12$ , CHCl<sub>3</sub>). ESI-HRMS ( $m/z$ ): calcd. for [C<sub>41</sub>H<sub>49</sub>BrN<sub>4</sub>O<sub>8</sub> + H]<sup>+</sup> 805.28065; obsd. 805.28113.

**4-((2-bromo-4-((4*R*,7*S*)-3-cyano-2-methyl-5-oxo-7-propyl-1,4,5,6,7,8-hexahydroquinolin-4-yl)-6-ethoxyphenoxy)methyl)-*N*-(16-oxo-3,6,9,12-tetraoxa-15-azaoctadec-17-yn-1-yl) benzamide (p-78b).** Yield: 9 mg, 11  $\mu$ mol, quant. <sup>1</sup>H NMR (600 MHz, CDCl<sub>3</sub>):  $\delta$  7.82 (d,  $J = 8.2$  Hz, 2H, 2 × CH<sub>ar</sub>), 7.60 (d,  $J = 8.1$  Hz, 2H, 2 × CH<sub>ar</sub>), 7.09 (d,  $J = 3.8$  Hz, 1H, NH), 7.02 (s, 1H, NH), 6.91 (d,  $J = 1.6$  Hz, 1H, CH<sub>ar</sub>), 6.81 (d,  $J = 1.8$  Hz, 1H, CH<sub>ar</sub>), 6.65 (s, 1H, NH), 5.04 (s, 2H, CH<sub>2</sub>), 4.55 (s, 1H, CH), 4.15 - 4.08 (m, 2H, CH<sub>2</sub>), 3.71 - 3.66 (m, 10H, 5 × CH<sub>2</sub>), 3.65 - 3.62 (m, 2H, CH<sub>2</sub>), 3.60 - 3.57 (m, 4H, 2 × CH<sub>2</sub>), 3.52 (t,  $J = 5.0$  Hz, 2H, CH<sub>2</sub>), 3.44 - 3.39 (m, 2H, CH<sub>2</sub>), 2.78 (s, 1H, CH), 2.52 - 2.32 (m, 3H, CH<sub>2</sub>, CH<sub>2</sub>-H<sup>a</sup>), 2.23 - 2.17 (m, 1H, CH), 2.16 - 2.08 (m, 4H, CH<sub>3</sub>, CH<sub>2</sub>-H<sup>b</sup>), 1.43 (t,  $J = 7.0$  Hz, 3H, CH<sub>3</sub>), 1.39 - 1.31 (m, 4H, 2 × CH<sub>2</sub>), 0.90 (t,  $J = 6.9$  Hz, 3H, CH<sub>3</sub>). <sup>13</sup>C NMR (151 MHz, CDCl<sub>3</sub>):  $\delta$  195.71, 167.68, 152.80, 152.49, 149.42, 144.76, 144.16, 142.24, 141.17, 134.19, 128.40, 127.26, 123.04, 119.32, 118.15, 113.02, 110.18, 88.47, 77.54, 74.01, 73.53, 70.64, 70.35, 70.34, 70.09, 69.41, 64.72, 43.49, 39.96, 39.71, 38.29, 37.51, 33.93, 33.82, 19.95, 18.75, 14.98, 14.19.  $[\alpha]_D^{20} = -58^\circ$  ( $c = 0.18$ , CHCl<sub>3</sub>). ESI-HRMS ( $m/z$ ): calcd. for [C<sub>43</sub>H<sub>53</sub>BrN<sub>4</sub>O<sub>9</sub> + H]<sup>+</sup> 849.30687; obsd. 849.30715.



**General procedure for the synthesis of fluorescent ligands (o-/m-/p-79a,b).** Compound **78** (5-10  $\mu$ mol, 1 eq) and azido-BODIPY-benzyl<sup>26</sup> (1 eq) were dissolved in degassed DCM/H<sub>2</sub>O (2 mL, 1:1, v/v) and aqueous solutions of sodium ascorbate (1 eq) and CuSO<sub>4</sub> (20 mol%) were added. The resulting mixture was stirred vigorously for 3 h, after which TLC indicated complete conversion of the reaction. The solvents were evaporated *in vacuo*, and the residue was taken

up in DCM and purified by silica column chromatography (0% → 5% MeOH in DCM) to yield the fluorescent ligand as a purple solid.  $R_f = 0.5$  (10:1 DCM:MeOH). FT-IR (thin film)  $\nu$  3302, 2923, 2363, 2342, 1648, 1607, 1497, 1458, 1387, 1256, 1145, 1044 cm<sup>-1</sup>.

**Fluorescent ligand (o-79a).** Yield: 5.6 mg, 4.1  $\mu$ mol, 59%. <sup>1</sup>H NMR (600 MHz, CDCl<sub>3</sub>):  $\delta$  8.05 (s, 1H, CH<sub>trz</sub>), 7.86 (d,  $J = 8.4$  Hz, 2H, 2 × CH<sub>ar</sub>), 7.61 (s, 1H, CH<sub>ar</sub>), 7.52 (s, 2H, 2 × NH), 7.35 (s, 3H, 3 × CH<sub>ar</sub>), 7.30 - 7.22 (m, 3H, 3 × CH<sub>ar</sub>), 7.19 (d,  $J = 7.2$  Hz, 2H, 2 × CH<sub>ar</sub>), 7.08 (s, 2H, CH<sub>ar</sub>, NH), 6.97 (d,  $J = 3.8$  Hz, 1H, CH<sub>ar</sub>), 6.92 (d,  $J = 8.2$  Hz, 2H, 2 × CH<sub>ar</sub>), 6.84 (s, 1H, CH<sub>ar</sub>), 6.79 (s, 1H, CH<sub>ar</sub>), 6.55 (d,  $J = 3.7$  Hz, 1H, CH<sub>ar</sub>), 5.91 (s, 1H, NH), 5.18 - 5.09 (m, 2H, CH<sub>2</sub>), 4.61 (s, 2H, CH<sub>2</sub>), 4.53 (s, 1H, CH), 4.39 (d,  $J = 5.6$  Hz, 2H, CH<sub>2</sub>), 4.05 - 3.89 (m, 4H, 2 × CH<sub>2</sub>), 3.69 - 3.52 (m, 16H, 8 × CH<sub>2</sub>), 2.82 - 2.75 (m, 2H, CH<sub>2</sub>), 2.52 (s, 3H, CH<sub>3</sub>), 2.47 - 2.25 (m, 7H, 3 × CH<sub>2</sub>, CH<sub>2</sub>-H<sup>a</sup>), 2.18 (s, 3H, CH<sub>3</sub>), 2.14 (s, 1H, CH), 2.10 - 2.02 (m, 4H, CH<sub>3</sub>, CH<sub>2</sub>-H<sup>b</sup>), 1.31 - 1.26 (m, 7H, CH<sub>3</sub> + 2 × CH<sub>2</sub>), 0.88 (d,  $J = 6.4$  Hz, 3H, CH<sub>3</sub>). <sup>13</sup>C NMR (151 MHz, CDCl<sub>3</sub>):  $\delta$  195.67,

171.56, 169.25, 159.73, 159.15, 155.33, 152.74, 149.80, 145.25, 143.36, 142.45, 140.31, 138.14, 137.11, 135.09, 134.61, 134.09, 130.99, 130.93, 130.71, 130.12, 128.85, 128.60, 128.40, 128.05, 127.87, 127.67, 126.26, 125.85 (HSQC cross-coupling), 123.17, 122.88, 118.47, 118.12, 114.28, 112.52, 109.95, 87.96, 72.82, 70.63, 70.57, 70.50, 70.47, 69.96, 69.73, 64.52, 63.96, 47.57 (HSQC cross-coupling), 43.82, 43.46, 40.08, 38.07, 37.50, 36.45, 33.88, 33.57, 29.84, 20.17, 19.91, 18.52, 14.70, 14.20, 13.37, 9.78. ESI-HRMS ( $m/z$ ): calcd. for  $[C_{71}H_{80}BBrF_2N_{10}O_{10} + H]^+$  1361.53761; obsd. 1361.54005.

**Fluorescent ligand (o-79b).** Yield: 9.5 mg, 7  $\mu$ mol, 57%.  $^1H$  NMR (600 MHz,  $CDCl_3$ ):  $\delta$  8.05 (s, 1H,  $CH_{trz}$ ), 7.86 (d,  $J = 8.5$  Hz, 2H,  $2 \times CH_{ar}$ ), 7.62 - 7.58 (m, 1H,  $CH_{ar}$ ), 7.56 (s, 1H, NH), 7.50 (s, 1H, NH), 7.39 - 7.32 (m, 3H,  $3 \times CH_{ar}$ ), 7.29 - 7.21 (m, 3H,  $3 \times CH_{ar}$ ), 7.18 (d,  $J = 7.2$  Hz, 3H,  $2 \times CH_{ar}$ , NH), 7.08 (s, 1H,  $CH_{ar}$ ), 6.97 (d,  $J = 3.8$  Hz, 1H,  $CH_{ar}$ ), 6.93 (d,  $J = 8.5$  Hz, 2H,  $2 \times CH_{ar}$ ), 6.83 (s, 1H,  $CH_{ar}$ ), 6.79 (s, 1H,  $CH_{ar}$ ), 6.54 (d,  $J = 3.8$  Hz, 1H,  $CH_{ar}$ ), 5.94 (s, 1H, NH), 5.15 (s, 2H,  $CH_2$ ), 4.61 (s, 2H,  $CH_2$ ), 4.53 (s, 1H, CH), 4.39 (d,  $J = 5.6$  Hz, 2H,  $CH_2$ ), 4.01 (t,  $J = 5.1$  Hz, 2H,  $CH_2$ ), 3.99 - 3.89 (m, 2H,  $CH_2$ ), 3.66 - 3.53 (m, 20H,  $10 \times CH_2$ ), 2.79 (t,  $J = 7.4$  Hz, 2H,  $CH_2$ ), 2.52 (s, 3H,  $CH_3$ ), 2.44 - 2.25 (m, 7H,  $3 \times CH_2$ ,  $CH_2-H^a$ ), 2.18 (s, 3H,  $CH_3$ ), 2.13 (s, 1H, CH), 2.10 - 2.03 (m, 4H,  $CH_3$ ,  $CH_2-H^b$ ), 1.31 - 1.25 (m, 7H,  $CH_3$ ,  $2 \times CH_2$ ), 0.87 (t,  $J = 6.3$  Hz, 3H,  $CH_3$ ).  $^{13}C$  NMR (151 MHz,  $CDCl_3$ ):  $\delta$  195.68, 171.58, 169.32, 159.73, 159.16, 155.33, 152.75, 149.91, 145.29, 143.41, 142.52, 140.30, 138.15, 136.99, 135.09, 134.61, 134.22, 130.93, 130.91, 130.70, 130.14, 128.84, 128.54, 128.31, 128.04, 127.87, 127.66, 126.26, 125.85, 123.16, 122.95, 119.41, 118.46, 118.10, 114.28, 112.57, 109.84, 87.92, 72.83, 70.64, 70.56, 70.52, 70.45, 64.51, 63.95, 47.71, 43.81, 43.48, 40.06, 39.15, 38.15, 37.52, 36.44, 33.89, 33.54, 29.93, 20.18, 19.91, 18.51, 14.69, 14.21, 13.37, 9.78. ESI-HRMS ( $m/z$ ): calcd. for  $[C_{73}H_{84}BBrF_2N_{10}O_{11} + H]^+$  1405.56383; obsd. 1405.56658.

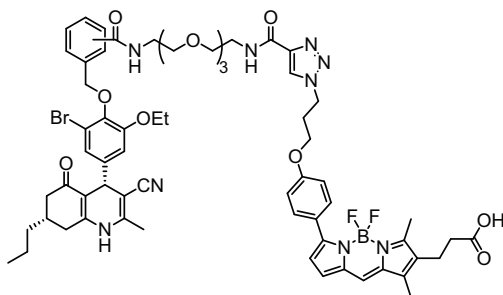
**Fluorescent ligand (m-79a).** Yield: 6.9 mg, 5.1  $\mu$ mol, 51%.  $^1H$  NMR (600 MHz,  $CDCl_3$ ):  $\delta$  8.03 (s, 1H,  $CH_{trz}$ ), 8.01 (s, 1H,  $CH_{ar}$ ), 7.85 (d,  $J = 8.6$  Hz, 2H,  $2 \times CH_{ar}$ ), 7.75 (d,  $J = 7.7$  Hz, 1H,  $CH_{ar}$ ), 7.62 (d,  $J = 7.5$  Hz, 1H,  $CH_{ar}$ ), 7.56 (s, 1H, NH), 7.41 (t,  $J = 7.6$  Hz, 1H,  $CH_{ar}$ ), 7.29 - 7.25 (m, 3H,  $3 \times CH_{ar}$ ), 7.25 - 7.21 (m, 1H,  $CH_{ar}$ ), 7.18 (d,  $J = 7.2$  Hz, 2H,  $2 \times CH_{ar}$ ), 7.08 (s, 1H,  $CH_{ar}$ ), 7.06 (s, 1H, NH), 7.01 (s, 1H, NH), 6.96 (d,  $J = 3.7$  Hz, 1H,  $CH_{ar}$ ), 6.93 - 6.90 (m, 3H,  $3 \times CH_{ar}$ ), 6.81 (s, 1H,  $CH_{ar}$ ), 6.54 (d,  $J = 3.8$  Hz, 1H,  $CH_{ar}$ ), 5.94 (s, 1H, NH), 5.05 - 4.98 (m, 2H,  $CH_2$ ), 4.58 (t,  $J = 6.6$  Hz, 2H,  $CH_2$ ), 4.54 (s, 1H, CH), 4.39 (d,  $J = 5.6$  Hz, 2H,  $CH_2$ ), 4.15 - 4.06 (m, 2H,  $CH_2$ ), 3.98 (t,  $J = 5.3$  Hz, 2H,  $CH_2$ ), 3.70 - 3.63 (m, 12H,  $6 \times CH_2$ ), 3.61 (s, 4H,  $2 \times CH_2$ ), 2.78 (t,  $J = 7.4$  Hz, 2H,  $CH_2$ ), 2.51 (s, 3H,  $CH_3$ ), 2.44 - 2.27 (m, 7H,  $3 \times CH_2$ ,  $CH_2-H^a$ ), 2.17 (s, 3H,  $CH_3$ ), 2.13 (s, 1H, CH), 2.09 - 2.01 (m, 4H,  $CH_3$ ,  $CH_2-H^b$ ), 1.42 (t,  $J = 6.9$  Hz, 3H,  $CH_3$ ), 1.30 - 1.25 (m, 4H,  $2 \times CH_2$ ), 0.86 (t,  $J = 6.5$  Hz, 3H,  $CH_3$ ).  $^{13}C$  NMR (151 MHz,  $CDCl_3$ ):  $\delta$  195.80, 171.59, 167.80, 160.28, 159.66, 159.19, 155.40, 152.77, 149.84, 145.12, 144.12, 143.35, 142.36, 140.26, 138.16, 138.14, 135.09, 134.79, 134.58, 131.29, 130.92, 130.66, 128.85, 128.64, 128.07, 127.87, 127.66, 126.92, 126.89, 126.20, 125.83, 123.16, 122.96, 119.47, 118.49, 118.10, 114.29, 112.98, 109.95, 88.09, 74.14, 70.72, 70.69, 70.55, 70.45, 69.93, 69.80, 64.69, 63.96, 47.67, 43.82, 43.48, 39.98, 39.09, 38.25, 37.52, 36.45, 33.92, 33.60, 29.91, 20.18, 19.88, 18.55, 14.96, 14.19, 13.36, 9.77. ESI-HRMS ( $m/z$ ): calcd. for  $[C_{71}H_{80}BBrF_2N_{10}O_{10} + H]^+$  1361.53761; obsd. 1361.54020.

**Fluorescent ligand (m-79b).** Yield: 3 mg, 2.1  $\mu$ mol, 60%.  $^1H$  NMR (600 MHz,  $CDCl_3$ ):  $\delta$  8.06 (s, 1H,  $CH_{trz}$ ), 7.99 (s, 1H,  $CH_{ar}$ ), 7.86 (d,  $J = 8.8$  Hz, 2H,  $2 \times CH_{ar}$ ), 7.77 (d,  $J = 7.8$  Hz, 1H,  $CH_{ar}$ ), 7.64 (d,  $J = 7.6$  Hz, 1H,  $CH_{ar}$ ), 7.60 (s, 1H, NH), 7.44 - 7.40 (m, 1H,  $CH_{ar}$ ), 7.31 - 7.21 (m, 3H,  $3 \times CH_{ar}$ ), 7.19 (d,  $J = 6.9$  Hz, 2H,  $2 \times CH_{ar}$ ), 7.09 - 7.05 (m, 1H,  $CH_{ar}$ ), 7.03 (s, 1H, NH), 6.97

(d,  $J = 4.0$  Hz, 1H, CH<sub>ar</sub>), 6.95 - 6.88 (m, 3H, 3 × CH<sub>ar</sub>), 6.85 (s, 1H, NH), 6.81 (d,  $J = 1.8$  Hz, 1H, CH<sub>ar</sub>), 6.54 (d,  $J = 4.0$  Hz, 1H, CH<sub>ar</sub>), 5.86 (s, 1H, NH), 5.02 (d,  $J = 6.8$  Hz, 2H, CH<sub>2</sub>), 4.60 (t,  $J = 6.9$  Hz, 2H, CH<sub>2</sub>), 4.54 (s, 1H, CH), 4.40 (d,  $J = 5.7$  Hz, 2H, CH<sub>2</sub>), 4.13 - 4.07 (m, 2H, CH<sub>2</sub>), 3.99 (t,  $J = 5.7$  Hz, 2H, CH<sub>2</sub>), 3.66 - 3.60 (m, 20H, 10 × CH<sub>2</sub>), 2.79 (t,  $J = 7.5$  Hz, 2H, CH<sub>2</sub>), 2.52 (s, 3H, CH<sub>3</sub>), 2.45 - 2.29 (m, 7H, 3 × CH<sub>2</sub>, CH<sub>2</sub>-H<sup>a</sup>), 2.18 (s, 3H, CH<sub>3</sub>), 2.15 (s, 1H, CH), 2.11 - 2.04 (m, 4H, CH<sub>3</sub>, CH<sub>2</sub>-H<sup>b</sup>), 1.43 - 1.41 (m, 3H, CH<sub>3</sub>), 1.31 - 1.27 (m, 4H, 2 × CH<sub>2</sub>), 0.89 - 0.87 (m, 3H, CH<sub>3</sub>). <sup>13</sup>C NMR (151 MHz, CDCl<sub>3</sub>): δ 195.75, 171.56, 167.76, 160.32, 159.68, 159.20, 155.43, 152.79, 149.67, 144.99, 144.18, 143.42, 142.28, 140.27, 138.12, 135.11, 134.80, 134.60, 131.35, 130.93, 130.67, 130.06, 128.86, 128.65, 128.08, 127.90, 127.69, 127.00, 126.91, 126.22, 125.84, 123.17, 122.96, 119.42, 118.49, 118.11, 114.30, 113.00, 110.02, 88.22, 74.20, 70.75, 70.66, 70.62, 70.50, 70.42, 69.99, 69.91, 64.70, 63.97, 47.67, 43.85, 43.48, 39.97, 39.12, 38.23, 37.54, 36.48, 33.93, 33.66, 29.85, 20.17, 19.90, 18.59, 14.96, 14.20, 13.37, 9.78. ESI-HRMS ( $m/z$ ): calcd. for [C<sub>73</sub>H<sub>84</sub>BBrF<sub>2</sub>N<sub>10</sub>O<sub>11</sub> + H]<sup>+</sup> 1405.56383; obsd. 1405.56641.

**Fluorescent ligand (p-79a).** Yield: 2.8 mg, 2 μmol, 29%. <sup>1</sup>H NMR (600 MHz, CDCl<sub>3</sub>): δ 8.03 (s, 1H, CH<sub>trz</sub>), 7.85 (d,  $J = 8.7$  Hz, 2H, 2 × CH<sub>ar</sub>), 7.77 (d,  $J = 7.9$  Hz, 2H, 2 × CH<sub>ar</sub>), 7.57 (d,  $J = 7.9$  Hz, 3H, 2 × CH<sub>ar</sub>, NH), 7.31 - 7.22 (m, 3H, 3 × CH<sub>ar</sub>), 7.19 (d,  $J = 7.1$  Hz, 2H, 2 × CH<sub>ar</sub>), 7.08 (s, 1H, CH<sub>ar</sub>), 6.97 (d,  $J = 4.0$  Hz, 2H, CH<sub>ar</sub>, NH), 6.94 - 6.88 (m, 3H, 3 × CH<sub>ar</sub>), 6.80 (d,  $J = 1.4$  Hz, 1H, CH<sub>ar</sub>), 6.55 (d,  $J = 4.0$  Hz, 1H, CH<sub>ar</sub>), 6.50 (s, 1H, NH), 5.87 (s, 1H, NH), 5.02 (s, 2H, CH<sub>2</sub>), 4.57 (s, 2H, CH<sub>2</sub>), 4.54 (s, 1H, CH), 4.40 (d,  $J = 5.6$  Hz, 2H, CH<sub>2</sub>), 4.13 - 4.06 (m, 2H, CH<sub>2</sub>), 3.97 (t,  $J = 5.2$  Hz, 2H, CH<sub>2</sub>), 3.68 - 3.61 (m, 16H, 8 × CH<sub>2</sub>), 2.79 (t,  $J = 7.4$  Hz, 2H, CH<sub>2</sub>), 2.52 (s, 3H, CH<sub>3</sub>), 2.47 - 2.26 (m, 7H, 3 × CH<sub>2</sub>, CH<sub>2</sub>-H<sup>a</sup>), 2.16 (d,  $J = 16.8$  Hz, 4H, CH<sub>3</sub>, CH), 2.09 (d,  $J = 10.2$  Hz, 4H, CH<sub>3</sub>, CH<sub>2</sub>-H<sup>b</sup>), 1.41 (t,  $J = 6.9$  Hz, 3H, CH<sub>3</sub>), 1.34 - 1.27 (m, 4H, 2 × CH<sub>2</sub>), 0.89 (t,  $J = 6.7$  Hz, 3H, CH<sub>3</sub>). <sup>13</sup>C NMR (151 MHz, CDCl<sub>3</sub>): δ 195.68, 171.57, 167.67, 159.61, 159.23, 155.49, 152.81, 149.36, 144.77, 144.16, 142.14, 141.07, 140.22, 138.12, 135.09, 134.56, 134.23, 130.92, 130.65, 128.87, 128.41, 128.29, 128.11, 127.90, 127.70, 127.17, 126.16, 125.79 (HSQC cross-coupling), 123.15, 122.97, 119.28, 118.54, 118.16, 114.31, 112.98, 110.14, 88.40, 74.00, 70.75, 70.73, 70.59, 70.43, 69.96, 69.89, 64.71, 63.98, 47.52 (HSQC cross-coupling), 43.86, 43.46, 39.96, 39.09, 38.21, 37.51, 36.48, 33.91, 33.73, 29.85, 20.17, 19.91, 18.66, 14.96, 14.19, 13.38, 9.79. ESI-HRMS ( $m/z$ ): calcd. for [C<sub>71</sub>H<sub>80</sub>BBrF<sub>2</sub>N<sub>10</sub>O<sub>10</sub> + H]<sup>+</sup> 1361.53761; obsd. 1361.54010.

**Fluorescent ligand (p-79b).** Yield: 4.6 mg, 3.3 μmol, 65%. <sup>1</sup>H NMR (600 MHz, CDCl<sub>3</sub>): δ 8.05 (s, 1H, CH<sub>trz</sub>), 7.85 (d,  $J = 8.4$  Hz, 2H, 2 × CH<sub>ar</sub>), 7.78 (d,  $J = 7.4$  Hz, 2H, 2 × CH<sub>ar</sub>), 7.61 (d,  $J = 7.9$  Hz, 1H, NH), 7.57 (d,  $J = 7.6$  Hz, 2H, 2 × CH<sub>ar</sub>), 7.30 - 7.23 (m, 3H, 3 × CH<sub>ar</sub>), 7.19 (d,  $J = 7.2$  Hz, 2H, 2 × CH<sub>ar</sub>), 7.08 (s, 2H, CH<sub>ar</sub>, NH), 6.96 (d,  $J = 3.8$  Hz, 1H, CH<sub>ar</sub>), 6.95 - 6.89 (m, 3H, 3 × CH<sub>ar</sub>), 6.80 (s, 1H, CH<sub>ar</sub>), 6.70 (s, 1H, NH), 6.54 (d,  $J = 3.8$  Hz, 1H, CH<sub>ar</sub>), 5.92 (s, 1H, NH), 5.05 - 4.99 (m, 2H, CH<sub>2</sub>), 4.61 (s, 2H, CH<sub>2</sub>), 4.54 (s, 1H, CH), 4.39 (d,  $J = 5.5$  Hz, 2H, CH<sub>2</sub>), 4.14 - 4.05 (m, 2H, CH<sub>2</sub>), 3.99 (s, 2H, CH<sub>2</sub>), 3.67 - 3.61 (m, 20H, 10 × CH<sub>2</sub>), 2.79 (t,  $J = 7.4$  Hz, 2H, CH<sub>2</sub>), 2.52 (s, 3H, CH<sub>3</sub>), 2.44 - 2.25 (m, 7H, 3 × CH<sub>2</sub>, CH<sub>2</sub>-H<sup>a</sup>), 2.18 (s, 4H, CH<sub>3</sub>, CH), 2.11 - 2.05 (m, 4H, CH<sub>3</sub>, CH<sub>2</sub>-H<sup>b</sup>), 1.41 (t,  $J = 6.9$  Hz, 3H, CH<sub>3</sub>), 1.35 - 1.29 (m, 4H, 2 × CH<sub>2</sub>), 0.88 (t,  $J = 6.6$  Hz, 3H, CH<sub>3</sub>). <sup>13</sup>C NMR (151 MHz, CDCl<sub>3</sub>): δ 195.72, 171.59, 167.51, 159.68, 159.20, 155.41, 152.81, 149.52, 144.88, 144.15, 142.20, 141.11, 140.27, 138.15, 135.09, 134.59, 134.16, 130.93, 130.69, 128.86, 128.39, 128.08, 127.89, 127.68, 127.22, 126.20, 125.84 (HSQC cross-coupling), 123.16, 123.01, 118.50, 118.14, 114.30, 112.97, 110.14, 88.33, 73.99, 70.76, 70.60, 70.47, 70.36, 64.72, 63.98, 47.53 (HSQC cross-coupling), 43.84, 43.47, 39.95, 38.23, 37.51, 36.46, 33.91, 33.71, 29.85, 20.18, 19.92, 18.64, 14.97, 14.20, 13.38, 9.78. ESI-HRMS ( $m/z$ ): calcd. for [C<sub>73</sub>H<sub>84</sub>BBrF<sub>2</sub>N<sub>10</sub>O<sub>11</sub> + H]<sup>+</sup> 1405.56383; obsd. 1405.56634.



**General procedure for the synthesis of fluorescent ligands (*m*-/*p*-80a).** Compound **78** (5–6  $\mu\text{mol}$ , 1 eq) and azido-BODIPY-acid **88** (1 eq) were dissolved in degassed DCM/ $\text{H}_2\text{O}$  (2 mL, 1:1, v/v) and aqueous solutions of sodium ascorbate (1.2 eq) and  $\text{CuSO}_4$  (20 mol%) were added. The resulting mixture was stirred vigorously for 2 h, after which TLC indicated complete conversion of the reaction. The solvents were evaporated *in vacuo*, and the residue was taken up in DCM

and purified by silica column chromatography (0%  $\rightarrow$  5% MeOH in DCM) to yield the fluorescent ligand as a purple solid.

**Fluorescent ligand (*m*-80a).** Yield: 2.4 mg, 1.9  $\mu\text{mol}$ , 38%.  $^1\text{H}$  NMR (600 MHz,  $\text{CDCl}_3/\text{MeOD}$ ):  $\delta$  8.28 (s, 1H,  $\text{CH}_{\text{trz}}$ ), 7.98 (s, 1H,  $\text{CH}_{\text{ar}}$ ), 7.85 (d,  $J = 8.8$  Hz, 2H,  $2 \times \text{CH}_{\text{ar}}$ ), 7.77 (d,  $J = 7.8$  Hz, 1H,  $\text{CH}_{\text{ar}}$ ), 7.72 (d,  $J = 7.5$  Hz, 1H,  $\text{CH}_{\text{ar}}$ ), 7.45 (t,  $J = 7.7$  Hz, 1H,  $\text{CH}_{\text{ar}}$ ), 7.20 (s, 1H,  $\text{CH}_{\text{ar}}$ ), 7.01 (d,  $J = 4.0$  Hz, 1H,  $\text{CH}_{\text{ar}}$ ), 6.94 (d,  $J = 8.9$  Hz, 2H,  $2 \times \text{CH}_{\text{ar}}$ ), 6.89 (dd,  $J = 5.8, 1.9$  Hz, 2H,  $2 \times \text{CH}_{\text{ar}}$ ), 6.55 (d,  $J = 4.1$  Hz, 1H,  $\text{CH}_{\text{ar}}$ ), 5.02 (s, 2H,  $\text{CH}_2$ ), 4.66 (t,  $J = 6.9$  Hz, 2H,  $\text{CH}_2$ ), 4.54 (s, 1H, CH), 4.16 - 4.09 (m, 2H,  $\text{CH}_2$ ), 4.06 (dd,  $J = 11.5, 5.9$  Hz, 2H,  $\text{CH}_2$ ), 3.72 - 3.57 (m, 16H,  $8 \times \text{CH}_2$ ), 2.75 (t,  $J = 7.8$  Hz, 2H,  $\text{CH}_2$ ), 2.53 (s, 3H,  $\text{CH}_3$ ), 2.52 - 2.33 (m, 7H,  $3 \times \text{CH}_2$ ,  $\text{CH}_2\text{-H}^{\text{a}}$ ), 2.26 (s, 3H,  $\text{CH}_3$ ), 2.20 (s, 1H, CH), 2.15 - 2.08 (m, 4H,  $\text{CH}_3$ ,  $\text{CH}_2\text{-H}^{\text{b}}$ ), 1.44 (t,  $J = 7.0$  Hz, 3H,  $\text{CH}_3$ ), 1.41 - 1.33 (m, 4H,  $2 \times \text{CH}_2$ ), 0.95 - 0.88 (m, 3H,  $\text{CH}_3$ ).  $^{13}\text{C}$  NMR (151 MHz,  $\text{CDCl}_3/\text{MeOD}$ ):  $\delta$  196.62, 174.73, 168.42, 159.24, 158.90, 154.97, 152.45, 151.41, 145.81, 143.74, 142.50, 139.98, 137.66, 134.82, 134.25, 134.18, 131.24, 130.46, 130.12, 128.27, 127.78, 126.74, 126.57, 125.97, 125.82, 122.96, 122.86, 118.59, 118.00, 117.63, 113.88, 112.42, 108.92, 87.03, 73.92, 70.27, 70.18, 70.00, 69.87, 69.44, 69.21, 64.33, 63.86, 47.59, 42.93, 39.61, 38.78, 38.03, 37.00, 33.65, 33.42, 32.48, 29.49, 19.54, 19.23, 17.38, 14.34, 13.57, 12.61, 9.07. ESI-HRMS ( $m/z$ ): calcd. for  $[\text{C}_{64}\text{H}_{73}\text{BBrF}_2\text{N}_9\text{O}_{11} + \text{H}]^+$  1272.47468; obsd. 1272.47697.

**Fluorescent ligand (*p*-80a).** Yield: 4.5 mg, 3.5  $\mu\text{mol}$ , 59%.  $^1\text{H}$  NMR (600 MHz,  $\text{CDCl}_3/\text{MeOD}$ ):  $\delta$  8.26 (s, 1H,  $\text{CH}_{\text{trz}}$ ), 7.88 - 7.80 (m, 4H,  $4 \times \text{CH}_{\text{ar}}$ ), 7.62 (d,  $J = 8.3$  Hz, 2H,  $2 \times \text{CH}_{\text{ar}}$ ), 7.24 (s, 1H,  $\text{CH}_{\text{ar}}$ ), 7.02 (d,  $J = 4.1$  Hz, 1H,  $\text{CH}_{\text{ar}}$ ), 6.94 (t,  $J = 5.9$  Hz, 2H,  $2 \times \text{CH}_{\text{ar}}$ ), 6.89 (s, 2H,  $2 \times \text{CH}_{\text{ar}}$ ), 6.56 (d,  $J = 4.1$  Hz, 1H,  $\text{CH}_{\text{ar}}$ ), 5.02 (s, 2H,  $\text{CH}_2$ ), 4.65 (s, 2H,  $\text{CH}_2$ ), 4.53 (s, 1H, CH), 4.17 - 4.08 (m, 2H,  $\text{CH}_2$ ), 4.05 (t,  $J = 5.7$  Hz, 2H,  $\text{CH}_2$ ), 3.71 - 3.61 (m, 16H,  $8 \times \text{CH}_2$ ), 2.75 (t,  $J = 7.8$  Hz, 2H,  $\text{CH}_2$ ), 2.55 - 2.50 (m, 4H,  $\text{CH}_3$ ,  $\text{CH}_2\text{-H}^{\text{a}}$ ), 2.48 - 2.36 (m, 6H,  $3 \times \text{CH}_2$ ), 2.26 (s, 3H,  $\text{CH}_3$ ), 2.21 (d,  $J = 7.5$  Hz, 1H, CH), 2.17 - 2.10 (m, 4H,  $\text{CH}_3$ ,  $\text{CH}_2\text{-H}^{\text{b}}$ ), 1.44 (t,  $J = 7.0$  Hz, 3H,  $\text{CH}_3$ ), 1.41 - 1.34 (m, 4H,  $2 \times \text{CH}_2$ ), 0.94 - 0.91 (m, 3H,  $\text{CH}_3$ ).  $^{13}\text{C}$  NMR (151 MHz,  $\text{CDCl}_3$ ):  $\delta$  196.68, 174.72, 168.30, 160.54, 159.05, 158.81, 154.83, 152.33, 151.53, 145.78, 143.52, 142.44, 140.72, 139.92, 134.74, 134.12, 133.40, 130.33, 129.99, 127.88, 127.85, 127.74, 126.92, 126.87, 125.85, 125.65, 122.94, 122.73, 119.25, 117.89, 117.51, 113.73, 112.18, 108.70, 86.90, 73.60, 70.14, 70.05, 69.84, 69.72, 69.30, 69.13, 64.16, 63.68, 47.30, 42.78, 39.50, 38.59, 37.96, 36.87, 33.54, 33.32, 32.32, 29.39, 19.46, 19.10, 17.25, 14.22, 13.46, 12.48, 8.94.

#### Synthesis of propargyl glycine extended FSH $\beta$ 33-53 peptides (*C*-,*N*-81).

Protected peptides were synthesized on an ABI-433A (Applied Biosystems, division of Perkin-Elmer) automated peptide synthesizer using a standard Fmoc-based protocol. The peptides were prepared on a 100  $\mu\text{mol}$  scale starting from Rink amide resin. Deprotection, coupling and capping steps were

performed as follows:

- Removal of the Fmoc-group with 20% piperidine in NMP for 3 × 3 min.
- NMP wash
- Coupling of the appropriate amino acid (5 eq) with HCTU (5 eq) as the coupling agent, DiPEA (10 eq) as the base, in NMP as the solvent for 1 h.
- NMP wash
- Capping of remaining free amines with 5% (v/v) Ac<sub>2</sub>O and DiPEA (0.1 M) in NMP, for 3 min.
- NMP and DCM wash

After the final coupling and deprotection step, all acid-labile protecting groups were removed and the peptide cleaved from the resin by treatment with TFA/H<sub>2</sub>O/TIS (95:2.5:2.5; v/v/v). Purification by RP-HPLC and lyophilizing from AcOH/H<sub>2</sub>O yielded the peptides as white fluffy powders.

**H-PraYTRDLVYKDPARPKIQTSTF-CONH<sub>2</sub> (N-81).** Yield: 38.3 mg, 15 μmol, 15%. ESI-HRMS (*m/z*): calcd. for [C<sub>120</sub>H<sub>189</sub>N<sub>33</sub>O<sub>33</sub> + 2H]<sup>2+</sup> 1311.71523; obsd. 1311.71429.

**H-YTRDLVYKDPARPKIQTSTFPra-CONH<sub>2</sub> (C-81).** Yield: 22 mg, 8.4 μmol, 8%. ESI-HRMS (*m/z*): calcd. for [C<sub>120</sub>H<sub>189</sub>N<sub>33</sub>O<sub>33</sub> + 2H]<sup>2+</sup> 1311.71523; obsd. 1311.71414.

**General procedure for the click reaction between azido-monomeric ligand *m*-74a,b and alkyne FSHβ33-53 peptides (C-,N-82a,b).** To a solution of **81** (1.5-2 μmol, 1 eq) and *m*-74 (1.1 eq) in dioxane/water (5:1; v/v) aqueous solutions of sodium ascorbate (2 eq) and CuSO<sub>4</sub> (20 mol%) were added. The mixture was stirred for 20 h, upon which LC/MS showed complete consumption of the peptide starting material. The solvents were removed *in vacuo*, and DCM was added to the residue, thereby extracting most of the remaining DHP-monomer. The crude product was purified on a Superdex-30 size exclusion column (30% ACN/ 0.05% TFA) and lyophilized to give the heterodimeric product. *R<sub>f</sub>* = 0.3 (1:1:1:1 H<sub>2</sub>O:n-BuOH:EtOAc:AcOH)

**H-Pra(-*m*-DHP)YTRDLVYKDPARPKIQTSTF-CONH<sub>2</sub> (N-82a).** Yield: 5 mg, 1.5 μmol, 69%. LC/MS analysis (linear gradient 10 → 90% ACN) *t<sub>R</sub>*: 5.84 min, ESI-MS (*m/z*): [M + 2 TFA]<sup>2+</sup>: 1814.13. ESI-HRMS (*m/z*): calcd. for [C<sub>158</sub>H<sub>236</sub>BrN<sub>39</sub>O<sub>40</sub> + 2H]<sup>2+</sup> 1701.84869; obsd. 1701.84959.

**H-Pra(-*m*-DHP)YTRDLVYKDPARPKIQTSTF-CONH<sub>2</sub> (N-82b).** Yield: 2.95 mg, 0.86 μmol, 50%. LC/MS analysis (linear gradient 10 → 90% ACN) *t<sub>R</sub>*: 5.86 min, ESI-MS (*m/z*): [M + 2 TFA]<sup>2+</sup>: 1836.00. ESI-HRMS (*m/z*): calcd. for [C<sub>160</sub>H<sub>240</sub>BrN<sub>39</sub>O<sub>41</sub> + 2H]<sup>2+</sup> 1723.86180; obsd. 1723.86189.

**H-YTRDLVYKDPARPKIQTSTFPra(-*m*-DHP)-CONH<sub>2</sub> (C-82a).** Yield: 2.7 mg, 0.79 μmol, 51%. LC/MS analysis (linear gradient 10 → 90% ACN) *t<sub>R</sub>*: 5.93 min, ESI-MS (*m/z*): [M + 2 TFA]<sup>2+</sup>: 1813.33. ESI-HRMS (*m/z*): calcd. for [C<sub>158</sub>H<sub>236</sub>BrN<sub>39</sub>O<sub>40</sub> + 2H]<sup>2+</sup> 1701.84869; obsd. 1701.84845.

**H-YTRDLVYKDPARPKIQTSTFPra(-*m*-DHP)-CONH<sub>2</sub> (C-82b).** Yield: 3.69 mg, 1.07 μmol, 69%. LC/MS analysis (linear gradient 10 → 90% ACN) *t<sub>R</sub>*: 5.94 min, ESI-MS (*m/z*): [M + 2 TFA]<sup>2+</sup>: 1835.87. ESI-HRMS (*m/z*): calcd. for [C<sub>160</sub>H<sub>240</sub>BrN<sub>39</sub>O<sub>41</sub> + 2H]<sup>2+</sup> 1723.86180; obsd. 1723.86146.

## References

- [1] Hoogendoorn, S.; Verkaik, S.; van Doormalen, E.; van der Marel, G. A.; van Koppen, C.; Timmers, C. M.; Overkleeft, H. S. contributed to the work described in this chapter.
- [2] Jacoby, E.; Bouhelal, R.; Gerspacher, M.; Seuwen, K. *ChemMedChem* **2006**, *1*, 760–782.
- [3] Pierce, K. L.; Premont, R. T.; Lefkowitz, R. J. *Nat. Rev. Mol. Cell Biol.* **2002**, *3*, 639–650.
- [4] Vassart, G.; Pardo, L.; Costagliola, S. *Trends Biochem. Sci.* **2004**, *29*, 119–126.

- [5] Pierce, J. G.; Parsons, T. F. *Annu. Rev. Biochem.* **1981**, *50*, 465–495.
- [6] Dierich, A.; Sairam, M. R.; Monaco, L.; Fimia, G. M.; Gansmuller, A.; LeMeur, M.; Sassone-Corsi, P. *Proc. Natl. Acad. Sci. U. S. A.* **1998**, *95*, 13612–13617.
- [7] Lei, Z.; Mishra, S.; Zou, W.; Xu, B.; Foltz, M.; Li, X.; Rao, C. V. *Mol. Endocrinol.* **2001**, *15*, 184–200.
- [8] Themmen, A. P.; Huhtaniemi, I. T. *Endocr. Rev.* **2000**, *21*, 551–583.
- [9] Szkudlinski, M. W.; Fremont, V.; Ronin, C.; Weintraub, B. D. *Physiol. Rev.* **2002**, *82*, 473–502.
- [10] Guo, T. *Expert Opin. Ther. Patents* **2005**, *15*, 1555–1564.
- [11] Heitman, L. H.; IJzerman, A. P. *Med. Res. Rev.* **2008**, *28*, 975–1011.
- [12] Hanssen, R. G. J. M.; Timmers, C. M. **2006**, EP Patent 1,427,733.
- [13] Pelletier, J. C.; Rogers, J.; Wrobel, J.; Perez, M. C.; Shen, E. S. *Bioorg. Med. Chem.* **2005**, *13*, 5986–5995.
- [14] Wrobel, J.; Jetter, J.; Kao, W.; Rogers, J.; Di, L.; Chi, J.; Peréz, M. C.; Chen, G.-C.; Shen, E. S. *Bioorg. Med. Chem.* **2006**, *14*, 5729–5741.
- [15] Maclean, D.; Holden, F.; Davis, A. M.; Scheuerman, R. A.; Yanofsky, S.; Holmes, C. P.; Fitch, W. L.; Tsutsui, K.; Barrett, R. W.; Gallop, M. A. *J. Comb. Chem.* **2004**, *6*, 196–206.
- [16] Guo, T. et al. *Bioorg. Med. Chem. Lett.* **2004**, *14*, 1713–1716.
- [17] Guo, T.; Adang, A. E.; Dong, G.; Fitzpatrick, D.; Geng, P.; Ho, K.-K.; Jibilian, C. H.; Kultgen, S. G.; Liu, R.; McDonald, E.; Saionz, K. W.; Valenzano, K. J.; van Straten, N. C. R.; Xie, D.; Webb, M. L. *Bioorg. Med. Chem. Lett.* **2004**, *14*, 1717–1720.
- [18] Grima Poveda, P. M.; Karstens, W. F. J.; Timmers, C. M. *WO Patent* **2006**, 2006117368(A1).
- [19] van Koppen, C. J.; Verboost, P. M.; van de Lagemaat, R.; Karstens, W.-J. F.; Loozen, H. J.; van Achterberg, T. A.; van Amstel, M. G.; Brands, J. H.; van Doornmalen, E. J.; Wat, J.; Mulder, S. J.; Raafs, B. C.; Verkaik, S.; Hanssen, R. G.; Timmers, C. M. *Biochem. Pharmacol.* **2013**, *85*, 1162–1170.
- [20] Simoni, M.; Gromoll, J.; Nieschlag, E. *Endocr. Rev.* **1997**, *18*, 739–773.
- [21] Radu, A.; Pichon, C.; Camparo, P.; Antoine, M.; Allory, Y.; Couvelard, A.; Fromont, G.; Hai, M. T. V.; Ghinea, N. N. *Engl. J. Med.* **2010**, *363*, 1621–1630.
- [22] Anzalone, L.; Hirsch, J. A. *J. Org. Chem.* **1985**, *50*, 2128–2133.
- [23] Tornøe, C. W.; Christensen, C.; Meldal, M. *J. Org. Chem.* **2002**, *67*, 3057–3064.
- [24] Rostovtsev, V. V.; Green, L. G.; Fokin, V. V.; Sharpless, K. B. *Angew. Chem. Int. Ed. Engl.* **2002**, *41*, 2596–2599.
- [25] Belleau, B.; Malek, G. *J. Am. Chem. Soc.* **1968**, *90*, 1651–1652.
- [26] van Delft, P.; Meeuwenoord, N. J.; Hoogendoorn, S.; Dinkelaar, J.; Overkleeft, H. S.; van der Marel, G. A.; Filippov, D. V. *Org. Lett.* **2010**, *12*, 5486–5489.
- [27] Verdoes, M.; Florea, B. I.; Hillaert, U.; Willems, L. I.; van der Linden, W. A.; Sae-Heng, M.; Filippov, D. V.; Kisselev, A. F.; van der Marel, G. A.; Overkleeft, H. S. *ChemBioChem* **2008**, *9*, 1735–1738.
- [28] Santa Coloma, T. A.; Dattatreya Murty, B.; Reichert Jr, L. E. *Biochemistry* **1990**, *29*, 1194–1200.
- [29] Sluss, P. M.; Krystek Jr, S. R.; Andersen, T. T.; Melson, B. E.; Huston, J. S.; Ridge, R.; Reichert Jr, L. E. *Biochemistry* **1986**, *25*, 2644–2649.
- [30] Zhang, X.-y.; Chen, J.; Zheng, Y.-f.; Gao, X.-l.; Kang, Y.; Liu, J.-c.; Cheng, M.-j.; Sun, H.; Xu, C.-j. *Cancer Res.* **2009**, *69*, 6506–6514.
- [31] Santa-Coloma, T. A.; Crabb, J. W.; Reichert Jr, L. E. *Mol. Cell. Endocrinol.* **1991**, *78*, 197–204.
- [32] Terrillon, S.; Bouvier, M. *EMBO Rep.* **2004**, *5*, 30–34.
- [33] Milligan, G. *Mol. Pharmacol.* **2004**, *66*, 1–7.
- [34] Szidonya, L.; Cserző, M.; Hunyady, L. *J. Endocrinol.* **2008**, *196*, 435–453.
- [35] Fan, Q. R.; Hendrickson, W. A. *Nature* **2005**, *433*, 269–277.
- [36] Kizuka, H.; Hanson, R. *J. Med. Chem.* **1987**, *30*, 722–726.
- [37] Portoghese, P. S. *J. Med. Chem.* **2001**, *44*, 2259–2269.
- [38] Bongers, K. M.; Hoogendoorn, S.; van Koppen, C. J.; Timmers, C. M.; Overkleeft, H. S.; van der Marel, G. A. *ChemMedChem* **2009**, *4*, 2098–2102.
- [39] Urizar, E.; Montanelli, L.; Loy, T.; Bonomi, M.; Swillens, S.; Gales, C.; Bouvier, M.; Smits, G.; Vassart, G.; Costagliola, S. *EMBO J* **2005**, *24*, 1954–1964.
- [40] Marsh, I. R.; Bradley, M. *Tetrahedron* **1997**, *53*, 17317 – 17334.
- [41] Bongers, K. M.; van den Berg, R. J.; Heitman, L. H.; IJzerman, A. P.; Oosterom, J.; Timmers, C. M.; Overkleeft, H. S.; van der Marel, G. A. *Bioorg. Med. Chem.* **2007**, *15*, 4841 – 4856.





# 7

## Small-molecule fluorescent agonists for the follicle-stimulating hormone receptor<sup>1</sup>

Fluorescent agonists for cell surface receptors allow visualization of the interaction between the ligand and its receptor as well as the processes that are set in motion by receptor activation. This chapter describes the synthesis of a diverse set of fluorescent, low molecular weight ligands for the follicle-stimulating hormone receptor (FSHR), based on a dihydropyridine (DHP) agonist. The fluorescent ligands were shown to be potent FSHR agonists, able to activate receptor signaling with nanomolar potencies and to effect receptor internalization at higher concentrations. The nature of the dye was shown to be of great importance for the selectivity of compound uptake. Although all compounds were internalized by FSHR-expressing cells, only the transport of Cy5-conjugated DHP **96** was mediated by the FSHR. The fluorescent DHP-Cy5 agonist was selectively taken up by FSHR-expressing cells in complex with the receptor, opening up possibilities for the targeted delivery of drugs into the endolysosomal pathway of FSHR-expressing cells.

## 7.1 Introduction

The use of fluorescent ligands to study receptor-related processes is an emerging field. Advancements in fluorescence-based microscopy techniques, such as confocal laser scanning microscopy and fluorescence correlation microscopy, have opened up ways to study ligand-protein interactions at the single cell or even single molecule level.<sup>2,3</sup> When the fluorescent ligand retains the pharmacological properties of the parent ligand, real-time visualization of receptor binding, internalization, trafficking and recycling is enabled.<sup>4</sup> Several fluorescent probes for G protein-coupled receptors (GPCRs) have emerged in the literature. Most of these employ peptide-based ligands, mainly because the attachment of a fluorophore to a peptide is a relatively minor increase in bulk and molecular weight compared to the attachment of a dye to a small-molecule ligand.<sup>5,6</sup> Baker *et al.* have evaluated multiple low molecular weight fluorescent ligands (both agonists and antagonists) for the study of adenosine A1 receptors. They have shown that both the choice of linker to separate the dye and the ligand and the nature of the fluorophore can have a profound influence on the pharmacological properties of the probes.<sup>7</sup> Where antagonistic probes can be used to study ligand-receptor binding, agonistic probes are useful tools for the study of receptor internalization. Kozma *et al.* have synthesized a variety of adenosine A3 receptor agonists incorporating different fluorophores, and found specific accumulation of fluorescence in cells expressing the receptor for one of the probes.<sup>8</sup>

The follicle-stimulating hormone receptor (FSHR) is a member of the GPCR family and plays an important role in human reproduction.<sup>9</sup> Activation of this receptor by its endogenous ligand follicle-stimulating hormone (FSH) leads to the dissociation of the bound G<sub>s</sub> protein and subsequent activation of adenylyl cyclase. To prevent overstimulation of the receptor, the C-terminal domain is phosphorylated which leads to binding of  $\beta$ -arrestins and uptake of the receptor-ligand complex in clathrin-coated pits.<sup>10-12</sup> The FSHR is mainly present on granulosa cells in the ovaries and on Sertoli cells in the testes, but expression has also been found on newly formed blood vessels of a variety of tumors.<sup>13,14</sup> As such, fluorescent ligands for the FSHR could be used as diagnostic tumor markers. Fluorescent agonists for the FSHR could also be used to study ligand-induced internalization and trafficking of the receptor (Figure 6.1, Chapter 6). Only one example of a fluorescent ligand for the FSHR has appeared in the literature and this is based on the FSH $\beta_{33-53}$  peptide ligand, also described in Chapter 6. Although FITC-FSH $\beta_{33-53}$  was taken up more efficiently in cells expressing the FSHR compared to cells without the receptor, the agonistic properties of this fluorescent peptide and its ability to induce receptor endocytosis were not investigated.<sup>15</sup> Dihydropyridines (DHPs) are a class of low molecular weight agonists for the FSHR which are very potent and selective.<sup>16,17</sup> Their pharmacological signaling properties have been investigated in depth and it has been shown that these allosteric ligands are able to induce receptor internalization.<sup>17</sup> In Chapter 6 the structure-activity relationship of different modes of attachment of a conjugation handle onto the parent DHP scaffold was examined. From these studies, it became clear that *meta*-substituted monomeric ligand

*m*-74a, with PEG spacer length  $n=3$  was the most promising lead for further conjugation. Attachment of a fluorescent BODIPY dye to this monomeric ligand resulted in a first series of fluorescent agonists for the FSHR. However, from this SAR study it also became clear that small modifications of the dye could have a big influence on the potency of the ligand. For instance, an additional benzyl group to mask the free carboxylic acid of the BODIPY dye did lead to a 3-4 fold decrease in agonistic potency.

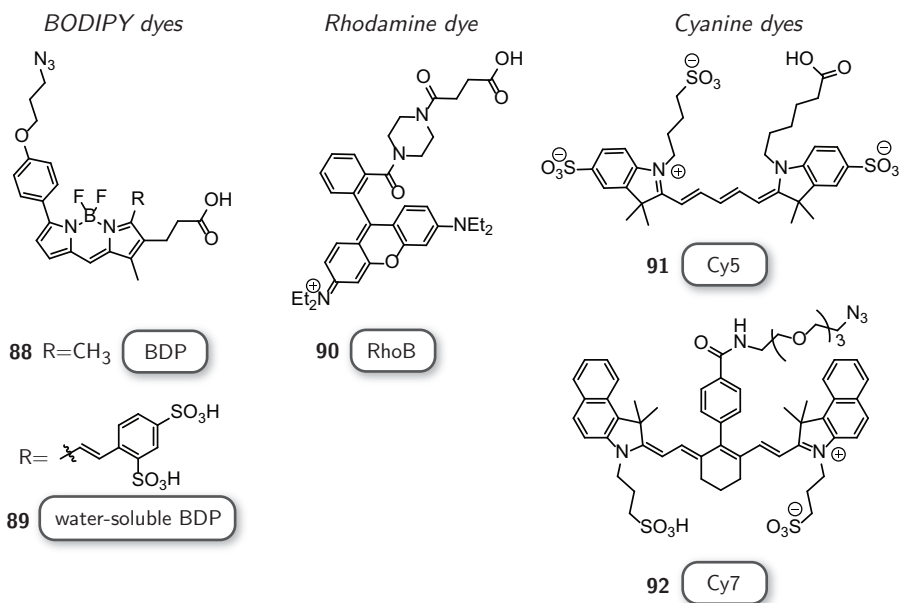


**Figure 7.1:** Overview of the different fluorescent dyes used in this study.

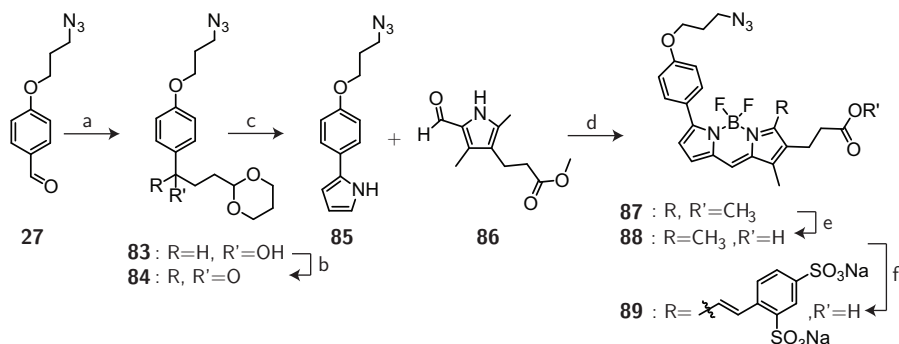
For cell or tissue imaging, organic dyes with red-shifted fluorescence absorption and emission wavelengths are favored, because of lower levels of autofluorescence in the red end of the spectrum. Figure 7.1 shows the structures of the fluorophores that were used in this study for the development of fluorescent FSHR agonists. Among these are dyes from three different classes: BODIPY dyes, cyanine dyes as well as a rhodamine dye. Emission wavelengths of these dyes vary between  $\sim 580$  nm (BODIPY-TMR **88**, Rhodamine B **90**) and  $>750$  nm (Cy7 **92**)<sup>18</sup> and especially the physicochemical properties are expected to be quite different. The synthesis of a water-soluble, red-shifted variant of bifunctional azido-BODIPY-acid<sup>19</sup> is described, with the aim to reduce the lipophilicity while conserving the optimal fluorescence properties associated with the BODIPY core.<sup>20</sup> In this study fluorescent ligands for the FSHR of various nature were synthesized and evaluated for their agonistic potencies in a luciferase assay. Fluorescence-activated cell sorting (FACS) was used to determine whether these probes were internalized by cells expressing the FSHR. Furthermore, fluorescence confocal microscopy was used to study ligand-induced receptor endocytosis and trafficking of the receptor-ligand complex. These experiments addressed the question what the requirements are to develop a low molecular weight agonist for the

FSHR that retains the profile of the parent DHP **55**, while shedding light on the intricate biological process of receptor activation.

## 7.2 Results and Discussion

**Synthesis.** The various dyes that were used for the synthesis of fluorescent-DHP probes are shown in Figure 7.1. The bifunctional BODIPY dye **88** has been previously reported by Verdoes *et al.*<sup>19</sup> Analogous to the work described in Chapter 3,<sup>21</sup> it was rationalized that a water-soluble derivative of this BODIPY could be obtained by employment of a Knoevenagel condensation reaction with disulfonic acid benzaldehyde. The obvious advantage hereof would be an increased hydrophilicity compared to the regular BODIPY, which might have a beneficial effect in terms of background fluorescence arising from aspecific membrane-interactions. Also, extension of the conjugated system by the Knoevenagel condensation reaction has previously been shown to lead to a red-shift in fluorescence.<sup>21</sup>

**Scheme 7.1:** Optimized synthetic route towards azido-BODIPY-acid **88** followed by a Knoevenagel condensation to obtain bifunctional water-soluble BODIPY **89**



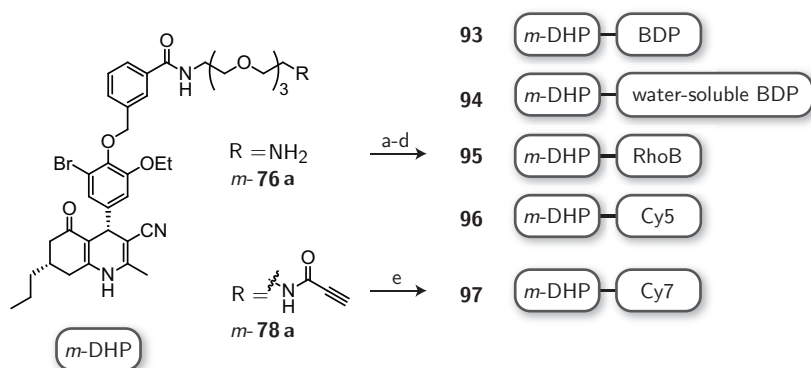
Reagents and conditions: [a] (1,3-dioxan-2-ylethyl)-magnesium bromide (0.5 M in THF), THF, 0 °C → rt, 70%; [b] MnO<sub>2</sub>, DCM, 79%; [c] NH<sub>4</sub>OAc, acetic acid; [d] i) HBr (aq), MeOH; ii) TEA, BF<sub>3</sub> · OEt<sub>2</sub>, DCE, 90 °C, **87**: 44% from **84** and hydrolyzed **88**: 10%; [e] Me<sub>3</sub>SnOH, toluene, reflux, 86%; [f] i) 4-formyl-1,3-benzenedisulfonic acid disodium salt, acetic acid, pyrrolidine, MeOH, 72 °C, ii) Dowex-Na<sup>+</sup>, 62%.

Scheme 7.1 shows the followed synthetic route towards water-soluble dye **89**. For this, the synthesis of intermediate **88** was optimized. The Grignard reaction of azidobenzaldehyde **27** with (1,3-dioxane-2-ylethyl)-magnesium bromide was conducted at 0 °C → rt instead of -10 °C → rt and for a shorter period of time, which significantly diminished elimination of the azide by action of the Grignard agent as a base, resulting in 70% yield of compound **83**. Oxidation with manganese oxide gave ketone **84** that was subjected to a very large excess of ammonium acetate (100 eq) in acetic acid to prevent byproduct formation during the Paal-Knorr pyrrole synthesis. Pyrrole **85** proved to be very sensitive to air and was used without excessive purification procedures in the condensation reaction with pyrrole aldehyde **86**.<sup>22</sup> The intermediate HBr salt was subjected to base and BF<sub>3</sub> · OEt<sub>2</sub>

under reflux conditions resulting in 44% yield of methyl ester **87** and an additional 10% of hydrolyzed BODIPY **88**, starting from **84**. The methyl ester was saponified in high yield (86%) using  $\text{Me}_3\text{SnOH}$ . This improves the existing route that employed an ethyl ester that required harsh conditions for saponification resulting in moderate yields (35%).<sup>19</sup> Knoevenagel condensation of azido-BODIPY-acid **88** with 4-formyl-1,3-benzendisulfonic acid using acetic acid and pyrrolidine in methanol was followed by ion-exchange over Dowex- $\text{Na}^+$  to give the sodium salt of water-soluble BODIPY **89** in 62% yield.

Both rhodamine B **90**<sup>23</sup> and Cy5 **91**<sup>24</sup> (Figure 7.1) were synthesized according to literature procedures and contained a carboxylic acid for ligation to the DHP agonist. To minimize the differences in structures between the fluorescent probes, the bifunctional BODIPY dyes **88** and **89** were also conjugated via their acid moieties. The only exception was Cy7 **92** which was synthesized with an additional azido-PEG spacer attached to the bulky core<sup>18</sup> to diminish potential steric interactions. As shown in Scheme 7.2 standard peptide coupling reagents were used to couple amino-DHP *m*-**76a** (Chapter 6) to the various dyes, resulting in "DHP-BDP" **93**, "DHP-water-soluble BDP" **94**, "DHP-RhoB" **95** and "DHP-Cy5" **96**. Cy7 dye **92** was used in a Cu(I)-catalyzed click reaction<sup>25,26</sup> with alkyne-DHP *m*-**78a** to give "DHP-Cy7" **97**. Yields varied between 40% and 92%, depending on ease of purification of the fluorescent ligands.

**Scheme 7.2:** Synthesis of fluorescent low molecular weight agonists based on *meta*-DHP **64**



Reagents and conditions: [a] azido-BODIPY acid **88**, EDC · HCl, HOBT, TEA, DCM, 48%; [b] water-soluble BODIPY **89**, EDC · HCl, HOBT, TEA, DMF, 92%; [c] Rhodamine B-acid **90**, EDC · HCl, HOBT, DiPEA, DMF, 82%; [d] Cy5-acid **91**, PyBOP, DiPEA, DMF, 55%; [e] azido-Cy7 **92**,  $\text{CuSO}_4$ , sodium ascorbate, dioxane/ $\text{H}_2\text{O}$ , 40%.

**Biological evaluation.** Fluorescent DHP ligands **93-97** were evaluated for their agonistic activity in a CRE-luciferase assay. CHO cells stably expressing the human FSHR and a CRE-luciferase reporter gene were cultured for 4 h in the presence of increasing concentration of probe. Cells were lysed and the cAMP-driven expression of luciferase was detected by the addition of a luminescent substrate. Effects were normalized against the maximum response obtained with recombinant FSH (200 pM). CHO cells without recep-

tor but with the reporter gene were used to control for non-receptor-mediated increases in cAMP levels and no response above background was detected in the control CHO cells for all compounds tested at the highest concentration. Representative dose-response curves are shown in Figure 7.2. All compounds were full agonists for the FSHR.

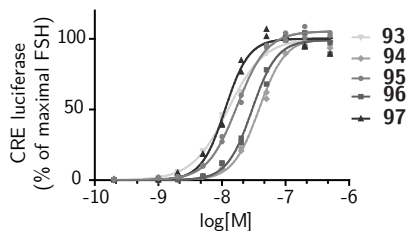


**Figure 7.2:** Agonistic dose-response curves of fluorescent ligands **93** - **97** on CHO cells stably expressing the human FSHR. The response was normalized against the maximal effect obtained with rFSH (200 pM). Representative curves are shown of at least three independent experiments performed in duplicate.

values of 24-35 nM. Overall, fluorescent ligands could be synthesized with low nanomolar potencies and without great differences between fluorophores used. Studies on other receptors have been reported where the nature of the fluorophore had a strong influence on the potency of the ligand.<sup>8,27</sup> The use of spacers to separate the ligand and dye is therefore often a requirement. The small differences in potency found here are in agreement with the previous SAR study which led to the identification of a PEG-spacer with three ethylene glycol units as the optimal spacer (Chapter 6) to connect bulk to the DHP lead compound.

**Table 7.1:** Mean agonistic potency ( $EC_{50}$ ) values of fluorescent ligands on CRE-luciferase activity in CHO cells stably expressing hFSHR and a CRE-luciferase reporter gene.

| Compound     | $EC_{50}$ (nM) | p $EC_{50}$ | $N$ | Compound  | $EC_{50}$ (nM) | p $EC_{50}$ | $N$ |
|--------------|----------------|-------------|-----|-----------|----------------|-------------|-----|
| <i>m-74a</i> | 6              | 8.22 ± 0.10 | 3   | <b>95</b> | 35             | 7.45 ± 0.51 | 3   |
| <b>93</b>    | 8              | 8.10 ± 0.11 | 5   | <b>96</b> | 15             | 7.82 ± 0.09 | 5   |
| <b>94</b>    | 24             | 7.62 ± 0.14 | 3   | <b>97</b> | 25             | 7.60 ± 0.12 | 3   |

The mean  $EC_{50}$  values are calculated from the p $EC_{50}$  (mean ± SEM) values from  $N$  independent experiments performed in duplicate. The value for monomeric ligand *m-74a* from Chapter 6 is given for comparison.

With potent agonistic fluorescent ligands in hand, it was investigated whether these compounds could be used to induce FSHR internalization, and whether this would result in selective uptake of these ligands in the endolysosomal pathway of cells expressing the receptor. A combination of fluorescence-activated cell sorting (Figure 7.3) and confocal fluorescence microscopy (Figure 7.4) was used to study the uptake of the fluorescent agonists in U2OS-FSHR cells stably expressing the rat FSHR fused to the N-terminus of

As can be seen in Table 7.1, DHP-BDP **93** was the most potent agonist of the series with an  $EC_{50}$  value of 8 nM. This is an improvement over the fluorescent ligand **80a** ( $EC_{50}$  = 26 nM) described in Chapter 6, which employed the azide-ligation handle of the bifunctional BO-DIPY dye to attach the DHP-ligand. Next best was the Cy5 derivative **96** with an  $EC_{50}$  value of 15 nM, still a very potent agonist for the FSHR. Attachment of the more bulky fluorophores rhodamine B, Cy7 or the water-soluble BODIPY resulted in slightly higher  $EC_{50}$

enhanced green fluorescent protein (eGFP). As a biological control, wild-type U2OS cells that do not express the FSHR were used. To test the ability of the ligands to induce receptor internalization, U2OS-FSHR cells were incubated with 10  $\mu$ M of compound for 2 h. It has been shown before that concentrations of about two orders of magnitude higher than the EC<sub>50</sub> found in the luciferase assay are needed to induce ~50% receptor internalization by FSH and low molecular weight FSHR agonists.<sup>17,28</sup> In case of a lipophilic, LMW agonist, the presence of serum albumin in the medium can lead to a rightward shift in dose-response curves because of binding of the compound to the serum.<sup>29</sup> Since no serum was included in the luciferase assay and 10% FCS was used for the internalization assay, this difference might also result in the much higher dose required in the internalization assay. Furthermore, receptors from different species were used in the luciferase (human) versus internalization (rat) assays, which might have an influence on the potency of the ligand. In the study by van Koppen *et al.*, this was thoroughly evaluated for a compound of the same DHP class, and no differences in potency were found between rat and human FSHR.<sup>17</sup> As shown in Figure 7.4A, vehicle-treated cells showed mainly membrane fluorescence, whereas treatment with the endogenous ligand recombinant human FSH (rFSH, 12 nM) led to the translocation of the receptor from the membrane to bright intracellular vesicles, indicative of endocytosis. Treatment with the fluorescent ligands did also result in the internalization of the receptor as seen by GFP fluorescence. Except for compound **97**, which could not be detected with this microscope, bright ligand fluorescence was present inside the cells. Apparent from the micrographs are the non-homogeneous levels of receptor expression in these cells, as judged by the intensity of the GFP signal. The intracellular fluorescence intensities for compounds **93-95** did not seem to correlate well with the presence or absence of GFP signal, which prompted further experiments.

The best agonists **93**, **96** and the Cy7-derivative **97** were subjected to flow cytometry analysis to quantitatively correlate receptor expression levels with compound uptake/binding. To diminish potential background staining due to high concentrations of fluorophore, the concentration was lowered to 1  $\mu$ M and U2OS-FSHR or U2OS cells were incubated for 2 h. Cells were thoroughly washed and a single-cell suspension in PBS was analyzed by FACS. The median fluorescence intensities of untreated versus compound-treated U2OS-FSHR cells are shown in Figure 7.3B. The GFP signal was constant throughout the experiments, indicating that no alterations in receptor expression levels were induced by the compounds. A low fluorescence signal, due to autofluorescence, was detected in untreated cells in BODIPY and Cy5 detection channels, and fluorescence increased ~1000-fold upon treatment with compound DHP-BDP or DHP-Cy5. For DHP-Cy7 the increase was much less (untreated MFI: 5, treated MFI: 12), probably also because of suboptimal detection options for this near-IR dye.<sup>18</sup> Comparison of cells with and without receptor led to interesting observations. An overlay of the histograms of U2OS-FSHR vs U2OS cells (Figure 7.3C) showed similar shifts in population fluorescence for DHP-BDP and DHP-Cy7, indicating that the compounds were taken up or binding to the cells, irrespective of the presence of receptor. The population of U2OS-FSHR cells treated with fluorescent agonist DHP-

Cy5 on the other hand, was >10-fold more fluorescent than the population of non-receptor cells. This finding was further confirmed by quadrant analysis of 2D ligand-fluorescence versus GFP-fluorescence intensity plots (Figure 7.3D, Table 7.2). Only for DHP-Cy5 **96** a linear relationship was found between receptor expression and compound fluorescence (Figure 7.3D). Quantitative quadrant analysis is given in Table 7.2. For all three channels (BODIPY, Cy5 and Cy7) quadrants were set such that 90-100% of the untreated U2OS cells were negative for both GFP and dye fluorescence and 90-93% of untreated U2OS-FSHR cells were positive for GFP but negative for dye fluorescence. Whereas 98% of the treated

**Table 7.2:** Quadrant analysis of FACS data.

| Compound             | Quadrant | untreated (%)       |                     | treated (%)         |                     |
|----------------------|----------|---------------------|---------------------|---------------------|---------------------|
|                      |          | U2OS                | U2OS-FSHR           | U2OS                | U2OS-FSHR           |
| DHP-BDP<br><b>93</b> | UL       | 0.06 ± 0.01         | 0.01 ± 0.01         | <b>99.83 ± 0.06</b> | 7.25 ± 1.14         |
|                      | UR       | 0.08 ± 0.03         | 0.09 ± 0.02         | 0.11 ± 0.02         | <b>92.64 ± 1.07</b> |
|                      | LL       | <b>99.82 ± 0.03</b> | 6.36 ± 0.88         | 0.06 ± 0.05         | 0.03 ± 0.02         |
|                      | LR       | 0.05 ± 0.03         | <b>93.54 ± 0.87</b> | 0.00                | 0.08 ± 0.06         |
| DHP-Cy5<br><b>96</b> | UL       | 0.00                | 0.00                | 1.56 ± 0.19         | 0.59 ± 0.35         |
|                      | UR       | 0.03 ± 0.03         | 0.00                | 0.02 ± 0.01         | <b>88.08 ± 2.79</b> |
|                      | LL       | <b>99.87 ± 0.06</b> | 6.15 ± 0.83         | <b>98.36 ± 0.21</b> | 6.10 ± 1.26         |
|                      | LR       | 2.43 ± 2.33         | <b>93.94 ± 0.9</b>  | 0.06 ± 0.02         | 5.24 ± 1.85         |
| DHP-Cy7<br><b>97</b> | UL       | 9.99 ± 0.64         | 0.14 ± 0.13         | <b>73.35 ± 4.44</b> | 2.84 ± 0.33         |
|                      | UR       | 0.07 ± 0.00         | 3.38 ± 2.52         | 0.09 ± 0.03         | <b>51.35 ± 0.6</b>  |
|                      | LL       | <b>89.92 ± 0.65</b> | 5.91 ± 0.31         | 26.56 ± 4.46        | 3.28 ± 0.42         |
|                      | LR       | 0.02 ± 0.01         | <b>90.58 ± 2.95</b> | 0.00                | 42.63 ± 0.21        |

U2OS or U2OS-FSHR cells were either untreated or treated with 1 μM of compound and analyzed by FACS. Contourplots of GFP vs fluorophore fluorescence were divided in quadrants (UL: upper left; UR: upper right; LL: lower left; LR: lower right) as shown in Figure 7.3 D. Percentages (mean ± SEM) calculated for three independent experiments performed in duplo are given. The main population in each group is typeset in boldface.

U2OS cells were negative for both GFP and Cy5 fluorescence upon treatment with compound **96**, 99% and 73% of the control cells became positive for BODIPY and Cy7 fluorescence upon treatment with **93** or **97**, respectively. In case of receptor-expressing cells, 88% of the DHP-Cy5 treated cells became double positive, 93% of the DHP-BDP treated cells and only 51% of the DHP-Cy7 treated cells. When the brightest population of cells in the GFP channel was selected and marked in the cell populations in the respective dye fluorescent channels, as shown in Figure 7.3E, a clear correlation was again found between the amount of receptor and the amount of compound fluorescence for compound DHP-Cy5 but not for the other two compounds. FACS data do not provide information on the localization of the fluorescent signal, therefore from these experiments it can not be concluded whether the compounds are taken up by the cells or merely binding. However, it can be concluded that only for compound DHP-Cy5 a clear relationship was found between dye fluorescence intensities and FSHR expression levels, without considerable background in cells that do not express the receptor. An important difference between the Cy5 and BODIPY dyes used in this study is their lipophilicity. The Cy5 dye **91** contains three nega-



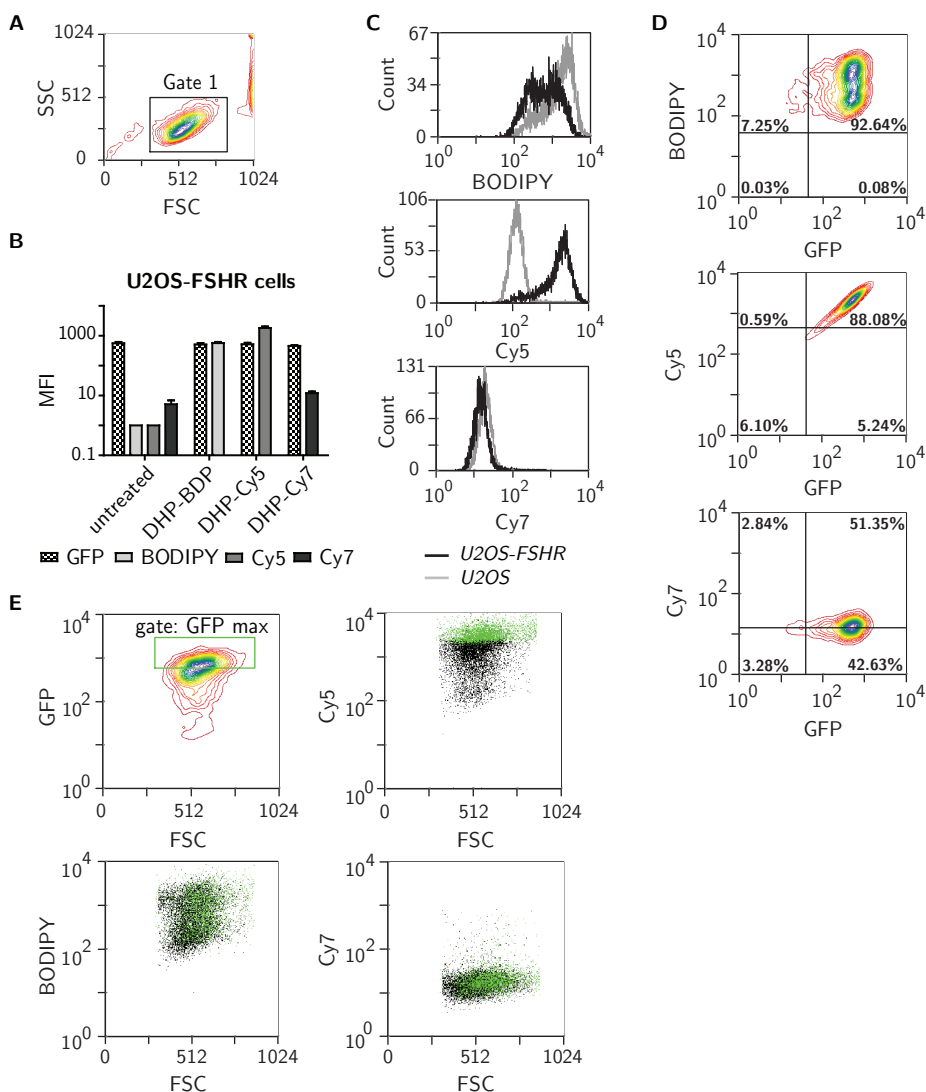


**Figure 7.3: FACS analysis.** U2OS-FSHR (GFP channel) and U2OS cells were treated with 1  $\mu$ M *m*-DHP-BDP **93** (BODIPY channel), *m*-DHP-Cy5 **96** (Cy5 channel) or *m*-DHP-Cy7 **97** (Cy7 channel). After treatment (2 h, 37  $^{\circ}$ C, 5%  $\text{CO}_2$ ), cells were washed with PBS (2 x) and harvested. A single cell suspension in PBS ( $5 \cdot 10^5$  cells/mL) was measured on a BD FACSCanto II FACS apparatus. Representative plots are shown from three independent experiments measured in duplo. A) Forward scatter (FSC) vs side scatter (SSC) plot used to set Gate 1; all subsequent data analysis was performed on cells within this gate. Sample size within Gate 1 > 10000 cells. B) Median fluorescence intensities (MFI) (mean  $\pm$  SEM,  $N=3$ ) of (un)treated U2OS-FSHR cells show similar GFP levels, but increased fluorescence in the corresponding fluorescence channel (compared to control) upon treatment with one of the compounds. C) Overlays of the histograms of treated U2OS-FSHR (black) and control U2OS (grey) show that treatment with compounds **93** and **97**, but not **96**, resulted in a similar fluorescent shift for both cell lines. D) Representative contour plots of dye fluorescence vs GFP of treated U2OS-FSHR cells, including the quadrants that were used for the data shown in Table 7.2. E) The correlation between the intensity of GFP versus dye fluorescence was further examined by selection of an additional gate "GFP max". Cells within this gate are marked green in the population (black) of each dye in its corresponding channel. Only for compound **96** it was found that cells with maximum FSHR-GFP levels correspond to those cells that have maximum dye fluorescence.

tively charged sulfonate groups and is highly water-soluble, whereas BODIPY dye **88** is uncharged and very lipophilic.<sup>20</sup> Table 7.3 reflects the lipophilicity of the compounds in calculated logD{7.4} values. Calculation of accurate values for the BODIPY dyes is hindered by the ambiguity of the structure because of the coordinate bond between boron and nitrogen. It is clear though that both Cy7 and BODIPY containing compounds (**97** and **93**) have much higher logD values than the corresponding Cy5 analogue **96**. This result illustrates that even though the physicochemical properties of these dyes in this case do not influence the agonistic potency of the fluorescent ligands, they have a major influence on the binding/uptake characteristics.

**Table 7.3:** Calculated logD{7.4} values.

| Compound              | logD{7.4} | dye class | Compound  | logD{7.4} | dye class     |
|-----------------------|-----------|-----------|-----------|-----------|---------------|
| <i>m</i> - <b>74a</b> | 4.7       | none      | <b>95</b> | 4.0       | Rhodamine B   |
| <b>93</b>             | 5.8       | BODIPY    | <b>96</b> | 3.6       | cyanine (Cy5) |
| <b>94</b>             | 1.4       | BODIPY    | <b>97</b> | 8.6       | cyanine (Cy7) |

logD values at pH 7.4 were calculated using MarvinSketch. The values for the compounds containing a BODIPY dye (**93** and **94**) are less reliable due to structural ambiguity caused by the coordinate bond between boron and nitrogen.

The ability of DHP-BDP **93** and DHP-Cy5 **96** to induce receptor internalization as well as the intracellular localization of the probes was further examined by confocal fluorescence microscopy. Illustrative examples of micrographs are shown in Figure 7.4B and D, and quantification of FSHR internalization and global fluorescence levels under the different conditions used is shown in Figure 7.5. BDP-DHP **93** was shown to induce receptor internalization in U2OS-FSHR cells as seen by the appearance of green intracellular vesicles. Similar levels of internalization were found as when the cells were treated with rFSH, confirming that DHP-BDP is a potent, functional FSHR agonist able to induce cAMP-mediated signaling as well as subsequent receptor internalization. BODIPY fluorescence was observed intracellularly in the perinuclear region in membrane-like structures, most likely corresponding to the membranes of the endoplasmic reticulum (ER) or Golgi apparatus.<sup>30,31</sup> Colocalization analysis of BODIPY fluorescence and GFP (receptor) fluorescence as shown in Figure 7.5C and Table 7.4 indicated that only moderate colocalization existed between the two dyes.<sup>32</sup> Indeed, the same intracellular localization pattern was seen when control U2OS cells were treated with the compound at 37 °C (Figure 7.4B, right panel). No difference in fluorescence levels was found between cells expressing the receptor and wild-type cells (Figure 7.5B), confirming the FACS data. When U2OS-FSHR cells were treated with compound at 4 °C, receptor internalization was inhibited (Figure 7.4B, middle panel and Figure 7.5A), as well as compound uptake. Receptor internalization is an active process, and the rate of internalization is dependent on the temperature.<sup>33</sup> The fact that also compound uptake was abolished at low temperature, indicates that the compound was not (only) taken up by passive diffusion but that other, active, processes played a role. Although diffusion through the cell membrane could be expected to be slowed down at lower

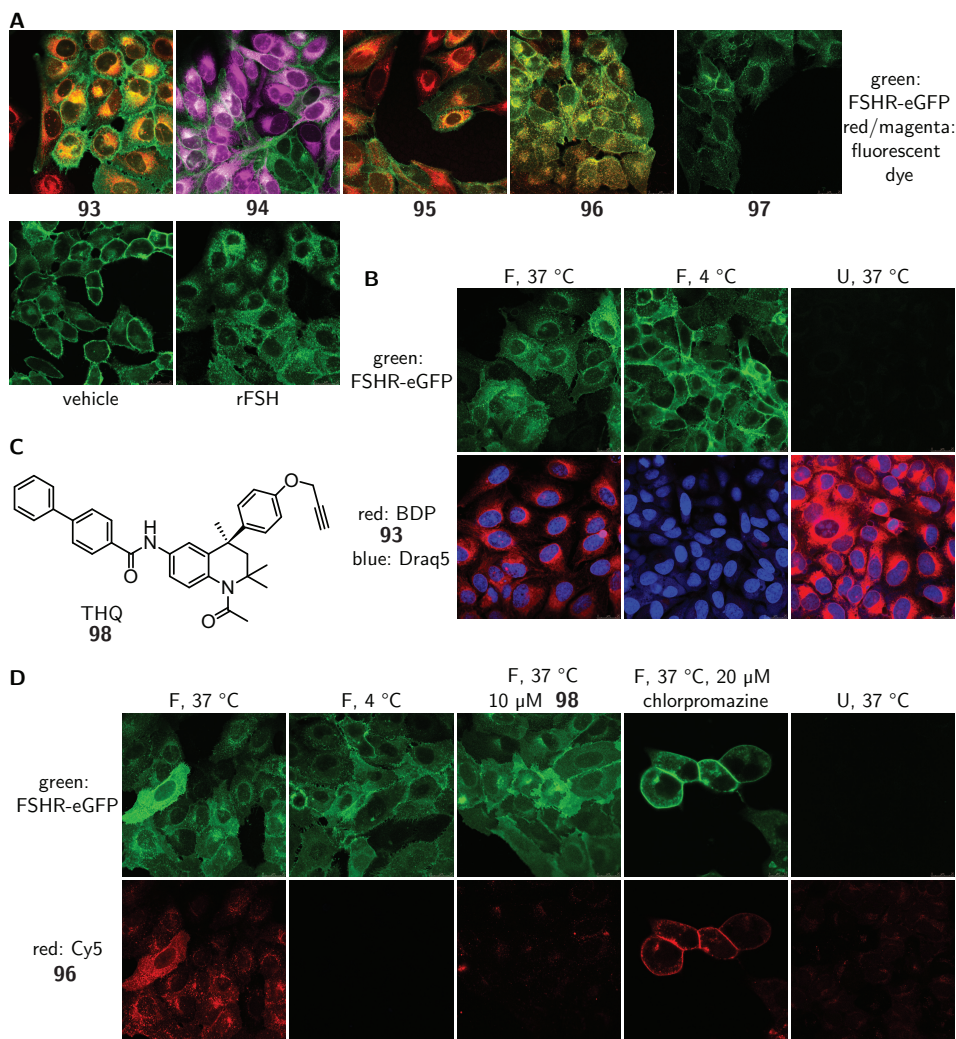


**Figure 7.4: Compound uptake and FSHR internalization analysis by confocal microscopy.** U2OS-FSHR (F) or wild-type U2OS (U) cells were incubated with compounds for 2 h, 37 °C. A) Representative micrographs of U2OS-FSHR cells that were treated with 10 μM of indicated compounds show receptor internalization (green), but high compound background fluorescence in all cells (red/magenta). B) Treatment of U2OS-FSHR cells with DHP-BODIPY **93** (1 μM) at 4 °C, prevented receptor internalization as well as the uptake of the compound. Control U2OS cells at 37 °C became brightly red fluorescent when treated with compound **93**, indicating that the uptake process is temperature-dependent, but not FSHR selective. C) Chemical structure of previously reported small-molecule FSHR antagonist, THQ **98**. D) Only DHP-Cy5 **96** (1 μM) was shown to induce receptor internalization in combination with selective uptake in receptor vs non-receptor cells (left vs right panels). Furthermore, uptake was inhibited at 4 °C (second left panel), by pre-incubation with THQ **98** (10 μM, middle panel) and by inhibition of receptor-internalization by chlorpromazine (CPZ, 20 μM, second right panel).

temperatures as well, this would not explain the complete lack of compound fluorescence at 4 °C. Based on this data, though, it is very unlikely that the internalization is FSHR-mediated. As shown in Figure 7.4A, the intracellular localization of compounds **94** and **95** is very similar to that found for **93**. Since the membranes of ER and Golgi provide a lipophilic environment inside the cell it is perhaps not surprising that the fluorescent ligands incorporating apolar dyes **93** and **95** (calc. log D{7.4}: 5.8 and 4 respectively, Table 7.3) accumulate here.<sup>30</sup> Apparently, the incorporation of the two sulfonic acid groups in BODIPY dye **89** is enough to make ligand **94** soluble in water and much more hydrophilic (logD{7.4} 1.4), but not to prevent it from binding to membrane structures. Most probably, a complex interplay between structural properties such as lipophilicity, charge and polar surface area as well as, potentially, affinity of the BODIPY core for certain membrane substituents or biomolecules forms the basis for the results obtained.

From the FACS analysis it was already apparent that DHP-Cy5 **96** was a better suited candidate for selective uptake by the FSHR than DHP-BDP **93** and its characteristics were further examined by confocal microscopy. At 1 μM concentration and 37 °C, the compound was shown to induce receptor internalization to comparable levels as DHP-BDP and rFSH (Figure 7.4D, Figure 7.5A). Compound fluorescence was also observed in intracellular vesicles, in stark contrast to the fluorescence pattern found for DHP-BDP (Figure 7.4D vs B). Colocalization analysis (Figure 7.5C, Table 7.4) showed strong colocalization between the receptor and the ligand,<sup>32</sup> as well as a higher intensity correlation quotient (ICQ) compared to DHP-BDP (0.2852 vs 0.1994, dependent staining:  $0 \leq x \leq 0.5$ ).<sup>34</sup> Treatment at 4 °C did not lead to receptor internalization, whereas total levels of GFP fluorescence remained constant, showing that this was not due to alterations in expression levels (Figure 7.5A,B). No Cy5 fluorescence was observed under these conditions, which indicates that the compound was taken up in an active manner. It is however, somewhat surprising that there was no or very little membrane fluorescence of compound **96** bound to the receptor detectable at 4 °C. It has been described that binding of FSH to the receptor becomes increasingly reversible at low temperatures. Also, the free energy of binding was calculated to be endothermic at temperatures below 12.5 °C.<sup>35</sup> This, in combination with the washing protocols might result in complete dissociation of possibly low levels of bound ligand to the membrane. Future experiments should therefore include an 'in between' temperature such as 16 °C to study receptor binding while internalization is still slowed down. Control U2OS cells treated with 1 μM of DHP-Cy5 did not show any intracellular Cy5 fluorescence, in accordance with the FACS data. These experiments strongly suggest FSHR-mediated uptake of DHP-Cy5 in the endolysosomal pathway of cells expressing this receptor. Control experiments with the Cy5 dye **91** alone or in combination with rFSH did not result in intracellular Cy5 fluorescence, proving that ligand binding to the receptor is a requirement for its uptake (data not shown). Additional proof was provided with the use of another low molecular weight ligand for the FSHR of the tetrahydroquinoline (THQ) class of receptor antagonists (Figure 7.4C).<sup>36,37</sup>

Pre-incubation of U2OS-FSHR cells with 10 μM THQ **98**<sup>36</sup> for 1 h, 37 °C, followed by in-

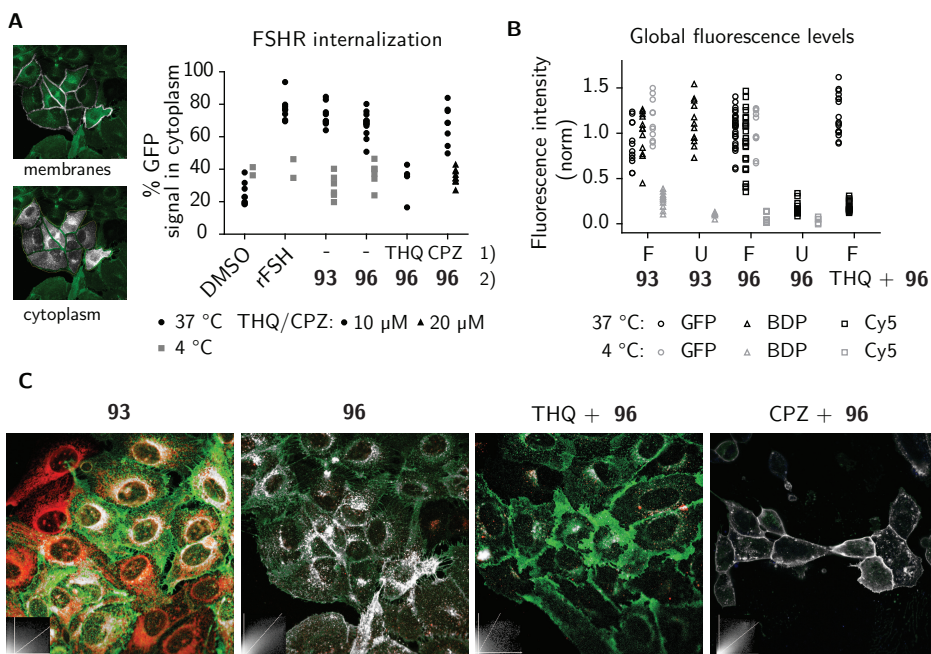


**Figure 7.5: Quantitative analysis of receptor internalization, global fluorescence and colocalization.** Confocal images of U2OS-FSHR (F) or U2OS (U) cells that were treated with 1 μM DHP-BODIPY **93** or DHP-Cy5 **96** were quantified using ImageJ. Each data point represents an analyzed picture from three independent experiments. A) FSHR internalization was determined by the ratio between GFP signal on the membrane and in the cytoplasm. Only at 37 °C FSHR-internalization was observed, and this could be inhibited by pre-treatment of the cells with FSHR-antagonist **98** or chlorpromazine (20 μM). left: Images showing the different ROIs (white) that were set to define membranes or cytoplasm, see the Experimental Section for more details on image analysis. B) Global fluorescence levels were determined to exclude effects of the compounds on total receptor levels (GFP signal) and to quantify the amount of aspecific compound uptake via active (37 °C, U2OS cells) or passive (4 °C) processes. C) Colocalization analysis of FSHR-eGFP with **93** or **96** under various conditions. Overlays showing colocalized pixels in white are shown; insert: fluorescence scatter plot. Values for different colocalization parameters are given in Table 7.4.

cubation with DHP-Cy5 (1 μM, 2 h, 37 °C) strongly blocked receptor internalization and reduced DHP-Cy5 uptake to background levels (Figure 7.4D, middle panel, Figure 7.5). The relatively high dose of THQ **98** (10 μM) compared to DHP-Cy5 (1 μM) was chosen because its antagonistic potency (IC<sub>50</sub>: 39 nM) is lower than the agonistic potency of DHP-Cy5 (EC<sub>50</sub>: 8 nM). Colocalization analysis (Figure 7.5C, Table 7.4) confirmed that the low levels of remaining Cy5 fluorescence were due to aspecific background. THQ is an allosteric antagonist of the FSHR<sup>37</sup> and one explanation would be that the compound competes for the same binding pocket as DHP on the receptor, thereby preventing binding of DHP-Cy5 and subsequent activation and internalization of the receptor. Alternatively, binding of the antagonist might result in a conformational shift of the receptor for which the agonist has reduced affinity. Further research is needed to elucidate the effect of THQ on DHP binding. In a final experiment, receptor internalization was blocked by pre-incubation with



**Table 7.4:** Colocalization analysis of *m*-DHP-BODIPY **93** and *m*-DHP-Cy5 **96** with eGFP-FSHR.

|                       | n (N)  | Rr             | M1             | M2             | ICQ            |
|-----------------------|--------|----------------|----------------|----------------|----------------|
| <b>93</b>             | 12 (3) | 0.4838 ± 0.023 | 0.9072 ± 0.010 | 0.9409 ± 0.009 | 0.1994 ± 0.011 |
| <b>96</b>             | 22 (5) | 0.7271 ± 0.008 | 0.9460 ± 0.005 | 0.9164 ± 0.007 | 0.2852 ± 0.005 |
| 10 μM THQ + <b>96</b> | 6 (2)  | 0.4637 ± 0.029 | 0.9027 ± 0.014 | 0.5942 ± 0.019 | 0.1658 ± 0.004 |
| 10 μM CPZ + <b>96</b> | 10 (2) | 0.7314 ± 0.013 | 0.9476 ± 0.006 | 0.9225 ± 0.008 | 0.2906 ± 0.006 |
| 20 μM CPZ + <b>96</b> | 9 (2)  | 0.7581 ± 0.020 | 0.9437 ± 0.010 | 0.9254 ± 0.007 | 0.3352 ± 0.005 |

n(N): number of pictures n from N independent experiments analyzed. Rr: Pearson's colocalization coefficient. Manders overlap coefficients (M) M1: red; M2: green. ICQ: intensity correlation quotient. Mean +/- SEM is given.

chlorpromazine, a cationic amphiphilic drug that interferes with clathrin-mediated endocytosis.<sup>38</sup> Inhibition is concentration-dependent and also varies with the cell line used.<sup>38-41</sup> Initial experiments were conducted with 10 μM of chlorpromazine, but this did not prevent agonist-induced receptor endocytosis (Figure 7.5A). The concentration was increased to 20 μM, which inhibited receptor internalization, but was clearly also toxic to the cells as seen by profound changes in morphology. Although receptor internalization could be blocked under these conditions, DHP-Cy5 was still able to bind to the FSHR as shown by strong colocalized fluorescence on the membranes of the cells (Figure 7.4D, Figure 7.5C, Table 7.4). Taken together, these results indicate that DHP-Cy5 induced FSHR internalization in a clathrin-mediated fashion. This process could be inhibited by pre-blocking the receptor (signaling) with the antagonist THQ, by disrupting clathrin-coated pit formation, or by lowering the temperature. Furthermore, internalization of the receptor also led to the selective uptake of the bound fluorescent agonist into intracellular vesicles of FSHR-expressing cells.

## 7.3 Conclusion

The follicle-stimulating hormone receptor is very important in human reproduction and has also been implied to play a role in tumor angiogenesis. As such, fluorescent FSHR ligands would be valuable tools for receptor-visualization, to study receptor-mediated processes, and ultimately, to visualize whether targeting of this receptor is a viable method for selective delivery of drugs to FSHR-expressing tumors. The aim of the present study was to synthesize and evaluate low molecular weight fluorescent analogues of the FSHR agonist DHP **55**. Using the information provided by the SAR study in Chapter 6 five fluorescent DHP ligands, incorporating dyes from different classes (BODIPY, rhodamine and cyanine dyes), were synthesized. Evaluation in a luciferase assay showed these ligands to be nanomolar potent agonists for the FSHR. U2OS cells stably expressing a GFP-tagged version of the FSHR were used to address questions regarding ligand-induced receptor internalization and subsequent uptake of the ligand in the endocytic pathway. All fluorescent agonists were able to induce receptor endocytosis as seen by receptor fluorescence, but

only one of the compounds, DHP-Cy5 (**96**) was selectively internalized together with the receptor. This illustrates that even when agonistic potency is unaffected by the physicochemical nature of the dye, other pharmacological parameters can be greatly altered. DHP-Cy5 was not taken up by control U2OS cells without receptor or at low temperature in receptor-expressing cells. Furthermore, internalization of both ligand and receptor could be inhibited by pharmacological intervention with either a LMW FSHR antagonist or with chlorpromazine, an inhibitor of clathrin-mediated endocytosis. This study once more shows that the incorporation of a dye can have a large influence on the properties of a small molecule. By tuning the nature of the dye, a highly nanomolar potent fluorescent agonist for the FSHR was successfully developed which was endocytosed in an FSHR-dependent fashion. This opens up the possibility of selective drug targeting via agonist-induced FSHR internalization, which will be explored in Chapter 8.

## 7.4 Experimental Section

**Cell culture conditions.** All cells were grown in a humidified atmosphere in 5% CO<sub>2</sub> at 37 °C. CHO cells stably expressing the human FSH receptor together with a luciferase reporter gene (CHO-hFSHR\_luc cells) and control cells without receptor but with luciferase gene (CHO\_luc cells) were provided by MSD, Oss, The Netherlands. Cells were cultured in Dulbecco's Modified Eagle's Medium (DMEM) and Ham's F12 medium (1:1) with glutamine, penicillin/streptomycin (0.1 mg/mL) and fetal calf serum (FCS). CHO-hFSHR\_luc cells were maintained under constant selection with Hygromycin B (0.8 mg/mL). Cells were subcultured twice weekly at a ratio of 1:10-1:15. U2OS cells stably expressing the rat FSHR fused to the N-terminus of eGFP (U2OS-FSHR cells) were obtained from MSD, Oss, The Netherlands (FSHR redistribution assay, Biolumage). Cells were grown in DMEM (high glucose (4.5 g/L) and with stable glutamine, Invitrogen), pen/strep (0.1 mg/mL), G418 (0.5 mg/mL) and FCS (10%). Wild-type U2OS cells were grown under the same conditions, without G418. Cells were subcultured twice weekly at a ratio of 1:8-1:10.

**Measurement of CRE-induced luciferase expression.** CHO\_luc or CHO-hFSHR\_luc cells were cultured to ~80% confluency before use in the assay. On the day of the experiment, cells were harvested using enzyme-free dissociation solution (Millipore), counted (Biorad TC10 automated cell counter) and resuspended in assay medium (DMEM-F12 (1:1), without phenol-red, with pen/strep (0.1 mg/mL) supplied with 1 µg/mL bovine insulin (Tebu-Bio) and 5 µg/mL human apo-transferrin (Sigma)) to a concentration of  $7.5 \times 10^5$  cells/mL. Experiments were conducted in 96-wells white Optiplates (Perkin Elmer) and each well contained 30 µL of test compound, recombinant FSH (200 pM final concentration, positive control) or assay medium (negative control), 30 µL of assay medium and 30 µL cell suspension. Final concentration of DMSO was 1% for all compounds, including controls. After 4 h of stimulation, 50 µL Neolite (PerkinElmer) was added to each well and luminescence signal was detected on a Microbeta Trilux 1450 Luminescence Counter (PerkinElmer). To control for non-FSHR mediated effects on intracellular cAMP levels, highest compound concentrations used in the dose-response experiments (typically 1 µM) were tested on CHO\_luc cells. Data was analyzed using GraphPad Prism 5 (GraphPad Software, La Jolla, USA), and values were normalized to the maximal effect obtained for recombinant human FSH (200 pM, rFSH, Org32489, gift from MSD,

Oss, The Netherlands). Each experiment was performed on duplicate plates and mean  $\pm$  SEM values of at least three independent experiments are given.

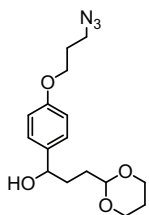
**Fluorescence-activated cell sorting.** U2OS or U2OS-FSHR cells were cultured as described under "Cell culture". Cells were seeded onto 6-well plates (400,000 cells/well) and cultured for 48 h, before start of the experiment. Compounds (as 2x stock solution in culture medium) **93**, **96** or **97** were added to the cells (1  $\mu$ M final concentration) and the cells were incubated for 2 h (37 °C, 5% CO<sub>2</sub>). Cells were washed with ice-cold PBS (2x) and harvested using enzyme-free dissociation solution (Millipore). After centrifugation (5 min, 1200 rpm), the pellet was resuspended in PBS to obtain a single-cell suspension of  $\sim 1 \times 10^6$  cells/mL. Cells were transferred to a 96-wells plate and samples measured using a BD FACSCanto II flow cytometer (BD Biosciences, San Jose, USA). The following laser/filter settings were used: GFP (FSHR):  $\lambda_{\text{ex}}$ : 488 nm,  $\lambda_{\text{em}}$ : 530/30 nm; BODIPY (**93**):  $\lambda_{\text{ex}}$ : 488 nm,  $\lambda_{\text{em}}$ : 585/42 nm; Cy5 (**96**):  $\lambda_{\text{ex}}$ : 633 nm,  $\lambda_{\text{em}}$ : >670 nm; Cy7 (**97**):  $\lambda_{\text{ex}}$ : 633 nm,  $\lambda_{\text{em}}$ : 780/60 nm and values were compensated using the instrumentation software and mono-stained controls. Data was analyzed using FCS Express 4 Flow Research Edition (De Novo Software, LA, USA). All samples were measured twice and values were calculated from three independent experiments with a sample size  $\sim 10000$  cells.

**Uptake and FSHR internalization microscopy experiments.** U2OS-FSHR or U2OS cells were maintained as described under "Cell culture". 48 h before the experiment, cells were harvested (Trypsin-EDTA), counted and seeded onto sterile Labtek II 4- or 8-chamber borosilicate coverglass systems (Fisher Emergo) at a density of 25-50  $\times 10^4$  cells/well. On the day of the experiment, cells were incubated with the indicated concentration of compound (10 or 1  $\mu$ M) or rFSH (12 nM) for 2 h at 37 or 4 °C, before being washed with PBS (2x), fixed (4% formaldehyde in PBS), washed again (PBS) and nuclei stained with Draq5 (Thermo Scientific) (optional, only when the compound fluorescence is detected in the dsRed channel). Cells were imaged on a Leica TCS SPE confocal microscope, using GFP (FSHR), dsRed (BODIPY, rhodamine) or Cy5 (Cy5, water-soluble BODIPY, Draq5) filter settings ( $\lambda_{\text{ex}}$  488, 532 or 635 nm) with optimized detection range to exclude bleed-through of dye signal in different channels. For competition experiments, cells were pre-incubated for 1 h with THQ **98** (10  $\mu$ M) or chlorpromazine (10 or 20  $\mu$ M), before addition of DHP-Cy5 **96** (1  $\mu$ M) to the medium. Images were taken under the same settings (laser power, gain, offset, pinhole) and were analyzed using ImageJ. Global fluorescence was determined either for the whole picture or for a specific region of interest (ROI), which only included regions with cells present, and corrected for the selected area. Intensities were normalized to an average of  $\sim 1$  for untreated or rFSH-treated U2OS-FSHR cells (GFP signal), DHP-BODIPY **93**- treated U2OS-FSHR cells (BODIPY signal), or DHP-Cy5 **96**- treated U2OS-FSHR cells (Cy5 signal), since these can be regarded as positive controls. The percentage of GFP fluorescence signal on the membranes compared to that in the cytoplasm was determined by selection of membranes (typically 5-7 cells/image that were inside the focal plane) with the brush tool (ROI: 'membranes'), followed by the creation of a ROI that included the selected cells (ROI: 'cells'). Two greyscale images were then thresholded according to Yen,<sup>42</sup> followed by selection of the 'membranes' ROI in each picture which was then either cleared (giving 'cytoplasm') or cleared outside (giving 'membranes'). Fluorescence intensities of cells/membranes within the ROI were measured and calculated as a fraction of total GFP signal (membrane+cytoplasm = 100%). For representative images showing the selected ROIs, see Figure 7.5. Colocalization was calculated on background-corrected images using the intensity correlation analysis and colocalization threshold plugins.



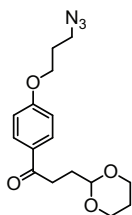
## Synthesis

**General.** All reagents were of commercial grade and used as received unless stated otherwise. Reaction solvents were of analytical grade and when used under anhydrous conditions stored over flame-dried 3 Å molecular sieves. Dichloromethane was distilled over CaH<sub>2</sub> prior to use. Solvents used for column chromatography were of technical grade and distilled before use. All moisture and oxygen sensitive reactions were performed under an argon atmosphere. Flash chromatography was performed on silica gel (Screening Devices BV, 0.04-0.063 mm, 60 Å). Reactions were routinely monitored by TLC analysis on DC-alufolien (Merck, Kieselgel60, F254) with detection by UV-absorption (254/366 nm) where applicable and spraying with a solution of (NH<sub>4</sub>)<sub>6</sub>Mo<sub>7</sub>O<sub>24</sub> · 4 H<sub>2</sub>O (25 g/l) and (NH<sub>4</sub>)<sub>4</sub>Ce(SO<sub>4</sub>)<sub>4</sub> · 2 H<sub>2</sub>O (10 g/l) in 10% sulfuric acid in water followed by charring at ~ 150 °C. 1H and 13C NMR spectra were recorded on a Bruker AV-400 (400 MHz) or Bruker DMX-600 (600 MHz). Chemical shifts are given in ppm ( $\delta$ ) relative to the residual solvent peak or TMS (0 ppm) as internal standard. Coupling constants are given in Hz. Peak assignments are based on 2D <sup>1</sup>H-COSY and <sup>13</sup>C-HSQC NMR experiments. IR measurements (thin film) were conducted on an IRaffinity-1 apparatus and evaluated using IRSolutions software (Shimadzu, Kyoto, Japan). LC-MS measurements were conducted on a Thermo Finnigan LCQ Advantage MAX ion-trap mass spectrometer (ESI<sup>+</sup>) coupled to a Surveyor HPLC system (Thermo Finnigan) equipped with a standard C18 (Gemini, 4.6 mmD × 50 mL, 5  $\mu$  particle size, Phenomenex) analytical column and buffers A: H<sub>2</sub>O, B: ACN, C: 0.1% aq.TFA. High resolution mass spectra were recorded on a LTQ Orbitrap (Thermo Finnigan) mass spectrometer equipped with an electrospray ion source in positive mode (source voltage 3.5 kV, sheath gas flow 10 mL min<sup>-1</sup>, capillary temperature 250 °C) with resolution R=60000 at m/z 400 (mass range m/z=150-2000) and dioctylphthalate (m/z = 391.28428) as a "lock mass". The high resolution mass spectrometer was calibrated prior to measurements with a calibration mixture (Thermo Finnigan). For reversed-phase HPLC purification of the final compounds a Gilson automated HPLC system equipped with a C18 semiprep column (Gemini C18, 250x10 mm, 5  $\mu$  particle size, Phenomenex) was used.

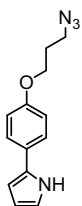


**1-(4-(3-azidopropoxy)phenyl)-3-(1,3-dioxan-2-yl)propan-1-ol (83).** Azidobenzaldehyde **27** (1.54 g, 7.5 mmol) was dissolved in dry THF (30 mL) and cooled to 0 °C in an ice-bath. Grignard reagents (1,3-dioxan-2-ylethyl)-magnesium bromide (0.5 M in THF, 15.5 mL, 7.75 mmol, 1.03 eq) was dropwise added over 1 h. The mixture was stirred for an additional h, while warming up to rt. TLC analysis indicated complete conversion of the reaction, so the reaction was quenched by addition of NH<sub>4</sub>OAc (sat aq, 20 mL), followed by extraction with EtOAc (3 × 50 mL). The combined organic layers were dried over MgSO<sub>4</sub>, filtered and concentrated under reduced pressure. The crude product was purified by silica column chromatography

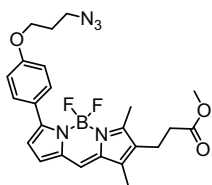
(20% EtOAc in toluene) resulting in compound **83** as a colorless oil in 70% yield (1.68 g, 5.2 mmol).  $R_f$  = 0.3 (2:1 toluene:EtOAc). <sup>1</sup>H NMR (400 MHz, CDCl<sub>3</sub>):  $\delta$  7.28 - 7.21 (m, 2H, 2 × CH<sub>ar</sub>), 6.90 - 6.73 (m, 2H, 2 × CH<sub>ar</sub>), 4.61 (dd,  $J$  = 7.1, 5.8 Hz, 1H, CH), 4.53 (t,  $J$  = 4.8 Hz, 1H, CH), 4.12 - 4.04 (m, 2H, CH<sub>2</sub>), 4.01 (t,  $J$  = 5.9 Hz, 2H, CH<sub>2</sub>), 3.77 - 3.66 (m, 2H, CH<sub>2</sub>), 3.49 (t,  $J$  = 6.7 Hz, 2H, CH<sub>2</sub>), 2.80 (s, 1H, OH), 2.12 - 1.96 (m, 3H, CH<sub>2</sub>, CH<sub>2</sub>-H<sup>a</sup>), 1.91 - 1.78 (m, 2H, CH<sub>2</sub>), 1.78 - 1.55 (m, 2H, CH<sub>2</sub>), 1.35 - 1.25 (m, 1H, CH<sub>2</sub>-H<sup>b</sup>). <sup>13</sup>C NMR (101 MHz, CDCl<sub>3</sub>):  $\delta$  157.96, 137.26, 127.13, 114.35, 102.07, 73.63, 66.93, 64.56, 48.29, 33.40, 31.60, 28.83, 25.72. FT-IR (thin film)  $\nu$  3447, 2960 (N<sub>3</sub>), 2854, 2094, 1611, 1512, 1241, 1136 cm<sup>-1</sup>. LC/MS analysis (linear gradient 10 → 90% ACN)  $t_R$ : 7.46 min, ESI-MS ( $m/z$ ): [M + H]<sup>+</sup>: 321.93. ESI-HRMS ( $m/z$ ): calcd. for [C<sub>16</sub>H<sub>23</sub>N<sub>3</sub>O<sub>4</sub> + H]<sup>+</sup> 322.17163; obsd. 322.17661.



**1-(4-(3-azidopropoxy)phenyl)-3-(1,3-dioxan-2-yl)propan-1-one (84).** Alcohol **83** (1.28 g, 4 mmol) was dissolved in dry DCM (40 mL) and  $\text{MnO}_2$  (3.47 g, 40 mmol, 10 eq) was added. The mixture was stirred for 24 h at room temperature, after which another 10 eq of  $\text{MnO}_2$  were added (3.47 g, 40 mmol) and the reaction continued for 20 h. Upon completion, the mixture was filtered over a plug of celite and concentrated. Purification by silica column chromatography (10  $\rightarrow$  20% EtOAc in PE) resulted in compound **84** as a colorless oil that solidified over time, in 79% yield (1.01 g, 3.16 mmol).  $R_f = 0.5$  (1:1 PE:EtOAc).  $^1\text{H NMR}$  (400 MHz,  $\text{CDCl}_3$ ):  $\delta$  7.96 (d,  $J = 8.8$  Hz, 2H, 2  $\times$   $\text{CH}_{\text{ar}}$ ), 6.92 (d,  $J = 8.8$  Hz, 2H, 2  $\times$   $\text{CH}_{\text{ar}}$ ), 4.66 (t,  $J = 5.0$  Hz, 1H, CH), 4.20 - 4.02 (m, 4H, 2  $\times$   $\text{CH}_2$ ), 3.88 - 3.68 (m, 2H,  $\text{CH}_2$ ), 3.53 (t,  $J = 6.6$  Hz, 2H,  $\text{CH}_2$ ), 3.06 (t,  $J = 7.3$  Hz, 2H,  $\text{CH}_2$ ), 2.14 - 1.96 (m, 5H, 2  $\times$   $\text{CH}_2$ ,  $\text{CH}_2$ -H<sup>a</sup>), 1.44 - 1.17 (m, 1H,  $\text{CH}_2$ -H<sup>b</sup>).  $^{13}\text{C NMR}$  (101 MHz,  $\text{CDCl}_3$ ):  $\delta$  198.25, 162.52, 130.45, 130.36, 114.18, 101.23, 66.98, 64.79, 48.20, 32.37, 29.59, 28.76, 25.90. FT-IR (thin film)  $\nu$  2960 ( $\text{N}_3$ ), 2854, 2360, 2098, 1675, 1600, 1508, 1252, 1134  $\text{cm}^{-1}$ . LC/MS analysis (linear gradient 10  $\rightarrow$  90% ACN)  $t_R$ : 8.51 min, ESI-MS ( $m/z$ ):  $[\text{M} + \text{H}]^+$ : 320.07. ESI-HRMS ( $m/z$ ): calcd. for  $[\text{C}_{16}\text{H}_{21}\text{N}_3\text{O}_4 + \text{H}]^+$  320.16048; obsd. 320.16035.

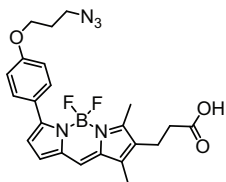


**2-(4-(3-azidopropoxy)phenyl)-1H-pyrrole (85).** Ketone **84** (1.2 g, 3.8 mmol) was dissolved in glacial acetic acid (30 mL) and  $\text{NH}_4\text{OAc}$  (30 g, 380 mmol, 100 eq) was added. The mixture was heated to reflux for 7 h and then allowed to cool to rt, before being poured into ice-water (100 mL). The solution was neutralized with  $\text{Na}_2\text{CO}_3$  and extracted with DCM (3  $\times$  50 mL). The combined organic layers were dried ( $\text{Na}_2\text{SO}_4$ ), filtered and concentrated. The mixture was purified by silica column chromatography (0  $\rightarrow$  10% EtOAc in PE) yielding both pyrrole **85** and acetoxypropane as an impurity. Because of the instable nature of the pyrrole it was used as such, without any further purifications.  $R_f = 0.45$  (4:1 toluene:EtOAc).  $^1\text{H NMR}$  (400 MHz,  $\text{CDCl}_3$ ):  $\delta$  8.77 (s, 1H, NH), 7.38 (d,  $J = 8.7$  Hz, 2H, 2  $\times$   $\text{CH}_{\text{ar}}$ ), 6.86 (d,  $J = 8.7$  Hz, 2H, 2  $\times$   $\text{CH}_{\text{ar}}$ ), 6.76 (d,  $J = 1.2$  Hz, 1H,  $\text{CH}_{\text{ar}}$ ), 6.45 (s, 1H,  $\text{CH}_{\text{ar}}$ ), 6.29 (dd,  $J = 5.5, 2.7$  Hz, 1H,  $\text{CH}_{\text{ar}}$ ), 3.99 (t,  $J = 6.0$  Hz, 2H,  $\text{CH}_2$ ), 3.49 (t,  $J = 6.7$  Hz, 2H,  $\text{CH}_2$ ), 2.04 - 2.00 (m, 2H,  $\text{CH}_2$ ).  $^{13}\text{C NMR}$  (101 MHz,  $\text{CDCl}_3$ ):  $\delta$  156.98, 131.71, 125.97, 124.94, 118.23, 114.70, 109.52, 104.60, 64.43, 48.04, 28.57.

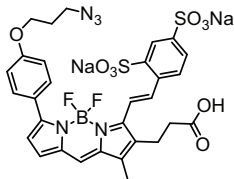


**1,3-dimethyl-2-(2-methoxycarbonylethyl)-5-(4-(3-azido-propoxy)-phenyl)-4,4-difluoro-4-bora-3a,4a-diaza-s-indacene (87).** Azido-pyrrole **130** (crude, 3.8 mmol) was dissolved in MeOH (30 mL) and carboxyaldehyde pyrrole **86**<sup>22</sup> (794 mg, 3.8 mmol, 1 eq) was added. After cooling of the mixture to 0  $^\circ\text{C}$ , HBr (48% in  $\text{H}_2\text{O}$ , 430  $\mu\text{L}$ , 1 eq) was added and the reaction continued for 1.5 h at 0  $^\circ\text{C}$ . The crude purple HBr salt was filtered off, dissolved and co-evaporated with DCE (3  $\times$  50 mL). To a solution of the crude HBr-salt (1.65 g, 3.2 mmol) in DCE (20 mL) were added TEA (1.3 mL, 9.6 mmol, 3 eq) and  $\text{BF}_3\cdot\text{OEt}_2$  (2 mL, 16 mmol, 5 eq) and the mixture was heated to 90  $^\circ\text{C}$  for 15 min, before being concentrated *in vacuo* and purified by silica column chromatography (0  $\rightarrow$  2% EtOAc in toluene, followed by 10% EtOAc in toluene + 1% AcOH). After purification both the title BODIPY-methyl ester **87** (812 mg, 1.69 mmol, 44% over 3 steps) and hydrolyzed azido-BODIPY-acid **88** (185 mg, 0.4 mmol, 10%) were obtained as purple solids.  $R_f = 0.6$  (4:1 toluene:EtOAc).  $^1\text{H NMR}$  (400 MHz,  $\text{CDCl}_3$ ):  $\delta$  7.86 (d,  $J = 8.8$  Hz, 2H, 2  $\times$   $\text{CH}_{\text{ar}}$ ), 7.05 (s, 1H,  $\text{CH}_{\text{ar}}$ ), 6.94 (d,  $J = 8.8$  Hz, 2H, 2  $\times$   $\text{CH}_{\text{ar}}$ ), 6.91 (d,  $J = 4.1$  Hz, 1H,  $\text{CH}_{\text{ar}}$ ), 6.51 (d,  $J = 4.0$  Hz, 1H,  $\text{CH}_{\text{ar}}$ ), 4.06 (t,  $J = 5.9$  Hz, 2H,  $\text{CH}_2$ ), 3.65 (s, 3H,  $\text{CH}_3$ ), 3.49 (t,  $J = 6.7$  Hz, 2H,  $\text{CH}_2$ ), 2.69 (t,  $J = 7.7$  Hz, 2H,  $\text{CH}_2$ ), 2.52 (s, 3H,  $\text{CH}_3$ ), 2.43 (t,  $J = 7.7$  Hz, 2H,  $\text{CH}_2$ ), 2.16 (s, 3H,  $\text{CH}_3$ ), 2.03 (p,  $J = 6.3$  Hz, 2H,  $\text{CH}_2$ ).  $^{13}\text{C NMR}$  (101 MHz,  $\text{CDCl}_3$ ):  $\delta$  172.89, 159.49, 159.13, 155.52, 139.82, 135.05, 134.31, 130.78, 130.74,

130.70, 129.93, 128.03, 125.71, 123.00, 118.30, 114.22, 64.50, 51.75, 48.24, 33.84, 28.76, 19.46, 13.12, 9.54. ESI-HRMS ( $m/z$ ): calcd. for  $[C_{24}H_{26}BF_2N_5O_3 + H]^+$  482.21695; obsd. 482.21711.

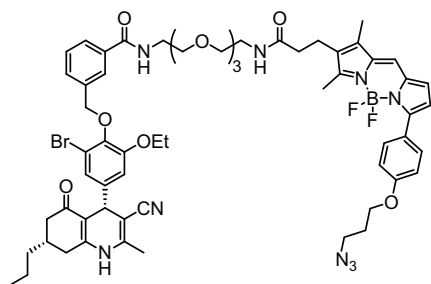


**1,3-dimethyl-2-(2-carboxyethyl)-5-(4-(3-azido-propoxy)-phenyl)-4,4-difluoro-4-bora-3a,4a-diaza-s-indacene (88).** BODIPY **87** (120 mg, 0.25 mmol) was dissolved in toluene (20 mL). After addition of  $Me_3SnOH$  (99 mg, 0.55 mmol, 2.2 eq) the mixture was heated to reflux for 3h and subsequently stirred for 16 h at rt. The organic layer was washed with HCl (aq, 0.1 M, 3 × 30 mL), water (1 × 30 mL), dried ( $MgSO_4$ ), filtered and concentrated under reduced pressure. Silica column chromatography (0 → 0.1% AcOH in 30% EtOAc in toluene) afforded azido-BODIPY-acid (100 mg, 0.21 mmol, 86%) as a purple solid.  $R_f = 0.3$  (4:1 toluene:EtOAc + AcOH).  $^1H$  NMR (400 MHz,  $CDCl_3$ ):  $\delta$  7.87 (d,  $J = 8.9$  Hz, 2H, 2 ×  $CH_{ar}$ ), 7.08 (s, 1H,  $CH_{ar}$ ), 6.99 - 6.91 (m, 3H, 3 ×  $CH_{ar}$ ), 6.53 (d,  $J = 4.1$  Hz, 1H,  $CH_{ar}$ ), 4.09 (t,  $J = 5.9$  Hz, 2H,  $CH_2$ ), 3.52 (t,  $J = 6.7$  Hz, 2H,  $CH_2$ ), 2.71 (t,  $J = 7.6$  Hz, 2H,  $CH_2$ ), 2.54 - 2.46 (m, 5H,  $CH_3$ ,  $CH_2$ ), 2.19 (s, 3H,  $CH_3$ ), 2.06 (p,  $J = 6.3$  Hz, 2H,  $CH_2$ ).  $^{13}C$  NMR (101 MHz,  $CDCl_3$ ):  $\delta$  178.49, 159.59, 159.07, 155.85, 139.86, 135.17, 134.34, 130.85, 129.60, 128.24, 125.78, 123.14, 118.53, 114.31, 64.57, 48.34, 33.90, 28.86, 19.30, 13.22, 9.71. ESI-HRMS ( $m/z$ ): calcd. for  $[C_{23}H_{24}BF_2N_5O_3 + H]^+$  468.20130; obsd. 468.20170.

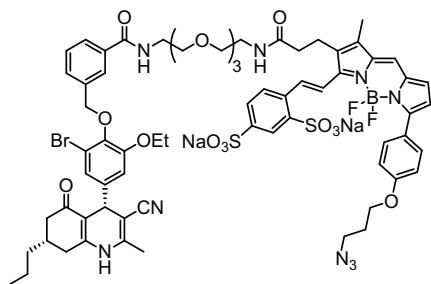


**1-methyl-2-(2-carboxyethyl)-3-[sodium styryl-2,4-disulfonate]-5-(4-(3-azido-propoxy)-phenyl)-4,4-difluoro-4-bora-3a,4a-diaza-s-indacene (89).** BODIPY **88** (51 mg, 0.11 mmol) was dissolved in MeOH (5 mL) and 4-formyl-1,3-benzenedisulfonic acid, disodium salt hydrate (34 mg, 0.11 mmol, 1 eq) was added followed by acetic acid (63  $\mu$ L, 1.1 mmol, 10 eq) and pyrrolidine (92  $\mu$ L, 1.1 mmol, 10 eq). After heating at 72 °C for 2 h, an additional 0.5 eq of benzaldehyde (16 mg, 0.05 mmol) was added. All starting BODIPY was consumed after 5 h, so the mixture was concentrated

and co-evaporated with toluene under reduced pressure. Repeated silica column chromatography (10 → 30% MeOH in DCM) followed by cation exchange over Dowex- $Na^+$  with water as the eluents yielded the sodium salt of sulfonated-BODIPY **89** in 62% yield (53 mg, 0.068 mmol) as a dark blue powder.  $R_f = 0.2$  (3:1 DCM:MeOH + AcOH).  $\lambda_{abs}$ (10  $\mu$ M in MeOH): 609 nm; (10  $\mu$ M in  $H_2O$ ): 601 nm.  $\lambda_{em}$ (100 nM in MeOH/ $H_2O$ ): 637 nm.  $^1H$  NMR (400 MHz, MeOD):  $\delta$  8.55 (d,  $J = 16.9$  Hz, 1H,  $CH=$ ), 8.50 (d,  $J = 1.4$  Hz, 1H,  $CH_{ar}$ ), 7.95 (d,  $J = 8.9$  Hz, 2H, 2 ×  $CH_{ar}$ ), 7.92 - 7.85 (m, 2H, 2 ×  $CH_{ar}$ ), 7.72 (d,  $J = 16.8$  Hz, 1H,  $CH=$ ), 7.42 (s, 1H,  $CH_{ar}$ ), 7.12 (d,  $J = 4.2$  Hz, 1H,  $CH_{ar}$ ), 7.02 (d,  $J = 8.9$  Hz, 2H, 2 ×  $CH_{ar}$ ), 6.68 (d,  $J = 4.2$  Hz, 1H,  $CH_{ar}$ ), 4.13 (t,  $J = 6.0$  Hz, 2H,  $CH_2$ ), 3.53 (t,  $J = 6.7$  Hz, 2H,  $CH_2$ ), 3.18 - 3.12 (m, 2H,  $CH_2$ ), 2.57 (t,  $J = 7.3$  Hz, 2H,  $CH_2$ ), 2.30 (s, 3H,  $CH_3$ ), 2.06 (p,  $J = 6.4$  Hz, 2H,  $CH_2$ ).  $^{13}C$  NMR (101 MHz, MeOD):  $\delta$  181.86, 161.22, 157.74, 154.19, 145.62, 144.65, 141.78, 138.06, 137.93, 136.73, 135.60, 133.98, 132.04, 130.02, 128.78, 127.22, 126.81, 126.51, 123.93, 123.42, 120.16, 115.30, 65.96, 49.34, 38.10, 29.80, 23.27, 9.57. ESI-HRMS ( $m/z$ ): calcd. for  $[C_{30}H_{28}BF_2N_5O_9S_2 + Na]^+$  738.12818; obsd. 738.12853.



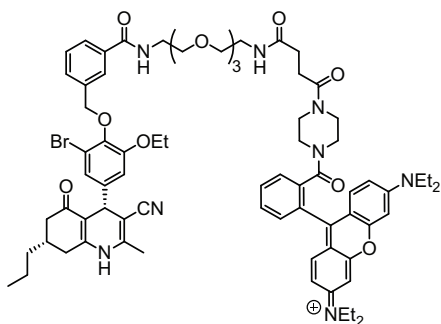
***m*-DHP-BODIPY-N3 (93).** To a solution of amino-DHP *m*-76a (8 mg, 10.6  $\mu$ mol) and azido-BODIPY-acid **88** (6 mg, 10.6  $\mu$ mol) in DCM (1 mL) were added EDC (4 mg, 21  $\mu$ mol, 2 eq), HOBt (2.8 mg, 21  $\mu$ mol, 2 eq) and TEA (3  $\mu$ L, 21  $\mu$ mol, 2 eq). The mixture was stirred for 3 h at room temperature, and subsequently washed with HCl (aq, 1 M, 2  $\times$  5 mL), water (1  $\times$  5 mL), dried (MgSO<sub>4</sub>), filtered and concentrated *in vacuo*. Purification by silica column chromatography (0  $\rightarrow$  5% MeOH in DCM), gave the product as a purple solid (6.2 mg, 5.1  $\mu$ mol, 48%).  $R_f$  = 0.3 (20:1 DCM:MeOH). <sup>1</sup>H NMR (600 MHz, CDCl<sub>3</sub>):  $\delta$  7.98 (d,  $J$  = 1.8 Hz, 1H, CH<sub>ar</sub>), 7.88 - 7.84 (m, 2H, 2  $\times$  CH<sub>ar</sub>), 7.76 (dt,  $J$  = 7.8, 1.4 Hz, 1H, CH<sub>ar</sub>), 7.62 (dt,  $J$  = 7.8, 1.3 Hz, 1H, CH<sub>ar</sub>), 7.41 (t,  $J$  = 7.7 Hz, 1H, CH<sub>ar</sub>), 7.09 (s, 1H, CH<sub>ar</sub>), 6.98 - 6.94 (m, 3H, 3  $\times$  CH<sub>ar</sub>), 6.91 (d,  $J$  = 2.0 Hz, 1H, NH), 6.87 (d,  $J$  = 5.6 Hz, 1H, CH<sub>ar</sub>), 6.80 (d,  $J$  = 2.0 Hz, 1H, CH<sub>ar</sub>), 6.53 (d,  $J$  = 4.1 Hz, 1H, CH<sub>ar</sub>), 6.45 (s, 1H, CH<sub>ar</sub>), 6.15 (t,  $J$  = 5.6 Hz, 1H, NH), 5.02 (d,  $J$  = 2.0 Hz, 2H, CH<sub>2</sub>), 4.55 (s, 1H, CH), 4.13 - 4.07 (m, 4H, 2  $\times$  CH<sub>2</sub>), 3.67 - 3.62 (m, 6H, 3  $\times$  CH<sub>2</sub>), 3.61 - 3.59 (m, 2H, CH<sub>2</sub>), 3.56 - 3.52 (m, 4H, 2  $\times$  CH<sub>2</sub>), 3.50 - 3.47 (m, 2H, CH<sub>2</sub>), 3.41 (t,  $J$  = 5.1 Hz, 2H, CH<sub>2</sub>), 3.34 - 3.29 (m, 2H, CH<sub>2</sub>), 2.72 (t,  $J$  = 7.2 Hz, 2H, CH<sub>2</sub>), 2.50 (s, 3H, CH<sub>3</sub>), 2.45 (dd,  $J$  = 16.1, 4.0 Hz, 1H, CH<sub>2</sub>-H<sup>a</sup>), 2.32 - 2.24 (m, 4H, 2  $\times$  CH<sub>2</sub>), 2.18 (d,  $J$  = 7.2 Hz, 4H, CH<sub>3</sub>, CH), 2.10 - 2.05 (m, 6H, CH<sub>3</sub>, CH<sub>2</sub>-H<sup>b</sup>, CH<sub>2</sub>), 1.42 (t,  $J$  = 7.0 Hz, 3H, CH<sub>3</sub>), 1.35 - 1.28 (m, 4H, 2  $\times$  CH<sub>2</sub>), 0.91 - 0.87 (m, 3H, CH<sub>3</sub>). <sup>13</sup>C NMR (151 MHz, CDCl<sub>3</sub>):  $\delta$  195.63, 171.89, 167.72, 159.80, 159.62, 155.46, 152.79, 149.35, 144.73, 144.14, 142.28, 140.15, 138.10, 135.05, 134.78, 134.58, 131.31, 130.87, 128.71, 128.01, 127.07, 126.71, 125.91, 123.01, 122.96, 119.27, 118.43, 118.07, 114.35, 113.03, 110.15, 88.41, 74.19, 70.56, 70.36, 70.29, 69.96, 69.83, 64.71, 64.65, 48.38, 43.48, 39.92, 39.45, 38.28, 37.54, 36.27, 33.93, 33.76, 28.92, 20.09, 19.93, 18.65, 14.96, 14.19, 13.34, 9.77. ESI-HRMS ( $m/z$ ): calcd. for [C<sub>61</sub>H<sub>71</sub>BBF<sub>2</sub>N<sub>9</sub>O<sub>9</sub> + H]<sup>+</sup> 1202.46920; obsd. 1202.47131.



***m*-DHP-water-soluble BODIPY (94).** To a solution of amino-DHP *m*-76a (8 mg, 10  $\mu$ mol) and water-soluble BODIPY-acid **89** (7.8 mg, 10  $\mu$ mol) in DMF (1 mL) were added EDC (4 mg, 20  $\mu$ mol, 2 eq), HOBt (2.8 mg, 20  $\mu$ mol, 2 eq) and TEA (7.5  $\mu$ L, 75  $\mu$ mol, 5 eq). The mixture was stirred for 4 h at room temperature, before the same amounts of EDC, HOBt and TEA were added again. After 48 h the reaction was finished, the solvent removed *in vacuo* and the residue purified by silica column chromatography (5  $\rightarrow$  25% MeOH in DCM). Crystallization

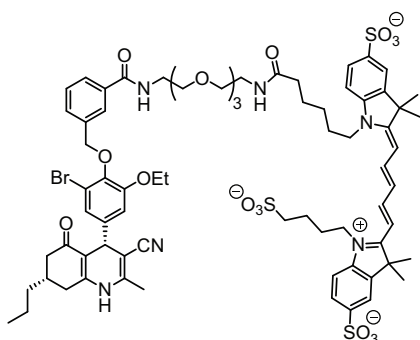
from DCM/MeOH/Et<sub>2</sub>O, followed by lyophilization from water gave the product as a dark blue solid (13.4 mg, 9.2  $\mu$ mol, 92%).  $R_f$  = 0.5 (5:1 DCM:MeOH). <sup>1</sup>H NMR (600 MHz, MeOD):  $\delta$  8.52 (d,  $J$  = 1.7 Hz, 1H, CH<sub>ar</sub>), 8.43 (d,  $J$  = 16.9 Hz, 1H, =CH), 8.39 (s, 1H, NH), 8.31 (t,  $J$  = 5.4 Hz, 1H, NH), 7.95 - 7.88 (m, 4H, 4  $\times$  CH<sub>ar</sub>), 7.84 (d,  $J$  = 8.2 Hz, 1H, CH<sub>ar</sub>), 7.72 (s, 1H, CH<sub>ar</sub>), 7.70 (d,  $J$  = 10.8 Hz, 1H, =CH), 7.63 (d,  $J$  = 7.6 Hz, 1H, CH<sub>ar</sub>), 7.42 (s, 1H, CH<sub>ar</sub>), 7.39 (t,  $J$  = 7.7 Hz, 1H, CH<sub>ar</sub>), 7.14 (d,  $J$  = 4.2 Hz, 1H, CH<sub>ar</sub>), 7.02 (d,  $J$  = 8.9 Hz, 2H, 2  $\times$  CH<sub>ar</sub>), 6.90 (d,  $J$  = 1.8 Hz, 1H, CH<sub>ar</sub>), 6.86 (d,  $J$  = 1.7 Hz, 1H, CH<sub>ar</sub>), 6.69 (d,  $J$  = 4.2 Hz, 1H, CH<sub>ar</sub>), 4.85 (s, 2H, CH<sub>2</sub>), 4.47 (s, 1H, CH), 4.14 (t,  $J$  = 6.0 Hz, 2H, CH<sub>2</sub>), 4.06 - 3.99 (m, 2H, CH<sub>2</sub>), 3.59 - 3.50 (m, 14H, 7  $\times$  CH<sub>2</sub>), 3.45 (q,  $J$  = 5.5 Hz, 2H, CH<sub>2</sub>), 3.40 - 3.36 (m, 2H, CH<sub>2</sub>), 3.12 - 3.04 (m, 2H, CH<sub>2</sub>),

2.61 - 2.53 (m, 3H, CH<sub>2</sub>, CH<sub>2</sub>-H<sup>a</sup>), 2.46 - 2.38 (m, 2H, CH<sub>2</sub>-H<sup>a</sup>, CH<sub>2</sub>-H<sup>b</sup>), 2.26 (s, 3H, CH<sub>3</sub>), 2.19 - 2.13 (m, 1H, CH), 2.11 (s, 3H, CH<sub>3</sub>), 2.10 - 2.03 (m, 3H, CH<sub>2</sub>, CH<sub>2</sub>-H<sup>b</sup>), 1.40 - 1.33 (m, 7H, CH<sub>3</sub>, 2 × CH<sub>2</sub>), 0.90 (t, *J* = 6.9 Hz, 3H, CH<sub>3</sub>). <sup>13</sup>C NMR (151 MHz, MeOD): δ 198.30, 175.53, 170.12, 161.34, 158.56, 154.04, 153.69, 153.22, 147.55, 145.82, 145.16, 144.43, 144.25, 141.54, 139.14, 138.14, 137.64, 136.19, 135.54, 134.63, 132.53, 132.05, 131.72, 130.65, 129.32, 128.85, 128.29, 127.79, 127.08, 126.54, 126.48, 124.18, 124.12, 123.18, 120.61, 120.38, 118.65, 115.28, 113.61, 109.90, 88.23, 75.13, 71.12, 71.08, 71.05, 71.01, 70.94, 70.62, 65.94, 65.58, 49.28, 43.99, 40.84, 40.46, 39.61, 38.07, 37.45, 34.74, 33.51, 29.72, 23.63, 20.84, 18.00, 15.08, 14.36, 9.28. ESI-HRMS (*m/z*): calcd. for [C<sub>68</sub>H<sub>75</sub>BBBrF<sub>2</sub>N<sub>9</sub>O<sub>15</sub>S<sub>2</sub> + H]<sup>+</sup> 1451.41413; obsd. 1451.41666.



***m*-DHP-Rhodamine B (95).** Amino-DHP *m*-76a (8 mg, 10 μmol) was added to a pre-activated solution of Rhodamine B-acid<sup>23</sup> **90** (6.1 mg, 10 μmol), EDC (3.8 mg, 20 μmol, 2 eq), HOBt (2.7 mg, 20 μmol, 2 eq) and DiPEA (3.3 μL, 20 μmol, 2 eq) in DMF (1 mL). The mixture was stirred for 16 h at room temperature, before addition of another equivalent of EDC (2 mg, 10 μmol) and DiPEA (1.5 μL, 10 μmol). After an additional 6 h, the solvent was removed *in vacuo* and the residue purified by silica column chromatography (0 → 7% MeOH in DCM).

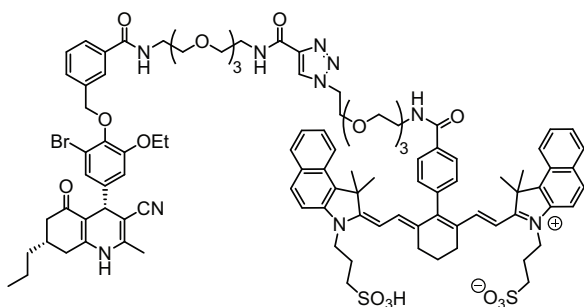
The product was obtained as a bright pink solid (11 mg, 8.2 μmol, 82%). *R<sub>f</sub>* = 0.9 (5:1 DCM:MeOH). <sup>1</sup>H NMR (600 MHz, CDCl<sub>3</sub>): δ 7.98 (s, 1H, CH<sub>ar</sub>), 7.81 (s, 1H, CH<sub>ar</sub>), 7.69 - 7.58 (m, 3H, 3 × CH<sub>ar</sub>), 7.50 (s, 1H, CH<sub>ar</sub>), 7.39 (t, *J* = 7.7 Hz, 1H, CH<sub>ar</sub>), 7.35 - 7.28 (m, 1H, CH<sub>ar</sub>), 7.18 (s, 2H, 2 × CH<sub>ar</sub>), 6.95 - 6.78 (m, 4H, 4 × CH<sub>ar</sub>), 6.72 (d, *J* = 7.3 Hz, 2H, 2 × CH<sub>ar</sub>), 5.01 - 4.86 (m, 2H, CH<sub>2</sub>), 4.53 (s, 1H, CH), 4.10 - 4.00 (m, 2H, CH<sub>2</sub>), 3.72 - 3.15 (m, 32H, 16 × CH<sub>2</sub>), 2.97 - 2.84 (m, 1H, CH<sub>2</sub>-H<sup>a</sup>), 2.57 - 2.33 (m, 6H, 2 × CH<sub>2</sub>, CH<sub>2</sub>-H<sup>superb</sup>, CH<sub>2</sub>-H<sup>a</sup>), 2.24 (s, 3H, CH<sub>3</sub>), 2.13 (s, 1H, CH), 2.07 - 1.96 (m, 1H, CH<sub>2</sub>-H<sup>(b)</sup>), 1.44 - 1.22 (m, 19H, 5 × CH<sub>3</sub>, 2 × CH<sub>2</sub>), 0.85 (t, *J* = 6.8 Hz, 3H, CH<sub>3</sub>). <sup>13</sup>C NMR (151 MHz, CDCl<sub>3</sub>): δ 196.30, 167.72, 167.63, 157.85, 155.74, 152.94, 152.76, 147.72, 143.81, 143.67, 138.14, 135.04, 134.87, 132.21, 131.30, 130.41, 130.27, 128.74, 128.54, 127.82, 127.26, 126.84, 123.32, 120.62, 117.73, 114.29, 114.11, 113.88, 112.58, 108.57, 96.45, 86.10, 74.21, 70.64, 70.55, 70.39, 70.21, 69.78, 64.59, 46.27, 44.84, 43.68, 42.07, 41.80, 39.97, 39.37, 38.46, 37.63, 34.00, 33.15, 30.77, 28.50, 19.93, 18.31, 14.97, 14.27, 12.74. ESI-HRMS (*m/z*): calcd. for [C<sub>74</sub>H<sub>90</sub>BrN<sub>8</sub>O<sub>11</sub>]<sup>+</sup> 1347.58865; obsd. 1347.59066.



***m*-DHP-Cy5 (96).** Amino-DHP *m*-76a (5 mg, 6.6  $\mu$ mol, 1.1 eq) was added to a pre-activated solution of Cy5-acid<sup>24</sup> **91** (5 mg, 6  $\mu$ mol), PyBOP (3.4 mg, 6.6  $\mu$ mol, 1.1 eq) and DiPEA (3  $\mu$ L, 18  $\mu$ mol, 3 eq) in DMF (1 mL). The mixture was stirred for 3 h at room temperature, before the solvent was removed *in vacuo* and the residue purified by RP-HPLC (25  $\rightarrow$  45% ACN in 12', buffer A: 10 mM NH<sub>4</sub>OAc) or silica column chromatography (0  $\rightarrow$  2% H<sub>2</sub>O in 40% MeOH in CHCl<sub>3</sub>). Crystallization from DCM/MeOH/hexanes and lyophilization from H<sub>2</sub>O yielded the product as a bright blue solid (5 mg, 3.3  $\mu$ mol, 55%).

$R_f = 0.7$  (1:1:1 EtOAc:n-BuOH:AcOH:H<sub>2</sub>O). <sup>1</sup>H

NMR (600 MHz, MeOD):  $\delta$  8.27 (td,  $J = 13.0, 8.1$  Hz, 2H, 2  $\times$  =CH), 8.03 (s, 1H, CH<sub>ar</sub>), 7.92 - 7.85 (m, 4H, 4  $\times$  CH<sub>ar</sub>), 7.79 (d,  $J = 7.8$  Hz, 1H, CH<sub>ar</sub>), 7.68 (d,  $J = 7.6$  Hz, 1H, CH<sub>ar</sub>), 7.46 (t,  $J = 7.7$  Hz, 1H, CH<sub>ar</sub>), 7.37 (d,  $J = 8.8$  Hz, 1H, CH<sub>ar</sub>), 7.28 (d,  $J = 8.2$  Hz, 1H, CH<sub>ar</sub>), 6.89 (dd,  $J = 15.7, 1.8$  Hz, 2H, 2  $\times$  CH<sub>ar</sub>), 6.68 (t,  $J = 12.4$  Hz, 1H, =CH), 6.39 (d,  $J = 13.7$  Hz, 1H, =CH), 6.31 (d,  $J = 13.7$  Hz, 1H, =CH), 5.00 (s, 2H, CH<sub>2</sub>), 4.58 (s, 1H, SO<sub>3</sub>H), 4.47 (s, 1H, CH), 4.17 - 4.10 (m, 2H, CH<sub>2</sub>), 4.10 - 4.04 (m, 4H, 2  $\times$  CH<sub>2</sub>), 3.69 - 3.56 (m, 10H, 5  $\times$  CH<sub>2</sub>), 3.56 - 3.51 (m, 2H, CH<sub>2</sub>), 3.45 (t,  $J = 5.4$  Hz, 2H, CH<sub>2</sub>), 3.29 - 3.26 (m, 2H, CH<sub>2</sub>), 2.90 (t,  $J = 6.8$  Hz, 2H, CH<sub>2</sub>), 2.60 (dd,  $J = 16.8, 4.5$  Hz, 1H, CH<sub>2</sub>-H<sup>a</sup>), 2.47 - 2.40 (m, 2H, CH<sub>2</sub>-H<sup>b</sup>, CH<sub>2</sub>-H<sup>a</sup>), 2.17 (t,  $J = 7.3$  Hz, 3H, CH<sub>2</sub>, CH), 2.15 - 2.09 (m, 4H, CH<sub>3</sub>, CH<sub>2</sub>-H<sup>b</sup>), 1.99 - 1.93 (m, 4H, 2  $\times$  CH<sub>2</sub>), 1.80 - 1.70 (m, 14H, 4  $\times$  CH<sub>3</sub>, CH<sub>2</sub>), 1.67 - 1.62 (m, 2H, CH<sub>2</sub>), 1.41 (t,  $J = 7.0$  Hz, 3H, CH<sub>3</sub>), 1.39 - 1.34 (m, 4H, 2  $\times$  CH<sub>2</sub>), 0.95 - 0.88 (m, 3H, CH<sub>3</sub>). <sup>13</sup>C NMR (151 MHz, MeOD):  $\delta$  198.37, 175.80, 175.35, 175.15, 170.07, 156.31, 156.10, 154.16, 153.67, 147.56, 145.27, 144.93, 144.81, 144.49, 143.41, 143.34, 142.64, 142.60, 139.34, 135.82, 132.62, 129.58, 128.45, 128.09, 128.04, 128.01, 124.31, 121.33, 120.47, 118.74, 113.78, 111.72, 111.62, 109.98, 105.52, 105.33, 88.30, 75.27, 71.59, 71.57, 71.28, 71.19, 70.57, 70.53, 65.75, 50.59, 50.53, 45.07, 43.80, 40.97, 40.30, 39.79, 38.19, 36.63, 34.88, 33.57, 28.15, 27.89, 27.34, 27.13, 26.50, 23.53, 20.97, 18.06, 15.23, 14.47. LC/MS analysis (linear gradient 10  $\rightarrow$  90% ACN)  $t_R$ : 6.67 min, ESI-MS ( $m/z$ ): [M + H]<sup>+</sup>: 1501.27. ESI-HRMS ( $m/z$ ): calcd. for [C<sub>73</sub>H<sub>91</sub>BrN<sub>6</sub>O<sub>17</sub>S<sub>3</sub> + H]<sup>+</sup> 1501.48385; obsd. 1501.48711.



***m*-DHP-Cy7 (97).** Alkyne-DHP *m*-78a (5.3 mg, 6.6  $\mu$ mol) in dioxane (0.5 mL) was added to a solution of azido-Cy7 **92** (7.22 mg, 6.7  $\mu$ mol) in dioxane/H<sub>2</sub>O (1 mL, 1:1, v/v). After addition of aqueous solutions of sodium ascorbate (130  $\mu$ L 100 mM, 13  $\mu$ mol, 2 eq) and CuSO<sub>4</sub> (13  $\mu$ L 100 mM, 1.3  $\mu$ mol, 20 mol%) the mixture was stirred for 16 h under an argon atmosphere. Upon completion, the solvent was removed under

reduced pressure and the residue purified by silica column chromatography (4  $\rightarrow$  20% MeOH in CHCl<sub>3</sub> + 0.5% H<sub>2</sub>O). Crystallization from DCM/MeOH/hexanes and lyophilization from H<sub>2</sub>O/dioxane yielded the product as a green solid (4.9 mg, 2.6  $\mu$ mol, 40%).  $R_f = 0.4$  (22:8:0.5 CHCl<sub>3</sub>:MeOH:H<sub>2</sub>O). <sup>1</sup>H NMR (600 MHz, MeOD):  $\delta$  8.33 (s, 1H, CH<sub>trz</sub>), 8.19 - 8.13 (m, 2H, CH<sub>ar</sub>), 8.01 (d,  $J = 8.6$

Hz, 2H, CH<sub>ar</sub>), 7.96 - 7.90 (m, 5H, 5 × CH<sub>ar</sub>), 7.75 (d, *J* = 7.7 Hz, 1H, CH<sub>ar</sub>), 7.61 (d, *J* = 8.8 Hz, 3H, 3 × CH<sub>ar</sub>), 7.51 (t, *J* = 7.6 Hz, 2H, 2 × CH<sub>ar</sub>), 7.45 - 7.37 (m, 5H, 5 × CH<sub>ar</sub>), 7.28 (d, *J* = 14.0 Hz, 2H, 2 × =CH), 6.89 (dd, *J* = 19.3, 1.8 Hz, 2H, 2 × CH<sub>ar</sub>), 6.38 (d, *J* = 14.0 Hz, 2H, 2 × =CH), 4.93 (s, 2H, CH<sub>2</sub>), 4.52 - 4.48 (m, 2H, CH<sub>2</sub>), 4.46 (s, 1H, CH), 4.43 - 4.36 (m, 4H, 2 × CH<sub>2</sub>), 4.10 - 4.00 (m, 2H, CH<sub>2</sub>), 3.84 - 3.66 (m, 8H, 4 × CH<sub>2</sub>), 3.64 - 3.44 (m, 22H, 11 × CH<sub>2</sub>), 2.97 (t, *J* = 6.8 Hz, 4H, 2 × CH<sub>2</sub>), 2.78 (d, *J* = 5.6 Hz, 4H, 2 × CH<sub>2</sub>), 2.58 (dd, *J* = 16.7, 4.4 Hz, 1H, CH<sub>2</sub>-H<sup>a</sup>), 2.47 - 2.36 (m, 2H, CH<sub>2</sub>-H<sup>b</sup>, CH<sub>2</sub>-H<sup>a</sup>), 2.25 (p, *J* = 6.8 Hz, 4H, 2 × CH<sub>2</sub>), 2.20 - 2.03 (m, 7H, CH<sub>3</sub>, CH<sub>2</sub>, CH<sub>2</sub>-H<sup>b</sup>, CH), 1.49 (d, *J* = 7.4 Hz, 12H, 4 × CH<sub>3</sub>), 1.39 - 1.32 (m, 7H, CH<sub>3</sub>, 2 × CH<sub>2</sub>), 0.90 (t, *J* = 6.8 Hz, 3H, CH<sub>3</sub>). <sup>13</sup>C NMR (151 MHz, MeOD): δ 198.29, 174.57, 170.01, 169.53, 162.51, 161.94, 154.14, 153.60, 148.38, 147.49, 145.28, 144.47, 144.41, 143.78, 141.03, 139.29, 135.79, 135.52, 134.48, 133.30, 133.20, 132.57, 131.77, 131.23, 131.08, 129.52, 129.32, 128.89, 128.62, 128.35, 127.96, 127.93, 125.86, 124.30, 123.32, 120.47, 118.76, 113.78, 112.07, 109.99, 101.12, 88.34, 75.22, 71.64, 71.57, 71.52, 71.41, 71.38, 71.28, 70.65, 70.56, 70.48, 70.07, 65.72, 51.74, 51.47, 44.14, 43.90, 41.29, 40.98, 40.04, 39.80, 38.20, 34.87, 33.56, 27.69, 25.87, 24.33, 22.61, 20.96, 18.07, 15.21, 14.48. LC/MS analysis (linear gradient 10 → 90% ACN) t<sub>R</sub>: 8.90 min, ESI-MS (*m/z*): [M + H]<sup>+</sup>: 1891.53. ESI-HRMS (*m/z*): calcd. for [C<sub>100</sub>H<sub>117</sub>BrN<sub>10</sub>O<sub>18</sub>S<sub>2</sub> + H]<sup>+</sup> 1890.72784; obsd. 1890.72949.

## References

- [1] Hoogendoorn, S.; Gold, H. K.; Rood, M. T. M.; van Puijvelde, G. H. M.; van der Marel, G. A.; van Koppen, C.; Timmers, C. M.; Overkleeft, H. S. contributed to the work described in this chapter.
- [2] Mackenzie, J. F.; Daly, C. J.; Pediani, J. D.; McGrath, J. C. *J. Pharmacol. Exp. Ther.* **2000**, *294*, 434–443.
- [3] Hausteiner, E.; Schwille, P. *Annu. Rev. Biophys. Biomol. Struct.* **2007**, *36*, 151–169.
- [4] Leopoldo, M.; Lacivita, E.; Berardi, F.; Perrone, R. *Drug Discov. Today* **2009**, *14*, 706–712.
- [5] Middleton, R. J.; Kellam, B. *Curr. Opin. Chem. Biol.* **2005**, *9*, 517–525.
- [6] Daly, C. J.; McGrath, J. C. *Pharmacol. Ther.* **2003**, *100*, 101–118.
- [7] Baker, J. G.; Middleton, R.; Adams, L.; May, L. T.; Briddon, S. J.; Kellam, B.; Hill, S. J. *Br. J. Pharmacol.* **2010**, *159*, 772–786.
- [8] Kozma, E.; Gizewski, E. T.; Tosh, D. K.; Squarzialupi, L.; Auchampach, J. A.; Jacobson, K. A. *Biochem. Pharmacol.* **2013**.
- [9] Dierich, A.; Sairam, M. R.; Monaco, L.; Fimia, G. M.; Gansmuller, A.; LeMeur, M.; Sassone-Corsi, P. *Proc. Natl. Acad. Sci. U. S. A.* **1998**, *95*, 13612–13617.
- [10] Maria de Fatima, M. L.; Liu, X.; Nakamura, K.; Benovic, J. L.; Ascoli, M. *Mol. Endocrinol.* **1999**, *13*, 866–878.
- [11] Ferguson, S. S. *Pharmacol. Rev.* **2001**, *53*, 1–24.
- [12] Marion, S.; Kara, E.; Crepieux, P.; Piketty, V.; Martinat, N.; Guillou, F.; Reiter, E. *J. Endocrinol.* **2006**, *190*, 341–350.
- [13] Simoni, M.; Gromoll, J.; Nieschlag, E. *Endocr. Rev.* **1997**, *18*, 739–773.
- [14] Radu, A.; Pichon, C.; Camparo, P.; Antoine, M.; Allory, Y.; Couvelard, A.; Fromont, G.; Hai, M. T. V.; Ghinea, N. N. *Engl. J. Med.* **2010**, *363*, 1621–1630.
- [15] Zhang, X.-y.; Chen, J.; Zheng, Y.-f.; Gao, X.-l.; Kang, Y.; Liu, J.-c.; Cheng, M.-j.; Sun, H.; Xu, C.-j. *Cancer Res.* **2009**, *69*, 6506–6514.
- [16] Grima Poveda, P. M.; Karstens, W. F. J.; Timmers, C. M. *WO Patent* **2006**, 2006117368(A1).
- [17] van Koppen, C. J.; Verbost, P. M.; van de Lagemaat, R.; Karstens, W.-J. F.; Loozen, H. J.; van Achterberg, T. A.; van Amstel, M. G.; Brands, J. H.; van Doornmalen, E. J.; Wat, J.; Mulder, S. J.; Raafs, B. C.; Verkaik, S.; Hanssen, R. G.; Timmers, C. M. *Biochem. Pharmacol.* **2013**, *85*, 1162–1170.
- [18] Lee, H.; Mason, J. C.; Achilefu, S. *J. Org. Chem.* **2006**, *71*, 7862–7865.

- [19] Verdoes, M.; Florea, B. I.; Hillaert, U.; Willems, L. I.; van der Linden, W. A.; Sae-Heng, M.; Filippov, D. V.; Kisselev, A. F.; van der Marel, G. A.; Overkleeft, H. S. *ChemBioChem* **2008**, *9*, 1735–1738.
- [20] Gonçalves, M. S. T. *Chem. Rev.* **2008**, *109*, 190–212.
- [21] Hoogendoorn, S.; Blom, A. E. M.; Willems, L. I.; van der Marel, G. A.; Overkleeft, H. S. *Org. Lett.* **2011**, *13*, 5656–5659.
- [22] Boiadjiev, S. E.; Lightner, D. A. *J. Heterocycl. Chem.* **2003**, *40*, 181–185.
- [23] Nguyen, T.; Francis, M. B. *Org. Lett.* **2003**, *5*, 3245–3248.
- [24] Mujumdar, R. B.; Ernst, L. A.; Mujumdar, S. R.; Lewis, C. J.; Waggoner, A. S. *Bioconjug. Chem.* **1993**, *4*, 105–111.
- [25] Tornøe, C. W.; Christensen, C.; Meldal, M. *J. Org. Chem.* **2002**, *67*, 3057–3064.
- [26] Rostovtsev, V. V.; Green, L. G.; Fokin, V. V.; Sharpless, K. B. *Angew. Chem. Int. Ed. Engl.* **2002**, *41*, 2596–2599.
- [27] Li, L.; Kracht, J.; Peng, S.; Bernhardt, G.; Buschauer, A. *Bioorg. Med. Chem. Lett.* **2003**, *13*, 1245–1248.
- [28] Kishi, H.; Krishnamurthy, H.; Galet, C.; Bhaskaran, R. S.; Ascoli, M. *J. Biol. Chem.* **2002**, *277*, 21939–21946.
- [29] Paone, D. V. et al. *J. Med. Chem.* **2007**, *50*, 5564–5567.
- [30] Terasaki, M.; Song, J.; Wong, J. R.; Weiss, M. J.; Chen, L. B. *Cell* **1984**, *38*, 101–108.
- [31] Teiten, M.; Bezdetnaya, L.; Morliere, P.; Santus, R.; Guillemin, F. *Br. J. Cancer* **2003**, *88*, 146–152.
- [32] Zinchuk, V.; Wu, Y.; Grossenbacher-Zinchuk, O. *Scientific reports* **2013**, *3*, 1–5.
- [33] Fletcher, P. W.; Reichert, L. E. *Mol. Cell. Endocrinol.* **1984**, *34*, 39–49.
- [34] Li, Q.; Lau, A.; Morris, T. J.; Guo, L.; Fordyce, C. B.; Stanley, E. F. *J. Neurosci.* **2004**, *24*, 4070–4081.
- [35] Andersen, T. T.; Curatolo, L. M.; Reichert, L. E. *Mol. Cell. Endocrinol.* **1983**, *33*, 37–52.
- [36] Bongers, K. M.; Hoogendoorn, S.; van Koppen, C. J.; Timmers, C. M.; Overkleeft, H. S.; van der Marel, G. A. *ChemMedChem* **2009**, *4*, 2098–2102.
- [37] van Straten, N. C.; van Berkel, T. H.; Demont, D. R.; Karstens, W.-J. F.; Merckx, R.; Oosterom, J.; Schulz, J.; van Someren, R. G.; Timmers, C. M.; van Zandvoort, P. M. *J. Med. Chem.* **2005**, *48*, 1697–1700.
- [38] Wang, L.-H.; Rothberg, K. G.; Anderson, R. *J. Cell Biol.* **1993**, *123*, 1107–1117.
- [39] Rejman, J.; Oberle, V.; Zuhorn, I.; Hoekstra, D. *Biochem. J* **2004**, *377*, 159–169.
- [40] Sun, X.; Yau, V. K.; Briggs, B. J.; Whittaker, G. R. *Virology* **2005**, *338*, 53–60.
- [41] Okuyama, M.; Laman, H.; Kingsbury, S. R.; Visintin, C.; Leo, E.; Eward, K. L.; Stoeber, K.; Boshoff, C.; Williams, G. H.; Selwood, D. L. *Nat. Methods* **2007**, *4*, 153–159.
- [42] Yen, J.-C.; Chang, F.-J.; Chang, S. *IEEE Trans. Image Process.* **1995**, *4*, 370–378.



# 8

## Small-molecule FSHR agonists as targeting agents for BNCT<sup>1</sup>

**B**oron neutron capture therapy (BNCT) is a binary therapy based on the ability of boron-10 to efficiently capture thermal neutrons. When sufficiently high levels of <sup>10</sup>B are accumulated within tumor tissues, these can be destroyed with minimal damage to the surrounding tissue. This chapter presents a targeting strategy for carboranes, suited for BNCT because of their high boron-content, by covalent attachment to a follicle-stimulating hormone receptor (FSHR) agonist. The presence of the FSHR on tumor-associated tissues has been demonstrated and agonist-induced internalization of the FSHR-ligand complex would result in selective delivery of the BNCT agent into the tumor cells. Five *m*-DHP-fluorophore-carborane constructs were synthesized and evaluated for their ability to activate the FSHR. All constructs were FSHR agonists with an EC<sub>50</sub> value below 100 nM, and able to induce receptor-internalization. The Cy5-containing construct **116** was shown to be endocytosed, at least partially, in a receptor-dependent fashion, illustrating the potential of DHP-conjugates for the targeted delivery of BNCT or other cytotoxic agents to FSHR-expressing cells.

## 8.1 Introduction

Boron neutron capture therapy (BNCT) is a binary anticancer therapy based on the ability of the boron-10 isotope to efficiently capture low-energy thermal neutrons. Both  $^{10}\text{B}$  and slow neutrons are in themselves relatively harmless to cells and tissues, whereas a combination of both leads to a nuclear reaction resulting in the release of lethal, high-energy  $\alpha$ -particles and  $^7\text{Li}$  ions (Figure 8.1A). These particles release all their energy along a trajectory of  $\leq 10\ \mu\text{m}$ , corresponding to the approximate diameter of a cell. Meaning that if high doses of boron-10 could be selectively accumulated within tumor tissues, focused irradiation of these tissues would provide a very efficient and localized means to kill the tumor cells.<sup>2-4</sup> Current clinically used BNCT agents include sodium mercaptoundecahydro-*closo*-dodecaborate (BSH) and (L)-4-dihydroxy-borophenylalanine (BPA) (Figure 8.1B) which are mainly used in the treatment of brain tumors.<sup>5</sup> The primary consideration in the design of novel BNCT agents is the requirement of high local concentrations of boron inside the tumor. It has been calculated that  $\sim 20\ \mu\text{g}\ ^{10}\text{B}/\text{g}$  tumor is needed for the therapy to be effective.<sup>6</sup> Agents containing a relatively high amount of boron are therefore favored, as well as delivery systems that allow the targeting of the BNCT agent to the tumor cells.<sup>7</sup>

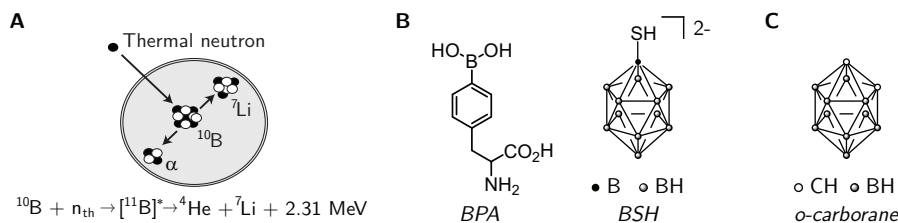


**Figure 8.1:** A) General principle of BNCT. B) BNCT agents BPA and BSH. C) Structure of *ortho*-carborane.

Over the last decades, the polyhedral dicarba-*closo*-dodecaboranes (carboranes), with the general formula  $\text{C}_2\text{B}_{10}\text{H}_{12}$ , have gained much interest as potential BNCT agents because of their high boron content. Furthermore, they are catabolically stable and ample organic chemical methods are available for their derivatization.<sup>8,9</sup> The most frequently used carborane is *ortho*-carborane, with the two carbon atoms adjacent to each other (Figure 8.1C), that can be synthesized from a variety of alkynes and decaborane and is commercially available. Carboranes are very lipophilic in nature, comparable to the adamantane group, and slightly larger than a rotating phenyl group.<sup>10</sup> Conjugates of carborane and a variety of biomolecules, such as carbohydrates,<sup>11</sup> amino acids,<sup>12</sup> nucleosides<sup>13</sup> and porphyrins,<sup>14</sup> for BNCT have been described.<sup>4,8</sup>

Ovarian cancer is the fifth cause of cancer-related death in women and cancer survival rates are much lower than for other types of cancers.<sup>15</sup> The most common form is ovarian epithelial cancer, which arises from the ovarian surface epithelium.<sup>16</sup> The factors that lead to the onset and progression of the tumor are debated, but there is a body of evidence indicative of a role for the gonadotropins (luteinizing hormone, LH and follicle

stimulating hormone, FSH) and their receptors.<sup>17,18</sup> While the main expression site of the follicle-stimulating hormone receptor (FSHR) in normal physiology is in granulosa cells of the ovaries,<sup>19</sup> the presence of the FSHR on both normal and tumor ovarian surface epithelium cells has been demonstrated.<sup>20–23</sup> The presence of the FSHR on ovarian cancer cells has been exploited for targeted delivery of cytotoxic drugs to the receptor. Zhang *et al.* have made use of FSH $\beta$ -peptides conjugated to nanoparticles to deliver paclitaxel to the tumor site.<sup>24,25</sup> The recent notion that the FSHR is also expressed by vascular endothelial cells of a wide range of tumors implicates that this receptor might have broader functions in carcinogenesis than previously recognized.<sup>26</sup>

In the previous Chapters 6 and 7, targeting of the FSHR has been investigated with the use of a small-molecule agonist for the receptor. By appropriate introduction of a spacer to the dihydropyridine (DHP) agonist,<sup>27,28</sup> nanomolar potent functionalized ligands were established. It was also shown that incorporation of a fluorophore led to very potent fluorescent ligands that could be used as diagnostic tools to study receptor-related processes. The ultimate goal of the research was to arrive at the targeted delivery of BNCT agents to FSHR-expressing tumor cells, by use of the low molecular weight ligand (Figure 6.2, Chapter 6). Selective accumulation of carboranes in cells via the FSHR, followed by localized irradiation with thermal neutrons would allow for a very efficient anti-tumor strategy with minimal damage to surrounding tissues. In this chapter, chemical strategies for functionalization of *ortho*-carborane are presented as well as the synthesis and biological evaluation of carborane-containing fluorescent ligands for the FSHR.

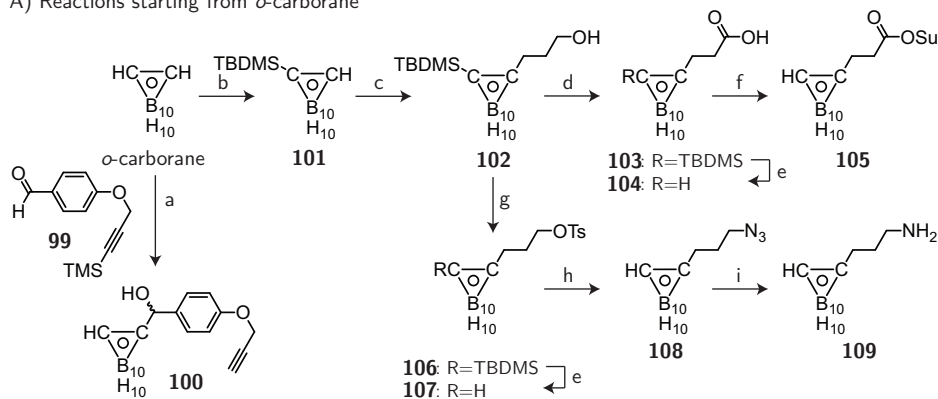
## 8.2 Results and Discussion

**Synthesis.** Incorporation of carboranes into larger constructs requires the presence of a ligation handle on the carborane core. To keep a high level of flexibility in the design of the final constructs, *ortho*-carboranes containing a variety of different groups for further conjugation were synthesized (Scheme 8.1). Commercially available *o*-carborane was used, and reacted with TMS-protected propargyloxy benzaldehyde **99** and TBAF to give deprotected alkyne-functionalized carbinol **100** as a racemic mixture.<sup>29</sup> Use of unprotected propargyloxy benzaldehyde did not result in product formation and the low yield of the reaction (24%) was likely due to the concomitant deprotection of the silyl group, which occurred faster than the addition of carborane to the aldehyde. Reaction times were kept short because of the reported cage-degradation upon prolonged exposure of the carborane cage to fluoride ions.<sup>8,30</sup> Carboranes containing other functionalities were synthesized from a common precursor, alcohol **102**.<sup>31</sup> The CH-groups of *o*-carborane are weakly acidic ( $pK_a = 22.0$ ) and can be deprotonated using a strong base such as *n*-butyllithium. The lithium mono-anion of carborane is unstable and disintegrates to the more stable di-anion and *o*-carborane, leading to di-substitution of the carborane cage.<sup>8</sup> With the use of the bulky TBDMS protective group, this could be prevented.<sup>32</sup> Subsequent oxidation of alcohol **102** using reported conditions ( $\text{NaIO}_4$ ,  $\text{RuCl}_3 \cdot 3 \text{H}_2\text{O}$ ) was high yielding (86%), but complete

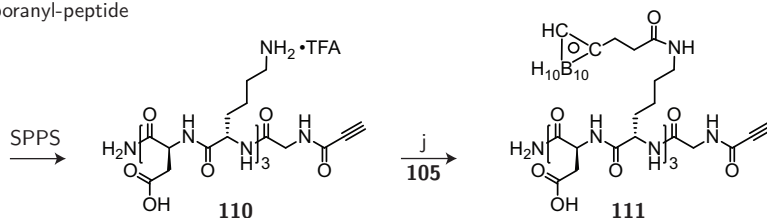
removal of the ruthenium catalyst proved cumbersome. Alternative conditions using mild TEMPO/BAIB oxidation were chosen and resulted in a clean conversion to acid **103** in 96% yield.<sup>33</sup> Subsequent deprotection of the TBDMS group was accomplished using TBAF under acidic conditions in near quantitative yield. The activated ester **105** was obtained in 88% yield and was used to synthesize carborane peptide **111** (Scheme 8.1B). The peptide scaffold **110** was synthesized using standard Fmoc-based solid-phase peptide synthesis (SPPS) and was designed with three aspartic acid residues to compensate for the hydrophobicity of the three incorporated carborane moieties. Also the peptide contained a terminal alkyne for use in subsequent Cu(I)-catalyzed Huisgen 1,3-dipolar cycloaddition.<sup>34,35</sup> The route towards azide and amine functionalized *o*-carborane started from common intermediate **102**, which was tosylated, TBDMS-deprotected with TBAF, and reacted with sodium azide to give azido-*o*-carborane **108** in good overall yields. The Staudinger reduction of azide **108** to primary amine **109** was low yielding, mainly because of deboronated by-products.<sup>8</sup> With functionalized carboranes in hand, five *m*-DHP-fluorophore-carborane constructs were

**Scheme 8.1:** Synthetic routes towards functionalized carboranes.

A) Reactions starting from *o*-carborane



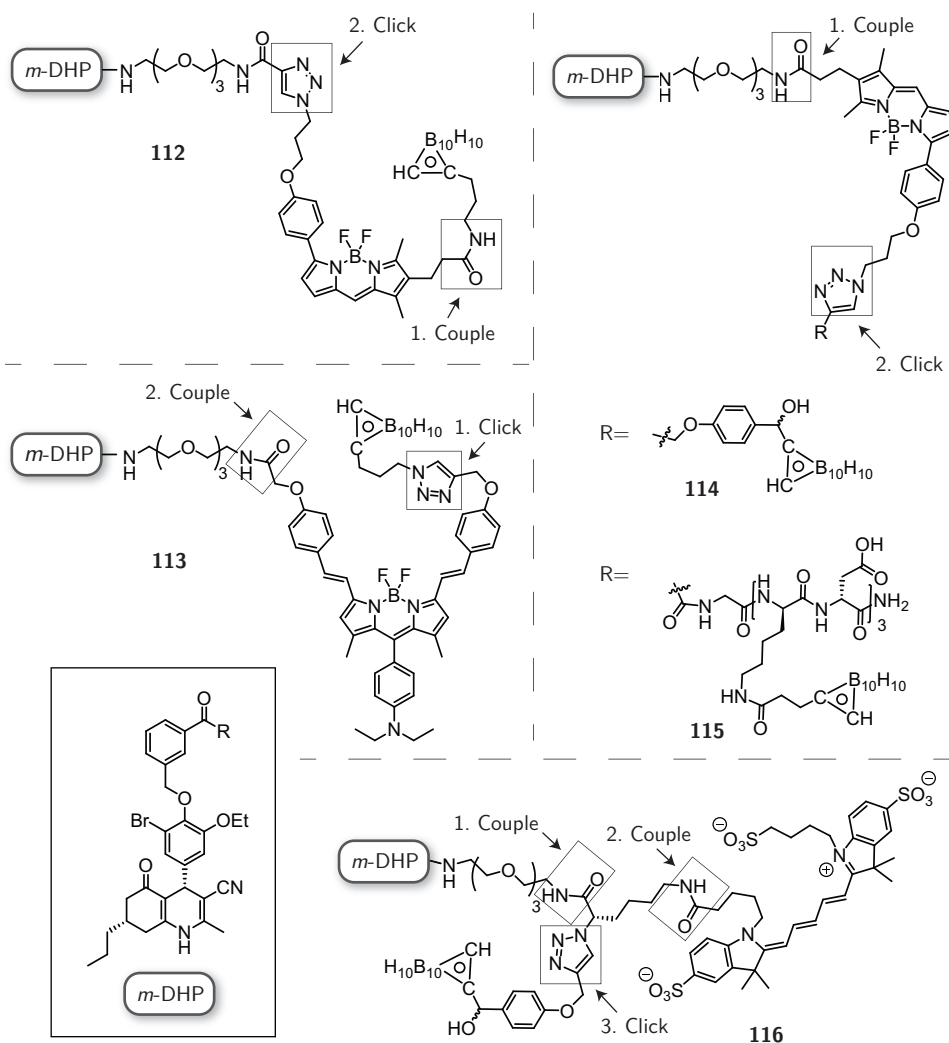
B) Carboranyl-peptide



Reagents and conditions: [a] TBAF, **99**, THF, 24%; [b] i) *n*-BuLi, toluene/Et<sub>2</sub>O, 0 °C → rt; ii) TBDMS-Cl, toluene/Et<sub>2</sub>O, 87%; [c] i) *n*-BuLi, THF; ii) trimethyleneoxide, THF, 86%; [d] TEMPO, BAIB, DCM/H<sub>2</sub>O, 96%; [e] TFA, TBAF, THF, -78 °C → rt, **104**: 98%, **107**: 84 %; [f] *N*-hydroxysuccinimide, EDC · HCl, DCM, 88%; [g] *p*-tosylchloride, DMAP, TEA, DCM, 96%; [h] sodium azide, TBAI, acetone, reflux, 97%; [i] PPh<sub>3</sub>, toluene/H<sub>2</sub>O, 29%; [j] carborane-OSu **105**, DiPEA, DMF, quant.

synthesized (Scheme 8.2). Different fluorophores and modes of attachment were chosen to find the optimal combination of dye and carborane that would yield a potent agonist. Amino-carborane **109** was reacted with bifunctional azido-BODIPY-OSu dye **36**<sup>36</sup> and subsequently clicked to alkyne-containing monomeric DHP ligand *m*-**131a** (Chapter 6) to give compound **112**. Alternatively, the other side of the BODIPY was used for ligation to the ligand (**93**, Chapter 7), which was then clicked to either alkyne-carborane **100** or carboranyl

**Scheme 8.2:** Overview of the different *meta*-DHP-fluorophore-carborane constructs that were synthesized.



All compounds were synthesized using orthogonal Cu(I)-catalyzed Huisgen [3+2] cycloaddition ("click") and peptide coupling conditions in the order indicated. See the Experimental section for experimental details of each step.

peptide **111** to yield compounds **114** and **115**, respectively. Although the bifunctional BO-DIPY dye is a very convenient dye for incorporation in larger constructs because of its two orthogonal ligation handles, studies using fluorescent ligand DHP-BDP **93** in Chapter 7 indicated that it was not selectively taken up by FSHR-expressing cells. pH-activatable dyes, that become fluorescent at acidic pH have been used as tools to selectively visualize the uptake of compounds in the endolysosomal pathway (Chapter 2).<sup>37,38</sup> Therefore, by attachment of a pH-activatable dye to the FSHR-agonist, it might be possible to distinguish between FSHR-mediated uptake of the construct and uptake by other processes, leading to the ER/Golgi localization (Chapter 7). Bifunctional pH-activatable dye **32** (Chapter 3), was clicked to azido-carborane **108**, the methyl ester on the BODIPY dye was saponified using mild basic conditions and the resulting carboxylic acid was coupled to amino-DHP *m*-**76a** yielding pH-activatable construct **113**. Attachment of a carborane to the DHP-Cy5 **96** (Chapter 7) required the addition of an extra ligation handle. Amino-DHP *m*-**76a** was coupled to 2-azido-6-(Boc-amino)hexanoic acid, the Boc group was removed and Cy5 **91**<sup>39</sup> was coupled using PyBOP. Crude azido-DHP-Cy5 was clicked to alkyne-carborane **100** in water/dioxane and the final construct **116** was isolated using column chromatography.

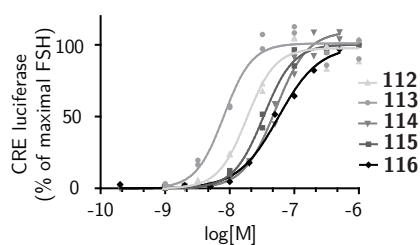


**Figure 8.2:** Agonistic dose-response curves of carborane-containing fluorescent ligands **112** - **116** on CHO cells stably expressing the human FSHR and CRE-inducible luciferase. The response was normalized against the maximal effect obtained with rFSH (200 pM). Representative curves of at least three independent experiments performed in duplicate are shown.

potency ( $EC_{50}$ ) values of the compounds (Table 8.1).

All constructs were shown to be full agonists for the receptor with potencies ranging between 7.6 nM (**113**) and 88 nM (**114**). Except for the pH-activatable compound (**113**), attachment of the fluorophore-carborane led to an order of magnitude decrease in potency, compared to monomeric ligand *m*-**74a**. Attachment of bulk, as for the carboranyl peptide, was well tolerated, again confirming that quite large extensions to the DHP core can be made without detrimental effects on its potency. Although slightly less potent than the parent molecule,  $EC_{50}$  values still were in a useful range for further experiments. To induce receptor internalization, much higher concentrations in the assay are needed than the  $EC_{50}$  values found in a luciferase assay, which is why only very potent agonists are feasible

**Biological evaluation.** The five DHP-fluorophore-carborane constructs were assessed for their agonistic potency on the FSHR using a CRE-luciferase assay. CHO cells stably expressing the human FSHR and a luciferase-reporter gene, were incubated with increasing concentrations of the compounds for 4 h (37 °C, 5% CO<sub>2</sub>). The luminescent signal, corresponding to receptor activation, was measured and the resulting dose-response curves are depicted in Figure 8.2. From these curves, the  $pEC_{50}$  values were obtained that were used to calculate the mean agonistic po-

**Table 8.1:** Mean agonistic potency (pEC<sub>50</sub> and EC<sub>50</sub>) values of carborane-containing fluorescent ligands in increasing CRE-mediated luciferase activity in CHO cells stably expressing hFSHR and a CRE-luciferase reporter gene.

| Compound     | EC <sub>50</sub> (nM) | pEC <sub>50</sub> | N | Compound   | EC <sub>50</sub> (nM) | pEC <sub>50</sub> | N |
|--------------|-----------------------|-------------------|---|------------|-----------------------|-------------------|---|
| <i>m-74a</i> | 6                     | 8.22 ± 0.10       | 3 | <b>114</b> | 88                    | 7.06 ± 0.14       | 3 |
| <b>112</b>   | 18                    | 7.74 ± 0.11       | 3 | <b>115</b> | 38                    | 7.42 ± 0.09       | 3 |
| <b>113</b>   | 8                     | 8.12 ± 0.11       | 3 | <b>116</b> | 45                    | 7.35 ± 0.04       | 4 |

The mean EC<sub>50</sub> values are calculated from the pEC<sub>50</sub> (mean ± SEM) values from *N* independent experiments performed in duplicate. The value for monomeric ligand *m-74a* from Chapter 6 is given for comparison.

candidates.<sup>27</sup> At higher concentrations these small molecules form aggregates (as seen by bell-shaped curves in a luciferase assay (data not shown)) and background fluorescence by nonspecific interaction between the dyes and cell membranes increases.

The ability of BODIPY-based compounds **113-115** to induce receptor endocytosis was studied using an internalization assay. U2OS cells stably expressing a green fluorescent eGFP-tagged FSHR (U2OS-FSHR cells) were used for this purpose. Without stimulation, the receptor is mainly present on the cell membrane, whereas activation leads to the occurrence of fluorescence in intracellular vesicles, indicative of endocytosis.<sup>27</sup> As illustrated in Figure 8.3, treatment of U2OS-FSHR cells with 10 μM of compounds **113-115** indeed led to translocation of the receptor from the membrane to the cytoplasm (GFP signal, middle panels). At this concentration some membrane fluorescence remained, indicating that 1 μM was not sufficient to induce full receptor internalization. For comparison, negative (DMSO only) and positive (recombinant FSH, rFSH) controls are depicted as well. Somewhat surprisingly, incorporation of a pH-activatable BODIPY dye in compound **113** did not result in selective fluorescence (Figure 8.3, upper left panel). Fluorescence was less than for the "always on" BODIPY-containing compound **114** (middle left panel), but still fluorescence was predominantly visible in membrane-like structures. This finding is in accordance with a recent paper entitled 'pH-sensitive fluorescent dyes: are they really pH-sensitive in cells?', where Zhang *et al.* have found that fluorescence of an pH-activatable aza-BODIPY dye was activated by intracellular membranes.<sup>40</sup> In contrast to the very large and polar mannose cluster-containing constructs described in Chapter 2 or the antibody-conjugates of Urano *et al.*,<sup>37,38</sup> which are not taken up by cells by other means than via receptor-mediated endocytosis, the DHP-pH-activatable BODIPY-carborane construct described here is much more lipophilic and could be expected to be taken up via different routes, leading to their localization in the ER and Golgi regions of the cell. Also, the binding kinetics of these ligands are not known, and since they are non-covalently bound to the receptor, they might dissociate quickly once internalized and diffuse out of the endolysosomal vesicles into the cytoplasm. Further research is needed to fully understand the mechanisms by which the BODIPY-containing DHP ligands are taken up by cells and trafficked to the membrane-rich regions of the cell. Comparison of the constructs containing only one carborane (**114**) or the carboranyl peptide (**115**) clicked to DHP-BDP, showed a different fluorescence pattern



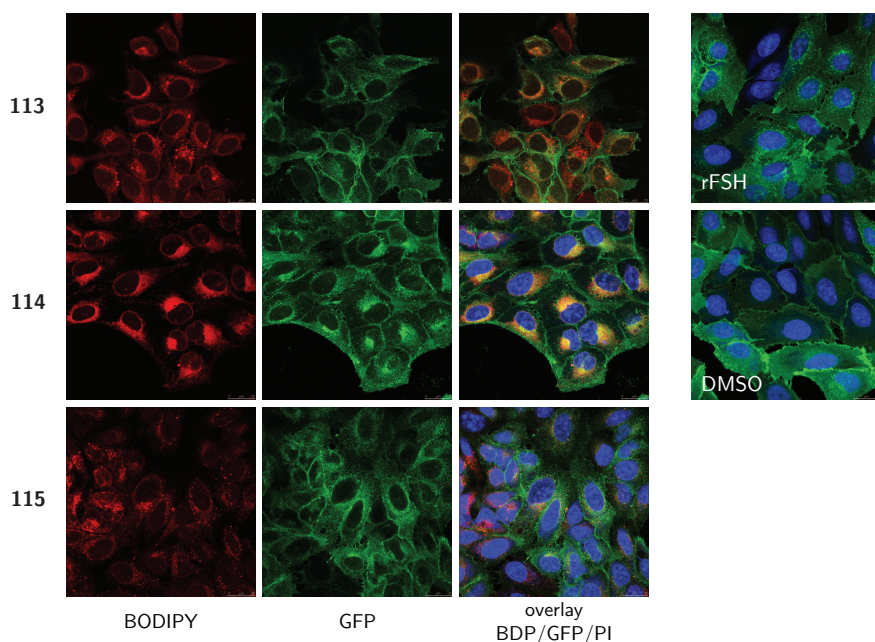


**Figure 8.3: Confocal fluorescence microscopy analysis of BODIPY-containing ligands.** U2OS-FSHR cells were treated with 10  $\mu\text{M}$  of compounds **113**, **114** or **115** for 2 h, followed by fixation with 4% formaldehyde in PBS. Treatment led to internalization of the receptor (GFP, green), but no selective uptake of the compounds (BODIPY, red) was found. Positive (rFSH) and negative (DMSO) controls are given for comparison.

for the larger peptide-containing compound **115** (lower left panel, Figure 8.3). No correlation with the GFP signal of the receptor was observed and areas without cells showed the same fluorescence pattern (not shown), most likely representing compound aggregates. In combination with the results described in Chapter 7, it can be concluded that the choice for BODIPY dyes in these constructs resulted in nonselective cellular uptake of these ligands.

The uptake characteristics of the much more hydrophilic Cy5-containing carborane ligand were next examined using fluorescence-activated cell sorting (FACS). Either receptor-expressing cells (U2OS-FSHR) or wild-type cells (U2OS) were incubated for 2 h with 1  $\mu\text{M}$  of DHP-Cy5-carborane **116**, washed and analyzed by flow cytometry. As can be seen in Figure 8.4A, which shows an overlay of the Cy5-fluorescence histograms of both cell lines, cells with receptor were slightly more fluorescent than those without. To examine whether this difference was correlated to receptor expression levels, the population of U2OS-FSHR cells with highest GFP-fluorescence levels (and thus receptor expression) was selected and depicted in green in the Cy5 scatterplot (Figure 8.4B). Indeed, cells with the highest levels of receptors were also highest in Cy5 fluorescence, a similar result as found for the fluorescent DHP-Cy5 **96** discussed in Chapter 7. Quadrant analyses of GFP vs Cy5 density plots for U2OS-FSHR and control U2OS cells are depicted in Figure 8.4C. A linear relationship between the intensity of Cy5 and GFP was found, but only for higher receptor



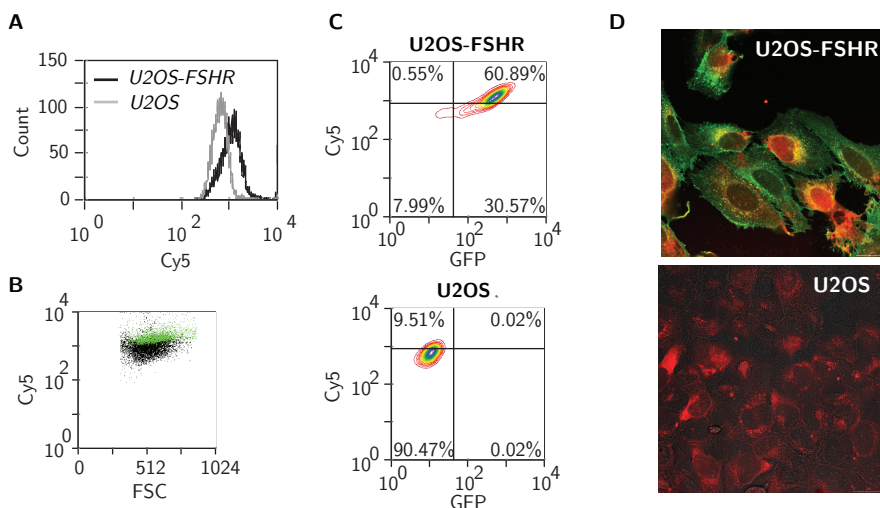


**Figure 8.4: Uptake of 116 (2 h, 1  $\mu$ M) in U2OS cells with or without FSHR-eGFP studied by FACS analysis (A-C) and confocal fluorescence microscopy (D).** A) Overlay of the histograms of treated U2OS-FSHR (black) and U2OS (grey) cells shows a slightly bigger shift in population mean for receptor cells compared to control cells. B) Scatterplot of Cy5 fluorescence vs forward scatter. Cells with maximum GFP levels are depicted in green. C) Representative contour plots of Cy5 vs GFP of treated U2OS-FSHR and U2OS cells, including the quadrants that were used to calculate the population percentages in each quadrant (mean, N=3). D) Confocal microscopy images of treated U2OS or U2OS-FSHR cells. Green corresponds to GFP (FSHR) and red to Cy5 (ligand) fluorescence. Overlying pixels are stained yellow for clarity, but no colocalization analysis was conducted.

expression levels. Attachment of the very apolar carborane clearly resulted in much increased background levels in untransfected cells or cells with low receptor expression in the U2OS-FSHR cell population. Confocal fluorescence microscopy of U2OS-FSHR cells showed receptor internalization and a non-homogeneous distribution of intracellular Cy5 fluorescence (Figure 8.4D). Control U2OS cells treated with compound **116** were also fluorescent, in accordance with the FACS data. Due to the non-uniform compound fluorescence in the cells, a detailed colocalization analysis was not conducted. Taken together, these results indicate that it is indeed possible to make larger constructs of the DHP-ligand to target a BNCT agent to FSHR-expressing cells. In the design of such constructs polarity should be an important parameter and care should be taken to compensate for the extremely lipophilic nature of the carborane cage.

### 8.3 Conclusion

Targeting of carboranes to FSHR expressing tumors presents a promising approach to selectively deliver high levels of boron-10 needed for BNCT. The constructs described in this chapter made use of the DHP low molecular weight agonist as targeting entity, combined with a fluorophore, either BODIPY or cyanine dye based, for visualization. Incorporation of one or more *o*-carborane moieties was successfully accomplished by the synthesis of a va-

riety of functionalized carboranes. The resulting DHP-fluorophore-carborane ligands were able to activate the FSHR, as determined by a luciferase assay, with slightly lower potencies than the monomeric or fluorescent ligands that were reported in the previous chapters. At higher (1  $\mu\text{M}$ ) concentrations of ligand, the receptor was (partially) internalized, as seen by the appearance of green intracellular vesicles in an FSHR-internalization assay. Fluorescence of BODIPY-based ligands was detected intracellularly in membrane structures when one *o*-carborane was introduced, and fluorescent clumps were visible in the medium when the larger carboranyl peptide-containing ligand **115** was added to the cells, indicative of aggregation. In case of Cy5-based ligand **116**, a linear correlation between the intensity of receptor fluorescence and the intensity of Cy5-ligand fluorescence was found using FACS. Unfortunately, background levels in untransfected cells were high and the intracellular fluorescence pattern in U2OS-FSHR cells was ambiguous. These findings illustrate the potential of the DHP ligand as targeting entity of cytotoxic drugs to tumors expressing the FSHR, while also exemplifying that the properties of the drug influence the construct as a whole.

## 8.4 Experimental Section

**Cell culture conditions.** All cells were grown in a humidified atmosphere in 5%  $\text{CO}_2$  at 37  $^\circ\text{C}$ . CHO cells stably expressing the human FSH receptor together with a luciferase reporter gene (CHO-hFSHR\_luc cells) and control cells without receptor but with luciferase gene (CHO\_luc cells) were provided by MSD, Oss, The Netherlands. Cells were cultured in Dulbecco's Modified Eagle's Medium (DMEM) and Ham's F12 medium (1:1) with glutamine, penicillin/streptomycin (pen/strep, 0.1 mg/mL) and fetal calf serum (FCS). CHO-hFSHR\_luc cells were maintained under constant selection with Hygromycin B (0.8 mg/mL). Cells were subcultured twice weekly at a ratio of 1:10-1:15. U2OS cells stably expressing the rat FSHR fused to the N-terminus of eGFP (U2OS-FSHR cells) were obtained from MSD, Oss, The Netherlands (FSHR redistribution assay, Biolumage). Cells were grown in DMEM (high glucose (4.5 g/L) and with stable glutamine, Invitrogen), pen/strep (0.1 mg/mL), G418 (0.5 mg/mL) and FCS (10%). Wild-type U2OS cells were grown under the same conditions, without G418. Cells were subcultured twice weekly at a ratio of 1:8-1:10.

**Measurement of CRE-induced luciferase expression.** CHO\_luc or CHO-hFSHR\_luc cells were cultured to ~80% confluency before use in the assay. On the day of the experiment, cells were harvested using enzyme-free dissociation solution (Millipore), counted (Biorad TC10 automated cell counter) and resuspended in assay medium (DMEM-F12 (1:1), without phenol-red, with pen/strep (0.1 mg/mL) supplied with 1  $\mu\text{g}/\text{mL}$  bovine insulin (Tebu-Bio) and 5  $\mu\text{g}/\text{mL}$  human apo-transferrin (Sigma)) to a concentration of  $7.5 \times 10^5$  cells/mL. Experiments were conducted in 96-wells white Optiplates (Perkin Elmer) and each well contained 30  $\mu\text{L}$  of test compound, recombinant FSH (200 pM final concentration, positive control) or assay medium (negative control), 30  $\mu\text{L}$  of assay medium and 30  $\mu\text{L}$  cell suspension. Final concentration of DMSO was 1% for all compounds, including controls. After 4 h of stimulation, 50  $\mu\text{L}$  Neolite (PerkinElmer) was added to each well and luminescence signal was detected on a Microbeta Trilux 1450 Luminescence Counter (PerkinElmer). To control for non-FSHR mediated effects on intracellular cAMP levels, highest compound concentrations used in the dose-response experiments (typically 1  $\mu\text{M}$ ) were tested on CHO\_luc cells. Data was analyzed using GraphPad Prism 5 (GraphPad Software, La Jolla, USA), and values were normalized to the maximal effect obtained for recombinant human FSH (200 pM, rFSH, Org32489, gift from MSD,

Oss, The Netherlands). Each experiment was performed on duplicate plates and mean  $\pm$  SEM values of at least three independent experiments are given.

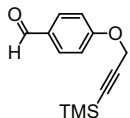
**Fluorescence-activated cell sorting.** U2OS or U2OS-FSHR cells were cultured as described under "Cell culture". Cells were seeded onto 6-well plates (400,000 cells/well) and cultured for 48 h, before start of the experiment. Compound **116** (as 2x stock solution in culture medium) was added to the cells (1  $\mu$ M final concentration) and the cells were incubated for 2 h (37 °C, 5% CO<sub>2</sub>). Cells were washed with ice-cold PBS (2x) and harvested using enzyme-free dissociation solution (Millipore). After centrifugation (5 min, 1200 rpm), the pellet was resuspended in PBS to obtain a single-cell suspension of  $\sim 1 \times 10^6$  cells/mL. Cells were transferred to a 96-wells plate and samples measured using a BD FACSCanto II flow cytometer (BD Biosciences, San Jose, USA). The following laser/filter settings were used: GFP (FSHR):  $\lambda_{\text{ex}}$ : 488 nm,  $\lambda_{\text{em}}$ : 530/30 nm; Cy5 (**96**):  $\lambda_{\text{ex}}$ : 633 nm,  $\lambda_{\text{em}}$ : >670 nm and values were compensated using the instrumentation software and mono-stained controls. Data was analyzed using FCS Express 4 Flow Research Edition (De Novo Software, LA, USA). All samples were measured twice and values were calculated from three independent experiments with a sample size of  $\sim 10000$  cells.

**Uptake and FSHR internalization microscopy experiments.** U2OS-FSHR or U2OS cells were maintained as described under "Cell culture". 48 h before the experiment, cells were harvested (Trypsin-EDTA), counted and seeded onto sterile Labtek II 4- or 8-chamber borosilicate coverglass systems (Fisher Emergo) at a density of 25-50  $\times 10^4$  cells/well. On the day of the experiment, cells were incubated with compound (10  $\mu$ M) for 2 h at 37 °C, before being washed with PBS (2x), fixed (4 % formaldehyde in PBS), washed again (PBS) and nuclei stained with propidium iodide (optional, only when the compound fluorescence is detected in the dsRed channel). Cells were imaged on a Leica TCS SPE confocal microscope, using GFP (FSHR), dsRed (**114**, **115**) or Cy5 (**113**, **116**) filter settings ( $\lambda_{\text{ex}}$  488, 532 or 635 nm) with optimized detection range to exclude bleed-through of dye signal in different channels. Images were colored using ImageJ.

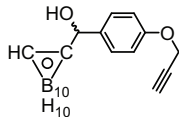
## Synthesis

**General.** All reagents were of commercial grade and used as received unless stated otherwise. Reaction solvents were of analytical grade and when used under anhydrous conditions stored over flame-dried 3 Å molecular sieves. Dichloromethane was distilled over CaH<sub>2</sub> prior to use. Solvents used for column chromatography were of technical grade and distilled before use. All moisture and oxygen sensitive reactions were performed under an argon atmosphere. Flash chromatography was performed on silica gel (Screening Devices BV, 0.04-0.063 mm, 60 Å). Reactions were routinely monitored by TLC analysis on DC-alufolien (Merck, Kieselgel60, F254) with detection by UV-absorption (254/366 nm) where applicable and spraying with a solution of (NH<sub>4</sub>)<sub>6</sub>Mo<sub>7</sub>O<sub>24</sub> · 4 H<sub>2</sub>O (25 g/l) and (NH<sub>4</sub>)<sub>4</sub>Ce(SO<sub>4</sub>)<sub>4</sub> · 2 H<sub>2</sub>O (10 g/l) in 10% sulfuric acid in water followed by charring at 150 °C. 1H and 13C NMR spectra were recorded on a Bruker AV-400 (400 MHz) or Bruker DMX-600 (600 MHz). Chemical shifts are given in ppm ( $\delta$ ) relative to the residual solvent peak or TMS (0 ppm) as internal standard. Coupling constants are given in Hz. LC-MS measurements were conducted on a Thermo Finnigan LCQ Advantage MAX ion-trap mass spectrometer (ESI+) coupled to a Surveyor HPLC system (Thermo Finnigan) equipped with a standard C18 (Gemini, 4.6 mmD  $\times$  50 mmL, 5 $\mu$  particle size, Phenomenex) analytical column and buffers A: H<sub>2</sub>O, B: ACN, C: 0.1% aq.TFA. High resolution mass spectra were recorded on a LTQ Orbitrap (Thermo Finnigan) mass spectrometer equipped with an electrospray ion source in positive mode (source voltage 3.5 kV, sheath gas flow 10 mL min<sup>-1</sup>, capillary temperature 250 °C) with resolution R=60000 at m/z 400 (mass range m/z=150-2000) and dioctylphthalate (m/z =

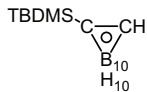
391.28428) as a "lock mass". The high resolution mass spectrometer was calibrated prior to measurements with a calibration mixture (Thermo Finnigan). For reversed-phase HPLC purification of the final compounds a Gilson automated HPLC system equipped with a C18 semiprep column (Gemini C18, 250x10 mm, 5 $\mu$  particle size, Phenomenex) was used.



**4-(3-Trimethylsilyl-propargyloxy)benzaldehyde (99).** 4-hydroxybenzaldehyde (0.37 g, 3 mmol) was dissolved in acetone (15 mL). Potassium carbonate (0.58 g, 4.2 mmol, 1.4 eq) was added and the mixture was refluxed at 65 °C for 30 min. 3-Bromo-1-trimethylsilylpropyne (0.54 mL, 3.3 mmol, 1.1 eq) was added and the mixture was refluxed for 6 h. The solvent was removed *in vacuo* and the residue was dissolved in water (10 mL) and extracted with EtOAc (4x). The combined organic layers were dried (MgSO<sub>4</sub>), filtered and concentrated under reduced pressure. Purification by silica column chromatography (1 → 2% EtOAc in PE) yielded the product as a colourless oil (0.50 g, 2.13 mmol, 71%).  $R_f$  = 0.74 (5:1 toluene:EtOAc). <sup>1</sup>H NMR (400 MHz, CDCl<sub>3</sub>):  $\delta$  9.75 (s, 1H, O=CH), 7.70 (d,  $J$  = 8.8 Hz, 2H, 2  $\times$  CH<sub>ar</sub>), 6.94 (d,  $J$  = 8.8 Hz, 2H, 2  $\times$  CH<sub>ar</sub>), 4.63 (s, 2H, CH<sub>2</sub>), 0.05 (s, 9H, 3  $\times$  CH<sub>3</sub>). <sup>13</sup>C NMR (101 MHz, CDCl<sub>3</sub>):  $\delta$  190.37, 162.35, 131.56, 130.24, 114.99, 98.93, 93.45, 56.57, -0.53. FT-IR (thin film)  $\nu$  1734, 1693, 1508, 1265, 1163, 1033, 846, 731, 702 cm<sup>-1</sup>. ESI-HRMS ( $m/z$ ): calcd. for [C<sub>13</sub>H<sub>16</sub>O<sub>2</sub>Si + H]<sup>+</sup> 233.09923; obsd. 233.09922.

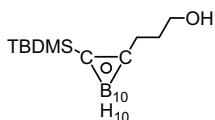


**4-((prop-2-yn-1-yloxy) phenyl) (1',2'-dicarba-closo-dodecaboran(12)-1'-yl) methanol (100).** *o*-Carborane (72 mg, 0.5 mmol) was dissolved in dry THF (2 mL). Tetra-*n*-butylammonium fluoride (1M in THF, 1.5 mL, 1.5 mmol, 3 eq) was added and the mixture was stirred at rt for 5 min. Subsequently, a solution of **99** (0.13 g, 0.55 mmol, 1.1 eq) in THF (1 mL) was added dropwise. After stirring for 5 min, more **99** (0.55 M in THF, 0.25 mmol, 0.5 eq) was added and the mixture was stirred for 5 min. The reaction was quenched with NH<sub>4</sub>Cl (sat aq, 2 mL), followed by extraction with diethyl ether (3  $\times$  2 mL). The combined organic layers were dried (MgSO<sub>4</sub>), filtered and concentrated under reduced pressure. Purification by silica column chromatography (2 → 5% EtOAc in PE) yielded the product as a racemic mixture (36 mg, 0.12 mmol, 24%).  $R_f$  = 0.42 (4:1 PE:EtOAc). <sup>1</sup>H NMR (400 MHz, CDCl<sub>3</sub>):  $\delta$  7.27 (d,  $J$  = 8.6 Hz, 2H, 2  $\times$  CH<sub>ar</sub>), 6.98 (d,  $J$  = 8.8 Hz, 2H, 2  $\times$  CH<sub>ar</sub>), 5.21 (s, 1H, CH), 4.70 (d,  $J$  = 2.4 Hz, 2H, CH<sub>2</sub>), 3.80 (s, 1H, BCH), 2.98 - 1.35 (m, 10H, 10  $\times$  BH), 2.54 (t,  $J$  = 2.4 Hz, 1H,  $\equiv$ CH). <sup>13</sup>C NMR (101 MHz, CDCl<sub>3</sub>):  $\delta$  158.47, 131.61, 128.06, 115.13, 78.94, 78.21, 76.08, 74.78, 59.44, 56.02. <sup>11</sup>B NMR (128 MHz, CDCl<sub>3</sub>):  $\delta$  -3.40, -4.37, -8.70, -9.26, -11.07, -12.47, -14.00. FT-IR (thin film)  $\nu$  3298 ( $\equiv$ C-H)), 2924, 2573 (B-H)), 1608, 1508, 1219, 1174, 1018, 825 cm<sup>-1</sup>.

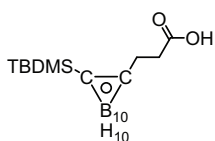


**1-(tert-Butyldimethylsilyl)-1,2-dicarba-closo-dodecaborane (101).** To a solution of *o*-carborane (2.88 g, 20.0 mmol, 1 eq) in dry toluene and Et<sub>2</sub>O (18 mL, 2:1, v/v) was added *n*-BuLi (2.5 M in hexane, 8.4 mL, 21.0 mmol, 1.05 eq) at 0 °C under an argon atmosphere. The solution immediately became turbid and was stirred for 2 h while gradually warming to rt. The mixture was cooled again to 0 °C and TBDMSCl (3.32 g, 22.0 mmol, 1.1 eq) in a 3 mL solution of toluene and Et<sub>2</sub>O (2:1, v/v) was added with a syringe and stirred overnight at rt. After addition of water (50 mL), the aqueous layer was extracted with Et<sub>2</sub>O (3  $\times$  50 mL). The combined organic layers were dried over MgSO<sub>4</sub>, filtered and concentrated *in vacuo*. Flash column chromatography (0 → 30% EtOAc in PE) afforded **101** as a colourless oil, which solidified to a white powder upon standing (4.48 g, 17.3 mmol, 87%).  $R_f$  = 0.8 (19:1 pentane:EtOAc). <sup>1</sup>H NMR (400 MHz, CDCl<sub>3</sub>):  $\delta$  3.44 (s, 1H, CHB), 3.24 - 1.38 (m, 10H, 10  $\times$  BH), 1.02 (s, 9H, 3  $\times$  CH<sub>3</sub>), 0.23 (s, 6H, 2  $\times$  CH<sub>3</sub>). <sup>13</sup>C NMR (101 MHz, CDCl<sub>3</sub>):  $\delta$  66.16,

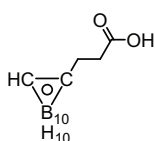
60.39, 27.11, 19.45, -4.42.  $^{11}\text{B}$  NMR (128 MHz,  $\text{CDCl}_3$ ):  $\delta$  0.18, -1.88, -7.10, -10.81, -12.34, -13.32. FT-IR (thin film)  $\nu$  3080 (BC-H), 2976, 2961, 2937, 2863, 2611, 2589, 2566 (B-H), 1468, 1364, 1265, 1256, 1072, 1030, 1003, 872  $\text{cm}^{-1}$ . ESI-HRMS ( $m/z$ ): calcd. for  $[\text{C}_8\text{H}_{26}\text{B}_{10}\text{Si} + \text{CH}_3\text{CN} + \text{H}]^+$  300.31452; obsd. 300.31492.



**1-(*tert*-Butyldimethylsilyl)-2-(3'-hydroxypropyl)-1,2-dicarba-closo-dodecaborane (101).** Compound **101** (2.59 g, 10.0 mmol) was dissolved in dry THF (50 mL) and *n*-BuLi (1.6 M in hexane, 6.88 mL, 11.0 mmol, 1.1 eq) was added slowly. Reaction mixture changed from colorless to bright orange/red. After stirring for 1 h, trimethylene oxide (1.30 mL, 20.0 mmol, 2 eq) was added and the mixture was stirred overnight at room temperature under an argon atmosphere. Subsequently, *n*-BuLi (1.6 M in hexane, 1.56 mL, 2.5 mmol, 0.25 eq) and trimethylene oxide (0.33 mL, 5.0 mmol, 0.5 eq) were added and the mixture was stirred for 3 h. The mixture was diluted with diethyl ether and washed with water (1  $\times$  40 mL). After the layers were separated, the aqueous layer was extracted with diethyl ether (2  $\times$  30 mL) and the combined organic layers were dried ( $\text{MgSO}_4$ ), filtered and concentrated under reduced pressure. Flash column chromatography (5  $\rightarrow$  25% EtOAc in PE) afforded the alcohol **102** as a white powder (3.08 g, 8.6 mmol, 86%).  $R_f = 0.3$  (4:1 PE:EtOAc).  $^1\text{H}$  NMR (400 MHz,  $\text{CDCl}_3$ ):  $\delta$  3.61 (t,  $J = 5.9$  Hz, 2H,  $\text{CH}_2$ ), 3.09 - 1.58 (m, 10H, 10  $\times$  BH), 2.39 - 2.30 (m, 2H,  $\text{CH}_2$ ), 1.81 - 1.72 (m, 2H,  $\text{CH}_2$ ), 1.51 (s, 1H, OH), 1.06 (s, 9H, 3  $\times$   $\text{CH}_3$ ), 0.33 (s, 6H, 2  $\times$   $\text{CH}_3$ ).  $^{13}\text{C}$  NMR (101 MHz,  $\text{CDCl}_3$ ):  $\delta$  81.40, 76.58, 61.71, 34.74, 33.08, 27.72, 20.48, -2.35.  $^{11}\text{B}$  NMR (128 MHz,  $\text{CDCl}_3$ ):  $\delta$  0.09, -4.06, -7.43, -10.42. FT-IR (thin film)  $\nu$  3560, 3323, 2936, 2569 (B-H), 1466, 1258, 1057 (C-O), 838 (Si- $\text{CH}_3$ )  $\text{cm}^{-1}$ . ESI-HRMS ( $m/z$ ): calcd. for  $[\text{C}_{11}\text{H}_{32}\text{B}_{10}\text{OSi} + \text{CH}_3\text{CN} + \text{H}]^+$  358.35639; obsd. 358.35701.

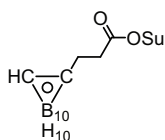


**3-1'-[2'-(*tert*-Butyldimethylsilyl)-1'-2'-dicarba-closo-dodecaboranyl] propionic acid (103).** To a solution of alcohol **102** (0.95 g, 3.00 mmol, 1 eq) in  $\text{DCM}/\text{H}_2\text{O}$  (15 mL, 2:1, v/v) under an argon atmosphere at rt, were added TEMPO (96 mg, 0.60 mmol, 0.2 eq) and bis(acetoxy)iodobenzene (2.42 g, 7.50 mmol, 2.5 eq). The resulting orange mixture was stirred vigorously for 1.5 h, before being quenched with  $\text{Na}_2\text{S}_2\text{O}_3$  (sat aq, 15 mL). Water (15 mL) was added and the aqueous layer was extracted with  $\text{DCM}$  (3  $\times$  50 mL). The combined organic layers were dried over  $\text{MgSO}_4$ , filtered and concentrated *in vacuo*. Flash column chromatography (10  $\rightarrow$  30% EtOAc in PE + 1% AcOH) afforded the carboxylic acid **103** as a white powder (2.87 mmol, 0.95 g, 96%).  $R_f = 0.5$  (2:1 PE:EtOAc + AcOH).  $^1\text{H}$  NMR (400 MHz,  $\text{CDCl}_3$ ):  $\delta$  10.86 (s, 1H, COOH), 3.38 - 1.43 (m, 10H, 10  $\times$  BH), 2.67 - 2.52 (m, 4H, 2  $\times$   $\text{CH}_2$ ), 1.07 (s, 9H, 3  $\times$   $\text{CH}_3$ ), 0.34 (s, 6H, 2  $\times$   $\text{CH}_3$ ).  $^{13}\text{C}$  NMR (101 MHz,  $\text{CDCl}_3$ ):  $\delta$  177.47, 79.37, 76.42, 34.15, 32.26, 27.63, 20.51, -2.39.  $^{11}\text{B}$  NMR (128 MHz,  $\text{CDCl}_3$ ):  $\delta$  0.39, -3.65, -7.28, -10.23. FT-IR (thin film)  $\nu$  3043, 2974, 2938, 2866, 2575 (B-H), 1714 (C=O), 1472, 1429, 1368, 1296, 1259, 1085, 1004, 928, 908, 858, 834  $\text{cm}^{-1}$ . ESI-HRMS ( $m/z$ ): calcd. for  $[\text{C}_{11}\text{H}_{30}\text{B}_{10}\text{O}_2\text{Si} + \text{CH}_3\text{CN} + \text{H}]^+$  372.33565; obsd. 372.33603.



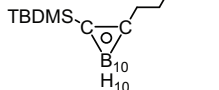
**3-(1-(1',2'-Dicarba-closo-decaboranyl)propionic acid (104).** Carboxylic acid **103** (435 mg, 1.32 mmol, 1 eq) was dissolved in dry THF (10 mL) under an argon atmosphere and cooled to  $-78$   $^\circ\text{C}$ . TFA (98  $\mu\text{L}$ , 1.32 mmol, 1 eq) was added followed by dropwise addition of TBAF (1M in THF, 1.58 mL, 1.58 mmol, 1.2 eq). After stirring for 5 min the cooling bath was removed and the reaction was allowed to warm to rt overnight.  $\text{Et}_2\text{O}$  (20 mL) was added and the organic layer was washed with HCl (aq, 1 M, 3  $\times$  30 mL). The combined aqueous layers were extracted with  $\text{Et}_2\text{O}$  (2  $\times$  60 mL) and the ether layers were combined, dried over  $\text{MgSO}_4$ , filtered and concentrated under

reduced pressure. Silica column chromatography (10 → 30% EtOAc in PE + 1% AcOH) yielded the carboxylic acid **104** as a white powder (281 mg, 1.30 mmol, 98%).  $R_f = 0.3$  (2:1 PE:EtOAc + AcOH).  $^1\text{H NMR}$  (400 MHz,  $\text{CDCl}_3$ ):  $\delta$  10.30 (s, 1H, COOH), 3.67 (s, 1H, BCH), 3.13 - 1.44 (m, 10H, 10 × BH), 2.67 - 2.54 (m, 4H, 2 ×  $\text{CH}_2$ ).  $^{13}\text{C NMR}$  (101 MHz,  $\text{CDCl}_3$ ):  $\delta$  176.93, 73.66, 61.74, 33.22, 32.43.  $^{11}\text{B NMR}$  (128 MHz,  $\text{CDCl}_3$ ):  $\delta$  -2.03, -5.45, -9.27, -11.71, -12.82. FT-IR (thin film)  $\nu$  3053, 2926, 2580 (B-H), 1696 (C=O), 1436, 1320, 1236, 1223, 1197, 1127, 1077, 1019, 1001, 908, 724  $\text{cm}^{-1}$ . ESI-HRMS ( $m/z$ ): calcd. for  $[\text{C}_5\text{H}_{16}\text{B}_{10}\text{O}_2 + \text{CH}_3\text{CN} + \text{H}]^+$  258.24917; obsd. 258.24944.



**3-(1',2'-Dicarba-closo-decaboranyl)propionic acid *N*-hydroxysuccinimide ester (105).**

Carboxylic acid **104** (80 mg, 0.37 mmol, 1 eq) in dry DCM (3 mL) was treated with *N*-hydroxysuccinimide (170 mg, 1.48 mmol, 4 eq) and EDC (283 mg, 1.48 mmol, 4 eq) and stirred for 3 h. DCM (10 mL) was added and the organic phase was washed with HCl (aq, 0.5 M, 3 × 10 mL), dried over  $\text{Na}_2\text{SO}_4$ , filtered and concentrated *in vacuo*. Silica column chromatography (5 → 40% EtOAc in PE) afforded the OSu ester **105** (102 mg, 0.33 mmol, 88%) as a white powder.  $R_f = 0.9$  (4:1 PE:EtOAc).  $^1\text{H NMR}$  (400 MHz,  $\text{CDCl}_3/\text{MeOD}$ ):  $\delta$  3.82 (s, 1H, BCH), 3.01 - 1.33 (m, 10H, 10 × BH), 2.85 - 2.70 (m, 6H,  $\text{CH}_2$ , 2 ×  $\text{CH}_2\text{-OSu}$ ), 2.58 (t,  $J = 7.6$  Hz, 2H,  $\text{CH}_2$ ).  $^{13}\text{C NMR}$  (101 MHz,  $\text{CDCl}_3/\text{MeOD}$ ):  $\delta$  169.39, 166.97, 72.92, 61.68, 31.96, 30.35, 25.49.  $^{11}\text{B NMR}$  (128 MHz,  $\text{CDCl}_3/\text{MeOD}$ ):  $\delta$  -2.21, -5.52, -9.36, -11.88, -12.84. FT-IR (thin film)  $\nu$  3060, 2953, 2928, 2852, 2580 (B-H), 1818, 1785, 1736, 1429, 1386, 1359, 1299, 1203, 1071, 1047, 994, 881, 811, 724  $\text{cm}^{-1}$ . ESI-HRMS ( $m/z$ ): calcd. for  $[\text{C}_9\text{H}_{19}\text{B}_{10}\text{NO}_4 + \text{CH}_3\text{CN} + \text{H}]^+$  355.26555; obsd. 355.26572.

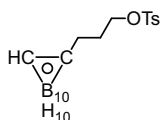


**3-[2'-(*tert*-Butyldimethylsilyl)-1',2'-dicarba-closo-dodecaboran(12)-1'-yl]-propyl 4-methylbenzenesulfonate (106).**

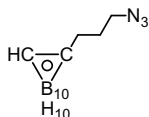
Compound **102** (0.32 g, 1 mmol) was dissolved in DCM (12.5 mL). Subsequently, *p*-tosylchloride (0.21 g, 1.1 mmol, 1.1 eq), triethylamine (0.28 mL, 2.0 mmol, 2 eq) and 4-dimethylaminopyridine (60 mg, 0.5 mmol, 0.5 eq) were added. After stirring for 3 h at room temperature, TLC showed completion of the reaction. The reaction mixture was washed with HCl (aq, 1 M, 3 × 10 mL) and brine (1 × 10 mL), followed by extraction of the aqueous layer with DCM (3 × 10 mL). The organic layers were combined, dried ( $\text{MgSO}_4$ ), filtered and concentrated under reduced pressure. Purification by silica column chromatography (2 → 3% EtOAc in PE) yielded the product as a white powder (0.45 g, 0.96 mmol, 96%).  $R_f = 0.6$  (5:1 PE:EtOAc).  $^1\text{H NMR}$  (400 MHz,  $\text{CDCl}_3$ ):  $\delta$  7.75 (d,  $J = 8.3$  Hz, 2H, 2 ×  $\text{CH}_{\text{ar}}$ ), 7.36 (d,  $J = 8.1$  Hz, 2H, 2H, 2 ×  $\text{CH}_{\text{ar}}$ ), 3.99 (t,  $J = 5.6$  Hz, 2H,  $\text{CH}_2$ ), 3.11 - 1.42 (m, 10H, 10 × BH), 2.46 (s, 3H,  $\text{CH}_3$ ), 2.34 - 2.25 (m, 2H,  $\text{CH}_2$ ), 1.91 - 1.80 (m, 2H,  $\text{CH}_2$ ), 1.03 (s, 9H, 3 ×  $\text{CH}_3$ ), 0.30 (s, 6H, 2 ×  $\text{CH}_3$ ).  $^{13}\text{C NMR}$  (101 MHz,  $\text{CDCl}_3$ ):  $\delta$  145.30, 132.86, 130.13, 128.00, 80.11, 76.60, 68.87, 34.30, 29.51, 27.66, 21.80, 20.47, -2.38.  $^{11}\text{B NMR}$  (128 MHz,  $\text{CDCl}_3$ ):  $\delta$  0.21, -3.79, -7.34, -10.28. FT-IR (thin film)  $\nu$  2937, 2571 (B-H), 1361 ( $\text{SO}_2$ ), 1176 ( $\text{SO}_2$ ), 927, 837, 817, 663  $\text{cm}^{-1}$ .

**3-[1',2'-Dicarba-closo-dodecaboran(12)-1'-yl]-propyl 4-methylbenzenesulfonate (107).**

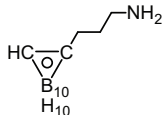
Compound **106** (1.00 g, 2.12 mmol) was dissolved in THF (25 mL) and cooled to  $-78$  °C. After addition of TBAF (1 M in THF, 2.5 mL, 2.5 mmol, 1.2 eq), the mixture was gradually warmed to room temperature and stirred for 30 min. Subsequently, the mixture was diluted with diethyl ether, washed with HCl (aq, 1 M, 3 × 20 mL) and brine (1 × 20 mL), dried ( $\text{MgSO}_4$ ), filtered and concentrated under reduced pressure. Purification by silica column chromatography (2 → 30% EtOAc in PE) yielded the product as a white powder (0.63 g, 1.78 mmol, 84%).  $R_f = 0.35$  (5:1 PE:EtOAc).  $^1\text{H NMR}$  (400 MHz,



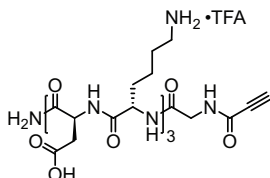
$\text{CDCl}_3$ ):  $\delta$  7.77 (d,  $J = 7.5$  Hz, 2H,  $2 \times \text{CH}_{\text{ar}}$ ), 7.37 (d,  $J = 7.6$  Hz, 2H,  $2 \times \text{CH}_{\text{ar}}$ ), 4.02 - 3.97 (m, 2H,  $\text{CH}_2$ ), 3.53 (s, 1H, BCH), 3.00 - 1.35 (m, 10H,  $10 \times \text{BH}$ ), 2.47 (s, 3H,  $\text{CH}_3$ ), 2.31 - 2.23 (m, 2H,  $\text{CH}_2$ ), 1.86 - 1.81 (m, 2H,  $\text{CH}_2$ ).  $^{13}\text{C}$  NMR (101 MHz,  $\text{CDCl}_3$ ):  $\delta$  145.42, 132.73, 130.17, 128.02, 73.98, 68.69, 61.76, 34.39, 28.74, 21.82.  $^{11}\text{B}$  NMR (128 MHz,  $\text{CDCl}_3$ ):  $\delta$  -2.25, -5.63, -9.25, -11.98, -13.03. FT-IR (thin film)  $\nu$  3062, 2579 (B-H), 1354 ( $\text{SO}_2$ ), 1173 ( $\text{SO}_2$ ), 921, 839, 659  $\text{cm}^{-1}$ .



**1-(3-Azidopropyl)-1,2-dicarba-closo-dodecaborane (107).** Compound **107** (0.64 g, 1.8 mmol) was dissolved in acetone (100 mL). Sodium azide (0.58 g, 8.9 mmol, 5 eq) and tetrabutylammonium iodide (cat.) were added and the mixture was refluxed overnight at 65 °C. After concentration of the mixture, the residue was dissolved in water (30 mL) and the compound was extracted with diethyl ether (3  $\times$  20 mL). Subsequently, the combined organic layers were dried ( $\text{MgSO}_4$ ), filtered and concentrated *in vacuo*. Purification by silica column chromatography (1  $\rightarrow$  5% EtOAc in PE) yielded the azide as a white powder (0.39 g, 1.73 mmol, 97%).  $R_f = 0.5$  (5:1 PE:EtOAc).  $^1\text{H}$  NMR (400 MHz,  $\text{CDCl}_3$ ):  $\delta$  3.58 (s, 1H, BCH), 3.31 (t,  $J = 6.3$  Hz, 2H,  $\text{CH}_2$ ), 3.03 - 1.46 (m, 10H,  $10 \times \text{BH}$ ), 2.31 - 2.25 (m, 2H,  $\text{CH}_2$ ), 1.80 - 1.69 (m, 2H,  $\text{CH}_2$ ).  $^{13}\text{C}$  NMR (101 MHz,  $\text{CDCl}_3$ ):  $\delta$  74.41, 61.64, 50.25, 35.32, 28.71.  $^{11}\text{B}$  NMR (128 MHz,  $\text{CDCl}_3$ ):  $\delta$  -2.30, -5.72, -9.26, -11.76, -13.03. FT-IR (thin film)  $\nu$  3065, 2577 (B-H), 2096 ( $\text{N}_3$ ), 1450, 1260, 1018, 721  $\text{cm}^{-1}$ .



**1-(3-Aminopropyl)-1,2-dicarba-closo-dodecaborane (109).** Compound **108** (68 mg, 0.3 mmol) and triphenylphosphine (94 mg, 0.36 mmol, 1.2 eq) were dissolved in toluene (3 mL). After stirring for 1 h, water (2 mL) was added and conversion to a white suspension occurred slowly. The mixture was stirred for 3 h and again water (2 mL) was added, followed by stirring for 3 h. Subsequently, the mixture was diluted with both EtOAc (4 mL) and water (4 mL) and the layers were separated. The aqueous layer was extracted with EtOAc (3  $\times$  8 mL). The combined organic layers were dried ( $\text{Na}_2\text{SO}_4$ ), filtered and concentrated *in vacuo*. Purification by silica column chromatography (10  $\rightarrow$  20% MeOH in DCM + 0.1% AcOH) yielded the product as a white powder (17 mg, 0.087 mmol, 29%).  $R_f = 0.7$  (1:1:1 EtOAc:H<sub>2</sub>O:n-BuOH:AcOH).  $^1\text{H}$  NMR (400 MHz,  $\text{CDCl}_3/\text{MeOD}$ ):  $\delta$  4.58 (s, 1H, BCH), 3.00 - 1.44 (m, 10H,  $10 \times \text{BH}$ ), 2.89 (t,  $J = 8$  Hz, 2H,  $\text{CH}_2$ ), 2.44 - 2.31 (m, 2H,  $\text{CH}_2$ ), 1.95 - 1.76 (m, 2H,  $\text{CH}_2$ ).  $^{13}\text{C}$  NMR (101 MHz,  $\text{CDCl}_3/\text{MeOD}$ ):  $\delta$  75.85, 63.98, 39.68, 35.36, 28.41.  $^{11}\text{B}$  NMR (128 MHz,  $\text{CDCl}_3/\text{MeOD}$ ):  $\delta$  1.88, -3.04, -5.00, -6.12, -8.66, -9.82, -10.86, -12.11, -13.33. FT-IR (thin film)  $\nu$  3444 (N-H), 3014, 2576 (B-H), 1614, 1498, 1068, 1018, 721  $\text{cm}^{-1}$ . ESI-HRMS ( $m/z$ ): calcd. for  $[\text{C}_5\text{H}_{19}\text{B}_{10}\text{N} + \text{H}]^+$  202.25934; obsd. 202.25948.



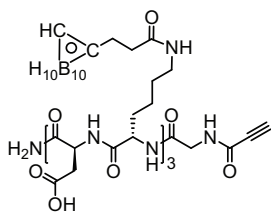
**$\text{NH}_2\text{CO}(\text{Asp-Lys})_3\text{Gly-propargyl}$  (110).** Starting from Tentagel S Rink resin (0.25 mmol) the peptide (Asp(t-Bu)-Lys(Boc))<sub>3</sub>-Gly-Fmoc was synthesized using an ABI-433A (Applied Biosystems, division of Perkin-Elmer) automated peptide synthesizer. Each cycle consisted of the following consecutive steps:

- Fmoc removal (20% piperidine in NMP (3  $\times$  3 min)).
  - NMP wash.
  - Coupling of the appropriate amino acid (1 mmol, 4 eq) with HCTU (4 eq) as the coupling agent and DiPEA (4 eq) as the base in NMP for 1 h.
  - NMP wash.
  - capping of the remaining amines with  $\text{Ac}_2\text{O}$  (5% v/v), DiPEA (0.1 M) in NMP for 3 min.
  - NMP and DCM wash.
- The last coupling was manually performed on  $\sim 0.05$  mmol resin as follows:



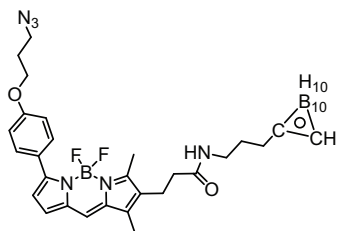
- Removal of the Fmoc groups with 20% piperidine in NMP for 20 min while shaking.
- Washing with NMP (2x), DCM (2x), NMP (1x).
- Coupling of propionic acid (16  $\mu$ L, 0.25 mmol, 5 eq) with EEDQ (62 mg, 0.25 mmol, 5 eq) in NMP for 1 h, while shaking.
- Washing with NMP (2x), DCM (2x), NMP (1x).

The peptide was globally deprotected and cleaved off the resin by treatment with 2% TIS in TFA for 3  $\times$  30 min, precipitated from ice-cold Et<sub>2</sub>O and spinned down to give a white pellet. Lyophilizing from water/ACN/*t*-BuOH yielded the peptide (33 mg, 28  $\mu$ mol, 56%). <sup>1</sup>H NMR (400 MHz, MeOD):  $\delta$  4.72 (dd, *J* = 8.6, 5.0 Hz, 1H, CH), 4.68 - 4.59 (m, 2H, 2  $\times$  CH), 4.33 - 4.18 (m, 3H, 3  $\times$  CH), 4.05 - 3.86 (m, 2H, CH<sub>2</sub>), 3.74 (s, 1H,  $\equiv$ CH), 3.06 - 2.76 (m, 12H, 6  $\times$  CH<sub>2</sub>), 2.03 - 1.75 (m, 6H, 3  $\times$  CH<sub>2</sub>), 1.75 - 1.63 (m, 6H, 3  $\times$  CH<sub>2</sub>), 1.57 - 1.43 (m, 6H, 3  $\times$  CH<sub>2</sub>). <sup>13</sup>C NMR (101 MHz, MeOD):  $\delta$  175.53, 174.81, 174.55, 174.29, 174.26, 174.09, 173.91, 173.80, 173.65, 171.97, 155.35, 77.87, 77.07, 55.79, 55.63, 55.18, 52.24, 52.03, 51.37, 43.91, 40.59, 40.53, 40.46, 36.62, 35.97, 35.89, 31.56, 31.34, 28.02, 27.88, 27.83, 23.74, 23.62, 23.50. ESI-HRMS (*m/z*): calcd. for [C<sub>35</sub>H<sub>57</sub>N<sub>11</sub>O<sub>14</sub> + H]<sup>+</sup> 856.41592; obsd. 856.41613.



**Carboranyl-peptide (111).** Peptide **110** (26 mg, 22  $\mu$ mol) was suspended in DMF (7 mL) and carborane-OSu **105** (34 mg, 0.1 mmol, 4 eq) and DiPEA (28  $\mu$ L, 0.15 mmol, 6 eq) were added. The product dissolved in DMF and LC/MS analysis indicated complete conversion after 15 h. The product was crashed out of the solution with ice-cold Et<sub>2</sub>O, collected and lyophilized from dioxane. Analysis showed that the product (34 mg, 0.022 mmol, quant) was sufficiently pure (~90%) to be used in the next step without any further purification.

<sup>1</sup>H NMR (400 MHz, CDCl<sub>3</sub>/MeOD):  $\delta$  4.78 - 4.71 (m, 1H, CH), 4.24 - 4.06 (m, 6H, 3  $\times$  CH<sub>α</sub>, 3  $\times$  BCH), 3.93 (q, *J* = 16.3 Hz, 2H, CH<sub>2</sub>), 3.70 (s, 1H,  $\equiv$ CH), 3.24 - 3.12 (m, 6H, 3  $\times$  CH<sub>2</sub>), 3.01-1.46 (m, 30H, 30  $\times$  BH), 2.96 - 2.79 (m, 6H, 3  $\times$  CH<sub>2</sub>), 2.63 - 2.55 (m, 6H, 3  $\times$  CH<sub>2</sub>), 2.47 - 2.38 (m, 6H, 3  $\times$  CH<sub>2</sub>), 1.91 - 1.76 (m, 6H, 3  $\times$  CH<sub>2</sub>), 1.50 (s, 6H, 3  $\times$  CH<sub>2</sub>), 1.42 - 1.33 (m, 6H, 3  $\times$  CH<sub>2</sub>). <sup>13</sup>C NMR (101 MHz, CDCl<sub>3</sub>/MeOD):  $\delta$  174.20, 173.44, 173.22, 173.09, 172.69, 172.59, 172.50, 171.48, 171.42, 170.48, 153.79, 76.51, 75.51, 74.68, 62.02, 55.19, 54.78, 54.64, 51.13, 50.89, 50.01, 42.56, 39.08, 39.01, 38.81, 35.58, 35.30, 35.10, 34.90, 33.04, 30.33, 30.15, 29.89, 28.50, 28.37, 22.83, 22.74, 22.66. <sup>11</sup>B NMR (128 MHz, CDCl<sub>3</sub>/MeOD):  $\delta$  -2.58, -5.83, -9.64, -11.88. LC/MS analysis (linear gradient 10  $\rightarrow$  90% ACN) *t*<sub>R</sub>: 10.69 min, ESI-MS (*m/z*): [M + H]<sup>+</sup>: 1451.73. ESI-HRMS (*m/z*): calcd. for [C<sub>50</sub>H<sub>99</sub>B<sub>30</sub>N<sub>11</sub>O<sub>17</sub> + H]<sup>+</sup> 1451.03027; obsd. 1451.03482.

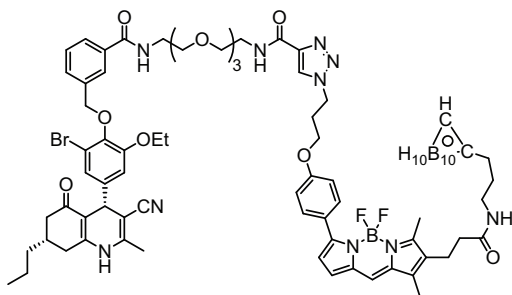


**Azido-BODIPY-carborane (132).** Amino-carborane **109** (5.8 mg, 29  $\mu$ mol, 1.1 eq) and azido-BODIPY-OSu **36** (14.6 mg, 26  $\mu$ mol, 1 eq) were dissolved in DMF (1 mL) and DiPEA (5  $\mu$ L, 29  $\mu$ mol, 1 eq) was added. After 3 h the reaction was concentrated and co-evaporated with toluene. Purification by silica column chromatography (0  $\rightarrow$  60% EtOAc in PE) yielded BODIPY-carborane (10 mg, 15  $\mu$ mol) as a purple solid in 56% yield. *R*<sub>f</sub> = 0.2 (1:1 PE:EtOAc) <sup>1</sup>H NMR (400 MHz, CDCl<sub>3</sub>):  $\delta$  7.89 - 7.84 (m, 2H, 2  $\times$  CH<sub>ar</sub>), 7.11

(s, 1H, CH<sub>ar</sub>), 6.99 (d, *J* = 4.1 Hz, 1H, CH<sub>ar</sub>), 6.98 - 6.95 (m, 2H, 2  $\times$  CH<sub>ar</sub>), 6.56 (d, *J* = 4.1 Hz, 1H, CH<sub>ar</sub>), 5.40 (t, *J* = 6.0 Hz, 1H, NH), 4.11 (t, *J* = 5.9 Hz, 2H, CH<sub>2</sub>), 3.62 - 3.57 (m, 1H, BCH), 3.54 (t, *J* = 6.6 Hz, 2H, CH<sub>2</sub>), 3.14 (q, *J* = 6.6 Hz, 2H, CH<sub>2</sub>), 3.00-1.00 (m, 10H, 10  $\times$



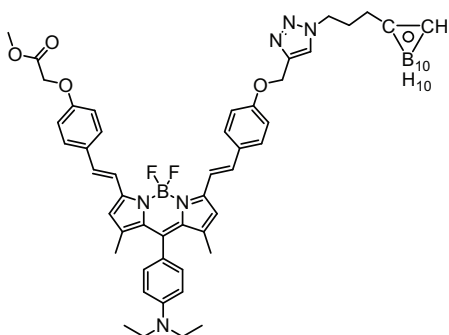
BH), 2.75 (t,  $J = 7.0$  Hz, 2H, CH<sub>2</sub>), 2.49 (s, 3H, CH<sub>3</sub>), 2.28 (t,  $J = 7.1$  Hz, 2H, CH<sub>2</sub>), 2.21 (s, 3H, CH<sub>3</sub>), 2.12 - 2.04 (m, 4H, 2 × CH<sub>2</sub>), 1.65 - 1.52 (m, 2H, CH<sub>2</sub>). <sup>13</sup>C NMR (101 MHz, CDCl<sub>3</sub>):  $\delta$  172.24, 171.58, 159.73, 158.98, 156.21, 139.79, 135.21, 134.21, 130.88, 130.17, 128.63, 125.63, 123.05, 118.93, 114.37, 74.53, 64.61, 61.49, 48.36, 38.66, 36.56, 35.22, 29.84, 29.40, 28.89, 25.52, 20.15, 13.29, 9.79. <sup>11</sup>B NMR (128 MHz, CDCl<sub>3</sub>):  $\delta$  1.12 (t), -2.40, -5.78, -9.42, -11.88, -13.08. LC/MS analysis (linear gradient 50 → 90% ACN)  $t_R$ : 9.54 min, ESI-MS ( $m/z$ ): [M + H]<sup>+</sup>: 630.53.



***m*-DHP-BODIPY-carborane (112).** *Meta*-

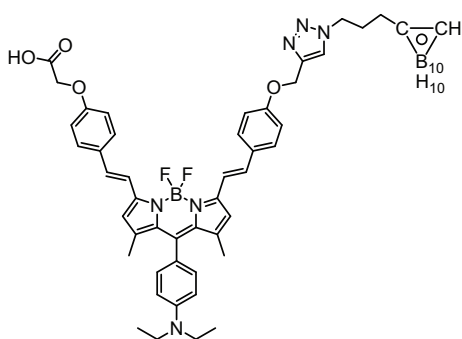
DHP-alkyne *m*-78a (6 mg, 7.5  $\mu$ mol, 1.2 eq) and azido-BODIPY-carborane 132 (3.9 mg, 6  $\mu$ mol, 1 eq) were dissolved in DCM (1.5 mL) and water (1 mL), and sodium ascorbate (aq, 1.2 eq) and CuSO<sub>4</sub> (aq, 20mol%) were added. After 3 h the reaction was finished, the organic layer was washed with water (2 × 5 mL), dried (Na<sub>2</sub>SO<sub>4</sub>), filtered and concentrated. Purification by silica column chromatography (0 → 3% MeOH in DCM)

yielded DHP-BODIPY-carborane (5.8 mg, 4  $\mu$ mol) as a purple solid in 67% yield.  $R_f = 0.2$  (10:1 DCM:MeOH) <sup>1</sup>H NMR (600 MHz, CDCl<sub>3</sub>):  $\delta$  8.05 (s, 1H, CH<sub>trz</sub>), 8.01 (s, 1H, CH<sub>ar</sub>), 7.84 (d,  $J = 8.8$  Hz, 2H, 2 × CH<sub>ar</sub>), 7.75 (d,  $J = 7.7$  Hz, 1H, CH<sub>ar</sub>), 7.62 (d,  $J = 7.6$  Hz, 1H, CH<sub>ar</sub>), 7.56 (s, 1H, NH), 7.41 (t,  $J = 7.7$  Hz, 1H, CH<sub>ar</sub>), 7.10 (s, 1H, CH<sub>ar</sub>), 6.99 - 6.94 (m, 2H, CH<sub>ar</sub>, NH), 6.94 - 6.89 (m, 3H, 3 × CH<sub>ar</sub>), 6.82 (d,  $J = 1.8$  Hz, 1H, CH<sub>ar</sub>), 6.55 (d,  $J = 4.1$  Hz, 1H, CH<sub>ar</sub>), 5.76 (s, 1H, NH), 5.02 (s, 2H, CH<sub>2</sub>), 4.60 (t,  $J = 6.6$  Hz, 2H, CH<sub>2</sub>), 4.54 (s, 1H, CH), 4.14 - 4.07 (m, 2H, CH<sub>2</sub>), 4.00 (q,  $J = 6.7, 4.9$  Hz, 2H, CH<sub>2</sub>), 3.70 - 3.57 (m, 17H, 8 × CH<sub>2</sub>, BCH), 3.13 (q,  $J = 6.6$  Hz, 2H, CH<sub>2</sub>), 2.90-1.10 (m, 10H, 10 × BH), 2.74 (t,  $J = 7.1$  Hz, 2H, CH<sub>2</sub>), 2.48 (s, 3H, CH<sub>3</sub>), 2.46 - 2.30 (m, 5H, 2 × CH<sub>2</sub>, CH<sub>2</sub>-H<sup>a</sup>), 2.28 (t,  $J = 7.2$  Hz, 2H, CH<sub>2</sub>), 2.21 (s, 3H, CH<sub>3</sub>), 2.17 - 2.13 (m, 1H, CH), 2.11 - 2.03 (m, 6H, CH<sub>3</sub>, CH<sub>2</sub>, CH<sub>2</sub>-H<sup>b</sup>), 1.61 - 1.51 (m, 2H, CH<sub>2</sub>), 1.42 (t,  $J = 6.9$  Hz, 3H, CH<sub>3</sub>), 1.34 - 1.22 (m, 4H, 2 × CH<sub>2</sub>), 0.87 (t,  $J = 6.9$  Hz, 3H, CH<sub>3</sub>). <sup>13</sup>C NMR (151 MHz, CDCl<sub>3</sub>):  $\delta$  195.77, 172.09, 167.81, 160.30, 159.43, 159.26, 155.75, 152.79, 149.75, 145.10, 144.15, 143.36, 142.33, 140.09, 138.17, 135.15, 134.81, 134.38, 131.31, 130.95, 130.49, 128.68, 128.47, 126.91, 126.11, 125.86, 123.13, 122.98, 118.80, 118.10, 114.33, 113.01, 110.04, 88.17, 74.65, 74.16, 70.74, 70.71, 70.58, 70.48, 69.91, 69.80, 64.73, 63.99, 61.53, 47.67, 43.51, 40.01, 39.14, 38.59, 38.28, 37.54, 36.41, 35.28, 33.95, 33.69, 29.90, 29.44, 20.17, 19.91, 18.62, 14.98, 14.20, 13.35, 9.81. <sup>11</sup>B NMR (128 MHz, CDCl<sub>3</sub>):  $\delta$  1.12 (t), -2.41, -5.56, -9.44, -11.88. LC/MS analysis (linear gradient 50 → 90% ACN)  $t_R$ : 9.17 min, ESI-MS ( $m/z$ ): [M + H]<sup>+</sup>: 1457.60. ESI-HRMS ( $m/z$ ): calcd. for [C<sub>69</sub>H<sub>90</sub>B<sub>11</sub>BrF<sub>2</sub>N<sub>10</sub>O<sub>10</sub> + H]<sup>+</sup> 1457.71414; obsd. 1457.71636.



**1,7-dimethyl-3-[(E)-4-(2-methoxy-2-oxoethoxy)styryl]-5-[(E)-4-((1-(3-[1',2'-dicarba-closo-dodecaboran(12)-1'-yl]-propyl)-1H-1,2,3-triazol-4-yl)methoxy)styryl]-8-[4-(N,N-diethylamino)phenyl]-4,4-difluoro-4-bora-3a,4a-diaza-s-indacene (133).** BODIPY **32** (7 mg, 9.8  $\mu\text{mol}$ ) and azido-carborane **108** (2.3 mg, 10.1  $\mu\text{mol}$ , 1.03 eq) were dissolved in DCM (1 mL). The mixture was put under an argon atmosphere, followed by the addition of sodium ascorbate (2 mg, 9.8  $\mu\text{mol}$ ) and a catalytic amount of copper(II)sulfate. The mixture was stirred at rt for 1 h when TLC analysis showed completion. The

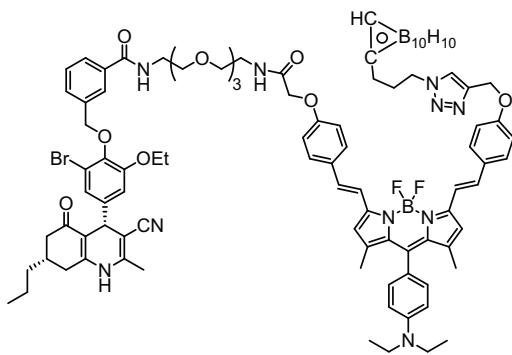
product was purified by silica column chromatography (0.2  $\rightarrow$  0.4% MeOH in DCM). Crystallization from DCM/hexanes yielded the product as blue crystals (8.8 mg, 9.36  $\mu\text{mol}$ , 93%).  $R_f = 0.8$  (1:1 PE : EtOAc)  $^1\text{H}$  NMR (400 MHz,  $\text{CDCl}_3$ ):  $\delta$  7.67 - 7.53 (m, 7H, 4  $\times$   $\text{CH}_{\text{ar}}$ , 3  $\times$  =CH), 7.18 (d,  $J = 16.2$  Hz, 2H, 2  $\times$  =CH), 7.05 (d,  $J = 8.7$  Hz, 2H, 2  $\times$   $\text{CH}_{\text{ar}}$ ), 6.99 (d,  $J = 8.8$  Hz, 2H, 2  $\times$   $\text{CH}_{\text{ar}}$ ), 6.93 (d,  $J = 8.8$  Hz, 2H, 2  $\times$   $\text{CH}_{\text{ar}}$ ), 6.75 (d,  $J = 8.8$  Hz, 2H, 2  $\times$   $\text{CH}_{\text{ar}}$ ), 6.61 (s, 2H, 2  $\times$  =CH), 5.25 (s, 2H,  $\text{CH}_2$ ), 4.68 (s, 2H,  $\text{CH}_2$ ), 4.33 (t,  $J = 6.5$  Hz, 2H,  $\text{CH}_2$ ), 3.83 (s, 3H,  $\text{CH}_3$ ), 3.52 (s, 1H, BCH), 3.41 (q,  $J = 7.0$  Hz, 4H, 2  $\times$   $\text{CH}_2$ ), 3.00 - 1.45 (m, 10H, 10  $\times$  BH), 2.26 - 2.18 (m, 2H,  $\text{CH}_2$ ), 2.18 - 2.06 (m, 2H,  $\text{CH}_2$ ), 1.58 (s, 3H,  $\text{CH}_3$ ), 1.57 (s, 3H,  $\text{CH}_3$ ), 1.21 (t,  $J = 7.0$  Hz, 6H, 2  $\times$   $\text{CH}_3$ ).  $^{13}\text{C}$  NMR (101 MHz,  $\text{CDCl}_3$ ):  $\delta$  169.31, 158.76, 158.41, 152.16, 152.06, 148.33, 144.60, 142.43, 142.36, 140.54, 134.99, 134.88, 134.22, 130.89, 130.46, 129.47, 129.08, 122.83, 121.46, 118.21, 118.02, 117.36, 115.25, 115.06, 112.05, 73.78, 65.46, 62.14, 61.82, 52.51, 49.20, 44.51, 35.09, 29.83, 15.13, 12.54.  $^{11}\text{B}$  NMR (128 MHz,  $\text{CDCl}_3$ ):  $\delta$  1.17 (t), -2.16, -5.43, -9.18, -11.93, -12.83. FT-IR (thin film)  $\nu$  2964, 2580 (B-H), 1749, 1598, 1508, 1481, 1197, 1161, 987, 817  $\text{cm}^{-1}$ . ESI-HRMS ( $m/z$ ): calcd. for  $[\text{C}_{48}\text{H}_{59}\text{B}_{11}\text{F}_2\text{N}_6\text{O}_4 + \text{H}]^+$  941.57349; obsd. 941.57629.



**1,7-dimethyl-3-[(E)-4-(carboxymethoxy)styryl]-5-[(E)-4-((1-(3-[1',2'-dicarba-closo-dodecaboran(12)-1'-yl]-propyl)-1H-1,2,3-triazol-4-yl)methoxy)styryl]-8-[4-(N,N-diethylamino)phenyl]-4,4-difluoro-4-bora-3a,4a-diaza-s-indacene (134).** A solution of LiOH (0.2 mg, 25.5  $\mu\text{mol}$ , 3 eq) in water (1 mL) was added to a solution of **133** (8 mg, 8.5  $\mu\text{mol}$ ) in THF (2 mL). The mixture was stirred for 4 h at rt, followed by addition of a solution of LiOH (0.1 mg, 13  $\mu\text{mol}$ , 1.5 eq) in water (8.5  $\mu\text{L}$ ). After 1 h at rt, the mixture was diluted with diethyl ether and acidified with HCl (aq, 1 M). The aqueous

layer was extracted with diethyl ether (3  $\times$  1.5 mL) and EtOAc (3  $\times$  1.5 mL). The combined organic layers were dried ( $\text{Na}_2\text{SO}_4$ ), filtered and concentrated under reduced pressure. Subsequently, the product was purified by silica column chromatography (2  $\rightarrow$  6% MeOH in DCM). Crystallization from DCM/hexanes yielded the product as blue crystals (6.1 mg, 6.6  $\mu\text{mol}$ , 78%).  $R_f = 0.2$  (1:1 EtOAc:PE + 0.01% AcOH)  $^1\text{H}$  NMR (400 MHz,  $\text{CDCl}_3/\text{MeOD}$ ):  $\delta$  7.97 (s, 1H, =CH), 7.63 - 7.53 (m, 6H, 4  $\times$   $\text{CH}_{\text{ar}}$ , 2  $\times$  =CH), 7.28 (d,  $J = 16.1$  Hz, 2H, 2  $\times$  =CH), 7.12 - 7.03 (m, 4H, 4  $\times$   $\text{CH}_{\text{ar}}$ ), 6.99 (d,  $J = 8.5$  Hz, 2H, 2  $\times$   $\text{CH}_{\text{ar}}$ ), 6.83 (d,  $J = 8.6$  Hz, 2H, 2  $\times$   $\text{CH}_{\text{ar}}$ ), 6.70 (s, 2H, 2  $\times$  =CH), 5.24 (s, 2H,  $\text{CH}_2$ ), 4.67 (s, 2H,  $\text{CH}_2$ ), 4.41 (t,  $J = 6.6$  Hz, 2H,  $\text{CH}_2$ ), 4.26 (s, 1H, BCH), 3.45 (q,  $J = 7.0$  Hz, 4H, 2  $\times$   $\text{CH}_2$ ), 3.02 - 1.11 (m, 10H, 10  $\times$  BH), 2.31 - 2.24 (m, 2H,  $\text{CH}_2$ ), 2.17 - 2.08 (m, 2H,  $\text{CH}_2$ ),

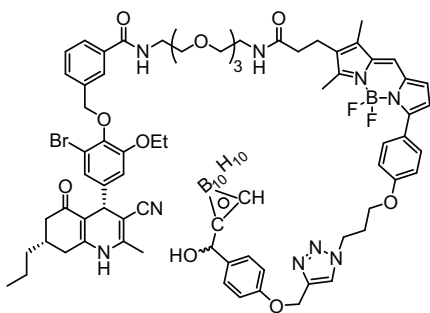
1.61 (s, 6H, 2 × CH<sub>3</sub>), 1.22 (t, *J* = 7.0 Hz, 6H, 2 × CH<sub>3</sub>). <sup>13</sup>C NMR (151 MHz, CDCl<sub>3</sub>/MeOD): δ 158.95, 152.34, 152.14, 148.54, 144.31, 142.73, 142.59, 140.64, 135.46, 135.23, 134.27, 134.22, 130.58, 129.55, 129.12, 123.70, 121.50, 117.81, 117.71, 117.57, 117.48, 115.36, 115.24, 112.34, 74.18, 62.20, 61.87, 44.63, 34.89, 29.89, 15.08, 12.44. <sup>11</sup>B NMR (128 MHz, CDCl<sub>3</sub>/MeOD): δ 1.18 (t), -2.48, -5.65, -9.36, -11.85, -13.00. FT-IR (thin film) *v* 2958, 2586 (B-H), 1734, 1600, 1458, 1489, 1199, 1165, 991. cm<sup>-1</sup>. ESI-HRMS (*m/z*): calcd. for [C<sub>47</sub>H<sub>57</sub>B<sub>11</sub>F<sub>2</sub>N<sub>6</sub>O<sub>4</sub> + H]<sup>+</sup> 927.55784; obsd. 927.56012.



### *m*-DHP-pH dependent BODIPY-carborane

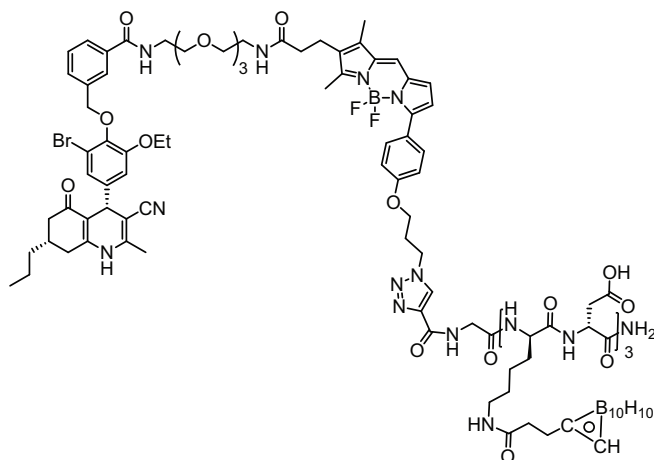
(113). To a solution of amino-DHP *m*-76a (3 mg, 4 μmol, 1.2 eq) and BODIPY-carborane-acid 134 (3 mg, 3.2 μmol, 1 eq) in DCM (1 mL) were added EDC (1.2 mg, 6.4 μmol, 2 eq), HOBT (0.87 mg, 6.4 μmol, 2 eq) and DiPEA (1.1 μL, 6.4 μmol, 2 eq). The mixture was stirred for 16 h at room temperature, and subsequently washed with HCl (aq, 1 M, 2 × 5 mL), water (1 × 5 mL), dried (Na<sub>2</sub>SO<sub>4</sub>), filtered and concentrated under reduced pressure. Purification by silica column chromatography (0.2 → 5%

MeOH in DCM), followed by crystallization from DCM/hexanes yielded the product as blue crystals (2.8 mg, 1.7 μmol, 53%). *R*<sub>f</sub> = 0.6 (10:1 DCM:MeOH) <sup>1</sup>H NMR (600 MHz, CDCl<sub>3</sub>): δ 7.98 (s, 1H, CH<sub>ar</sub>), 7.79 (d, *J* = 7.8 Hz, 1H, CH<sub>ar</sub>), 7.64 - 7.52 (m, 6H, 6 × CH<sub>ar</sub>), 7.45 - 7.40 (m, 1H, CH<sub>ar</sub>), 7.26 - 7.13 (m, 7H, 7 × CH<sub>ar</sub>), 7.09 (s, 1H, CH<sub>ar</sub>), 7.04 - 6.97 (m, 3H, 2 × CH<sub>ar</sub>, NH), 6.97 - 6.88 (m, 3H, 2 × CH<sub>ar</sub>, NH), 6.83 - 6.72 (m, 3H, 2 × CH<sub>ar</sub>, NH), 6.63 (d, *J* = 6.0 Hz, 1H, CH<sub>ar</sub>), 5.25 (s, 2H, CH<sub>2</sub>), 5.03 (s, 2H, CH<sub>2</sub>), 4.51 (s, 2H, CH<sub>2</sub>), 4.49 (s, 1H, CH), 4.32 (t, *J* = 6.6 Hz, 2H, CH<sub>2</sub>), 4.14 - 4.07 (m, 2H, CH<sub>2</sub>), 3.68 - 3.48 (m, 19H, 9 × CH<sub>2</sub>, BCH), 3.45 - 3.41 (m, 2H, CH<sub>2</sub>), 2.48 - 1.80 (m, 22H, 4 × CH<sub>2</sub>, CH<sub>3</sub>, CH, 10 × BH), 1.59 (s, 6H, 2 × CH<sub>3</sub>), 1.42 (t, *J* = 7.0 Hz, 3H, CH<sub>3</sub>), 1.32 - 1.16 (m, 10H, 2 × CH<sub>2</sub>, 2 × CH<sub>3</sub>), 0.90 - 0.83 (m, 3H, CH<sub>3</sub>). <sup>13</sup>C NMR (151 MHz, CDCl<sub>3</sub>): δ 195.69, 168.19, 167.67, 159.00, 157.99, 152.80, 149.70, 145.00, 144.45, 144.14, 142.38, 138.03, 135.47, 134.89, 131.25, 130.98, 130.21, 129.19, 129.06, 128.73, 128.37, 127.26, 126.60, 125.44, 123.02, 122.99, 119.42, 118.18, 118.08, 117.71, 115.36, 115.25, 113.01, 109.97, 88.13, 74.22, 73.84, 70.70, 70.68, 70.45, 70.00, 69.72, 68.77, 68.24, 67.53, 64.75, 62.13, 61.85, 51.06, 49.22, 43.46, 39.94, 38.97, 38.26, 37.60, 35.05, 33.98, 33.66, 29.85, 19.90, 18.55, 15.18, 14.97, 14.23. <sup>11</sup>B NMR (128 MHz, CDCl<sub>3</sub>/MeOD): δ 1.19 (t), -2.24, -5.53, -9.21, -11.92. ESI-HRMS (*m/z*): calcd. for [C<sub>85</sub>H<sub>104</sub>B<sub>11</sub>BrF<sub>2</sub>N<sub>10</sub>O<sub>10</sub> + 2H]<sup>2+</sup> 832.41548; obsd. 832.41631.



***m*-DHP-BODIPY-carborane (114).** Compound **93** (2.73 mg, 2.27  $\mu\text{mol}$ ) and alkyne-carborane **100** (0.83 mg, 2.72  $\mu\text{mol}$ , 1.2 eq) were dissolved in DCM (1 mL) and sodium ascorbate (aq, 4.54  $\mu\text{mol}$ , 2 eq) and  $\text{CuSO}_4$  (aq, 0.45  $\mu\text{mol}$ , 20 mol%) were added. The mixture was stirred for 16 h, and subsequently washed with water ( $2 \times 5$  mL), dried ( $\text{MgSO}_4$ ), filtered and concentrated *in vacuo*. Purification by silica column chromatography (0  $\rightarrow$  4% MeOH in DCM), gave the product as a purple solid (2.56 mg, 1.7  $\mu\text{mol}$ , 75%).  $R_f = 0.6$  (10:1 DCM:MeOH)  $^1\text{H}$  NMR (600 MHz,  $\text{CDCl}_3/\text{MeOD}$ ):  $\delta$  7.97 (s, 1H,

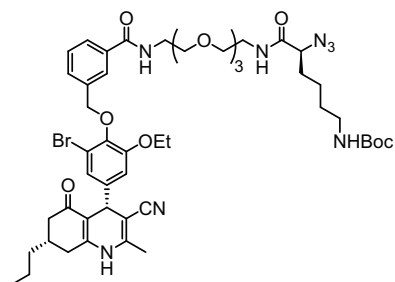
$\text{CH}_{\text{ar}}$ ), 7.85 (d,  $J = 8.9$  Hz, 2H,  $2 \times \text{CH}_{\text{ar}}$ ), 7.80 (s, 1H,  $\text{CH}_{\text{trz}}$ ), 7.75 (d,  $J = 7.8$  Hz, 1H,  $\text{CH}_{\text{ar}}$ ), 7.71 (d,  $J = 7.7$  Hz, 1H,  $\text{CH}_{\text{ar}}$ ), 7.44 (t,  $J = 7.7$  Hz, 1H,  $\text{CH}_{\text{ar}}$ ), 7.26 (d,  $J = 8.7$  Hz, 2H,  $2 \times \text{CH}_{\text{ar}}$ ), 7.19 (s, 1H,  $\text{CH}_{\text{ar}}$ ), 6.99 (d,  $J = 4.1$  Hz, 1H,  $\text{CH}_{\text{ar}}$ ), 6.97 - 6.92 (m, 4H,  $4 \times \text{CH}_{\text{ar}}$ ), 6.90 - 6.87 (m, 2H,  $2 \times \text{CH}_{\text{ar}}$ ), 6.55 (d,  $J = 4.1$  Hz, 1H,  $\text{CH}_{\text{ar}}$ ), 5.19 (s, 2H,  $\text{CH}_2$ ), 5.13 (s, 1H, CH), 5.01 (s, 2H,  $\text{CH}_2$ ), 4.65 (t,  $J = 6.8$  Hz, 2H,  $\text{CH}_2$ ), 4.53 (s, 1H, CH), 4.15 - 4.09 (m, 2H,  $\text{CH}_2$ ), 4.08 (s, 1H, BCh), 4.04 (t,  $J = 5.7$  Hz, 2H,  $\text{CH}_2$ ), 3.96 (s, 1H, OH), 3.66 - 3.60 (m, 8H,  $4 \times \text{CH}_2$ ), 3.58 - 3.56 (m, 2H,  $\text{CH}_2$ ), 3.52 - 3.49 (m, 2H,  $\text{CH}_2$ ), 3.44 (t,  $J = 5.2$  Hz, 2H,  $\text{CH}_2$ ), 3.32 (t,  $J = 5.2$  Hz, 2H,  $\text{CH}_2$ ), 2.79 - 1.68 (m, 10H,  $10 \times \text{BH}$ ), 2.73 (t,  $J = 7.5$  Hz, 2H,  $\text{CH}_2$ ), 2.51 (s, 4H,  $\text{CH}_3$ ,  $\text{CH}_2\text{-H}^{\text{a}}$ ), 2.48 - 2.43 (m, 3H,  $\text{CH}_2$ ,  $\text{CH}_2\text{-H}^{\text{a}}$ ), 2.40 - 2.35 (m, 1H,  $\text{CH}_2\text{-H}^{\text{b}}$ ), 2.31 (t,  $J = 7.5$  Hz, 2H,  $\text{CH}_2$ ), 2.22 (s, 4H,  $\text{CH}_3$ , CH), 2.16 - 2.09 (m, 4H,  $\text{CH}_3$ ,  $\text{CH}_2\text{-H}^{\text{b}}$ ), 1.43 (t,  $J = 7.0$  Hz, 3H,  $\text{CH}_3$ ), 1.39 - 1.33 (m, 4H,  $2 \times \text{CH}_2$ ), 0.94 - 0.90 (m, 3H,  $\text{CH}_3$ ).  $^{13}\text{C}$  NMR (151 MHz,  $\text{CDCl}_3/\text{MeOD}$ ):  $\delta$  197.15, 173.36, 168.92, 160.09, 159.46, 158.80, 155.37, 152.99, 151.95, 146.38, 144.26, 144.05, 143.11, 140.69, 138.24, 135.32, 134.84, 134.68, 133.12, 131.80, 131.02, 130.96, 128.86, 128.40, 128.28, 127.22, 127.11, 126.38, 124.32, 123.42, 119.93, 118.50, 118.18, 114.78, 114.47, 112.99, 109.44, 87.58, 86.80, 80.63, 74.46, 74.18, 70.68, 70.65, 70.31, 70.26, 70.01, 69.92, 64.88, 64.39, 61.90, 59.74, 47.74, 43.50, 40.08, 39.59, 38.62, 37.57, 36.17, 33.98, 33.06, 29.95, 20.46, 20.10, 17.97, 14.92, 14.16, 13.16, 9.59. LC/MS analysis (linear gradient 10  $\rightarrow$  90% ACN)  $t_R$ : 11.54 min, ESI-MS ( $m/z$ ):  $[\text{M} + \text{H}]^+$ : 1508.27. ESI-HRMS ( $m/z$ ): calcd. for  $[\text{C}_{73}\text{H}_{91}\text{B}_{11}\text{BrF}_2\text{N}_9\text{O}_{11} + \text{H}]^+$  1508.71841; obsd. 1508.71380.



***m*-DHP-BODIPY-carboranyl peptide (115).**

*m*-DHP-BODIPY-azide **93** (4 mg, 3.5  $\mu$ mol) and carboranyl peptide **111** (6.85 mg, 4.7  $\mu$ mol, 1.3 eq) were dissolved in dioxane (1 mL) and sodium ascorbate (aq, 9.4  $\mu$ mol, 2 eq) and CuSO<sub>4</sub> (aq, 0.9  $\mu$ mol, 20 mol%) were added. The mixture was stirred for 16 h and concentrated *in vacuo*. Purification by silica column chromatography (10  $\rightarrow$  50% MeOH in DCM), followed by lyophilizing from

dioxane/H<sub>2</sub>O gave the product as a purple solid (7.36 mg, 2.8  $\mu$ mol, 79%). <sup>1</sup>H NMR (600 MHz, CDCl<sub>3</sub>/MeOD):  $\delta$  8.45 (s, 1H, CH<sub>trz</sub>), 7.99 (s, 1H, CH<sub>ar</sub>), 7.85 (d, *J* = 8.2 Hz, 2H, 2  $\times$  CH<sub>ar</sub>), 7.77 (d, *J* = 7.6 Hz, 1H, CH<sub>ar</sub>), 7.70 (d, *J* = 7.2 Hz, 1H, CH<sub>ar</sub>), 7.45 (t, *J* = 7.3 Hz, 1H, CH<sub>ar</sub>), 7.26 (s, 1H, CH<sub>ar</sub>), 7.01-6.88 (m, 5H, 5  $\times$  CH<sub>ar</sub>), 6.56 (s, 1H, CH<sub>ar</sub>), 5.01 (s, 2H, CH<sub>2</sub>), 4.52 (s, 4H, 4  $\times$  CH), 4.40-4.20 (m, 6H, 3  $\times$  BCH, 3  $\times$  CH), 4.19 - 3.96 (m, 6H, 3  $\times$  CH<sub>2</sub>), 3.76 - 3.41 (m, 16H, 8  $\times$  CH<sub>2</sub>), 3.24 - 3.08 (m, 6H, 3  $\times$  CH<sub>2</sub>), 2.79 - 0.81 (m, 96H, 5  $\times$  CH<sub>3</sub>, 24  $\times$  CH<sub>2</sub>, CH, 30  $\times$  BH). LC/MS analysis (linear gradient 10  $\rightarrow$  90% ACN) *t*<sub>R</sub>: 11.98 min, ESI-MS (*m/z*): [M + H]<sup>2+</sup>: 1327.40. ESI-HRMS (*m/z*): calcd. for [C<sub>111</sub>H<sub>170</sub>B<sub>31</sub>BrF<sub>2</sub>N<sub>20</sub>O<sub>26</sub> + H]<sup>+</sup> 2653.49555; obsd. 2653.49652.

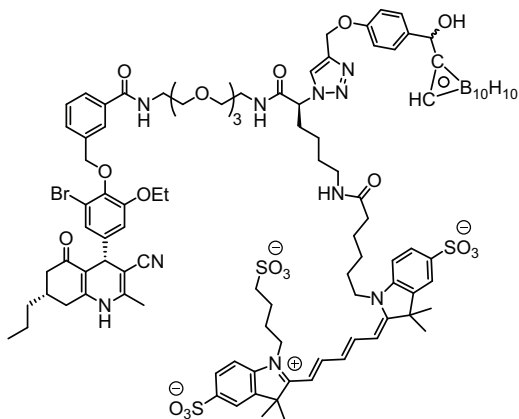


***tert*-Butyl (16-azido-1-(3-((2-bromo-4-(*4R,7S*)-3-cyano-2-methyl-5-oxo-7-propyl-1,4,5,6,7,8-hexahydroquinolin-4-yl)-6-ethoxyphenoxy)methyl)phenyl)-1,15-dioxo-5,8,11-trioxo-2,14-diazaisocosa-20-yl) carbamate (135).**

Amino-DHP *m*-76a (9 mg, 12  $\mu$ mol) *N*H<sub>Boc</sub> was added to a pre-activated solution of (*S*)-(-)-2-Azido-6-(Boc-amino)hexanoic acid (dicyclohexyl ammonium) salt (6 mg, 13  $\mu$ mol, 1.1 eq), EDC (5 mg, 26  $\mu$ mol, 2.2 eq), HOBT (3.5 mg, 26  $\mu$ mol, 2.2 eq) and TEA (3.6  $\mu$ L, 26  $\mu$ mol, 2.2 eq) in DCM (2 mL). The mixture was stirred for 3 h at room temperature, before being purified by silica

column chromatography (0  $\rightarrow$  5% MeOH in DCM), yielding compound **135** as a colorless solid (9 mg, 8.9  $\mu$ mol, 74%). <sup>1</sup>H NMR (400 MHz, CDCl<sub>3</sub>):  $\delta$  8.03 (s, 1H, CH<sub>ar</sub>), 7.77 (d, *J* = 7.7 Hz, 1H, CH<sub>ar</sub>), 7.65 (d, *J* = 7.5 Hz, 1H, CH<sub>ar</sub>), 7.45 (t, *J* = 7.7 Hz, 1H, CH<sub>ar</sub>), 7.19 (s, 1H, NH), 6.93 (s, 2H, CH<sub>ar</sub>, NH), 6.84 - 6.76 (m, 2H, CH<sub>ar</sub>, NH), 5.04 (s, 2H, CH<sub>2</sub>), 4.69 (s, 1H, NH), 4.56 (s, 1H, CH), 4.13 (dd, *J* = 6.9, 2.7 Hz, 2H, CH<sub>2</sub>), 3.96 - 3.84 (m, 1H, CH<sub>α</sub>), 3.77 - 3.29 (m, 16H, 8  $\times$  CH<sub>2</sub>), 3.10 (d, *J* = 5.7 Hz, 2H, CH<sub>2</sub>), 2.52 - 2.27 (m, 3H, CH<sub>2</sub>, CH<sub>2</sub>-H<sup>a</sup>), 2.24 - 2.02 (m, 5H, CH<sub>3</sub>, CH<sub>2</sub>-H<sup>b</sup>, CH), 2.03 - 1.74 (m, 4H, 2  $\times$  CH<sub>2</sub>), 1.54 - 1.38 (m, 14H, 4  $\times$  CH<sub>3</sub>, CH<sub>2</sub>), 1.36 - 1.24 (m, 4H, 2  $\times$  CH<sub>2</sub>), 0.88 (t, *J* = 6.7 Hz, 3H, CH<sub>3</sub>). <sup>13</sup>C NMR (101 MHz, CDCl<sub>3</sub>):  $\delta$  195.68, 174.63, 169.51, 167.83, 152.79, 149.73, 144.97, 144.19, 142.38, 138.30, 134.81, 131.34, 128.69, 126.86, 123.06, 119.36, 118.09, 113.13, 110.08, 88.31, 74.16, 70.71, 70.68, 70.46, 70.43, 69.96, 69.60, 64.75, 64.22, 43.53, 40.01, 39.38, 38.33, 37.56, 33.98, 33.77, 31.88, 29.83, 28.59, 22.78, 19.92, 18.64, 14.97, 14.17. FT-IR (thin film)  $\nu$  3285, 2928, 2872, 2104 (N<sub>3</sub>), 1648, 1533, 1497, 1385, 1275, 1126, 1045

cm<sup>-1</sup>. LC/MS analysis (linear gradient 10 → 90% ACN)  $t_R$ : 9.79 min, ESI-MS ( $m/z$ ): [M + H]<sup>+</sup>: 1009.00. ESI-HRMS ( $m/z$ ): calcd. for [C<sub>49</sub>H<sub>67</sub>BrN<sub>8</sub>O<sub>10</sub> + H]<sup>+</sup> 1007.42363; obsd. 1007.42397.



***m*-DHP-Cy5-carborane (116).** Compound **135** (3 mg, 3 μmol) was dissolved in DCM (2 mL) and TFA (0.5 mL) was added. After 1 h the solvents were removed *in vacuo*, followed by co-evaporation with toluene (3 ×). After silica column chromatography (0 → 10 % MeOH in DCM + 1% TEA) the resulting free amine (LC/MS analysis (linear gradient 10 → 90% ACN)  $t_R$ : 7.34 min, ESI-MS ( $m/z$ ): [M + H]<sup>+</sup>: 909.20) was used directly for the coupling with a pre-activated mixture of Cy5 **91** (1.9 mg, 2.2 μmol), PyBOP (1.3 mg, 2.5 μmol) and DiPEA (1.1 μL, 6.6 μmol) in DMF (1 mL). The mixture was stirred overnight, before being concentrated *in vacuo*. Crude azido-DHP-Cy5

(LC/MS analysis (linear gradient 10 → 90% ACN)  $t_R$ : 7.58 min, ESI-MS ( $m/z$ ): [M + H]<sup>+</sup>: 1655.40) was dissolved in water (0.5 mL) and carborane **100** (0.83 mg, 2.72 μmol) in dioxane (0.5 mL) and aqueous solutions of sodium ascorbate (4.5 μmol) and CuSO<sub>4</sub> (0.45 μmol) were added. After 16 h, the solvents were removed under reduced pressure and compound **116** was isolated by silica column chromatography (0 → 2% H<sub>2</sub>O in 40% MeOH in CHCl<sub>3</sub>) as a blue solid (1.33 mg, 0.68 μmol, 31% over 3 steps). <sup>1</sup>H NMR (600 MHz, MeOD): δ 8.32 - 8.18 (m, 3H, 2 × CH=, CH<sub>trz</sub>), 8.02 (s, 1H, CH<sub>ar</sub>), 7.92 - 7.86 (m, 4H, 4 × CH<sub>ar</sub>), 7.79 (d,  $J$  = 7.6 Hz, 1H, CH<sub>ar</sub>), 7.67 (d,  $J$  = 7.6 Hz, 1H, CH<sub>ar</sub>), 7.45 (t,  $J$  = 7.7 Hz, 1H, CH<sub>ar</sub>), 7.41 - 7.35 (m, 1H, CH<sub>ar</sub>), 7.31 - 7.24 (m, 3H, 3 × CH<sub>ar</sub>), 6.99 (d,  $J$  = 8.7 Hz, 2H, 2 × CH<sub>ar</sub>), 6.95 - 6.86 (m, 2H, 2 × CH<sub>ar</sub>), 6.64 (t,  $J$  = 12.3 Hz, 1H, CH=), 6.39 (d,  $J$  = 13.6 Hz, 1H, CH=), 6.33 (d,  $J$  = 13.6 Hz, 1H, CH=), 5.35 - 5.30 (m, 1H, CH), 5.15 (d,  $J$  = 10.8 Hz, 3H, CH<sub>2</sub>, CH), 5.01 (s, 2H, CH<sub>2</sub>), 4.47 (s, 1H, CH), 4.41 (s, 1H, BCH), 4.16 - 4.03 (m, 6H, 3 × CH<sub>2</sub>), 3.68 - 3.55 (m, 12H, 6 × CH<sub>2</sub>), 3.55 - 3.51 (m, 2H, CH<sub>2</sub>), 3.51 - 3.45 (m, 2H, CH<sub>2</sub>), 3.11 - 3.04 (m, 2H, CH<sub>2</sub>), 2.91 (s, 2H, CH<sub>2</sub>), 2.60 (dd,  $J$  = 16.8, 4.4 Hz, 1H, CH<sub>2</sub>-H<sup>a</sup>), 2.47 - 2.39 (m, 2H, CH<sub>2</sub>-H<sup>b</sup>, CH<sub>2</sub>-H<sup>a</sup>), 2.20 - 2.05 (m, 9H, CH<sub>3</sub>, 2 × CH<sub>2</sub>, CH<sub>2</sub>-H<sup>b</sup>, CH), 1.96 (s, 4H, 2 × CH<sub>2</sub>), 1.82 - 1.78 (m, 4H, 2 × CH<sub>2</sub>), 1.72 (d,  $J$  = 7.7 Hz, 12H, 4 × CH<sub>3</sub>), 1.67 - 1.60 (m, 4H, 2 × CH<sub>2</sub>), 1.51 - 1.43 (m, 2H, CH<sub>2</sub>), 1.40 - 1.13 (m, 7H, 2 × CH<sub>2</sub>, CH<sub>3</sub>), 0.92 (t,  $J$  = 6.8 Hz, 3H, CH<sub>3</sub>). <sup>13</sup>C NMR (151 MHz, MeOD): δ 198.38, 175.68, 175.39, 175.07, 170.22, 170.11, 160.07, 156.27, 156.01, 154.16, 153.68, 147.56, 145.28, 144.97, 144.87, 144.78, 144.48, 143.43, 143.31, 142.66, 142.58, 139.34, 135.81, 134.43, 132.61, 129.59, 129.41, 128.39, 128.10, 128.02, 124.80, 124.31, 121.32, 120.46, 118.76, 115.50, 113.80, 111.72, 111.61, 109.99, 105.63, 105.39, 88.31, 82.22, 75.28, 75.13, 71.57, 71.31, 71.24, 70.55, 70.19, 65.76, 65.02, 62.53, 61.22, 51.70, 50.60, 45.08, 44.14, 40.98, 40.65, 39.79, 39.76, 38.20, 36.76, 34.89, 33.58, 33.25, 29.60, 28.18, 27.87, 27.38, 27.13, 26.55, 23.99, 23.54, 20.97, 18.07, 15.24, 14.48. LC/MS analysis (linear gradient 10 → 90% ACN)  $t_R$ : 9.65 min, ESI-MS ( $m/z$ ): [M + H]<sup>+</sup>: 1959.67. ESI-HRMS ( $m/z$ ): calcd. for [C<sub>91</sub>H<sub>122</sub>B<sub>10</sub>BrN<sub>10</sub>O<sub>20</sub>S<sub>3</sub>]<sup>+</sup> 1959.81596; obsd. 1959.81972.

## References

- [1] Hoogendoorn, S.; Blom, A. E. M.; Mock, E. D.; van der Marel, G. A.; van Koppen, C.; Timmers, C. M.; Overkleeft, H. S. contributed to the work described in this chapter.
- [2] Barth, R. F.; Soloway, A. H.; Fairchild, R. G.; Brugger, R. M. *Cancer* **1992**, *70*, 2995–3007.
- [3] Barth, R. F.; Coderre, J. A.; Vicente, M. G. H.; Blue, T. E. *Clin. Cancer Res.* **2005**, *11*, 3987–4002.
- [4] Soloway, A. H.; Tjarks, W.; Barnum, B. A.; Rong, F.-G.; Barth, R. F.; Codogni, I. M.; Wilson, J. G. *Chem. Rev.* **1998**, *98*, 1515–1562.
- [5] Yamamoto, T.; Nakai, K.; Matsumura, A. *Cancer Lett.* **2008**, *262*, 143–152.
- [6] Barth, R. F.; Vicente, M.; Harling, O. K.; Kiger III, W.; Riley, K. J.; Binns, P. J.; Wagner, F. M.; Suzuki, M.; Aihara, T.; Kato, I.; Kawabata, S. *Radiat. Oncol.* **2012**, *7*, 1–21.
- [7] Calabrese, G.; Nesnas, J. J.; Barbu, E.; Fatouros, D.; Tsiouklis, J. *Drug discov. today* **2012**, *17*, 153–159.
- [8] Valliant, J. F.; Guenther, K. J.; King, A. S.; Morel, P.; Schaffer, P.; Sogbein, O. O.; Stephenson, K. A. *Coord. Chem. Rev.* **2002**, *232*, 173–230.
- [9] Hawthorne, M. F. *Angew. Chem. Int. Ed. Engl.* **1993**, *32*, 950–984.
- [10] Fauchere, J.; Do, K. Q.; Jow, P.; Hansch, C. *Experientia* **1980**, *36*, 1203–1204.
- [11] Tietze, L. F.; Bothe, U. *Chem Eur J* **1998**, *4*, 1179–1183.
- [12] Varadarajan, A.; Hawthorne, M. F. *Bioconjug. Chem.* **1991**, *2*, 242–253.
- [13] Lesnikowski, Z. J.; Shi, J.; Schinazi, R. F. *J. Organomet. Chem.* **1999**, *581*, 156–169.
- [14] Miura, M.; Gabel, D.; Oenbrink, G.; Fairchild, R. G. *Tetrahedron Lett.* **1990**, *31*, 2247–2250.
- [15] Siegel, R.; Naishadham, D.; Jemal, A. *CA: a cancer journal for clinicians* **2013**, *63*, 11–30.
- [16] Holschneider, C. H.; Berek, J. S. *Semin. Surg. Oncol.* **2000**, *19*, 3–10.
- [17] Choi, J.-H.; Wong, A. S.; Huang, H.-F.; Leung, P. C. *Endocr. Rev.* **2007**, *28*, 440–461.
- [18] Mertens-Walker, I.; Baxter, R. C.; Marsh, D. J. *Cancer Lett.* **2012**, *324*, 152–159.
- [19] Simoni, M.; Gromoll, J.; Nieschlag, E. *Endocr. Rev.* **1997**, *18*, 739–773.
- [20] Parrott, J. A.; Doraiswamy, V.; Kim, G.; Mosher, R.; Skinner, M. K. *Mol. Cell. Endocrinol.* **2001**, *172*, 213–222.
- [21] Zheng, W.; Magid, M. S.; Kramer, E. E.; Chen, Y.-T. *Am. J. Pathol.* **1996**, *148*, 47.
- [22] Zheng, W.; Lu, J. J.; Luo, F.; Zheng, Y.; Feng, Y.-j.; Felix, J. C.; Lauchlan, S. C.; Pike, M. C. *Gynecol. Oncol.* **2000**, *76*, 80–88.
- [23] Brodowska, A.; Laszczyńska, M.; Brodowski, J.; Masiuk, M.; Starczewski, A. *Histol. Histopathol.* **2012**, *27*, 241.
- [24] Zhang, X.-y.; Chen, J.; Zheng, Y.-f.; Gao, X.-l.; Kang, Y.; Liu, J.-c.; Cheng, M.-j.; Sun, H.; Xu, C.-j. *Cancer Res.* **2009**, *69*, 6506–6514.
- [25] Zhang, X.; Chen, J.; Kang, Y.; Hong, S.; Zheng, Y.; Sun, H.; Xu, C. *Int. J. Pharm.* **2013**, *453*, 498–505.
- [26] Radu, A.; Pichon, C.; Camparo, P.; Antoine, M.; Allory, Y.; Couvelard, A.; Fromont, G.; Hai, M. T. V.; Ghinea, N. *N. Engl. J. Med.* **2010**, *363*, 1621–1630.
- [27] van Koppen, C. J.; Verbost, P. M.; van de Lagemaat, R.; Karstens, W.-J. F.; Loozen, H. J.; van Achterberg, T. A.; van Amstel, M. G.; Brands, J. H.; van Doornmalen, E. J.; Wat, J.; Mulder, S. J.; Raafs, B. C.; Verkaik, S.; Hanssen, R. G.; Timmers, C. M. *Biochem. Pharmacol.* **2013**, *85*, 1162–1170.
- [28] Grima Poveda, P. M.; Karstens, W. F. J.; Timmers, C. M. *WO Patent* **2006**, 2006117368(A1).
- [29] Nakamura, H.; Aoyagi, K.; Yamamoto, Y. *J. Am. Chem. Soc.* **1998**, *120*, 1167–1171.
- [30] Tomita, H.; Luu, H.; Onak, T. *Inorg. Chem.* **1991**, *30*, 812–815.
- [31] Ahrens, V. M.; Frank, R.; Stadlbauer, S.; Beck-Sickinger, A. G.; Hey-Hawkins, E. *J. Med. Chem.* **2011**, *54*, 2368–2377.
- [32] Gomez, F. A.; Hawthorne, M. F. *J. Org. Chem.* **1992**, *57*, 1384–1390.
- [33] Parrott, M. C.; Marchington, E. B.; Valliant, J. F.; Adronov, A. *J. Am. Chem. Soc.* **2005**, *127*, 12081–12089.
- [34] Tornøe, C. W.; Christensen, C.; Meldal, M. *J. Org. Chem.* **2002**, *67*, 3057–3064.
- [35] Rostovtsev, V. V.; Green, L. G.; Fokin, V. V.; Sharpless, K. B. *Angew. Chem. Int. Ed. Engl.* **2002**, *41*, 2596–2599.
- [36] Verdoes, M.; Florea, B. I.; Hillaert, U.; Willems, L. I.; van der Linden, W. A.; Sae-Heng, M.; Filippov, D. V.; Kisselev, A. F.; van der Marel, G. A.; Overkleeft, H. S. *ChemBioChem* **2008**, *9*, 1735–1738.
- [37] Urano, Y.; Asanuma, D.; Hama, Y.; Koyama, Y.; Barrett, T.; Kamiya, M.; Nagano, T.; Watan-

- abe, T.; Hasegawa, A.; Choyke, P. L.; Kobayashi, H. *Nat. Med.* **2009**, *15*, 104–9.
- [38] Hoogendoorn, S.; Habets, K. L.; Passemard, S.; Kuiper, J.; van der Marel, G. A.; Florea, B. I.; Overkleeft, H. S. *Chem. Commun.* **2011**, *47*, 9363–9365.
- [39] Mujumdar, R. B.; Ernst, L. A.; Mujumdar, S. R.; Lewis, C. J.; Waggoner, A. S. *Bioconjug. Chem.* **1993**, *4*, 105–111.
- [40] Zhang, X.-X.; Wang, Z.; Yue, X.; Ma, Y.; Kiesewetter, D. O.; Chen, X. *Mol. Pharm.* **2013**, *10*, 1910–1917.



# 9

## From LMW to HMW ligands: fluorescently tagged FSH by sortase-mediated ligation<sup>1</sup>

The heterodimeric follicle-stimulating hormone (FSH) consists of a common  $\alpha$ -subunit and a unique  $\beta$ -subunit which are non-covalently linked to each other. The C-terminus of the FSH $\beta$ -subunit is not involved in receptor binding and was selected for introduction of a sortase recognition sequence (LPETGG) and a His<sub>10</sub>-affinity tag. "FSH-LPETGG" was recombinantly expressed in HEK293 cells, semi-purified and subjected to sortase-mediated ligation with a synthetic sortagging nucleophile (GGG-BDP-MC) to provide fluorescent "FSH-BDP-MC". This protein was shown to be a full FSHR agonist with comparable potency as wild-type FSH in stimulating cAMP production. FSH-BDP-MC was able to induce FSHR-GFP internalization, and was trafficked together with its receptor in the endolysosomal pathway as determined by fluorescence colocalization. The versatility of a synthetic nucleophile combined with the selectivity and potency of the endogenous ligand opens up novel possibilities for the study and manipulation of FSH- and FSHR-related processes.

## 9.1 Introduction

The glycoprotein follicle-stimulating hormone (FSH), which is secreted by the pituitary gland, has important functions in human reproduction. FSH is a heterodimeric protein that shares its  $\alpha$ -subunit with the closely related proteins human chorionic gonadotrophin (hCG), luteinizing hormone (LH) and thyroid-stimulating hormone (TSH). The unique  $\beta$ -subunit confers its selectivity for the follicle-stimulating hormone receptor (FSHR), present on granulosa cells in the ovaries and Sertoli cells in the testes.<sup>2</sup> The two subunits are non-covalently bound to each other, and an intricate network of disulfide bridges in each subunit allows for a strong interaction between the two.<sup>3,4</sup> Disruption of disulfide bonds Cys20-104 or Cys28-82 in the FSH $\beta$  subunit, by mutation of the cysteines forming the bridge, prevents correct folding of the subunit and heterodimer formation.<sup>5</sup> In mammals, FSH is present as many different isoforms. Two *N*-linked glycosylation sites are present on both the FSH $\alpha$  (Asn-52 and Asn-78) and FSH $\beta$  (Asn-7 and Asn-24) chains and the core structures and degree of sulfation and sialylation of the *N*-glycans are very heterogeneous.<sup>2,6</sup> Numerous functions of FSH glycosylation have been reported, such as proper protein folding, assembly and secretion and circulation half-lives.<sup>7-11</sup> FSH is used clinically for the treatment of anovulatory females and in assisted reproduction techniques (in-vitro fertilization, intracytoplasmic sperm injection).<sup>12,13</sup> Originally, urine preparations containing FSH were used, which have increased in purity and FSH content over the years. With the development of a recombinant system for the production of FSH, access was gained to highly pure protein with good batch-to-batch consistency.<sup>13-16</sup> Functionally important posttranslational modifications of recombinant human FSH (Puregon) produced by eukaryotic Chinese hamster ovary (CHO) cells are remarkably similar to urinary or pituitary derived FSH.<sup>17</sup>

Besides the well-established importance of the glycoproteins and their receptors in reproduction, they are thought to be implicated in cancer pathogenesis. The presence of the FSHR on ovarian surface epithelial tumor cells has been reported,<sup>18,19</sup> as well as the unexpected finding of ubiquitous FSHR expression on vascular endothelial cells of a variety of tumors.<sup>20</sup> Visualization of the FSHR therefore presents an opportunity for tumor diagnostics, whereas targeting of cytotoxic drugs to FSHR-expressing tumors enables therapeutic intervention. In Chapters 6-8 a targeting strategy has been described based on a small-molecule synthetic agonist for the FSHR. High ligand efficiency, oral bioavailability, metabolic stability and synthetic access to large quantities of a chemically defined structure (and derivatives) are amongst the arguments in favor of the use of a low molecular weight ligand. However, in terms of receptor selectivity and potency the endogenous protein ligand is hard to beat.

The aim of the research described in this chapter is to combine the selectivity and potency of FSH as a targeting ligand with the flexibility of synthetic 'cargo', e.g. a fluorescent dye, peptide or drug. Sortase-mediated ligation, also termed 'sortagging', was the envisaged method of choice to accomplish this. The bacterial enzyme Sortase A binds to its C-terminal recognition sequence on a target protein and catalyzes the transpeptidation with

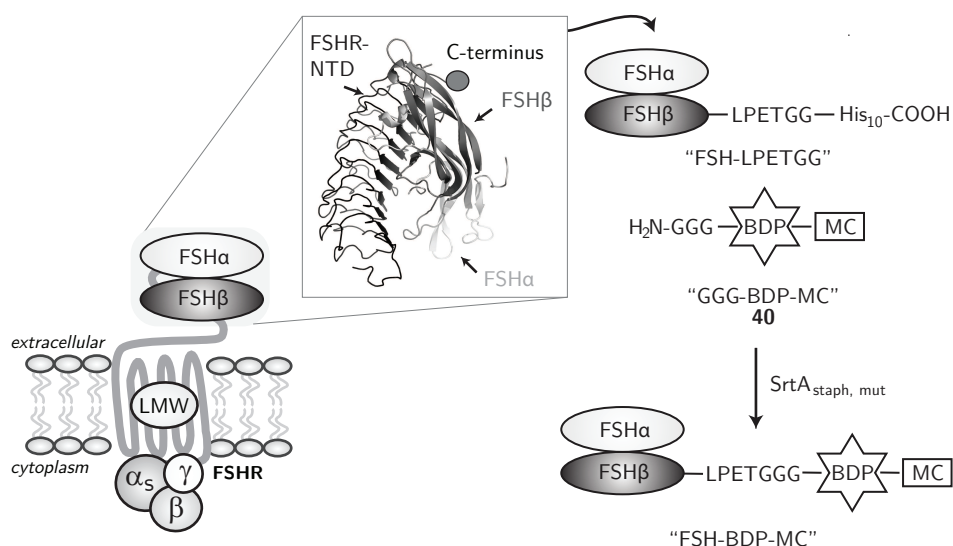


**Figure 9.1:** Left: Schematic representation of heterodimeric FSH bound to the N-terminal domain (NTD) and a LMW ligand to the transmembrane domain of the FSHR. Detail: Reported crystal structure of FSH bound to the receptor shows that the C-terminus of FSH $\beta$  is not involved in receptor binding.<sup>21,22</sup> Structure was made with PyMOL and the grey ball at the C-terminus indicates the ligation site. Right: Sortase-mediated ligation described in this chapter.

a (synthetic) triglycine nucleophile (Figure 9.1).<sup>23,24</sup> A recombinant version of FSH with a C-terminally extended  $\beta$ -subunit has been reported with retention of receptor binding and biological activity.<sup>25,26</sup> In addition, crystallographic data of FSH bound to the ectodomain of the receptor support the hypothesis that the FSH $\beta$  C-terminus is not involved in receptor binding (Figure 9.1).<sup>21,22</sup> In this chapter, sortase-mediated ligation of a synthetic fluorescent peptide to the C-terminus of the FSH $\beta$ -subunit of recombinant FSH is described. Functional assays are used to determine what the pharmacological properties of fluorescently labeled FSH are and whether this holds promise for use in future applications of FSHR visualization and targeting.

## 9.2 Results and Discussion

**Expression and sortagging of FSH-LPETGG.** Recombinant human FSH suited for sortase-mediated ligation ("FSH-LPETGG") was expressed using two plasmids, one encoding the wild-type FSH  $\alpha$ -subunit and one the FSH $\beta$ -subunit containing a C-terminal sortase sequence (LPETGG) and His<sub>10</sub>-tag for purification purposes. Chinese hamster ovary (CHO) cells and human embryonic kidney (HEK293) cells are eukaryotic expression systems capable of introducing the required posttranslational modifications on the protein and have been used before for the expression of fully active, recombinant FSH.<sup>14,27</sup> Small scale transfection experiments in both cell lines were performed and the presence of FSH-LPETGG in

cell lysates and medium was determined by immunoblotting. From these experiments, it became apparent that both the heterodimeric FSH-LPETGG as well as monomeric FSH $\beta$ -LPETGG were secreted into the medium. In previous reports on recombinant FSH expression it was noted that intact heterodimeric protein is secreted efficiently from the cells, but monomeric, wild-type FSH $\beta$  very slowly and to a smaller extent.<sup>14</sup> However, fusion of a hCG-derived peptide to the FSH $\beta$  C-terminus led to much higher levels of FSH $\beta$ -CG $\beta$  secretion.<sup>26</sup> The enhanced secretion of FSH $\beta$ -LPETGG might thus be due to its C-terminal extension. Assembly of the subunits appeared to be more efficient in HEK293 cells than in CHO cells, based on the ratio of dimeric protein and FSH $\beta$  that were secreted, and thus these cells were selected for larger scale expression experiments.

Adherent HEK293T cells were transiently co-transfected with FSH $\alpha$  and FSH $\beta$ -LPETGG cDNA and from 24 h after transfection, cells were cultured in serum-free medium. Medium was collected and refreshed every 24 h and FSH-LPETGG expression was detected using antibodies against FSH $\alpha$  and FSH $\beta$  (Figure 9.3A). The detected bands were very diffuse, indicating the presence of multiple isoforms, and higher in molecular weight than wild-type recombinant FSH (rFSH, Org32489), because of the C-terminal extension. For clarity, a schematic representation of all subsequent purification and sortagging steps is given in Figure 9.2. Medium containing FSH-LPETGG was pooled, concentrated and subjected to Ni-affinity purification (Figure 9.3B). Recombinant FSH-LPETGG and monomeric FSH $\beta$ -LPETGG were captured very efficiently by a Ni-NTA agarose column, since no FSH-derived protein was detected in both the flow-through (FT) and washing steps (wash) from the column. Elution from the resin using imidazole resulted in a semi-pure protein preparation consisting of FSH-LPETGG, FSH $\beta$ -LPETGG (as seen by immunoblotting), and some remaining other proteins.

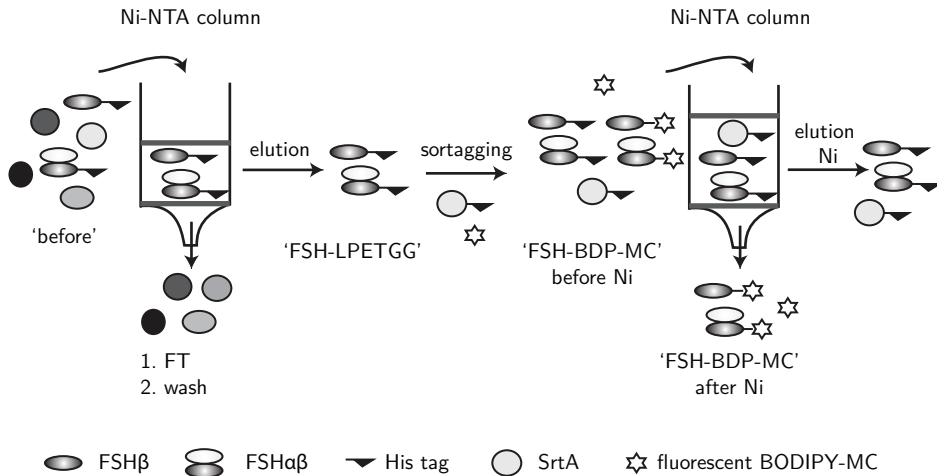


**Figure 9.2: Schematic representation of the purification, sortagging and second purification steps on FSH-LPETGG.** From each step, a sample was taken and subjected to SDS-PAGE analysis, as shown in Figure 9.3 B and C.

Semi-purified FSH-LPETGG was subjected to sortase-mediated ligation using Sortase A (SrtA) from *Staphylococcus aureus*, containing three mutations (P94S/D160N/ K196T).<sup>28</sup> As described in Chapter 4, this triple mutant SrtA has enhanced affinity for the LPETGG sequence, which makes it much more suited for use in very diluted samples. As a nucleophile, "GGG-BDP-MC" **40** (Scheme 4.1, Chapter 4) was used, enabling fluorescent visualization because of the BODIPY dye ("BDP") while also containing a large peptide-based synthetic mannose cluster ("MC", Chapter 2) as model cargo. The ligation reaction was carried out for 2h at 37 °C with a large excess of nucleophile (100 μM), to diminish the potential hydrolysis reaction (Figure 4.3, Chapter 4). Then, Ni-NTA agarose beads were added to the mixture to capture any remaining His-tagged starting proteins, SrtA and the SrtA-FSH intermediate. Everything C-terminally of the threonine residue in the sortase sequence was cleaved off during the transpeptidation (Figure 9.1) so the product "FSH-BDP-MC" was not captured by the Ni-NTA resin (Figure 9.3). After nickel-affinity purification, heterodimeric FSH-BDP-MC was obtained as determined by in-gel fluorescence scanning and immunoblotting against the  $\alpha$ - and  $\beta$ -subunits. Reduction of the protein sample with dithiothreitol (DTT), resulted in the disappearance of the higher molecular weight band and appearance of one lower running band, confirming the presence of heterodimeric protein (Figure 9.3).

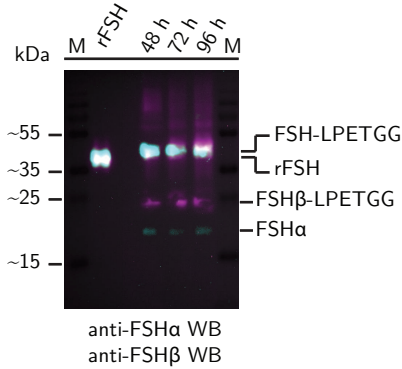
**Table 9.1:** Protein concentrations of FSH-LPETGG and FSH-BDP-MC

|                   | FSH (μg/mL) <sup>a</sup> | [FSH] (nM)            | Total protein (mg/mL) | %FSH/total protein |
|-------------------|--------------------------|-----------------------|-----------------------|--------------------|
| <b>FSH-LPETGG</b> | 14; 9                    | 284; 180 <sup>b</sup> | 1.8; 1.2              | 0.3; 0.3           |
| <b>FSH-BDP-MC</b> | 12; 8                    | 244; 167 <sup>b</sup> | 1.5; 1.6              | 0.3; 0.2           |
| <b>rFSH</b>       |                          | 112                   | 2.5                   | 0.1                |

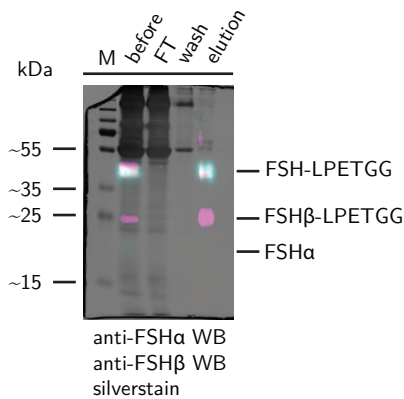
<sup>a</sup>Concentrations (μg/mL) were determined using an FSH-ELISA assay. Values of two separate expression and sortagging experiments are given. <sup>b</sup>Calculated using estimated MW of 50 kDa.

The amounts of FSH-LPETGG and FSH-BDP-MC obtained were estimated by a sandwich ELISA assay against FSH $\beta$  (Table 9.1). Based on the expected increase in weight by the C-terminal extension and the observed gelshift, an estimated molecular weight of 50 kDa for FSH-LPETGG/FSH-BDP-MC was assumed to calculate the FSH concentration (nM) (Table 9.1). The given values might be a slight overestimation of the actual heterodimer concentration, because of potential cross-reactivity of the free  $\beta$ -subunit, present in both samples besides the heterodimer, in the ELISA assay. The recombinant wild-type human FSH (rFSH) preparation, which was used as a positive control throughout the experiments, is stabilized by the use of bovine serum albumin (BSA) as an additive. As seen in Table 9.1, the estimated percentage FSH/total protein in the sample after Ni-affinity purification of both FSH-LPETGG and FSH-BDP-MC was similar to that of the rFSH stock. Since the absolute amounts of FSH-BDP-MC obtained were ~2.6/1.8 μg (2 independent experiments, corresponding to 35-40% yield of the sortase reaction) no further purification procedures were conducted and the protein preparation was used as such. As can be seen in Figure 9.3C,

## A) Expression of FSH-LPETGG



## B) Ni-affinity purification of FSH-LPETGG



## C) Sortase-mediated ligation of FSH-LPETGG

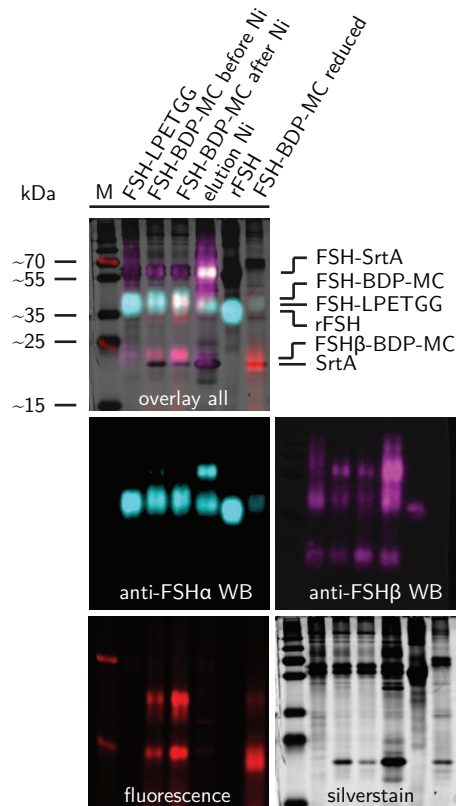


**Figure 9.3: Expression, purification and sortase-mediated ligation of FSH-LPETGG.** A) Medium of HEK293T cells transiently transfected with FSH $\alpha$  and FSH $\beta$ -LPETGG ( $t=0$ ) was refreshed every 24 h and the presence of heterodimeric FSH-LPETGG as well as the respective monomers in the medium was detected using monoclonal antibodies against FSH $\alpha$  (cyan) or FSH $\beta$  (magenta). B) Combined and concentrated medium of A) was treated with Ni-NTA agarose to capture all His-tagged proteins, washed and subsequently eluted with imidazole to yield semi-purified FSH-LPETGG, also containing FSH $\beta$ -LPETGG. C) Sortase-mediated ligation of semi-purified FSH-LPETGG (as in B) with GGG-BDP-MC followed by removal of SrtA, SrtA-FSH intermediate, unreacted FSH-LPETGG and FSH $\beta$ -LPETGG using Ni-NTA agarose, yields fluorescently labeled FSH-BDP-MC (as well as FSH $\beta$ -BDP-MC). Fluorescent proteins were detected by in-gel fluorescence scanning (red) and FSH-derived proteins were visualized using immunoblotting against FSH $\alpha$  (cyan) or FSH $\beta$  (magenta). Total protein was detected using silverstain, however, due to the low abundance of recombinant FSH in these samples and the heterogeneity of their glycosylation pattern, no distinguishable band for the various rFSH constructs was found. Reduction of the mixture with DTT (5 mM, 1 h, 37 °C) resulted in dissociation of the heterodimer as seen by in-gel fluorescence ('FSH-BDP-MC reduced').

some FSH-sortase intermediate and unreacted FSH-LPETGG was eluted from the nickel beads ('elution Ni'), thus optimization of the reaction conditions might lead to a slightly improved yield.

**Biological evaluation of FSH-LPETGG and FSH-BDP-MC.** Agonistic activities of the FSH-LPETGG and FSH-BDP-MC proteins were determined in a CRE-luciferase assay. For this, CHO cells stably transfected with the human FSHR and a CRE-luciferase reporter construct were treated with various concentrations (as calculated from the values given in Table 9.1) of the recombinant proteins for 4 h (37 °C, 5 % CO<sub>2</sub>). The resulting dose-response curves, depicted in Figure 9.4 (left), were very similar for both proteins and control rFSH. The mean agonistic potencies (EC<sub>50</sub>) calculated from the pEC<sub>50</sub> values determined from the fitted curves, were 5 pM for both constructs (Figure 9.4), indicating that these C-terminal modifications could be introduced without influencing the potency of the protein.

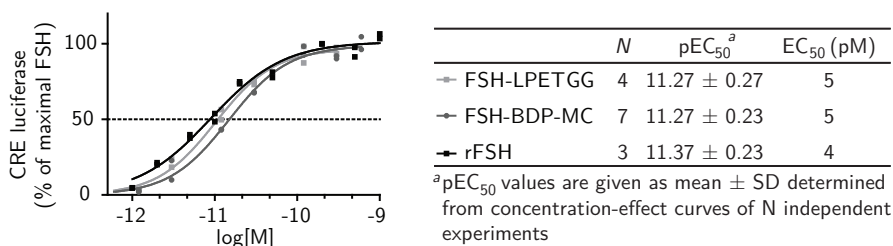


**Figure 9.4: Luciferase assay.** Agonistic activities of FSH-LPETGG, FSH-BDP-MC and rFSH on CHO cells stably expressing human FSHR and CRE-luciferase reporter. left: Representative dose-response curves of the effect normalized to the maximal luciferase activity induced by rFSH. right: EC<sub>50</sub> values of the different constructs.

Upon activation of the receptor, signaling cascades are set in motion which result in the phosphorylation of the FSHR.<sup>29</sup> It is believed that this leads to sequestering by  $\beta$ -arrestins and the internalization of the receptor-ligand complex in clathrin-coated pits, thereby preventing overstimulation of the receptor.<sup>30–32</sup> The ability of the FSH-LPETGG and FSH-BDP-MC proteins to induce receptor internalization was examined next with the use of U2OS cells that stably express the rat FSHR conjugated to enhanced green fluorescent protein (eGFP) (U2OS-FSHR cells). The percentage of GFP fluorescence signal inside the cytoplasm was calculated as a measure for receptor internalization (Figure 9.5A). Untreated cells showed bright membrane fluorescence and only ~30% of the receptor fluorescence was localized inside the cell, as observed before (Chapter 7). Treatment with FSH-LPETGG or FSH-BDP-MC (11–14 nM) for 2 h induced receptor internalization to the same extent as rFSH (~80%) as seen by bright intracellular vesicles (Figure 9.5A,C). The total levels of GFP fluorescence and BODIPY fluorescence were quantified (Figure 9.5B) and this showed that the total amount of receptor, either on the membrane or internalized, remained constant throughout the experiments. Only for FSH-BDP-MC bright intracellular BODIPY fluorescent signal was detected (Figure 9.5B,C). Since a large excess of nucleophile GGG-BDP-MC 40 was employed in the sortase reaction, control experiments were conducted to show that



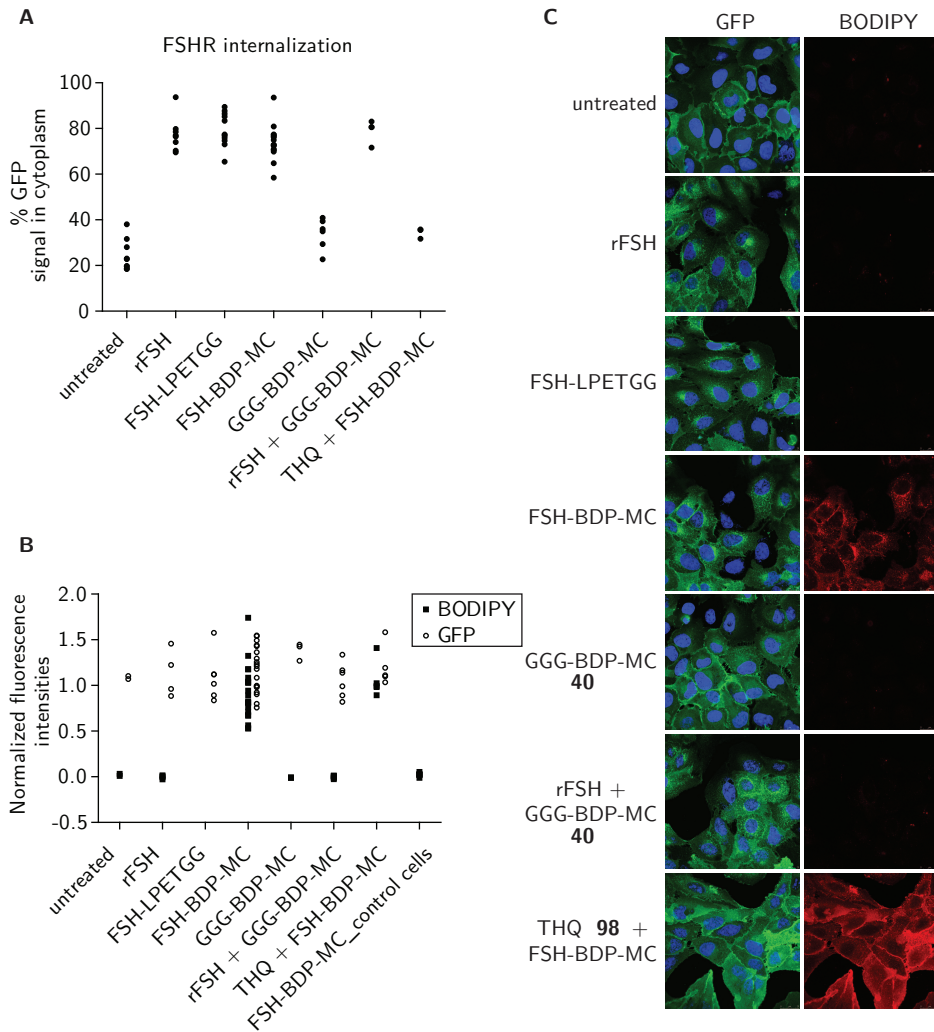


**Figure 9.5: Confocal microscopy of FSHR internalization and FSH-BDP-MC uptake.** U2OS cells stably expressing eGFP-conjugated rat FSHR were incubated with rFSH, FSH-LPETGG or FSH-BDP-MC (11-14 nM), GGG-BDP-MC (3  $\mu$ M) or a combination of rFSH (11 nM) and GGG-BDP-MC (3  $\mu$ M) for 2 h, 37  $^{\circ}$ C, 5%  $\text{CO}_2$ . For competition experiment cells were pre-treated with THQ 98 (10  $\mu$ M, 1 h) followed by incubation with FSH-BDP-MC (4 nM, 2 h). Cells were washed, fixed (4% formaldehyde in PBS) and imaged using a confocal fluorescence microscope. Images were analyzed A) for the relative amount of receptor (GFP signal) inside the cytoplasm versus on the cell membrane as a measure for receptor internalization and B) for total GFP (receptor expression levels) and BODIPY signal intensities. Values were normalized to give mean GFP $\sim$ 1 for untreated and rFSH-treated cells and mean BODIPY $\sim$ 1 for MC-BDP-GGG treated cells. Each dot represents a picture analyzed from  $N=1$  (THQ + FSH-BDP-MC) to  $N=5$  (FSH-BDP-MC) independent experiments. C) Representative images of all conditions showing receptor localization (GFP, green) and compound/protein uptake/binding (BODIPY, red). Blue: Draq5 nuclear stain.



the remaining nucleophile in the sample was not at the basis of receptor internalization and intracellular BODIPY fluorescence. Cells were incubated with 3  $\mu\text{M}$  of compound **40**, corresponding to the maximum concentration that could be present in the FSH-BDP-MC sample. As shown in Figure 9.5A-C, this did not result in receptor internalization or any increase in BODIPY levels above autofluorescence background levels. Also, concomitant exposure of U2OS-FSHR cells to rFSH (11 nM) and nucleophile **40** (3  $\mu\text{M}$ ) resulted in rFSH-induced receptor internalization, but not in uptake of the nucleophile. These experiments confirm the covalent attachment of GGG-BDP-MC to FSH, resulting in agonistically active and fluorescent FSH-BDP-MC. It can not be excluded that remaining FSH $\beta$ -BDP-MC is partly responsible for the observed effects. Wild-type FSH $\beta$  reportedly is able to bind the FSHR albeit with a 100-fold less affinity, and literature evidence points to the heterodimeric protein as the only biologically active species.<sup>33</sup> Treatment of control U2OS cells without FSHR with FSH-BDP-MC did not result in any intracellular BODIPY fluorescence (Figure 9.5B), confirming the receptor-mediated uptake of the protein.

A low molecular weight FSHR antagonist has been reported that is based on the tetrahydroquinoline (THQ) scaffold and binds to an allosteric binding site on the receptor (Figure 9.1).<sup>34,35</sup> Using a THQ-derivative, compound **98** (Figure 7.4C, Chapter 7), in combination with the low molecular weight fluorescent agonist DHP-Cy5 **96** (Chapter 7) resulted in inhibition of DHP-Cy5 induced FSHR internalization. Furthermore, no Cy5 fluorescence was observed indicating that THQ also prevented DHP-Cy5 from FSHR binding. An analogous experiment was conducted with THQ **98** (10  $\mu\text{M}$ ) and FSH-BDP-MC (4 nM) and the results are shown in Figure 9.5. THQ was able to antagonize FSHR-internalization, but unable to inhibit binding of FSH-BDP-MC to the receptor as seen by very bright BODIPY membrane labeling. Colocalization analyses of receptor GFP fluorescence and FSH BODIPY fluorescence for conditions with and without THQ are given in Figure 9.6 and Table 9.2. In both cases strong colocalization was found, with values above 0.84 for Pearson's colocalization coefficient and high intensity correlation quotients of  $\sim 0.33$  (dependent staining:  $0 \leq x \leq 0.5$ ).<sup>36,37</sup> This further confirmed the specific interaction between FSH-BDP-MC and the FSHR. In a final experiment, the low molecular weight agonist DHP-Cy5 **96** and FSH-BDP-MC were combined. As shown in Figure 9.6B, this led to the colocalization of all three fluorophores in intracellular vesicles, establishing that these two agonists share the same target receptor, but not the binding site. Interestingly, some of the intracellular vesicles were only positive for GFP and not for either ligand. This could reflect an intracellular population of receptors or it could be caused by dissociation of the ligand from the receptor during endocytosis and trafficking. Time-course studies could be used to examine this in more detail.

Reports on the internalization and trafficking of the FSH-FSHR complex so far have made use of radio-labeled [<sup>125</sup>I] or [<sup>131</sup>I]-FSH and immunostaining techniques for receptor visualization.<sup>38-41</sup> Some of these indicate that the FSHR is recycled back to the membrane intact, while FSH is trafficked to the lysosomes and degraded,<sup>40</sup> and others report recycling of the intact FSH-FSHR complex.<sup>41</sup> The experiments in this study support the use of

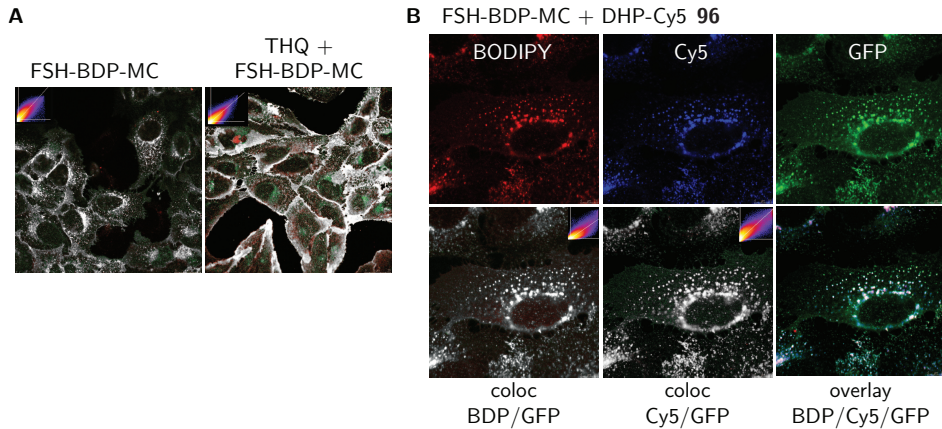


**Figure 9.6: Colocalization of FSH-BDP-MC with eGFP-FSHR.** A) Overlays of pictures shown in Figure 9.5 for FSH-BDP-MC (left) and THQ + FSH-BDP-MC (right) showing colocalized pixels in white. Insert: fluorescence scatterplot. Colocalization parameters are given in Table 9.2. B) Concomitant treatment of U2OS-FSHR cells with HMW ligand FSH-BDP-MC (14 nM) and LMW ligand DHP-Cy5 **96** (1  $\mu$ M) (Chapter 7) led to internalization of the receptor and colocalization of all three fluorophores.

**Table 9.2:** Colocalization analysis of FSH-BDP-MC with eGFP-FSHR.

|                               | n (N)  | Rr                 | M1                 | M2                 | ICQ                |
|-------------------------------|--------|--------------------|--------------------|--------------------|--------------------|
| FSH-BDP-MC<br>THQ <b>98</b> + | 18 (5) | 0.8448 $\pm$ 0.033 | 0.9368 $\pm$ 0.013 | 0.9689 $\pm$ 0.013 | 0.3372 $\pm$ 0.018 |
| FSH-BDP-MC                    | 8 (1)  | 0.8401 $\pm$ 0.035 | 0.9629 $\pm$ 0.010 | 0.9729 $\pm$ 0.012 | 0.3271 $\pm$ 0.021 |

n(N): number of pictures n from N independent experiments analyzed. Rr: Pearson's colocalization coefficient. Manders overlap coefficients (M) M1: red; M2: green. ICQ: intensity correlation quotient. Mean  $\pm$  SD is given.

fluorescently labeled FSH as a suited alternative for an in-depth study on the intracellular localization and trafficking of FSH after internalization.

### 9.3 Conclusion

The expression of a recombinant heterodimeric protein potentially has many pitfalls because of the crucial assembly step. In this study a sorttagging competent version of follicle-stimulating hormone, FSH-LPETGG, was expressed in HEK293T cells. The intact heterodimer was secreted from the cells into the medium, as well as the free FSH $\beta$ -LPETGG subunit. Since both proteins contained the His<sub>10</sub>-tag and the sortase sequence, separation of the two was not possible with the little protein material that was obtained. Sortase-mediated ligation of the semi-pure protein preparation with a synthetic nucleophile, GGG-BDP-MC **40**, resulted in the formation of FSH-BDP-MC. This protein was shown to be fully active on the FSHR in terms of G<sub>s</sub>-signaling and receptor internalization. Moreover, strong

colocalization of the protein and the receptor under various conditions was established, both in intracellular vesicles and on the cell membrane, proving the interaction between the two. Fluorescently labeled FSH might find applications in the study of FSH-FSHR trafficking and in FSHR visualization on (tumor) cells. Furthermore, by introduction of the mannose cluster as a model for 'cargo', it has been shown that large synthetic molecules are tolerated at the FSH $\beta$  C-terminus without compromising activity. The challenge now lies in the optimization of protein expression and purification procedures to obtain larger quantities of defined protein preparations. The synthetic nature of the sortagging nucleophile allows for easy exchange of this cluster with a variety of other drugs (such as the carboranyl peptide discussed in Chapter 8) or biological modulators. Combined with the inherent selectivity and potency of FSH for the FSHR this might present a very powerful approach for targeted drug delivery.

## 9.4 Experimental Section

**Cell culture conditions.** All cells were grown in a humidified atmosphere in 5% CO<sub>2</sub> at 37 °C. CHO cells stably expressing the human FSH receptor together with a luciferase reporter gene (CHO-hFSHR\_luc cells) and control cells without receptor but with luciferase gene (CHO\_luc cells) were provided by MSD, Oss, The Netherlands. Cells were cultured in Dulbecco's Modified Eagle's Medium (DMEM) and Ham's F12 medium (1:1) with glutamine, penicillin/streptomycin (pen/strep, 0.1 mg/mL) and FCS. CHO-hFSHR\_luc cells were maintained under constant selection with Hygromycin B (0.8 mg/mL). Cells were subcultured twice weekly at a ratio of 1:10-1:15. U2OS cells stably expressing the rat FSHR fused to the N-terminus of eGFP (U2OS-FSHR cells) were purchased from Thermo Scientific (FSHR redistribution assay, Pierce Biotechnology). Cells were grown in DMEM (high glucose) supplemented with L-glutamine (2 mM), pen/strep (0.1 mg/mL), G418 (0.5 mg/mL) and FCS (10%). Wild-type U2OS cells were grown under the same conditions, without G418. Cells were subcultured twice weekly at a ratio of 1:8-1:10. Adherent HEK293T cells were cultured in DMEM (high glucose, 4.5 g/L) supplemented with pen/strep (0.1 mg/mL) and NBS (10%, iron-supplemented, HyClone, Thermo Scientific).

**FSH ELISA assay.** Amounts of recombinant FSH in the various samples were estimated using an FSH ELISA kit (IBL international GmbH, Germany) per manufacturer's protocol. This kit encompasses a solid-phase sandwich ELISA against human FSH $\beta$ . An estimated molecular weight of 50 kDa was used to calculate molarities for FSH-LPETGG and FSH-BDP-MC samples.

**Cloning, expression and purification of FSH-LPETGG-His<sub>10</sub>.** The cDNA of FSH- $\alpha$  was amplified by PCR with a forward primer: 5'-CATAAGCTTACCATGGATTACTACAG AAAATATGCAGCTATC TTTCTGGTCACATTG TCGGTGTTTCTG CATGTTCT CCATTCGGCTCCTGAT GTGCAGGATT GCCCAGAAT GCACG-3' containing a *Hind*III site and a reverse primer: 5'-CATGGATCCGGTAC CT-TAAGATTTG TGATAATAACAA GTACTGCAG TGGCACGCC GTGTGGTTCTCCAC TTTGAAAC-CCCCATT ACTGTGACCCTGTTATA TGATTTAGC-3' containing a *Bam*HI site. The fragment was subcloned into *Hind*III-*Bam*HI-digested pcDNA3.1(+) and sequenced in both directions (282-FSH $\alpha$ ). The cDNA of FSH- $\beta$  was amplified by PCR with a forward primer: 5'-CATGCTAGCTAAGCTTTG

GTACCGCCGC CACCATGAAGAC ACTGCAGTTTTTCTTCC-3' containing a *Hind*III site and a reverse primer: 5'-ATCTCTAGA TTAGTGGTGATG GTGATGAT GATGGTGTGGTATTGATCCTCTTCTGAGAT GAGTTTTTGTCTGT ACAACCGCCGGTCT CGGCAGTTCTTTTCATTTACCAAAGG-3' introducing a C-terminal sortase sequence, Myc-tag, His-tag and a *Xba*I site. The fragment was subcloned into *Hind*III - *Xba*I-digested pcDNA3.1 Hygro(+) and sequenced in both directions (288-FSH $\beta$ -LPETGG-Myc-His). HEK293T cells were transfected by addition of a pre-made mixture of polyethylenimine (PEI, 25 kDa linear, Polysciences Inc.) and plasmids encoding FSH $\alpha$  (282-FSH $\alpha$ ) and FSH $\beta$ -LPETGG-His<sub>10</sub> (288-FSH $\beta$ -LPETGG-Myc-His) (ratio PEI:DNA 3:1, ratio  $\alpha$ : $\beta$  1:1). After 24 h, cells were cultured in serum-free DMEM (high glucose + 0.1 mg/mL pen/strep). Medium was collected every 24 h and concentrated using Amicon stirred ultracentrifugation devices equipped with 10 kDa MWCO filters. Small samples were analyzed to determine expression levels and fractions containing FSH-LPETGG-His<sub>10</sub> were combined. Briefly, native sample loading buffer (5  $\mu$ L 4 $\times$ , no  $\beta$ -mercaptoethanol) was added to samples (15  $\mu$ L,  $\sim$ 20 $\times$  concentrated) and proteins were separated, without boiling the samples, on 12.5% SDS-PAGE, followed by transfer to a PVDF membrane using a Biorad Trans-blot Turbo transfer system. Membranes were blocked (1 h, rt, 5% milk in TBS + 0.1% Tween-20) and incubated (o/n, 4  $^{\circ}$ C) with primary antibodies against either FSH $\alpha$  (1:1000 mouse monoclonal anti-FSH $\alpha$  antibody [ME.111], ab9500, Abcam) or FSH $\beta$  (1:800 mouse monoclonal anti-FSH antibody [SP107], ab21587, Abcam). Membranes were washed (3 $\times$  20' TBST) and incubated with secondary antibody (1:5000 goat anti-mouse IgG-HRP, sc-2005, Santa Cruz Biotech), followed by extensive washing (3 $\times$  20' TBST, 1  $\times$  20' TBS) and developing (luminol, ECL enhancer, H<sub>2</sub>O<sub>2</sub>). Luminescent signal was detected using a Chemidoc XRS (Biorad). Image analysis and artificial coloring was done with ImageJ. In all experiments, rFSH was included as a positive control.

After concentrating and pooling, 5 $\times$  Ni-binding buffer was added (100 mM Tris pH 8.0, 750 mM NaCl, 100 mM imidazole) and the solution was applied on a Ni-NTA column (1 mL bed volume, Qiagen), which was pre-equilibrated with binding buffer. The sample was allowed to flow by gravity, and the flow-through was applied again to the column to ensure complete binding of all His-tagged proteins ("FT"). After binding, the column was washed with 10 column volumes (CV) of binding buffer (20 mM Tris, pH 8.0, 150 mM NaCl, 20 mM imidazole) ("wash"). The bound His-tagged proteins were eluted with 4 CV of elution buffer (20 mM Tris pH 8.0, 150 mM NaCl, 500 mM imidazole) and concentrated/buffer exchanged to 20 mM Tris pH 8.0, 150 mM NaCl using Amicon ultracentrifuge tubes (10 kDa MWCO, Millipore). Each step was monitored by SDS-PAGE/WB to detect the presence of recombinant FSH. Also, gels were silverstained for total protein loading. This procedure yielded semi-pure FSH-LPETGG-His<sub>10</sub>, including monomeric FSH $\beta$ -LPETGG-His<sub>10</sub>.

**Sortase-mediated ligation of FSH-LPETGG-His<sub>10</sub> with GGG-BDP-MC (40).** Transpeptidation reactions on FSH-LPETGG-His<sub>10</sub> were carried out for 2 h, 37  $^{\circ}$ C, in the presence of mutant P94S/D160N/K196T SrtA<sub>staph</sub><sup>28</sup> (11  $\mu$ M), sortase ligand **40** (100  $\mu$ M) in sortase reaction buffer (65  $\mu$ L 50 mM Tris, 150 mM NaCl, 10 mM CaCl<sub>2</sub>, pH 7.5). Then, nickel-binding buffer (5 $\times$ : 100 mM Tris pH 8.0, 750 mM NaCl, 100 mM imidazole) was added and the mixture applied to Ni-NTA agarose beads (100  $\mu$ L bed volume) to capture remaining His-tagged starting materials, FSH-SrtA intermediates and SrtA. After binding for 20 min at rt, the beads were spinned down (5 min, 14000 g) and the supernatant was collected. The beads were washed twice with 1 $\times$  binding buffer, and the washes were combined with the supernatant, yielding FSH-BDP-MC (35-40%, based on ELISA of 2 independent experiments). Beads were eluted with elution buffer (20 mM Tris pH 8.0, 150 mM NaCl, 500 mM imidazole). All steps were analyzed using 12.5% SDS-PAGE followed by fluorescence scanning (Chemidoc MP, Biorad), western blot analysis or silverstaining, as described above. As a control for the presence of heterodimeric fluorescent protein, a small aliquot of FSH-BDP-MC was reduced by

addition of 50 mM Tris, pH 7.5, 0.5 mM EDTA, 25 mM NaCl and 5 mM DTT for 1 h, rt, and this was also included on gel. Gel analysis and artificial coloring was done with ImageJ and overlays were made in Adobe Photoshop.

**Measurement of CRE-induced luciferase expression.** CHO<sub>luc</sub> or CHO-hFSHR<sub>luc</sub> cells were cultured to ~80% confluency before use in the assay. On the day of the experiment, cells were harvested using enzyme-free dissociation solution (Millipore), counted (Biorad TC10 automated cell counter) and resuspended in assay medium (DMEM-F12 (1:1), without phenol-red, with pen/strep (0.1 mg/mL) supplied with 1 µg/mL bovine insulin (Tebu-Bio) and 5 µg/mL human apo-transferrin (Sigma)) to a concentration of  $7.5 \times 10^5$  cells/mL. Experiments were conducted in 96-wells white Optiplates (Perkin Elmer) and each well contained 30 µL of recombinant FSH, 30 µL of assay medium and 30 µL cell suspension. After 4 h of stimulation, 50 µL Neolite (PerkinElmer) was added to each well and luminescence signal was detected on a Microbeta Trilux 1450 Luminescence Counter (PerkinElmer). To control for non-FSHR mediated effects on intracellular cAMP levels, highest concentrations of dose-response curves were tested on CHO<sub>luc</sub> cells. As a positive control, forskolin (3 µM, gift from the Medicinal Chemistry department, Leiden University) was included. Data was analyzed using GraphPad Prism 5 (GraphPad Software, La Jolla, USA), and values were normalized to the maximal effect obtained for recombinant human FSH (200 pM, rFSH, Org32489, gift from MSD, Oss, The Netherlands). Each experiment was performed on duplicate plates and mean  $\pm$  sd values of at least three independent experiments are given.

**Uptake and FSHR internalization microscopy experiments.** U2OS-FSHR or U2OS cells were maintained as described under "Cell culture". 48 h before the experiment, cells were harvested (Trypsin-EDTA), counted and seeded onto sterile Labtek II 4- or 8-chamber borosilicate coverglass systems (Fisher Emergo) at a density of  $25\text{-}50 \times 10^4$  cells/well. On the day of the experiment, cells were incubated with the indicated recombinant FSH (11-14 nM) for 2 h, before being washed with PBS (2x), fixed (4 % formaldehyde in PBS), washed again (PBS) and nuclei stained with Draq5 (Thermo Scientific). Cells were imaged on a Leica TCS SPE confocal microscope, using GFP (FSHR), dsRed (BODIPY) or Cy5 (Draq5) filter settings ( $\lambda_{\text{ex}}$  488, 532 or 635 nm) with optimized detection range to exclude bleed-through of dye signal in different channels. For competition experiments, cells were pre-incubated for 1 h with THQ 98 (10 µM), before addition of FSH-BDP-MC (4 nM) to the medium. For dual uptake experiments, cells were incubated with a combination of small molecule agonist DHP-Cy5 96 (1 µM) or sortase ligand 40 (3 µM) and FSH-BDP-MC (14 nM) or rFSH (11 nM). Images were taken under the same settings (laser power, gain, offset, pinhole) and were analyzed using ImageJ. Global fluorescence was determined either for the whole picture or for a specific ROI, which only included regions with cells present, and corrected for the selected area. Intensities were normalized to an average of ~1 for untreated or rFSH-treated cells (GFP signal) or FSH-BDP-MC-treated cells (BODIPY signal), since these can be regarded as positive controls. The percentage of GFP fluorescence signal on the membranes compared to in the cytoplasm was determined by selection of membranes (typically 5-7 cells/image that were inside the focal plane) with the brush tool (ROI:'membranes'), followed by the creation of a ROI that included the selected cells (ROI:'cells'). Two greyscale images were then thresholded according to Yen,<sup>42</sup> followed by selection of the 'membranes' ROI in each picture which was then either cleared (giving 'cytoplasm') or cleared outside (giving 'membranes'). Fluorescence intensities of cells/membranes within the ROI were measured and calculated as a fraction of total GFP signal (membrane+cytoplasm = 100%). For representative images showing the selected ROIs, see Chapter 7, Figure 7.5. Colocalization was calculated on background-corrected images using the intensity correlation analysis and colocalization threshold plugins.

## References

- [1] Hoogendoorn, S.; den Dulk, H.; van der Marel, G. A.; Brouwer, J.; Overkleeft, H. S. contributed to the work described in this chapter.
- [2] Pierce, J. G.; Parsons, T. F. *Annu. Rev. Biochem.* **1981**, *50*, 465–495.
- [3] Dias, J. A.; Van Roey, P. *Arch. Med. Res.* **2001**, *32*, 510–519.
- [4] Fox, K. M.; Dias, J. A.; Van Roey, P. *Mol. Endocrinol.* **2001**, *15*, 378–389.
- [5] Hirooka, T.; Maassen, D.; Berger, P.; Boime, I. *Endocrinology* **2000**, *141*, 4751–4756.
- [6] Ulloa-Aguirre, A.; Timossi, C.; Damián-Matsumura, P.; Dias, J. A. *Endocrine* **1999**, *11*, 205–215.
- [7] Flack, M. R.; Froehlich, J.; Bennet, A. P.; Anasti, J.; Nisula, B. C. *J. Biol. Chem.* **1994**, *269*, 14015–14020.
- [8] Thotakura, N. R.; Blithe, D. L. *Glycobiology* **1995**, *5*, 3–10.
- [9] Baenziger, J. U.; Green, E. D. *Biochim. Biophys. Acta* **1988**, *947*, 287–306.
- [10] Barrios-De-Tomasi, J.; Timossi, C.; Merchant, H.; Quintanar, A.; Avalos, J.; Andersen, C. Y.; Ulloa-Aguirre, A. *Mol. Cell. Endocrinol.* **2002**, *186*, 189–198.
- [11] Morell, A. G.; Gregoriadis, G.; Scheinberg, I. H.; Hickman, J.; Ashwell, G. *J. Biol. Chem.* **1971**, *246*, 1461–1467.
- [12] Daya, S. *Fertil. Steril.* **2002**, *77*, 711–714.
- [13] Simoni, M.; Nieschlag, E. *Reprod. Med. Rev.* **1995**, *4*, 163–178.
- [14] Keene, J. L.; Matzuk, M. M.; Otani, T.; Fauser, B.; Galway, A. B.; Hsueh, A.; Boime, I. *J. Biol. Chem.* **1989**, *264*, 4769–4775.
- [15] Out, H. J.; Mannaerts, B. M.; Driessen, S. G.; Bennink, H. J. C. *Hum. Reprod. Update* **1996**, *2*, 162–171.
- [16] Loumaye, E.; Campbell, R.; Salat-Baroux, J. *Hum. Reprod. Update* **1995**, *1*, 188–199.
- [17] Olijve, W.; de Boer, W.; Mulders, J. W.; van Wezenbeek, P. M. *Mol. Hum. Reprod.* **1996**, *2*, 371–382.
- [18] Zheng, W.; Lu, J. J.; Luo, F.; Zheng, Y.; Feng, Y.-j.; Felix, J. C.; Lauchlan, S. C.; Pike, M. C. *Gynecol. Oncol.* **2000**, *76*, 80–88.
- [19] Zheng, W.; Magid, M. S.; Kramer, E. E.; Chen, Y.-T. *Am. J. Pathol.* **1996**, *148*, 47.
- [20] Radu, A.; Pichon, C.; Camparo, P.; Antoine, M.; Allory, Y.; Couvelard, A.; Fromont, G.; Hai, M. T. V.; Ghinea, N. *N. Engl. J. Med.* **2010**, *363*, 1621–1630.
- [21] Jiang, X.; Liu, H.; Chen, X.; Chen, P.-H.; Fischer, D.; Sriraman, V.; Henry, N. Y.; Arkininstall, S.; He, X. *Proc. Natl. Acad. Sci. U. S. A.* **2012**, *109*, 12491–12496.
- [22] Fan, Q. R.; Hendrickson, W. A. *Nature* **2005**, *433*, 269–277.
- [23] Popp, M. W.; Antos, J. M.; Grotenbreg, G. M.; Spooner, E.; Ploegh, H. L. *Nat. Chem. Biol.* **2007**, *3*, 707–708.
- [24] Tsukiji, S.; Nagamune, T. *ChemBioChem* **2009**, *10*, 787–798.
- [25] LaPolt, P.; Nishimori, K.; Fares, F.; Perlas, E.; Boime, I.; Hsueh, A. *Endocrinology* **1992**, *131*, 2514–2520.
- [26] Fares, F. A.; Suganuma, N.; Nishimori, K.; LaPolt, P. S.; Hsueh, A.; Boime, I. *Proc. Natl. Acad. Sci. U. S. A.* **1992**, *89*, 4304–4308.
- [27] Flack, M.; Bennet, A.; Froehlich, J.; Anasti, J.; Nisula, B. *J. Clin. Endocrinol. Metab.* **1994**, *79*, 756–760.
- [28] Chen, I.; Dorr, B. M.; Liu, D. R. *Proc. Natl. Acad. Sci. U. S. A.* **2011**, *108*, 11399–11404.
- [29] Nakamura, K.; Krupnick, J. G.; Benovic, J. L.; Ascoli, M. *J. Biol. Chem.* **1998**, *273*, 24346–24354.
- [30] Marion, S.; Kara, E.; Crepieux, P.; Piketty, V.; Martinat, N.; Guillou, F.; Reiter, E. *J. Endocrinol.* **2006**, *190*, 341–350.
- [31] Ferguson, S. S. *Pharmacol. Rev.* **2001**, *53*, 1–24.
- [32] Maria de Fatima, M. L.; Liu, X.; Nakamura, K.; Benovic, J. L.; Ascoli, M. *Mol. Endocrinol.* **1999**, *13*, 866–878.
- [33] Sluss, P. M.; Krystek Jr, S. R.; Andersen, T. T.; Melson, B. E.; Huston, J. S.; Ridge, R.; Reichert Jr, L. E. *Biochemistry* **1986**, *25*, 2644–2649.
- [34] Bonger, K. M.; Hoogendoorn, S.; van Koppen, C. J.; Timmers, C. M.; Overkleeft, H. S.; van der Marel, G. A. *ChemMedChem* **2009**, *4*, 2098–2102.
- [35] van Straten, N. C.; van Berkel, T. H.; Demont, D. R.; Karstens, W.-J. F.; Merks, R.; Oosterom, J.; Schulz, J.; van Someren, R. G.; Timmers, C. M.; van Zandvoort, P. M. *J. Med. Chem.* **2005**, *48*, 1697–1700.

- [36] Zinchuk, V.; Wu, Y.; Grossenbacher-Zinchuk, O. *Scientific reports* **2013**, *3*, 1–5.
- [37] Li, Q.; Lau, A.; Morris, T. J.; Guo, L.; Fordyce, C. B.; Stanley, E. F. *J. Neurosci.* **2004**, *24*, 4070–4081.
- [38] Dias, J. A. *Biol. Reprod.* **1986**, *35*, 49–58.
- [39] Cohen, B. D.; Bariteau, J. T.; Magenis, L. M.; Dias, J. A. *Endocrinology* **2003**, *144*, 4393–4402.
- [40] Shimizu, A.; Kawashima, S. *J. Biol. Chem.* **1989**, *264*, 13632–13638.
- [41] Krishnamurthy, H.; Kishi, H.; Shi, M.; Galet, C.; Bhaskaran, R. S.; Hirakawa, T.; Ascoli, M. *Mol. Endocrinol.* **2003**, *17*, 2162–2176.
- [42] Yen, J.-C.; Chang, F.-J.; Chang, S. *IEEE Trans. Image Process.* **1995**, *4*, 370–378.





# 10

## Summary, Work in Progress and Future Prospects

Cell surface receptors function as communication channels between the outside and inside of the cell. In response to ligand binding and activation, a variety of signaling cascades is brought into action. In order to prevent overstimulation of the system, this might eventually result in endocytosis of the ligand-receptor complex from the cell membrane to intracellular compartments. Besides, some types of receptors recycle constitutively between the cell membrane and the intracellular environment, independent of ligand activation. Chapter 1 describes different strategies that make use of synthetic small molecules as targeting devices for cell surface receptors, to either visualize the endocytic processes or to deliver cargo to an intracellular compartment. Successful examples include certain types of G protein-coupled receptors, lectin binding receptors and the folate receptor. Receptors belonging to the first two categories are central to the work described in this thesis.

The mannose receptor (MR) belongs to the family of C-type lectins and is expressed by immune cells such as dendritic cells (DCs) and macrophages to recognize and capture pathogens that contain mannosylated glycoproteins on their surface.<sup>1,2</sup> A previous report by Hillaert *et al.*, described a synthetic mannose containing peptide, termed 'mannose cluster' (MC), that was used to target the cysteine protease activity-based probe DCG-04 to DCs, via the mannose receptor. A BODIPY dye was included in the construct to visualize the labeled lysosomal cathepsins.<sup>3</sup> In Chapter 2 this work was extended by the use of pH-activatable BODIPY dyes, which are quenched at neutral or basic pH and become fluorescent once protonated in acidic cellular compartments.<sup>4</sup> Different MC-pH-activatable BODIPY-DCG-04 constructs were synthesized and evaluated for their *in vitro* pH-dependency, their ability to bind cathepsins and their *in situ* fluorescence properties. The con-

structs were found to have similar  $pK_a$ -values as the original BODIPY dyes published by Urano *et al.* and similar lysate cathepsin labeling as the 'always on' MC-BDP-DCG-04 probe. The main advantage of the incorporation of pH-activatable BODIPY dyes in the constructs became apparent by live-cell imaging experiments of dendritic cells incubated with these probes. Indeed, fluorescence only occurred in intracellular vesicles, without any background in the medium, enabling real-time visualization of receptor endocytosis and trafficking.<sup>5</sup>

The proven utility of the pH-activatable BODIPY dyes in Chapter 2 prompted the development of a novel series of these dyes as described in Chapter 3. With the use of a Knoevenagel-like condensation reaction, pH-activatable dyes containing an azide, alkyne or carboxylic acid ligation handle could be synthesized. Double, consecutive, Knoevenagel condensation was employed to arrive at asymmetric, bifunctional pH-activatable dyes that either contained an additional ligation handle or a charged, polar group to increase water-solubility. These dyes were shown to have similar pH-dependency profiles but red-shifted absorbance and emission maxima compared to the previously reported dyes, making them more suited for imaging applications.<sup>6</sup> An area that could benefit from the use of pH probes is that of glucosidase profiling. Activity-based probes for the lysosomal enzyme  $\beta$ -glucocerebrosidase (GBA1) have been described, based on the cyclophellitol inhibitor.<sup>7</sup> Attachment of a pH-activatable BODIPY dye to cyclophellitol would enable selective visualization of the acidic cellular compartments where GBA1 resides and could potentially be used to 'probe' the pH of these compartments in normal and diseased (Gaucher) states. Furthermore, such probes could be used for a detailed study of recombinant GBA1 (Cerezyme) uptake and trafficking along the endolysosomal pathway of Gaucher cells. To investigate this, a set of pH-activatable BODIPY-cyclophellitol probes **117** were synthesized (Figure 10.1), based on the BODIPY dyes developed in Chapter 3.

Azido-cyclophellitol was synthesized as previously reported and attached to BODIPYs **29a-c,e** via Cu(I)-catalyzed click reaction (Figure 10.1A).<sup>7,8</sup> *In vitro* characterization of the pH-dependency of these probes showed no alterations compared to the unconjugated dyes, confirming that attachment of these dyes via their conjugation handles could be done without changing their pH profile (Figure 10.1B). In addition, *in vitro* biological evaluation showed that these probes had comparable potencies for inhibition of GBA1 as the BODIPY-cyclophellitol probes published by Witte *et al.*<sup>7</sup> Pre-incubation of recombinant GBA1 with known inhibitors conditurolo B epoxide (CBE), cyclophellitol or BODIPY-cyclophellitol abolished labeling with probes **117**, confirming that these bound to the active site of the protein. Also, labeling of recombinant GBA1 with probes **117** only occurred between pH 3.5 and pH 7.0, with optimal labeling around pH 5.5, which coincides with the pH activity profile for GBA1 towards the fluorogenic substrate 4-methylumbelliferyl  $\beta$ -D-glucopyranoside.<sup>7</sup> Thus, potent activity-based pH-activatable probes for GBA1 had been developed which were put to use in microscopy experiments to visualize endogenous lysosomal GBA1 or the uptake and trafficking of pre-labeled Cerezyme into the lysosomal pathway of dendritic cells. These preliminary experiments showed, however, that the *in-situ* pH-dependency of

these probes did not correlate to the profiles found *in vitro*. Fluorescence was predominantly detected in membranous areas of the cells when these probes were added to cells, even at 10 nM concentrations. No vesicular staining, characteristic of endolysosomes, was observed and when binding of the probes to GBA1 was prevented by pre-incubation with CBE, this resulted in the same fluorescence pattern. Incubation of dendritic cells with pre-labeled Cerezyme also resulted only in non-specific fluorescence although substoichiometric amounts of probe were used for labeling to ascertain that no unbound probe was present in solution. The pH-dependency profiles of these probes in a more complex system such as a cell or the active site of a protein are clearly not as evident as in a test tube. It is very well possible that these dyes are 'activated' by apolar membrane constituents, leading to the background fluorescence.<sup>9</sup> On the other hand, appropriately positioned acidic or basic residues in the enzyme's active site might protonate or deprotonate the BODIPY dye leading to an increase or decrease in fluorescence which is not correlated to the pH of the organelle. Similar results were obtained when a pH-activatable dye was used in Chapter 8 illustrating that the *in situ* pH-dependency should be carefully evaluated for each novel construct.

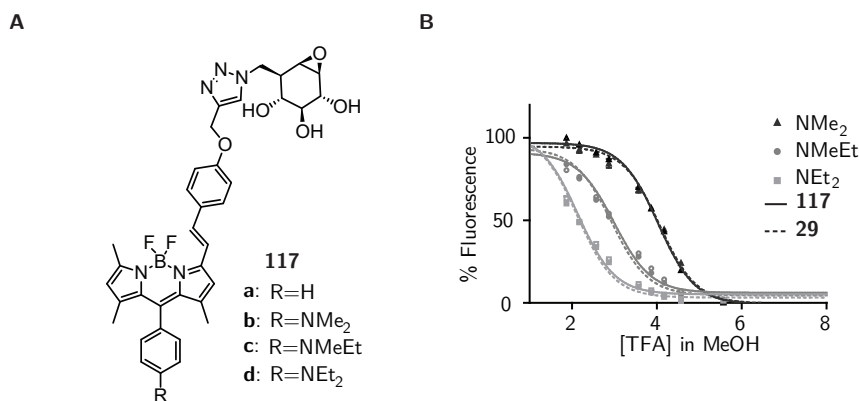


**Figure 10.1:** A) Structure of (pH-activatable) BODIPY-cyclophellitol probes **117a-d**. B) Comparison of fluorescence intensity vs p[TFA] curves for unconjugated BODIPYs **29b,c,e** and probes **117b-d**.

In Chapter 4, the mannose cluster was again used as a targeting entity towards mannose-binding lectins on dendritic cells. However, instead of the delivery of a synthetic activity-based probe as in Chapter 2, the research in this chapter was aimed at the targeted delivery of a 70 kDa protein, Heat shock protein 70 (Hsp70). Recombinant Hsp70 with a C-terminal extension containing a sortase A recognition sequence (LPETGG) and a His-affinity tag, was expressed and purified to yield Hsp70-LPETGG. Synthetic triglycine nucleophiles containing either a BODIPY dye (GGG-BDP **38**) or a BODIPY dye linked to the mannose cluster (GGG-BDP-MC **40**) were synthesized and used for small-scale optimization of the sortase-mediated ligation. Large scale sortase-mediated ligation of Hsp70-LPETGG and GGG-BDP-MC was conducted using the optimized conditions, resulting in the formation of Hsp70-BDP-MC. Repeated chromatography steps were needed for complete removal of

the excess of nucleophile, which would otherwise interfere in the uptake experiments. Purified Hsp70-BDP-MC was subsequently shown to be taken up in a mannose-receptor dependent fashion by dendritic cells. Its presence in intracellular vesicles was demonstrated by fluorescence confocal microscopy. The next step would be to determine what the functional consequences are of targeted delivery of Hsp70 into the endolysosomal pathway. Hsp70 has been shown to have a stabilizing effect on lysosomes with clinical potential in the treatment of Niemann Pick disease, a lysosomal storage disorder.<sup>10</sup> It is of great interest to determine whether the stabilizing effects of Hsp70 also affect other lysosomal enzymes, such as GBA1. Hsp70-BDP-MC would be an excellent candidate to study this in Gaucher cells, which are macrophage-like cells that express the mannose receptor. Potential outcomes of Hsp70-assisted (mutant) GBA1 stabilization include enhanced catalytic activity, diminished protein turnover resulting in longer half-lives or increased levels of correctly folded (and thus catalytically active) protein. The activity of GBA1 could be addressed with the activity-based cyclophellitol or aziridine probes.<sup>7,11</sup> Lipid analysis of lysosomal sphingolipids provides an additional means to look at the effects of Hsp70 on GBA1 activity. Control experiments with recombinant Hsp70 without the mannose cluster can be used to measure the additional effects induced by targeted delivery via the mannose receptor. The research described in Chapter 4 should be easily extendable to other proteins, and sortase-mediated ligation of a synthetic mannose cluster to other proteins might present an alternative to glycan remodeling for delivery to MR-expressing cells.

Although the research described in Chapters 2 and 4 illustrates the convenience of the synthetic mannose cluster, it is undisputedly a very artificial ligand compared to natural occurring mannosides. Whereas the mannose receptor is known for its broad ligand specificity,<sup>1</sup> other mannose-binding C-type lectins such as DC-SIGN and DC-SIGNR have been shown to have narrower specificity and a strong preference for high mannose oligosaccharides.<sup>12</sup> Synthetic oligomannosides, containing different amounts of mannoses, could be used to examine substrate specificity of the different C-type lectins. Furthermore, if taken up in the endocytic pathway, these could be substrates for lysosomal mannosidases, leading to degradation of the glycan and subsequent release of the cargo attached to it. In analogy with the research presented in Chapter 2, three  $\text{man}_{n=1/3/7}$ -BODIPY-DCG-04 constructs were synthesized with the aim of targeting mannose-binding C-type lectins present on dendritic cells (Figure 10.2A). Lysate labeling experiments showed concentration-dependent labeling of cathepsins as seen for other DCG-04 derivatives (Figure 10.2B). Both the  $\text{man}_3$ - (**119**) and  $\text{man}_7$ -oligomannoside (**120**) constructs were taken up by dendritic cells, as seen by confocal microscopy and SDS-PAGE cathepsin labeling (Figure 10.2C). Competition with mannan abolished the labeling, indicating that uptake was receptor-dependent. The  $\text{man}_1$ -BDP-DCG-04 construct **118** however was poorly taken up and many aspecific background bands were detected (data not shown). Further experiments using specific blocking antibodies against the mannose receptor or DC-SIGN are needed to determine which receptor is responsible for the uptake of the  $\text{man}_3$ - and  $\text{man}_7$ -BDP-DCG-04 compounds.

In Chapter 5 a synthetic route towards the mannose-6-phosphate analogue of the man-

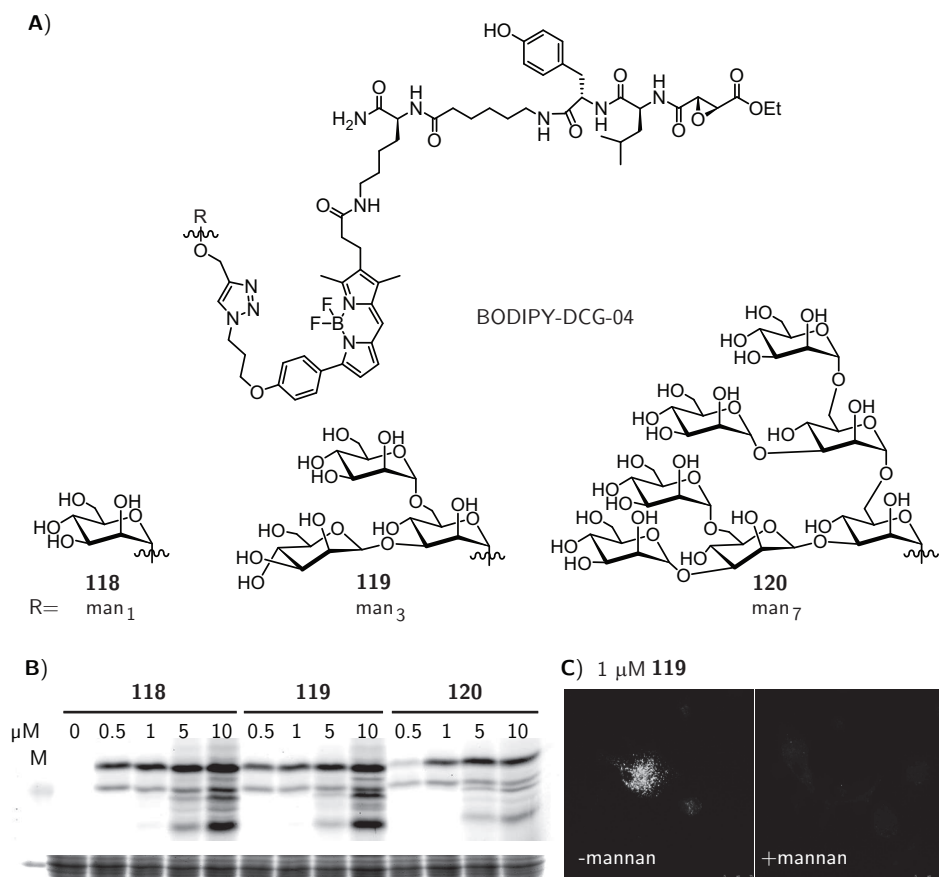


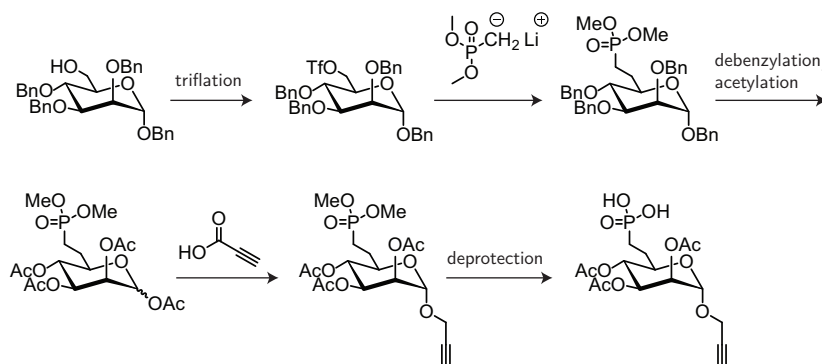
**Figure 10.2:** A) Structures of man<sub>1</sub>-, man<sub>3</sub>-, and man<sub>7</sub>-BODIPY-DCG-04. B) Concentration-dependent labeling of cathepsins with probes **118-120**. Mouse liver lysate (10 μg) was labeled with indicated concentrations of probes at pH 5.5 for 1 h, 37 °C, resolved on 12.5% SDS-PAGE and scanned for fluorescence. C) Confocal fluorescence microscopy analysis of compound **119** uptake. Mouse immature dendritic cells were incubated with 1 μM of probe **136** (2 h, 37 °C) in the presence or absence of mannan (3 mg/mL, 1 h, 37 °C pre-incubation), washed and imaged.

nose cluster was described. The resulting mannose-6-phosphate cluster (M6PC) was conjugated to BODIPY-DCG-04 to study its uptake and trafficking in the endolysosomal pathway. Introduction of the M6PC did not interfere with cathepsin labeling, as shown by lysate labeling experiments. Introduction of the phosphates led to the uptake in dendritic cells via other means than the mannose receptor, since uptake could not be inhibited by addition of mannan. Furthermore, M6PC-BDP-DCG-04 was taken up by COS cells, a fibroblast-like cell line, as seen by fluorescence microscopy, flow cytometry and cathepsin labeling experiments, whereas the mannose cluster analogue was inactive. Uptake of M6PC-BDP-DCG-04 in COS cells was shown to be inhibited by addition of mannose-6-phosphate, confirming that the uptake was mediated by the mannose-6-phosphate receptor. These results indicate that by a synthetic modification the receptor-binding characteristics of a ligand can be com-

pletely altered. Glycoengineering of recombinant enzymes, such as already successfully employed for glucocerebrosidase in Gaucher disease, is a viable method for improved targeting and efficiency of enzyme replacement therapy. Delivery of recombinant enzymes to various endothelial cells that are affected by Pompe or Fabry disease most likely occurs via the CI-MPR. Although both the cation-dependent and the cation-independent mannose-6-phosphate receptors cycle to and from the cell membrane, it has been shown that only the CI-MPR is able to bind ligands at the surface, because of the pH-dependency for ligand binding of the CD-MPR.<sup>13,14</sup>

Literature examples make use of oxime ligation of a synthetic M6P-bearing oligosaccharide to recombinant acid  $\alpha$ -glucosidase<sup>15,16</sup> or introduction of an IGF-II derived peptide fused to human  $\beta$ -glucuronidase<sup>17</sup> to target these enzymes to the CI-MPR. Sortase-mediated ligation of a sortagging ligand containing the mannose-6-phosphate cluster might provide an alternative to these methods in targeting the CI-MPR. In line with the work in Chapter 4, introduction of the mannose-6-phosphate cluster on Hsp70 would allow for targeted delivery of Hsp70 into Niemann-Pick fibroblast.

**Scheme 10.1:** Proposed route for the synthesis of a propargyl mannose-6-phosphonate building block.



A potential drawback of the use of mannose-6-phosphate containing ligands is their susceptibility to dephosphorylation by phosphatases. To prevent this, synthetic M6P analogues have been proposed that retain receptor affinity but are not recognized by dephosphorylating enzymes. Of these, the isosteric mannose-6-phosphonate was shown to be the most promising candidate.<sup>18–22</sup> Synthesis of propargyl mannose-6-phosphonate, followed by click reaction to the common peptide scaffold of the mannose and mannose-6-phosphate cluster, would provide a means for the development of a mannose-6-phosphonate cluster with, presumably, the same binding characteristics as the M6PC, but enhanced stability. Preliminary experiments in the development of such a cluster have shown that the anomeric propargyl group, which was installed early in the synthetic route towards propargyl mannose(-6-phosphate), is likely to interfere with the installment of the C-phosphonate and limits the choice of suitable protective groups. Therefore, a synthetic route where the propargyl is introduced in a later stage should present a more viable alternative, as shown

in Scheme 10.1. The acetyl protected sugar could be employed directly in the click reaction with resin bound **48**, followed by Fmoc removal and coupling with propiolic acid as a click handle, before cleaving the cluster from the resin. Mild basic hydrolysis of the acetlys as described for the benzoyls on the mannose-6-phosphate cluster should result in a fully deprotected mannose-6-phosphonate cluster, containing a click handle for further conjugation.

In Chapters 6-9 various approaches towards targeting of the follicle-stimulating hormone receptor (FSHR) were described. The first three chapters concerned the use of low molecular weight ligands, based on the agonistic dihydropyridine **55** core structure, as targeting ligands, whereas in the last chapter, Chapter 9, the endogenous ligand FSH was employed. To arrive at potent agonists containing a ligation handle for further conjugation, a structure-activity relationship (SAR) study was performed in Chapter 6. Evaluation of the synthesized compounds in a luciferase assay led to the identification of *meta*-DHP **74a**, with PEG spacer length  $n=3$ , as the optimal monomeric ligand. Further conjugation of this ligand to either another copy of the DHP agonist, FSH $\beta_{33-53}$  peptide or fluorescent BODIPY dye resulted in homo- and hetero-dimeric ligands as well as fluorescent ligands. Evaluation of these compounds showed that attachment of bulk to the optimized DHP ligand was tolerated without big loss in potency. No clear bivalency effect was observed for the dimeric compounds. Somewhat surprisingly, the monomeric FSH $\beta_{33-53}$  peptides were inactive in the luciferase assay. A fluorescent analogue of FSH $\beta_{33-53}$  has been used by Zhang *et al.* and was shown to be selectively taken up by FSHR expressing cells. In that study, the naturally occurring cysteine in the sequence was used as the ligation site for attachment of a FITC dye, whereas this residue was replaced by a serine in the peptides described in Chapter 6 and an additional propargyl glycine residue was added as a click handle.<sup>23</sup> The FSH $\beta_{33-53}$  sequence is part of a loop structure in FSH $\beta$  which is believed to play a role in conferring receptor selectivity.<sup>24,25</sup> It would be of interest to use circular dichroism (CD) to examine the secondary structure of the monomeric peptides **81** as well as the heterodimeric DHP-FSH $\beta_{33-35}$  ligands. Comparison to the known structural elements in the wildtype FSH $\beta_{33-53}$  sequence might provide an explanation for the lack of agonistic activity of compounds **81**.<sup>26</sup>

In Chapter 7 several fluorescent ligands based on the optimal *meta*-DHP structure from Chapter 6 were synthesized and evaluated for their agonistic potencies for the FSHR. It was shown that both DHP-BODIPY (**93**) and DHP-Cy5 (**96**) were low nanomolar potent agonists for the FSHR, capable of inducing receptor internalization. However, the internalization properties of the ligands themselves turned out to be highly dependent on the nature of the fluorophore. Only when the charged and hydrophilic cyanine dye was used other non-FSHR mediated endocytic processes could be prevented, resulting in the selective uptake of DHP-Cy5 in cells expressing the FSHR, in an FSHR-mediated fashion. This selective fluorescent agonist could find its use in the study of internalization and trafficking of the receptor-ligand complex and as a diagnostic tool to visualize the FSHR on healthy and tumor cells. Based on the knowledge gained in this chapter, it would be interesting



to synthesize a Cy5-derivative of low molecular weight antagonist THQ **98**. A selective fluorescent antagonist might find its use in cell-surface receptor visualization, without inducing the biological effects as done by an agonist. Additional in depth pharmacological experiments with DHP-Cy5 should include a selectivity profile for the FSHR versus the closely related TSHR or LHR. Also, microscopy experiments at 16 °C instead of 4 °C to study receptor binding without internalization are recommended. Immunostaining for markers of the various endolysosomal compartments together with colocalization analysis might reveal the intracellular route of the ligand-receptor complex. The use of antagonist THQ or chlorpromazine in an luciferase assay might give further insight in the action of these agents on DHP-induced FSHR signaling as opposed to internalization.

Receptor-mediated endocytosis of the fluorescent agonists reported in Chapter 7 opened up the way for the development of carborane containing analogues described in Chapter 8. Uptake of DHP-fluorophore-carborane constructs in the endolysosomal pathway of FSHR-expressing cells would provide a means for the selective delivery of a high concentration of boron needed for boron neutron capture therapy (BNCT). Several BODIPY-based constructs were synthesized, as well as one Cy5 construct. All compounds were agonists for the FSHR, albeit with slightly lower potencies than their fluorescent counterparts in Chapter 7. Again, only the Cy5 containing DHP-Cy5-carborane was shown to be taken up by cells in an FSHR-dependent fashion, although much higher background levels in non-receptor cells were observed than for DHP-Cy5 **96**. The highly lipophilic nature of the carborane cage most likely is at the basis of this result, increasing the lipophilicity of the construct as a whole.<sup>27</sup> A possible solution for this would be to convert the *closo*-carborane cage to its charged *nido*-analogue, an approach met with success in the development of water-soluble carborane-thymidine analogues for BNCT.<sup>28</sup> Alternative cytotoxic drugs might be attached to the DHP core to ensure their delivery in FSHR-expressing cells. Examples might include doxorubicin, a DNA intercalating drug of the anthracycline family, or paclitaxel, a mitotic inhibitor of the taxane diterpene family. Since the site of action of these drugs is not within the endolysosomes, the incorporation of a scissile linker that is cleaved either at acidic pH (e.g. hydrazone, *cis*-aconityl) or by action of a lysosomal enzyme (e.g. cathepsin B) might prove essential.<sup>29,30</sup> Although these drugs are both structurally quite different from the cargo that has been introduced onto the DHP ligand in this thesis, their molecular weights are well within the limits of what could successfully be attached without loss in potency. Considering their polarities, doxorubicin might be the best candidate since it is soluble in water (10 mg/mL), in contrast to paclitaxel which is water-insoluble.<sup>31</sup>

Besides its use as a BNCT agent, there has been interest in the carborane cage as a pharmacophore. Due to its size and lipophilicity *ortho*-carborane is often used as a mimic for either a phenyl or an adamantane group.<sup>32-34</sup> Because of its non-classical electron distribution, the CH-groups are weakly acidic whereas the BH-vertices are considered hydridic in nature. This allows for the participation of the BH-groups in dihydrogen bonding with typical proton donors.<sup>33,35,36</sup> Besides, stacking interaction between the acidic C-H hydrogens



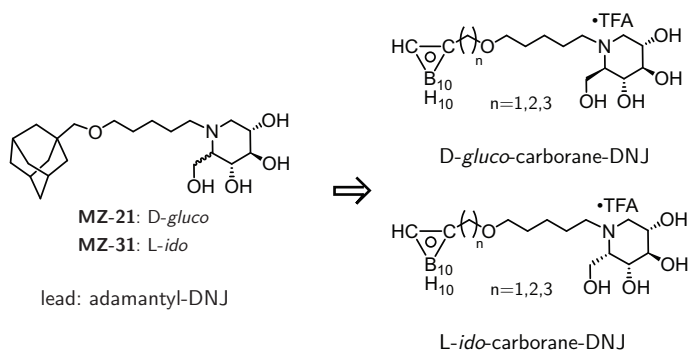


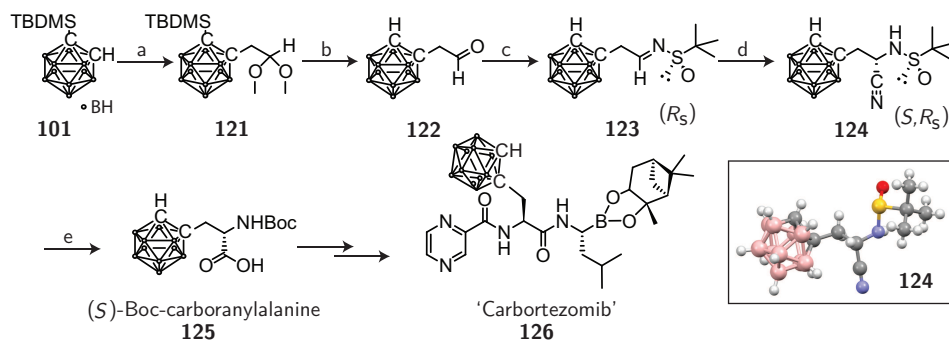
**Figure 10.3:** Carboranyl derivatives of adamantyl-deoxynojirimicin (MZ-21 and MZ-31), incorporating different alkyl spacers.

and the aromatic  $\pi$ -system of a benzene ring have been described, providing another means of a potential favorable interaction between *o*-carborane and other (bio)molecules.<sup>37,38</sup> The various functionalized carboranes described in Chapter 8 were an excellent starting point for the design of bio-active molecules containing a carborane as phenyl or adamantyl mimic. The first set of compounds were carborane-containing analogues of previously reported adamantyl-deoxynojirimicin, a potent inhibitor of the enzymes glucosyl ceramide synthase (GCS), glucocerebrosidase (GBA1) and  $\beta$ -glucosidase 2 (GBA2) involved in glycosphingolipid metabolism.<sup>39</sup> Six different analogues were synthesized, which shared the pentyl-oxy spacer connected to either *D-gluco*- or *L-ido*-deoxynojirimicin (DNJ), but with varying lengths ( $n=1-3$ ) of alkyl spacers attached to the *o*-carborane core (Figure 10.3). Biological evaluation showed these to be very potent inhibitors of all three enzymes, with similar trends in enzyme selectivity profiles as observed for adamantyl-DNJs (MZ-21 and MZ-31, Figure 10.3) but with a smaller influence of the spacer length (data not shown).

In a second example, the carborane cage was introduced as a mimic for a phenyl group in the proteasome inhibitor bortezomib (Scheme 10.2). This peptide-based inhibitor contains a phenylalanine residue, which, according to the crystal structure of the inhibitor in the proteasome  $\beta 1$  and  $\beta 5$  subunits, is not involved in binding.<sup>40</sup> A novel synthetic route towards carboranylalanine was designed based on the asymmetric Strecker reaction, using CsF and TMSCN, on a chiral carborane sulfinimine.<sup>41,42</sup> The absolute stereochemistry of the cyanosulfinamides was established by X-ray crystallography, confirming the anti-addition of the cyanide with respect to the sulfoxide. Both stereoisomers of Boc-protected carboranylalanine were readily obtainable in high yields and enantioselectivity via this route (Scheme 10.2). *In situ* formation of the activated OSu-ester, followed by reaction with L-boronoleucine, Boc-removal and TBTU coupling with 2-pyrazinecarboxylic acid resulted in reasonable yields of bortezomib analogue, "carbortezomib". Competition experiments between this novel inhibitor and a fluorescently tagged pan-reactive proteasome activity-based probe (MVB003)<sup>43</sup> showed concentration-dependent inhibition by carbortezomib of the proteasome  $\beta 1$  and  $\beta 5$  subunits as well as the immunoproteasome

analogues  $\beta 1i$  and  $\beta 5i$ . The epoxomicin-based MVB003 is a covalent, irreversible probe where (car)bortezomib is a covalent, reversible inhibitor. Upon prolonged exposure of bortezomib-labeled proteasome to MVB003, the fluorescent signal increased because of this inequality. It is therefore necessary to use a different assay, such as a fluorogenic substrate assay, to determine the  $IC_{50}$  values of carbortezomib for the different subunits. These two examples showed that the incorporation of carborane in structurally diverse molecules can lead to potent bio-active compounds. It would be of interest to use these compounds in a more complex environment, such as in cells or in organisms, to examine their pharmacokinetic and pharmacodynamic properties.

**Scheme 10.2:** Synthetic route towards carbortezomib **126**. Insert: crystal structure of (*S*,*R*<sub>s</sub>)-cyanosulfonamide **124**.



Reagents and conditions: [a] *n*-BuLi, 1-bromo-2,2-dimethoxyethane, Et<sub>2</sub>O, 96%; [b] i) TBAF, TFA, THF; ii) 37% HCl, AcOH, 93%; [c] (*R*)-*tert*-butylsulfonamide, DCM, 94%; [d] TMSCN, CsF, DMF, -50 °C, 98% overall (dr: 93:7), 48% after crystallization (de: >99%); [e] i) 6M HCl, H<sub>2</sub>O, Δ; ii) Boc<sub>2</sub>O, Et<sub>3</sub>N, THF/H<sub>2</sub>O, 85%.

The research described in Chapter 9, employed sortase-mediated ligation to attach fluorescent cargo to recombinant FSH-LPETGG. Successful ligation resulted in fluorescent FSH-BDP-MC, which was shown to be a picomolar potent FSHR agonist in a luciferase assay and capable of inducing receptor internalization at low nanomolar concentrations. Bright BODIPY fluorescence was observed inside the cells, colocalized with the GFP signal of the GFP-tagged receptor. No background was observed in control cells without FSHR, confirming the selective uptake of this protein together with its receptor. This would thus present a feasible alternative for the use of the LMW DHP agonist in FSHR visualization and targeting. Furthermore, because FSH and DHP bind to allosteric binding sites on the receptor, fluorescent analogues of both could be used in the same experiment as shown in Figure 9.6, Chapter 9. In the study by van Koppen *et al.* it was shown that the presence of DHP Org 214444-0 increased FSH binding to the receptor.<sup>44</sup> It would be of interest to also conduct a detailed study of internalization kinetics and EC<sub>50</sub> values for DHP-Cy5 and FSH-BDP-MC alone and in combination.

Due to low expression levels of FSH-LPETGG and the presence of free FSH $\beta$ -LPETGG which also contained the His-affinity tag and sortase sequence it was not possible to ob-

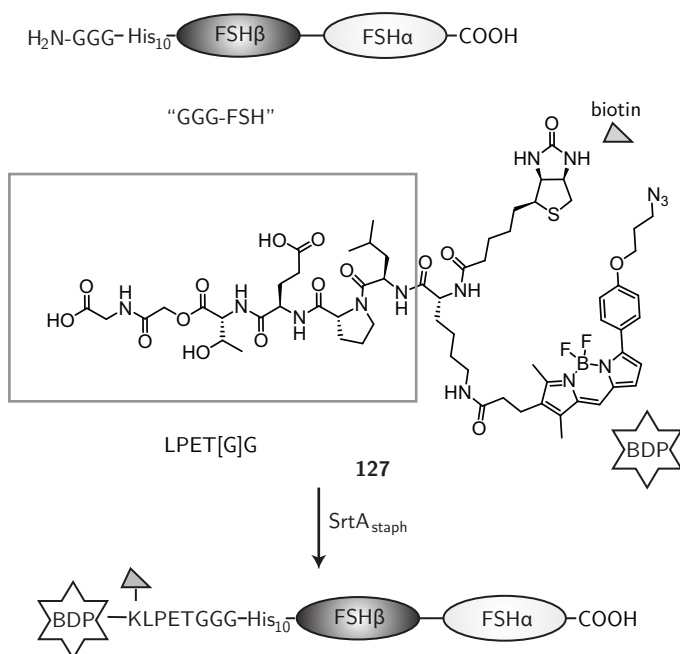


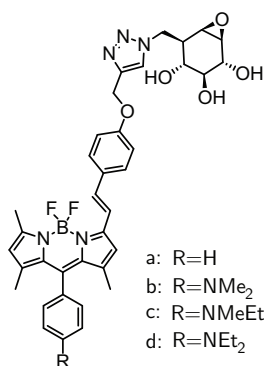
**Figure 10.4:** N-terminal sort tagging using a single chain variant of FSH and depsipeptide 127.

tain a pure FSH-BDP-MC protein preparation. An alternative approach would be to make use of a single chain variant of FSH, which would circumpass the assembly step and would therefore result in the presence of only the intact, full-length, protein.<sup>45,46</sup> Single chain variants, with the C-terminus of FSH $\beta$  fused either directly or via a linker sequence to the N-terminus of FSH $\alpha$  are as active as the heterodimeric protein.<sup>47</sup> The N- $\beta$ -C-N- $\alpha$ -C conformation is based on the notion that the C-terminus of the  $\alpha$ -subunit of the glycoprotein hormones is crucial for receptor binding and activity.<sup>46,48</sup> A sort tagging-compatible variant of a single chain FSH was designed, which contained three additional glycine residues at the N-terminus of FSH $\beta$  allowing for N-terminal sort tagging.<sup>49</sup> A depsipeptide sortase sequence containing both a biotin and BODIPY dye, compound 127, was synthesized as sort tagging partner (Figure 10.4).<sup>50</sup> However, transfection of HEK293 cells with the single chain construct did not result in any observable protein expression and only proteins of lower molecular weight were detected, possibly indicative of splice variants. Alternative expression systems could be considered as well as the incorporation of alternative linker sequences between the sortase sequence and the N-terminus of FSH $\beta$ , which might result in more stable transcripts.

## 10.1 Experimental Section

### Synthesis

**General.** All reagents were of commercial grade and used as received unless stated otherwise. Reaction solvents were of analytical grade and when used under anhydrous conditions stored over flame-dried 3 Å molecular sieves. Dichloromethane was distilled over CaH<sub>2</sub> prior to use. Solvents used for column chromatography were of technical grade and distilled before use. All moisture and oxygen sensitive reactions were performed under an argon atmosphere. Flash chromatography was performed on silica gel (Screening Devices BV, 0.04–0.063 mm, 60 Å). Reactions were routinely monitored by TLC analysis on DC-alufolien (Merck, Kieselgel60, F254) with detection by UV-absorption (254/366 nm) where applicable and spraying with a solution of (NH<sub>4</sub>)<sub>6</sub>Mo<sub>7</sub>O<sub>24</sub> · 4 H<sub>2</sub>O (25 g/l) and (NH<sub>4</sub>)<sub>4</sub>Ce(SO<sub>4</sub>)<sub>4</sub> · 2 H<sub>2</sub>O (10 g/l) in 10% sulfuric acid in water followed by charring at ~150 °C. <sup>1</sup>H, <sup>13</sup>C NMR and <sup>31</sup>P spectra were recorded on a Bruker AV-400 (400 MHz) or Bruker DMX-600 (600 MHz). Chemical shifts are given in ppm (δ) relative to the residual solvent peak or TMS (0 ppm) as internal standard. Coupling constants are given in Hz. Peak assignments are based on 2D <sup>1</sup>H-COSY and <sup>13</sup>C-HSQC NMR experiments. Chloroform was neutralized by filtration over basic Al<sub>2</sub>O<sub>3</sub> before use with t-butyl-protected phosphates. IR measurements (thin film) were conducted on an IRaffinity-1 apparatus and evaluated using IRSolutions software (Shimadzu, Kyoto, Japan). LC-MS measurements were conducted on a Thermo Finnigan LCQ Advantage MAX ion-trap mass spectrometer (ESI+) coupled to a Surveyor HPLC system (Thermo Finnigan) equipped with a standard C18 (Gemini, 4.6 mmD × 50 mmL, 5 μ particle size, Phenomenex) analytical column and buffers A: H<sub>2</sub>O, B: ACN, C: 0.1% aq.TFA. High resolution mass spectra were recorded on a LTQ Orbitrap (Thermo Finnigan) mass spectrometer equipped with an electrospray ion source in positive mode (source voltage 3.5 kV, sheath gas flow 10 mL min<sup>-1</sup>, capillary temperature 250 °C) with resolution R=60000 at m/z 400 (mass range m/z=150–2000) and dioctylphthalate (m/z = 391.28428) as a "lock mass". The high resolution mass spectrometer was calibrated prior to measurements with a calibration mixture (Thermo Finnigan). For reversed-phase HPLC purification of the final compounds an automated HPLC system equipped with a C18 semiprep column (Gemini C18, 250×10 mm, 5 μ particle size, Phenomenex) was used. HPLC-MS purifications were performed on an Agilent Technologies 1200 series automated HPLC system with a Quadropole MS 6130, equipped with a semi-preparative Gemini C18 column (Phenomenex, 250×10, 5 μ particle size). Optical rotations were measured on a Propol automatic polarimeter (Sodium D-line, λ = 589 nm).



### General procedure for the synthesis of (pH-activatable) BODIPY-cyclophellitol (**117a-d**).

Azidocyclophellitol (1 eq) and BODIPY-alkyne **29** (1 eq) were dissolved in *t*-BuOH/toluene/H<sub>2</sub>O (1–2 mL, 1:1:1, v/v/v) and sonicated for 30 min under argon. CuSO<sub>4</sub> (0.1 eq, 100 mM in H<sub>2</sub>O) and sodium ascorbate (0.15 eq, 100 mM in H<sub>2</sub>O) were added and the mixture was heated to 80 °C. After 2 h an additional amount of CuSO<sub>4</sub> (0.1 eq) and sodium ascorbate (0.15 eq) were added. After 2 h the mixture was concentrated *in vacuo* and co-evaporated with toluene. HPLC-MS purification and lyophilizing from *t*-BuOH/H<sub>2</sub>O resulted in **117a-d** as purple powders. *R*<sub>f</sub> = 0.35 (9:1 DCM:MeOH).

**'always on'-BODIPY-cyclophellitol (117a).** Yield: 2.74 mg, 4.1  $\mu\text{mol}$ , 26%.  $^1\text{H}$  NMR (600 MHz, MeOD):  $\delta$  8.13 (s, 1H,  $\text{CH}_{\text{trz}}$ ), 7.57 (dd,  $J = 7.4, 5.0$  Hz, 5H,  $5 \times \text{CH}_{\text{ar}}$ ), 7.50 (d,  $J = 16.2$  Hz, 1H,  $\text{CH}=\text{}$ ), 7.38 - 7.30 (m, 3H,  $\text{CH}=\text{}$ ,  $2 \times \text{CH}_{\text{ar}}$ ), 7.07 (d,  $J = 8.8$  Hz, 2H,  $2 \times \text{CH}_{\text{ar}}$ ), 6.75 (s, 1H, CH), 6.08 (s, 1H, CH), 5.24 (s, 1H,  $\text{OCH}_2$ ), 4.67 (dd,  $J = 13.9, 8.6$  Hz, 2H,  $\text{NCH}_2$ ), 3.62 (d,  $J = 8.2$  Hz, 1H, CH), 3.24 (dd,  $J = 10.0, 8.2$  Hz, 1H, CH), 3.15 (t,  $J = 9.8$  Hz, 1H, CH), 3.07 - 3.00 (m, 2H,  $2 \times \text{CH}$ ), 2.53 (s, 3H,  $\text{CH}_3$ ), 2.42 (td,  $J = 9.2, 8.5, 4.5$  Hz, 1H, CH), 1.46 (s, 3H,  $\text{CH}_3$ ), 1.42 (s, 3H,  $\text{CH}_3$ ).  $^{13}\text{C}$  NMR (151 MHz, MeOD):  $\delta$  160.69, 155.86, 154.79, 144.84, 144.16, 143.78, 141.83, 137.34, 136.39, 133.93, 132.80, 131.34, 130.40, 130.25, 129.90, 129.50, 126.38, 122.12, 118.69, 118.07, 116.43, 116.33, 78.23, 72.53, 68.70, 62.49, 57.59, 55.44, 50.96, 44.68, 14.78, 14.64, 14.53. ESI-HRMS ( $m/z$ ): calcd. for  $[\text{C}_{36}\text{H}_{36}\text{BF}_2\text{N}_5\text{O}_5 + \text{H}]^+$  668.28503; obsd. 668.28553.

**pH-activatable BODIPY-cyclophellitol (117b).** Yield: 5.44 mg, 7.66  $\mu\text{mol}$ , 30%.  $^1\text{H}$  NMR (600 MHz, MeOD):  $\delta$  8.15 (s, 1H,  $\text{CH}_{\text{trz}}$ ), 7.56 (d,  $J = 8.7$  Hz, 2H,  $2 \times \text{CH}_{\text{ar}}$ ), 7.49 (d,  $J = 16.3$  Hz, 1H,  $1 \times \text{CH}=\text{}$ ), 7.33 (d,  $J = 16.4$  Hz, 1H,  $1 \times \text{CH}=\text{}$ ), 7.11 (d,  $J = 8.6$  Hz, 2H,  $2 \times \text{CH}_{\text{ar}}$ ), 7.07 (d,  $J = 8.7$  Hz, 2H,  $2 \times \text{CH}_{\text{ar}}$ ), 6.91 (d,  $J = 8.6$  Hz, 2H,  $2 \times \text{CH}_{\text{ar}}$ ), 6.74 (s, 1H, CH), 6.07 (s, 1H, CH), 5.24 (s, 2H,  $\text{OCH}_2$ ), 4.87 (dd,  $J = 13.8, 3.8$  Hz, 1H,  $\text{NCH}_2\text{-H}^{\text{a}}$ ), 4.67 (dd,  $J = 13.9, 8.6$  Hz, 1H,  $\text{NCH}_2\text{-H}^{\text{b}}$ ), 3.62 (d,  $J = 8.2$  Hz, 1H, CH), 3.26 - 3.20 (m, 1H, CH), 3.14 (t,  $J = 9.8$  Hz, 1H, CH), 3.03 (d,  $J = 6.3$  Hz, 8H,  $2 \times \text{CH}$ ,  $2 \times \text{NCH}_3$ ), 2.52 (s, 3H,  $\text{CH}_3$ ), 2.42 (td,  $J = 9.2, 8.7, 2.5$  Hz, 1H, CH), 1.57 (s, 3H,  $\text{CH}_3$ ), 1.52 (s, 3H,  $\text{CH}_3$ ).  $^{13}\text{C}$  NMR (151 MHz, MeOD):  $\delta$  160.56, 155.31, 154.13, 152.61, 144.86, 144.22, 143.96, 143.37, 136.73, 134.64, 133.59, 131.45, 130.11, 129.79, 126.37, 123.37, 121.81, 118.29, 116.42, 113.69, 78.23, 72.53, 68.69, 62.49, 57.58, 55.45, 50.95, 44.67, 40.55, 15.07, 14.84, 14.62. FT-IR (thin film)  $\nu$  3300.0, 1599.8, 1539.5, 1505.8  $\text{cm}^{-1}$ . LC/MS analysis (linear gradient 10  $\rightarrow$  90% ACN)  $t_{\text{R}}$ : 7.80 min, ESI-MS ( $m/z$ ):  $[\text{M} + \text{H}]^+$ : 711.33. ESI-HRMS ( $m/z$ ): calcd. for  $[\text{C}_{38}\text{H}_{41}\text{BF}_2\text{N}_6\text{O}_5 + \text{H}]^+$  711.32723; obsd. 711.32738.

**pH-activatable BODIPY-cyclophellitol (117c).** Yield: 2.43 mg, 3.35  $\mu\text{mol}$ , 18%.  $^1\text{H}$  NMR (600 MHz, MeOD):  $\delta$  8.15 (s, 1H,  $\text{CH}_{\text{trz}}$ ), 7.56 (d,  $J = 8.7$  Hz, 2H,  $2 \times \text{CH}_{\text{ar}}$ ), 7.49 (d,  $J = 16.4$  Hz, 1H,  $\text{CH}=\text{}$ ), 7.32 (d,  $J = 16.3$  Hz, 1H,  $\text{CH}=\text{}$ ), 7.08 (dd,  $J = 11.3, 8.7$  Hz, 4H,  $4 \times \text{CH}_{\text{ar}}$ ), 6.89 (d,  $J = 8.7$  Hz, 2H,  $2 \times \text{CH}_{\text{ar}}$ ), 6.74 (s, 1H, CH), 6.07 (s, 1H, CH), 5.24 (s, 2H,  $\text{OCH}_2$ ), 4.87 (dd,  $J = 13.9, 3.8$  Hz, 1H,  $\text{NCH}_2\text{-H}^{\text{a}}$ ), 4.67 (dd,  $J = 13.9, 8.6$  Hz, 1H,  $\text{NCH}_2\text{-H}^{\text{b}}$ ), 3.62 (d,  $J = 8.2$  Hz, 1H, CH), 3.51 (q,  $J = 7.0$  Hz, 2H,  $\text{CH}_2$ ), 3.24 (dd,  $J = 9.9, 8.2$  Hz, 1H, CH), 3.14 (t,  $J = 9.9$  Hz, 1H, CH), 3.04 (q,  $J = 3.8$  Hz, 2H,  $2 \times \text{CH}$ ), 2.99 (s, 3H,  $\text{NCH}_3$ ), 2.52 (s, 3H,  $\text{CH}_3$ ), 2.42 (td,  $J = 9.8, 4.3$  Hz, 1H, CH), 1.58 (s, 3H,  $\text{CH}_3$ ), 1.54 (s, 3H,  $\text{CH}_3$ ), 1.16 (t,  $J = 7.0$  Hz, 3H,  $\text{CH}_3$ ).  $^{13}\text{C}$  NMR (151 MHz, MeOD):  $\delta$  160.56, 155.27, 154.09, 151.14, 144.87, 144.21, 143.97, 143.49, 136.69, 134.67, 133.62, 131.46, 130.23, 129.79, 126.37, 122.92, 121.80, 118.28, 116.42, 113.63, 78.24, 72.53, 68.70, 62.49, 57.59, 55.45, 50.96, 47.61, 44.68, 37.72, 15.08, 14.84, 14.61, 11.22. FT-IR (thin film)  $\nu$  3025.7, 2362.3, 1600.6, 1539.2, 1158.8, 1065.7  $\text{cm}^{-1}$ . LC/MS analysis (linear gradient 10  $\rightarrow$  90% ACN)  $t_{\text{R}}$ : 7.21 min, ESI-MS ( $m/z$ ):  $[\text{M} + \text{H}]^+$ : 725.33. ESI-HRMS ( $m/z$ ): calcd. for  $[\text{C}_{39}\text{H}_{43}\text{BF}_2\text{N}_6\text{O}_5 + \text{H}]^+$  725.34288; obsd. 725.34305.

**pH-activatable BODIPY-cyclophellitol (117d).** Yield: 3.46 mg, 4.68  $\mu\text{mol}$ , 14%.  $^1\text{H}$  NMR (600 MHz, MeOD):  $\delta$  8.13 (s, 1H,  $\text{CH}_{\text{trz}}$ ), 7.55 (d,  $J = 8.7$  Hz, 2H,  $2 \times \text{CH}_{\text{ar}}$ ), 7.49 (d,  $J = 16.3$  Hz, 1H,  $\text{CH}=\text{}$ ), 7.31 (d,  $J = 16.3$  Hz, 1H,  $\text{CH}=\text{}$ ), 7.06 (dd,  $J = 8.8, 3.2$  Hz, 4H,  $4 \times \text{CH}_{\text{ar}}$ ), 6.85 (d,  $J = 8.7$  Hz, 2H,  $2 \times \text{CH}_{\text{ar}}$ ), 6.72 (s, 1H, CH), 6.06 (s, 1H, CH), 5.23 (s, 2H,  $\text{OCH}_2$ ), 4.67 (dd,  $J = 13.9, 8.6$  Hz, 2H,  $\text{NCH}_2$ ), 3.62 (d,  $J = 8.1$  Hz, 1H, CH), 3.45 (q,  $J = 7.0$  Hz, 4H,  $2 \times \text{CH}_2$ ), 3.24 (dd,  $J = 9.9, 8.2$  Hz, 1H, CH), 3.15 (t,  $J = 9.8$  Hz, 1H, CH), 3.04 (d,  $J = 3.7$  Hz, 2H,  $2 \times \text{CH}$ ), 2.52 (s, 3H,  $\text{CH}_3$ ), 2.42 (td,  $J = 9.1, 8.6, 4.4$  Hz, 1H, CH), 1.60 (s, 3H,  $\text{CH}_3$ ), 1.56 (s, 3H,  $\text{CH}_3$ ), 1.20 (t,  $J = 7.0$  Hz, 6H,  $2 \times \text{CH}_3$ ).  $^{13}\text{C}$  NMR (151 MHz, MeOD):  $\delta$  160.54, 155.20, 154.03, 149.80, 144.87,

144.21, 143.97, 143.62, 136.63, 134.70, 133.65, 131.47, 130.34, 129.78, 126.37, 122.32, 121.78, 118.26, 116.41, 113.22, 78.23, 72.53, 68.70, 62.49, 57.59, 55.45, 50.95, 45.35, 44.67, 31.12, 15.11, 14.88, 14.62, 12.71. FT-IR (thin film)  $\nu$  1653.9, 1506.0  $\text{cm}^{-1}$ . LC/MS analysis (linear gradient 10  $\rightarrow$  90% ACN)  $t_R$ : 6.62 min, ESI-MS ( $m/z$ ):  $[\text{M} + \text{H}]^+$ : 739.47. ESI-HRMS ( $m/z$ ): calcd. for  $[\text{C}_{40}\text{H}_{45}\text{BF}_2\text{N}_6\text{O}_5 + \text{H}]^+$  739.35853; obsd. 739.35866.

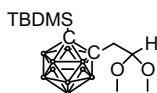
**Synthesis of Man<sub>1</sub>-BODIPY-DCG-04 (118).** Propargyl mannose (1.75 mg, 8  $\mu\text{mol}$ ) and BODIPY-DCG-04 **22** (8.6 mg, 7.6  $\mu\text{mol}$ ) were dissolved in DMF/H<sub>2</sub>O (3 mL, 1:1 v/v) and sodium ascorbate (160  $\mu\text{L}$ , 100 mM in H<sub>2</sub>O, 2 eq) and CuSO<sub>4</sub> (16  $\mu\text{L}$ , 100 mM in H<sub>2</sub>O, 0.2 eq) were added. The resulting mixture was stirred for 2 h at room temperature, before being concentrated and co-evaporated with toluene. Purification by HPLC-MS (A: 25 mM NH<sub>4</sub>OAc, B: linear gradient 20  $\rightarrow$  35% ACN in 12') and lyophilization from H<sub>2</sub>O yielded the final compound (4.3 mg, 3.2  $\mu\text{mol}$ , 42%).  $R_f = 0.9$  (2:1 DCM:MeOH) <sup>1</sup>H NMR (600 MHz, CDCl<sub>3</sub>/MeOD):  $\delta$  8.02 (s, 1H, CH<sub>trz</sub>), 7.92 (t,  $J = 5.6$  Hz, 1H, NH), 7.86 (d,  $J = 7.5$  Hz, 2H, 2  $\times$  CH<sub>ar</sub>), 7.83 (d,  $J = 7.6$  Hz, 1H, NH), 7.76 (t,  $J = 5.6$  Hz, 1H, NH), 7.40 (s, 1H, CH<sub>ar</sub>), 7.06 (d,  $J = 4.1$  Hz, 1H, CH<sub>ar</sub>), 7.01 (d,  $J = 8.5$  Hz, 2H, 2  $\times$  CH<sub>ar</sub>), 6.95 (d,  $J = 8.9$  Hz, 2H, 2  $\times$  CH<sub>ar</sub>), 6.69 (d,  $J = 8.5$  Hz, 2H, 2  $\times$  CH<sub>ar</sub>), 6.59 (d,  $J = 4.1$  Hz, 1H, CH<sub>ar</sub>), 4.80 (d,  $J = 12.4$  Hz, 1H, CH<sub>2</sub>-H<sup>a</sup>), 4.67 - 4.60 (m, 3H, CH<sub>2</sub>, CH<sub>2</sub>-H<sup>b</sup>), 4.45 (t,  $J = 7.5$  Hz, 1H, CH), 4.40 - 4.36 (m, 1H, CH), 4.30 - 4.19 (m, 3H, CH<sub>2</sub>, CH), 4.08 (t,  $J = 5.8$  Hz, 2H, CH<sub>2</sub>), 3.85 (dd,  $J = 11.8, 2.1$  Hz, 1H, CH<sub>2</sub>-H<sup>a</sup>), 3.82 - 3.77 (m, 1H, CH), 3.74 - 3.65 (m, 3H, CH<sub>2</sub>-H<sup>b</sup>, 2  $\times$  CH), 3.64 - 3.55 (m, 3H, 3  $\times$  CH), 3.15 - 3.11 (m, 3H, CH<sub>2</sub>, CH<sub>2</sub>-H<sup>a</sup>), 3.06 - 3.01 (m, 1H, CH<sub>2</sub>-H<sup>b</sup>), 2.99 - 2.93 (m, 1H, CH<sub>2</sub>-H<sup>a</sup>), 2.86 - 2.80 (m, 1H, CH<sub>2</sub>-H<sup>b</sup>), 2.75 (t,  $J = 7.4$  Hz, 2H, CH<sub>2</sub>), 2.50 (s, 3H, CH<sub>3</sub>), 2.42 (p,  $J = 6.5$  Hz, 2H, CH<sub>2</sub>), 2.33 (t,  $J = 7.3$  Hz, 2H, CH<sub>2</sub>), 2.25 (s, 3H, CH<sub>3</sub>), 2.21 - 2.16 (m, 2H, CH<sub>2</sub>), 1.78 - 1.69 (m, 1H, CH<sub>2</sub>-H<sup>a</sup>), 1.62 - 1.48 (m, 6H, 2  $\times$  CH<sub>2</sub>, CH<sub>2</sub>-H<sup>b</sup>, CH), 1.46 - 1.41 (m, 2H, CH<sub>2</sub>), 1.41 - 1.35 (m, 2H, CH<sub>2</sub>), 1.31 - 1.29 (m, 5H, CH<sub>2</sub>, CH<sub>3</sub>), 1.22 - 1.15 (m, 2H, CH<sub>2</sub>), 0.92 (d,  $J = 6.4$  Hz, 3H, CH<sub>3</sub>), 0.88 (d,  $J = 6.4$  Hz, 3H, CH<sub>3</sub>). <sup>13</sup>C NMR (151 MHz, CDCl<sub>3</sub>/MeOD):  $\delta$  177.02, 176.02, 174.68, 173.56, 172.96, 168.66, 168.31, 160.68, 160.59, 157.16, 156.37, 145.22, 141.69, 136.49, 135.67, 131.84, 131.81, 131.78, 131.68, 131.30, 129.27, 128.81, 127.14, 125.60, 124.63, 119.12, 116.19, 115.14, 100.70, 74.84, 72.42, 71.93, 68.54, 65.67, 63.19, 62.90, 60.64, 56.36, 54.34, 54.11, 53.33, 53.14, 48.49, 41.56, 40.15, 40.12, 38.14, 36.86, 36.58, 32.64, 30.93, 29.87, 29.74, 27.32, 26.39, 25.80, 24.17, 23.29, 22.02, 21.29, 14.35, 13.28, 9.62. ESI-HRMS ( $m/z$ ): calcd. for  $[\text{C}_{65}\text{H}_{88}\text{BF}_2\text{N}_{11}\text{O}_{17} + \text{H}]^+$  1344.64935; obsd. 1344.65139.

**Synthesis of Man<sub>3</sub>-BODIPY-DCG-04 (119).** Man<sub>3</sub>-propargyl (2.4 mg, 4.5  $\mu\text{mol}$ ) and BODIPY-DCG-04 **22** (5.12 mg, 4.5  $\mu\text{mol}$ ) were dissolved in DMF/H<sub>2</sub>O (2 mL) and sodium ascorbate (90  $\mu\text{L}$ , 100 mM in H<sub>2</sub>O, 2 eq) and CuSO<sub>4</sub> (2.2  $\mu\text{L}$ , 100 mM in H<sub>2</sub>O, 0.5 eq) were added. The resulting mixture was stirred for 1 h at room temperature, before being concentrated and co-evaporated with toluene. Purification by HPLC-MS (A: 25 mM NH<sub>4</sub>OAc, B: linear gradient 20  $\rightarrow$  35% ACN in 12') and lyophilization from H<sub>2</sub>O yielded the final compound (1.8 mg, 1.1  $\mu\text{mol}$ , 24 %).  $R_f = 0.25$  (1:1 DCM:MeOH). <sup>1</sup>H NMR (600 MHz, MeOD):  $\delta$  8.08 (s, 1H, CH<sub>trz</sub>), 7.88 (d,  $J = 8.9$  Hz, 2H, 2  $\times$  CH<sub>ar</sub>), 7.43 (s, 1H, CH<sub>ar</sub>), 7.07 (d,  $J = 4.0$  Hz, 1H, CH<sub>ar</sub>), 7.01 (d,  $J = 8.5$  Hz, 2H, 2  $\times$  CH<sub>ar</sub>), 6.97 (d,  $J = 8.9$  Hz, 2H, 2  $\times$  CH<sub>ar</sub>), 6.69 (d,  $J = 8.5$  Hz, 2H, 2  $\times$  CH<sub>ar</sub>), 6.62 (d,  $J = 4.1$  Hz, 1H, CH<sub>ar</sub>), 5.05 (s, 1H, CH), 4.85 - 4.77 (m, 3H, CH<sub>2</sub>-H<sup>a</sup>, 2  $\times$  CH), 4.69 - 4.61 (m, 3H, CH<sub>2</sub>, CH<sub>2</sub>-H<sup>b</sup>), 4.45 (t,  $J = 7.6$  Hz, 1H, CH), 4.38 (dd,  $J = 9.3, 5.7$  Hz, 1H, CH), 4.29 - 4.23 (m, 3H, CH<sub>2</sub>, CH), 4.09 (t,  $J = 5.9$  Hz, 2H, CH<sub>2</sub>), 4.05 (d,  $J = 2.5$  Hz, 1H, CH), 3.98 - 3.90 (m, 2H, CH<sub>2</sub>-H<sup>a</sup>, CH), 3.88 - 3.54 (m, 17H, CH<sub>2</sub>-H<sup>b</sup>, 2  $\times$  CH<sub>2</sub>, 12  $\times$  CH), 3.16 - 3.09 (m, 3H, CH<sub>2</sub>, CH<sub>2</sub>-H<sup>a</sup>), 3.07 - 2.99 (m, 1H, CH<sub>2</sub>-H<sup>b</sup>), 2.99 - 2.93 (m, 1H, CH<sub>2</sub>-H<sup>a</sup>), 2.86 - 2.80 (m, 1H, CH<sub>2</sub>-H<sup>b</sup>), 2.76 (t,  $J = 7.3$  Hz, 2H, CH<sub>2</sub>), 2.51 (s, 3H, CH<sub>3</sub>), 2.42 (p,  $J = 6.5$  Hz, 2H, CH<sub>2</sub>), 2.33 (t,  $J = 7.3$  Hz, 2H, CH<sub>2</sub>), 2.26 (s, 3H, CH<sub>3</sub>), 2.20 - 2.14 (m, 2H, CH<sub>2</sub>), 1.77 - 1.70 (m, 1H, CH<sub>2</sub>-H<sup>a</sup>), 1.64 - 1.47 (m, 6H, 2  $\times$  CH<sub>2</sub>, CH<sub>2</sub>-H<sup>b</sup>, CH),

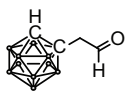
1.47 - 1.41 (m, 2H, CH<sub>2</sub>), 1.41 - 1.35 (m, 2H, CH<sub>2</sub>), 1.32 - 1.29 (m, 5H, CH<sub>2</sub>, CH<sub>3</sub>), 1.20 - 1.15 (m, 2H, CH<sub>2</sub>), 0.92 (d,  $J = 6.4$  Hz, 3H, CH<sub>3</sub>), 0.88 (d,  $J = 6.4$  Hz, 3H, CH<sub>3</sub>). <sup>13</sup>C NMR (151 MHz, MeOD):  $\delta$  177.14, 176.13, 174.79, 173.69, 173.08, 168.74, 168.43, 165.61, 163.01, 160.81, 160.67, 157.29, 156.48, 150.29, 145.18, 142.19, 136.59, 135.75, 131.90, 131.77, 131.36, 129.35, 128.91, 127.23, 125.71, 124.73, 119.16, 116.24, 115.22, 103.97, 101.33, 100.79, 80.67, 74.96, 74.39, 73.70, 72.66, 72.46, 72.10, 71.27, 68.80, 68.64, 67.48, 67.14, 65.75, 63.23, 62.91, 60.71, 56.47, 54.38, 54.21, 53.42, 53.19, 41.62, 40.20, 38.19, 36.91, 36.63, 32.71, 31.05, 29.95, 29.82, 27.40, 26.48, 25.88, 24.25, 23.30, 22.02, 21.34, 14.35, 9.59. LC/MS analysis (linear gradient 10% → 90% ACN)  $t_R$ : 6.53 min, ESI-MS ( $m/z$ ): [M + H]<sup>+</sup>: 1668.40.

**Synthesis of Man<sub>7</sub>-BODIPY-DCG-04 (120).** Man<sub>7</sub>-propargyl (4 mg, 3.4  $\mu$ mol) and BODIPY-DCG-04 **22** (3.8 mg, 3.4  $\mu$ mol) were dissolved in H<sub>2</sub>O/DMF (2 mL, 1:1 v/v) followed by addition of sodium ascorbate (68  $\mu$ L, 100 mM in H<sub>2</sub>O, 2 eq) and CuSO<sub>4</sub> (6.8  $\mu$ L, 100 mM in H<sub>2</sub>O, 0.2 eq). The resulting mixture was stirred for 8 h at room temperature, before being concentrated and co-evaporated with toluene. Purification by HPLC-MS (A: 25 mM NH<sub>4</sub>OAc, B: linear gradient 20 → 35% ACN in 12') and lyophilization from H<sub>2</sub>O yielded man<sub>7</sub>-BDP-DCG-04 (2.5 mg, 1.1  $\mu$ mol, 32%).  $R_f = 0.4$  (1:1:1 EtOAc: H<sub>2</sub>O: *n*-BuOH: AcOH). <sup>1</sup>H NMR (600 MHz, MeOD):  $\delta$  8.28 (s, 1H), 8.09 (d,  $J = 8.1$  Hz, 1H), 7.95 (s, 1H), 7.90 - 7.85 (m, 2H), 7.79 (t,  $J = 5.6$  Hz, 1H), 7.42 (s, 1H), 7.07 (d,  $J = 4.1$  Hz, 1H), 7.01 (d,  $J = 8.5$  Hz, 2H), 6.98 (d,  $J = 8.9$  Hz, 2H), 6.69 (d,  $J = 8.5$  Hz, 2H), 6.62 (d,  $J = 4.1$  Hz, 1H), 5.11 (s, 1H), 5.07 (s, 1H), 4.99 (s, 1H), 4.81 - 4.64 (m, 8H), 4.50 - 4.43 (m, 1H), 4.41 - 4.36 (m, 1H), 4.31 - 4.23 (m, 3H), 4.19 (d,  $J = 2.8$  Hz, 1H), 4.12 - 4.07 (m, 4H), 4.03 - 3.53 (m, 41H), 3.16 - 3.10 (m, 3H), 3.07 - 3.02 (m, 1H), 3.00 - 2.94 (m, 1H), 2.88 - 2.80 (m, 1H), 2.76 (t,  $J = 7.3$  Hz, 2H), 2.51 (s, 3H), 2.44 (q,  $J = 6.4$  Hz, 2H), 2.34 (t,  $J = 7.2$  Hz, 2H), 2.26 (s, 3H), 2.21 - 2.17 (m, 2H), 1.78 - 1.71 (m, 1H), 1.66 - 1.47 (m, 6H), 1.47 - 1.41 (m, 2H), 1.41 - 1.36 (m, 2H), 1.33 - 1.28 (m, 5H), 1.23 - 1.17 (m, 2H), 0.92 (d,  $J = 6.4$  Hz, 3H), 0.88 (d,  $J = 6.4$  Hz, 3H). ESI-HRMS ( $m/z$ ): calcd. for [C<sub>101</sub>H<sub>148</sub>BF<sub>2</sub>N<sub>11</sub>O<sub>47</sub> + H]<sup>+</sup> 2317.96965; obsd. 2317.97256.

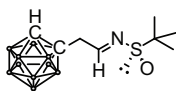
**2-{ 2'-[1'-(*tert*-Butyldimethylsilyl)-1',2'-dicarba-closo-dodecaboranyl]} -1,1-dimethoxyethane (121).** To a solution of TBDMS-carborane **101** (4.27 g, 16.5 mmol, 1 eq) in Et<sub>2</sub>O (60 mL) was added *n*-BuLi (2.5 M in hexane, 7.9 mL, 19.8 mmol, 1.2 eq) at rt under an argon atmosphere. The solution was stirred for 1.5 h turning from colourless to yellow. The mixture was cooled to 0 °C after which 2-bromo-1,1-dimethoxyethane (2.9 mL, 24.8 mmol, 1.5 eq) was added and the solution was stirred for 16 h at rt. After addition of water (200 mL), the aqueous layer was extracted with Et<sub>2</sub>O (3 × 200 mL) and the combined organic layers were washed with brine (1 × 500 mL). The organic phase was dried over MgSO<sub>4</sub>, filtered and concentrated *in vacuo*. Flash column chromatography (100% pentane → 8% EtOAc in pentane) yielded acetal **121** as a colourless oil (5.47 g, 15.7 mmol, 96%).  $R_f = 0.6$  (19:1 pentane:EtOAc). <sup>1</sup>H NMR (400 MHz, CDCl<sub>3</sub>):  $\delta$  4.42 (t,  $J = 5.0$  Hz, 1H, CH), 3.31 (s, 6H, 2 × OCH<sub>3</sub>), 2.47 (d,  $J = 5.0$  Hz, 2H, CH<sub>2</sub>), 3.18 - 1.44 (m, 10H, BH), 1.07 (s, 9H, 3 × CH<sub>3</sub>), 0.33 (s, 6H, 2 × CH<sub>3</sub>). <sup>13</sup>C NMR (101 MHz, CDCl<sub>3</sub>):  $\delta$  103.11, 77.43, 76.10, 53.44, 41.48, 27.66, 20.45, -2.32. <sup>11</sup>B NMR (128 MHz, CDCl<sub>3</sub>):  $\delta$  0.34, -3.42, -7.32, -10.18. FT-IR (thin film)  $\nu$  2953, 2934, 2864, 2610, 2567 (B-H), 1474, 1465, 1446, 1395, 1383, 1365, 1257, 1190, 1120, 1084, 1057, 941, 930, 910, 876, 837, 818, 794, 775, 731 cm<sup>-1</sup>. ESI-HRMS ( $m/z$ ): calcd. for [C<sub>12</sub>H<sub>34</sub>B<sub>10</sub>O<sub>2</sub>Si + CH<sub>3</sub>CN + H]<sup>+</sup> 388.36695; obsd. 388.36781.



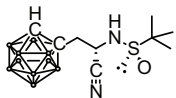




**2-(1',2'-Dicarba-closo-dodecaboranyl)-ethanal (122).** Acetal **121** (5.47 g, 15.7 mmol, 1 eq) was dissolved in THF (60 mL) and cooled to  $-78\text{ }^{\circ}\text{C}$  under an argon atmosphere. TFA (1.17 mL, 15.7 mmol, 1 eq) was added followed by the dropwise addition of TBAF (1 M in THF, 18.8 mL, 18.8 mmol, 1.2 eq). The mixture was allowed to warm up for 1 h, after which the cooling bath was removed and stirring was continued at rt. After 3 h TLC showed complete conversion of the starting material and water (200 mL) was added. The aqueous layer was extracted with  $\text{Et}_2\text{O}$  ( $2 \times 200\text{ mL}$ ). The combined organic layers were washed with brine ( $1 \times 400\text{ mL}$ ), dried over  $\text{MgSO}_4$ , filtered and concentrated. The deprotected carborane was dissolved in 25 mL AcOH at rt under an argon atmosphere and HCl (37% v/v in water, 3.9 mL, 47.1 mmol, 3 eq.) was added carefully. TLC showed complete conversion after 3 h and after the addition of toluene (100 mL), the mixture was concentrated to dryness under reduced pressure. Water (100 mL) was added and extracted with  $\text{Et}_2\text{O}$  ( $2 \times 100\text{ mL}$ ). The combined organic layers were washed with sat. aq.  $\text{NaHCO}_3$  ( $1 \times 200\text{ mL}$ ), brine ( $1 \times 200\text{ mL}$ ), dried over  $\text{MgSO}_4$ , filtered and concentrated *in vacuo*. Flash column chromatography (10%  $\rightarrow$  40% EtOAc in pentane) afforded aldehyde **122** as a colourless oil (2.69 g, 14.4 mmol, 92%). Deprotected acetal:  $R_f = 0.6$ ; aldehyde:  $R_f = 0.3$  (9:1 pentane:EtOAc). FT-IR (thin film)  $\nu$  3059 (BC-H), 2572 (B-H), 1726 (C=O), 1395, 1244, 1124, 1079, 1044, 1018, 1000, 959, 943, 940, 908, 881, 722  $\text{cm}^{-1}$ .  $^1\text{H}$  NMR (400 MHz,  $\text{CDCl}_3$ ):  $\delta$  9.57 (t,  $J = 1.9\text{ Hz}$ , 1H, O=CH), 4.17 (s, 1H, BCH), 3.29 (d,  $J = 1.8\text{ Hz}$ , 2H,  $\text{CH}_2$ ), 3.07 - 1.48 (m, 10H, BH).  $^{13}\text{C}$  NMR (101 MHz,  $\text{CDCl}_3$ ):  $\delta$  194.53, 67.44, 60.20, 48.29.  $^{11}\text{B}$  NMR (128 MHz,  $\text{CDCl}_3$ ):  $\delta$  -2.06, -4.64, -8.91, -11.08, -12.69. ESI-HRMS ( $m/z$ ): calcd. for  $[\text{C}_4\text{H}_{14}\text{B}_{10}\text{O} + \text{CH}_3\text{CN} + \text{H}_2\text{O} + \text{H}]^+$  246.24917; obsd. 246.24940.



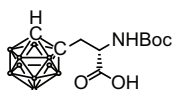
**(R)-(-)-N-[2-(1',2'-Dicarba-closo-dodecaboranyl)ethylidene]-tert-butyl-sulfonamide (123).** To a solution of aldehyde **122** (0.96 g, 5.18 mmol, 1 eq) in DCM (30 mL) was added (*R*)-tert-butylsulfonamide (0.69 g, 5.7 mmol, 1.1 eq) and anhydrous  $\text{CuSO}_4$  (2.7 g, 16.6 mmol, 3.2 eq.) at rt under an argon atmosphere for 16 h. The suspension was vacuum filtrated over a Whatman cellulose filter, washed with DCM and concentrated under reduced pressure. Flash column chromatography (10%  $\rightarrow$  50% EtOAc in pentane) afforded sulfinimine **123** as a white powder (1.41 g, 4.88 mmol, 94%). mp  $143\text{--}145\text{ }^{\circ}\text{C}$ .  $R_f = 0.8$  (1:3 pentane:EtOAc).  $[\alpha]_D^{20} = -231.4\text{ }^{\circ}\text{C}$  ( $c = 1.0$ , DCM). FT-IR (thin film)  $\nu$  3028 (BC-H), 2978, 2966, 2590, 2581 (B-H), 1627 (N=H), 1472, 1455, 1428, 1393, 1365, 1181, 1099, 1057, 1019, 995, 723, 704  $\text{cm}^{-1}$ .  $^1\text{H}$  NMR (400 MHz,  $\text{CDCl}_3$ ):  $\delta$  7.93 (t,  $J = 5.3\text{ Hz}$ , 1H, N=CH), 3.84 (s, 1H, BCH), 3.54 - 3.29 (m, 2H,  $\text{CH}_2$ ), 3.16 - 1.48 (m, 10H, BH), 1.21 (s, 9H,  $3 \times \text{CH}_3$ ).  $^{13}\text{C}$  NMR (101 MHz,  $\text{CDCl}_3$ ):  $\delta$  162.29, 69.85, 60.55, 57.73, 42.69, 22.55.  $^{11}\text{B}$  NMR (128 MHz,  $\text{CDCl}_3$ ):  $\delta$  -1.82, -4.92, -8.87, -11.31, -12.69. ESI-HRMS ( $m/z$ ): calcd. for  $[\text{C}_8\text{H}_{23}\text{B}_{10}\text{NOS} + \text{H}]^+$  290.25763; obsd. 290.257910.



**(R<sub>s</sub>)-(+)-N-[(S)-1-cyano-2-(1',2'-dicarba-closo-dodecaboranyl)ethyl]-tert-butylsulfonamide (124).** Sulfinimine **123** (1.01 g, 3.50 mmol, 1 eq) was dissolved in DMF (18 mL) and cooled to  $-50\text{ }^{\circ}\text{C}$  under an argon atmosphere. CsF (0.69 g, 4.60 mmol, 1.3 eq.) was added, followed by the dropwise addition of TMSCN (0.57 mL, 4.60 mmol, 1.3 eq.). The mixture turned bright yellow and stirring was continued at  $-50\text{ }^{\circ}\text{C}$ . After 24 h additional TMSCN (0.13 mL, 1.10 mmol, 0.3 eq) was added and stirring was continued at  $-50\text{ }^{\circ}\text{C}$  for 60 h. TMSCN (0.3 eq) was added two times more after 92 h and 97 h until TLC showed complete conversion of the starting material after 99 h. The reaction was quenched with a sat. aq.  $\text{NH}_4\text{Cl}$  solution (30 mL) and water (60 mL) was added. The aqueous layer was extracted with EtOAc ( $3 \times 100\text{ mL}$ ) and the combined organic layers were washed with brine ( $1 \times 300\text{ mL}$ ), dried over  $\text{MgSO}_4$ , filtered and concentrated *in vacuo*. The product was co-



evaporated three times with toluene to remove leftover DMF which gave cyanosulfonamide **124** as an orange/yellow solid which was pure according to  $^1\text{H-NMR}$  analysis in a diastereomeric ratio of 93:7 (1.09 g, 3.43 mmol, 98%). Recrystallization from EtOH/pentane at  $-20\text{ }^\circ\text{C}$  afforded cyanosulfonamide **124** as yellow crystals (0.54 g, 1.69 mmol, 48%) as a single diastereomer ( $de > 99\%$ ). mp  $170\text{ }^\circ\text{C}$ .  $R_f = 0.5$  (1:1 pentane: EtOAc).  $[\alpha]_D^{20} = -59.4^\circ$  ( $c = 2.2$ , MeOH). FT-IR (thin film)  $\nu$  3451, 3400, 3059 (BC-H), 2982, 2573 (B-H), 2319, 2071, 1471, 1456, 1439, 1366, 1118, 1024, 986, 907, 880, 851, 825, 795, 723  $\text{cm}^{-1}$ .  $^1\text{H NMR}$  (400 MHz, MeOD):  $\delta$  4.70 (s, 1H, BCH), 4.50 (dd,  $J = 9.1, 5.0$  Hz, 1H, CH), 3.00 (dd,  $J = 15.4, 9.2$  Hz, 1H,  $\text{CH}_2\text{-H}^a$ ), 2.89 (dd,  $J = 15.4, 5.0$  Hz, 1H,  $\text{CH}_2\text{-H}^b$ ), 3.20 - 1.47 (m, 10H, BH), 1.25 (s, 9H,  $3 \times \text{CH}_3$ ).  $^{13}\text{C NMR}$  (101 MHz, MeOD):  $\delta$  119.17, 72.15, 63.68, 58.21, 48.03, 42.18, 22.68.  $^{11}\text{B NMR}$  (128 MHz, MeOD):  $\delta$  -2.36, -4.97, -9.33, -11.71, -12.71. ESI-HRMS ( $m/z$ ): calcd. for  $[\text{C}_9\text{H}_{24}\text{B}_{10}\text{N}_2\text{OS} + \text{H}]^+$  317.26853; obsd. 317.26905.



**(S)-(-)-N-Boc-o-Carboranylalanine(125)**. Cyanosulfonamide **124** (520 mg, 1.64 mmol, 1 eq) was dissolved in 6 M HCl (aq., 6 mL) at rt and refluxed for 4.5 h.

The mixture was co-evaporated three times with toluene to remove all solvent to afford the unprotected amino acid as the HCl salt. Subsequently, the amino acid was redissolved in THF/water (6 mL, 1:1, v/v) at rt under an argon atmosphere and  $\text{Boc}_2\text{O}$  (536 mg, 2.46 mmol, 1.5 equiv.) and  $\text{Et}_3\text{N}$  (0.92 mL, 6.56 mmol, 4 eq) were added and the mixture was stirred for 16 h. The solvent was removed under reduced pressure and co-evaporated with toluene (3x). Flash column chromatography (100% EtOAc  $\rightarrow$  30% MeOH in EtOAc) gave the Boc-protected amino acid as an off-white powder (462 mg, 1.39, 85%).  $R_f = 0.3$  (EtOAc + 3 drops AcOH).  $[\alpha]_D^{20} = -19.7^\circ$  ( $c = 2.3$ , MeOH). FT-IR (thin film)  $\nu$  3061 (BC-H), 2981, 2932, 2585 (B-H), 1716 (C=O), 1511, 1395, 1370, 1290, 1255, 1158, 1069, 1022, 851, 781, 725  $\text{cm}^{-1}$ .  $^1\text{H NMR}$  (400 MHz, MeOD):  $\delta$  4.52 (s, 1H, BCH), 4.15 (d,  $J = 8.8$  Hz, 1H, CH $\alpha$ ), 2.92 (d,  $J = 15.2$  Hz, 1H,  $\text{CH}_2\text{-H}^a$ ), 2.64 (dd,  $J = 15.0, 10.6$  Hz, 1H,  $\text{CH}_2\text{-H}^b$ ), 3.14 - 1.56 (m, 10H, BH), 1.46 (s, 9H,  $3 \times \text{CH}_3$ ).  $^{13}\text{C NMR}$  (101 MHz, MeOD):  $\delta$  157.67, 80.90, 74.51, 63.18, 54.60, 39.55, 28.71.  $^{11}\text{B NMR}$  (128 MHz, MeOD):  $\delta$  -2.64, -5.55, -9.57, -11.40, -13.00. ESI-HRMS ( $m/z$ ): calcd. for  $[\text{C}_{10}\text{H}_{25}\text{B}_{10}\text{NO}_4 + \text{CH}_3\text{CN} + \text{H}]^+$  373.31250; obsd. 373.31299.

## References

- [1] Stahl, P. D. *Curr. Opin. Immunol.* **1992**, *4*, 49–52.
- [2] Sallusto, F.; Cella, M.; Danieli, C.; Lanzavecchia, A. *J. Exp. Med.* **1995**, *182*, 389–400.
- [3] Hillaert, U.; Verdoes, M.; Florea, B.; Saragliadis, A.; Habets, K.; Kuiper, J.; Van Calenbergh, S.; Ossendorp, F.; van der Marel, G.; Driessen, C.; Overkleeft, H. *Angew. Chem. Int. Ed. Engl.* **2009**, *48*, 1629.
- [4] Urano, Y.; Asanuma, D.; Hama, Y.; Koyama, Y.; Barrett, T.; Kamiya, M.; Nagano, T.; Watanabe, T.; Hasegawa, A.; Choyke, P. L.; Kobayashi, H. *Nat. Med.* **2009**, *15*, 104–9.
- [5] Hoogendoorn, S.; Habets, K. L.; Passemard, S.; Kuiper, J.; van der Marel, G. A.; Florea, B. I.; Overkleeft, H. S. *Chem. Commun.* **2011**, *47*, 9363–9365.
- [6] Hoogendoorn, S.; Blom, A. E. M.; Willems, L. I.; van der Marel, G. A.; Overkleeft, H. S. *Org. Lett.* **2011**, *13*, 5656–5659.
- [7] Witte, M. D. et al. *Nat. Chem. Biol.* **2010**, *6*, 907–913.
- [8] Hansen, F. G.; Bundgaard, E.; Madsen, R. *J. Org. Chem.* **2005**, *70*, 10139–10142.
- [9] Zhang, X.-X.; Wang, Z.; Yue, X.; Ma, Y.; Kiesewetter, D. O.; Chen, X. *Mol. Pharm.* **2013**, *10*, 1910–1917.
- [10] Kirkegaard, T.; Roth, A. G.; Petersen, N. H.; Mahalka, A. K.; Olsen, O. D.; Moilanen, I.; Zylicz, A.; Knudsen, J.; Sandhoff, K.; Arenz, C.; Kinnunen, P. K.; Nylandsted, J.; Jäättelä, M. *Nature* **2010**, *463*, 549–553.

- [11] Kallemeijn, W. W. et al. *Angew. Chem. Int. Ed. Engl.* **2012**, *124*, 12697–12701.
- [12] Mitchell, D. A.; Fadden, A. J.; Drickamer, K. *J. Biol. Chem.* **2001**, *276*, 28939–28945.
- [13] Stein, M.; Zijderhand-Bleekemolen, J. E.; Geuze, H.; Hasilik, A.; Von Figura, K. *EMBO J* **1987**, *6*, 2677.
- [14] Watanabe, H.; Grubb, J. H.; Sly, W. S. *Proc. Natl. Acad. Sci. U. S. A.* **1990**, *87*, 8036–8040.
- [15] Zhu, Y.; Jiang, J.-L.; Gumlaw, N. K.; Zhang, J.; Bercury, S. D.; Ziegler, R. J.; Lee, K.; Kudo, M.; Canfield, W. M.; Edmunds, T.; Jiang, C.; Mattaliano, R. J.; Cheng, S. H. *Mol. Ther.* **2009**, *17*, 954–963.
- [16] Zhu, Y.; Li, X.; Mcvie-Wylie, A.; Jiang, C.; Thurberg, B.; Raben, N.; Mattaliano, R.; Cheng, S. *Biochem. J* **2005**, *389*, 619–628.
- [17] LeBowitz, J. H.; Grubb, J. H.; Maga, J. A.; Schmiel, D. H.; Vogler, C.; Sly, W. S. *Proc. Natl. Acad. Sci. U. S. A.* **2004**, *101*, 3083–3088.
- [18] Berkowitz, D. B.; Maiti, G.; Charette, B. D.; Dreis, C. D.; MacDonald, R. G. *Org. Lett.* **2004**, *6*, 4921–4924.
- [19] Fei, X.; Connelly, C. M.; MacDonald, R. G.; Berkowitz, D. B. *Bioorg. Med. Chem. Lett.* **2008**, *18*, 3085–3089.
- [20] Vidil, C.; Morère, A.; Garcia, M.; Barragan, V.; Hamdaoui, B.; Rochefort, H.; Montero, J.-L. *Eur. J. Org. Chem.* **1999**, *1999*, 447–450.
- [21] Khanjin, N. A.; Montero, J.-L. *Tetrahedron Lett.* **2002**, *43*, 4017–4020.
- [22] Gary-Bobo, M.; Nirdé, P.; Jeanjean, A.; Morère, A.; Garcia, M. *Curr. Med. Chem.* **2007**, *14*, 2945.
- [23] Zhang, X.; Chen, J.; Kang, Y.; Hong, S.; Zheng, Y.; Sun, H.; Xu, C. *Int. J. Pharm.* **2013**, *453*, 498–505.
- [24] Roth, K. E.; Dias, J. A. *Mol. Cell. Endocrinol.* **1995**, *109*, 143–149.
- [25] Westhoff, W.; Slootstra, J.; Puijk, W.; Kuperus, D.; Flinterman, J.; Schaaper, W.; Onk, H.; Meloen, R. *J. Reprod. Immunol.* **1996**, *30*, 133–149.
- [26] Agris, P. F.; Guenther, R. H.; Sierzputowska-Gracz, H.; Easter, L.; Smith, W.; Hardin, C. C.; Santa-Coloma, T. A.; Crabb, J. W.; Reichert Jr, L. E. *J. Protein Chem.* **1992**, *11*, 495–507.
- [27] Yamamoto, K.; Endo, Y. *Bioorg. Med. Chem. Lett.* **2001**, *11*, 2389–2392.
- [28] Byun, Y.; Yan, J.; Al-Madhoun, A. S.; Johnsamuel, J.; Yang, W.; Barth, R. F.; Eriksson, S.; Tjarks, W. *Appl. Radiat. Isot.* **2004**, *61*, 1125–1130.
- [29] Trail, P. A.; Willner, D.; Hellström, K. E. *Drug Dev. Res.* **1995**, *34*, 196–209.
- [30] Trail, P. A.; King, D. H.; Dubowchik, G. M. *Cancer Immunol. Immunother.* **2003**, *52*, 328–337.
- [31] Singla, A. K.; Garg, A.; Aggarwal, D. *Int. J. Pharm.* **2002**, *235*, 179–192.
- [32] Valliant, J. F.; Guenther, K. J.; King, A. S.; Morel, P.; Schaffer, P.; Sogbein, O. O.; Stephenson, K. A. *Coord. Chem. Rev.* **2002**, *232*, 173–230.
- [33] Scholz, M.; Hey-Hawkins, E. *Chem. Rev.* **2011**, *111*, 7035–7062.
- [34] Issa, F.; Kassiou, M.; Rendina, L. M. *Chem. Rev.* **2011**, *111*, 5701–5722.
- [35] Siegbahn, P. E.; Eisenstein, O.; Rheingold, A. L.; Koetzle, T. F. *Acc. Chem. Res.* **1996**, *29*, 348–354.
- [36] Fanfrlík, J.; Lepšík, M.; Horinek, D.; Havlas, Z.; Hobza, P. *ChemPhysChem* **2006**, *7*, 1100–1105.
- [37] Blanch, R. J.; Williams, M.; Fallon, G. D.; Gardiner, M. G.; Kaddour, R.; Raston, C. L. *Angew. Chem. Int. Ed. Engl.* **1997**, *36*, 504–506.
- [38] Raston, C. L.; Cave, G. W. *Chem Eur J* **2004**, *10*, 279–282.
- [39] Overkleeft, H. S.; Renkema, G. H.; Neele, J.; Vianello, P.; Hung, I. O.; Strijland, A.; van der Burg, A. M.; Koomen, G.-J.; Pandit, U. K.; Aerts, J. M. *J. Biol. Chem.* **1998**, *273*, 26522–26527.
- [40] Groll, M.; Berkers, C. R.; Ploegh, H. L.; Ovaa, H. *Structure* **2006**, *14*, 451 – 456.
- [41] Li, B.-F.; Yuan, K.; Zhang, M.-J.; Wu, H.; Dai, L.-X.; Wang, Q. R.; Hou, X.-L. *J. Org. Chem.* **2003**, *68*, 6264–6267.
- [42] Ferreira, F.; Botuha, C.; Chemla, F.; Pérez-Luna, A. *Chem. Soc. Rev.* **2009**, *38*, 1162–1186.
- [43] Kolodziejek, I.; Misaš-Villamil, J. C.; Kaschani, F.; Clerc, J.; Gu, C.; Krahn, D.; Niessen, S.; Verdoes, M.; Willems, L. I.; Overkleeft, H. S.; Kaiser, M.; van der Hoorn, R. A. *Plant Physiol.* **2011**, *155*, 477–489.
- [44] van Koppen, C. J.; Verbost, P. M.; van de Lagemaat, R.; Karstens, W.-J. F.; Loozen, H. J.; van Achterberg, T. A.; van Amstel, M. G.; Brands, J. H.; van Doornmalen, E. J.; Wat, J.; Mulder, S. J.; Raafs, B. C.; Verkaik, S.; Hanssen, R. G.; Timmers, C. M. *Biochem. Pharmacol.* **2013**, *85*, 1162–1170.
- [45] García-Echeverría, C.; Imbach, P.; France, D.; Fürst, P.; Lang, M.; Noorani, M.; Scholz, D.; Zimmermann, J.; Furet, P. *Bioorg. Med. Chem. Lett.* **2001**, *11*, 1317 – 1319.

- [46] Ben-Menahem, D. *J. Neuroendocrinol.* **2004**, *16*, 171–177.
- [47] Sugahara, T.; Sato, A.; Kudo, M.; Ben-Menahem, D.; Pixley, M. R.; Hsueh, A. J.; Boime, I. *J. Biol. Chem.* **1996**, *271*, 10445–10448.
- [48] Parsons, T. F.; Pierce, J. G. *J. Biol. Chem.* **1979**, *254*, 6010–6015.
- [49] Antos, J. M.; Chew, G.-L.; Guimaraes, C. P.; Yoder, N. C.; Grotenbreg, G. M.; Popp, M. W.-L.; Ploegh, H. L. *J. Am. Chem. Soc.* **2009**, *131*, 10800–10801.
- [50] Williamson, D. J.; Fascione, M. A.; Webb, M. E.; Turnbull, W. B. *Angew. Chem. Int. Ed. Engl.* **2012**, *124*, 9511–9514.



# Samenvatting

## Een chemisch biologische aanpak voor doelgerichte ligand-medicijn constructen

Membraangebonden receptoren aan de buitenkant van een cel functioneren als een communicatiekanaal tussen de intra- en extracellulaire ruimte. Als een receptor wordt geactiveerd door binding van een ligand, leidt dit tot een scala aan intracellulaire signaleringcascades. Om te voorkomen dat de cel te sterk gestimuleerd raakt, kan het ligand-receptor complex geïnternaliseerd worden, van de membraan naar intracellulaire compartimenten. Synthetische liganden die selectief kunnen binden aan een bepaald type receptor kunnen potentieel ingezet worden om een fluorescent molecuul of een medicijn te sturen naar de cel van interesse. In hoofdstuk 1 worden verschillende strategieën besproken voor het gebruik van synthetische liganden voor receptoren. Deze liganden worden ofwel gebruikt voor visualisatie van ligand binding en het transport van het ligand-receptor complex door de cel, ofwel om doelgerichte therapie mogelijk te maken.

De mannose receptor (MR) behoort tot de familie van C-type lectine-bindende receptoren en wordt tot expressie gebracht door cellen van het immuunsysteem, zoals dendritische cellen en macrofagen. Glycoeiwitten op pathogenen worden herkend door de MR en vervolgens geïnternaliseerd en afgebroken, wat leidt tot een immuunrespons. In een eerdere studie is een synthetisch ligand beschreven, het zogenaamde mannose cluster (MC), dat kan binden aan de MR. Dit cluster is vastgemaakt aan een fluorescente remmer van lysosomale cathepsines (BODIPY-DCG-04) en dit leidde tot de selectieve opname van het construct in dendritische cellen. In hoofdstuk 2 wordt op dit onderzoek voortgeborduurd met de synthese van een aantal vergelijkbare constructen. Door gebruik te maken van pH-afhankelijke BODIPYs kon het proces van opname bestudeerd worden zonder te wassen, omdat de constructen alleen fluorescent zijn in een zuur milieu, zoals in de lysosomen. Er kon worden aangetoond dat de constructen cathepsines remmen, zowel in lysaat als in de cel, en dat de opname in dendritische cellen receptor-afhankelijk is.

Het bewezen nut van de pH-afhankelijke BODIPYs in hoofdstuk 2 leidde tot de ontwikkeling van een nieuwe serie kleurstoffen, zoals beschreven in hoofdstuk 3. Door gebruik te maken van een Knoevenagel-achtige condensatiereactie konden pH-afhankelijke BODIPYs worden gesynthetiseerd met verschillende handvatten voor verdere conjugatie, zoals een azide, alkyn of zuurgroep. Door middel van twee, elkaar opvolgende, Knoevenagel-reacties kon bovendien een extra handvat of een water oplosbare groep geïntroduceerd

---

worden. De gesynthetiseerde kleurstoffen hadden een vergelijkbare pH-afhankelijkheid als die beschreven in hoofdstuk 2. Bovendien waren de excitatie- en emissiespectra verschoven richting het rood, wat deze stoffen zeer geschikt maakt voor microscopie toepassingen.

In hoofdstuk 4 wordt het mannose cluster wederom gebruikt als doelgericht ligand voor de mannose receptor. Echter, in plaats van een klein molecuul zoals in hoofdstuk 2 werd er nu een 70 kDa groot eiwit, Hsp70, aan vastgemaakt. Recombinant Hsp70, voorzien van een C-terminale extensie met een sortase A herkenningsequentie (LPETGG) en een His-affiniteitssequentie erin, werd tot expressie gebracht en gezuiverd. Vervolgens werd dit 'Hsp70-LPETGG' eiwit geligeerd aan dan wel BODIPY, dan wel BODIPY-mannose cluster met behulp van het bacteriële enzym sortase. De reactie werd eerst geoptimaliseerd op kleine schaal en vervolgens op grote schaal uitgevoerd. Het product, Hsp70-BDP-MC, werd gezuiverd en vervolgens toegevoegd aan het medium van dendritische cellen. Er kon worden aangetoond dat dit eiwit werd opgenomen door de cellen met behulp van microscopie. Blokkering van de receptor (met het natuurlijk voorkomende ligand mannan) zorgde ervoor dat Hsp70-BDP-MC niet meer werd opgenomen, wat een indicatie is voor receptor-gemedieerde opname.

In hoofdstuk 5 werd onderzocht of een synthetische verandering van het mannose cluster er toe kon leiden dat een andere receptor dan de mannose receptor bereikt werd. Daarvoor werd een mannose-6-fosfaat cluster (M6PC) ontworpen en gesynthetiseerd en wederom geconjugeerd aan BODIPY-DCG-04. Cathepsine labelingsexperimenten in lever lysaat lieten zien dat introductie van de fosfaatgroepen op het cluster geen effect had op de labelingsefficiëntie. Experimenten met COS cellen lieten zien dat M6PC-BODIPY-DCG-04, in tegenstelling tot MC-BODIPY-DCG-04, door de cellen werd opgenomen, wat resulteerde in de labeling van lysosomale cathepsines. Voorbehandeling van de COS cellen met mannose-6-fosfaat remde de opname van het construct, wat aangeeft dat het construct inderdaad via de mannose-6-fosfaat receptor werd opgenomen. Voorbehandeling van dendritische cellen met mannan, om de mannose receptor te blokkeren, resulteerde niet in remming van de opname. In conclusie toonden deze experimenten aan dat door een kleine synthetische modificatie de receptor selectiviteit van het ligand kon worden veranderd van de mannose receptor naar de mannose-6-fosfaat receptor.

In de hoofdstukken 6-9 worden verschillende strategieën besproken om doelgerichte moleculen voor de follikelstimulerend hormoon (FSH) receptor te ontwikkelen. In de eerste drie hoofdstukken worden laag moleculair gewicht (LMW) liganden gebruikt, gebaseerd op een eerder gepubliceerde dihydropyridine (DHP) agonist en in hoofdstuk 9 het endogene hormoon FSH. In hoofdstuk 6 werd een reeks aan verbindingen gebaseerd op DHP gesynthetiseerd om erachter te komen wat de beste plek was om het molecuul te functionalisieren zonder de activiteit op de receptor aan te tasten. De gesynthetiseerde verbindingen werden getest in een luciferase assay en hieruit kon een structuur-activiteitsrelatie worden gedestilleerd. Het bleek dat *meta*-gefunctionaliseerde DHPs in combinatie met een polyethyleenglycol linker van lengte  $n=3$  de meest potente agonisten opleverde. Met deze bouwsteen konden dimere en fluorescente FSH receptor agonisten worden gemaakt zon-

der dat dit ten koste ging van de activiteit.

Hoofdstuk 7 beschrijft het onderzoek naar de meest optimale kleurstof om vast te maken aan het ligand geïdentificeerd in hoofdstuk 6. Verschillende kleurstoffen konden worden geïntroduceerd wat resulteerde in potente fluorescente agonisten. Deze agonisten waren tevens in staat om de receptor te laten internaliseren, zoals gedemonstreerd in een microscopie internalisatie assay. Het bleek echter dat de meeste van deze fluorescente liganden ook geïnternaliseerd werden in cellen die geen receptor expressie hadden. Alleen in het geval van de hydrofiele en geladen kleurstof Cy5 werd het resulterende ligand DHP-Cy5 selectief via de FSH receptor opgenomen. Deze stof is daarmee een zeer geschikte kandidaat als diagnostisch gereedschap om de aanwezigheid van de FSH receptor op bijvoorbeeld eierstoktumorcellen aan te tonen. Of het mogelijk is om naast een fluorescente kleurstof ook een medicijn te sturen naar cellen die de FSH receptor tot expressie brengen met behulp van het DHP ligand, is beschreven in hoofdstuk 8. Verscheidene moleculen werden gesynthetiseerd welke naast de DHP en de kleurstof ook een of meerdere carboranen bevatten. Carboranen kunnen gebruikt worden in een tweedelige therapie genaamd "boron neutron capture therapy (BNCT)" voor de bestrijding van kanker. Helaas bleek dat het toevoegen van de vette carboraan structuur resulteerde in de aspecifieke opname van de constructen in cellen die geen receptor bevatten. Een lage mate van selectiviteit kon alleen worden bereikt door Cy5 als kleurstof te gebruiken.

Om te voorkomen dat iedere (kleine) modificatie van het ligand grote invloed heeft op de opname eigenschappen, kan worden gekozen voor een hoog moleculair gewicht (HMW) ligand. Deze strategie is beschreven in hoofdstuk 9 waar sortase werd gebruikt om FSH fluorescent te labelen met BODIPY-MC. Het resulterende FSH-BDP-MC bleek een zeer potente agonist voor de FSH receptor en werd bovendien zeer selectief, samen met de receptor, door de cellen opgenomen. Het werk beschreven in dit proefschrift is samengevat in hoofdstuk 10 en er is tevens een vooruitblik geschetst voor mogelijk vervolgonderzoek. Concluderend laat het hier beschreven onderzoek zien dat doelgerichte moleculen zeer waardevol zijn in het selectief sturen van fluorescente of therapeutisch interessante moleculen naar receptoren op specifieke cellen of weefsels.

# List of Publications

**Novel endogenous peptide agonists of cannabinoid receptors.** Gomes, I., Grushko, J. S., Golebiewska, U., Hoogendoorn, S., Gupta, A., Heimann, A. S., Ferro, E. S., Scarlata, S., Fricker, L. D., Devi, L. A. *FASEB J.* **2009**, 23:3020-3029

**Synthesis and pharmacological evaluation of dimeric follicle-stimulating hormone receptor antagonists.** Bongers, K. M., Hoogendoorn, S., van Koppen, C. J., Timmers, C. M., Overkleeft, H. S., van der Marel, G. A. *ChemMedChem* **2009**, 4:2098-2102

**Synthesis of oligoribonucleic acid conjugates using a cyclooctyne phosphoramidite.** Van Delft, P., Meeuwenoord, N. J., Hoogendoorn, S., Dinkelaar, J., Overkleeft, H. S., van der Marel, G. A., Filippov, D. V. *Org. Lett.* **2010**, 12:5486-5489

**Development of selective LH receptor agonists by heterodimerization with a FSH receptor antagonist.** Bongers, K. M., Hoogendoorn, S., van Koppen, C. J., Timmers, C. M., van der Marel, G. A., Overkleeft, H. S. *ACS Med. Chem. Lett.* **2011**, 2:85-89

**Targeted pH-dependent fluorescent activity-based cathepsin probes.** Hoogendoorn, S., Habets, K. L., Passemar, S., Kuiper, J., van der Marel, G. A., Florea, B. I., Overkleeft, H. S. *Chem. Commun.* **2011**, 47: 9363-9365

**Synthesis of pH-activatable red fluorescent BODIPY dyes with distinct functionalities.** Hoogendoorn, S., Blom A. E. M., Willems, L. I., van der Marel, G. A., Overkleeft, H. S. *Org. Lett.* **2011**, 13: 5656-5659

**Hypersensitive response to over-reactive cysteines.** Hoogendoorn, S., Willems, L., Florea, B., Overkleeft, H. *Angew. Chem. Int. Ed. Engl.* **2011**, 50: 5434-5436

**Bioorthogonal chemistry: Applications in activity-based protein profiling.** Willems, L. I., van der Linden, W. A., Li, N., Li, K.-Y., Liu, N., Hoogendoorn, S., van der Marel, G. A., Florea, B. I., Overkleeft, H. S. *Acc. Chem. Res.* **2011**, 44: 718-729

**Two-step bioorthogonal activity-based proteasome profiling using copper-free click reagents: A comparative study.** Van der Linden, W. A., Li, N., Hoogendoorn, S., Ruben, M., Verdoes, M., Guo, J., Boons, G.-J., van der Marel, G. A., Florea, B. I., Overkleeft, H. S. *Bioorg. Med. Chem.* **2012**, 20:662-666

**Identification of Novel DAG-lipase- $\alpha$  Inhibitors with Unprecedented Selectivity in Brain Using Comparative ABPP and In Silico Design.** Baggelaar, M. P., Janssen, F. J., van Esbroeck, A. C. M., den Dulk, H., Allara, M., Hoogendoorn, S., McGuire, R., Florea, B., Meeuwenoord, N., van den Elst, H., Visser, L., van der Marel, G. A., Brouwer, J., Doherty, P., Di Marzo, V., Overkleeft, H.S., van der Stelt, M. *Angew. Chem. Int. Ed. Engl.* **2013**, DOI: 10.1002/anie.201306295



# Curriculum Vitae

Sascha Hoogendoorn werd op 1 augustus 1984 geboren te Amsterdam. Zij behaalde in 2002 het VWO diploma (profielen Natuur & Gezondheid en Natuur & Techniek) aan het Erasmus College te Zoetermeer en begon in dat jaar aan de bacheloropleiding Scheikunde aan de Universiteit Leiden. In 2004 begon zij tevens aan de bacheloropleiding Bio-Farmacologische Wetenschappen aan dezelfde universiteit. In het kader van beide bachelorprogramma's werd in 2005 een korte onderzoeksstage verricht naar nieuwe allosterische modulators voor de A<sub>3</sub> adenosine receptor in de Farmacochemie vakgroep onder begeleiding van dr. J. Brussee en prof. dr. A. P. IJzerman.

In 2006 begon zij aan de masteropleiding Chemistry (track 'Design and Synthesis'). Haar hoofdvakstage, getiteld 'Synthesis and biological evaluation of dimeric FSHR/LHR modulators', voerde zij uit in de vakgroep Bio-Organische Synthese onder begeleiding van dr. K. M. Bongers, prof. dr. G. A. van der Marel en prof. dr. H. S. Overkleeft. Dit werk werd bekroond met de Unilever Research Prijs. Van april tot oktober 2008 werd in het kader van de bijvakstage het onderzoek getiteld 'Molecular mechanisms of CB1 receptor activation - studies using the novel peptide antagonist hemopressin and its analogues' uitgevoerd in de groep van prof. dr. L. A. Devi aan Mount Sinai School of Medicine (New York, USA). In november 2008 werd het Master of Science diploma 'cum laude' behaald.

Van januari 2009 tot september 2013 werd als assistent in opleiding het onderzoek beschreven in dit proefschrift uitgevoerd in de vakgroep Bio-Organische Synthese onder leiding van prof. dr. G. A. van der Marel en prof. dr. H. S. Overkleeft. Tevens werd een gedeelte van het beschreven werk uitgevoerd in de vakgroep Medische Biochemie (AMC, Amsterdam) onder leiding van dr. R. G. Boot en prof. dr. J. M. F. G. Aerts. Delen van dit onderzoek zijn gepresenteerd door middel van posters op de jaarlijkse NWO-CW 'Design and Synthesis' conferenties (2009, 2010, 2012) en CHAINS (2011) welke tweemaal werden bekroond met een posterprijs (2010, 2011). Posterpresentaties werden gegeven op het IPS congres (San Diego, USA, 2011) en tijdens de EMBO Chemical Biology congressen (Heidelberg, Duitsland, 2010, 2012). Daarnaast werd op het EMBO Chemical Biology congres (2012) een mondelinge presentatie gegeven. In 2009 heeft de auteur deelgenomen aan de zomerschool 'New horizons in synthetic methodology' van de HRSMC graduate school.

Thans is de auteur van dit proefschrift werkzaam als onderzoeker in de groep van prof. J. K. Chen, Stanford School of Medicine, USA.